ARMY COMMUNICATIONS RESEARCH AND DEVELOPMENT COMMAND -- ETC F/G 9/1 PROCEEDINGS OF THE INTERNATIONAL WIRE AND CABLE SYMPOSIUM (28TH--ETC(U) AD-A081 428 NOV 79 NL UNCLASSIFIED 1 of 5 AD-AO8I428 1 0 -- j ì

Proceedings of the



28th INTERNATIONAL WIRE & CABLE SYMPOSIUM

NOVEMBER 13 THRU 15 1979





SPONSORED BY THE

Approved for public released
Distribution Unlimited

U S Army Communications Research and Development Command Fort Monmouth, New Jersey



REPORT DOCUMENTA		READ INSTRUCTIONS BEFORE COMPLETING FORM
REPORT NUMBER N/A	2. GOVT ACCESSION	NO. 3. RECIPIENT'S CATALOG NUMBER
TITLE (and Subtitle)		5. TYPE OF REPORT & PERIOD COVERED
Proceedings of the Inte	rnational Wire and	Final 13-15 November
Cherry Hill, New	Jersey on	6. PERFORMING ORG. REPORT NUMBER
various November 13,		9 8. CONTRACT OR GRANT NUMBER(6)
		None
US Army Communications R&D C Fiber Optic Team (DRDCO-COM- Multichannel Trans Div, CENC	Command RM-1)	10. PROGRAM ELEMENT, PROJECT, TASK AREA & WORK UNIT NUMBERS 111.62701 AH92 612701, H92.MA.11,21
. CONTROLLING OFFICE NAME AND ADDRE US Army Communications R&D C	command 🖫 🗼 📑	NOVEMBER 1979
Fiber Optic Team (DRDCO-COM- Multichannel Trans Div., CEN		13. NUMBER OF PAGES
MONITORING AGENCY NAME & ADDRESS(I	f different from Controlling Office	15. SECURITY CLASS. (of this report)
SAME AS ABOVE	111457	UNCLASSIFIED
	(410)	15a. DECLASSIFICATION/DOWNGRADING SCHEDULE
DISTRIBUTION STATEMENT (at the abetract		rept.
16 1627×14	4192	
Supplementary Notes Proceedings of technical pap Cable Symposium sponsored an & Development Command	nnually by US Army C	ommunications Research
KEY WORDS (Continue on reverse side if necesside Aerospace electronics, cable cable materials, cable performance, interconnections, mix wire insulation, wire materials.)	e design, cable eval ormance, cable testi litary electronics,	ng, electronic wiring, fiber
· · · · · · · · · · · · · · · · · · ·	Cable Symposium is to ngs include fifty on wire and cable, mand allation, application essing, wire/mable d	e papers (51) in the field terials, testing, evaluation, ons, fire retardancy, fiber

DD 1 JAN 73 1473 EDITION OF 1 NOV 68 IS OBSOLETE

UNCLASSIFIED

REPORT DOCUMENTA	READ INSTRUCTIONS BEFORE COMPLETING FORM		
REPURT NUMBER	2. GOVT ACCESSION NO	. 3. RECIPIENT'S CATALOG NUMBER	
4. TITLE (and Subtitle) Proceedings of the 28th Inte Cable Symposium 1979	5. TYPE OF REPORT & PERIOD COVERED Final 13-15 November 6. PERFORMING ORG. REPORT NUMBER N/A		
7. AUTHOR(*) Various	6. CONTRACT OR GRANT NUMBER(s)		
9. PERFORMING ORGANIZATION NAME AND A US Army Communications R&D C Fiber Optic Team (DRDCO-COM- Multichannel Trans Div, CENC	10. PROGRAM ELEMENT, PROJECT, TASK AREA & WORK UNIT NUMBERS 1L1.62701.AH92 612701.H92.MA.11.21		
US Army Communications R&D C Fiber Optic Team (DRDCO-COM-	ommand	12. REPORT DATE November 1979	
Multichannel Trans Div., CEN	13. NUMBER OF PAGES 400		
14. MONITORING AGENCY NAME & ADDRESS(1) SAME AS ABOVE	15. SECURITY CLASS. (of this report) UNCLASSIFIED 15. DECLASSIFICATION/DOWNGRADING SCHEDULE		

16. DISTRIBUTION STATEMENT (of this Report)

Approved for Public Release: Distribution Unlimited.

17. DISTRIBUTION STATEMENT (of the abstract entered in Block 20, if different from Report)

18. SUPPLEMENTARY NOTES

Proceedings of technical papers presented at 28th International Wire and Cable Symposium sponsored annually by US Army Communications Research & Development Command

- 19. KEY WORDS (Continue on reverse side if necessary and identify by block number)

 Aerospace electronics, cable design, cable evaluation, cable manufacture,
 cable materials, cable performance, cable testing, electronic wiring, fiber
 optics, interconnections, military electronics, telephone communications,
 wire insulation, wire materials, wire testing.
- 20. ABSTRACT (Continue on reverse side if necessary and identity by block number)

 The International Wire and Cable Symposium is the only symposium of its kind in the world. The proceedings include fifty one papers (51) in the field of electrical and electronic wire and cable, materials, testing, evaluation, connections, splicing, installation, applications, fire retardancy, fiber optics, manufacturing, processing, wire/mable design and manufacturing.

DD 1 JAN 73 1473 EDITION OF THOU 65 IS OBSOLETE

UNCLASSIFIED

SECURITY CLASSIFICATION OF THIS PAGE (When Date Entered)

REPORT DOCUMENTATION I	PAGE	READ INSTRUCTIONS BEFORE COMPLETING FORM	
REPORT NUMBER N/A	2. GOVT ACCESSION NO.	3. RECIPIENT'S CATALOG NUMBER	
4. TITLE (and Subtitle) Proceedings of the 28th Internatio Cable Symposium 1979	5. TYPE OF REPORT & PERIOD COVERED Final 13-15 November 6. PERFORMING ORG. REPORT NUMBER N/A		
7. Author(*) Various	8. CONTRACT OR GRANT NUMBER(s)		
9. PERFORMING ORGANIZATION NAME AND ADDRESS US Army Communications R&D Command Fiber Optic Team (DRDCO-COM-RM-1) Multichannel Trans Div, CENCOMS	10. PROGRAM ELEMENT. PROJECT, TASK AREA & WORK UNIT NUMBERS 111.62701.AH92 612701.H92.MA.11.21		
11. CONTROLLING OFFICE NAME AND ADDRESS US Army Communications R&D Command		12. REPORT DATE November 1979	
Fiber Optic Team (DRDCO-COM-RM-1) Multichannel Trans Div., CENCOMS	13. NUMBER OF PAGES 400		
14. MONITORING AGENCY NAME & ADDRESS(If ditterent SAME AS ABOVE	15. SECURITY CLASS. (of this report) UNCLASSIFIED 15a. DECLASSIFICATION/DOWNGRADING SCHEDULE		

16. DISTRIBUTION STATEMENT (of this Report)

Approved for Public Release: Distribution Unlimited.

- 17. DISTRIBUTION STATEMENT (of the abstract entered in Block 20, if different from Report)
- Proceedings of technical papers presented at 28th International Wire and Cable Symposium sponsored annually by US Army Communications Research & Development Command
- 19. KEY WORDS (Continue on reverse side if necessary and identity by block number)
 Aerospace electronics, cable design, cable evaluation, cable manufacture,
 cable materials, cable performance, cable testing, electronic wiring, fiber
 optics, interconnections, military electronics, telephone communications,
 wire insulation, wire materials, wire testing.
- 20. ABSTRACT (Continue on reverse side if necessary and identity by block number)

 The International Wire and Cable Symposium is the only symposium of its kind in the world. The proceedings include fifty one papers (51) in the field of electrical and electronic wire and cable, materials, testing, evaluation, connections, splicing, installation, applications, fire retardancy, fiber optics, manufacturing, processing, wire/mable design and manufacturing.

DD , FORM 1473 EDITION OF 1 NOV 65 IS OBSOLETE

UNCLASSIFIED

SECURITY CLASSIFICATION OF THIS PAGE (When Data Entered)

REPORT DOCUMENTATION	READ INSTRUCTIONS BEFORE COMPLETING FORM			
f. REPORT NUMBER N/A	2. GOVT ACCESSION NO.	3. RECIPIENT'S CATALOG NUMBER		
4. TITLE (and Subtitle) Proceedings of the 28th Interna Cable Symposium 1979	5. TYPE OF REPORT & PERIOD COVERED Final 13-15 November 6. PERFORMING ORG. REPORT NUMBER N/A			
7. AUTHOR(*) Various	8. CONTRACT OR GRANT NUMBER(s) - None			
US Army Communications R&D Comm Fiber Optic Team (DRDCO-COM-RM- Multichannel Trans Div, CENCOMS	10. PROGRAM ELEMENT, PROJECT, TASK AREA & WORK UNIT NUMBERS 1L1.62701.AH92 612701.H92.MA.11.21			
US Army Communications R&D Comm		12. REPORT DATE November 1979		
Fiber Optic Team (DRDCO-COM-RM-Multichannel Trans Div., CENCOM	13. NUMBER OF PAGES 400			
14. MONITORING AGENCY NAME & ADDRESS(II dill SAME AS ABOVE	15. SECURITY CLASS. (of this report) UNCLASSIFIED 15. DECLASSIFICATION/DOWNGRADING SCHEDULE			

16. DISTRIBUTION STATEMENT (of this Report)

Approved for Public Release: Distribution Unlimited.

- 17. DISTRIBUTION STATEMENT (of the abstract entered in Block 20, if different from Report)
- Proceedings of technical papers presented at 28th International Wire and Cable Symposium sponsored annually by US Army Communications Research & Development Command
- 19. KEY WORDS (Continue on reverse side if necessary and identify by block number)
 Aerospace electronics, cable design, cable evaluation, cable manufacture,
 cable materials, cable performance, cable testing, electronic wiring, fiber
 optics, interconnections, military electronics, telephone communications,
 wire insulation, wire materials, wire testing.
- 20. ABSTRACT (Continue on reverse side if necessary and identity by block number)

 The International Wire and Cable Symposium is the only symposium of its kind in the world. The proceedings include fifty one papers (51) in the field of electrical and electronic wire and cable, materials, testing, evaluation, connections, splicing, installation, applications, fire retardancy, fiber optics, manufacturing, processing, wire/mable design and manufacturing.

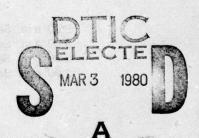
DD 1 JAN 73 1473 EDITION OF 1 NOV 65 IS OBSOLETE

UNCLASSIFIED

PROCEEDINGS OF 28th INTERNATIONAL WIRE AND CABLE SYMPOSIUM

Sponsored by
US Army Communications Research and Development Command
(CORADCOM) Fort Monmouth, N. J.

Cherry Hill, New Jersey November 13, 14 and 15, 1979



APPROVED FOR PUBLIC RELEASE: DISTRIBUTION UNLIMITED

organise at as a same. After the emposium stane population again at the

addressed of appropriate sensor characteristics of penetral sensor and conference of penetral sensor and conference of the conference of t

28th INTERNATIONAL WIRE AND CABLE SYMPOSIUM

SYMPOSIUM COMMITTEE

Elmer F. Godwin, Chairman, USA CORADCOM (201) 544-2770
Adolf Asam, ITT Electro-Optical Products Division
Ken Bow, Dow Chemical USA
Leo M. Chattler, DCM International Corporation
Michael DeLucia, David W. Taylor Naval Ship R&D Center
Marta Farago, Northern Telecom Ltd.
Irving Kolodny, General Cable Corporation
William Korcs, Shell Development Company
John Lelivelt, USA CORADCOM
Frank Short, Belden Corporation
George Webster, Bell Labs

ADVISORY

Joe Neigh, AMP, Inc.

TECHNICAL SESSIONS

bnammod mampolova Tuesday, 13 November 1979 Boli British 1900 ymna 20

9:30 a.m. Session I:	Tutorial - Wire and Cable Industry As
	Others See Us

2:00	p.m.	Session	II:	Cable Design I
2:00	p.m.	Session	111:	Testing

Wednesday, 14 November 1979

9:00 a.m.	Session	IV:	Cable Materials & Reclamation
9:00 a.m.	Session '	V: 6	Cable Design II
2:00 p.m.	Session '	VI:	Connections for Telecommunications
2:00 p.m.	Session '	VII:	Cable Applications

Thursday, 15 November 1979

9:00 a.m	. Session	VIII:	Fire Considerations
9:00 a.m	Session	IX:	Optical Fiber
2:00 p.m	. Session	X:	Optical Cable

PAPERS

Responsibility for the contents rests upon the authors and not the symposium committee or its members. After the symposium, all the publication rights of each paper are reserved by their authors, and requests for republication of a paper should be addressed to the appropriate author. Abstracting is permitted, and it would be appreciated if the symposium is credited when abstracts or papers are republished. Requests for individual copies of papers should be addressed to the authors.



MESSAGE FROM THE CHAIRMAN

Accession For

NTIS GRANT
DDC TAB
Unamounce:
Justificati

By
Distribution

Availability Codes

Availand/or
special

Welcome to the 28th International Wire and Cable Symposium (IWCS). During the past year, your Chairman and Co-Chairman retired from Government Service. It has been my pleasure to be associated with the IWCS for the past sixteen (16) years, serving as its Co-Chairman or Chairman for the last seven years. During the past seven years, I have been most gratified by the enthusiasm and cooperation of the committee members who worked so diligently in the planning and conduct of these symposia. I hope to continue my association with the committee and symposium.

I am pleased to report that last year's symposium (27th) was again a tremendous success, both in attendance and in favorable responses received on the technical presentations. The attendance of approximately 1600 consisted of 218 international representatives from twenty three countries. Twenty four of the fifty three papers presented were by representatives from nine different countries. The increase each year in international representation is indeed encouraging.

The response to the call for papers was tremendous again this year with many excellent abstracts submitted for consideration. Nine technical sessions and a tutorial session are included in the program. A timely topic and distinguished panel members should make the tutorial session entitled "Wire and Cable Industry as Others See Us" an interesting and informative session.

The committee continues to look for ways to improve the activities of the symposium. We are constantly exploring new ideas and innovations for technical growth and to promote the interchange of information, as well as provide a convivial environment for its attendees. Your comments and suggestions are solicited and warranted in order to maintain the prestigious position the symposium has obtained in the worldwide wire and cable community.

I wish to express my appreciation to all committee members for their dedicated efforts and cooperation. The ultimate credit for the success of the symposium belongs to the committee and to the many individual governmental and industrial organizations that provide technical assistance and/or contributions. The committee solicits the continued support of all members of the wire and cable industry to ensure success in years to come.

ELMER F. GODWIN Chairman

PROCEEDINGS

INTERNATIONAL WIRE & CABLE SYMPOSIUM

BOUND-AVAILABLE AT CORADCOM

20th	International	Wire &	Cable	Symposium	Proceedings	_	1971 -	\$ 4.00
21st	International	Wire &	Cable	Symposium	Proceedings	_	1972 -	5.00
22nd	International	Wire &	Cable	Symposium	Proceedings	_	1973 -	6.00
23rd	International	Wire &	Cable	Symposium	Proceedings	_	1974 -	7.00
24th	International	Wire &	Cable	Symposium	Proceedings	_	1975 -	7.00
25th	International	Wire &	Cable	Symposium	Proceedings	-	Not Avail	able
26th	International	Wire &	Cable	Symposium	Proceedings	_	1977 -	7.00
27th	International	Wire &	Cable	Symposium	Proceedings	_	1978 -	8.00
*28th	International	Wire &	Cable	Symposium	Proceedings	-	1979 -	10.00
*Extra	copies 1-3 \$1	0.00; ne	xt 4-10	\$8.00; next	11 and above :	\$5.0	0 each.	

Make check or bank draft **PAYABLE in US** dollars to the **INTERNATIONAL WIRE** & **CABLE SYMPOSIUM** and forward request to:

Mr. E. F. Godwin, Chairman
International Wire & Cable Symposium
US Army Communications R&D Command
ATTN: DRDCO-COM-RM-1
Fort Monmouth, NJ 07703
USA

PHOTOCOPIES—AVAILABLE AT DEPARTMENT OF COMMERCE

Photocopies are available for complete sets of papers for 1964 and 1966 thru 1978. Information on prices and shipping charges should be requested from the:

US Department of Commerce
National Technical Information Service
Springfield, Virginia 22151
USA

Include Title, Year and "AD" Number.

13th Annual Wire & Cable Symposium (1964)	- A	D 7	87164	
15th Annual Wire & Cable Symposium (1966)	- 4	DA	00660	1
16th International Wire & Cable Symposium (1967)	- 4	D 7	87165	
17th International Wire & Cable Symposium (1968)	- 4	D 7	87166	
18th International Wire & Cable Symposium (1969)	- 4	D 7	87167	
19th International Wire & Cable Symposium Proceedings 1970	- 4	D 7	14985	
20th International Wire & Cable Symposium Proceedings 1971	- 4	D 7	33399	
21st International Wire & Cable Symposium Proceedings 1972	- 4	D 7	52908	
22nd International Wire & Cable Symposium Proceedings 1973				
23rd International Wire & Cable Symposium Proceedings 1974	- 4	DA	00325	1
24th International Wire & Cable Symposium Proceedings 1975				
25th International Wire & Cable Symposium Proceedings 1976				
26th International Wire & Cable Symposium Proceedings 1977				
27th International Wire & Cable Symposium Proceedings 1978				
Kwix Index of Technical Papers, International Wire & Cable				
Symposium (1952 - 1975)	- A	D A	02755	8

HIGHLIGHTS OF THE 27TH INTERNATIONAL WIRE AND CABLE SYMPOSIUM

NOVEMBER 14, 15, 16, 1978 CHERRY HILL HYATT HOUSE, CHERRY HILL, N.J.



Banquet Guest Speaker—Dr. G. P. Dinneen, Assistance Secretary of Defense (Comm. Commano, Control and Intelligence).



Members - Tutorial Session (L to R): R. Flores, REA; J. C. Storry, GTE; F. Banks, Bell Canada; H. Anderson, Yankee Group and T. Farrell, 3M CO. - Session Chairman.



T. Pfeiffer, Tech. Dir., CORADCOM, Fort Monmouth.



Awards presented to T. McManus, Northern Telecom, Canada; and R. Beveridge, Saskatchewan, Telecomm. Canada, for outstanding tech. paper; and W. Schmacher, AMP Inc. for best presentation.



Col. E. R. Weidner, Jr., Chief of Staff, CORADCOM, Fort Monmouth.



Committee members J. Neigh, AMP Inc.; and T. Farrell, 3M Co. with retirement certificate.

CANDID SCENES AT THE 27TH IWCS





AWARDS

Best Presentation

Outstanding Technical Paper

Method

H. Lubars and J. A. Olszewski, General Cable Corp—"Analysis of Structural Return Loss in CATV Coaxial Cable"	1968	N. Dean, B.I.C.C.—"The Development of Fully Filled Cables for the Distribution Network"
J. B. McCann, R. Sabia and B. Wargotz, Bell Laboratories—"Characterization of Filler and Insulation in Waterproof Cable"	1969	J. D. Kirk, Alberta Government Telephones— "Progress and Pitfalls of Rural Buried Cable"
D. E. Setzer and A. S. Windeler, Bell Laboratories—"A Low Capacitance Cable for the T2 Digital Transmission Line"	1970	Dr. O. Leuchs, Kable and Metalwerke—"A New Self-Extinguishing Hydrogen Chloride Binding PVC Jacketing Compound for Cables"
R. Iyenger, R. McClean and T. McManus, Bell Northern Research—"An Advanced Multi-Unit Coaxial Cable for Tool PCM Systems"	1971	S. Nordblad, Telefonaktiebolaget LM Erics- son—"Multi-Paired Cable of Nonlayer Design for Low Capacitance Unbalance Telecommunication Network"
		N. Kojima, Nippon Telegraph and Telephone— "New Type Paired Cable for High Speed PCM Transmission"
J. B. Howard, Bell Laboratories—"Stabilization Problems with Low Density Polyethylene Insulations"	1972	S. Kaufman, Bell Laboratories—"Reclamation of Water-Logged Buried PIC Telephone Cable"
Dr. H. Martin, Kabelmetal—"High Power Radio Frequency Coaxial Cables, Their Design and Rating"	1973	R. J. Oakley, Northern Electric Co., Ltd.—"A Study into Paired Cable Crosstalk"
D. Doty, AMP Inc.—"Mass Wire Insulation Displacing Termination of Flat Cable"	1974	G. H. Webster, Bell Laboratories—"Material Savings by Design in Exchange and Trunk Telephone Cable"
T. S. Choo, Dow Chemical U.S.A.—"Corrosion Studies on Shielding Materials for Underground Telephone Cables"	1975	J. E. Wimsey, United States Airforce—"The Bare Base Electrical Systems"
N. J. Cogelia, Bell Telephone Laboratories and G. K. Lavoie and J. F. Glahn, US Department of Interior—"Rodent Biting Pressure and Chemical Action and Their Effects on Wire and Cable Sheath"	1976	Michael DeLucia, Naval Ship Research and Development Center—"Highly Fire-Retardant Navy Shipboard Cable"
Thomas K. McManus, Northern Telecom Canada Ltd. and R. Beveridge, Saskatchewan Telecom- munications, Canada—"A New Generation of Filled Core Cable"	1977	William L. Schmacher, AMP Inc.—"Design Considerations for Single Fiber Connector"
Fumio Suzuki, Shizuyoshi Sato, Akinori Mori and Yoichi Suzuki; Sumitomo Electric Industries, Ltd., Japan-Microcoaxial Cables Insulated with Highly Expanded Polyethylene By Chemical Blowing	1978	Richard C. Mondello, Bell Labs.—"Design and Manufacture of An Experimental Lightguide Cable For Undersea Transmission Systems"

CONTRIBUTORS

Abbey Plastics Corp.

Hudson, MA

Abbott Industries, Inc.

Leominster, MA

AFA Industries/Arnold Field Assoc.

The Fullkura Cable Works, Inc.

Cavitt Wire & Cable Co. Inc

Hackensack, NJ

Alambres Y Cables Venezolanos,

C.A.Alcave

Caracas, Venezuela

First Way, Wembley, Middlesex, Eng.

Allied Chemical Corp.

Morristown, NJ

Amercable Corp.

El Dorado, AR

American Hoechst Corp.

Leominster, MA

The Anaconda Co. Aluminum Div., Mill Prod.

Louisville, KY

Anaconda/Continental Wire & Cable

York, PA

Andrew Corp.

Orland Park, IL

ARCO Chemical Co.

Philadelphia, PA

Arco Polymers

Philadelphia, PA

Arvey Corp.

Cedar Grove, NJ

Austral Standard Cables Pty. Ltd.

Clayton, Victoria, Australia

Bell Canada (Ontario Region)

Toronto, Ontario, Can.

Belding Corticelli Thread Co.

Putnam, CT

Berkshire Electric Cable Co.

Leeds, MA

Berk-Tek, Inc.

Reading, PA

B. F. Goodrich Chemical Div.

Cleveland, OH

BICC Telecommunication Cables Ltd.

Prescot, Merseyside, England

Boston Insulated Wire & Cable Co. Ltd.

Hamilton, Ontario, Can.

BP Chemicals

Geneva, Switzerland

BP Chemicals (Suisse) SA

Geneva, Switzerland

C. W. Brabender Instruments Inc.

S. Hackensack, NJ

Brand-Rex Company

Willimantic, CT 06226

Breen Color Concentrates, Inc.

The Celker Com.

Lambertville, NJ 08530

The Bridge Mfg. Co.

Enfield, CT

Burgess Pigment Co.

Sandersville, GA

Cable Consultants Corp.

Larchmont, NY

Cabot Corp.

Billerica, MA

Cable Equipment Corp.

New York, NY

Cables de Comunicaciones S.A.

Zaragonza, Spain

Camden Wire Co. Inc.

Camden, NY

Campbell Technical Waxes Ltd.

Kent, England

Canada Wire & Cable Ltd.

Winnipeg, Manitoba, Can.

Canadian Industries Ltd.

Willowdale, Ontario, Can.

Carlew Chemicals, Ltd.

Montreal, Can.

R. E. Carroll, Inc.

Trenton, NJ

Cary Chemicals Inc.

Edison, NJ

Central Tool & Machine Co., Inc.

Bridgeport, CT

Chase & Sons, Inc.

Randolph, MA

Chemplast Inc.

Wayne, NJ

Cities Service, Chester Cable Operations

Chester, NY

Cida Geigy

Ardsley, NY

Cities Service Co., Colors & Specialties

Tulsa, OK

Colonial Rubber Works Inc.

Dyersburg, TN

Colorite Plastics Co., Div. of Dart Indust.

Ridgefield, NJ

Comm/Scope, Co.

Catawba, NC

Communications Technology Corp.

Los Angeles, CA

Conoco Chemicals Co.

Houston, TX

Copperweld Bimetallics Group

Pittsburgh, PA

Corning Glass Works

Corning, NY

Credit Lyonnais

Paris, France

Crellin Plastics

Chatham, NY

Dainichi-Nippon Cables Ltd.

Tokyo, Japan

Davis-Standard

Pawcatuck, CT

The Delker Corp.

Branford, CT

Delphi Wire & Cable

Folcroft, PA

Diamond Shamrock Alberta Gas Ltd.

Snowden, Montreal, Can.

Diamond Shamrock Corp.

Cherry Hill, NJ

Disco Inc.

Ringwood, NJ

Dow Chemical Corp.

Midland, MI

Dow Corning Corp.

Midland, MI

E.I. du Pont de Nemours Co.

Wilmington, DE

DuPont of Canada Ltd.

Toronto, Can.

Dussek Bros. Australia

Regents Park, Australia

Dussek Bros. (Canada) Ltd.

Belleville, Ontario, Can.

Duncan M. Gillies Co. Inc.

West Boylston, MA

Eastman Chemical Products Inc.

Kingsport, TN

Economy Cable Grip Co., Inc.

So. Norwalk, CT

G + W Elco Corp.

Huntingdon, PA

Electroconductores C.A.

Caracas. Venezuela

The Electric Wire & Cable Co. of Israel Ltd., Haifa

Haifa, Israel

Essex Group inc.

Decatur, IL

Ets. Pourtier Pere & Fils

Romainville, France

Exxon Chemical Co. USA

Houston, TX

Fabricon Manufacturing Ltd.

Belleville, Ontario, Can.

Felten & Guilleaume Carlswerk AG

Koln, W. Germany

Firestone Plastics Co.

Pottstown, PA

Firestone Plastics Co.

Pottstown, PA

Forumlabs Industrial Inks

Escondido, CA

Freeport Kaolin Co. ashoW seel DipotersuO

NYC. NY

The Fujikura Cable Works

Chiba, Japan

CONTRIBUTORS

The Fujikura Cable Works, Inc.

Tokyo, Japan

Gavitt Wire & Cable Co. Inc.

Brookfield, MA

Gavlick Machinery Corp.

Bristol, CT

GE Co.- Silicone Products Div.

Waterford, NY

Gem Gravure Co. Inc.

West Hanover, MA

General Cable Corp.

Greenwich, CT

General Electric Co.

Waterford, NY

General Telephone & Electronics Corp.

Stamford, CT

G. M. Gest Inc.

Quebec, Can.

W. L. Gore & Associates, Inc.

Newark, DE

Great American Chem. Co.

Fitchburg, MA

Guill Tool & Engineering Co. Inc.

West Warwick, RI

Harbour Industries, Inc.

Shelburne, VT

High Voltage Engineering Corp.

Burlington, MA

Hitachi Cable, Ltd.

Tokyo, Japan

HiTemp Wires, Inc.

Hauppauge, NY

J. M. Huber Corp.

Borger, TX

Hudson Wire Co.

Ossining, NY

ICI Americas Inc. Base and America Shares Diluga

Wilmington, DE

Insulation/Circuits, Lake Publishing Corp.

THE AUDBROAD RUST

Libertyville, IL

Kabmatik AB

Stockholm, Vaellingby, Sweden

Kenrich Petrochemicals Inc.

Bayonne, NJ

LaBarge, Inc.

Irving, CA 92714

Lamart Corp. 160 notice the emitodate T 0018

Clifton, NJ

Laribee Wire Man. Co.

Camden, NY

3M Company

St. Paul, MN

Maillefer Company

South Hadley, MA

Manning Paper Co.

Troy, NY

Micro-Tek Corp.

Cinnaminson, NJ

Monsanto Ind. Chem. Co.

St. Louis, MO

The Montgomery Company

Windsor Locks, CT

H. Muehlstein & Co.

Greenwich, CT

Nesor Alloy Corp.

West Caldwell, NJ

New England Printed Tape Co.

Pawtucket, RI

New York Telephone Co.

New York, NY

NFK Kabel B.V.

Delft, The Netherlands

Nippon Telegraph & Telephone Public Corp.

Tokyo, Japan

NL Industries

Hightstown, NJ

Nokia Electronics Inc.

Atlanta, GA

Nonotuck Man. Co.

South Hadley, MA

Northeast Wire Co. Inc.

Holyoke, MA

Northern Petrochemical Co.

Des Plaines, IL

Northern Telecom Canada Ltd.

Lachine, Quebec, Can.

Noury Chemical Corp.

Burt, NY

Oak Materials Group

Hoosick Falls, NY

The Okonite Company

Ramsev, NJ

Olex Cables Ltd.

Tottenham, Victoria, Australia

Omega Wire Inc.

Camden, NY

Pacific Petrochemicals Ltd.

Downsview, Ontario, Can.

Packard Electric Div. GMC

Warren, OH

Pantasote Inc.

Passaic, NJ

Pennwalt Corporation

Philadelphia, PA

Penreco

Butler, PA

A. E. Petsche Co. Inc.

Arlington, TX

Phalo Corp.

Shrewsbury, MA

Phelps Dodge Int'l Corp.

Coral Gables, FL

Phelps Dodge Thailand Ltd.

Bangkok, Thailand

Phillips Cables Ltd.

Vancouver, B.C., Can.

Phillips Chemical Co.

Pasadena, TX

Pirelli Cimo Corp.

Allendale, NJ

Pirelli SA ball ashow gnissiperficested off?

Sao Paulo, Brazil

Plastoid Corporation (Appellate) Islandee T

New York, NY

Plymouth Rubber Co., Inc.

Canton, MA

Plymouth Wire & Cable Co.

Worcester, MA

Polymer Services, Inc. and American American

East Brunswick, NJ

PPG Industries, Inc. on Warrante West of the State of the

Chicago, IL

Prestolite Wire Division

Hudson, MA

Radiation Dynamics Inc.

Melville, NY

Radix Wire Co. Issue O to the Doors T

Cleveland, OH

Raychem Corp.

Menlo Park, CA

Reichhold Chemicals, Inc.

Hackettstown, NJ/Mansfield, MA

Reliable Electric Co.

Franklin Park, IL

The Rochester Corp.

Culpeper, VA

The Rockbestos Co.

New Haven, CT

John Royle & Sons

Paterson, NJ

SCAL

Paris, France

Shell Chemical Co.

Houston, TX

Siecor Optical Cables Inc.

Horseheads, NY

SILEC

Paris, France

Siemens AG

Munich, W. Germany

Societe Anonyme de Telecommunications

Paris, France

Southwest Chemical & Plastics

Seabrook, TX

Southwire Co.

Carrollton, GA

Sterling Davis Electric

Wallingford, CT

Sumitomo Electric Industries Ltd.

Osaka, Japan

Sun Chemical Corp., Facile Div.

Paterson, NJ

Sun Petroleum Products Co.

Philadelphia, PA

Superior Cable Corp.

Hickory, NC

Systems Communications Cable Inc.

Phoenix, AZ

Syncro Machine Co.

Perth Amboy, NJ

The Swiss Insulating Works Ltd.

Breitenbach, Switzerland

Technical Coatings Co.

Nutley, NJ

Teknor Apex Co. And And Indiana Andrew 19

Pawtucket, RI

Telecom Australia Headquarters

Melbourne, Australia

Teledyne Thermatics

Elm City, NC

Teledyne Western Wire & Cable - N. ogsowii.)

Los Angeles, CA

Telephone Cables Ltd.

Dagenham, England

Tenneco Chemicals Co.

Piscataway, NJ

Tensolite Co., Div. of Carlisle Corp.

Buchanan, NY

Tekronix Inc.

Beaverton, OR

Thermax Wire Corp.

Flushing, NY

Times Fiber Communications, Inc.

Wallingford, CT

Torpedo Wire & Strip, Inc.

Pittsfield, PA

Trea Industries Inc.

N. Kingstown, RI

Ube Industries Ltd.

New York, NY

Unifos Kemi AB viscos and viscos from an T

Stenungsund, Sweden

Union Carbide Corp.

Hackensack, NJ

Union Carbide Corp.

New York, NY

US Steel Corp. On the Transmission of the Steel Corp.

Pittsburgh, PA

Wardwell Braiding Machine Co.

NAK Kebel B.V.

Central Falls, RI

Western Electric

Norcross, GA

G. Whitfield Richards Co.

Philadelphia, PA

Whitmor Wire & Cable Corp.

No. Hollywood, CA 91605

Wilcom Products, Inc.

Laconia, NH 03246

Wilson Products Inc.

Neshanic Station, NJ

Wire Journal

Guilford, CT

Wyre Wynd Inc.

Jewett City, CT

Wyrough & Loser, Inc. Street S

Trenton, NJ

The Zippertubing Co.

Los Angeles, CA

VINDHER OF AN YEAR ON A TABLE O	F CONTENTS
	seriar Lich Suden Englisht und Hubertine und Fluggeschlichen Zusten 2. Bernes Lich Lunden Konflugt
Tuesday, November 13, 1979—9:30 am Hunterdon and Cumberland Rooms	A SIMPLIFIED METHOD FOR COMPARING INSULA- TION CUT-THROUGH RESISTANCE OF BACKPANEL WIRES, P. Hubis, W.L. Gore & Associates Inc
SESSION I: Tutorial WIRE AND CABLE INDUSTRY AS OTHERS SEE US	A TIME DOMAIN CROSSTALK TEST FOR COAXIAL CABLES, R.M. Brooks, W.J. Stephens, Post Office Telecommunications, Ipswich, England
Chairperson: Irv Kolodny, General Cable Corp. Panel Members: Mr. R. Callahan, Editor/Publisher, Wire Technology & Wire Industry News	LCSS MEASUREMENT SYSTEM OPERATING IN THE FREQUENCY RANGE 100 MHz TO 300 MHz COVER-ING THE TEMPERATURE RANGE 2°C to 40°C, P.C. Francis, Bakelite Zylonite Ltd., Stirlingshire, Scotland and G.J. Hill, Electrical Research Association, Surrey
Mr. L. Perlman, Director, Com- modities Research Unit Limited Mr. John Kessler, President of	England
Kessler Marketing Intelligence Mr. George Farley, Executive Editor Electrical Wholesaling, McGraw-Hill	L.J. Hall, J. Lynch and R. Pirotta, Telecom Australia, Melbourne, Australia
A PLANICARRINAN POWSH AND DENISTOLOSIDE PARTICAL ARTHUR.	Laboratories
Tuesday, November 13, 1979—2:00 pm Gloucester Room	Wednesday, November 14, 1979—9:00 am Gloucester Room
SESSION II: CABLE DESIGN I	SESSION IV: CABLE MATERIALS & RECLAMATION
Chairperson: Ken Bow, Dow Chemical USA	Chairperson: Bill Korcz, Shell Development Co.
MULTI-LAYER SHIELD DESIGN AND PERFORMANCE EVALUATION CONSIDERATIONS, J. Kincaid and G. Flaim, Belden Corp. 1 VINYLIDENE CHLORIDE COPOLYMER SHEATHING FOR IMPROVED FLAME RESISTANCE, R.J. Streu, R.C.	RECYCLING OF PVC FROM CABLE AND WIRE SCRAP, E. Scalco and R.L. Decker, Bell Laboratories, R.C. Donovan and A.F. Rodde, Western Electric 96 AN ATTEMPT AT RECYCLING POLYOLEFINS FROM WIRE AND CABLE SCRAP, J.A. Falter and E. Scalco,
Devereaux, W.E. Brown, Dow Chemical USA	Bell Laboratories A METHOD FOR RESTABILIZATION OF ANTIOXIDANT DEPLETED LOW DENSITY POLYETHYLENE CON- DUCTOR INSULATION, F.R. Wight, Bell Laboratories,
DESIGN AND EVALUATION OF HIGH STRENGTH SUBMARINE CABLE FOR OCEAN TOWING, S. Ta- chigami, J. Nakajima, H. Umezu, S. Kikkawa, M. Okubo, H. Kawazoe, The Furukawa Electric Co., To-	REHABILITATION OF BURIED AIR-CORE PIC CABLE PLANT, R.P. Collins and W.S. Pesto, Bell Laboratories 118
REINFORCED SELF-SUPPORTING CABLE - A NEW ALTERNATIVE IN PROTECTED AERIAL PLANT FACILITIES, P.J. Reale, Jr., L. Borowicz, Western	THE RELATION BETWEEN THE FOAMING MECHAN- ISM AND THE VISCOELASTIC PROPERTIES OF HIGH DENSITY POLYETHYLENES FOR EXPANDED COM- MUNICATION CABLES, M. Matsui and Y. Morita.
Electric Co	Dainichi-Nippon Cables Ltd., Hyogo-ken, Japan 126 EFFECT OF THERMAL AGING ON THE FLEXIBILITY AND CONDUCTIVITY OF PLATED AND UNPLATED COPPER CONDUCTORS, T. Inagaki, Hudson Wire
Cables, Ltd., Itami, Japan	Company 137
Tuesday, November 13, 1979—2:00 pm Hunterdon Room	Wednesday, November 14, 1979—9:00 am Hunterdon Room
SESSION III: TESTING	SESSION V: CABLE DESIGN II
Chairperson: Frank Short, Belden Corp.	Chairperson: Leo Chattler, DCM International Corp.
TRANSMISSION & CROSSTALK MEASUREMENTS ON INSTALLED MULTIPAIR CABLE, T. Nantz, Bell Laboratories, Norcross	ON THE NEED FOR METALLIC SCREENS IN THE SHEATHS OF TELEPHONE LOCAL-LOOP CABLES, H.J.C. Spencer and G.A. Bartlett, Post Office Telecommunications, London, England

THE DEVELOPMENT AND MEASUREMENT OF A WIDE	COM	APPLICATION OF SEISMOLOGY IN TELEPHONY,	
BAND 12 PAIR CABLE, H.L. Baker, Rediffusion Engineering Ltd., Surrey, England; J.D. Hinchliffe and R. Mullins, Reliance Cords & Cables, Ltd., London,		L. Ance and J. McCann, Rural Electrification Administration	273
England	153		
NON-CONTACT INK JET PRINTER FOR CABLE SHEATH MARKING, W. Newton, Western Electric	160		
NEW ALUMINUM SHEATH CABLE USED FOR ELEC-	18 A 5	Thursday, November 15, 1979-9:00 am	
TROMAGNETIC SHIELDING, Y. Yamazaki, T. Ideguchi and S. Masaki, Nippon Telegraph & Telephone Public		Hunterdon Room	
Corp., Tokyo, Japan	165	SECOND A SECOND	
A SHOCK-ABSORBING JACKET FOR TELECOM- MUNICATIONS CABLE, H.M. Hutson, Rural Elec-		SESSION VIII: FIRE CONSIDERATIONS	
trification Administration	174	Chairperson: Michael DeLucia, David W. Taylor No.	aval
and R.L. Beauchamp, Northern Telecom Canada Ltd.,		Ship Research and Development Cer	nter
Montreal, Quebec, Canada	179	LOW SMOKE AND FLAME SPREAD CABLES, L.J.	
Wednesday, November 14, 1979—2:00 pm		Przybyla, E.J. Coffey Underwriters Laboratories,	
Gloucester Room		S. Kaufman and M.M. Yocum, Bell Laboratories, J.C. Reed and D.B. Allen, E.I. DuPont DeNemours	
SESSION VI: CONNECTIONS FOR		and Co	281
TELECOMMUNICATIONS		DEVELOPMENT OF FLAME-RESISTANT CABLES FOR INSTRUMENTATION AND COMMUNICATION, Y. Ta-	
Chairperson: George Webster, Bell Laboratories		kahashi, T. Yamamoto and K. Nakano, The Fujikura Cable Works Ltd., Tokyo, Japan	292
64 AMORANA		A FLAME RESISTANT POWER AND CONTROL CABLE	232
CORRELATION BETWEEN LABORATORY TESTS AND TEST SITE RESULTS OF TELECOMMUNICATION		INSULATION FOR MODERN ELECTRICAL APPLICATIONS, E. Kingsbury, A. Bruhin and A.F. Wu, General	
CABLES, SPLICES AND CLOSURES, G. Boscher and		Electric Co	299
W. Giebel, Siemens AG, Munchen, Germany MODERN CONSTRUCTION METHODS TO COMBAT	184	ALL LIQUID FIRE RETARDANT URETHANE CASTING RESINS, M. Brauer and T. Kroplinski, NL Industries Inc.	305
THE RISING IN-PLACE COSTS OF UNDERGROUND		PERFORMANCE OF POLYVINYL CHLORIDE COM-	218
CABLES, T.M. Kochansky, GTE Service Corp., SIMPLIFIED PRECONNECTORIZED CABLE SYSTEM	191	MUNICATION CABLES IN A MODIFIED STEINER TUNNEL TEST I.L. Waderhra, IBM Corp.,	312
FOR THE INTERNATIONAL TELEPHONE MARKET, J.		Pagu Tagunturu Mater Wall Asia Inninegal	
Prosper and J.Z. Avalos, Cables de Communicaciones S.A., Zaragoza, Spain	201		
MULTI FIBER OPTICAL CONNECTOR COMPONENT			
CHARACTERIZATION, D.Q. Snyder, Western Electric	209	Thursday, November 15, 1979—9:00 am	
IN-THE-FIELD CONNECTIONS WITH FIBER OPTIC CABLES, A.J. Moss, J.H. Aumiller and J. Uradnisheck,		Gloucester Room	
E.I. DuPont DeNemours & Co.,	212	SESSION IX: OPTICAL FIBER	
THE RESERVE OF A WARM EAST SUBJECT OF THE PROPERTY OF THE PROP			
Wednesday, November 14, 1979–2:00 pm Hunterdon Room		Chairperson: Adolph Asam, ITT Electro-Opti Products Division	cal
nunterdon Room		Walkshire San	
SESSION VII: CABLE APPLICATIONS	alest "	IMPROVEMENT AND APPLICATION OF POLYMER CLAD OPTICAL FIBER FOR COMMUNICATION USE.	
Chairman Mont Chairm Nadalan Talana III		N. Ohmori, H. Kajioda, T. Shimada, S. Shinzawa and K.	EPE
Chairperson: Marta Farago, Northern Telecom, Lt.	a.	Takeda, Hitachi Cable Corp., Tokyo, Japan	319
LIGHTNING, TRANSIENT AND ELECTROMAGNETIC		CABLE, C. Schlef, P. Narasimham, and S.M. Oh, ITT	007
DISTRUBANCES IN THE SWEDISH DEFENCE TELECOMMUNICATION NETWORK, K. Egeland and		Electro-Optical Products Division EFFECTS OF SINGLE-MODE FIBER NA ON OPTICAL	327
H. Mork, L.M. Ericsson Network Dept., Stockholm,	005	AND MECHANICAL PROPERTIES, F.I. Akers, A.R.	
Sweden A COMPARISON OF THE PROPERTIES OF FOAM AND	225	Asam and M.S. Maklad, ITT Electro-Optical Products Division	333
FOAM-SKIN INSULATION IN FILLED CABLES, J.P.			
	222	RECENT ADVANCES IN HIGH STRENGTH OPTICAL	
Garmon and L.E. Davis, Superior Cable Corporation ANALYSIS OF LONG TERM STABILITY OF EXPANDED	232	RECENT ADVANCES IN HIGH STRENGTH OPTICAL FIBERS HAVING SURFACE COMPRESSION, M.S. Maklad, A.R. Asam and F.I. Akers, ITT Electro-Optical	
Garmon and L.E. Davis, Superior Cable Corporation ANALYSIS OF LONG TERM STABILITY OF EXPANDED INSULATION IN FILLED CABLES, M. Tenzer and J.	232	FIBERS HAVING SURFACE COMPRESSION, M.S. Maklad, A.R. Asam and F.I. Akers, ITT Electro-Optical Products Division	340
Garmon and L.E. Davis, Superior Cable Corporation ANALYSIS OF LONG TERM STABILITY OF EXPANDED INSULATION IN FILLED CABLES, M. Tenzer and J. Olszewski, General Cable Corp., Union, New Jersey and I. Kolodny, General Cable Corp.	232	FIBERS HAVING SURFACE COMPRESSION, M.S. Maklad, A.R. Asam and F.I. Akers, ITT Electro-Optical Products Division PROTECTION AND RELIABILITY OF OPTICAL FIBER ARC FUSION SPLICING, T. Arai, O. Watanabe and K.	340
Garmon and L.E. Davis, Superior Cable Corporation ANALYSIS OF LONG TERM STABILITY OF EXPANDED INSULATION IN FILLED CABLES, M. Tenzer and J. Olszewski, General Cable Corp., Union, New Jersey and I. Kolodny, General Cable Corp.		FIBERS HAVING SURFACE COMPRESSION, M.S. Maklad, A.R. Asam and F.I. Akers, ITT Electro-Optical Products Division PROTECTION AND RELIABILITY OF OPTICAL FIBER ARC FUSION SPLICING, T. Arai, O. Watanabe and K. Inada, Fujikura Cable Works Ltd., Chiba-ken, Japan; S.	340
Garmon and L.E. Davis, Superior Cable Corporation ANALYSIS OF LONG TERM STABILITY OF EXPANDED INSULATION IN FILLED CABLES, M. Tenzer and J. Olszewski, General Cable Corp., Union, New Jersey and I. Kolodny, General Cable Corp. COMPARTMENTALIZED LONGITUDINAL WATER-PROOF CABLES, D.J. Dekker, J. Bruining and G.A. Schuring, Netherlands Postal & Telecommunications	244	FIBERS HAVING SURFACE COMPRESSION, M.S. Maklad, A.R. Asam and F.I. Akers, ITT Electro-Optical Products Division PROTECTION AND RELIABILITY OF OPTICAL FIBER ARC FUSION SPLICING, T. Arai, O. Watanabe and K. Inada, Fujikura Cable Works Ltd., Chiba-ken, Japan; S. Seikai and M. Hirai, Ibaraki Electrical Communication Laboratory, N.T.T., Ibaraki-ken, Japan	340
Garmon and L.E. Davis, Superior Cable Corporation ANALYSIS OF LONG TERM STABILITY OF EXPANDED INSULATION IN FILLED CABLES, M. Tenzer and J. Olszewski, General Cable Corp., Union, New Jersey and I. Kolodny, General Cable Corp. COMPARTMENTALIZED LONGITUDINAL WATER-PROOF CABLES, D.J. Dekker, J. Bruining and G.A.		FIBERS HAVING SURFACE COMPRESSION, M.S. Maklad, A.R. Asam and F.I. Akers, ITT Electro-Optical Products Division PROTECTION AND RELIABILITY OF OPTICAL FIBER ARC FUSION SPLICING, T. Arai, O. Watanabe and K. Inada, Fujikura Cable Works Ltd., Chiba-ken, Japan; S. Seikai and M. Hirai, Ibaraki Electrical Communication	

Thursday, November 15, 1979—2:00 pm Gloucester Room

SESSION X: OPTICAL CABLE

Chairperson: Irv Kolodny, General Cable Corp.

INSTALLATION AND FIELD MEASUREMENT EQUIPMENT FOR OPTICAL COMMUNICATION CABLES, F. Krahn, W. Meininghaus, D. Rittich, K. Serapins, and H. Gladenbeck, Felten & Guilleaume Carlswerke AG, Koln, Germany

INSTALLED FIBER OPTIC CABLES, J.B. Masterson.	
General Cable Corp	36
HIGH DENSITY MULTICORE-FIBER CABLE, S. Inao, T.	
Sato, H. Hondo, M. Ogai, S. Sentsui, A. Otake and K.	
Yoshizaki, The Furukawa Electric Co., Tokyo, Japan; K.	
Ishihara and N. Uchida, Ibaraki Electrical Communica-	
tion Laboratory, Ibaraki, Japan	370
STRESS-STRAIN BEHAVIOR OF OPTICAL FIBER CA-	
BLES, P.R. Bark, Siecor Optical Cables Ltd., Oestreich	
and G. Zeidler, Siemens AG, Munich, Germany DESIGN AND PERFORMANCE OF A CROSS-PLY	385
LIGHTGUIDE CABLE SHEATH, P.F. Gagen and M.R.	20:
Santana, Bell Laboratories	39

MULTI-LAYER SHIELD DESIGN AND PERFORMANCE EVALUATION CONSIDERATIONS

J. W. Kincaid, Jr.

G. Flaim

Belden Corporation Geneva, Illinois

ABSTRACT

Six different multi-layer shield designs are presented. The shield designs are evaluated on twisted pair cable. Measured transfer impedance data is presented for the frequency range 100 KHz - 50 MHz. The shield uniformity voltage is defined as the voltage of one conductor of the pair with respect to the other (differential voltage) during the transfer impedance test. The data presented includes the transfer impedance and shield uniformity voltage after flexing.

INTRODUCTION

The multi-layer shield is typically a composite of one or more braided wire layers and one or more aluminum/polyester laminated tape layers. In practice this shield type is designed for coaxial as well as twinaxial (shielded balanced pair) cable. Cost and/or performance considerations tend to rule out the use of single layer shields for certain applications. For example, both the high cost of metallic wire and a frequency (increasing) dependent transfer impedance are application limiting factors for the braided wire shields. Relatively poor physical strength, high d.c. resistance, and possible inductive coupling or slot antenna effect are application limiting factors for the laminated tape shield. However, when the wire braid and laminated tape are designed in a multi-layer shield improved performance characteristics are obtained.

This paper reports on four tape shield designs and two tape plus braid shield designs. The designs are not considered to be optimal but have been chosen to demonstrate basic performance characteristics. Performance evaluation of the prototype shield designs is limited to measured transfer impedance and measured shield uniformity voltage. The shield uniformity voltage is defined and the effect of the drain wire, commonly used in tape shields, on transfer impedance is discussed. Performance degradation is determined after 500 cycles and 1000 cycles of cable flex.

PROTOTYPE SHIELD DESIGN

The characteristics of the shield design and the prototype designation are given in Table 1. The shields were spirally applied over a common twisted pair design. The twisted pair characteristics are given in Table 2. Prototypes B, Z, M, and D were jacketed with a pvc compound. However, the braided prototype cables were not jacketed.

Table 1 - Multi-layer shield construction.

SHIELD CHARACTERISTIC	PROTOTYPE DESIGNATION						
	В	в-в	z	м	D	D-B	BRAID
TAPE WIDTH	5/8"	5/8"	1"	1"	1"	1"	
NUMBER OF .00035" ALUMINUM LAYERS	1	1	1	2	2	2	-
NUMBER OF .0005" POLYESTER LAYERS	1	1	1	2	1	1	ě.,
EDGE FOLD	No	No	Yes	Yes	Yes	Yes	
BRAID: 68% 16 X 4 X #34 TC	No	Yes	No	No	No	Yes	Yes

Table 2 - Twisted pair construction.

•	WISTED PAIR CONSTRUCTION	
CONDUCTOR GAGE	#22 (7 x #30 TC)	
INSULATION TYPE	POLYPROPYLENE	
INSULATION THICKNESS	.010"	
LAY LENGTH	2*	
IMPEDANCE	28 OHMS, 60 OHMS	

PERFORMANCE MEASUREMENT

Transfer Impedance Equipment

To measure transfer impedance of shielded pair cable, a fixture was developed with features similar to both the Simons terminated triaxial fixture (1) and the IEC (2) fixture.

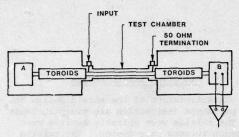


Figure 1 - Triaxial transfer impedance measuring device.

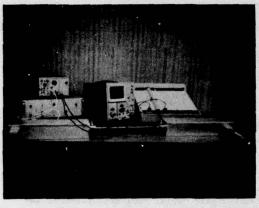


Figure 3 - Photograph of test equipment used for transfer impedance measurement.

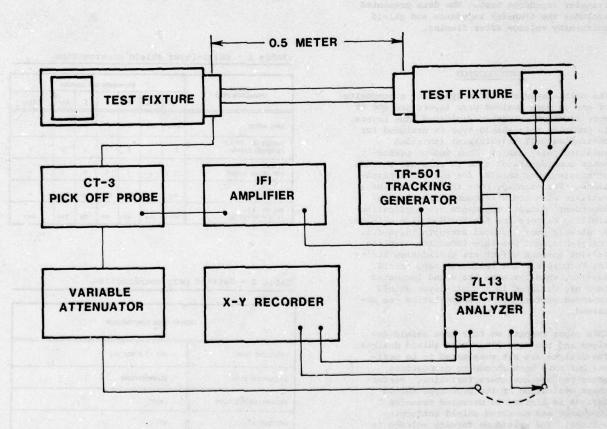


Figure 2 - Equipment block diagram for transfer impedance measurement.

The resulting triaxial device diagrammed in Figure 1 uses toroids to terminate and isolate the outer system. Input current is applied directly to the sample shield under test. Sample lengths were short enough and the test frequencies were low enough so that the outer system could be terminated in a 50 ohm load. The equipment set-up is diagrammed in Figure 2 and photographed in Figure 3.

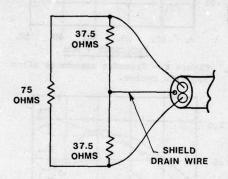


Figure 4 - Rosistor termination network.

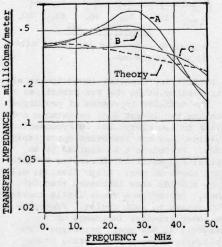


Figure 5 - Transfer impedance of stainless steel tube.

To be sure the equipment was operating properly, the transfer impedance of a stainless steel tube was measured. The measurement (curve C, Figure 5) was made with a coaxial cable core inside the tube. The measurement was repeated with the coaxial core replaced by a twisted pair. With the twisted pair, the measurement was made in two ways: 1) the pair was terminated with the network of Figure 4 at one end and the conductors were shorted together at the oposite end. The voltage from the two shorted conductors to ground was measured (curve A, Figure 5) with a differential probe. 2) The pair conductors were shorted together at each end of the cable and terminated to ground through a 28 ohm resistor. The voltage from the two shorted conductors to ground was measured (curve B, Figure 5) with the differential probe. The results of these measurements and the theoretical transfer impedance of the stainless steel tube are given in Figure 5. With the coaxial cable core, the measured transfer impedance is very close to the theoretical value for a uniform thin wall tube. However, the results obtained with the pair inside the tube indicates coaxial cable shield transfer impedance is different from twisted pair cable shield transfer impedance. This is an area that needs further study.

Prototype Shield Measurement Procedure

The prototype cables were teminated (point A in Figure 1) with the balanced network shown in Figure 4. To obtain transfer impedance and shield uniformity voltage, voltage measurements were made at the opposite end of the cable (point B in Figure 1) which was not terminated. Three voltage measurements were made. These are the voltage of each conductor with respect to ground while the other conductor is open circuited and the voltage of one conductor with respect to the other. A high input impedance differential probe was used. The first two voltage measurements were used to calculate two transfer impedance values for the shielded pair cable. If the shield is uniform and the pair is balanced, these two values should be very close to each other. However, when the shield is not uniform or the pair is not well balanced, these values will not be equal. Assuming pair balance is not a factor, the shield uniformity voltage is given by the differential voltage of the pair conductors.

Flex Test Procedure

The unbraided prototype cables were subjected to flex test after which transfer impedance and shield uniformity were measured. The flex test is diagrammed in Figure 6. Approximately 40 cm of the cable length was flexed. The cable was under approximately 10 pounds of tension during the test. The cables were flexed 500 cycles and 1000 cycles.

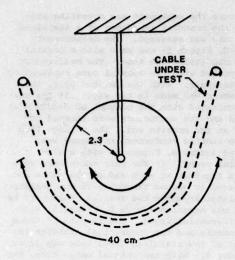


Figure 6 - Flex test diagram.

PRESENTATION OF RESULTS

Transfer impedance versus tape prototype shield design. Figures 7, 8, and 9 present the transfer impedance for 0 cycles, 500 cycles, and 1000 cycles, respectively, of flexing for prototypes B, M, Z, and D. Transfer impedance for one of the pair conductors only is presented for clarity. The simplified electrical equivalent for the shield cross-sections shown in Figure 10 facilitates interpretation of the graphs. Prototypes D, M, and Z approximate closed tube shields due to the tape edge folding. However, the seal

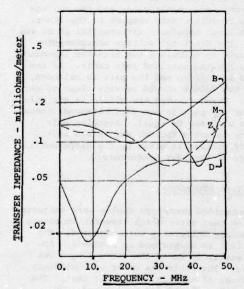


Figure 7 - Transfer impedance after zero flex cycles.

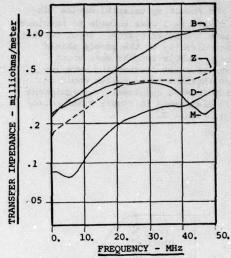


Figure 8 - Transfer impedance after 500 flex cycles.

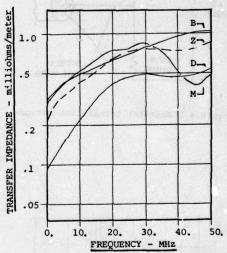


Figure 9 - Transfer impedance after 1000 flex cycles.

is not perfect and transfer impedance is already increasing at 50 MHz for prototypes M and Z. The transfer impedance of prototype D, which has the lowest d.c. resistance and is similar to two closed but interconnected tube shields, has not increased appreciably at 50 MHz. Prototype B is similar to an open spiral and exhibits increasing transfer impedance above 20 MHz. After flexing, all prototype shields show increased transfer impedance. Prototype B shows little increase from 500 cycles to 1000 cycles. Prototype D shows lower transfer impedance up to approximately 42 MHz where prototype M becomes slightly lower. In general, prototype D provides lower transfer impedance before and after flexing.

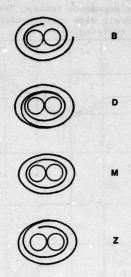


Figure 10 - Simplified shield electrical cross-section.

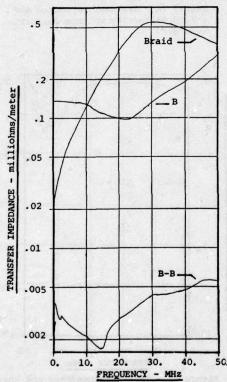


Figure 11 - Transfer impedance for braid plus tape shields.

Transfer impedance for braid plus tape prototype shield designs. Figure 11 presents transfer impedance for the braid shield, for prototype B and prototype B-B. Adding the braid to prototype B reduces the transfer impedance by approximately two orders of magnitude. Between approximately 10 MHz and 50 MHz prototype B has lower transfer impedance than the braid shield.

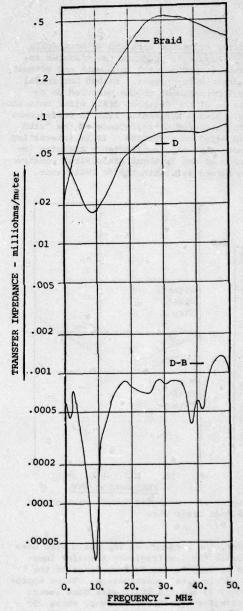


Figure 12 - Transfer impedance for braid plus tape shields.

Figure 12 presents transfer impedance for the braid shield, for prototype D and prototype D-B. Again adding the braid reduces transfer impedance by approximately two orders of magnitude. However, prototype D has lower transfer impedance than the braid shield between approximately 3 MHz and 50 MHz. In general, the braid plus tape prototype shield designs have much lower transfer impedance than either the braid or tape alone.

Transfer impedance with and without drain wire. Figure 13 presents the transfer impedance of prototype B both with and without the drain wire present. Dashed horizontal line I corresponds to the measured dc resistance of the "without drain wire" construction. Dashed horizontal line II corresponds to the measured dc resistance of the "with drain wire" construction. It is interesting to note that the low frequency transfer impedance of the "without drain wire" construction agrees well with the dc resistance.

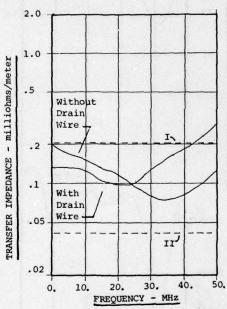


Figure 13 - Transfer impedance with and without drain wire.

However, the presence of the drain wire does not cause the low frequency transfer impedance to drop to the dc resistance of the "with drain wire" construction. Below approximately 25 MHz the drain wire does lower the transfer impedance; however, above 25 MHz, the transfer impedance was greater with the drain wire. This trend was observed for each of the prototype designs. The difference

in transfer impedance between "with" and "without" drain wire constructions diminishes after flex cycle aging.

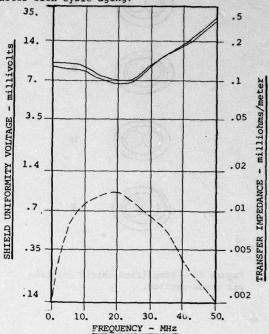


Figure 14 - Transfer impedance and shield uniformity voltage for prototype B.

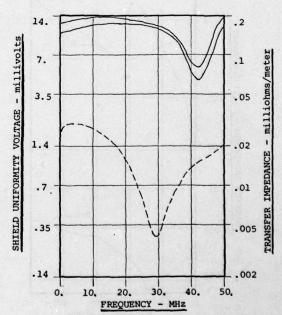


Figure 15 - Transfer impedance and shield uniformity voltage for prototype M.

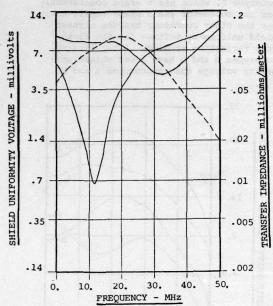


Figure 16 - Transfer impedance and shield uniformity voltage for prototype Z.

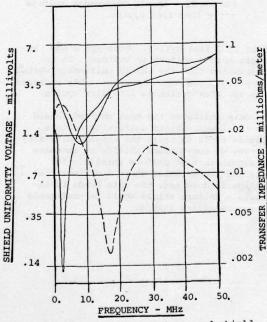


Figure 17 - Transfer impedance and shield uniformity voltage for prototype D.

Shield uniformity voltage versus tape prototype shield design, Figures 14, 15, 16, and 17 present transfer impedance (right hand ordinate) for both of the pair conductors of prototype B, M, Z, and D, respectively, and also shield uniformity voltage (left hand ordinate) for each prototype design. The shield uniformity voltage is indicated by the dashed line in each figure. The simplified tape wrapping and folding equivalent diagram for the shield cross-sections shown in Figure 18 facilitates interpretation of the data. Prototype B has two wraps around almost the entire circumference. The transfer impedance determined from voltage measurements of each pair conductor is quite similar. For prototype M which has 2, 4, and 5 wraps at various locations on the circumference, the difference in transfer impedance for each conductor is greater than for prototype B and the shield uniformity voltage is also greater. For prototype Z and D, there is significant variation in the transfer impedance for each conductor at low frequencies. However, at frequencies above 25 MHz for prototype Z and above 8 MHz for prototype D, the transfer impedance is generally increasing. For prototype D, the shield uniformity voltage does increase to a peak at approximately 30 MHz.

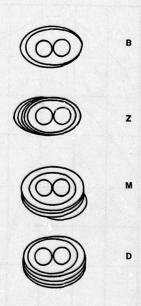


Figure 18 - Simplified shield wrap and fold cross-section.

Figures 19, 20, and 21 present the shield uniformity voltage for 0 cycles, 500 cycles, and 1000 cycles, respectively, of flexing for prototypes B, M, Z, and D.

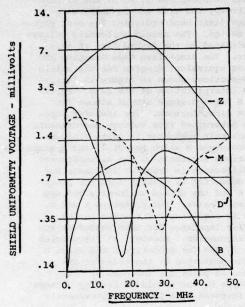


Figure 19 - Shield uniformity voltage after zero flex cycles.

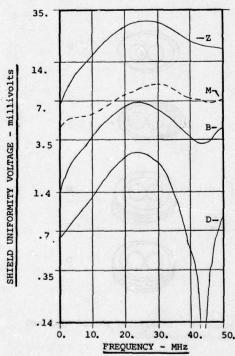


Figure 20 - Shield uniformity voltage after 500 flex cycles.

Prototype Z, which has 5 wraps consistently near one conductor and 2 wraps consistently near the other conductor has the highest shield uniformity voltage for the flex cycle variations studied. After flexing, prototypes B and D have lower shield uniformity voltage than prototypes Z and M.

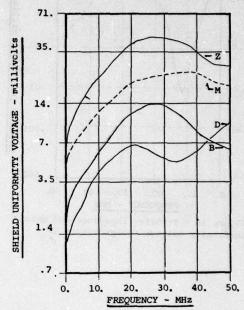


Figure 21 - Shield uniformity voltage after 1000 flex cycles.

After 1000 flex cycles, prototype B has the lowest shield uniformity voltage. It is interesting that the shield uniformity voltage for prototype B does not appreciably increase from 500 flex cycles to 1000 flex cycles.

The data indicates the most uniform shield has the lowest shield uniformity voltage. Flexing tends to cause the shield uniformity voltage of non-uniform shields to increase more than that of uniform shields. For balanced transmission where a differential voltage is detected, the data tends to indicate a uniform shield would be preferable to a non-uniform shield.

CONCLUSION

Transfer impedance before flex cycle aging. The prototype design determines the transfer impedance.

- a. Braid plus tape prototypes B-B and D-B have lower transfer impedance than either prototype B or prototype D, respectively. Transfer imepdance is reduced by approximately two orders of magnitude.
- b. Prototypes B and D have lower transfer impedance than the braid over the frequency range 10 MHz to 50 MHz and 3 MHz to 50 MHz, respectively.
- c. Prototype D generally has the lowest transfer impedance for the tape prototype designs. (Exceptions are evident in Figure 7.)
- d. Transfer impedance is modified by the presence of the drain wire. At low frequencies the transfer impedance is greater than the d.c. resistance of the drain wire would indicate. At high frequencies, the transfer impedance is greater if the drain wire is present than if absent.

Transfer impedance after flex cycle aging.

- A. All prototype designs tested have greater transfer impedance after flexing than before flexing.
- B. The prototype design determines the amount of increase in transfer impedance due to flexing.
 - a. Prototype D has the lowest transfer impedance up to approximately 42 MHz at which frequency prototype M has slightly lower transfer impedance.
 - b. Prototype D transfer impedance is approximately as low after 1000 flex cycles as is prototypes Z and B transfer impedance after 500 flex cycles.
- C. After sufficient flexing, the measured transfer impedance tends to approach a common value.
 - a. Prototype B transfer impedance increases only slightly from 500 flex cycles to 1000 flex cycles.
 - b. Prototypes B, Z, and M transfer impedance is approximately the same at frequencies below 30 MHz after 1000 flex cycles.

Shield uniformity voltage

A. Shield uniformity voltage is defined as the differentail voltage between the pair conductors during the transfer impedance test.

- B. Shield uniformity voltage is an indicator of how well balanced the pair is and also how uniform or symmetric the shield is with respect to each conductor. For well balanced pairs, the shield uniformity voltage indicates shield uniformity. The smaller the differential voltage, the more uniform the shield.
- C. Shield nonuniformity causes the transfer impedance values calculated from voltage measurements on each conductor to be unequal. The effect is minimal for prototypes B and M but pronounced for prototypes Z and D.

The multi-layer shield is an important shield type which is being designed for many video and digital data transfer applications. It is anticipated that the usage of multi-layer shields will increase to obtain improved performance and meet increasingly stringent EMI/RFI restrictions.

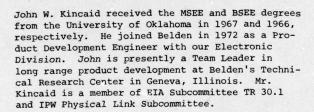
REFERENCES

- K. A. Simons, "Relating Transfer Impedance to Coaxial Cable Radiation," 23rd International Wire and Cable Symposium, Atlantic City, New Jersey, December, 1974.
- International Electrotechnical Commission, "Publication 96-1, Radio Frequency Cables," Geneva, Switzerland, 1971.

ACKNOWLEDGEMENTS

The authors acknowledge the contribution of the Facile Division of Sun Chemical Corporation.







Gino Flaim received a BSEE degree from the University of Illinois in 1976. He joined Belden in 1978 as a Product Development Engineer and is currently engaged in shielding studies. Prior to joining Belden, Gino worked for General Telephone and Electronics.

VINYLIDENE CHLORIDE COPOLYMERS FOR IMPROVED FLAME RESISTANCE

W. E. Brown,

R. C. Devereaux,

R. J. Streu

The Dow Chemical Company Midland, Michigan

ABSTRACT

A rubber modified vinylidene chloride copolymer has been developed to combine the inherently good burn resistant properties of polyvinylidene chloride into a compound with good low temperature properties. An oxygen index of 36% and an NBS smoke density of 265 have been combined with impact resistance and flexibility at -15°C by incorporating a modifying rubber phase to minimize the plasticizer level previously necessary for good low temperature performance.

INTRODUCTION

Polymers and copolymers of vinylidene chloride (PVDC) possess some remarkably good physical properties that should lend themselves to uses in the wire and cable insulation industry. Outstanding among these properties are Saran's combustion characteristics. Saran polymers ignite with difficulty, burn sluggishly and contribute small fuel value while generating a light, white, wispy smoke and a stable char with no intermediate flaming drip stage. All of these characteristics would be desirable in many wire and cable applications, but unfortunately many of these characteristics are sacrificed by the additives necessary to make the material melt processable, while conveying to it the necessary physical properties of toughness and low temperature flexibility.

The development of a new rubber reinforcement technology has resulted in a vinylidene chloride copolymer extrusion resin which largely retains the good combustion characteristics without sacrifice of other physical properties. Cable jacketing has been extruded from this material, thus demonstrating in this early stage of development the practical application of a truly new form of PVDC.

It is interesting to note that PVDC was first considered by the Communication Wire and Cable Industry in 1939, but nothing came of these early evaluations. Presumably this was because the practical ways to process the resin capable of obtaining the handling and performance characteristics required in finished material had not been developed. In the meantime, the Saran family of molding and extrusion resins, dispersion coatings, particulates and films has been developed to a very high degree, principally for food packaging, paper coating and consumer applications largely concerned with the protection of food.

This paper deals with the properties of the new rubber modified PVDC, such that communications materials engineers may determine the potential utility of this material in the industry. The purpose here is to obtain early exposure to a large knowledgeable audience so that further development work can proceed along lines closely associated with future needs. Rapid improvements and modifications in such developmental materials are common, and indeed necessary, to get the maximum value from new technology.

COMBUSTION PROPERTIES

Polymers based on vinylidene chloride are inherently less flammable and smoke-producing than other commercially available polymers with the exception of polytetrafluoroethylene.

COMPARISON OF COMBUSTION PROPERTIES OF WELL KNOWN POLYMERS WITH PVDC

Polymer	LOI (1)	<u>Ds</u> (2)	VHc.
PVDC	70-80	50	4,220
ABS	18	600	
POLYSTYRENE	18	600	17,870
PVC	45	600	7,370
POLYETHYLENE	18	280	19,990
NYLON	25	-	0.0000000000000000000000000000000000000
PTFE	95	-	-

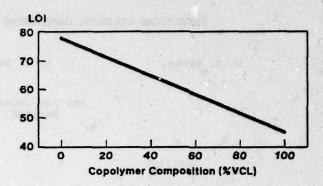
Stw/B

- (1) L.O.I. ASTM D2863-70
- (2) Ds NBS Smoke Density Chamber

The differences are primarily due to the high level of chlorine in the molecular structure, so there is less fuel for combustion.

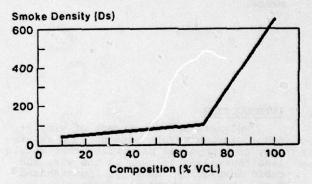
One of the most common materials for fire resistant applications is flexible polyvinyl chloride (PVC). This material is non-flammable when the ignition source is weak, such as a spark. Under fire conditions where there is a secondary source of fuel, the formulated polymer will burn readily, giving off copious amounts of smoke. The base polymer of PVC is quite fire resistant, having a desirable Limited Oxygen Index (L.O.I.) of about 45. Polyvinylidene chloride has a significantly higher oxygen index than PVC but has historically proven difficult to fabricate by conventional extrusion techniques. The existing method of improving the fabrication properties of polyvinylidene chloride (PVDC) is copolymerization with vinyl chloride. A comparison of vinylidene chloride-vinyl chloride copolymers with PVC shows a significant weight percent level of vinyl chloride can be incorporated in the polymer system to achieve processability while maintaining a maximum L.O. I.

EFFECT OF COMPOSITION ON LIMITING OXYGEN INDEX OF VDC/VCL COPOLYMERS



Polyvinyl chloride has historically been shown to give off large amounts of smoke. The polymers based on VDC yield substantially less smoke in useful compositional ranges of 80-95 percent vinylidene chloride.

COPOLYMER COMPOSITION VS SMOKE GENERATION FOR VDC/VCL COPOLYMERS



PVDC thermally decomposes by an entirely different mode than PVC. A quantitative mechanism for thermal dehydrochlorination of PVDC was proposed by Boyer (1) et al. They visualized a two-stage reaction initiating below 200°C. The polymer chain begins to liberate HCl, forming double bonds.

$$\{CH_2-CCl_2\}_n \triangle \{CH=CCl\}_n + nHCl$$

This step is followed by a crosslinking reaction, significantly restricting the melting and dripping of the polymer.

 $\{CH=CCl\}_n$ $\underline{\Delta}$ crosslinked aromatic products.

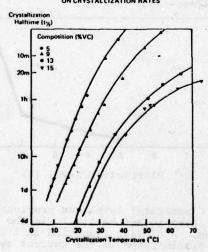
Further heating splits off a total of two molecules of HCl for each monomer unit, leaving a residue of nearly pure carbon. The HCl, which constitutes about 60% of the total mass, is colorless, non-combustible, and does not contribute to smoke. The carbon residue requires higher temperatures and abundant oxygen to burn. Further, the carbon residue is left in a feamed state, which is non-dripping, and can offer thermal insulation to the yet unburned material under the structure.

DEVELOPMENT OF A CABLE JACKETING MATERIAL

Vinylidene chloride-vinyl chloride copolymers would appear to be an excellent base from which to develop a fire resistant cable jacketing; however, there are several problems to be overcome.

Currently produced VDC copolymers are semi-crystalline in nature. The crystallinity is beneficial in that it leads to high heat distortion temperatures, and to a low degree of creep. It is detrimental in that it contributes to the brittleness of the polymer. Crystallinity can be reduced through copolymerization, but this can also reduce the crystallization rate to an unacceptably low level. Control of the copolymer composition can be exercised to optimize the level and rate of crystallization, allowing the VDC copolymer to crystallize before the final cable windup operation. Otherwise, severe blocking may occur.

EFFECT OF COMPOSITION ON CRYSTALLIZATION RATES

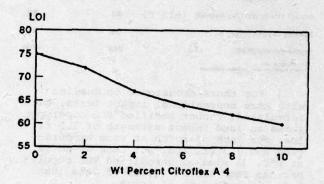


Another problem is the addition of plasticizers to achieve low temperature toughness. Depending on the application, the cable jacketing must show good toughness and flexibility to -15°C and prefer-

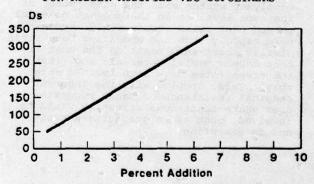
ably -30°C. Although the levels of plasticizer additives are not great by comparison to those required in PVC, they are the prime contributor to smoke and increased flammability.

Therefore, low temperature toughness and combustion properties are two primary considerations for development of an F.R. cable jacketing polymer. Previously available vinylidene chloride copolymers achieved relatively high L.O.I. values, but yielded high smoke density and poor impact strength at usable plasticizer levels.

PLASTICIZER LEVEL VS LIMITING OXYGEN INDEX OF RUBBER MODIFIED VDC COPOLYMER



PLASTICIZER LEVEL VS. SMOKE DENSITY FOR RUBBER MODIFIED VDC COPOLYMERS



A fundamental improvement in the low temperature properties of VDC copolymers is currently under development by addition of an impact modifying rubber phase (RMVDC). The base resin, although lower in L.O.I. than the current base VDC copolymers, so dramatically achieves low temperature toughness that substantial improvements in smoke density are possible. This is due to the ability to reduce

plasticizer level or change additives to less smoke producing moieties. Physical property comparisons with a standard PVC cable jacketing compound describes the improvements available with this new resin containing a typical formulation.

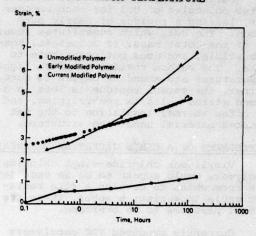
PHYSICAL PROPERTIES OF RUBBER MODIFIED VDC COPOLYMERS

	RM Saran' formulated	PVC
Tensile strength, psi		
Yield	1,700	
Ultimate	2,190	2,910
Elongation . %		
Yield	22	
Ultimate	250	245
Modulus, 2% offset, psi	41,000	6,800
100%, pei	1,500	1,920
Impact strength (Wiley Method) (-15	5°C) 44	50
Limiting oxygen index, %	36	29
Smoke density (NBS)	265	>500
"ST DESC/12 G-66		

For those accustomed to dealing with more conventional impact tests, the formulated, rubber modified VDC copolymer shows an Izod impact strength of 7.5 ft. lbs. per inch of notch at room temperature and 2.3 ft. lbs. per inch of notch at 0°C. A similar unmodified VDC copolymer has Izod impact values of less than 1 ft. lb. per inch of notch.

Early work on the creep behavior of rubber modified VDC using a different base copolymer system with the same rubber at the same level as in the present material showed that creep strain would increase more rapidly than the umodified base resin. Similar short-term tests on the most recent developmental materials show that the creep rates have been reduced sizeably. This, coupled with the inherent chemical resistance of Saran suggests uses where continuous stressing would be involved, such as in pressurized cable and in gasketing.

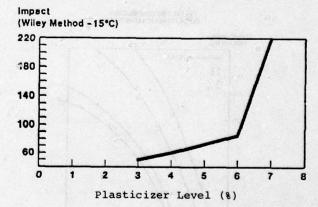
CREEP OF RMVDC 500 PSI ROOM TEMPERATURE



Currently, development of the reinforcement technology has not yet reached a level where it has been possible to cover the wide range of available properties. The following examples are included to provide currently available data on the rubber reinforced system.

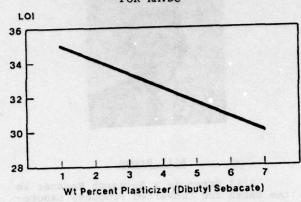
Low temperature impact on the improved system as a function of plasticizer level has been evaluated.

LOW TEMPERATURE IMPACT VS PLASTICIZER LEVEL FOR RUBBER MODIFIED VDC COPOLYMERS



Plasticizer level has previously been shown to affect L.O.I. in the PVDC system. A similar reduction in L.O.I. has been demonstrated in the current system.

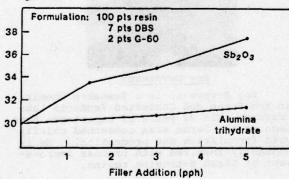
PLASTICIZER LEVEL VS. L.O.I. FOR RMVDC



Reduction in the oxygen index with plasticizer addition has resulted in the search for additives to modify the combustion and performance characteristics of the fabricated system. Commonly added flame suppressants such as antimony trioxide and aluminum trihydrate were evaluated for their effect on the system.

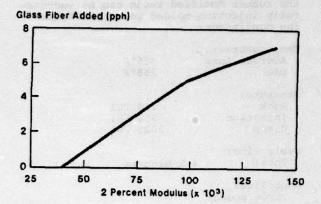
PLASTICIZER EFFECT ON L.O.I. FOR RMVDC

Oxygen Index



Sizeable increases in modulus can also be demonstrated by the addition of glass fibers during formulation.

GLASS FIBER ADDITION TO RMVDC



FABRICATION TECHNOLOGY

Melt processing is characteristically conducted in long length to diameter ratio extruders containing corrosion resistant steel barrels and screws. Handling of the new resin is not markedly different in this sense from other Saran materials. While it is true that extrusion experience with rubber modified VDC copolymers is limited to the developmental program of the past three years, it should also be noted that the total experience in extruding VDC copolymers worldwide exceeds 40 years and several billion pounds. More-over, recent developments in extrusion technology have boosted rates while decreasing thermal history to the point where thermal degradation should not be a consideration in any modern commercial conversion process.

For example, high barrier VDC copolymers have been extruded in 4 1/2" extruders, at rates exceeding 700 lbs. per hour, where similar materials were limited to about a 25 lb. per hour rate until the early 1950's. This equates to a 13 2/3% compounded growth rate in extrusion rate. On the other hand, it is true we have had no reason to attempt to push the rubber modified Saran in a cable jacketing line since the capacity hasn't been available. We believe that due to the similar extrudability of the modified VDC resins to previous systems, the extrusion needs of the cable jacketing industry are well within the capabilities of the current resin.

The same is probably not true in wire coating where much higher line speeds are needed and hence much faster crystallization rates in the resin itself.

Experience with injection molding has been limited to the formation of some small parts ranging in size from a few

grams to a few pounds. It appears that the rubber modified resin can be successfully injection molded under the following conditions:

Temperatures:

Average Zone 325°F Die 295°F

Pressure:

Back 110 PSI Injection 550 PSI Clamp 2025 PSI

Cycle Time:

Total 4.5 Minutes

Shot Size: Three pounds

The same necessities for corrosion resistant steel wherever the hot resin contacts the machinery prevail in injection molding as they do in extrusion.

Other uses for rubber modified VDC copolymers have been proposed in films, in multilayered structures, in fiber binding applications and a variety of uses associated with the more conventional molding and extrusion.

CONCLUSIONS

The recent development of a unique modification technology for vinylidene chloride copolymers has resulted in a system with an oxygen index of 36%, a smoke density of 265 and greatly enhanced flexibility and low temperature performance. These improvements coupled with a copolymer system that can be varied to provide specific performance requirements presents an opportunity to develop a cable jacketing system or other applications with improved burn resistant properties.

REFERENCES

- L. A. Matheson and R. F. Boyer, Ind. Eng. Chem., 44, 867, (1952).
- Dow Developed Variable Temperature/ Impact Strength Tester.

The content of this document is not intended to reflect hazards present by this, or any other material, under actual fire conditions.



Bill Brown

Bill Brown is a Research Manager in the Saran and Converted Products Laboratory of The Dow Chemical Company. His previous experience has included direction of the Molding and Extrusion section of Saran Research. Bill is currently involved in the new applications area. He received his B.S. degree from the State University of New York.



Roy Devereaux

Roy Devereaux is a Research Chemist in the Saran and Converted Products Laboratory. His 27 years of experience have been in the Saran area concerned chiefly with formulation and processing. He is presently involved with process improvement of Saran extrusion resins.



Bob Streu

Bob Streu is a Research Specialist in the Saran and Converted Products Laboratory. His previous experience has included compositional and property studies of vinylidene chloride copolymers. He is current responsible for research efforts in Emulsion and Rubber Modified Sarans. Bob is a graduate of Saginaw Valley State College.

POSITIVE TEMPERATURE COEFFICIENT MATERIALS FOR TELEPHONE CABLE REPAIR

Bruce Campbell

Raychem Corporation Menlo Park, CA

Introduction

At relatively high carbon black loading levels some polymers exhibit a positive temperature coefficient (PTC) of resistance which causes the resistance to rise sharply as the temperature approaches an anomaly point. This property, when used in a heat-shrinkable crosslinked polymer tape, makes it possible to perform telephone cable repairs without danger of damage to polyethylene-jacketed conductors employed in telephone cables.

The purpose of developing a temperature-regulating heat-shrinkable tape is to effect telephone cable repairs where a torch activated repair is either prohibited or impractical. The auxiliary junction between a lead sleeve and a polyethylene cable in underground plant is an example of a repair or construction requirement where use of a torch is prohibited; furthermore, the cable sheaths are of significantly different thermal conductivities. The current method of building this joint, which is usually pressurized, requires a craft-sensitive series of taping operations using both conformal elastomeric tapes and glass-reinforced tapes.

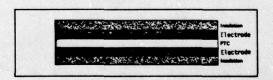
At the entry to a manhole, cables from the conduit run are often severely bent and thus develop cracks in the cable sheath at or inside the first few inches of the conduit. Existing repair techniques require removal of some or all of the concrete face of the manhole to gain access to the repair site. Even after the considerable expense of removing the concrete, the repair is insufficiently accessible for use of a torch to give satisfactory results.

The newly developed solution to these problems is a heat-shrinkable plastic tape with

self-limiting electrical heating properties, using in conjunction with a hot melt adhesive. The shrinking properties of the tape are achieved by using an expanded, cross-linked polymer. The shrinking properties allow the tape to be initially loosely wrapped about the repair site, while assuring a highly conformal wrap after the tape has shrunk. The self-limiting heating properties ensure that no part of the cable becomes overheated during the repair process.

The hot melt adhesive is designed to flow during heating, thus filling any irregularities in the cable sheath. The adhesive has been formulated to achieve adhesive bonding at bondline temperatures as low as $100^{\circ}\mathrm{C}$. The time/power/temperature characteristics of the tape are designed to provide the required amount of heat for sufficient time to heat the adhesive and substrate (cable sheath) adequately for adhesive bond formation. The adhesive bondline temperature, at the end of an $8\frac{1}{2}$ minute power cycle, is typically about $125^{\circ}\mathrm{C}$ and produces average bondline peel strengths of 25 pounds per linear inch for polyethylene cable sheaths and 35 pounds per linear inch for lead cable sheaths. The values cited are measured using a climbing drum procedure at two inches per minute crosshead speed at room ambient conditions. A cross section of the new heat-shrinkable plastic tape is shown in Figure I.

Figure I Cross-sectional view of tape



Heat is generated by resistive heating as current passes from one electrode to the other through the central PTC layer. As the tape heats, the resistance of the PTC layer increases. When the temperature of any part of the tape reaches the design limit, its resistance becomes sufficiently high that it produces only enough heat to maintain the desired control temperature. In a typical auxiliary repair, more heat will flow to the lead sheath (a higher conduction material) than to the

polyethylene sheath, thereby bringing the entire joint to a uniform temperature.

The positive temperature coefficient material is carbon black loaded polyolefin. While resistive heating with carbon black loaded polymers is relatively common, the resistance anomaly which can occur at a particular temperature was first noted in 1957¹. Its potential for use in a self-limiting heater was first published in 1969². Since that time, numerous authors have explored carbon black loaded polymers in search of explanations for the behavior of the material ³,4,5

An examination of Figure II shows that the resistance rise in the PTC layer is slight up to the anomaly point (130°C) at which temperature the rise becomes very steep.

Figure II

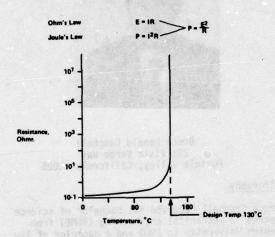


Figure II Resistance versus Temperature

The mechanism responsible for the phenomenon is thought to be the separation of the carbon conduction chains which exist at the crystalline/amorphous interfaces of the polymer⁶, due to sudden expansion of the polymer. This expansion and carbon separation occurs at or near the crystalline melting of the carbon black loaded polymer. Figure III diagramatically illustrates the phenomenon on a molecular level.

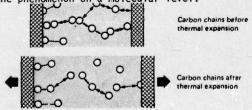


Fig. III Self-limiting action on molecular level: resistance changes according to temperature.

The positive temperature coefficient anomaly allows the tape, as it heats up, to exhibit a time dependent power curve. Figure IV shows a typical power curve.

Figure IV

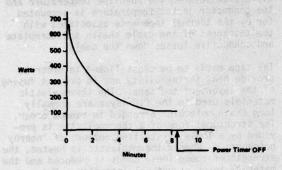
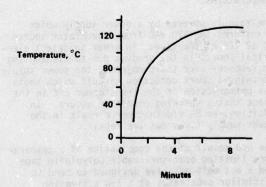


Figure IV Power versus Time

During an $8\frac{1}{2}$ minute heating cycle, the temperature at the bondline of the repair can be shown to rise so that the temperature is limited to approximately 125°C (Figure V).

Figure V



Adhesive Bondline Temperature versus Time

A STATE OF THE STA

The bondline temperature is important since higher temperatures will produce unacceptable heating of the conductor jackets. The softening or melting of those jackets could allow the conductors to push through the walls of the jacket with the resultant loss of insulating properties. Thermocouple monitoring of the conductor jackets shows that the jacket temperatures never exceed 90°C during the repair procedure. The 30°C difference between the bondline temperature and the conductor jacket temperature is accounted for by the thermal impedance associated with the thickness of the cable sheath and turnplate and conductive losses down the cable.

The tape needs to be cross-linked in order to provide heat shrinkability and to prevent fusing of the layers of the tape. The thermoplastic materials used in the PTC layer are normally long chain molecules arranged in random order. The structural form of a thermoplastic is provided by a loose crystalline network of "nearby neighbors." When a thermoplastic is heated, the strength of these loose bonds is reduced and the material loses structural integrity. The thermoplastic may be altered in form by movement between molecules, and upon cooling, the loose bonding will again occur and another solid structure will appear. If a thermoplastic material is exposed to high energy electron radiation, permanent cross-linking will occur by intermolecular joining of adjacent molecules. The cross-links are in addition to the loose bonds discussed above and are retained even above the melting point of the material. Thus, these cross-links will have the effect of trapping the carbon black particles in the matrix and holding them there even at elevated temperatures.

The tape is powered by a power supply which transforms the 120 VAC from a generator source to 12 VAC at the tape. In order to detect electrical shorts in the product due to mishandling or recovery over sharp objects, the power supply contains a spark detection circuit which shuts the primary side of the transformer off in the event that a sparking condition occurs. In addition, an $8\frac{1}{2}$ minute timer circuit in the power supply times out the repair.

The end result of the combination of a temperature limiting heat-shrinkable polyolefin tape and a hot melt adhesive designed to bond to dissimilar substrates at a low activation temperature, is a unique way to achieve repairs of telephone cables in environments where dependable repair techniques are lacking. The fact that the PTC materials can be employed as thermostatic switches activatable below the temperature which causes cable damage provides the designer with a novel tool for further construction and repair applications.

- ¹ G. G. Harman, Phys. Rev., 106, 1358 (1957).
- ² E. Andrich, Philips Tech. Rev., 30, 170 (1969).
- ³ J. Meyer, Polymer Eng. and Sci., 706, Vol. 14, No. 10, Oct., (1974)
- J. Meyer, Polymer Eng. and Sci., 462, Vol. 13, No. 6, Nov., (1973)
- ⁵ M. Narkis, A. Ram, R. Flashnes, Polymer Eng. and Sci., 649, Vol. 18, No. 8, June (1978).
- T. Speer, S. Kucklinca, IEEE, P.C.I.C. Conf. Proc., 50, (1975)



Bruce Donald Campbell 221 Vista Verde Way Portola Valley, California 94025

Biography

Bruce Campbell received his bachelor of science degree in mechanical engineering (BSME) from Lehigh University in 1960 and a bachelor of law degree (LLB) from the university of San Fernando Valley, College of Law in 1968. Mr. Campbell is presently employed as a product design manager for the Telecom Division, Raychem Corporation, Menlo Park, California.

Design and Evaluation of High-strength Submarine Cable for Ocean Towing

Mr. J. Nakajima Mr. M. Okubo Mr. S. Tachigami Mr. H. Kawazoe Mr. H. Umezu

Mr. S. Kikkawa

The Furukawa Electric Company, Ltd. Tokyo, Japan

Summary

Development of new resources, such as minerals, energy and foods which can be obtained from the ocean is one of the most important subjects of research for the future existence of mankind. Most cables used for such development are towed by a ship. They are not only forced to exhibit complex behaviors while towed by the ship but also are subjected to severe mechanical loads when the sensor is drawn out and winch-wound. These loads were theoretically analyzed and estimated, and the cable and the cable joint optimum to the towing system were developed.

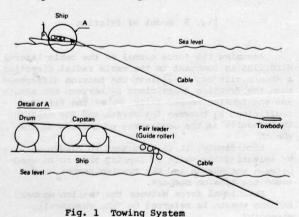
Against the estimated load factors, the basic mechanical and fatigue characteristics were checked, and the cable life was estimated.

Based on the desk and laboratory examinations, the practical towing test is currently under way using the improved cable and its joint for the confirmation of the basic quality. As a result, we have reached the conclusion that the developed towing cable system can be practically applied.

Outline of Towing System

Fig. 1 shows the outline of the towing system which has so far been studied. The towing cable consists of the sensor at the front end, the cable, the joint connecting the sensor and cable, and the onboard joint.

The onboard handling system consists of a take-up drum, double capstan and fair leader.



Load Estimation

Prior to designing the cable system, it is necessary to estimate the load at the time of cable use in terms of quantity. Taking the towing system into consideration, the theoretical analysis and the calculation of loads that are naturally expected to be imposed on the cable were performed. Namely, the loads are the tension occurring due to hydrodynamic drag, friction between the tension member and outer sheath to be required when the cable is wound by the capstan, variation of tension due to pitching and oscillation of the ship and slip-over-sheave loaded by the onboard handling system, such as the capstan.

Tension

Tension is the most basic load caused by the cable weight and hydrodynamic drag. Particularly, as the cable is lengthened and the towing speed is increased as in the current case, the tension becomes excessively great. The effect of the cable length and the ship speed on the towing tension and underwater configuration were examined. In the theoretical calculation the configuration of the underwater cable is assumed to be in a two dimensional uniform flow and the following equations can be obtained from the balance of forces in the directions of the Y axis and Z axis in Fig. 2.

$$dT/ds = \omega \sin \phi - Ft$$
 (1)

$$T d\phi/ds = \omega \cos \phi - Fn \qquad (2)$$

$$dY/ds = \cos \phi \tag{3}$$

$$dZ/ds = \sin \phi$$
 (4)

where Ft and Fn are drags in the tangential direction and normal direction, respectively. The following equations are given by the use of Pode model regarding the hydrodynamic drag.

$$Ft = \frac{1}{2} \rho t Cn V |V| f$$
 (5)

$$Fn = \frac{1}{2} \text{ pt Cn } V^2 \sin \phi |\sin \phi| \qquad (6)$$

where

t = cable diameter

Cn = normal drag coefficient

V = velocity of flow

f = Pode's constant

As the initial condition, assuming that the sensor keeps the horizontal condition from the fact that the specific weight of the sensor is equal to that of sea water, the following equations become true at the point of S = 0.

$$Y = Z = 0 \tag{7}$$

$$\phi = 0 \tag{8}$$

$$Fn = 0$$
 (9)

$$Ft = \frac{1}{2} \rho t' Cn v|v|f$$
 (10)

where t' = sensor diameter

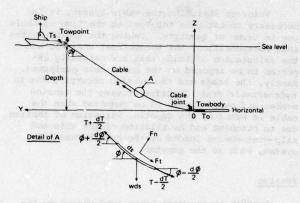


Fig. 2 Tow problem

The result of calculation obtained from the above equations is shown in Figs. 3 and 4. It has been confirmed that the result of calculation of tension and underwater configurations thus obtained nearly corresponds to the results of separately conducted towing tests.

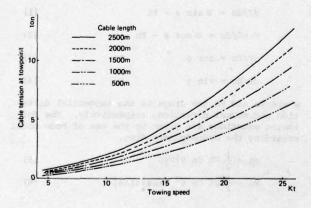


Fig. 3 Relation between cable tension and towing speed

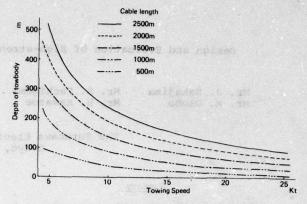


Fig. 4 Relation between cable depth and towing speed

Friction force

Since presently designed cable is of the double sheath structure wherein an outer sheath is provided over the tension member, the friction force must sufficiently withstand the shearing force between the outer sheath and the tension member when such cable is wound by the capstan. As shown in Fig. 5, as far as the model is concerned, the tension difference dT across the capstan which acts on the cable is guaranteed by the friction force between the sheath and the capstan.

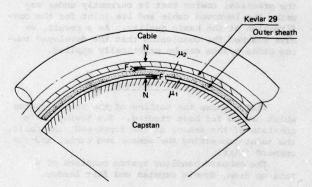


Fig. 5 Model of friction

Assuming the force normal to the cable lateral direction is constant in the cable radial direction, a sheath slip occurs against the tension difference when the friction coefficient μ_2 between the sheath and the tension member falls below the friction coefficient μ_1 between the sheath and the capstan. This results in the occurrence of bellows on the sheath.

Accordingly, it is important to assure $\mu_2>\mu_1$ by selecting the value of lapping tape to be used between the sheath and the tension member or between the tension members.

Frictional force between the tension member and the sheath is referred to "the sheath-slip-strength".

Analysis of unsteady state dynamic behavior of towing cable

Loads the towing cable would be subjected to under the water while towed by a ship were estimated and the unsteady state dynamic behavior was analyzed by the finite element method in order to examine the effects of the estimated loads on the The towing system under analysis cable life. consists of a towing cable and a neutrally buoyant towbody and it is thus set that the underwater cable configuration is two-dimensional, the movement of the towpoint changes in a sine curve as the ship pitching is expected and the sea water is incompressible and viscous. The tow cable and the towbody were divided into 30 elements having 31 nodes and the towbody was treated as an additional section of the characteristics different from the cable. The element is a two dimensional bar element and the deformation is represented by the six nodal displacements that permit extension, bending and rotation. Accordingly, the element displacement vector $\{d\}^e$ is given as follows.

$$\{\mathbf{d}\}^{\mathbf{e}} = \begin{Bmatrix} \mathbf{U}\mathbf{x} \\ \mathbf{U}\mathbf{y} \end{Bmatrix} = \begin{Bmatrix} \mathbf{N}\mathbf{x} \\ \mathbf{N}\mathbf{y} \end{Bmatrix} \begin{Bmatrix} \mathbf{U}\mathbf{x}_1 \\ \mathbf{U}\mathbf{y}_1 \\ \mathbf{0}_1 \\ \mathbf{U}\mathbf{x}_2 \\ \mathbf{U}\mathbf{y}_2 \\ \mathbf{0}_2 \end{Bmatrix}$$
(11)

It was so established that the function of displacement of the element in the x direction was linear and that in the y direction was third order. Nx and Ny are given by the following.

$$[Nx, Ny] = \begin{cases} 1 - \xi & 0 \\ 0 & 1 - 3\xi^2 + 2\xi^3 \\ 0 & (\xi - 2\xi^2 + \xi^3) \ell \\ \xi & 0 \\ 0 & 3\xi^2 - 2\xi^3 \\ 0 & (-\xi^2 + \xi^3) \ell \end{cases}$$
(12)

where

The element stiffness matrix is given by the following.

$$\begin{bmatrix} \frac{EA}{\ell} & \text{Symmetry} \\ 0 & \frac{12EI}{\ell^3} \\ 0 & \frac{6EI}{\ell^2} & \frac{4EI}{\ell} \end{bmatrix}$$

$$\begin{bmatrix} K \end{bmatrix}^e = \begin{bmatrix} -\frac{EA}{\ell} & 0 & 0 & \frac{EA}{\ell} \\ 0 & -\frac{12EI}{\ell^3} & -\frac{6EI}{\ell^2} & 0 & \frac{12EI}{\ell^3} \\ 0 & \frac{6EI}{\ell^2} & \frac{2EI}{\ell} & 0 & -\frac{6EI}{\ell^2} & \frac{4EI}{\ell} \end{bmatrix}$$
(13)

The element mass matrix is given by the fol-

$$[m]^{e} = \begin{cases} \frac{1}{3} & & \\ 0 & \frac{13}{35} & \text{Symmetry} \\ 0 & \frac{11\ell}{210} & \frac{\ell^{2}}{105} \\ \frac{1}{6} & 0 & 0 & \frac{1}{3} \\ 0 & \frac{9}{70} & \frac{13\ell}{420} & 0 & \frac{13}{35} \\ 0 - \frac{13\ell}{420} - \frac{\ell^{2}}{140} & 0 & -\frac{11\ell}{210} & \frac{\ell^{2}}{105} \end{cases}$$

$$(0A\ell)$$

The external force {f}e due to the cable weight is expressed by the following equation.

$$\{f\}^{e} = \begin{cases} fx \\ fy \end{cases} = \begin{cases} \sin \theta \\ \cos \theta \end{cases} \omega_{e}$$
 (15)

 ω_e = weight per unit length of cable in where

Nodal forces due to the distributed loading of the element are represented by the following equation.

element are represented by the following equa-

$$[\mathbf{F}]^{\mathbf{e}} = \int_{0}^{1} [\mathbf{N}]^{\mathbf{T}} {\{\mathbf{f}\}}^{\mathbf{e}} \mathbf{k} d\xi = \begin{bmatrix} \frac{1}{2} \sin \theta \\ \frac{1}{2} \cos \theta \\ \frac{1}{12} \cos \theta \\ \frac{1}{2} \sin \theta \\ \frac{1}{2} \cos \theta \\ -\frac{\ell^{2}}{12} \cos \theta \end{bmatrix} (\ell^{\omega}_{\mathbf{e}}) (16)$$

Considering only the drag force and assuming that the hydrodynamic force is proportional to the square of the velocity both in the normal and tangential components,

$$q_t = -\frac{\rho_f}{2} D C_t \dot{v}_x |\dot{v}_x| \qquad (17)$$

$$q_y = -\frac{\rho_f}{2} D c_n \dot{v}_y |\dot{v}_y|$$
 (18)

Ct = tangential drag coefficient

C_n = normal drag coefficient D = element diameter

 $\rho_{\rm f}$ = fluid density (Sea water)

The hydrodynamic force [Ff]e to be applied to the element was calculated by deforming as follows so as to permit the calculation by the use of Gauss's integration.

$$[\mathbf{F}_{\mathbf{f}}]^{\mathbf{e}} = \int_{0}^{k} [\mathbf{N}]^{\mathbf{T}} \{ \mathbf{q}_{\mathbf{y}}^{\mathbf{q}_{\mathbf{x}}} \} d\mathbf{x}$$
$$= \frac{k}{2} \int_{-1}^{1} [\mathbf{N}]^{\mathbf{T}} \{ \mathbf{q}_{\mathbf{x}} \} d\mathbf{n}$$
(19)

where $\eta = 2 \xi - 1$

Further, regarding the additional resistance which is created as the tow cable in the water is accelerated, since the added mass due to normal acceleration is all that is to be considered, the added mass {fg}e to be applied to the element is

$$\left\{ \mathbf{f}_{k} \right\}^{e} = \begin{cases} \mathbf{f}_{kx} \\ \mathbf{f}_{ky} \end{cases} = - \begin{bmatrix} 0 & 0 \\ 0 & \rho_{a} \end{bmatrix} \begin{bmatrix} \ddot{\mathbf{u}}_{x} \\ \ddot{\mathbf{u}}_{y} \end{bmatrix}$$
 (20)

where

 $\begin{array}{ll} \rho^{\,\prime}_{a} \; = \; C_m \rho_{fA} \\ C_{Ri} \; = \; added \; mass \; coefficient \\ \lambda \; = \; cross \; section \; of \; element \end{array}$

Then, the element mass matrix [m] e is combined with the element added mass matrix and the element virtual mass matrix [M]e is expressed as follows.

$$[M] \stackrel{e}{=} \begin{bmatrix} \frac{R_{\rho}}{3} \\ 0 & \frac{13}{35} \\ 0 & \frac{11\ell}{210} & \frac{\ell^2}{105} \\ \\ \frac{R_{\rho}}{6} & 0 & 0 & \frac{R_{\rho}}{3} \\ 0 & \frac{9}{70} & \frac{13\ell}{420} & 0 & \frac{13}{35} \\ 0 & -\frac{13\ell}{420} - \frac{\ell^2}{140} & 0 & -\frac{11\ell}{210} & \frac{\ell^2}{105} \end{bmatrix}$$
 where
$$R_{\rho} = \rho/(\rho + C_{m}\rho_{f})$$

 $R_{\rho} = \rho/(\rho + c_{m}\rho_{f})$ $\rho = cable density$

The above concludes the formulation of the element coordinate system.

Then, transformation to the global coordinate system is performed using the transformation matrix [T].

$$[T] = \begin{pmatrix} \cos\theta & \sin\theta & 0 & 0 & 0 & 0 \\ -\sin\theta & \cos\theta & 0 & 0 & 0 & 0 \\ 0 & 0 & 1 & 0 & 0 & 0 \\ 0 & 0 & 0 & \cos\theta & \sin\theta & 0 \\ 0 & 0 & 0 & -\sin\theta & \cos\theta & 0 \\ 0 & 0 & 0 & 0 & 0 & 1 \end{pmatrix}$$
(22)

After all values were transformed to the global coordinate system, the kinematic equation of the system

$$\Sigma[\mathbf{T}]^{\mathbf{T}}[K]^{\mathbf{e}}[\mathbf{T}]\mathbf{u} + \Sigma[\mathbf{T}]^{\mathbf{T}}[M]^{\mathbf{e}}[\mathbf{T}]\mathbf{u}$$

$$= \Sigma([\mathbf{F}] + [\mathbf{F}_{\mathbf{f}}]) \tag{23}$$

was numerically calculated by Newmark's β method taking β = 1/4. Table 1 was used as input data for the numerical analysis. Assuming the towpoint moved at

$$U_{X} = 10.28 t$$
 (24)

$$U_y = 2.5 \sin \frac{\pi}{5} t$$
 (25)

the each nodal displacement ($\mathbf{U_x}$, $\mathbf{U_y}$, θ) and the tow-point tension in the time increment of 0.01 sec were calculated up to 100 seconds. The results disclosed that the periodic tension change due to the pitching of the ship was about ±10% of mean tension as shown in Fig. 6.

Table 1 Properties used for the reference system

Item	Symbol	Cable	Towbody
Diameter r	n D	0.031	0.08
Mass kgs ² /m	4 P	173.35	104.52
Weight in water kg/r	n w	0.51	0.0
Stretch property k	9 EA	620000	620000
Bending property kgm	² EI	4	2
Normal drag coefficient	Cn	1.15	1.15
Tangential drag coefficient	Ct	0.01	0.01

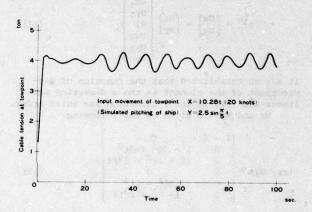


Fig. 6 Periodic tension change

Slip-over-sheave

Onboard handling system generally used consists mainly of a take-up drum and a double capstan. The number of cable turns around the capstan is determined by the friction coefficient between the cable and capstan, and by the drum take-up tension to be

For the model, the number of turns around the capstan is set to a sufficiently large value and it is assumed that the backward cable tension becomes so small as not to affect the cable slip-over-sheave fatigue. In considering the life, when the using conditions are assumed to be two times of winch winding and drawing out a day, 50-day towing a year and 10 year's service, the cable must withstand 1000 times of reciprocating slip-over-sheaves.

Not only the tension but also the tilt angle and capstan diameter are considered to affect the cable life. The tilt angle was set at 90 deg. and several values of capstan diameter were set.

Though the slip-over-sheave at the take-up drum and fair leader is naturally expected, the slip-over-sheave at the take-up drum and at the fair leader was neglected for the reason that its effect on the slip-over-sheave fatigue was considered to be sufficiently small due to small tension and large drum diameter at the take-up drum and due to small tilt angle at the fair leader.

Design of Cable and Joint

Cable diameter and specific weight were set at 31 mm and 1.7 respectively in order to reduce the towing tension and to assure easy handling on the ship.

Figs. 7 and 8 show the structure of the cable and cable joint currently designed. The cable consists of nylon-insulated 75-pair conductors, inner sheath, Kevlar 3-layer tension member, copper braid, outer sheath and layered lapping tapes.

Design characteristics of this cable are as follows. The design value of tensile strength was set at 24 tons taking the fatigue into account. Since the diameter and specific weight were restricted, a copper braid was provided between the outer sheath and tension member to adjust the specific weight. This copper braid contributes greatly to maintaining the required frictional force between the outer sheath and the tension member.

The cable joint is manufactured by pulling out the Kevlar from the cable at a certain angle and certain tension and curing epoxy resin. Its performance is found good.

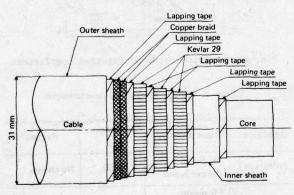


Fig. 7 Cable structure

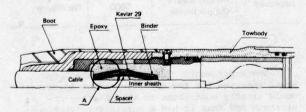


Fig. 8 Joint structure

Evaluation

For the evaluation of basic performance, the tensile test and sheath-slip strength test were conducted. For the verification of dynamic fatigue characteristics the oscillation test and slip-oversheave test were conducted.

Tension

The tensile strength testing method is shown in Fig. 9. The conventional high-tension cable tensile test employs the method wherein tension member is fixed at each end and the assembly thus obtained is installed to the tensile testing machine and a tensile force is directly applied. When the tension member is Kevlar, the optimum method at the present time is to pot-cure epoxy resin. Regarding the termination, the strength of epoxy resin to be used presents a problem for the reason to be mentioned later and the tensile strength is unavoidably limited. The tensile strength of the cable presently fabricated for trial is as large as 24 tons, and therefore, it cannot be confirmed by the conventional method.

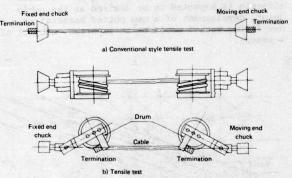


Fig. 9 Tensile test setup

Accordingly, the tensile test was conducted in such a way that a frictional force was produced by winding the cable around the drum and loads applied to the termination were alleviated. The number of turns was set at two in consideration of safety according to the following band-brake formula.

$$n = \frac{1}{2\pi} \frac{1}{\mu} \ln \left(\frac{T_1}{T_2} \right) = 1.2 \approx 2$$
 (26)

where

n = number of turns around drum

= friction coefficient between drum
and cable (=0.1)

T₁ = presumed breaking strength (=24 t)
T₂ = presumed tensile strength of termination with epoxy resin (=12 t)

Test results showed the average tensile strength was 23 tons and the designed value was nearly satisfied.

The tensile test of the cable joint was conducted in such a way as to replace the one end shown in Fig. 9 (b) illustrating the developed method by the cable joint. The average tensile strength of the cable joint was found to be 11.45 tons. This value is sufficient for the presumed load at the cable joint. However, it is noted that the cable joint was broken under the load as low as less than 50% of the cable strength. In an effort to discover the cause, cable joint internal stress analysis was conducted by employing the finite element method. Prior to the analysis, the cable joint to be examined (Fig. 8) was simplified as follows.

 a. As cable components, core, Kevlar and outer sheath are considered and others are neglected.

b. Kevlar is completely impregnated with epoxy resin.

c. All materials follow Hooke's law.
The result of analysis is shown in Fig. 10
with the A part enlarged in Fig. 8. The drawing
shows the cable joint internal stress distribution
when the tension is 6 tons. The length of the
reference arrow shows the ratio of stress to breaking strength represents 100%. It was found out by
this means that though the ratio was less than 30%
at the Kevlar part, it exceeded 100% at the epoxy
resin part. Thus the strength of epoxy resin constitutes a bottleneck of this fixing method.

As high tension corresponding to the cable strength is expected to be desired at the cable joint, development of a new potted material or a new fixing method would be an important subject of research.

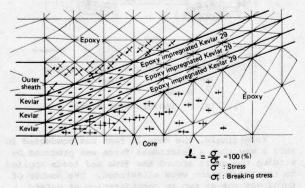


Fig. 10 Stress distribution in epoxy potted joint

Sheath-slip-strength and friction coefficient

For confirming whether the sheath-slipstrength discussed in Section (load estimation) is sufficient or not, it would be ideal to measure the friction coefficient at each layer for each tension and compare the resultant values. However, since there is no reliable measuring method, checking if bellows are produced or not by the sheathslip strength test (Fig. 11) was all that was conducted. The test was conducted in such a way that the cable was wound about a 1200 mm ø sheave (supposed to be the capstan) with a half turn, a constant tension was loaded and the sheave was caused to turn. The friction coefficient between two elements was compared by observing whether slip occurred between the sheath and sheave or between the sheath and tension member. The results of the experiments which were conducted using or not using the copper braid as a lapping tape between the tension member and sheath and changing sheath material are shown in Table 2.

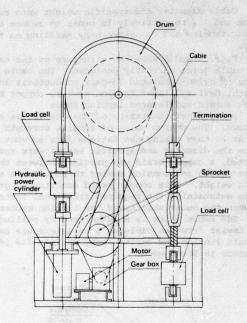


Fig. 11 Measuring setup of friction coefficient

Table 2 Outer sheath-slip-strength

Cable type	Cable structure	Back tension (kg)	Remark
Prototype I	PE sheath Copper braids	5000	No change
Prototype II	PE sheath No Copper braids	570	Sheath bellows
Improved	Rubber sheath Copper braids	5000	No change

The experiments clarified that the copper braid inserted for the specific weight adjustment would greatly contribute to the sheath-slip-strength and that it had a sufficient frictional force.

By measuring the tension difference across the cable while the sheave of this testing machine is driven, the friction coefficient between the cable and sheave can be found. This friction coefficient is one important factor for determining the number of turns about the capstan, take-up tension of the take-up drum and the capacity of those elements in the onboard handling system. For reference, the friction coefficient at each tension in the two cases when polyethylene is used as the sheath material and when rubber is used for that purpose is shown in Fig. 12.

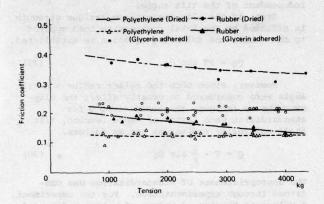


Fig. 12 Friction coefficient

Oscillation fatigue test

From the result of the load estimation previously mentioned, it is known that the tension changes in the towing cable while being towed. Separately conducted towing tests confirmed the occurrence of ±10 % tension change at Sea State 4. Though analysis has not yet been conducted to this date, it is confirmed that high frequency micro-oscillation is generated. The method and the results of the oscillation fatigue test are hereafter described.

Tension change testing method. The testing machine consists of a frame securing the cable, hydraulic power cylinder, hydraulic power unit, etc. and produces tension change by alternately changing the relief valves for setting high or low pressure with the solenoid valve and the timer. Test conditions were as follows.

Tension: 5 tons ±20%
Frequency: 0.67 Hz
Oscillation: 3.6 x 10⁶ cycles

Actual operation was taken into account in determining the oscillation cycles.

The test result was evaluated by subjecting the cable to the tensile test after the completion of the oscillation in the specified cycles and by observing whether or not change in tensile characteristics took place.

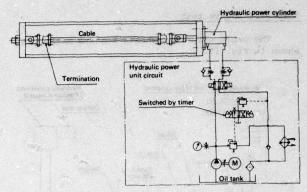


Fig. 13 Fatigue testing method by periodic tension change

Micro oscillation The micro oscillation testing method is shown in Fig. 14.

The testing machine consists of a frame having a span length of 37 m, a weight load device employing a lever and an electromagnetic oscillator generating high frequency micro oscillation. The test was conducted in such a way that approx. 37 m cable was provided between the spans, a specified tension was applied, the cable 6.3 m from the load end was held by the oscillator and the cable was given proper oscillation. The test conditions were as follows.

Tension: 5 tons
Resonance frequency: approx. 20 Hz
Maximum amplitude: $\pm 6 - 10$ mm
Oscillation: Max. 6 x 10^7 cycles

Operation was taken into account for determining the oscillation cycles.

As in the case of tension change, the test result was evaluated by subjecting the cable to the tensile test after the completion of a given oscillation cycles and by observing whether or not any change in tensile characteristics took place. As a result of both tension change and micro oscillation tests, there was no abnormality found in the cable appearance. The cable was further subjected to the tensile test and it was found that the tensile characteristics were not changed as compared with the condition before the oscillation. Thus, the cable was determined safe against oscillation.

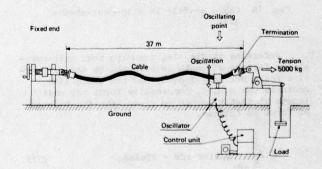


Fig. 14 Fatigue testing method by oscillation

Slip-over-sheave test

The cable slip-over-sheave testing method is shown in Fig. 15.

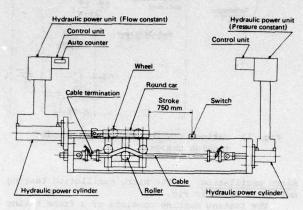


Fig. 15 Slip-over-sheave testing setup

The cable was subjected to a constant tension by means of a hydraulic power cylinder connected to the hydraulic power unit. This kept a constant pressure and reciprocating motion of the roller was provided by the hydraulic power cylinder connected to the constant flow hydraulic unit.

The reciprocating motion was switched by changing the direction of the solenoid valve in the hydraulic unit which drove the roller with microswitches provided at each end as a sensor.

The relative positions of the cable and the roller are shown in Fig. 16.

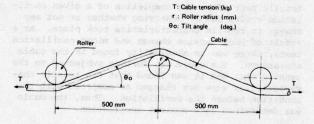


Fig. 16 Cable profile in slip-over-sheave test

Referring to Fig. 16, assuming that slip-oversheave fatigue strength is affected by the compressive force per unit length, and the cable line contacts the roller, compressive force per unit length at that time can be given from the balance of force as follows.

$$2 \int_{\frac{\pi}{2} - \theta_0}^{\frac{\pi}{2}} q_0 \sin\theta \cdot rd\theta = 2T \sin\theta_0$$
 (27)

where T = cable tension
r = roller radius
θ = cable tilt angle

$$2 \operatorname{rq}_{0} \left[-\cos \theta\right] \frac{\frac{\pi}{2}}{\frac{\pi}{2}} - \theta_{0} = 2 \operatorname{T} \sin \theta_{0}$$

$$q_{0} = \frac{\operatorname{T}}{r}$$
(28)

As seen, compressive force per unit length becomes a function of the tension and roller radius, and is independent of the tilt angle.

Then, if the slip-over-sheave fatigue strength is affected by the total compressive load applied to the cable, the following equation is established.

$$Q_0 = 2T \sin \theta_0 \tag{29}$$

However, since both the roller radius and tilt angle were considered to greatly affect the slip-over-sheave fatigue, the coefficient Q for standardizing each factor of cable tension, tilt angle and roller radius was set as follows.

$$Q = T \cdot \frac{1}{r} \sin \theta_0 \tag{30}$$

The appropriateness of standardization was confirmed through experimentation. For the experiment, 4 values of tension, 2 values of roller radius and 3 values of tilt angle were taken. The repetition cycles until the tension member was broken was found, and each condition was converted to 0 by Eq. (30). The experiment results are shown in Fig. 17. By the above experiment it was confirmed that each point was on the same curve and that the conversion of Eq. (30) was nearly appropriate. From the above results, in the currently set onboard system, it is taken that there is no problem in terms of slip-over-sheave fatigue since the tilt angle is very small in the fair leader and since the roller diameter is large and tension is small in the take-up drum. Therefore, fatigue on the capstan is solely considered.

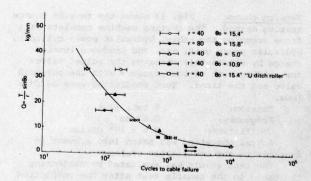


Fig. 17 Result of slip-over-sheave test

Table 3 Evaluation of cable useful life by slip-over-sheave test

	Number	Tension		Q	kg/mm			NC	ycles	100
k	of turns	kg	r = 750	600	500	400	r= 750	600	500	400
1	0	5000	6.7	8.3	10.0	12.5	1200	780	540	350
2	0.5	3400	4.5	5.7	6.8	8.5	2900	1700	1100	730
3	1.0	2400	3.2	4.0	4.8	6.0	104	5400	2500	1500
4	1.5	1600	2.1	2.7	3.2	4.0	00	104	10 ¹	5400
5	2.0	1100	1.5	1.8	2.2	2.8	00	∞	∞	10
6	2.5	760	1.0	1.3	1.5	1.9	00	∞	∞	∞
7	3.0	520	0.7	0.9	1.0	1.3	∞	00	∞	00
n	7 Σ 1/Nk k=1		n = 500				0.64	1.08	1.63	2.59
n;	7 E 1/N _k		n =	500			0.22	0.44	0.70	1.16

Table 3 shows tension at each turn of the capstan, the value of coefficient Q with respect to the roller radius and the cycles to failure at that time. When the value of Q is less than 2, it was neglected, based on the assumption that the effect on the fatigue would be small.

If Miner's hypothesis is established relating to slip-over-sheave fatigue,

$$\frac{n_1}{N_1} + \frac{n_2}{N_2} + \frac{n_3}{N_3} + \cdots + \frac{n_k}{N_k} = 1$$
 (31)

where

 $\mathbf{n_k} \; = \; \mathbf{number} \; \; \mathbf{of} \; \; \mathbf{slip\text{-}over\text{-}sheave} \; \; \mathbf{at} \; \; \mathbf{each} \\ \quad \quad \mathbf{tension} \\$

 N_k = number of slip-over-sheave until failure

In the case of the capstan,

$$n_1 = n_2 = \cdots = n_k = n$$

Accordingly, Eq. (31) can be rewritten as

$$n \sum_{k} \frac{1}{N_k} = 1 \tag{32}$$

When 10-year life is to be assured on the basis of the above setting, slip-over-sheave of 1000 reciprocations must be considered. In the present slip-over-sheave test, slip-over sheave is considered to comprise both-sides and a value of 500 reciprocations is set. If n = 500 in Eq. (32), $n_{\widetilde{k}} \ 1/N_k$ in Table 3 can be calculated from Eq. (32). When $n\Sigma (1/N_k) < 1$, it is safe against slip-over-sheave fatigue. Accordingly, if the winding tension is 5 tons and r=750, the cable will be broken in approx. 8 years. If the winding tension is 3.4 tons and r=500, the cable will withstand 10 years' use.

The appropriateness of this life estimation method has been confirmed by the slip-over-sheave fatigue test performed under equivalent conditions to the actual use, and the data are ready to be compared with those of practical towing tests being carried out at present.

It was confirmed as a result of disassembly investigation after the slip-over-sheave test that the cause of Kevlar break-down was Kevlar wear due to the rubbing of the tension member against the lapping tape or the tension member against the other one, as a result of the slip-over-sheave. Though Kevlar fibres are light, have high tensile strength, are strong against oscillation and are an excellent tension member, they are less resistant to wear due to compressive forces. To overcome this problem, improvement and modification are necessary.

As a result of the above mentioned evaluation, it was confirmed that the cable was sufficiently safe in terms of tensile strength and sheath-slip-strength as the static mechanical characteristics and in oscillation fatigue strength as the dynamic mechanical characteristic.

As for the Kevlar armored cable, it became clear that the slip-over-sheave is the most important factor affecting to the cable life. It will be very useful to follow up the examination by pinpointing its objective to slip-over-sheave fatigue.

Conclusions

Practical towing tests are now under way using the cable and cable joint disclosed here and it is confirmed that the basic characteristics are sufficiently satisfied.

As the result of a series of examinations, proper evaluation method of the towing cable as well as slip-over-sheave test, and design method of high-tension cable employing Kevlar were established.

However, there are subjects to be solved as the following.

- a. Enhancement of system reliability and the development of a more accurate life estimation method.
- b. For generalizing the cable evaluation method, establishment of a method to replace the gross cable load with the load of each component material so as to be able to represent the cable characteristics by the characteristics of component materials.

Design and evaluation techniques dealt with here are considered to be applicable not only to towing cables but also to general cables as well.

Acknowledgement

The authors would like to thank Mr. Shibata, Mr. Arai and Miss Ito for their great support. They also would like to thank management personnel who participated in this joint research.

References

- Alfred H. Keil. May, 1969. Stability and Motion Control of Ocean Vehicles. Copyright C 1969 by The Massachusetts Institute of Technology.
- A.P.K. De Zoysa. 1978. Steady-state Analysis of Undersea Cables. Ocean Engng. Vol.5, pp.209 ∿ 223 C Pergamon Press Limited.
- 3) J. Ketchman and Y.K. Lou. Application of the Finite Element Method to Towed Cable Dynamics. IEEE OCEAN pp. 98 ~ 107, 1975.
- R.L. Webster. Structural Response of Arbitrary Underwater Cable Systems.
 ASME, Vol. 1, pp. 43

 59, 1975.
- 5) M.J. Casarella and M. Parsons. Cable Systems Under Hydrodynamic Loading. Marine Technology Society Journal, Vol. 4, July/Aug. 1970, pp. 27 ∿ 44.
- R.L. Webster. Nonlinear Static and Dynamic Response of Underwater Cable Structures Using the Finite Element Method. paper OTC 2322, 1975.
- H.B. Amey, Jr. and G. Pomonik. Added Mass and Damping of Submerged Bodies Oscillating Near the Surface. paper OTC 1557, 1972.



JUN NAKAJIMA
The Furukawa Electric
Co., Ltd.
6-1 Marunouchi, 2-chome
Chiyoda-ku, Tokyo,
Japan

Mr. Nakajima graduated from Waseda Univ. 1962 with a B.Sc. in mechanical engineering. He has been engaged in research and development of telephone cables and the accessories.

Mr. Nakajima is now manager of Outside Plant Engineering Section of the Telecommunication Laboratories at The Furukawa Electric Co., Ltd. and a member of the Japan Society of Mechanical Engineers and also of the Institute of Electronics and Communication Engineers of Japan.



SHIGERU TACHIGAMI
The Furukawa Electric
Co., Ltd.
6-1 Marunouchi, 2-chome
Chiyoda-ku, Tokyo,
Japan

Mr. Tachigami graduated from Tohoku Univ. 1970 with a B.Sc. in mechanical engineering. Then he joined The Furukawa Electric Co., Ltd. and has been engaged in research and development of telephone cable and the accessories.

Mr. Tachigami is now chief engineer of Outside Plant Engineering Section of the Telecommunication Laboratories at The Furukawa Electric Co., Ltd.



SATORU KIKKAWA
The Furukawa Electric
Co., Ltd.
6-1 Marunouchi, 2-chome
Chiyoda-ku, Tokyo,
Japan

Mr. Kikkawa graduated from Yamanashi Univ. 1972 with a B.Sc. in mechanical engineering. Then he joined The Furukawa Electric Co., Ltd. and has been engaged in research and development of telephone cable and the accessories.

Mr. Kikkawa is now engineer of Outside Plant Dep. of the Telecommunication Div. at The Furukawa Electric Co., Ltd.



MASANORI OKUBO
The Furukawa Electric
Co., Ltd.
6-1 Marunouchi, 2-chome
Chiyoda-ku, Tokyo,
Japan

Mr. Okubo graduated from Waseda Univ. 1972 with a B.Sc. in electrical communication engineering. Then he joined The Furukawa Electric Co., Ltd. and has been engaged in research and development of telephone cables and manufacturing methods for telephone cables.

Mr. Okubo is now engineer of Engineering Section of the Telecommunication Div. at The Furukawa Electric Co., Ltd.



HARUO UMEZU
The Furukawa Electric
Co., Ltd.
6-1 Marunouchi, 2-chome
Chiyoda-ku, Tokyo,
Japan

Mr. Umezu graduated from Nihon Univ. 1972 with a B.Sc. in chemical engineering. Then he joined The Furukawa Electric Co., Ltd. and has been engaged in research and development of plastic material and manufacturing methods for telephone cables.

Mr. Umezu is now engineer of Material Engineering Section of the Telecommunication Laboratories at The Furukawa Electric Co., Ltd.



HIDEYO KAWAZOE
The Furukawa Electric
Co., Ltd.
6-1 Marunouchi, 2-chome
Chiyoda-ku, Tokyo,
Japan

Mr. Kawazoe graduated from Tokyo Univ. 1977 with a B.Sc. in mechanical engineering. Then he joined The Furukawa Electric Co., Ltd. and has been engaged in research and development of telephone cables and the accessories.

Mr. Kawazoe is now engineer of Outside Plant Engineering Section of the Telecommunication Laboratories at The Furukawa Electric Co., Ltd.

REINFORCED SELF-SUPPORTING CABLE

A NEW ALTERNATIVE IN PROTECTED AERIAL PLANT FACILITIES

P. J. Reale, Jr. and L. M. Borowicz, Jr.

Western Electric

Abstract

Protection of aerial cable facilities against sheath damage is a problem which telephone companies encounter daily. Sheath openings are caused by a variety of sources for which there is more than one solution. In order to reduce the amount of maintenance and installation effort associated with aerial plant in trouble prone areas, a reinforced self-supporting cable was designed.

Introduction

A review of current telecommunications publications will reveal discussions of advancements in technology and modern administrative techniques. Earth stations. fiber optics, and the implementation of the Serving Area Concept (SAC) or Rural Area Network Design (RAND) are all subjects which significantly impact on the telephone industry. While these topics may be interesting due to their novelty and future wide-scale applications, they do not address the more routine problems which the telephone operating companies encounter everyday. It is now time to direct attention to one of the less glamorous outside plant problems which must be solved in order to maintain a secure exchange area network, i.e. aerial cable sheath troubles. Due to its very nature, the aerial environment subjects cable to a wider range of potential trouble sources than either the buried or underground environments. Of course, lightning and gophers can play havoc with a buried cable due to the moisture surrounding the cable, and underground systems are jeopardized by the flooding of manholes. However,

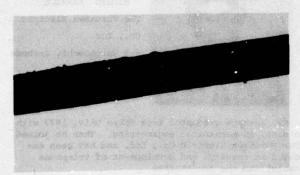


FIGURE 1: Squirrel damage to a polyethylene jacket removed from a cable which was in service.

aerial cables must contend with a continuing battle of endurance against the elements, animals and the people living in the area served by these facilities. Cable troubles resulting from sheath breaks can be caused by tree abrasion, construction site accidents, shotgun pellets, lashing wire, beetles and electrical burns from contact with power lines. While these sources of trouble may be discounted by some as being isolated incidents or causing only a miminal number of sheath breaks, the damage caused by animals has been documented.

A major source of cable damage in aerial plant has been attributed to the gray squirrel. Typically, in South Central Bell, one "squirrel trouble" may occur along every 1,500 feet of aerial cable. In one district alone, the repair of squirrel damage generated an expense of \$5,500 during July and August of 1975.

Similar destruction of facilities has been encountered in many other companies as well. The reasons for animal damage are not yet understood, however, the final result is that a maintenance expense estimated in the millions of dollars is incurred. Techniques have been adapted to deter animal damage on existing plant, however, the preventative solutions can also be costly. This was evidenced during 1974 in the Nassau County area served by New York Telephone where one-half million dollars were spent to avoid further damage from animals. While the squirrel has been responsible for much of the animal caused sheath breaks, woodpeckers are also believed to contribute to this destruction.

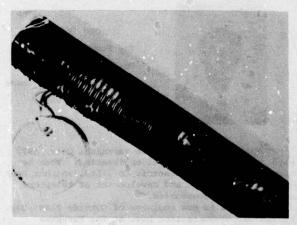


FIGURE 2: Woodpecker damage to a polyethylene jacket under a controlled environment.

Alternatives For Protecting Aerial Outside Plant

Usually, it is not possible to predict the precise location in which animals will attack aerial plant. Therefore, a cable is usually damaged first, then repaired and if similar sheath troubles occur in the area, it can then be expected that this trend will continue and that preventative measures need to be taken in order to thwart the efforts of squirrels and woodpeckers.

The alternatives available for consideration by the field engineers to protect existing aerial circuits are either to install a protective device around the repaired cable or if the cost of the repairs is greater than the cost of installing a new cable, the construction of new plant may be the desirable alternative.

There are several types of mechanical devices which can be installed on existing cable. These are commonly known as cable guards and are manufactured with either a circular or triangular cross-section.

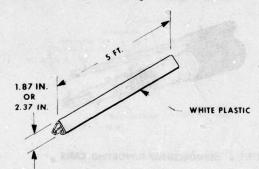


FIGURE 3: Self-locking cable guard

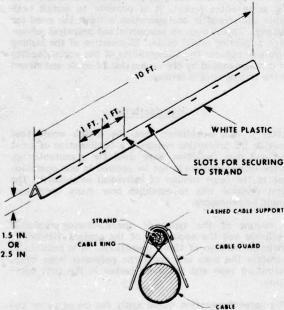


FIGURE 4: Secured cable guard

The basic concept of a cable guard is to provide a barrier of hard, slippery plastic around the cable which will prevent the animal from directly attacking the sheath. Thus, any damage is minimized and encountered by the cable guard and not the sheath.

If an area is known to have sheath troubles related to animals, a cable of more robust nature can be used when initially building the aerial facilities. Traditionally, a PASP (polyethylene-aluminum-steel-polyethylene) sheath design has been employed for this purpose. PASP has several features, which are not found in a single sheath aerial cable, that provide additional protection against animal attacks.

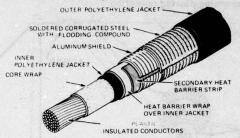


FIGURE 5

PASP CABLE

Moisture which enters a cable's outer sheath subsequent to damage is blocked by an inner polyethylene jacket surrounding the core, thus assuring continuity of service. The sheath also incorporates a layer of corrugated steel applied longitudinally. The advantage of this steel is greater impedance to further sheath penetration caused by the animal. The steel also provides the benefit of increased electromagnetic shielding at low frequencies.

Limitations of the Current Alternatives

While cable guards and the use of PASP cable have been proven effective in resisting sheath damage caused by animals, there are limitations associated with the use of these alternatives.

Cable guards are currently most advantageous for applications in which the telephone company is concerned with preventing additional damage to a cable which is already in plant. It is, of course, always possible to replace the damaged cable with a new double sheath cable, although this solution is normally economically feasible only when the cable has been severely damaged over a distance of many spans. Using cable guards in applications limited to existing cables, however, necessitates post facto identification of problem areas, i.e., the cable must incur some damage before preventative measures can be taken. Thus, elimination of all damage is not possible, and maintenance efforts must be expended to repair the cable until the decision is made to install the guards. While cable guards provide a successful method of preventing future sheath damage to an existing cable, they may require a large investment. For example, in Nassau County, the New York Telephone Company spent approximately three quarters of a million dollars on plastic cable guards during 1975 in order to prevent animal related sheath penetration.

In an effort to minimize sheath related maintenance costs and eliminate future expenditures for preventative devices, an alternative which is often employed is to install a PASP sheathed cable. While the cable guard solution is recommended for existing plant, the PASP solution is utilized for the construction of new plant in an area prone to sheath damage. Although the PASP alternative can reduce maintenance efforts by impeding the penetration of animals from reaching the cable's inner jacket, the installation of this cable still requires the placing of a support strand and necessitates the lashing operation. These two factors not only account for a high labor content in the installed cost of a PASP cable, but also result in a time consuming placing operation.

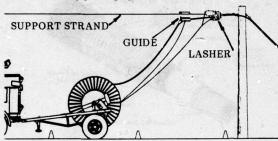


FIGURE 6: Lashing an aerial cable

Although the PASP cable solution is relied upon by many telephone companies, the motivation still exists for reducing installation costs and increasing productivity.

The Reinforced Self-Support Design

In an effort to decrease cable placing costs and augment installation productivity of protected aerial plant facilities, a reinforced self-supporting cable was designed.

The new design employs polyethylene insulated copper conductors in the construction of the cable core, and similer to the regular (single sheath) self-supporting cable, incorporates an undulated core. The undulations are waves in the core which permit it to expand with the sheath when the support strand is tensioned. This allows the cable to expand without incurring any strain in the conductors. Surrounding the undulated core is polyester core wrap, a corrugated aluminum shield covered by a polyethylene jacket. This inner sheath is similar to a single sheath, aluminum polyethylene (ALPETH), aircore aerial cable with the addition of a polyethylene copolymer coating

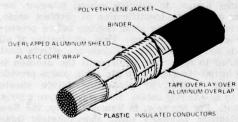


FIGURE 7 ALPETH SHEATH

on the aluminum shielding which increases the strength of the inner jacket and retards moisture migration.

A crepe paper wrap is applied around the ALPETH sheath which serves as a heat barrier during the subsequent soldering of the seam on a corrugated steel shield. The use of an ALPETH inner sheath has the advantage of separating the aluminum shielding from the surrounding steel shield with a polyethylene jacket, thus preventing the possibility of moisture-originating corrosion between the two metals.

The steel shield also gives the reinforced self-supporting design additional mechanical protection from the attacks of animals. The support member is a preformed 4 inch, extra high strength (EHS), class A galvanized steel strand which has a minimum breaking strength of 6,650 pounds. Both the steel shielding and the support strand are coated with a thermo-plastic flooding compound and an outer jacket of polyethylene is employed to unite the two components.

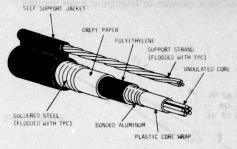


FIGURE 8 REINFORCED SELF-SUPPORTING CABLE

Because the cable and support strand are enclosed in the same outer jacket, it is possible to install both cable and strand in one operation without the need for lashing. This is both an economic and practical advantage in placing aerial cable. Elimination of the lashing wire also reduces the vulnerability of the aerial facility to damage caused by the separation of cable and strand if the lashing wire is broken.

Manufacturing

After it was established that the design would best provide the protection required, a combination of exist ing and new facilities were used for manufacturing. Since this sheath could not be applied in one operation due to the large number of individual components, the first decision was to establish how many operations would be necessary.

A review of the types of manufacturing facilities available and the economics of the project yielded an optimum number of three operations. It is possible to undulate the core and apply the polyester core wrap, aluminum tape and the inner jacket in the first operation.

The second operation would apply the crepe paper and the steel tape, while the third operation would provide the steel strand, the flooding compound and the polyethylene jacket.

THE POST OF THE PROPERTY OF THE PARTY OF THE

In the first operation the cable is received from the stranding operation on cable core trucks, undulated in the normal manner, and the plastic core wrap applied followed by application of the aluminum shield. This assembly is passed through the shield gap positioning device, which is required in order to assure that the aluminum edges are butted together prior to jacketing. A polyethylene jacket is then extruded about the aluminum and cooled. The entire cable is then placed on standard design shipping reels.

The second operation uses the shipping reel as a supply reel and passes the sub-cable through the steel tape sheathing line for application of the paper core wrap and the soldering of the steel tape. This assembly is then placed on a core truck.

In the final operation, the steel covered cable is flooded with thermo-plastic compound, the steel strand is supplied and flooded, and the final jacket applied.

Field Trial

In an effort to determine the outside plant feasibility of the reinforced self-support design, a field trial was commenced in Poughkeepsie, New York on October 7 and 8, 1976. The purpose of the field activities was to observe the installation of the cable for any problems encountered during placing, splice preparation or the splicing operation itself. Trials of this type also permit the evaluation of the product's compatibility with current telephone company practices and allow for direct interaction with the outside plant craftspersons, a factor which may highlight unanticipated inconveniences or problems. A longer term objective of the trial was to verify the cable's ability to reduce maintenance costs associated with repairing troubles resulting from the gnawing habits of rodents or other sources of sheath damage.



FIGURE 9: Field trial environment

The area of Poughkeepsie has several neighborhoods which experience a high incidence of animal related sheath troubles. Prior to the installation of the reinforced self-supporting cable, the field trial location had records of 14 service affecting troubles attributed to squirrel damage, which resulted in a total of 42 hours of lost service. Thus, this residential area was evaluated as a good candidate for a field trial location.

Two neighborhoods were finally selected for the installation of the new product which are established wooded areas. This environment is representiative of one which provides a good habitat for animal life such as squirrels. Two sizes of reinforced self-supporting cable were selected - 50 pair/26 gauge, and 200 pair/24 gauge - and were employed in a distribution application. A total of 2,200 feet of the 50 pair cable was installed in 14 spans, and was placed using the stationary reel method. For this operation, the cable reel was located near the initial pole of attachment and payed off as the cable was pulled through pole-mounted supports with a plastic rope. The supports incorporated a rotating sheave which allowed the cable to be pulled with minimal frictional resistance.

The installation was generally successful, with the only trouble occuring when the cable was pulled around a six-inch sheave at an angle of approximately 75°. This practice, however, is not in accordance with the recommended procedures for installing self-supporting cable which limit the angle to a maximum of 60°. This method, therefore, resulted in flattening the cable and damaging the jacket over the support strand.

Due to the robust nature of the sheath, one concern was the splicer's ability to open the four layers of the sheath while the cable was on the pole. However, during the field trial, the splicer was able to remove both plastic jackets and metallic shields as well as clean and ground the shield in approximately five minutes. Thus, the initial concern proved to be unwarranted.

The remaining 3,740 feet of the 200 pair/24 gauge cable was placed along the back property line of the telephone subscribers' residences which paralleled a private access road. Because this area was free from many interfaces, the moving reel method of installation was employed. In this case, the reel was mounted on a truck and payed off as the truck moved between poles.



FICURE 10: Placing the 200 pair 24 gauge cable

Almost three years after the field trial installation, the site was revisited. The area is served by several types of cable, both single and double sheath, and trouble reports in the area showed that animal related sheath damage was still a problem. In fact, the week prior to the reevaluation, squirrels attacked an area very close to the field trial location which is served by a regular self-supporting cable. While most of the damage was borne by the cable closures, some damage was experienced in the sheath adjacent to the damaged apparatus. The field trial cable, however, located in the same environment, had no reports of sheath damage. It is believed that efforts by the animal population to attack the reinforced, self-supporting cable were experienced although service was not interrupted as a result of any sheath openings due to the protective inner jacket.

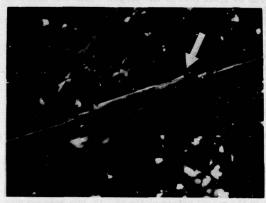


FIGURE 11: Closure damaged by squirrels

This highlights an important feature of the design: that of continuity of service after an opening in the outer sheath. Many times a service affecting trouble is temporarily cleared by transferring the subscriber to a good, vacant pair. While this method is beneficial for restoring service rapidly, it also allows the possibility of neglecting to repair the damaged sheath at a later date. Thus, the potential still exists for future service affecting troubles in the single sheath cable until the damage is located and repaired. With the reinforced design, damage to the outer sheath will result in neither interrupting present service nor necessitating sheath repair to prevent future troubles.

Conclusion

Reinforced self-support cable was initially designed in an effort to aid the telephone operating companies install aerial plant in an environment prone to damage from animals. In fact, the product was originally introduced as a self-supporting cable with "squirrel protection". Since its conception, however, additional applications for the product have been discovered. In addition to successfully reducing cable troubles due to sheath damage from squirrels, the cable design has also proved effective in reducing troubles caused by woodpeckers, shotgun pellets, tree abrasion, and other potential sources of mechanical sheath damage. In conjunction with the mechanical protection offered, reinforced self-support also provides additional protection against electromagnetic interferences such as

those produced by power transmission lines which cause noisy circuits. Although this cable was developed for protection against squirrels, it is effective in the exchange area aerial network to reduce maintenance expenses due to jacket damage from a variety of causes.

References

- "Economic Review of Rodenticide Usage in the U.S.", Arthur D. Little, Inc., May 20, 1976, Contract No. 68-01-2489.
- F. W. Horn and O. B. Cook, "The New Look in Aerial Cable", <u>Bell Laboratories Record</u>, October, 1964.

Acknowledgement

The authors would like to express their appreciation to N. J. Cogelia of Bell Laboratories for the use of the damaged cable samples and for his valuable advice in the preparation of this paper.

P. J. Reale, Jr. Western Electric 2000 Northeast Expressway Norcross, Georgia 30071



P. J. Reale, Jr. received a Bachelor of Mechanical Engineering degree from Georgia Institue of Technology in 1975. He was engaged in the engineering development of nickel-cadimium batteries with SAFT in Paris, France until 1978. Since this time he has been working in a planning engineer capacity on small pair size PIC cable with Western Electric, and is pursuing an M B.A. degree at Georgia State University in Atlanta.

L. M. Borowicz, Jr. Western Electric 2500 Broening Highway Baltimore, Maryland 21224

L. M. Borowicz, Jr. received his B.S. degree in Mechanical Engineering from the University of Maryland in 1969. He has since been with Western Electric in Baltimore where he is presently involved with the sheathing of communication cable.

A NEW MANUFACTURING PROCESS OF WAVEGUIDE BY APPLICATION OF A BONDED JACKET TECHNIQUE

Bv

Eiji Iri,

Michio Morishita,

Yutaka Ohuchi

Dainichi-Nippon Cables, Ltd. Osaka, Japan

SUMMARY

With improvements in the bonded jacket technique conventionally employed for telecommunication cables, we developed a process and equipment for manufacturing waveguides having a conductor lap joint of higher properties in an accurately controlled position and a bonded jacket retaining the desired cross sectional shape with high stability. The equipment for performing the process by a sequential operation comprises a tape supply, preformer, heat bonding assembly, main former, polyethylene extruder, cooling unit, pulling catapillar and take-up. The process and equipment provide waveguides with higher characteristics, at lower costs and with greater ease than heretofore possible, and are useful also for the production of pipes, telecommunication cables and coaxial cables.

1. Introduction

Waveguides or coaxial cables are generally used as antenna feeders for microwave telecommunication and broadcasting links. Research in recent years has been directed to improvements in the overall properties of waveguides and to the production of waveguides at reduced costs with increased ease. Focusing attention on the latter, we have made investigations on waveguides and developed a process and equipment for manufacturing waveguides with higher characteristics, at lower costs and with greater ease than heretofore possible. With improvements in the bonded jacket technique conventionally employed for telecommunication cables, the manufacturing process and equipment described in this paper provide a lap joint of higher properties for the conductor tape, permit accurate position control of the lap and assure stability of the bonded jacket in its cross sectional shape.

The process and equipment are useful not only for the manufacture of

waveguides but also for the production of pipes and tubes with high precision, the production of telecommunication cables with cores which are not resistant to external pressure or heat and the production of coaxial cables with high properties and low costs.

2. Manufacture

2.1 Process

The object of our research is to develop waveguides of the structure shown in Fig. 1. The waveguide comprises a metal tape with its thickness reduced to such extent that will not adversely affect the electrical characteristics of the waveguide, so as to render the waveguide easy to handle for installation and to assure savings in material. The metal tape is covered with a polyethylene jacket heatbonded to the tape and imparting mechanical strength to the tape. The process and

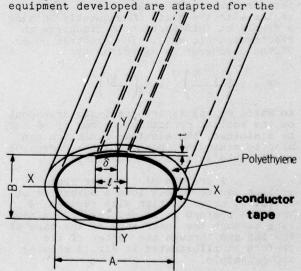


Fig.1.Cross sectional view of the waveguide

manufacture of such waveguides by a single process at reduced costs while fulfilling the above requirements.

(1) Lap of tape with improved bond

Since the waveguide is used at a high frequency and has a hollow interior, the lap of the conductor tape must be completely heat-bonded to fulfil the requirements of electrical and mechanical characteristics. Accordingly there is the necessity of using a tool for supporting the tape from inside and holding the tape in the desired cross sectional shape during heat bonding. The tool is fixed in position at all times and must be surfacetreated to avoid defacement of the inner surface of the waveguide.

(2) Position control of lap

The lap of the conductor tape in the waveguide (Fig. 1) is heat-bonded with thermoplastic resin which holds the over-lapping portions of the tape out of electrical contact with each other. waveguide is so designed as will be described below to avoid the leakage of electromagnetic waves from the non-contact portion. Suppose the inner edge of the tape at the lap is deviated from the minor axis Y-Y of the ellipse by a distance δ , and the metal layers at the lap are spaced apart by a distance t. It is then assumed that a slit of width t is present at the deviated position. When a dominant mode wave is transmitted through the waveguide, a surface current flows on the waveguide as seen in Fig. 2, with a component I_T of the current crossing the slit at right angles with the slit, consequently forming a dipole at this portion to discharge an electromagnetic wave. The electric power of the discharge is expressed by:

$$F = K_1 \left(\frac{I_T \cdot t}{\lambda} \right)^2 = K_2 \left(\frac{\delta \cdot t}{\lambda} \right)^2$$

in which K_1 and K_2 are constants dependent on the ambient conditions. Thus if δ can be minimized, the electric radiation can also be minimized, rendering the waveguide serviceable as such satisfactorily.

A preform of circular cross section can be formed into a waveguide of ellipical cross section with reduced δ when the preform is so deformed along the line through the inner edge of the tape at the lap and through the center of the preform as illustrated in Fig. 3 showing the principle.

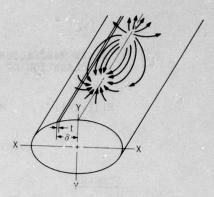


Fig.2. Current lines on the inner surface at the top of elliptical waveguide

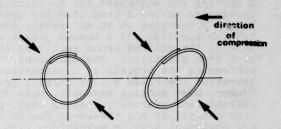


Fig. 3. Principle of lap-position control

(3) Assurance of specified elliptical cross section

If an elliptical tube made from a thin conductor tape is covered with hot polyethylene immediately after extrusion and then rapidly cooled, the polyethylene will thermally contract markedly, with the likelihood of collapsing the elliptical tube to a flat form. To inhibit this phenomenon to the greatest possible extent, the tube must be subjected to gradient cooling with a cooling tank divided into three zones.

2.2 Manufacturing equipment

The equipment for the bonded jacket process for telecommunication cables, which is unable to produce waveguides of the above structure, has been improved with provision of additional devices for the manufacture of the waveguides by a single process. Fig. 4 shows the improved equipment, which, although operated at a production speed of about members of members of the waveguides of a production speed of about members of members of members of members of the waveguides of a production speed of about members of members of members of the members

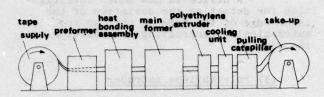


Fig.4. Manufacturing equipment

The equipment can be divided into eight large units which will be described below in detail.

(1) Tape supply

Fig. 5 shows a conductor tape comprising a metal layer which may be treated with a chromate when desired and a thermoplastic resin layer (of polyethylene hotmelt adhesive composition) bonded to one side of the metal layer. The conductor tape is wound on a drum with the metal layer positioned outside and paid off by a catapillar.

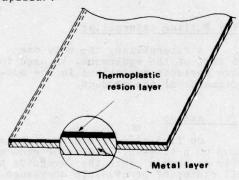


Fig.5. Conductor tape

(2) Preformer

The conductor tape is first made by a preformer into a tube of circular cross section in which the lap is less likely to sag since the inner edge of the tape must be completely bonded to the outer edge at the lap. The circular tube is subsequently formed into an elliptical tube.

The preformer comprises a tapered trough-shaped die for forming the tape to the shape of a trumpet, an overlapping die for further forming the tape into a circular tube with a specified lap, shape adjusting dies for dimensioning the tube to a predetermined outside diameter, etc.

The overlapping die is tapered

from inlet toward outlet and has a restraining plate for forcing one edge of the tape inside the other edge to provide a lap (Fig. 6).

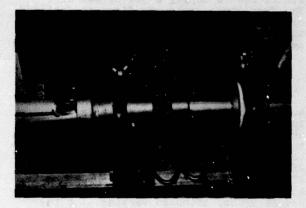


Fig.6. Overlapping die

A tubular core member is fixedly disposed concentrically with shape adjusting dies and extends further downstream from these dies through the circular tube, permitting the tube to retain its cross sectional shape (Fig. 7).

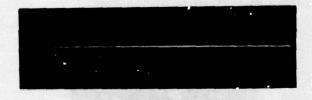


Fig.7. Core member

The core member is coated with Teflon over the outer surface to prevent the inner surface of the tube from defacement. A highly volatile lubricant is applied to the core member to reduce the friction involved. The lubricant completely vaporizes off at the subsequent heat bonding assembly and will not adversely affect the bonding of the lap.

(3) Heat bonding assembly

The circular tube shaped to the specified inside and outside diameters and lap dimension by the preformer is fed to a heat bonding assembly, in which the lap is bonded with the thermoplastic resin provided in this portion by being pressed on with four rolls and the tubular core

member extending through the tube.

The heat bonding assembly is provided with a 7-KW heater against which air is fed to supply a jet of hot air. The four press rolls are fixed as inclined circumferentially of the tube by a suitable to press the inner edge of the lap between the rolls and the core member.

(4) Main former

The tube with its lap heatbonded by the bonding assembly is shaped into a tube of specified elliptical cross section by a main former. At this time, the inner edge of the tape at the lap must be positioned in the vicinity of the minor axis of the elliptical cross section. (The deviation from the axis should be up to ± 2 mm, for example, for waveguides for use at 9 GHz, although varying with the waveguide size.)

The main former comprises two rolls positioned one above the other as spaced apart by an adjustable distance and each having a peripheral groove semielliptical in cross section to form a specified elliptical space between the rolls when they are arranged in combination as shown in Fig. 8. The forming rolls are angularly shiftable about the axis of the tube so that the tube can be formed as contemplated with ease.

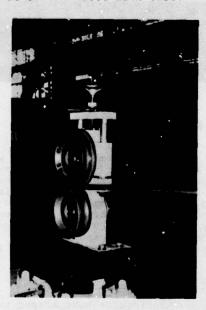


Fig.8. Forming rolls

A device is now under investigation for detecting the deviation of the inner edge of the tape at the lap and automatically controlling the position of the edge.

(5) Polyethylene extruder

The elliptical tube prepared is then covered with a polyethylene jacket. Hot polyethylene (200 $^{\circ}$ C) extruded from an extruder is heat-bonded to the thermoplastic resin coating on the outer surface of the tube.

(6) Cooling unit

The polyethylene jacket, if quenched, would abruptly shrink and deform the elliptical tube to a flat shape. To avoid this, the jacket is cooled gradually in a cooling tank divided into three zones each about 7 m in length, namely a first zone of air cooling, a second zone of hot water cooling (with a temperature gradient of 85 to 40°C/7m) and a third zone of cold water.

(7) Pulling caterpillar

A caterpillar, the only one driven unit of the equipment, is used to minimize periodic variations in the outside diameter of the product.

(8) Take-up

On finishing, the waveguide is wound up on a take-up. A drum of reduced diameter is usable since the waveguide has a small radius of permissible curvature.

2.3 Product

The waveguide produced by the process and equipment described above, named "elliptical laminate waveguide," is designed for use with marine radars (at a frequency of 9.3 to 9.5 GHz) and has been found to exhibit good characteristics. The waveguide generally has the following features:

- (a) The waveguide is comparable to existing rectangular waveguides (WRJ-9) in electrical characteristics.
- (b) It is flexible, lightweight and therefore easy to handle for installation.
- (c) It is easily connectable with a butt flange and a choke flange of the insertion type which assure water-

tight coupling (Fig. 9)

- (d) The aluminum conductor, when surfacetreated with a chromate, is highly resistant to corrosion due to salt water.
- (e) It is inexpensive.

(1) Construction

Table 1. Cross sectional dimension of the waveguide

Cross sect	elliptical shape		
Outside (mm)	major axis	approx. 34	
diameter	minor axis	approx. 20	
Inside	major axis A	approx. 27	
(mm) diameter	minor axis B	approx. 14	
Axis ratio B/A		approx. 0.5	
Width of overlap (mm)		approx. 10	
Thickness of polyethylene (mm)		approx. 2.5	

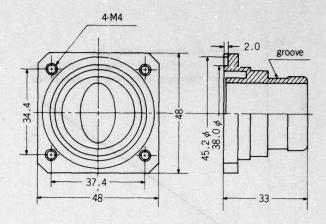
(2) Terminal ends

Since the polyethylene jacket is firmly bonded to the conductor tape and is not easily removable, the waveguide is made connectable with a wedge-shaped flange inserted into the waveguide, with silicone rubber filled in a groove at an insert portion of the flange, and fastened to the waveguide by a binding wire.

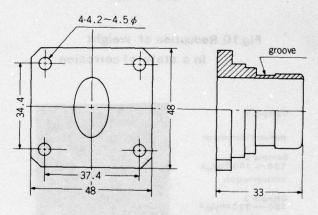
To ensure ease of connection for installation, a choke flange is also prepared. With an impedance transformer incorporated in the flange, the waveguide is connectable directly to a rectangular waveguide (WRJ-9).

(3) Resistance to salt water

The waveguide itself and the terminal joint are of watertight structure against ingress of salt water. However, since the waveguide is designed for use on ships or in coatal areas, salt-containing air is likely to enter the waveguide during coupling or installation and cause corrosion to the conductor portion. To avoid this, the conductor is surfacetreated with a chromate and made resistant to corrosion.



(1) Choke pressurizable flange



(2) Butt unpressurizable flange

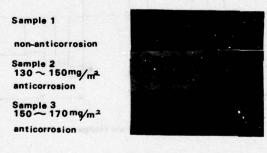
Fig.9. Flanges

Tapes thus treated uniformly can be used with ease and are heat-bonded at a low temperature in the process described, without impairing the treated surface. This is one of the features of the process.

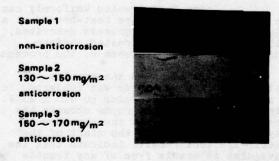
Fig. 10 shows the results obtained when the waveguide was subjected to a salt spray test according to JIS Z 2371. Fig. 11 presents photographs showing the corrosion developing in the specimen 15 days and 60 days after the start of the test. The test results indicate that the waveguide is usable free of any trouble when surface-treated with 150 to 170 mg/m² of surface treating agent containing a chromate.

O.30 — Non-anticorrosive aluminium tape — Anticorrosive (130~150mg/m²) aluminium tape — Anticorrosive (150~170mg/m²) aluminium tape O.20 — Anticorrosive (150~170mg/m²) aluminium tape Term of trial (days)

Fig.10. Reduction of weight in a state of corrosion



(1) After 15 days



(2) After 60 days

Fig.11. A state of corrosion in brine

(4) Electrical characteristics

Table 2 shows the electrical characteristics of the waveguide. When connected directly to a WRJ-9 rectangular waveguide, the waveguide has a V.S.W.R. characteristic of not higher than 1.10 in the frequency range of 9.30 to 9.50 GHz and of not higher than 1.07 especially in the range of 9.35 to 9.45 GHz. Since the waveguide has an elliptical cross section with an axis ratio of 0.5, the cut-off frequency is 6.5 GHz for dominant mode (eH1) and 11.9 GHz for primary higher mode (eH2).

Table 2. Electrical characteristics

Frequency band	(GHz)	9.30~9.50	
V.S.W.R.	mus de	≦1.10	
Attenuation constant (dB/m)		0.12	
Cutoff (GHz)	dominant mode	6.5	
frequency	higher mode	11.9	

The waveguide is comparable to seamless elliptical aluminum waveguides in frequency characteristics of attenuation constant. Fig. 12 shows measurements of the characteristics for the waveguide and corresponding values calculated for a seamless elliptical aluminum waveguide having the same axis ratio (0.5).

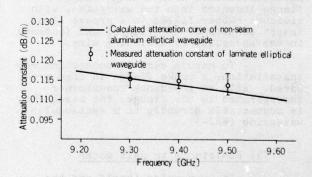


Fig.12. Frequency-dependent characteristics

(5) Mechanical characteristics

Table 3 shows the mechanical characteristics of the waveguide. The minimum bending radius and permissible torsion are the radius and the amount of torsion, respectively, to which the waveguide could be bent and twisted three times reciprocally in one direction and then opposite direction without entailing any variations in the V.S.W.R. characteristics. Since the waveguide requires a very small bending or twisting moment, is lightweight and therefore easy to handle, a mounting assembly shown in Fig. 13 are usable.

Table 3 Mechanical characteristics

AUGUST STREET OF STREET	E-plane	250
Min. bending radius (mm)	H-plane	250
Allowable twist	(deg./m)	180
	E-plane	450
Moment for min. bend (g·m)	H-plane	700
Moment for allowable twist	(g·m)	550
Allowable compression stress	(kg/cm²)	5.0
	waveguide	300
Max. tensile strength (kg)	termination	240
Allowable tensile strength	(kg)	100
Weight	(g/m)	230

(6) Environmental test

The waveguide is to be used on ships or coatal areas and will be subjected to vibrations caused by a marine engine or wind. When subjected to vibration test under the conditions listed in Table 4 and simulating such an environment, the waveguide exhibited satisfactory performance free of deterioration in the V.S.W.R. characteristics in the presence of vibrations in E and H planes.

The waveguide was further checked for variations in the V.S.W.R. characteristics and attenuation constant characteristics under 85 heat cycles simulating variations in the outdoor temperature and each involving temperature variations of from $-20^{\circ}\text{C} \longrightarrow +60^{\circ}\text{C} \longrightarrow -20^{\circ}\text{C}$ over a period of 6 hours. The specimens used were a 5-m long waveguide wound in the direction of E plane into a bundle of loops having a radius of 250 mm and tested for electrical characteristics, and wave-

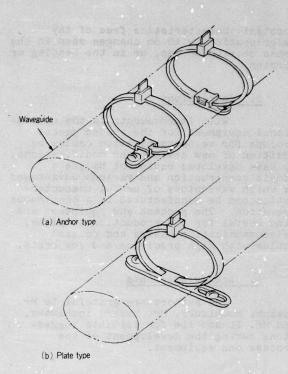


Fig.13. Mounting accessories

Table.4. Vibration test

Vibration test condition	Length of sample (cm)
E-plane vibration condition (1)+(2)+(3)	118
H-plane vibration condition $(1) + (2) + (3)$	118
Axial vibration condition $(1) + (2) + (3)$	234

Condition (1); $500 \sim 750 \text{cpm}$, $\pm 3 \text{mm}$, 40 minutes(2); $750 \sim 1800 \text{cpm}$, $\pm 1 \text{mm}$, 40 minutes(3); $1500 \sim 3000 \text{cpm}$, $\pm 0.2 \text{mm}$, 40 minutes

guides bent in the directions of E plane to a radius of 250mm, those bent in the direction of H plane to the same radius, and those twisted by 90° over a length of 500 mm, the bent or twisted specimens being checked for changes in the cross section and the lap, and for restoration from the bent or twisted state. The specimens were found to retain the desired V.S.W.R. characteristics and attenuation

constant characteristics free of any deterioration, with no changes seen in the cross section or lap, or in the bending or torsion.

3. Conclusions

With improvements in the conventional equipment for the bonded jacket process for telecommunication cables by addition of new devices and modifications, we have developed equipment having a simple construction and various advantages by which waveguides of useful characteristics can be manufactured by a continuous operation. The process and equipment are also useful for the production of pipes, telecommunication cables and coaxial cables with high precision and low costs.

4. Acknowledgements

The authors are grateful to Mr. Takashi Mochizuki, Mr. Masaru Yoshikawa, and Mr. Itsuzo Abe for valuable suggestions during the development of the process and equipment.

5. Authors



Eiji Iri

Dainichi-Nippon Cable, Ltd. 1, Kaichiku, Ikejiri, Itami, Hyogo, Japan

Mr. Iri graduated from Osaka Univ. 1973 with a M. Sc degree in Electrical engineering. Then he joined the Dainichi-Nippon Cables Ltd. and has been engaged in research and development of radio-frequency coaxial cables and waveguides.

he is now an engineer of Telecommunication Research Department of his company. He is also a member of the Institute of Electronics and Communications Engineers of Japan.



Michio Morishita

Dainichi-Nippon Cable, Ltd. 1, Kaichiku Ikejiri, Itami, Hyogo, Japan

Mr. Morishita graduated from Osaka Institute of Technology 1970 with a B. Sc degree in electrical engineering. Then he joined the Dainichi-Nippon Cable, Ltd. and has been engaged in research and development of waveguides.

He is now an engineer of Telecommunication Research Department of his company.



Yutaka Ohuchi

Dainichi-Nippon Cable, Ltd. Higashimukaijima Amagasaki, Japan

Mr. Ohuchi graduated from Tokyo Univ. of Agriculture and Technology 1970 with a B. Sc degree in mechanical engineering. Then he joined the Dainichi-Nippon Cable, Ltd. and engaged in manufacturing methods of Radio-frequency Cables and waveguides.

He is now an engineer of Mechanical Engineering Production Department of his company.

Transmission and Crosstalk Measurements on Installed Multipair Cable

T.D. Nantz

Bell Laboratories, Norcross, Georgia

Abstract

Transmission and crosstalk measurements on installed cables often complement laboratory measurements. For example, field measurements include "real world" placing, splicing, and upkeep effects, and make no assumptions about length scaling laws. This paper describes a portable computer-controlled field measurement system, consisting of commercially available equipment which is capable of measuring and analyzing insertion loss, input impedance, near-end crosstalk (NEXT) and far-end crosstalk (FEXT). Typical accuracies are 0.2 dB for loss, 1 dB for crosstalk and 1 to 2 % for impedance.

Introduction

T1, the first digital pair-gain system, was developed for use on voice frequency (VF) exchange-grade multipair cables. While T1 transmission on existing cable continues to grow, new cable designs optimized for digital transmission are now available as are new, higher capacity digital systems.[1]

These new systems and cables significantly increase the amount of cable electrical data needed. Each new digital system requires electrical characterization of all cable designs the system will use, and each new cable design requires characterization for all systems that might use the cable, including voice frequency (VF).

Resistance, mutual capacitance, delay, insertion loss, input impedance, near-end crosstalk (NEXT) and far-end crosstalk (FEXT) data provide the nucleus of information necessary for the system designer. Since the late 1960's, these measurements have been performed by computer-controlled laboratory equipment on 1000 to 2000 ft. reel lengths.[2,3] However, laboratory measurements do not include the effects of handling, splicing and maintenance, and they require assumptions concerning length scaling laws for

crosstalk. Field measurements on spliced repeater sections include all of the above effects, and can be made on discontinued designs no longer available for laboratory measurement. While laboratory measurements will continue to provide the bulk of cable data, field measurements can be used to complement the laboratory data.

This paper will describe a set of commercially available portable test equipment that we have used for transmission and crosstalk measurements on installed multipair cables. The remaining sections will provide a system overview, describe the measurement equipment, present test configurations and typical outputs, and show a practical example using this equipment to verify laboratory models of a new cable design. Instrument manufacturers and part numbers will not be used in the main body of the paper since several instruments are capable of making the required measurements. Appendix A contains manufacturer, part number, size, weight and power consumption on the equipment presently used in our test set-up.

System Overview

The system measures loss and phase under various conditions, and performs the calculations necessary to determine input impedance, NEXT, FEXT and insertion loss on installed cables. The key features of this system are portability, flexibility and immediacy of results. All system components may be placed in an 8 passenger van with the two rear seats removed, and the equipment is easily shipped from the laboratory to the field location. Total power consumption is less than 1800 watts. The system's computer provides flexibility by doing instrument calibrations, calculations, and data averaging, and by providing the capability to quickly change the measurement programs on-site. The flexibility of the instrument interface bus allows addition of other test instruments (RLC bridges, spectrum analyzers, etc.) with a minimum of delay. The computer also performs data analysis, and outputs both printed and graphical results in near "real time".

and the second property of the second

For descriptive purposes the system is divided into a basic measurement system and auxiliary equipment. The basic measurement system is used in all measurement configurations. It performs the loss and phase measurements, does the computations, and outputs the data. The auxiliary equipment is a set of components, portions of which are added to the basic system to make a particular measurement.

Basic Measurement System

The basic measurement system, shown in Figure 1, consists of a frequency synthesizer/network analyzer combination, a desktop computer, a printer and a plotter.

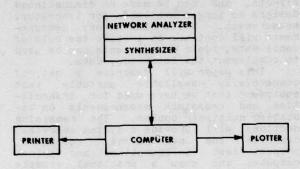


FIGURE 1. BASIC MEASUREMENT

The synthesizer (signal source) provides the test stimulus as well as tracking signals to the network analyzer (detector). The network analyzer actually performs the loss and phase measurements. The computer is the system controller. The printer and plotter provide hard copy of results.

The synthesizer provides sine wave outputs from 50 Hz to 13 MHz at up to +26 dBm. Frequency stability is 2 x 10-7 parts per month and resolution is 0.1 Hz. The output level accuracy is 0.05 dBm and resolution is 0.01 dBm. The synthesizer's output is 50 ohms unbalanced.

The network analyzer is a narrow-band tracking detector. Two input channels are available, A or B. The voltage measured is either the A channel, the B channel, or A-B. Phase measurements are relative channel A. Detector bandwidths of 10 Hz, 100 Hz, or 3 kHz are available. Normally, the 100 Hz bandwidth is used, but a high noise environment may require the use of 10 Hz bandwidth. to the Inputs network analyzer are unbalanced with a 1 megohm impedance. Feed hru terminations, 50 ohms, are used for all measurements described in this paper to give identical source and detector impedances. Since multipair cables are used in the balanced Since mode, transformers are used to provide mode conversion.

The network analyzer has a 100 dB dynamic range on each of three measurement ranges. The 100 dB dynamic range is not sufficient to fully characterize between unit NEXT or high frequency FEXT on typical repeater spans. By using the synthesizer's maximum output of +26 dBm and the network analyzer's most sensitive range, losses up to 133 dB can be measured.

Resolution is 0.01 dB and 0.01 degrees for loss and phase, respectively. Typical system accuracies are 0.2 dB and 0.2 degrees. These accuracies include the computer's data enhancement of instrument calibration and data averaging to reduce the effects of noise.

Measurements are made at the rate of two frequency points per second, including set-up of instruments by the computer, frequency output, settling times, and measurement and averaging of up to 20 readings.

The computer, system controller, has 24k bytes of read/write (RAM) memory and a built- in magnetic tape cartridge capable of storing 250k bytes of programs or data. The programming language is an interpreter language, similar to BASIC, which trans-lates the source-program instructions into machine code one instruction at a time as the program is executing. Although an interpreter language executes slower than a compiler language, it simplifies programming and debugging, and allows quick program changes. These features make the interpreter language ideal for field measurements where no two situations are exactly the same and unexpected situations may require a change in synthesizer output level or detector bandwith. The computer has built-in logarithmic, exponential, and trigonometric functions. Read Only Memories (ROMs) provided additional capabilities which permit the use of "for/next" loops, parameter passing to subroutines, memory conservation with special storage formats, printer and plotter interfacing, and string variable manipulation.

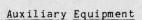
Interfaces to test instruments are via the IEEE-488 bus. The use of this bus relieves the measurement engineer from concern about the signals required to interface a particular instrument to the computer, allowing concentration on the measurement techniques. Using this bus, a new instrument can be easily integrated into the measurement system. This bus has proven popular since its introduction in 1975, and today, practically all measurement instruments offer it as an option.

The computer controls the measurement instruments, makes calibration corrections, stores data, and analyzes, prints and plots results. All of these operations are done on-site in virtually "real time", enabling correction of problems or

changes in the measurement plan in the field. Figure 2 is a photo demonstrating portability of the basic system.



FIGURE 2. BASIC MEASUREMENT SYSTEM



The basic measurement system is augmented by a instrument coupler, pair switch, data communication devices and a second synthesizer to perform the full complement of measurements - insertion loss, NEXT, FEXT, and input impedance.

The instrument coupler converts the

The instrument coupler converts the IEEE-488 bus format from the computer to the BCD format required by the pair switch. This conversion allows the switch to interface via the 488 bus.

The pair switch, Figure 3, automates the laborious tasks of pair connection for crosstalk measurements, and increases the number of combinations that can measured in a given time frame. switch is organized as two 5 by 5 (25 pair) matrices. Under computer control the switch connects one pair to the synthesizer and one pair to the network analyzer. For NEXT measurements the switch provides connections for within one between two 25 pair groups. Since for FEXT measurements the disturbing signal is injected at the far-end of the cable, the switch is automatically configured to select any one of 50 pairs and connect this pair to the network analyzer. Pairs which are not selected are terminated in a resistor.

The switch is not used in the measurement of insertion loss and input impedance since the number of connections is small enough to permit manual connection and the variations in path length and contact resistance of the switch would degrade the accuracy of the measurements.

The switching elements are hermetically sealed reed relays using rhodium-plated contacts. Minimum isolation between any two pairs is 114 dB at 150 kHz - degrading to 80 dB at 3.15 MHz.

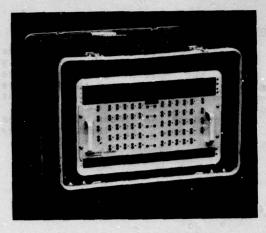


FIGURE 3. PAIR SWITCH

Measurements of input impedance and are performed with the signal source NEXT detector (synthesizer/network and analyzer) at the same end. However, measurement of FEXT and insertion loss require that the source and detector be located at opposite ends of the test section. FEXT and insertion loss measurements are performed by using a second identical synthesizer as the signal source. A second synthesizer is necessary since the network analyzer requires a synthesizer to provide tracking signals. The accuracy of the synthesizer outputs and frequency stability do not degrade the accuracy of loss measurements by more than 0.05 dB.

The computer controls the remote synthesizer through a pair of interfaces which convert the IEEE-488 bus signals to RS232 signals and a set of 4-wire pointto-point 1200 baud modems. Two cable pairs not in the test population connect the modems. The converters and modems are labeled "data communications" in Figures 6 and 8. The 1200 baud data transmission rate applies to all instruments on a particular 488 bus, since the bus data rate is controlled by the slowest instrument connected. This rate is sufficient for controlling the remote synthesizer where each frequency change requires less than 60 bytes of data, but it would more than double the measurement time (already 3 hours for FEXT on 1225 combinations at three frequencies) if the 1200 baud were applied to all transmissions between the computer the local synthesizer, network analyzer and switch; therefore, two 488 busses are used, one for the local equipment and the second for the remote equipment.

Input Impedance and NEXT Measurements

The measurements of input impedance and NEXT are performed by accessing only one end of the cable. Thus, only one operator is required, and the interface modems and second synthesizer are not used.

used.

The simplest use of the basic system is the measurement of input impedance (Figure 4).

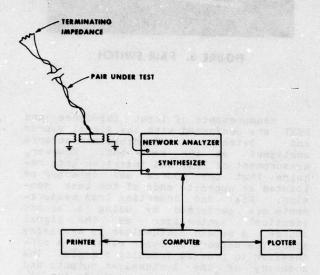
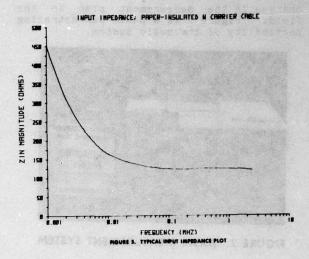


FIGURE 4. INPUT IMPEDANCE MEASUREMENT

The impedance of a terminated cable pair is obtained by measuring the loss and phase of a reference impedance bridged across the measurement terminals, and comparing this with the loss and phase obtained with the pair connected to the measurement terminals and the reference removed. Outputs include printed values of impedance and plots, such as that shown in Figure 5, of impedance magnitude versus frequency. Accuracy is between 1 and 2 % for most values of impedance. Pairs are manually connected directly to the measurement terminals. The measurement of 50 frequencies including output takes less than two minutes. The computer memory is sufficient to hold data for 25 pairs at 50 frequencies.



To measure NEXT, the pair switch and and instrument coupler are connected to the basic system (Figure 6).

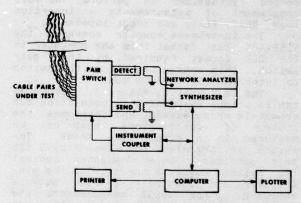


FIGURE 6. NEAR-END CROSSTALK (NEXT) MEASUREMENT

Pair selection and measurement are automatically handled by the computer. Prior to starting the crosstalk measurements the computer checks the switch and pair connections for poor contact resistance, opens, shorts and crosses. Sufficient memory is available to hold data for the 625 combinations between two 25 pair groups at four frequencies. Measurement time for this is about 20 minutes including data analysis and typical output as shown in Figure 7.

Mean Mdian S.D. Corr	NEXT- 0.1500 79.78 79.75 7.60 0.57	NEXT- 0.7720 68.54 68.50 8.01 0.66	NEXT- 1.5000 64.56 64.75 8.14 0.68	NEXT- 3.1500 59.89 59.75 9.22 0.52
No. of	points=	300,0000		
No. 1 2 3 4 5 6 7 8 9 10	dB P1 P2 102.1 1 20 101.8 3 18 101.7 7 21 101.2 15 23 99.4 17 21 98.8 11 16 97.3 4 10 97.2 16 21 97.1 18 22 96.1 3 20	Best 10 dB P1 P2 94.9 17 21 92.2 16 21 90.6 7 2 3 22 89.2 3 22 89.2 1 24 87.2 5 13 86.1 10 20 84.9 7 20 83.5 15 23 83.3 7 21	dB P1 P2 85.5 8 23 84.8 16 21 84.2 15 23 83.4 3 7 83.1 12 16 82.3 19 23 82.1 7 15 81.4 3 25 81.1 7 23 80.4 6 21	dB P1 P2 99.6 2 14 87.6 5 23 84.4 9 28 83.1 7 25 81.8 3 17 79.7 7 23 78.9 16 21 78.7 1 17 78.4 1 19 78.4 9 17
1 2 3 4 5 6 7 8 9 10 11 12 13 14 15	61.7 9 10 63.2 22 23 64.8 3 5 64.2 11 12 64.5 4 5 64.8 7 8 64.8 21 22 65.0 3 4 65.6 1 6 65.7 13 14 66.5 14 16 66.8 1 12 67.1 8 9	Morst 15 48.8 2 3 50.0 3 5 50.3 9 10 50.8 8 9 51.8 12 13 14 52.7 7 8 53.0 24 25 53.6 2 5 53.8 11 12 53.9 21 22 53.9 21 22 53.5 10 11	44,1 9 10 44,1 8 9 44,5 3 5 45,1 12 13 45,5 11 12 46,0 2 3 47,0 2 5 47,4 11 13 47,6 22 23 47,6 22 23 47,9 17 19 48,0 7 8 49,0 3 9 49,4 18 19 49,7 24 25 49,9 16 18	37, 4 8 9 38.5 2 3 38.5 9 10 38.7 7 8 39.6 12 13 40.9 11 12 41.9 13 14 42.0 4 5 42.1 24 25 43.1 17 19 43.5 2 5 43.7 22 23 43.8 11 13 43.8 22 25
1234 556 7789 9111 1231 1451 1671 1892 2232 245 Mean 9.D. Worst	PSUM- 0.1500 59.53 60.79 59.19 60.04 58.72 59.61 61.65 59.61 59.87 59.87 59.87 59.87 62.13 62.14 62.53 61.46 62.74 59.37 63.46 62.74 59.37 63.76 63.76 63.74	PSUM- 0.7720 49.81 46.03 44.72 49.17 45.51 50.30 49.26 49.26 45.46 45.46 45.46 45.46 45.46 46.96 46.96 46.97 46.74 45.46 46.96 46.96 46.97 50.74 49.79 52.03 49.66 50.78 50.78 48.68	PSUM- 1.5000 44.85 42.36 40.37 46.61 40.24 45.74 45.74 41.56 39.83 42.12 42.09 41.29 44.87 48.73 44.72 45.14 44.09 48.79 48.79 48.59 43.95 44.172 44.07 2.63 39.83	PSUM- 3.1500 40.93 36.29 34.55 39.57 35.16 39.80 36.85 34.13 33.44 36.99 37.03 35.65 37.91 40.20 40.52 41.02 43.21 42.56 38.54 40.62 39.00 37.08 39.00 37.08 39.42 40.62 39.00 37.08 39.00 37.08 39.42 40.62 39.00 37.08

The output includes mean, standard deviation (sigma) and minimum pair to pair values, best and worst pair combinations, power sum mean and sigma, and power sum values for each pair. A histogram is output for the convenience of the operator to check for possible "sports" in the data.

FEXT and Insertion Loss Measurements

These two measurements require equipment at both ends of the cable section under test. Two operators are used as well as the second synthesizer and data communications equipment. The operators coordinate their efforts over a "talk" circuit.

The data communications link remote synthesizer are added to the NEXT configuration to measure FEXT (Figure 8). The switch is automatically configured so that all 1225 combinations within a 50 pair group can be measured. As with the NEXT measurement, the computer checks the switch and connections prior to beginning crosstalk measurements. the disturbing pair is manually connected to the synthesizer at the far-end. The computer then selects the receive pairs and scans the frequencies. Insertion loss of each disturbing pair is measured and subtracted from the measured crosstalk loss to give equal-level FEXT data. The computer memory can hold 3 frequencies of 1225 combinations. Data output is similar to the NEXT output (Figure 7). Time for a 50 pair run (1225 combinations) at three frequencies is about 3 hours. This time could be reduced to just over 1 hour if a second switch were available for the farend connections.

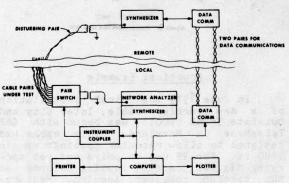
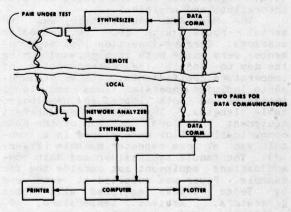


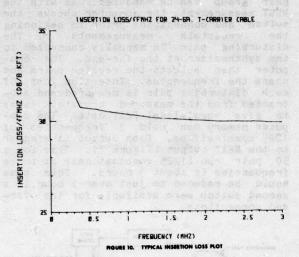
FIGURE B. FAR-END CROSSTALK (FEXT) MEASUREMENT

The configuration for insertion loss measurements, Figure 9, includes the basic system, the remote synthesizer, and the data communications link. Pairs are manually connected to the transformers.



MOURE 9. INSERTION LOSS MEASUREMENT

Typical outputs include printed loss values and plots of loss divided by the square root of frequency (Figure 10). A three term polynominal fit of insertion loss is also performed.



Practical Example

In June 1979 the first installation of a new carrier cable, Inter City and Outstate Trunk (ICOT), was begun with C&P Telephone in Maryland. This cable was designed to allow repeater spacings up to 9000 ft. For VF use on pairs not yet carrying digital traffic, loading is done at the carrier repeater spacing. Measurements were made on an installed repeater section of ICOT to validate predictions of loss and impedance made by laboratory design models. These models output primary and secondary cable constants, insertion loss and input impedance based on cable geometry and the material properties. Equations in the models are both theoretical and empirical.

The Maryland installation was an aerial route with 8000 ft. repeater spacings. Carrier insertion loss measurements were made both at night and during the day to enable the determination of temperature coefficients. The VF measurements included insertion loss and input impedance on both loaded and non-loaded cable lengths. The basic measurement equipment and local portion of the data communications link were placed in a rental van at one repeater manhole (Figure 11). The remote synthesizer and data communications equipment sat outside the far manhole. Power was supplied at each end by Telco trucks equipped with motor generators. Ambient temperature, DC resistance and capacitance were also measured.

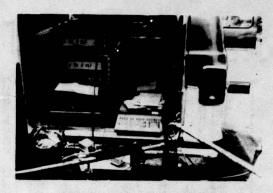


FIGURE 11. EQUIPMENT IN VAN

Table I compares predicted and measured T-Carrier performance. Engineering loss in Table I is the loss in dB/Kft at the maximum average capacitance allowed for the cable design. It is evaluated from a least squares fit to loss versus mutual capacitance.

Table I

Predicted Measured Difference

Engineering Loss (dB/kFt)

T1 3.6 3.6 0
T1C 5.2 5.1 2

Temperature Coefficient (dB/kFt/10 deg. F)

T1 0.044 0.040
T1C 0.055 0.053 10

Figure 12 gives a plot of predicted and measured loss from .2 to 3.0 MHz. The predicted loss in Figure 12 comes from the laboratory models with the DC resistance and capacitance matched to the measured values. Differences between the data and model are such that they appear as a single curve in the figure.

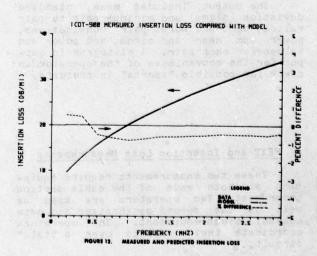
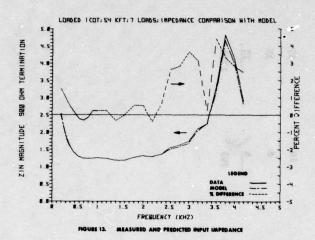


Figure 13 presents the data for predicted and measured input impedance for a 54 kFt. section with 7 load coils.



Results for all measurements show excellent agreement, generally within 3 %, and validate the laboratory models for this cable design. With the models validated, the system designers can confidently run perturbations to this cable design to check system margins against variations in cable manufacture.

Summary

A portable set of commercially available equipment has been described for use in field measurement of insertion loss, NEXT, FEXT and input impedance. A desktop computer acts as the system controller and provides flexibility in making measurements, analyzing data and interfacing instruments. This equipment has proved useful in characterizing both new and discontinued cable designs in several operating companies throughout the Bell System.

Acknowledgement

I would like to acknowledge the work of Mr. A. F. Judy of Bell Labs. Mr. Judy assembled the pasic measurement system, and provided valuable assistance in extending its usage through our many discussions.

References

- W. G. Nutt and J. P. Savage, Jr., "Multipair Cables for Digital Transmission," National Telecommunications Conference Record, December 1978.
- R. E. Anderson, "Computer Controlled Cable Measurements," Proceedings of the 21st International Wire and Cable Symposium, December 1972.
- J. Kreutzberg and T. D. Nantz, "Precision Insertion Loss Measurements and Data Analysis on Multipair Cable,"
 Proceedings of the 24th International Wire and Cable Symposium, November 1975.



T. D. Nantz received the BSEE from the University of Pennsylvania in 1968, and the MSEE from Northeastern University in 1973. He is currently a Member of Technical Staff at Bell Laboratories engaged in multipair cable development and characterization.

CONTRACTOR STATE OF THE PARTY O

APPENDIX A

may not et alle and a local to fed and a local to fed a local to fed a local to fed and a local to the constant and the constant and the local to th

Equipment, Manufacturer, Part Number, Size, Weight, and Power Consumption

Component	Manufacturer and Part Number	No. Req'd.	Dimensions (inch) Width, Height, Length	Weight (1bs.)	Power Consumption (watts)
Computer	Hewlett Packard-9825A	1	14-1/2, 4-1/2, 19	25	170
Printer	Hewlett Packard-9866B	1	17-1/2, 6, 15	07	250
Plotter	Hewlett Packard-9862A	1	19-1/2, 8-1/2, 19	.04	200
Synthesizer	Hewlett Packard-3330B	2	16-3/4, 7, 21-1/2	53	200
Network Analyzer	Hewlett Packard-3570A	1	16-3/4, 5-1/4, 21-1/2	20	230
Pair Switch	Matrix Systems 6584-H	1	19, 7, 19	09	300
Data Communica- tion Interface	Hewlett Packard-59403A	2	8-1/2, 4, 17	10	35
Modems	Bell System 202T	2	6, 4, 11-1/2	8	35
Instrument Coupler	Fairch:1d 4880	7	8-1/2, 3, 10.8	9	35
			TOTAL	363	1725

Promisers Lie Priedinos vienes Lie Priedinos Residentes Residentes

A SIMPLIFIED METHOD FOR COMPARING INSULATION CUT-THROUGH RESISTANCE OF BACKPANEL WIRES

Paul E. Hubis

Newark W. L. Gore & Associates, Inc.

Delaware

Abstract

Cut-through testing has long been used as an uncomplicated method to predict the mechanical toughness of insulation systems on electrical and electronic wiring. Methods have varied from dragging farm plows across buried cables to the use of precise and sensitive laboratory test instruments. As wire sizes grow smaller and mechanical requirements stricter, consistent and convenient cut-through testing becomes more difficult. The purpose of this article is to review a test method which has been developed specifically for insulation cutthrough testing of the wires used for wire-wrapping in computer and other electronic equipment. The development of this testing technique will be shown through the various stages of methods and equipment with a recommendation for a simple, laboratory quality device to consistently and conveniently perform these tests. Variables in both test equipment and wire tests will be discussed.

Section I. Introduction

The typical cut-through test in use has been the static load type. A dead weight is used to force an insulated conductor against a blade of specified sharpness for a particular period of time. At the end of the period, a "pass" or "fail" is determined by voltage breakdown tests, where the voltage potential is applied between the conductor and the blade. Some of these tests are cumbersome, time consuming to run, and very dependent upon the technique for applying the load.

In the case of the MIL-W-81822, "cold flow" test, the test device must remain undisturbed for ninety-six hours. Movement or vibration during the test period can cause failure in a wire that might normally have passed. For the "cut through" portion of the test, heavier loads are applied for a shorter duration, only one hour, but the outcome is more subject to the initial impact of the load coming to rest on the insulation.

Complicated arrangements have been made to eliminate the instantaneous load concentration

at test initiation. The use of rotating cams, lead shot or water transfer techniques have been used to solve the problem.

Regardless of the draw backs of "static" load testing, it does provide some measure of quality assurance, testing the minimum cut-through resistance of the wire. Consequently, it helps protect against costly insulation failure in the application.

Section II. Dynamic Testing

For comparison testing, a constantly increasing "dynamic" load provides much more data in a shorter period of time, taking the insulation to failure quickly. Development of this test technique has been fraught with some of the same dif-ficulties inherent in "static" load tests. The load must be applied smoothly, at a consistent and repeatable rate to minimize variability. In some cases, this has been accomplished through the use of increasing volumes of liquid or lead shot. More sophisticated tests are done using a quality tensile test machine such as an Instron machine.

Some dynamic test differences arise due to the difference between constant rate of penetration and constant rate of load increase. However, both methods have the advantage of controlled rate, not inherent in the static load test.

Section III. Dynamic Cut-Through Testing Development

Dynamic cut-through testing is certainly not new. It has been used for years by Bell Laboratories, the Canadian Standards Association, Sperry-Univac, and others to compare and qualify insulations.

Our efforts to develop a cut-through tester were aimed at a mechanized device which would be uncomplicated, yet give a smooth and pre-dictable variation to load. The outcome was the use of a constant speed drive screw supported by a lever.

As the drive screw rotates, it moves the load toward the end of the lever, creating a progressively heavier load at the fulcrum, where the wire is being tested. The mechnical advantage created by the lever, permits the use of a moving load much lighter than the load stress desired at the wire test point. Automatic shut-off at cutthrough stops the load, and a mreasurement is taken.

Later, a two station variable speed tester was built that had the ability to test two samples simultaneously. This device (Figure 1, Two Station Tester) has several other features:

- fully synchronized operation with automatic shut-off at cut-through;
- (2) asynchronous operation mode;
- (3) pre-set and variable speed either in the synchronized or asynchronous mode; and
- (4) direct load (LED) read-out in grams.

However, problems with blade-to-blade variability make this device difficult to calibrate and maintain calibration for extended periods of time. Vibration and heat, created by the stepper motor drives, compound the variability problem.

Section IV. A Single Station, Single Speed Cut-Through Tester

A simple, single station cut-through tester for wire-wrap (Figure 2, New Single Station Unit) shows the current single station design of cut-through tester, which is much more convenient to use; and provides reliable data consistently. Features of this machine include:

- (1) constant speed drive;
- (2) direct load read-out in kilograms;
- (3) automatic shut-off at cut-through failure (Figure 3 schematic);
- (4) easy changeability of cut-through blades; and
- (5) electrically heated blade.

Section V. Additional Comments on Cut-Through Testing

One difficulty that has not been totally resolved is that of the cut-through blade. Test results are highly dependent on the local sharpness of the blade. This puts strict requirements on the blade hardness and uniformity across the entire cutting surface. A fully satisfactory blade (one which is uniformly sharp and very durable) is difficult to find so that testing is still more qualitative than quantitative due to changes in the blade's surface over a period of time and changes from one blade to another. However, quantitative comparison tests can be run with great consistency over short periods of time before the blade's surface changes. Military Standard 414, "Sampling Procedures and Tables for Inspection by Variables for Percent Defective", may be effectively used in an inspection plan.

Another significant variable in cutthrough testing is the test temperature. Heating the blade electrically is a simple way to simulate this. Results from this kind of testing are extremely important for electronic equipment, which must function at elevated temperatures. High temperature areas occur in many surprising areas, such as in commercial computer equipment, where higher power and higher density integrated circuits are becoming commonplace. A project of ours is the continued evaluation of temperature effects on mechanical characteristics of wire for wire wrap. (Figure 4 shows the influence of elevated blade temperatures on three MIL-W-81822 wires.)

Other variables in dynamic cut-through testing include:

- failure detection and automatic shut-off circuit;
- (2) insulation wall thickness; and
- (3) insulation concentricity.

Summary

Cut-through testing for fine wires has been developed at this stage to a point where qualitative analysis can be made very accurately, and quantative results are only limited by the condition of the cut-through blade. Various materials and constructions can now be accurately compared to each other in this failure mode, which is most common in wire-wrap packaged electronic equipment. Additional work to develop better cut-through blades and more data about the effect of local temperatures will be done to improve the usefulness of cut-through testing as a means to project the durability of insulated wires in the harsh environment of sharp wire-wrap pins.

Biography

Paul E. Hubis is a Product Manager for W. L. Gore & Associates, Inc. at the Corporate Headquarters in Newark, Delaware, where he coordinates product development and marketing of wire wrappable products. His work includes improving and developing test methods consistent with the wire application. Mr. Hubis received a Bachelor of Arts degree from Washington College in 1966, and has been with W. L. Gore & Associates, Inc. since 1970, which is located at 555 Paper Mill Road, P.O. Box 8734, Newark, Delaware 19711.



FIGURE 1. TWO STATION TESTER

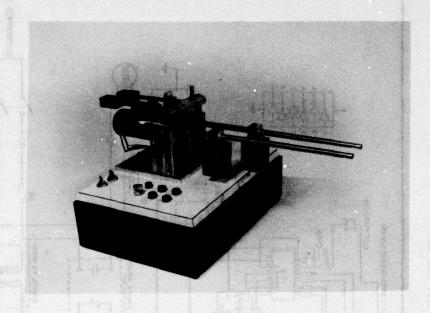
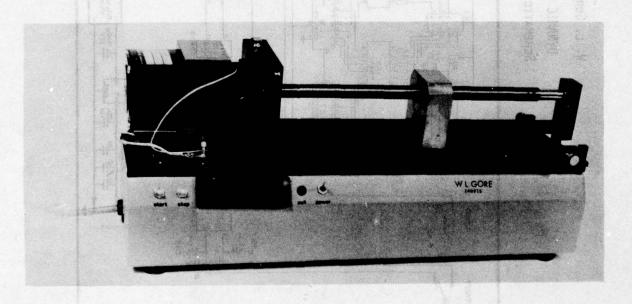


FIGURE 2. New SINGLE STATION UNIT



SCHEMATIC - SERIAL NO. 000F15

W. L. GORE & ASSOCIATES, INC.

DYNAMIC CUT-THROUGH TESTER

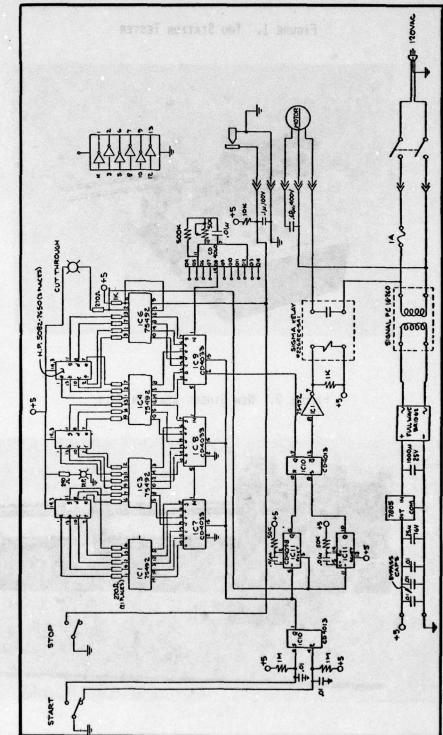


FIGURE 3.

DYNAMIC CUT-THROUGH RESISTANCE OF MIL-W-81822, 30 AWG WIRE AT ELEVATED TEMPERATURES

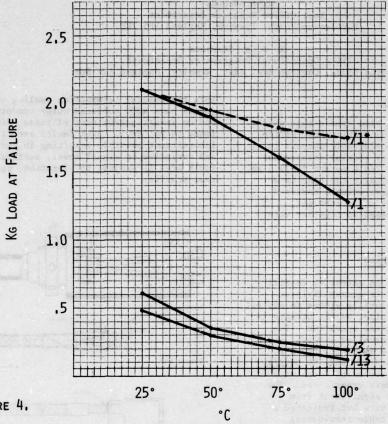


FIGURE 4.

**BLADE TEMPERATURE

*EXPERIMENTAL HIGH TEMPERATURE VERSION. **BLADE RADIUS <.001".

Acknowledgment

The author wishes to acknowledge the important contributions of:

Mr. G. Hansell, Development Mr. H. VanDeusen, Engineering Mrs. D. Sklodowski, Testing Mr. D. Fye, Manufacturing

A TIME DOMAIN CROSSTALK TEST FOR COAXIAL CABLES

R. M. Brooks
Post Office Research Department
Martlesham Heath, Ipswich, England IP5 7RE

W. J. B. Stephens
Post Office Operational Programming Department,
Carlton House, Carlton Ave. East, Wembley, England HA9 8QH

Summary

A description is given of a time domain test which, since its introduction by the British Post Office a year ago, has achieved considerable success in pinpointing individual faulty coaxial connections close to the repeaters in 1.2/4.4 mm and 2.6/9.5 mm coaxial cable systems. Basically the test is a near-end crosstalk measurement using a modified launch condition and a 10 ns pulse echo set. Measurement examples are presented together with initial field experience.

Introduction

The British Post Office has an extensive coaxial cable network installed for frequency division multiplex systems and it naturally wishes to exploit this available underground plant as the network is converted to high-speed digital operation. The initial assessment of the installed network, which in Britain is mainly 1.2/4.4 mm cable, proved satisfactory for the proposed 120 and 140 Mbit/s systems although a limited number of cases of poor near-end crosstalk (NEXT) were experienced. The levels encountered were not significant from a system impairment point of view but indicated a potential problem with the cable terminating arrangements shown in Fig. 1.

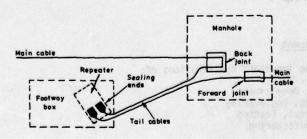


Fig 1 Typical cable termination arrangement for 1.2/4.4 mm cable

Both the coaxial termination sealing ends and back joints have soft soldered outer conductors, Fig 2, and on investigation some of these joints were found to be 'dry'. Such faults are likely to be intermittent possibly resulting in bursts of noise and variation in signal level, particularly if the fault area is subject to vibration, eg from heavy road traffic.

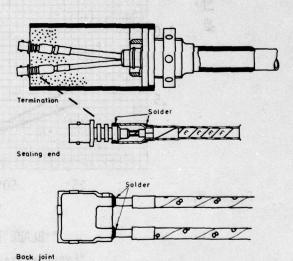


Fig 2 1.2/4.4 mm coaxial termination and back joint

For digital transmission bursts of errors or in severe cases loss of framing alignment could occur. In order to facilitate the smooth introduction of high speed digital transmission systems it was considered important to detect and rectify such faults. The forward joints and main cable to main cable joints are brazed and therefore were not considered to be a problem.

Conventional NEXT measurements are undertaken in the frequency domain and relate to the crosstalk between two coaxial circuits. Whilst the test serves a useful purpose in establishing the impairment of transmission systems due to crosstalk it is far from ideal as a general test for the following

THE PERSON STATES

reasons:

- unless faults exist in both coaxial pairs significant crosstalk cannot normally be detected.
- it is necessary to measure all pair combinations.
- the technique does not generally lend itself to the location of individual faults.
- d. above 1 MHz, measurement sensitivity of the order of 160 dB is required.
- e. the measurements are time consuming.

If, as is the case for the BPO coaxial network, the coaxial pair outer conductors are insulated from each other it is possible to overcome these problems by using a modified launch condition. In this technique, known as 'outer injection', the disturbing circuit is formed by the outer conductors of two coaxial pairs. Any signal coupled from the disturbing circuit into the coaxial pair under test is detected as crosstalk. This approach is similar in concept to the triaxial test for coaxial connectors 1. The resulting reduction in required measurement sensitivity has enabled pulse echo techniques to be employed without recourse to signal averaging. An advantage of using a time domain technique is that the fault position can be readily identified. In addition, provided that separate input and output ports are available, the same basic equipment as used for pulse echo testing can be employed. The BPO field test equipments use a 10 ns raised cosine pulse, which is sufficient to resolve the sealing end from the back joint and additionally is the correct pulse for return loss testing for 140 Mbit/s digital line systems.

Measurement Principles

Outer Injection

It is useful to approach the concept of outer injection by firstly considering NEXT. When the outer conductor thickness is much larger than the skin depth the NEXT between coaxial pairs with solid outer conductors is extremely small. In fact for 1.2/4.4 mm and 2.6/9.5 mm coaxial pairs NEXT attenuation would be expected to be greater than 160 dB for frequencies above approximately 1 MHz. In practice, if values lower than this occur the prime cause is not uniform crosstalk but crosstalk occurring at discrete points, namely at the site of faulty joints, connectors or cable damage. By restricting our attention to frequencies above 1 MHz we can ignore the uniform coupling mechanism.

If we consider two parallel coaxial pairs, the outer conductors of which are insulated from each other, then apart from the coaxial circuits an additional 'intermediate circuit' will be present². This circuit will be formed by the two outer conductors and insulating medium. The current flowing in the intermediate circuit will be confined by skin effect to the outermost surface region of the outer

conductors. Similarly the current flowing in the coaxial circuits will be confined to the inside surface region of the outer conductors. Provided the outer conductors are sufficiently thick little coupling will occur between these circuits.

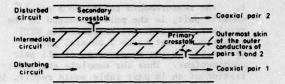


Fig 3 Crosstalk between coaxial pairs

However, under fault conditions (Fig 3), the signal transmitted down the disturbing circuit induces a signal in the intermediate circuit, via the fault, and this signal propagates in both directions. The intermediate circuit now acts as a disturbing circuit for the second coaxial circuit.

If a fault is present in the second coaxial circuit then a signal will be induced into the coaxial path and so crosstalk will be observed. It can be seen that for crosstalk to be present a fault must exist in the outer conductors of both coaxial circuits. In general the coaxial and intermediate circuits are weakly coupled and so the primary and secondary crosstalk magnitudes are small compared with their respective disturbing signals.

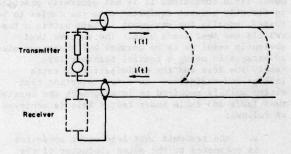


Fig 4 Principle of outer injection

If, for test purposes, the transmitter is connected directly to the 'intermediate circuit', this technique being known as 'outer injection' (Fig 4), certain benefits arise:

a. since one of the weak coupling mechanisms (ie the previously mentioned coupling between the disturbing circuit and intermediate circuit) has been removed the required measurement sensitivity is very much reduced, usually by at least 60 dB. This has allowed the use of pulse echo techniques with the prime advantage of ease of identification of

the crosstalk fault position. Unfortunately the attenuation of the outer injection transmission path is high and for 10 ns pulse testing on 1.2/4.4 mm cable only crosstalk faults within the first 50 m or so can be detected. However for the checking the end terminating arrangements a range of 10 m is normally adequate.

b. the measurements relate to a single coaxial pair, ie the pair connected to the receiver. By contrast conventional NEXT measurements relate to 2 coaxial pairs necessitating the measurement of all pair combinations. Thus the complete characterisation of an 18 pair cable would require 153 conventional NeXT measurements against 18 outer injection measurements. The amount of testing time is therefore very much reduced.

Obviously the concepts presented are somewhat simplified. In practice there will be more than two outer conductors within a cable structure and in addition other conductors will be present ie interstitial pairs and a metallic sheath. Usually there is a high coupling between the various circuits (other than coaxial) and this will complicate the intermediate circuit. In some ways this acts to the advantage of the outer injection technique in that for a particular coaxial pair under test the results are more or less independent of the choice of the injection circuit second conductor, which could in fact be the sheath conductor, if it is not earthed, or an interstitial conductor.

Measurement Consideration

Under field conditions it is not generally practical to directly connect equipment onto the cables to be tested, usually the equipment is kept within a test vehicle and test leads used. The receive lead obviously requires to be coaxial but there are also advantages in using a coaxial transmit lead, namely low loss and the minimisation of earth leakage and radiation. An outer injection transition unit is required to interconnect the coaxial test leads and cable under test. This is achieved as follows:

- a. the transmit test lead outer conductor is connected to the outer conductor of the pair under test.
- b. the transmit test lead inner conductor is connected to the outer conductor of a spare coaxial pair and is referred to as the transmit outer.

No attempt has been made to match the impedance of the transmit test lead to that of the outer injection circuit, since this is neither easy to achieve nor strictly necessary. The normal length of test lead used, 12 m, ensures that multiple echoes between the transition unit and pulse generator are displaced outside the time window of prime interest. The measurement configuration is shown in Fig 5.

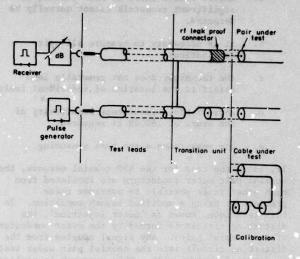


Fig 5 Schematic of pulse crosstalk measurement

It is important that the test lead and associated connectors in the receive path have negligible crosstalk coupling. Nowhere is this more important than the connection to the coaxial pair under test since a faulty indication could be interpreted as a faulty sealing end.

The transition unit will invariably generate external electromagnetic fields which will induce currents into the outer surfaces of the test leads and so receive equipment with good screening is required.

The impedance of the outer injection circuit is substantially different from that of the coaxial circuit. Whilst the coaxial impedance is approximately constant at 75 ohms over the frequency range 1-100 MHz, the impedance of the outer injection is variable. From a limited number of measurements on 1.2/4.4 mm coaxial terminations the impedance was found to steadily decrease from approximately 60 ohms at 1 MHz to 30 ohms at 40 MHz and then increase to 50 ohms at 100 MHz. This impedance characteristic is much as expected since, as the frequency increases the impedance will tend to reduce due to the decrease in the internal inductance of the conductors and the proximity effect3. However, within the cable terminating arrangement the coaxial pairs are splayed out resulting in an increase in impedance which will only be significant at the higher frequencies. Although it might have been preferable to calibrate the measurement in terms of the disturbing current the more practical approach appeared to be that of considering the crosstalk in terms of insertion loss. Comparison can therefore only be easily made where the impedance of the outer injection paths are approximately equal. In practice the impedance variations normally encountered will introduce a measurement uncertainty of 2 dB which is considered

acceptable. Calibration is achieved by looping the leads back and adjusting a variable attenuator to give a reference received voltage level. On connection to the pair under test the attenuator is re-adjusted to give a suitable display of the crosstalk voltage. By relating the received level to the reference level and taking into the account the attenuation removed, the crosstalk loss is obtained.

Test Equipment

Pulse Echo Test Set

Referring to Fig 5, the pulse generator, receiver and attenuator may be a proprietary pulse echo test set provided that the transmit and receive ports can be separated. In some cases this can be easily achieved by removing a hybrid bridge. Ideally to obtain adequate sensitivity the units should be capably of resolving the transmitted signal when it is attenuated by 100 dB. The BPO is currently using two types of equipment:

a. a 10 ns pulse echo set specially constructed by the BPO for testing cables for 60 MHz fdm and high bit rate digital application. The pulse generator of this unit is of the avalanche transistor type having an output pulse of approximately raised cosine shape with a peak pulse amplitude of 90 v into a 75 chm resistive load. The receiver consists of a proprietary 20 dB gain, high frequency amplifier and a sampling oscilloscope. Commercial versions of the tester are produced under licence from the BPO.

b. a modified commercial Time Domain Reflectometer 5 with a BPO built add-on unit, Fig 6.

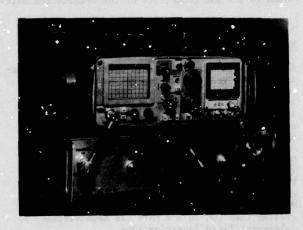


Fig 6 Pulse crosstalk field unit

Whilst the instrument adequately performs the measurements for which it was designed, modification was necessary to meet the requirements of the pulse crosstalk test; namely, isolating the transmit and receive circuitry improving the receiver screening and increasing the measurement sensitivity. The latter was achieved by using an external pulse generator similar to a. above; the relatively low amplitude output pulse from the instrument being used as a trigger. An added advantage of this approach is that the delay of the external pulse head and test leads is sufficient for the internal crosstalk of the trigger pulse to decay before the start of the measurements. Avalanche pulse generators usually have a significant coupling between the output and triggering ports for a time interval of the order of 1 us after avalanching has taken place. Reflections from the cable transmit circuit could therefore appear in the trigger circuit and be coupled into the receiver circuit by the instrument crosstalk. In order to avoid this situation it was necessary to ensure that the trigger path was unidirectional. This was achieved by using a fast switching transistor and a monostable as the input stage of the external pulse generator. For calibration purposes an additional 60 dB attenuator was required and this together with the pulse generator, battery pack, matching and overload protection circuits comprise the add-on unit. The Time Domain Reflectometer can be restored to its normal mode of operation by uncoupling the add-on unit and inserting a coaxial U-link at the appropriate point to couple together the transmit and receive circuits.

Test Leads

Test lead lengths of 12 m have been found to satisfy most field situations. Good screening is required since the receive lead is sensitive to pickup from the outer injection transition unit, radio broadcast signals etc. The desired amount of screening was attained by having a third braid woven over the pvc sheath of a double-braided flexible cable. Care was taken with the crimping of the braids onto the connectors as a poor connection becomes a source of extraneous crosstalk. Finally the leads were bonded together by a plastic coating to give greater robustness and better handling characteristics.

Transition Unit

The test leads are coupled to the cable under test by the outer injection transition unit; Fig 7 shows the type of unit used for 1.2/4.4 mm cable.

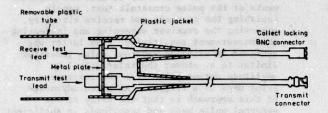


Fig 7 1.2/4.4 mm transition unit

The test leads connect onto two N type panel straight adaptors mounted onto a metal plate. To the other ports are attached two double-braided flexible leads 0.4 m in length. These leads provide a degree of flexibility for connection onto the cable under test and should be kept as short as is practical. The receive flexible lead is terminated in a specially developed collet locking BNC connector shown in Fig 8.

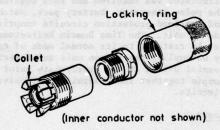


Fig 8 Collet locking BNC connector

As the locking ring is tightened the collet compresses down onto the outer conductor of the sealing end BNC female connector thereby ensuring a good connection. It was necessary to develop a special connector because BNC connectors do not reliably provide a good outer connection, particularly if any lateral force is present. At the end of the short flexible transmit lead is a male BNC connector where the inner to outer transition takes place, see Fig 9. This is achieved by truncating and isolating the screening braids. A capped crimping ferrule, previously soldered to a BNC back nut, is inserted over the insulation of the lead, the inner conductor projects through a small hole in the cap and is soldered to the ferrule thereby achieving the inner to outer transfer. The ferrule is crimped onto the lead thus securing, the connector. The body of the BNC connector, without the inner conductor pin, is then screwed into position. Finally a shrinkdown plastic coating is applied to the ferrule and part of the connector body. The N type connectors and mounting

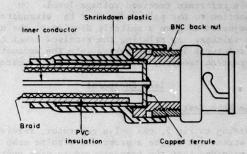


Fig 9 BNC transmit connector

metal plate are isolated from the repeater case and any other conductors by a partly removable plastic jacket. This maximises the current flow on the outer surface of the coaxial pair under test.

Calibration Unit

For calibration purposes it is necessary to effect a loop in the test leads. This could have been achieved by removing the transition unit and joining the leads together with a female-female N type connector. However this does not provide a check on the continuity of the transition unit. It is better to connect the transition unit to a reversing unit which restores the outer injection circuit back to a coaxial circuit i.e. an 'outer' to 'inner' transition or reversal takes place. This will have a negligible effect on the calibration provided the flexible leads are sufficiently short to be unresolvable by the pulse. The reversing unit can easily be constructed so that it can be connected either way round to the BNC connectors of the transistion unit.

Field Experience

Equipment Performance

Equipments have been in field operation for approximately one year and in general have performed well. Some initial problems were experienced due to the lack of robustness of the prototype collet locking connectors. The help of a commercial connector firm was enlisted who produced yersions having a greatly improved life expectancy.

Measurement Experience

From laboratory studies it was found that the crosstalk loss of correctly made joints, measured with an outer injected 10 ns pulse, should be greater than 100 dB and this has been verified by subsequent field investigations.

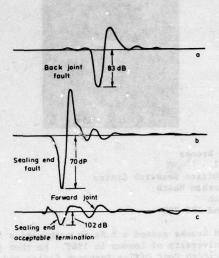


Fig 10 Pulse crosstalk measurements on an installed 1.2/4.4 mm cable

Typical measurements relating to outer conductor fault conditions are shown in Fig 10a and 10b. By way of comparison Fig 10c shows an acceptable response for a sealing end forward joint.

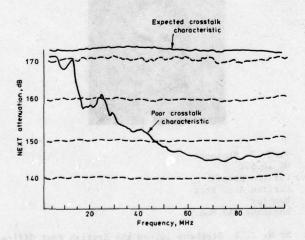


Fig 11 Conventional NEXT measurement on an installed 1.2/4.4 mm cable

Fig 11 shows examples of frequency domain NEXT measurements on cables with and without outer conductor faults.

The majority of testing has been concerned with the 1.2/4.4 mm cable network although some tests have also been undertaken on 2.6/9.5 mm cables. The types of fault encountered fall into two categories:

a. faults of an "open window" type.

These faults have mainly been partially open conductor seams, open back joint casings and spot soldered outer conductors.

b. faults of an intermittent nature

These faults have mainly been dry or cracked solder joints or the complete lack of solder altogether. Other faults include loose connector piece parts and scored outer conductors.

Faults of the open window type are stable and will not cause problems to digital transmission at 140 Mbit/s. To date the outer injection pulse crosstalk loss of such faults has been greater than 80 dB.

Dry joint type faults (type b) are notorious for providing long periods of virtually trouble-free operation between bouts of sporadic variation in contact resistance. Before oxides have had time to accumulate, such faults might be undetectable by any test but once developed outer injection pulse crosstalk losses between 60 and 70 dB could be obtained. If it is required to detect this type of fault in the early stages (i.e. where the measured value is greater than 90 dB) it does not seem possibly to easily differentiate between the two categories of fault, except by visual inspection after a location has been made.

At present the 100 dB specification is still under review but experience to date suggests that little change is likely to be made in the near future.

Conclusions

A description has been given of a simple but effective technique for the detection of near-end crosstalk faults in coaxial cable repeater sections. The main advantages of this technique, over conventional near end crosstalk measurements, are that discrete outer conductor faults can be easily located and the testing time is much reduced. Field test equipments, using 10 ns raised cosine pulses, have been in operation within the British Post Office for approximately one year and have performed well. The technique has proved to be the most sensitive test available for providing warning of incipient faults. It is therefore expected that with this increased measurement capability the general standard of jointing will improve.

Apart from field testing the technique has application for testing coaxial lead assemblies

during development and manufacture. This test has been incorporated into the BPO specification for the manufacture of 1.2/4.4 mm coaxial terminations and consideration is being given to incorporating the test into the installation specification for 1.2/4.4 mm coaxial cables.

Acknowledgement

We would like to acknowledge the work of our colleagues S Ahmad and E V T Perrins in the design of the collet-locking BNC connector and in test equipment production. Also we are grateful to the Director of Research and the Director of Operational Programming of the British Post Office for permission to publish this paper.

References

- FOWLER P: Screened Coaxial Cables for High Sensitivity Systems, IEEE Symposium On Electromagnetic Compatibility Montreux, May 1975, pp 291-6
- SCHELKUNOFF S A and ODARENKO T M: Crosstalk
 Between Coaxial Transmission Lines,
 Bell System Technical Journal,
 April 1937, pp 144-64
- GRIVET P: The Physics of Transmission Lines at High and Very High Frequencies, Academic Press, Vol 1, 1970
- Pulse Echo Test Set M85391, Decca Radar Ltd London, England
- Tektronix 1503 Time Domain Reflectometer Tektronix Inc., Beaverton, Oregon 97077, USA
- Connector No GE 37226062, Greenpar Ltd, Harlow, England
- 7. BROOKS R M and STEPHENS W J: A Pulse Crosstalk Method for the Detection of Incipient Faults in Coaxial Pair Cables, IEE Colloquium on Assessment of Media for Digital Transmission, 1 Oct 1978



R. M. Brooks R5.3.1 Post Office Research Centre Martlesham Heath Ipswich England IP5 7RE

Mr R M Brooks gained a B.Sc. in mathematics from the University of London in 1969. He then joined the British Post Office Research Centre and was engaged in research concerning submarine cable transmission systems. Between 1972 and 1978 he worked on theoretical studies and testing techniques for inland coaxial cable systems. He is currently working in the development of submerged optical fibre transmission systems.



W. J. B. Stephens OP 10.5.2 Carlton House Carlton Ave. East Wembley England, HA9 8QH

Mr W. J. B. Stephens joined the British Post Office Research Centre in 1942 and has been engaged in a variety of projects including submarine cable transmission systems, transformer design, telephone instrument design and external plant development. In 1971 he moved to the External Development Division of the BPO Operational Programming Department where he has responsibility for specialised testing of installed coaxial cables.

AN AUTOMATIC HIGH RESOLUTION DIELECTRIC LOSS MEASUREMENT SYSTEM OPERATING IN THE FREQUENCY RANGE 100 MHz TO 300 MHz COVERING THE TEMPERATURE RANGE 2 C to 40 C

P.C. FRANCIS

G.J. HILL

BXL POLYETHYLENE DIVISION, SCOTLAND.

ELECTRICAL RESEARCH ASSOCIATION, LONDON.

Abstract

An improved dielectric loss measurement system incorporating a re-entrant hybrid cavity operating in the frequency range 100 MHz to 300 MHz and using an air substitution technique is described. The system operation is under computer control. The system operating temperature range is 2°C to 40°C. Although designed for use with low loss polyethylene, the system can be used to evaluate most low loss polymers. The system is capable of resolving O.1 microradians in loss angle with reproducibility better than ± 0.3 microradians and absolute accuracy, traceable to National Standards, of ± 3 microradians or 5% whichever is the greater. Details of system design and calibration procedures in support of the above performance are given. The system is suitable for use in a Quality Control environment where rapid precise loss angle values are required on low loss

1. Introduction

The measurement of loss angle and permittivity of dielectric materials in the frequency range 100 MHz to 300 MHz using re-entrant cylindrical cavities was described in 1945. The accuracy of loss angle and permittivity achieved with the above system was of the order of ± 50 microradians and 1% respectively. Recent developments in low loss dielectrics such as polyethylene ($tan\delta = 50$ microradians at 30 MHz) has necessitated the development of apparatus and test methods capable of higher loss angle resolution and accuracy than have hitherto been required. Since apparatus operating in the frequency range 1 MHz to 100 MHz capable of loss angle measurement accuracy better than ± 3 m microradians exists², a test system operating above exists², a test system operating above 100 MHz and capable of comparable loss angle measurement accuracy was required for product development and quality assurance work. This paper describes the development of an automated high resolution dielectric loss measurement system

for operation in the frequency range 100 MHz to 300 MHz, and covering a temperature range 2°C to 40°C. The system performance is assessed at its centre operating frequency of 150 MHz to measure the loss angle of various grades of polyethylene at 23°C and 2°C respectively.

2. <u>Description of the Dielectric</u> <u>Loss Measurement System</u>

2.1 Development Objectives:

An integrated dielectric loss measurement system operating in the frequency range 100 MHz to 300 MHz has been developed on the basis of the following objectives:

- (a) To develop a dielectric loss measurement system capable of a loss angle resolution of 0.1 microradian with a reproducibility of ± 0.3 microradians over the frequency range 100 MHz to 300 MHz.
- (b) To achieve a measurement accuracy, traceable to National Standards, of ± 3 microradians or ± 5% whichever is the greater, over the same frequency range.
- (c) To base the dielectric loss measurement on the air substitution technique using a hybrid re-entrant cavity with a centre operational frequency of 150 MHz and covering the range 100 MHz to 300 MHz.
- (d) To develop the hybrid re-entrant cavity with the capability of variable temperature operation in the range 2°C to 40°C.

2.2 Apparatus:

A functional block diagram of the dielectric loss measurement system is shown on Fig. 1. The essential components comprise: a hybrid re-entrant cavity, cavity temperature control system, signal detector, signal source and a minicomputer.

The second second second second

Re-entrant axial cavity design. The outline design of the cavity for operation in the frequency range 100 MHz to 300 MHz is shown in Fig. 2 (a, b). The cavity is designed for variable temperature operation in a controlled dry atmosphere. Dry air is admitted to the cavity via a hole in the rear wall and vents to the atmosphere through the specimen port in the front of the cavity. No cover is provided for the specimen port but care has been taken to ensure that external changes have no effect upon the electric field in the cavity.

A high, reproducible value of 'Q' for the cavity is ensured by use of silver solder at all internal joints. The internal walls of the cavity are polished and goldplated to ensure a high reproducible value of Q. The upper variable electrode is moved by a non-rotating piston micrometer acting against a spring loading with an 'over-ride' mechanism to prevent disturbance of calibration by excessive pressures being generated should the electrodes come into contact with each other or the specimen. This micrometer can read to ± 0.2 µm.

Parallelism of the electrodes is ensured in three ways:

- (a) precision machining of all components during construction,
- (b) electrode faces are lapped optically flat,
- (c) final adjustment is made using an expanding ball gauge driving a linear voltage displacement transducer (LVDT).

The LVDT is also used to provide an analogue voltage output proportional to the position of the electrodes.

There is no precise method available for calculation of the inter-electrode capacitance due to uncertainties in the value of fringing capacitance appropriate to the re-entrant design. The method adopted is first to establish the approximate value of the electrode gap with an expanding ball gauge, set at 1250 µm: the nominal specimen thickness. The cavity is then resonated at a series of frequencies in the range 100-300 MHz. The resonant frequency (fo) and electrode micrometer setting (M:) are established at a minimum of five frequencies in this range.

The resonance equation describing the cavity performance:

$$\frac{1}{2\pi f_0 C_T} = Z_0 \tan \left(\frac{2\pi f_0 L}{c}\right) ----- (1)$$

where f_0 = frequency of resonance

Z₀ = system impedance

L = cavity length

C_T = inter-electrode capacitance

c = velocity of light in vacuo

has been modified to take account of the separate inductors in the two parts of the cavity and is then re-cast in terms of geometric and edge capacitances (Cg and Ce) between the electrodes where Cg is given by:

$$c_g = \mathcal{E} \mathcal{E}_o \frac{\pi}{4} \frac{D2}{t}$$
 -----(2)

where D = electrode diameter (mm)

t = electrode separation = $(Mx + \Delta)$ (μm)

Δ = micrometer zero error (μm)

Ce the edge or fringing capacitance is described by the Kirchoff³ approximation.

The total capacitance is now given by:

$$C_T = (Cg + \eta Ce) ---- (3)$$

where 'q' is a disposable parameter whose value lies between 1.0 and 2.0.

Equations (1) to (3) are then solved numerically for each set of values of (fo, Mx) to give the value of Δ with least variation across the frequency range. The optimum value of Δ is determined to a precision of \pm 0.1 µm using a computer programme which has been incorporated into the automated operation sequence. The value of Δ is re-established at each temperature at which measurements are made.

The resonant frequency of the cavity for a specimen of defined thickness and permittivity and with pre-determined inner and outer diameters, is controlled by the overlal length of the cavity. The design equation for the overall length 'L' in (mm) is:

$$L = \underbrace{0.8334 \times 10^3}_{f_0} \quad \left[\tan^{-1} \left\{ \underbrace{\frac{2119.8}{f_0 C_T}} - \tan (3.611f_0) \right\} \right] + (I_1 - t) - - - (4)$$

where I₁ = height of the base electrode (mm)

 f_0 = resonant frequency (MH2)

C_T = total inter-electrode capacitance (pF)

t = inter-electrode gap (mm) = $(Mo + \Delta)$ mm

The overall length 'L' of the above cavity is 222 mm. For a specimen whose

permittivity is 2.29 and thickness 1250 um and cavity inner and outer diameters of 37 mm and 128 mm respectively, the centre resonant frequency (fo) is 150 ± 1 MHz.

Cavity Temperature Control. Variations in temperature will have three effects upon the measurement:

- (a) the dielectric loss of the polyethylene itself will vary (by approximately -0.6 prad/°C rise in temperature);
- (b) the length of the cavity will alter, thus varying the value of Mx at which resonance occurs.

 Such changes as occur DURING a determination of Q will decrease the precision of measurement, but may be ignored due to the speed of measurement and temperature stability of the cavity. These changes in length will alter Q by approximately -2.5 x 10-3/°C.
- (c) the resistivity of the material of the cavity will alter, by approximately 5 x 10-3/°C, thus producing a variation in Q of approximately 2 ppm/°C. This last effect may be neglected in comparison with (a) and (b).

To achieve a loss angle resolution of \pm 0.1 microradians, the contribution due to uncertainties in temperature must be limited to \pm 0.05 µrad. This implies a knowledge and control of temperature to \pm 0.1°C over long periods and a short term variation (over a period of measurement) of considerably less.

The cavity is temperature controlled by a liquid coolant circulating in its internal channels (Fig. 2b) and provided with a supply of dry temperature controlled air. A conditioning enclosure and specimen support plate (Fig. 2a) is provided to ensure that the specimen can be conditioned in a dry atmosphere at the temperature of measurement and may be inserted into the cavity without coming into contact with the laboratory atmosphere. The range of operation is 2°C to 40°C with a guaranteed temperature sensitivity of ± 0.06°C.

Short term variations in temperature and temperature uniformity are dealt with by the cavity design. The use of a massive brass block with good thermal insulation reduces short term variations to the level shown in Fig. 3. To ensure that temperature control to better than \pm 0.1°C is achieved, and to enable computer correction of values of Q to be

achieved, a temperature sensor capable of displaying temperature changes of ± 0.02°C over the temperature range of operation is required. A platinum resistance thermometer has been adopted for this purpose so that accurate values of temperatures can be determined as well as any short term variations recorded. The temperature resolution is better than ± 0.01°C with an accuracy of better than 0.1°C over the temperature range 2 to 40°C. This thermometer has been interfaced with a digital voltmeter (DVM) and computer to give direct read-out and recording of cavity temperature.

Detector System. The detector specification is deduced from measurement resolution and accuracy criteria. The specification is shown in Table 1. The choice between detectors systems was narrowed to three devices identified: (A) Power meter with low-barrier Schottky detector with analogue output; (B) Power meter with low-barrier Shottky detector with digital output; (C) Low-barrier Shottky diode detector with square law load - which were examined for performance against the defined specification. The centre frequency of 300 MHz was chosen for the studies as none of the detectors showed pronounced variations over the range 100 MHz to 600 MHz and all are designed for use in 10 MHz to 12 GHz. The results of the evaluation are shown in Table 1.

Although detector system B showed the best performance, detector system C (Fig. 4) was selected on a cost effective basis. Detector system A did not meet specification.

The detector system is built into the cavity head as shown in Fig. 5. This ensures that minimum temperature drift and noise is produced from the detector and pre-amplifier which are both mounted in good thermal contact to the cavity within the temperature controlled enclosures. The pre-amplifier output is lOVdc at the peak of the cavity resonance spectrum, and is at sufficiently high level to be immune from stray pick-up. The detector incorporates an RF filter to minimise the output of RF signals.

High Frequency Source. A suitable source for this application must provide, over the frequency range of operation, a signal whose frequency and amplitude stability are compatible with the cavity Q and dimensional stability. The high frequency source with the stability performance shown in Table 2 fulfilled the above requirement.

The cavity is coupled to an H.F.

source and detector via two small aerials whose position and design are optimised to ensure that the Q is a maximum with sufficient transmission loss to ignore loading of the cavity.

Automation of Measurement System. To achieve the development objectives of loss angle resolution and accuracy, it is essential to carry out full system calibration, specimen measurement and calculations sensibly within fifteen minutes. Since these operations carried out manually would require a minimum of three man-hours, an automated measurement system has been developed.

When set to "automatic" the output function switch passes control for cavity operation to the computer. Two circuit boards inside the instrument receive the control data from the computer and implement operation of the cavity.

A 16-bit duplex interface from the computer to the first board sends control and data information from the computer. A 12-bit A.D.C. on this board receives the data and outputs a latched analog voltage via an amplifier, directly to the Varicap tuner of the source oscillator, thus providing frequency sweeping capability to the computer. (Frequency is read by the computer on a separate B.C.D. interface linked to a frequency counter.)

A further four bits of data from the computer are decoded to drive the second (relay) board. This board selects the output function for the display and data output interface, controls the operation of the switched attenuator and enables operation of the oscillator. No operator adjustments are required for this interface. (Fig. 6.)

The programme divides itself naturally into three sections:

- (i) Calibration procedures in which the zero error of the main micrometer is established, the edge capacitance for the electrodes calculated, and the LVDT set up.
- (ii) The system integrity for sample measurement is established. In this section, the resonant voltage drift rate, cavity temperature and relative humidity are measured and the noise present in the detector system and its subsequent electronics is established. Should any of the above parameters fall outside the specification set, the programme stops, indicating which parameter is out of specification. The final

calibration sequence establishes
the frequency dependence of the
circuit 'Q' of the unloaded cavity.
(Table 3.) A coupling factor
correction is introduced at this
stage to allow for slight deviations in the measured values from
the best fit to the (F) ourve.

(iii) In this section the operator is taken step by step through a dielectric loss measurement by means of prompting statements in the computer display and the value of tans calculated in terms of the measurement and calibration data stored in the computer.

At the selected test frequency, the unloaded cavity is tuned to resonance. The computer reads the peak signal output and the electrode position.

The frequency of the oscillator is then swept, under voltage control via a D/A converter, through the resonance curve and the frequency of the maximum output voltage precisely established. The cavity 'Q' is then established via a precision switched attenuator with the specimen 'OUT' of the cavity and again with the specimen 'IN' the cavity.

The dielectric loss angle $(\tan \delta)$ is calculated from the difference in circuit 'Q' between the conditions of specimen 'OUT' and specimen 'IN' together with test specimen thickness as in Equation 5.

Tan
$$\delta$$
 = $\frac{(Qo-Qi)}{(Qo,Qi)}$ x $\frac{(Mo+\Delta)}{(Ts+Mi-Mo)}$ x E -----(5)

where $Tan\delta$ = loss angle of specimen (microradians)

Qo = cavity Q, specimen 'OUT'

Qi = cavity Q, specimen 'IN'

Mo,Mi = electrode micrometer readings, at specimen 'OUT'/specimen 'IN' respectively (μ m)

Δ = electrode micrometer zero error (μm)

Ts = specimen thickness (µm)

E = edge capacitance correction factor

Experimental Work

Frequency dependence of cavity 'Q'

The frequency dependence of cavity 'Q' and 'Q' stability were determined in the frequency range 100 MHz to 300 MHz. The results are shown in Table 3.

Accuracy of cavity 'Q'

The accuracy of cavity Q was evaluated at different attenuator settings at 150 MHz. The results obtained are shown in Table 4.

Effect of specimen thickness

Variations in the specimen thickness can lead to two separate sources of error when measuring the dielectric loss:

- (a) Uncertainty in the value of Ts to be used in Equation 5 with the consequent uncertainty in the value of tans.
- (b) Actual variations in the value of Ts of the sample if the area under consideration is allowed to change due to slight variations in the sample position between measurements.

An automated specimen thickness measurement jig was developed to reduce the uncertainty in the value of specimen thickness (Ts) to a level which is compatible with loss angle resolution and accuracy requirements. The value of the specimen thickness (Ts) is measured with an accuracy of ± 0.2 µm, established by use of tungsten carbide slip gauges and a comparator capable of resolving 0.05 µm.

A plastic "specimen guide" attached to the specimen permits the specimen to be inserted in one position only.

System measurement performance

To evaluate the overall system performance, loss angle measurements were carried out at 150 MHz, the centre resonant frequency of the cavity. Measurements at 150 MHz were carried out at 23°C (Table 5) and 2°C (Table 6) respectively on low density polyethylene compounds referenced as follows:

P-E/A: Density 0.919g/cc, MFI 0.14dg/min. P-E/B: Density 0.919g/cc, MFI 0.16dg/min. P-E/C: Density 0.926g/cc, MFI 1.0 dg/min. P-E/D: Density 0.923g/cc, MFI 0.14dg/min.

Loss angle values in the frequency range 1 MHz - 65 MHz were also measured for the above compounds using a separate test set (2); Mathematical analysis showed that the curve of the format:

Tan δ = a + b \sqrt{f} (microradians) ----- (6 where Tan δ = loss angle (microradians) a,b = constants f = test frequency (MHz)

gave the best fit to the values measured

in the frequency range and was used to predict the loss angle values at 150 MHz shown in Table 5 and Fig. 7.

4. Summary of Performance of Complete System

Loss Angle Resolution and Reproducibility

From the design considerations discussed in Section 2.2, it is seen that the measurement system can resolve 0.1 microradian in loss angle.

The reproducibility is demonstrated by repeat measurements on the same specimen and repeat measurements at an interval of 48 hours. It is seen from that a reproducibility in terms of standard error of at least ± 0.3 microradians is seen to be achieved.

Accuracy of Measurement

The accuracy of measurement of the system has been demonstrated at the centre resonant frequency of 150 MHz using three criteria, i.e. (1) agreement of frequency dependence of measured Q with the theoretical value (Table 3); (2) reproducibility of Q measurement with different values of attenuation, each attenuator calibrated with an accuracy traceable to National Standards. Table 4 shows that the values of Q may be intercompared to better than 1% proving that the value at 150MHz is self consistent and may be used as a reference for comparison of Q measurements at other frequencies; (3) agreement of measured tans with values of tans calculated from an empircal tan6 = a + b√f law to within + 3 microradians or 5% whichever is the greater (Table 5).

. Conclusions

- 5.1 An automated dielectric loss measurement system has been developed which can make reproducible measurements of dielectric loss at 150 MHz to better than ± 0.3 microradians with an accuracy of ± 3 microradians or 5% whichever is the larger. Measurement in the frequency range 100-300 MHz may be performed with suitable samples by adjustment of the air gap between the specimen and the cavity electrodes without loss of precision.
- 5.2 The level of loss angle resolution and reproducibility achievable makes it possible to investigate small changes in dielectric loss properties due to changes in polymer structure, ageing effects, etc. The measurement system is also suitable for use in a Quality Assurance environment where rapid, precise test data is required.

- 5.3 The measurement system is capable of operation in the temperature range 2°C to 23°C. The temperature range may be extended up to 40°C without adversely effecting system performance.
- 5.4 The principal advantages of system automation come from the speed of measurement or calibration, which is achieved within 10 minutes. An added advantage comes in the question of æcuracy of measurement. Quick access to computing facilities enables the basic measurement of Cavity Q to be checked for accuracy before commencement of a measurement.

Acknowledgement

The apparatus described in this paper is the result of an Electrical Research Association project jointly sponsored by CENTRE NATIONAL D'ETUDES DES TELECOMMUNICATIONS, France; SODEFIN, France; STANDARD TELEPHONES AND CABLES LTD., Southampton; and BXL, Polyethylene Division, Scotland.

The authors wish to thank the sponsors for their co-operation in the project and for their permission to publish this paper.

References

- C.N. Works, T.W. Dakin, F.W. Boggs
 "A rescnant cavity method for
 measuring dielectric properties at
 ultra high frequencies", Proc. IRE,
 245-254, April 1945.
- G.J. Hill, P.C. Francis, "Determination of dielectric properties of low loss materials at radio frequencies", Proc. IEE, Vol. 129, pp 135-140, July 1975.
- Kirchhoff, G: On the Theory of Condensers, 'Monatsber. Akad. Wiss' (Berlin), March 1887, p.144: Collected Works, Barth (Leipzig), 1882, p.101.
- Hybrid Re-entrant Cavity Development Programme: Ref. ERA Project 3088.

And a sequence of the first first first first first for the control of the contro

TABLE 1

COMPARISON OF DETECTOR SYSTEMS AT 300 MHz

	Detector System	Noise	Drift Rate	Power Law 3dB step
Specified Value		20	100	<u>+</u> 0.05
A B C		11.1 [±] 1.4 8.7 [±] 0.2 18.0 [±] 2.0	124 [±] 21 32 [±] 10 62 [±] 30	3.044 [±] 0.001 3.002 [±] 0.001 3.000 [±] 0.001* 3.052 [±] 0.001**

Notes * At - 15 dBm input power } outside this range the detector is ** At - 25 dBm input power outside the present specification

TABLE 2

H.F. SOURCE SIGNAL STABILITY 100 MHz-500MHz

Frequency Drift	Ampl. Drift	'Noise'
$\frac{1}{f} \cdot \frac{df}{dt}$. $10^{-6}/s$	$\frac{1}{v} \frac{dv}{dt} \times 10^{-6}/s$	<u>∕uV</u> rms
0.001	1.11	11,2

The State of the S

TABLE 3

VARIATION OF CAVITY 'Q' WITH FREQUENCY

Frequency MHz	Theoretical 'Q'	Measured 'Q' (cavity under Automatic Control)
100	1686	1563
150	2069	1893
200	2384	2051
300	2920	2359

TABLE 4

ACCURACY OF CAVITY 'Q' AT 150 MHz

ttenuator (dB)	Cavity 'Q' Values
3.0	1899.6 [±] 5.7
4.0	1928.3 [±] 5.9
6.0 STHOOP-SHALOCK XELLIBATE	1891.7 [±] 7.3
10.0	1911.9 [±] 4.6
20.0	1917.9 [±] 6.5
, as felt, 33	1909.6 [±] 14.5 (Average)

TABLE 5

COMPARISON, AT 150 MHz/23°C, OF MEASURED LOSS ANGLE VALUES WITH THE LOSS VALUES PREDICTED FROM CURVE FITTING CALCULATIONS

HO. THOUGHE SOUNDE DIELECTRICLOSS IN ASUREMENT SYSTEM IDIAGRAMIAATICS

Compound Reference	Tan6 (uR) at 150 MHz/23°C / 35% RH		
Compound Reference	Measured *	Predicted from Eqn (3)	
LZJ			
P-E/A	157.4 ± 0.1	154.0 ± 4	
1.395.395.4 T.C.V.4	157.7 ± 0.1 **		
P-E/B	131.7 ± 0.2	128.7 ± 4	
P-E/C	102.9 ± 0.2	99.0 ± 3	
	103.1 ± 0.2 **	The second second	
	THE THE THE STREET STREET		
P-E/D	84.5 ± 0.2	84.0 ± 3	

^{*} Average values - Standard Error of five successive measurements.

TABLE 6

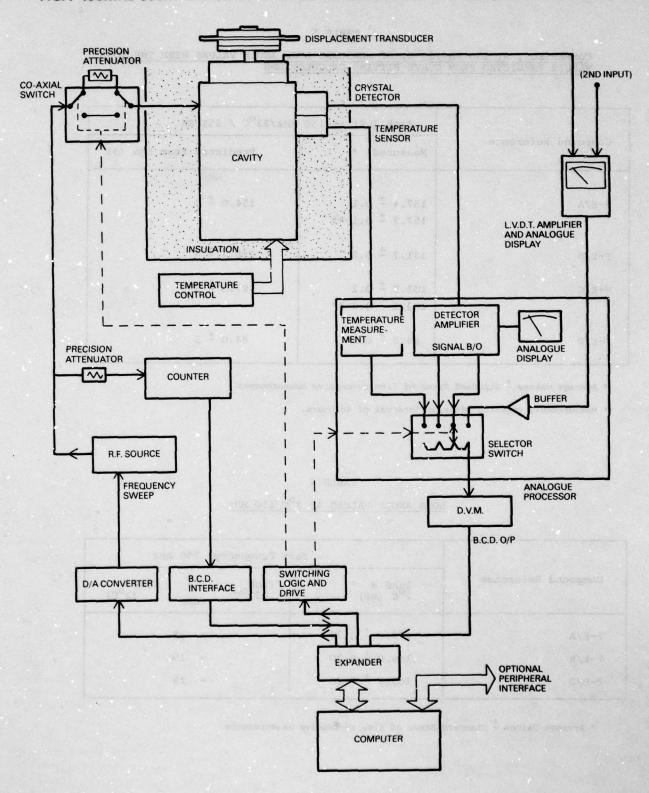
LOSS ANGLE VALUES AT 2^OC/150 MHz

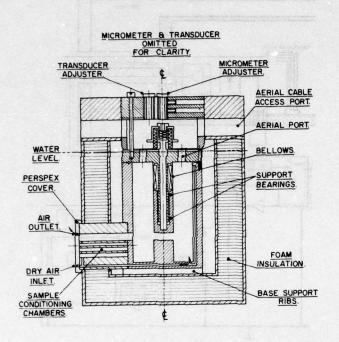
	Test Frequency: 150 MHz		
Compound Reference	Tans @ * 2°C (uR)	Tan6 - Tane (2°C)	
P-E/A	172.0 ± 0.30	- 15	
P-E/B	146.0 ± 0.30	- 15	
P-E/D	103.5 ± 0.20	- 19	

^{*} Average Values + Standard Error of five successive measurements

^{**} Measurements repeated after an interval of 48 hours.

FIG. 1 100MHz-300MHz DIELECTRIC LOSS MEASUREMENT SYSTEM (DIAGRAMMATIC)





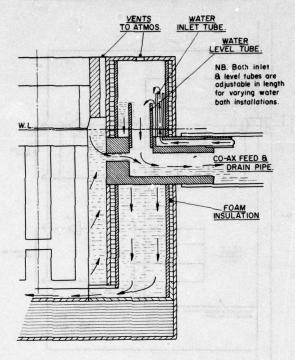
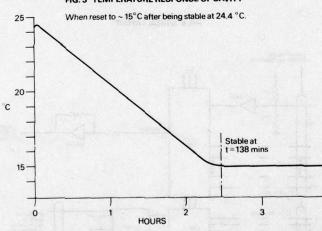
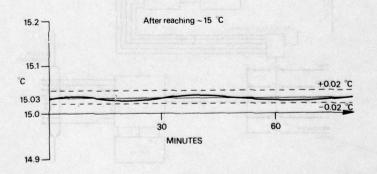
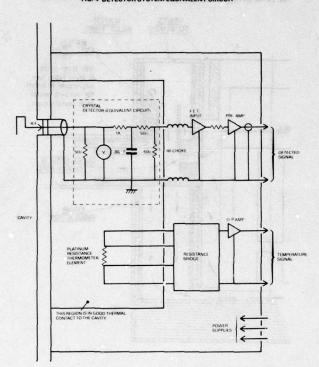


FIG. 3 TEMPERATURE RESPONSE OF CAVITY







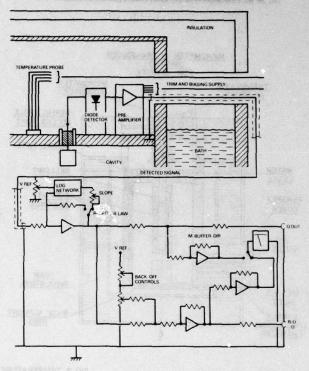
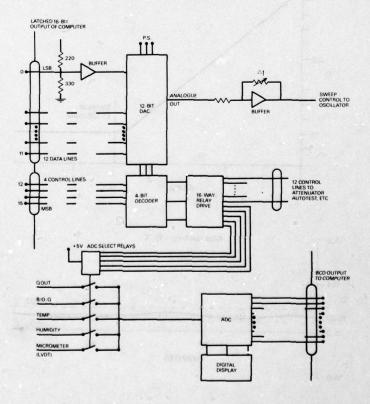
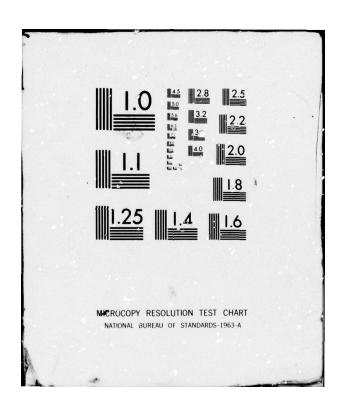
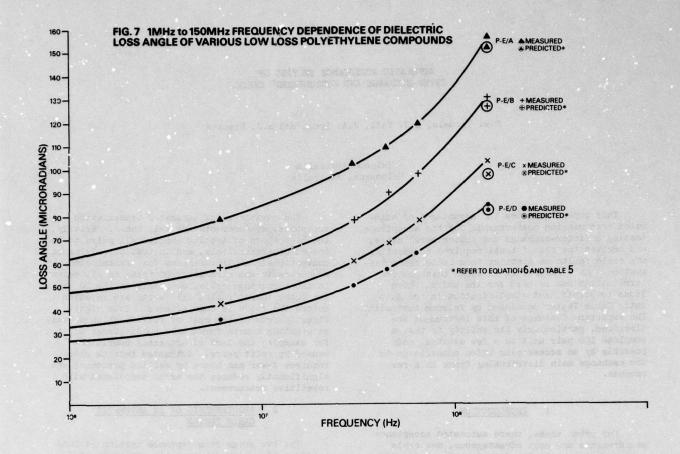


FIG. 6 DIGITAL LAYOUT



ARMY COMMUNICATIONS RESEARCH AND DEVELOPMENT COMMAND -- ETC F/G 9/1 PROCEEDINGS OF THE INTERNATIONAL WIRE AND CABLE SYMPOSIUM (28TH--ETC(U) AD-A081 428 NOV 79 UNCLASSIFIED NL 2 of 5 AD-A08I428 A 2 Q. 2 凮 a A







Mr. P.C. Francis, Bakelite Xylonite Limited, Inchyra Road, Grangemouth, FK3 9XG, Scotland.

Peter C. Francis joined the Physics and Physical Chemistry Section of Technical Department of Bakelite Ltd. in 1955. He was elected M. Institute of Physics, London in 1970 and is now Senior Product Technologist, Wire and Cable Group of BXL Polyethylene Division carrying out development and technical service work on polyethylene telephone cable insulation products. He has special responsibility for development of precision dielectric loss measurement techniques and their application.



Dr. G.J. Hill,
Electrical Research
Association,
Cleeve Road,
Leatherhead,
Surrey, England.

Dr. Hill is manager of the Flectronic Materials and Components Department at ERA Ltd., Leatherhead, U.K. He graduated in Physics from the University of Bristol in 1958 and was awarded the degree of PhD in 1962 for studies of the effects of pressure on the dielectric properties of solids. He was elected F.Inst.P. in 1970 and has published papers on the conducting properties of transition metal oxides, scanning electron microscopy and precision dielectric measurements.

AUTOMATIC ACCEPTANCE TESTING OF INTER-EXCHANGE AND SUBSCRIBERS' CABLE

M.W. Tisdale, L.J. Hall, J.A. Lynch and R.J. Pirotta

Telecom Australia Melbourne, Australia

This paper indicates the advantages of automated transmission measurements for the acceptance testing of inter-exchange and subscribers' cable, and derives the set of tests required to identify any cable faults as distinct from cable characterisation. As a result, it is shown that passive terminations can be used for the pairs, which leads to significant simplification in the Automatic Cable Tester developed by Telecom Australia. The important features of this instrument are discussed, particularly its ability to test a complete 100 pair unit in a few minutes, made possible by an access plug which connects on to the exchange main distributing frame in a few seconds.

1. INTRODUCTION

For urban areas, where automated acceptance measurements are most advantageous, new cable installations basically fall into two categories, namely inter-exchange (or junction) cables connecting exchanges (offices) together, and subscribers' cables which connect the telephone sets to the local exchanges.

New inter-exchange cables are initially installed loaded for voice frequency working. However, as the break-even distance(where digital carrier systems result in a lower circuit cost per unit distance) is reducing, as the traffic level grows, extra circuit capacity will be obtained by deloading groups of pairs and installing digital line equipment. Consequently, the acceptance testing of new inter-exchange or junction cables is done at voice frequencies, yet, such testing should identify any faults which, while only causing degradation at voice frequencies (and therefore perhaps going undetected if comprehensive testing is not used), would caus complete failure of digital carrier systems. It must be emphasised that acceptance testing is not designed to collect cable characterisation data for system design purposes, but solely to reveal faults due to cable manufacture and installation defects. Subscribers' cables are normally unloaded in urban areas, although where the distance from the subscriber to the local exchange is large, H88 pattern loading is employed. Accordingly, as for inter-exchange cable, testing is required to be done at voice frequencies.

The advantages of automated transmission acceptance measurements are well known. Briefly, the high speed of testing enables all pairs to be tested comprehensively, and instead of relying on conventional sampling schemes for transmission measurements and elementary DC tests on all pairs in inter-exchange cable, or solely on the DC tests for subscribers' cable, all faults are revealed before the cable is commissioned. This significantly reduces the cost of rectification as well as creating a more favourable public image due to, for example, the lack of crosstalk complaints caused by split pairs. Automated testing also requires fewer man hours by skilled personnel and significantly reduces the error associated with repetitive measurement.

2. REQUIREMENTS OF AN AUTOMATIC CABLE TESTER

The two areas of acceptance testing of installed cable which are most time consuming and error-prone are firstly, the connection of the equipment to the pairs under test and then secondly, the interpretation of results to determine if the required specification limit is met. Consequently any Automatic Cable Tester (ACT) must concentrate, at least initially, on these two aspects.

In Australia, all cable pairs entering the exchange are terminated on the main distributing frame (MDF) using a standard 100 pair link block. On one side of the block the incoming pairs are terminated, while on the other side, the pairs leading to the equipment are terminated. Connection between the corresponding wires on either side of the block is made by removable links. Figure 1 shows the current design of block which employs soldered connections. A new design of block is being introduced which uses wire wrap terminations but which will still enable the connection of equipment such as the ACT to it.

Early in the design of the ACT, the decision was made to connect to all of the 100 pairs terminated on an MDF link block in one operation by means of an MDF access plug. As a result, all 100 pairs and combinations of them could be tested in one cycle of operation of the ACT, without the need for further operator intervention. The maximum unit size of cables in

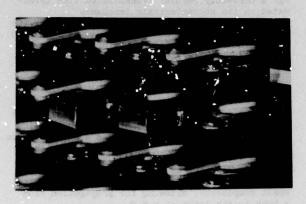
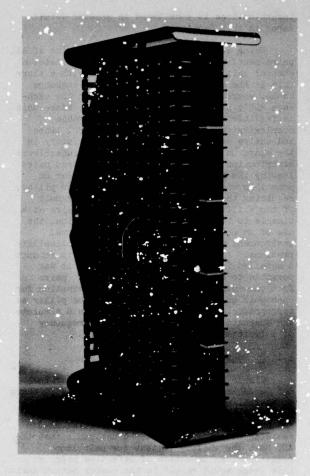


Fig. 1 The MDF Link Block (right) with a close-up of the terminating tags and removable links (above).

Australia is 100 pairs, and since faults between cable pairs in different units occur very infrequently and any one unit does not appear on more than one MDF link block, a cable can be comprehensively tested by simply attaching the MDF access plug to all of the link blocks on which units from that cable are terminated. The significant aspects of the design of the MDF access plug are considered in Section 4.

For acceptance testing purposes, an automated testing instrument should give a "go/no go" result when a measured parameter for a pair-to-pair combination is compared to a predetermined standard, and, only when that limit is exceeded, should a warning be given to the operator. This may take the form of the testing procedure stopping, with the pair number or numbers displayed or, if a printer is fitted, a print-out of the relevant information.

An additional requirement of any test instrument is that of minimum complexity to ensure maximum reliability and repairability under field conditions, as well as minimum cost, to ensure that as many instruments as needed can be obtained to enable all cables to be tested. Small size and weight are also significant. All the above factors were considered in the design of the Automatic Cable Tester. Having decided that the instrument must access 100 pairs in one operation, the next stage was to determine the minimum set of tests to be performed in order that all faults be revealed. This is discussed in detail in Section 3.



3. ACCEPTANCE TESTS REQUIRED

The first step in determining the minimum set of tests required to determine whether a cable is adequate for its intended purpose, is to define carefully that purpose. A multipair telecommunication caple is designed to provide between its two ends, for all of its pairs, an insertion loss versus frequency characteristic which lies between certain predefined limits when fed with a source and terminated by a load of specified impedances. In addition, each pair must not couple more than a predefined ratio of its signal power into any other pair nor receive more than that same ratio from any other pair. For digital systems, the situation is more complex than this, but can be expressed effectively in these terms. The input impedance versus frequency of each end of each pair must lic within required limits in order to ensure adequate transhybrid loss in two wire/four wire terminating sets when the pairs are used for bidirectional voice frequency working and to ensure that the insertion loss versus frequency characteristic is not impaired. This latter point is particularly important with digital systems. The interrelationship between input impedance and

insertion loss is considered in greater detail later in this Section.

Using automated equipment to determine if all pairs meet the above requirements, necessitates a control unit at one end of the route with & slave unit at the other end. With an inter-exchange cable, whereby all the pairs appear on the exchange ADF's at either end, the use of a slave unit is feasible, although it adds considerable complexity to the instrument, as control lines and active switching and measuring circuitry in the slave unit must be provided. For subscribers' distribution cable, a block of one hundred pairs leaving the MDF at the exchange may appear on more than one cross-connecting cabinet or pillar, requiring the use of more than one slave unit if the ability of the ACT to test 100 pairs at a time is to be fully realised. In addition, the use of an active slave unit in the external environment would undoubtedly lead to reliability problems. As a result, it was decided to conduct a detailed investigation as to whether it was possible to adequately acceptance test pairs from one end, using only a passive termination for each pair on the remote MDF, cabinet or pillar as appropriate. The termination unit would simulate the characteristic impedance versus frequency of a typical perfectly uniform pair.

3 1 DC Tests

Simple DC tests are traditionally carried out on cable pairs as external plant work is being completed. These tests are designed to ensure that there are no obvious defects such as open and short circuit pairs and poor insulation resistance. It was considered desirable that the ACT have the ability to test for pair loop resistance, as detection of defective pairs at this stage would result in the easier determination of the nature of faults than if the pair failed a later test.

3.2 <u>Insertion Loss, Return Loss and Input</u> <u>Impedance</u>

The mean and standard deviation of the insertion loss of pairs in the cable route, providing they do not contain any defects, are well known from calculation and characterisation measurements. As a result, the aim of acceptance testing is not to measure the actual insertior loss of the pair under test, but rather to determine whether the pair has any defect or defects which would cause it to be not a member of the ensemble for which the mean and standard deviation are known. In line with the aim of using orly a fixed termination for the pair under test and conducting measurements only from the sending end, it was necessary to determine a measurable parameter of the pair which is sensitive to any defects which would affect the insertion loss performance.

The input reflection coefficient p(f) at a frequency f of a transmission line is defined to be the ratio of the voltage V (0) of the reverse travelling wave (at the input x = 0), caused by reflections throughout the line, to the voltage

of the forward travelling wave at the input $V_{+}(0)$. For a perfectly regular transmission line terminated in its characteristic impedance Z_{0} at $x=\lambda$, the value of V(0) is zero and $V_{+}(0)$ is the total voltage on the line at the input V(0). At a point x away from the origin, the forward travelling wave is given by

$$V_{\perp}(x) = V_{\perp}(0) e^{-\gamma x}$$
 (3-1)

where $\gamma = \alpha + j\beta$, the propagation constant of the line. In a small length dx at x, irregularities in the structure of the line cause a small reverse travelling wave dV (x) to be generated, which adds to any reverse travelling wave already present, generated by irregularities between x and £. V (0) is the summation of all these small components, allowing for propagation from x back to the input at x = 0.

$$V_{-}(0) = \int_{x=0}^{k} dV_{-}(x) e^{-\gamma x}$$
 (3-2)

Consequently :-

$$\rho(f) = \frac{V_{-}(0)}{V_{+}(0)} = \int_{x=0}^{\ell} \frac{dV_{-}(x)}{V_{+}(x)} e^{-2\gamma x}$$
(3-3)

Denoting the characteristic impedance at x as $\mathbb{Z}^{\ell}(x)$, then

$$\frac{dV_{-}(x)}{V_{+}(x)} = d\rho(x) \stackrel{\Delta}{\Rightarrow} r(x)dx = \frac{\Sigma(x + dx) - \Sigma(x)}{\Sigma(x + dx) + \Sigma(x)}$$
(3-4)

There are a number of subtle points in this model which are fully described in Reference 1. In particular, the attenuation α of the line is slightly higher than α , the value which the line would have if there were no irregularities in its structure (that is, Z(x) = Z for all x). From Equation 3-4, r(x) is the reflection density function and is approximated by

$$r(x) = \frac{1}{2Z_0} \frac{dZ(x)}{dx}$$
 (3-5)

so that

$$\rho(f) = \int_{X=0}^{\ell} r(x) e^{-2\gamma x} dx$$
 (3-6)

For a lump loaded transmission line, the above analysis still applies where the changes of characteristic imredance (Equations 3-4 and 3-5) are due to irregularities in the transmission line, and its loading pattern, where these irregularities are superimposed upon the normal change in characteristic impedance with length, which a perfectly uniform loaded line exhibits.

Thus $\rho(f) = 0$ for a uniform line, loaded or not, but departures from uniformity caused, for example, by changes in the geometry of the pair or variations in the inductance and/or spacing of the loading coils, will cause $\rho(f)$ to be non-zero.

The input impedance Z of the line with an input reflection coefficient $\rho(f)$, given by Equation 3-6, is

$$Z_{in} = Z_{o}\left(\frac{1+\rho(f)}{1-\rho(f)}\right)$$
 (3-7)

$$\simeq$$
 Z₀ (1 + 2 \dot{p} (f))

so that

$$Z_{in} - Z_{o} = 2Z_{o} \rho(f)$$

$$= \int_{x=o}^{k} 2Z_{o} r(x) e^{-2\gamma x} dx$$
(3-8)

Now consider a measurement technique wherein the pair under test is made one arm of a bridge with the opposite arm being the characteristic impedance Z of the typical, perfectly uniform pair of the same type as the one under test. Then at any frequency f the ratio of the bridge output and excitation voltages VD and VS is given by:

$$\frac{V_D}{V_S} = K(Z_{in} - Z_o) = K 2Z_o \rho(f)$$

$$= K \int_{x=0}^{\ell} 2Z_o r(x) e^{-2\gamma x} dx \qquad (3-9)$$

where K is a constant.

Equation 3-9 shows that irregularities in the structure of the line can be determined by measurement of the reflection coefficient. By measurement over a sufficiently wide frequency band, it is possible to remove effectively the transform relation (that is, the e-2YX and integral) from Equation 3-9 and obtain the derivative of Z(x) for all x. This is the principle of the pulse echo tester and is discussed in greater detail in References 2 & 3. If the single frequency input to the bridge is replaced by a noise generator with a power density spectrum P(f) over a frequency range from f_1 to f_2 , then the average power at the bridge output is approximately:

$$P_{D} = 2P \int_{f_{1}}^{f_{2}} |K|^{2} |\rho(f)|^{2} df$$

$$P_{D} = P \int_{x=0}^{R} |r(x)|^{2} e^{-h\alpha} av^{x} dx$$
 (3-10)

where P_D is the total detected power and P is the (constant) power spectral density (considered to be one sided) and where α_{av} is the average attenuation across the band f_1 to f_2 . For loaded lines in particular, α is very close to constant across the voice frequency band, making the above approximation very close to exact. For non-loaded lines, over the voice frequency range, it is adequately accurate for the purposes of this discussion.

Equation 3-10 shows that the measurement of the input impedance difference from Z of a transmission line (using band limited white noise) effectively yields an exponentially weighted sum of the squared reflections on the line.

In Section 2, it was stated that the performance of the transmission line is well known if the line is uniform with length. An analysis of the type in Section 3.3 of Reference 1 indicates that Equation 3-10 effectively gives the summation of the attenuation increases due to irregularities in the line over both the frequency range f₁ to f₂ and the length of the line (although exponentially weighted).

The summation of the attenuation increases with frequency may be considered unacceptable at first, because the result does not distinguish between a large number of small wideband increases and between a small number of large narrowband increases. However, the characteristics of the human ear must be considered at this stage and it is well known that, even quite large but widely spaced narrowband increases in the insertion loss versus frequency performance of a voice transmission path, do not result in significant adverse effects, in the same manner that wideband increases, as long as they are small enough, do not create problems. It is wideband increases of fairly large magnitudes which cause transmission problems; the measurement of the differences in the input impedance with band limited noise responds most satisfactorily to these.

The exponential weighting with length is a problem which cannot be solved with any single ended measuring equipment using time invariant circuitry. Some modern high performance pulse echo testers for coaxial tubes use a time dependent filter coupled to the time base in order to correct for the attenuation which the pulse suffers in its propagation to the irregularity and return.

This level of complexity was not considered acceptable in the Automatic Cable Tester, as it rould have meant using a pulse generator rather than a noise generator, a time variant filter linked to the pulse generator time base, and an integrator to sum the reflections with distance (converted to time by the phase velocity). However, the minimum ralue for e in Equation 3-10 is 0.03 for a maximum of 7.5 dB loss for a voice

frequency inter-exchange route. Testing from both ends increases this minimum value to 0.18; however, such long length inter-exchange cable routes are unusual, the average loss being 4 dB, yielding 0.63 as the minimum value of the multiplier in Equation 3-10 when testing from both ends is employed. This value is considered quite acceptable in terms of the sensitivity which the ACT is required to have to attenuation increases due to irregularities in the middle of a route.

For the practical reasons indicated in Section 3, for subscribers' cable only one-way measurements, from the exchange MDF to the cabinet or pillar, are possible. The loss on these routes is such that the minimum value of the exponential weighting factor in Equation 3-10 still leaves adequate measurement sensitivity to detect remote and irregularities.

In summary then, measurement of the average noise power at the output of a bridge containing the pair under test and an impedance accurately simulating the characteristic impedance Z of the typical, perfectly uniform pair, when excited by a noise generator with a close to flat spectral density over an adequately wide band, effectively yields a result which is the summation of the attenuation increases due to the irregularities (return loss) both along the length of the pair and across the frequency band of excitation. Equations 3-8 and 3-10 also show that this noise power is the summation with frequency of the squared impedance mismatch of the pair relative to Z and is also a summation with frequency of the returned power ratio which is important in echo and stability calculations.

3.3 The Reference Impedance

The one remaining problem in this measurement technique is in obtaining a good simulation of the uniform line characteristic impedance Z across the frequency band from f, to f₂ (typically 300 Hz and 3400 Hz). In the ACT, this problem was solved by making use of a known good pai as the reference arm of the bridge. To determine whether a pair has adequate quality to be used as the reference (that is, whether it is close to Z across the frequency band), it is subjected to a comprehensive program of manual tests.

To this point, the tests considered have been on each pair alone, to determine whether it is an adequate transmission line for the purpose for which it is required. However, adequate transmission performence on each pair is a necessary, but not sufficient, condition for acceptable performance. The power coupling ratio from any pair to any other pair must be sufficiently small to prevent intelligible crosstalk. This power coupling ratio is normally expressed as the ratio of the voltages on the disturbed pair to the disturbing pair at both the sending end (near end crosstalk NEXT) and the receiving end (far end crosstalk ratio, FEXTR).

3.4 Crosstalk

- Crosstalk coupling is not dependent on transmission irregularities as some of the factors which cause irregularities within a pair will result in the coupling of power to and from other pairs. The most important example of this is when there are split pairs resulting from splicing errors. However, a pair which has acequate transmission performance, as based on the results of the band limited noise input impedance difference measurement (or relative return loss when the reference impedance is a known good pair), cannot be guaranteed to have acceptable crosstall performance. The two reasons for this are in
 - . There are mechanisms which cause crosstalk couplings, but which do not have a significant effect on transmission.
 - . The sensitivity of the input immedsace measurement is not adequate to detect minor defects which may cause both crosstalk and transmission irregularities. This is insignificant for transmission, but not for crosstalk coupling.

As a result, it was considered necessary to introduce a crosstalk measurement into the ACT. As the ACT can make measurements from only one end of a cable, with tre pairs terminated at the remote end by an impedance simulating their characteristic impedance, only NEXT can be measured.

The NEXT of two pairs of length & is given by

NEXT =
$$j2\pi f \int_{x=0}^{\ell} C_{N}(x)e^{-2\gamma x} dx$$
 (3-11)

where f is the frequency and $C_N(x)$ is the near end coupling density function such that, in a small length dx at x, the incremental NEXT is $j2\pi fC_N(x)dx$.

The far end crosstalk ratio is

FEXTR =
$$j2\pi f \int_{x=0}^{\ell} C_F(x) dx$$
 (3-12)

where $C_p(x)$ is the far end coupling density function. Both $C_p(x)$ and $C_p(x)$ can be related to the capacitance unbalance per unit length, K(x), and the inductance unbalance or effective mutual inductance per unit length, M(x).

$$c_{N}(x) = \frac{K(x)Z}{8} + \frac{M(x)}{Z_{o}}$$
 (3-13)

and
$$C_F(x) = \frac{K(x)Z_0}{8} - \frac{M(x)}{Z_0}$$
 (3-14)

For medium to high levels of unpalance, K(x) and M(x) are highly correlated and this can be approximated by :-

$$M(x) = \frac{K(x) L(ext)}{K_1C}$$
 (3-15)

where L(ext) is the external inductance per unit length, C is the mutual capacitance per unit length, and K_1 is a constant varying between 4 for adjacent pairs, dropping to less than 2 for pairs with one to two other pairs separating them. The important point, however, is that the above correlation on pair combinations with a medium to high level of coupling means that $C_{\rm p}(x)$ is not less than $C_{\rm p}(x)$, although at the low frequencies in use on subscribers' cable and particularly for loaded cable, $C_{\rm N}(x)$ and $C_{\rm F}(x)$ are close to being equal.

There is substantial merit in measuring an effective summation of crosstalk couplings along the length of the cable for the pair combination concerned, in a similar manner to that which has been done for reflections. The exponential weighting is inevitable for a measurement conducted from one end only; however, as explained earlier, this is quite tolerable, considering the practical advantages in measurement ease gained from so doing. However, whereas an adequately wide window of white noise was suitable to obtain the summation of irregularities on a single pair, to obtain the summation of crosstalk couplings between pairs, the disturbing pair would have to be excited by noise with a power density spectrum given by :-

$$P(f) = A/f^2$$
 with $f_1 < f < f_2$

where f is in the voice frequency range (3-16) and A is a constant (where f₂ - f₁ is adequately large). This "shaped" noise is necessary to compensate for the proportional-to-frequency term in the expression for NEXT (Equation 3-11).

This procedure was not implemented in the ACT for the following two reasons :-

- The difficulty in obtaining a power spectral density of the form given by Equation 3-16 was not considered compatible with the desire to keep the instrument as simple as possible.
- The network crosstalk requirements have been formulated for a frequency of 1600 Hz.

Accordingly, the NEXT is measured at 1600 Hz. This gives the actual crosstalk at 1600 Hz rather than the summation of the crosstalk couplings with length, and as such does not necessarily give a direct assessment of the FEXTR for the pair combination. However, at the low frequencies considered here (leading to fairly short electrical lengths for the cable unler test), the probability of the FEXTR being unacceptably nigh, while the NEXT is acceptable, is very low.

4. CABLE PAIR ACCESS

4.1 The MDF Link Block

The ability of the Automatic Cable Tester to rapidly and accurately test a large number of pairs is mainly due to the MDF Access Flug which convects to the 100 pair MDF link block shown in Figure 1. The MDF link block consists of two hundred split tags such that a wire connected to the line side of the tag is not electrically connected to the cachange side of the tag until a bridging link is inserted. The MDF link blocks are mounted vertically on the frame with the pairs of the inter-exchange or subscribers' cables terminated on the link side of the block with the internal exchange cabling terminated on the other. The two tags in the top left hand corner have the links in place.

4.2 The MDF Access Plug

With the links removed, the MDF access plug encases the link block and connects with the line side of the tags using the contact areas onto which the bridging links are slid. These contact arecs are smooth and uncontaminated by solder flux deposits and the like. As the wiring enters the link block from the rear, there is adequate room for the access plug to be brought up to and aligned with the required link block before moving the handles and driving the contactors home. The installed position of the access plug on a link block is shown in Figure 2. Considerable development work was required to ensure that a good contact is achieved on the 200 separate tags without risk of damage and that & definite "right home" feeling was transmitted to the operator as the plug is fully engaged.

The MDF access plug contains the switching circuitry which connects the signal generating and measuring equipment in the moster unit to the pairs to be tested. If switching were not employed in the access plug, a large 100 pair cable would be required between it and the master unit, with the following disadventages:-

- Such a cable is bulky and heavy, and there would be a considerable risk of damage to exchange equipment in its use.
- . As the cable could not be easily screened it would add its own component to crosstalk, thereby reducing accuracy (unless additional complex equipment were added in the master unit).
- . The additional plug and socket contacts required would reduce reliability

Switching is provided by reed relays, driven by a digital decoder controlled by the master unit. Figure 3 shows the circuitry in the access plug. Reed relays were chosen for the switching because there is a nigher degree of isolation attainable than with semiconductor switches and because there is a higher reliability, considering that the



Fig.2 MDF Access Plug Installed on MDF Link Block

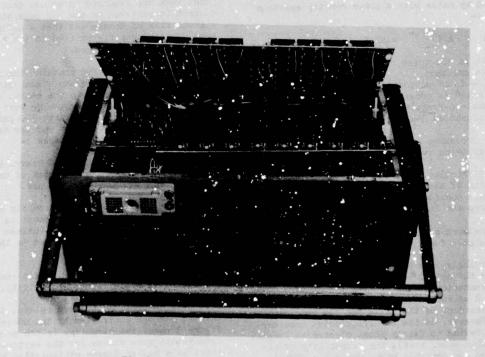


Fig. 3 Internal Circuitry of MDF Access Flug

switching elements could be exposed to stray voltages on the cable pairs to be tested. The operating time of the relays does not add significantly to the overall time required to test 100 pairs.

4.3 Far End Termination

For an inter-exchange cable, where the far ends of the pairs are also terminated on MDF link blocks, a passive version of the access plug containing the impedance simulation appropriate to the cable type is used. Normally, this is simply an 1200 Ω resistor for H88 pattern loaded pairs.

For subscribers' cable, the pairs can be terminated by means of a cabinet or pillar access plug which places the termination resistor across the pair. For loaded cable pairs this is again 1200 P but is 600 Ω for unloaded pairs. Although resistively terminating an unloaded pair is not as accurate as with loaded pairs (as the characteristic impedance varies far more with frequency for unloaded cable), it should be remembered that, in the relative return loss test, the pair under test is compared to a known good pair and that the threshold level of the fault detector, attached to the average power level detector on the measuring bridge output, is adjusted to suit the type of cable under test. Obviously the threshold is lower for inter-exchange than subscribers' cable,

5. THE MASTER UNIT

The master unit of the Automatic Cable Tester is shown in Figure 4. Although the instrument as shown is designed for partable operation, adaptor plates can be fitted to enable rack mounting, should this be required, although this option imposes the constraint that all the modules in the unit be accessible from the front panel.

Three modules are used in the master unit, namely, the signal generating module, the signal receiving module and the control module. Like the MDF access plug, the operation of the signal modules is fully determined by the control module, although to obtain an ergonomically satisfactory panel layout, the displays indicating the actual pair(s) under test and their signal level have been located on the appropriate signal modules. Conventional analogue and digital circuitry has been used throughout in order to achieve a high degree of reliability and repairability. A number of design features which bear mentioning are discussed below. As indicated in Section 3, the instrument was designed to perform two measurements, firstly, the voice band noise input impedance difference with respect to a standard impedance, and secondly, near end crosstalk attenuation at 1.6 kHz. These are performed on all 100 pairs for the first, and all combinations of the 100 pairs for the second. Both measurements require active circuitry at the sending end only, with the remote end being passively terminated.

However, the main feature of the ACT is that, it is, in effect, a switching unit which sequentially brings all combinations of two pairs to the terminals of the test equipment. For the above-mentioned tests, the test equipment for measuring the input impedance and NEXT is internal to the ACT; however, any two pairs can be accessed from the front panel by the switching circuitry so that additional tests can be conducted as required using the ACT simply as a pair selecting instrument. A test normally conducted in this manner is that of the DC loop resistance of all pairs, typically carried out before the AC measurements, in order to verify that all the 200 contacts in each of the MDF access plugs at the measuring and terminating ends are satisfactory (although of course the input impedance measurement would identify any faults).

For the impedance difference measurement, the reference impedance is taken as the input impedance of pair 1 (or any other pair), which has been thoroughly checked using conventional techniques. However, an alternative is to use an external reference which may be a pair from another cable which is identical to the one under test or a lumped simulation of Z, the nominal characteristic impedance. This is easily done by selecting pair 000 as the reference by the switches on the front panel of the ACT.

As it is intended to determine whether the cable under test meets required performance limits, the ACT is designed to give a "go/no go" result against predetermined limits for both the input inpedance difference and crosstalk measurements. The instrument cycles through all pairs or pair combinations as appropriate, stopping with a visual alarm when a "no go" result is detected. The operator then assesses the situation by noting the meter readings and arranging for further action. However, if there are two or more pairs which are split due to errors in splicing, then many pair combinations will have a crosstalk performance which is below specification.

As an aid to locating the pairs which are actually split, the threshold limit can be reduced from 65 cr 70 dB to say 40 dB with the result that, only when these defective pairs are tested, will the new limit be exceeded. After correcting the faults, the cable is again tested using the normal acceptance limits.

6. CCNCLUSION

This paper has described the philosoppy behind the selection of appropriate tests to determine the suitability of installed telecommunication cable pairs, both loaded and "mloaded, for voice frequency transmission.

It has beer shown that tests which require active circuitry only at one end, with a passive termination at the remote end, can give adequate information for acceptance purposes, particularly

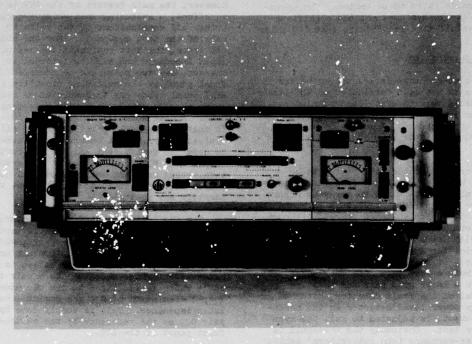


Fig. 4 The ACT Master Unit

if these tests are carried out from both ends. The use of these tests enabled an Automatic Cable Tester which is compact, reliable and relatively simple, and which can test 100 pairs in one operating cycle, to be developed. The heart of the instrument is the MDF access plug, controlled by the master unit, which makes contact with 100 pairs on the MDF link block, and then connects the pairs required for testing to the master unit.

As the ACT requires approximately six minutes to completely test a 100 pair unit (or an equivalent number of pairs from multiple smaller units), improved productivity, as well as accuracy, has been achieved in acceptance testing of both interexchange and subscribers' cable.

7. SPECIFICATIONS

Dimensions (including handles)

- . Master Unit : 500 mm \times 385 mm \times 165 mm (w \times d \times h)
- MDF Access Plug : 310 mm × 220 mm × 150 mm (w × d × h)
- . Number of Pairs Tested in One Operation

100, contained in one MDF link block.
Tests Conducted

Band Limited White Noise Input Impedance Difference against a known good pair or other reference impedance (Relative Return Loss, RRL), on all pairs. Near End Crosstalk (NEXT) for all pair combinations.

Testing Time

- . RRL 90 seconds for 100 pairs
- MEXT 270 seconds for all combinations of 100 pairs (normal and reverse from one end only).

8. ACKNOWLEDGEMENTS

The permission of the Chief General Manager, Australian Telecommunications Commission, (Telecom Australia) to publish this paper is gratefully acknowledged. In addition, the authors would like to acknowledge the assistance of Mr J.K. Lynch for his help in preparing the manuscript.

9. REFERENCES

- 1. L.J. Hall, "Return Loss and Transmission Distortion Due to Structural Irregularities in Coaxial Cable", 27th International Wire and Cable Symposium, 1978.
- 2. L.J. Hall, "Assessment of Telecom Australia Coaxial Cables for High Speed Digital Transmission", Symposium on Digital Communication Systems, University of New South Wales, December 1977.
- 3. P.I. Somlo, "The Locating Reflectometer", IEEE Trans. Microwave Theory and Techniques, Volume MTT-20, Number 2, 1972.



M.W. Tisdale, Telecom Australia, 28/570 Bourke St., Melbourne, Victoria, 3000 Australia

M.W. Tisdale joined Telecom Australia as a Technician-in-Training in 1957. Extensive field experience in the area of transmission measurements provided him with a sound knowledge of the necessary requirements of automatic cable measurement leading to his contribution to the overall design concepts which ensured the success of the project. He is currently Senior Technical Officer at Telecom Australia's External Practices Development Facility, Headquarters.



L.J. Hall, Telecom Australia, 28/570 Bourke St., Melbourne, Victoria, 3000 Australia

L.J. Hall joined Telecom Australia as a Cadet Engineer in 1971, graduating in Electrical Engineering from the University of New South Wales in 1974. From 1974 to 1977, he did postgraduate work at the University of New South Wales in the field of cable propagation. In late 1977, he became Senior Engineer, Bearer Characterisation and Measurement, Cable Design and Specifications Section, Headquarters.



J.A. Lynch, Telecom Australia, 159 Heidelberg Rd., Northcote, Victoria, 3070 Australia

J.A. Lynch joined Telecom Australia as a Technician-in-Training in 1958. From 1963 to 1975 he was involved in both field and laboratory measurements of the transmission performance characteristics of system bearers. His involvement in the Automatic Cable Tester, Electronic and Physical Design and Construction, was between 1975 and 1978. He is presently Senior Technical Officer, Transmission Measurements Section, Victoria.



R.J. Pirotta, Telecom Australia, 14 James St., Summer Hill, NSW, 2130 Australia

R.J. Pirotta graduated in Electrical Engineering from the University of Sydney in 1971 and then joined Telecom Australia, New South Wales administration. He has worked in the areas of carrier equipment commissioning and transmission measurements, which led to his involvement with the Automatic Cable Tester, particularly the MDF Access Plug. He is currently involved in the area of cable pretection in the Lines Practices and Protection Section, New South Wales.



L.A. Kiss, Telecom Australia, 28/570 Bourke St., Melbourne, Victoria, 3000 Australia

L.A. Kiss graduated in Mechanical Engineering from the University of Melbourne in 1971 and then joined the Lines Construction Branch of Telecom Australia Headquarters. He has been involved with the design, specification and installation practices of all components of external plant. Currently he is Senior Engineer, Cable Specifications, Cable Design and Specifications Section, Headquarters.

A SHORT TERM WATER RESISTANCE TEST FOR FILLED SERVICE WIRE

William C. Reed

Bell Telephone Laboratories Norcross, Georgia

Abstract

Water enters air spaces in incompletely filled waterproof service wire by two major processes. In one process, water moves rapidly into some voids causing air to be trapped and compressed. In the other process, water slowly displaces the air in the voids. The ultimate water ingress can be predicted from the water contribution of either process. This allows a short term quality control test for water resistance to be devised which examines only the rapid compression process. Using air to create an artificial hydrostatic pressure head, this process is forced to completion in a few minutes.

I. Introduction

Filled telephone service wire provides the buried service connection between a distribution cable and a subscriber. An example of a filled service wire is shown in Figure 1. It consists of two twisted pairs of color-coded, polyethylene-insulated, 22 gauge, copper conductors. The pairs are bundled into a polyester-wrapped core, protected by a corrugated bronze shield and covered by an extruded PVC jacket. All available space within the shield is flooded with a flame-retardant thermoplastic filling compound.

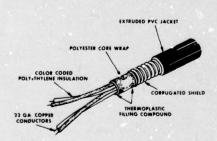


FIGURE 1. Filled Service Wire

The filling compound serves as a water barrier to block the radial and longitudinal distribution of water within the corrugated shield. Sufficient water within the shield can change the transmission characteristics of the wire and may even cause short circuits between exposed conductors. Therefore, filling the wire adequately during manufacture is an important requirement.

The degree of fill is monitored by a percent fill test and a 100 hour water immersion test. The percent fill test determines the fill of the wire core. The immersion test measures the average change in conductor capacitance to ground of a wire sample immersed under 1 foot of water, the core of the sample being exposed at two foot intervals by 1/2 inch slits.

These tests are not completely satisfactory. The percent fill test, which measures only the fill of the core, yields results that do not relate directly to capacitive changes caused by water anywhere under the shield. The immersion test is unrealistically long and the results are difficult to interpret.

This paper describes a single short term test which was developed to overcome these problems. The test is based on a theory for water ingress which is proven experimentally.

II. Test Methods

Experimental proof is obtained through two new tests similar to the percent fill and immersion tests above. The new percent fill test is based upon the total space available for fill. The new immersion test uses air pressure to force water into the wire structure rapidly, thereby reducing test time to a few minutes.

A. Percent Fill Test for Space Within the Shield

The percent fill test is performed on 12" wire samples which are carefully cut to length to avoid distortion of the sample.

The percent fill, F, is computed as follows:

$$F = \frac{W - W_{\text{tube}} - W_{\text{c}}}{\left(V_{\text{tube}} - V_{\text{c}}\right) \rho_{\text{f}}} \times 100\%$$
 (1)

where

W is the weight of the sample

W_{tube} is the weight of the sheath tube (the jacketed shield with core and filling compound removed)

W is the computed weight of the core materials except filling compound

V_{tube} is the volume of the sheath tube determined by filling the tube with a measured volume of water

V_c is the computed volume of the core materials except filling compound

of is the density of the filling compound.

Accuracy of test results is within 6%.

B. Pressurized Water Immersion Test

A pressure cell for rapid testing of service wire is shown in two views in Figure 2. The cell consists of a 3/4 inch diameter plastic pipe with associated valves, coupling, and adapters capable of withstanding 100 psi pressure.

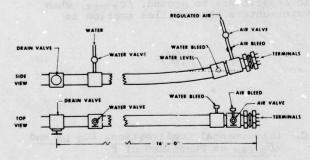


FIGURE 2. Pressure Cell for Water Resistance Test

Water fills the cell except for a small air space at one end. The small air space permits rapid changes in pressure while limiting the stored energy of the compressed air to a safe level.

A 15 foot wire sample is used for the test. The core is exposed at two foot intervals by 1/2 inch slits cut through the jacket and shield. At one end, the insulated conductors are bent over and taped to the jacket to prevent water from reaching bare

conductor ends. At the other end, the shield and each conductor are connected to the terminal plate.

The sample is sealed in the cell and the ground component of mutual capacitance of each conductor is measured. The cell is then filled with water. Opening the air valve instantaneously pressurizes the cell. Change in capacitance, ΔC_g , is monitored as a function of time.

III. Development of Relationship of Short Term ΔCg to Long Term water Ingress

A theory for water ingress into a wire structure will now be developed together with confirming experimental data. First, the processes of water entry are examined to predict the total volume of water, Vwater, which eventually enters the wire. Vwater depends on percent fill and water pressure and is directly proportional to the long term change in the ground component of mutual capacitance, $\Delta C_{\rm g}$ LT. $\Delta C_{\rm g}$ LT is shown to be related to a short term change, $\Delta C_{\rm g}$ ST, resulting from the rapid filling of voids which trap and compress air.

 $\Delta C_{\rm G}$ ST is measured in the short term test. This measurement may be compared to a test limit for properly filled wire and may be used to determine percent fill. Through percent fill, the long term change $\Delta C_{\rm G}$ LT can be calculated for any water pressure.

A. Water Ingress

If the wire is incompletely filled, water may collect in the unfilled space (voids). The total volume of air voids, $V_{\rm A}$, is the volume of missing compound. $V_{\rm A}$ may be expressed in terms of percent fill, F, as

$$v_{A} = \left(\frac{100-F}{100}\right)V \tag{2}$$

where V is the volume available for fill.

Water can enter only those voids which connect by a channel to the outside of the wire. The probability of the existence of a channel depends on F. It is 1 for F = 0% and 0 for F = 100%. Assuming that this probability is linearly related to F, the total volume of accessible voids, $V_{\rm A}$, is

$$V_{\mathbf{A}'} = V_{\mathbf{A}} \left(\frac{100 - F}{100} \right) \tag{3}$$

V_A' is composed of voids which completely fill with water if air is free to escape (open voids) and voids which partially fill if air is trapped (closed voids). Therefore

$$V_{A}' = V_{T} + V_{F} \tag{4}$$

where $V_{\rm T}$ is the total volume of closed voids and $V_{\rm F}$ is the total volume of open voids.

The probability for each type of void also depends on F. The probability for V_T is 0 for F = 0% and 1 for F = 100%. Assuming that this probability is also linearly related to F, V_T is given by

$$v_{T} = v_{A} \cdot \left(\frac{F}{100}\right) \tag{5}$$

When a wire initially under atmospheric pressure, P_A , is placed in water under a hydrostatic pressure of P_O , water moves into the accessible voids until equilibrium is established. Figure 3 illustrates the equilibrium condition. The air in V_T has been compressed to a volume of V_O at pressure P_O . Water fills the remainder of V_T and all of V_T .

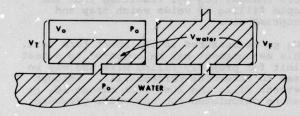


FIGURE 3. Equilibrium Condition, Water Pressure Equals Pressure of Compressed Trapped Air

The total volume of water which entered the voids, $V_{\mbox{Water}}$, may be written as

$$v_{\text{water}} = v_{\text{A}}' - \frac{P_{p}}{2} v_{\text{T}}$$
 (6)

By combining Equations (2), (3), (5), and (6) $V_{\mbox{water}}$ becomes

$$v_{\text{water}} = \left(\frac{100 - F}{100}\right)^2 \left[1 - \frac{P_A}{P_O} \frac{F}{100}\right] v$$
 (7)

The volume of water, $V_{\rm water}$, which finally enters a given length of wire is small (on the order of 10^{-1} in per foot). This volume is therefore difficult to measure directly. Its effect on the components of mutual capacitance, however, is quite large. The ground component is particularly sensitive.

B. ΔCq in the Long Term, ΔCg LT

Entry of water into the wire structure causes the ground component of the mutual

capacitance of each conductor, C_g , to increase. The average percent change, ΔC_g , is given by

$$\Delta C_{g} = \frac{1}{n} \sum_{i=1}^{i=n} \frac{C_{gi}(\text{wet}) - C_{gi}(\text{dry})}{C_{gi}(\text{dry})} \times 100$$
 (8)

where n is the number of conductors.

If water is distributed randomly throughout a wire, ΔC_g is proportional to the volume of the water. If water entry is complete, the amount of water, $V_{\rm water}$, is described by Equation (7). The expression for ΔC_g in the long term, ΔC_g LT, is then

$$\Delta C_{SLT} = \left(\frac{100-F}{100}\right)^2 \left[1 - \frac{P_A}{P_O} \frac{F}{100}\right] K$$
 (9)

where K is a constant of proportionality including V. K may be evaluated from the value of ΔC_{g} LT which occurs when an unfilled wire (F = 0%) is filled with water. For the wire shown in Figure 1, K = 273%.

If the distribution of water is not random but is arranged for maximum ΔC_g at a particular F, that arrangement will consist of sections of completely filled and completely unfilled wire. The maximum change in capacitance to ground, ΔC_g max, when water enters the unfilled section is

$$\Delta c_{g \text{ max}} = \left(\frac{100 - F}{100}\right) K \tag{10}$$

C. Experimental Confirmation, ΔC_g LT and ΔC_g max as Functions of F

 ΔC_g LT (Equation (9)) for $P_O=34.7$ psia and ΔC_g max (Equation (10)) are plotted as functions of F in Figure 4. Plotted also are the ΔC_g LT values for wire samples of various fills immersed in water at $P_O=34.7$ psia.

The data in general fits closely to the curve with some scatter. This scatter is caused by the accuracy of determining percent fill (±6%) and by the nonrandom distribution of water within the wire structure, e.g., missing fill over the core wrap. Note that no data points fall below the curve representing completely random distribution of voids.

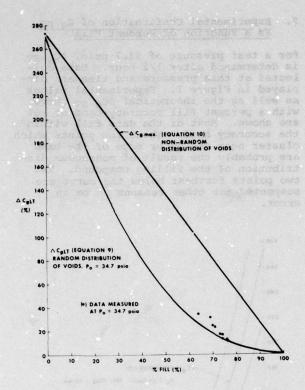


FIGURE 4. $\Delta C_{g\ LT}$ and $\Delta C_{g\ max}$ as Functions of Percent Fill, F

D. Experimental Confirmation, Contribution of Each Process to ΔC_q LT

 ΔC_g is plotted against time in Figure 5 for one wire sample having F = 77%. The sample was subjected to 34.7 psia for about 1400 minutes at which time pressure was reduced to atmospheric pressure. Reducing the pressure allows compressed air, trapped in some voids, to force water from the wire.

The total volume of water which eventually entered the wire is given by Equations (5) and (6) as

$$v_{\text{water}} = 0.67 \, V_{\text{A}}$$

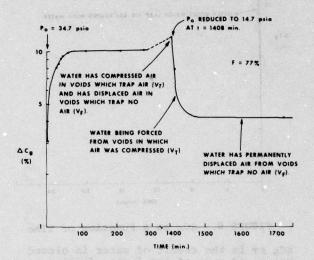
which gives rise to the long term change, $\Delta C_{\mbox{\scriptsize g}}$ $_{\mbox{\scriptsize LT}}.$

After pressure was reduced, only open voids were holding water. The total volume of these voids is given by Equations (4) and (5) as

$$V_{F} = 0.23 V_{A}'$$

which accounts for 34.3% of the long term change, $\Delta C_{\mathbf{q}}$ LT.

 $\Delta C_{\rm G~LT}$ from Figure 5 is experimentally determined to be 12.2% (at t = 1408 minutes). After pressure was reduced, $\Delta C_{\rm G}$ recovered to 4.2%. This compares favorably to the theoretical calculation of 4.18% (34.3% of $\Delta C_{\rm G~LT}$).



FIGURL 5. ACg as a Function of Time Showing the Effects of Both Types of Voids

E. ΔCq in the Short Term, ΔCq ST

The process of trapping and compressing the air in a void by entering water is completed rapidly, as shown in Appendix A. The time constant for this process is determined by the void and channel geometry and is inversely proportional to the square of the hydrostatic pressure

Open voids fill slowly with water. The time constant for this process depends on the pressure difference between the water inlet and air outlet channels of the void as well as the geometry of the void and its channels (see Appendix A).

The experimentally observed sharp knee in plots of ΔC_g vs. time, Figure 6, confirms the different time constants of these two processes. Before the knee, mostly closed voids are filled. After the knee, mostly open voids are filled.

The volumes of water contained in each type of void are functions of F and together determine ΔC_g LT. Because of these relationships, a short term measurement of ΔC_g at the knee of the curve, ΔC_g ST, can be used to predict ΔC_g LT.

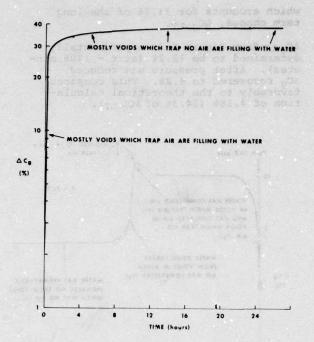


FIGURE 6. ΔC_g as a Function of Time

 ΔC_g ST is the result of water in closed voids and some of the faster filling open voids. The contribution of the open voids depends on the geometry of the air passages, and decreases with increasing fill. ΔC_g ST is proportional to the volume of water entering in the short term and

$$\Delta C_{q ST} \alpha \left(V_{water} - V_{F} \right) + \left(\frac{100 - F}{100} \right) V_{F}$$
 (11)

Since ΔC_g LT is proportional to V_{water} , then

$$\Delta C_{g ST} = \left[\frac{V_{water} - \left(\frac{F}{100}\right) V_{F}}{V_{water}} \right] \Delta C_{g LT}$$
 (12)

By combining Equations (2), (3), (4), (5), (7), (9), and (12), $\Delta C_{g~ST}$ may be expressed in terms of percent fill as

$$\Delta C_{g \text{ ST}} = \left(\frac{100 - F}{100}\right)^{2} \left[1 - \frac{P_{A}}{P_{O}} \left(\frac{F}{100}\right) - \frac{F}{100} \left(\frac{100 - F}{100}\right)\right] K \quad (13)$$

F. Experimental Confirmation of C_q ST as a Function of Percent Fill

For a test pressure of 34.7 psia, ΔC_g ST is determined after 1/2 hour. Data collected at this pressure and time are displayed in figure 7. Experimental values as well as the theoretical ΔC_g ST curve with a percent fill accuracy band of ±6% are shown. Most of the data fall within the accuracy band. Those few points which cluster near the upper edge of the band are probably the result of nonrandom distribution of the filling compound. The two points furthest below the curve are suspected for other reasons to be in error.

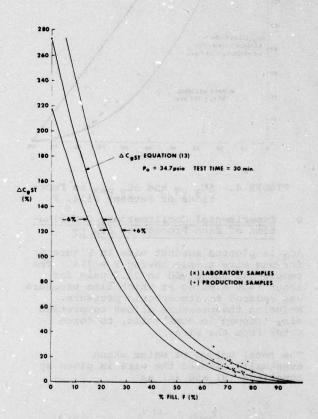


FIGURE 7. $\Delta C_{g \ ST}$ as a Function of Percent Fill, F

G. Determination of Test Requirements for $\frac{\Delta Cg}{\Delta T}$

Commercially produced samples over a period of 6 months were randomly selected and tested by the 100 hour water immersion test and the percent fill test described in Section II-B. The results indicated that the possibility of failing the 100 hour test increased abruptly below 62% fill.

Some of these samples were tested to determine ΔC_g ST. The data is shown in Figure 7. ΔC_g ST for most production samples is less than 20%. By Equation (13), C_g ST is calculated to be 19.8% for F = 62%, P_O = 34.7 psia. Equation (9) predicts that a wire with 62% fill immersed under 1 foot of water (15.1 psia) will experience a long term change, ΔC_g LT, of only 15.6%.

This study demonstrates that a well-manufactured sample of wire can be routinely produced to meet a short term test requirement of ΔC_q ST = 20% when subjected to 34.7 psia for 1/2 hour.

IV. Conclusion

The change in the ground component of mutual capacitance in the short term, $\Delta C_{\rm g}$ ST, is mainly the result of water entry into voids which trap air. Measurement of $\Delta C_{\rm g}$ ST may be used to determine the percent fill of the wire and to predict the long term change, $\Delta C_{\rm g}$ LT.

References

- C. J. Aloisio and E. D. Nelson, "Effect of Water and Petroleum Jelly Migration on Capacitance of Plastic Insulated Cables," 22nd International Wire and Cable Symposium, December 1973.
- H. Lamb, "Hydrodynamics," (New York: Dover, 1945) p. 585.
- H. B. Dwight, "Tables of Integrals and Other Mathematical Data," (New York: McMillan).

Appendix A

Time Constants for Water Ingress

The change, ΔC_g , as a result of water ingress is not instantaneous. It takes place over a period of time determined by the rate at which water enters voids in the filling compound of the wire.

A. Voids Which Trap Air

Consider a single cavity of volume V_{t} connected to the outside of the wire by a small passage. See Figure A1. At some time t the cavity contains some water, V_{w} , and some air, V_{a} , so that

$$v_t = v_w + v_a . (A1)$$

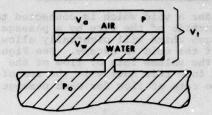


FIGURE Al. Water Flow into a Cavity Which Traps Air

At the time t water pressure, $P_{\rm O}$, has compressed the trapped air to a pressure $P_{\rm O}$. Water moves into the cavity until $P_{\rm O}$ = P and then $V_{\rm a}$ = $V_{\rm O}$. Assuming the compression to be isothermal

$$PV_a = P_O V_O \tag{A2}$$

From Poiseuille's Law, 2 the volume rate of flow of water into the cavity is

$$\frac{dv_{w}}{dt} = G(P_{O} - P)$$
 (A3)

where $\mathrm{d}V_{\mathrm{W}}/\mathrm{d}t$ is the volume rate of flow and G is a constant which includes the viscosity of water and the passage geometry.

By combining Equations (A2) and (A3), the volume rate of flow may be expressed as

$$\frac{dV_{w}}{dt} = G\left(P_{o} - \frac{P_{o}V_{o}}{V_{a}}\right) \tag{A4}$$

and

$$\frac{V_{t} - V_{w}}{V_{t} - V_{w} - V_{o}} dV_{w} = GP_{o} dt$$
 (A5)

To determine the volume of water, $V_{\rm W}$, in the cavity at any time, t, Equation (A5) is integrated.

$$\int_{0}^{V_{w}} \frac{v_{t} - v_{w}}{v_{t} - v_{w} - v_{o}} dv_{w} = \int_{0}^{t} GP_{o} dt$$
 (A6)

Evaluation of Equation (A6) yields a time constant, 3 τ_{t} , for the flow of water into a cavity which traps air and for the change, ΔC_g . The time constant

$$\tau_{t} = \frac{k}{GP_{o}^{2}} \tag{A7}$$

For elevated pressure, such as those used in testing, τ_t is small.

B. Voids Which Do Not Trap Air

Consider a void which is connected to the outside of the wire by a passage or passages which will eventually allow the air of the void to escape. See Figure A2. The volume rate of flow of the water into this cavity is the sum of the volume rate of flow for each passage, Qi.

$$\frac{\mathrm{d}\mathbf{v}_{\mathbf{w}}}{\mathrm{d}\mathbf{t}} = \sum_{j=1}^{n} Q_{j} \tag{A8}$$

where n is the number of passages.

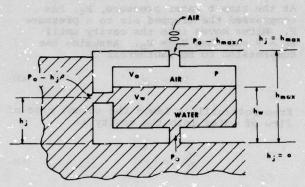


FIGURE A2. Water Flow into a Cavity
Which Allows Air to
Escape

The pressure at the jth opening, P_{oj} , is

$$P_{oj} = P_o - h_j \rho \tag{A9}$$

where h_j is the height of the entrance port above h_j = 0.

The volume rate of flow for each passage is now expressed as

$$Q_{j} = G_{j} \left(P_{Oj} - \left[P + \left(h_{w} - h_{j} \right) \rho \right] \right)$$
 (A10)

where $h_{\mathbf{w}}$ is the height of the water within the cavity referenced to h_j = 0 and ρ is the density of water.

Since air escapes, the pressure of the air in the cavity adjusts to the pressure of the water at the escape port. Thus,

$$P = P_{O} - h_{max} \rho \tag{A11}$$

where h_{max} is the vertical position of the escape port.

Combining Equations (A9), (A10), and (A11) the volume rate of flow for each passage is

$$Q_{j} = G_{j} (h_{max} - h_{w}) \rho$$
 (A12)

and the total volume rate of flow is

$$\frac{dV_{w}}{dt} = \sum_{j=1}^{n} G_{j}(h_{max} - h_{w})\rho$$
 (A13)

For a cavity with vertical sides $h_{\mathbf{W}}$ may be expressed in terms of $V_{\mathbf{W}}$ as

$$h_{W} = \frac{V_{W}}{A} \tag{A14}$$

where A is the cross sectional area of the cavity.

Equation (Al3) can now be solved to determine the volume of water, $V_{\rm W}$, in the cavity at any time, t. The solution is

$$\int_{0}^{V_{w}} \frac{dv_{w}}{\sum_{g_{j}} h_{max} \rho - \sum_{g_{j}} \frac{v_{w}}{A}} = \int_{0}^{t} dt$$
 (A15)

which yields the time constant for filling the cavity with water, $^3\ \tau_{\text{f}}$, as

$$\tau_{f} = \frac{p}{\sum_{j} G_{j} \rho}$$
 (A16)

or, since Ah_{max} is the volume of the cavity $\mathrm{V}_{\text{f}}\text{,}$

$$\tau_{f} = \frac{v_{f}}{\sum_{G_{j} \cap h_{max}}}$$
(A17)

where ρh_{max} is the hydrostatic pressure difference across the void. ρh_{max} is exceedingly small so that τ_f is generally large.

C. Time Constants and Water Ingress into a Wire

The preceding discussions concern only single cavities. A wire contains a number of cavities each with unique characteristics which determine its time constant for filling with water. As a consequence, any water dependent phenomena for the wire, examined and plotted as a function of time, will produce a curve which is a composite of the curves for the individual water filling processes.



William C. Reed is a member of the Multipair Cable and Wire Department, Bell Telephone Laboratories, Norcross, Georgia. He received a BA in mathematics and physics from Wittenberg University in 1959 and an MA in physics from Wake Forest University in 1969. He joined Bell Laboratories in 1970 and has worked on the design and development of test methods and test equipment for loop maintenance. His present responsibilities concern outside plant service and distribution wires.

RECYCLING OF PVC FFOM CABLE AND WIRE SCRAP

E. Scalco R. L. Decker R. C. Donovan A. F. Rodde

Bell Laboratories Mountain Avenue Murray Hill, N.J.

Western Electric Corporation 222 Broadway New York, New York

Abstract

A system is described which is capable of reclaiming poly(vinyl chloride) plastic from cable and wire scrap. The reclaimed material is subsequently refined using some novel techniques and is then reformulated to yield compounds which are useful in cable jacket applications: some reformulation variables are delineated. Evaluation of substantial factory trials and economic and environmental implications are discussed.

present the only such Bell System process in regular operation is reclamation and recycling ABS from unrepairable telephones. 6 In addition, a two-snot molding technology was developed for recycling scrap plastics in high quality applications.

The purpose of this paper is to relate how the Bell System developed a new technology for reclaiming PVC from post-consumer, or field, wire and cable scrap, and how the reclaim was refined and subsequently recompounded, such that the resulting material can be used to jacket new cables. This technology was achieved through coordinated efforts of personnel from Bell Laboratories, Nassau Recycle Corp. and WE Company.

Introduction

A significant part of Bell System plant is continually undergoing change. In outside plant old cables are removed and replaced. In customer premises telephones as well as associated station wire and small switching and other equipment are regularly installed, supplanted, relocated or removed. In central offices (CO's) old equipment is updated or replaced by new, and main-distributing frame connections are altered continuously.

A consequence of this activity is the annual generation of almost 400 million 1b. of post-consumer scrap. In addition, a much smaller, but significant amount of scrap is produced at Western Electric (WE) manufacturing facilities. The scrap contains many important materials such as copper, lead, precious metals, plastics, etc., and since 1931, Nassau Recycle Corporation (NRC) a subsidiary of WE Company, has been reclaiming and recycling much of the metals from this scrap for Bell System reuse. 1-4 In addition, for the

past several years, the Bell System has been artive in recycling acrylonitrile-styrene-butadiene (ABS) plastic from factory scrap, 5 while polyethylene (PE) and poly(vinyl chloride) [PVC] extruder purgings and cable sheath strippings from factory scrap have undergone primary recvcling. The above are some important examples of plastics PVC Cable and Wire Scrap

The Bell System uses plastics mainly as insulation and jacketing on transmission wire and cable, as cable conduit, and in telephone housings and cords. PVC is used primarily in telephone CO's and customer premises as wire insulation and cable jacket because of its inherent fire retardan y. Depending on the product end-use requirements, and the compound in use at the time, widely different types of vinyl compounds containing many additives are found in these installations. In addition, in CO's many of the wires insulated with PVC are also protected by a serving or braid of cotton which is coated by a fire retardant lacquer. Also, some other PVC wires are covered with a nylon jacket. In 1973 a new insulation was introduced to replace some of the textile covered wires. It uses a novel PVC compound which is crosslinked by high energy electron irradiation 8 (IPVC). A significant amount of power cable insulated with a variety of flame retardant rubbers are also located in CO's.

The reclamation process of much of the PVC cable and wire field scrap begins in the CO's where Operating Company personnel generate and collect scrap while installing new equipment, or making routine changes in the main distributing frame. It is then shipped to WE Regional Service Centers and then to NRC (Figures 1 and 2).

It is clear from the foregoing that although the major fraction of this scrap is PVC insulated wire, substantial amounts of other materials are also present including small quantities of

reclaimed from relatively clean scrap. However, reclamation of scrap plastic after consumer use and after it has been joined with other materials is a significantly more complex problem. At

telephone equipment, PE, pulp and rubber cables, old tools, small chassis, etc. Understandably, this complicates the recycling effort.

The Recycling Process

By virtue of economic, technical and environmental factors, the best approach for the reclamation was determined to be mechanical granulation (or chopping). Two different chopping systems have been installed at NKC's Staten Island, N.Y. and Gaston, S.C. facilities for the recovery of copper and for development and production trials on the recycling of PVC. The more recent one will be discussed.

The first phase involves considerable sorting to eliminate materials which may be injurious to the granulation equipment or may interfere with the recycling of copper and plastic (Figure 3).

After sorting, the post-consumer scrap is first cut to a size which can be accepted by the granulators where it is further reduced in size until it is liberated into its various components.

The succeeding phase, aspiration, is designed to remove liberated textile which becomes fluff-like after granulation. Aspiration ports are placed at various points in a mechanical system but the most effective are those located immediately after granulation.

The last phase has as its specific function the separation of the granulated copper and plastic into mainly three fractions: copper, plastic and middlings (pieces of wire whose insulation has not separated from the conductor). This is accomplished with a series of screener and gravity shaker tables. The resultant plastic fraction forms the starting material for the post-treatment, or refining steps (Figure 4).

Impurity Removal Processes

The chopped plastic issuing from the granulation system contains too many contaminants to be recycled without further treatment. The non-metal contaminants (4 %) are mainly textile, IPVC, rubber, phenolics, nylon and PE, while the metal contaminants, mostly copper, varies according to chopping conditions.

More than 90% of the plastic particles are larger than 40 mesh and the majority have sizes between 30 and 20 mesh. Since the contaminants have roughly the same size distribution, dry screening of the impurities proved ineffective.

Many separation techniques were studied: airgravity tables, fluidized beds, liquid systems, solvent processes, air elutriation, electrostatic separation, cryopulverizing, etc.. The efficiency of the separation systems of interest was always significantly de reased by the presence of textile fluff in the plastic. In addition, the fluff entraps copper and plastic particles. To liberate the plastic from the fluff a new process, called an air vortex aspirator, or more simply a Putfer, was conceived and developed (Figure 5). In the Puffer, the plastic fraction is subjected to a turbulent air stream with high shear and acceleration fields. The liberated textile and dust-like material are then separated from the plastic, copper and other "heavy" materials, by a counter-flow air elutriation column. This system has successfully reduced the textile and dust contaminants to very low levels and contributed significantly to the effectiveness of the downstream refining systems.

Next, an electrostatic separator (see Figure 6) is used to remove most of the conductive metallic impurities, including the middlings, from the plastic output stream of the Puffer. In this apparatus particles are sprayed by a corona discharge and deposited on a rotating grounded cylinder. The plastic particles retain their charge and adhere to the rotor, while the metals rapidly leak their charge to the rotor and are thrown from the rotor by centrifugal action. By staging several rotors, usually ~95% of the metals are removed. Criteria that the copper impurity must be reduced to a low level and that the processing costs must be low are satisfied by this process.

After the electrostatic separator, the impurity level in the plastic stream is typically about 2-3% consisting principally of rubber, IPVC, nylon, phenolics and middlings. These are removed by extrusion screening (Figure 7), and the contaminants level after this process is about 0.5% and, since the large particles are filtered (Figure 8) only small contaminants are present.

It had been learned that the finest screen meshes provide the most effective impurity removal but result in a rapid rise of extruder head pressure (Figure 9). Furthermore, using meshes finer than 60 yield material with improved appearance but without further improvement in significant properties, such as resistance to low temperature embrittlement (LTB)⁹ as shown in Figure 10.

Although in typical applications commercial screen changers are cycled manually after hours of production, this reclamation process requires screen changing every few minutes. To accomplish these frequent screen changes in a production environment new automatic screen changing equipment was developed.

The beneficial effect of contaminants, removed by the post-treatment processes cited above, on two properties of the resulting PVC reclaim is shown in Table 1. However, not only the amount, but also the type of contaminant removed seemed to be important (Figure 11).

Reformulation of the PVC Reclaim

Because of the relatively large quantity of this reclaim material becoming available in the near future, large volume applications seemed appropriate. Uses outside the Bell System seemed to be limited principally to garden hose core or to carpet backing. It was thus decided that an attempt should be made to use the reclaim in cable jacket applications where electrical and colorability requirements are substantially less than in primary insulation. However, PVC jacket materials used in the Bell System's communication cables have other very stringent requirements such as: excellent fire retardance: resistance to low temperature embritlement; resistance to tear, cut-through, and general installation and field abuse; good extrudability; etc.

The reclaim material was deficient in many of these requirements. However, it is not surprising that these deficiencies should exist in this reclaim if one considers that it results from a mixture of many FVC compounds, some of which had been in service for 25 years or longer, and which were formulated for widely different applications during an earlier technology. Moreover, the reclaim has been subjected to extensive mechanical and thermal stresses during the reclamation and extrusion screening operations, respectively.

Nevertheless, it was possible to reformulate, or recompound, this mixture of PVC compounds by admixing specific quantities of selective plasticizer, stabilizer, fire retardants, internal and external lubricants and colorants, such that the resulting properties would closely follow those of new compounds. Following are some illustrations of how some critical physical properties of the PVC reclaim are affected by incorporation of some of the additives listed above.

In order to achieve both good flame retardancy, as measured by limiting oxygen index 10 (LOI), and acceptable LTB, a very efficient plasticizer* was chosen so that only a small addition to the PVC reclaim was necessary. However, plasticizers of this type are flammable and therefore add to the flame retardation problem. Figure 12 shows that addition of 3 phr of the classical flame retardant, $\mathrm{Sb}_2\mathrm{C}_3$, to the PVC reclaim increases LOI from 27% to 29% ($\sim31\%$ was desirable for one significant application). Higher concentrations of Sb203 did not impart additional flame retardancy. It was found that an additional flame retardant, Al203.3H20, improved the LOI but had a negative effect on the LTB of PVC. Al203.3H20 is available as a fine powder and it was determined that, regardless of surface treatment (through the use of coupling agents), its particle size distribution dominated the effect on LTB, as shown in Figure 13. Clearly, in plasticized PVC the optimum average particle size is near 1.0 μm . Using material of this optimum size, its beneficial effect on LOI and its deletorious effect on LTB of PVC reclaim is shown in Figure 14. Although not shown in this figure,

Al₂O₃·3H₂O also had a significant adverse effect on the cut-through performance of PVC reclaim, as measured by Shear Resistance* test.

In applications where electrical resistivity had to be improved, a variety of clays and silicas were added to the PVC reclaim. However, as shown in the example of Figure 15, the improvement in resistivity was accompanied by a penalty of a large decrease in LTB.

Cabling Trials

Using the process outlined above PVC has been reclaimed from field scrap and recompounded in a production environment.

Cable jacket extrusion trials have been performed at the Atlanta and Baltimore Works involving over 60 thousand pounds of "reconstituted" PVC reclaim and over one million feet of cable. After extensive laboratory testing (see for example Tables 2 and 3), the cables have been sold to the Telephone Operating Companies where they are being successfully used.

The types of cable made included: nine different sizes of Central Office cables varying in size from 6 to 300 conductors of 22, 24 and 26 AWG; three different sizes of cable for customer premises; three different types of underground cable and one outside plant wire (see Figure 16).

All the above cables have performed well during manufacturing and on product tests, however, upon close scrutiny, small protrusions on the jacket surface can be detected; therefore, it is expected that, unless the present low level of residual contaminants in the reclaim, ~0.5% can be reduced economically, it is improbable that such cable jacket will be used widely in locations of high visibility in cuctomer's premises. It is expected, however, that the "reconstituted" reclaim will find wide usage in underground cables where flame retardance is required, in Central Office or switchboard cable, and possibly in other cables such as stub cables.

An exhaustive production cabling trial has shown that variation among ten 1,000 lb. lots of the "reconstituted" PVC reclaim is acceptable for normal WE plant manufacturing. The principal physical and chemical properties of each lot varied only within narrow limits as shown in Table 4.

Status of the Recycling System

NRC has expanded its facilities by constructing a new plant in Gaston, South Carolina and the scrap PVC wire and cable is reclaimed at this new

^{*} Permanence is also of primary importance, therefore a plasticizer of low volatility had to be selected.

The load required to cut through a 0.075" thick plaque of plastic with a steel wedge 1.0" in length, a 450 angle, with a 0.030" flat cutting edge and moving at 2.25"/min.

facility. As mentioned previously, by 1981 it is expected that about 15 million pounds of PVC $\,$ will be reclaimed yearly. This plastic can be recompounded at the WE-Baltimore Works or at outside compounders to meet specific needs of the WE cable plants. The overall economics of this reclamation have been examined and the potential net savings are substantial. A comparison of the energy consumption between reclaimed PVC and virgin PVC shows that the energy equivalent of 2 pounds of crude oil is saved for every pound of PVC recycled. Since the proposed recycling system poses no air or water pollution problems and decreases the solid waste significantly, it is an environmentally sound system. With Bell System scrap being an important supply of PVC for cable manufacture, the Bell System becomes less susceptible to the kind of material shortaces that every major industry experienced in 1974.

Summary and Conclusion

A system has been developed to recycle PVC plastic from scrap PVC wire and cable into cable jacket for new cable. The system is unique in that plastic from post-consumer scrap is recycled. Processes were developed for removing contaminants from the plastic and formulations were developed to recompound the plastic for high quality, primary applications. Production trials have demonstrated that the reclaimed plastic is suitable for cable jacket applications.

Acknowledgements

The work summarized herein would have been impossible without the close cooperation of many Bell System colleagues including engineers at NRC, WE Engineering and Research Center, Bell Laboratories at Atlanta, WE Baltimore Works, and WE Cable and Wire Products Engineering Control Center. Of major significance were the contributions of Messrs. A. Karp, and J. J. Taylor of Western Electric Engineering Research Center and Nassau Recycle Corporation, respectively.

References

- Donovan, R. C., Pompeo, A. J., Scalco, F., Bell Laboratories Record, <u>55</u>, 8 (1977).
- Donovan, R. C., Pompeo, A. J., Scalco, E., "Recycling PVC", presented to the Polymers and Energy Conservation Workshop, sponsored by U.S. Dept. of Energy, in Washington, D.C. (Nov. 3-4, 1977). Abstract TID-28553.
- Wehrenberg, R. H., II, Materials Engineering, 89, 3 (1979).
- " Waste Not Want Not", Telephony, <u>196</u>; 15 (1979).
- See for example, Beboington, G. H., 3PE Technical Papers, XXV, (1979).

- Hubbauer, P., Kern, H. E., SPE Technical Papers, XXV, (1979).
- Donovan, R. C., Rabe, K. S., Lord, H. A., Mammel, W. K., Pol. Eng. and Sci., <u>15</u>, 11 (Nov. 1975).
- See for example, Gladstone, H. M. and Loan, L. D., U.S. Pat. 3,623,940 (Nov. 30, 1971).
- 9. ASTM Standards, (D-746), Part 35.
- 10. ASTM Standards (D-2863), Part 35.
- Bell System Standard: The material is mixed at 205°C in a Plasticorder torque rheometer chamber until degradation is observed.

TABLE 1

Process	Non-Metallic Contaminants >250 Mesh (Wt. %)	LTB ¹	Process. 2 Stability (min.)
After Gross Sorting	5~10	13	5
After Sorting for PVC Reclamation	4.0	5	7
After Sorting + Puffer & Electrst.	Sep. 1.9	-2	13
After Sorting + Extrusion Screening	0.40	-8	20

- 1 Low Temperature Brittleness
- Plasticorder Processing Stability¹¹

TA	R	r.	E	2
***		м	**	-30

The second of th		
Low Temp. Impact	Reclaim	Virgin
Temp. (°C) - 13 (%) Failed	0	n
- 16	0	0
+ 18	0	0
- 23	20	20
U.L. Steiner Tunnel		
Flame spread (ft)	7.5	9.5
Smoke index	2330	2190
Oven Aging (Jacket)		
Retention of clong. (%)	74	72

TABLE 3

	Reclaim	Virgin
Low Temp. Impact		
Temp. (°C) -12 (% failed)	0	0
-18	, n	0
-23	10	80
U.L. 83 Flame Test	Pass	Pass
Progressive Cut-Through (1b-in/mil) 0.8	1.3
Instron Cut Through (1b/mil)	0.8	0.8
Abrasion (Revol./mil)	20	32

	TABLE 4			
		Average	Minimum	Maximum
Oxygen Index	+347 -	10 31.3	31.0	31.5
Low Temp, Brittleness	°c	-22	-21	-24
Shear Resistance	lb/in	600	530	670
Tear Strength	lb/in	460	400	500
Ult. Elongation		270	260	300
Ult. Tensile Strength.	psi	2050	1980	3140
Hardness, Sh. D.	units	45.6	45.0	46.0
Heat Distorsion	9	11.8	9.0	13.0
Ether Extractables	Wt. 9.	24.3	23.5	25.0
Contaminants >250 Mesh	Wt. 9.	0,23	0.12	1.4



Figure 1- Post-consumer Scrap at Nassau Recycle Corporation at Gaston, South Carolina



Figure 2- Unsorted PVC Scrap Wire and Cable

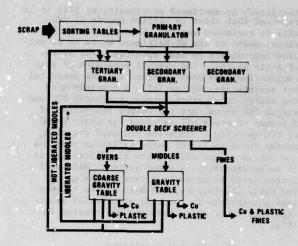


Figure 3- Flow Diagram of the Reclamation Process

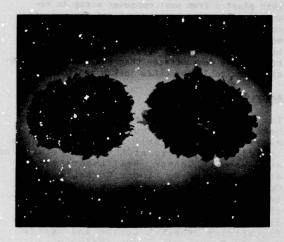


Figure 4- Plastic and Copper from the Chopping System

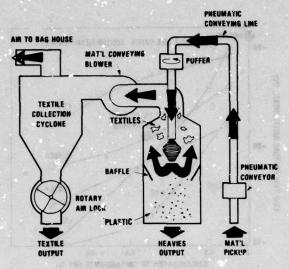


Figure 5- Air Vortex Separator (Puffer)
System

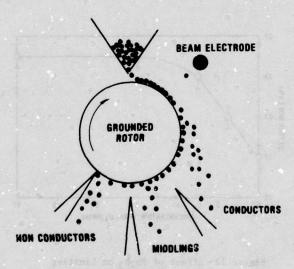


Figure 6- High Tension Separator

EXTRUSION AND SCREENING OF RECLAIMED PVC

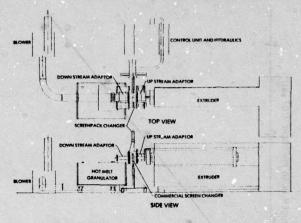


Figure 7- Schematic of Extruder With Automatic Screen Changer and Mot-Melt Granulator

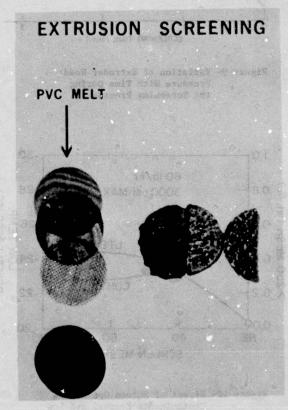


Figure 8- Screen From Filtering Extruder

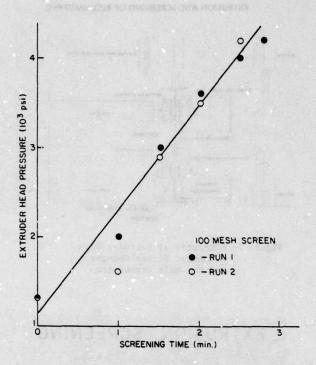


Figure 9- Variation of Extruder Head Pressure With Time During the Screening Process

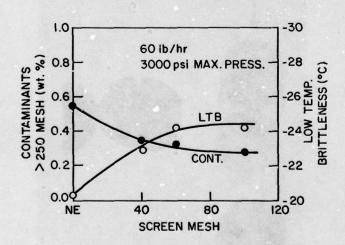


Figure 10- Effect of Screen Opening on Contaminants Removal and Low Temperature Brittleness (LTB) of Recompounded PVC Reclaimed from Carefully Sorted Scrap

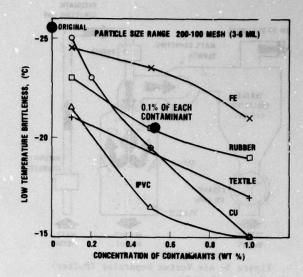


Figure 11- Effect of Type and Concentration of Contaminants on LTB of Flexible Virgin PVC

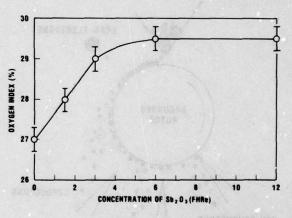


Figure 12- Effect of Sb₂O₃ on Limiting Oxygen Index (LOI) of Recompounded PVC Reclaim

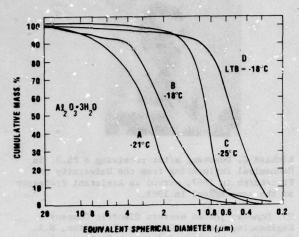


Figure 13- Effect of Particle Size of A1203.3H20 on LTB of Flexible PVC

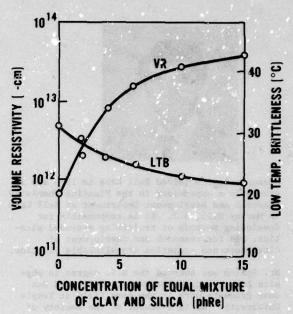


Figure 15- Effect of Equal Mixtures of Calcined Ciay and Fumed Silica on the Volume Resistivity and LTB of Recompounded PVC Reclaim

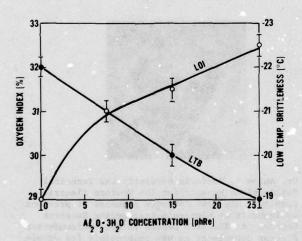


Figure 14- Effect of Al₂C₃·3H₂O on LOI and LTB of Recompounded PVC Reclaim



Figure 16- Types of Cable Jacketed With Recompounded Reclaimed PVC



Emanuele Scalco joined Bell Labs in 1963 and is presently a supervisor in the Plastics Chemistry Research and Development Department at Bell Labs in Murray Hill, N.J. He is responsible for developing methods of reclaiming extruded plastics, and for research and development of elastomers and radiation crosslinkable plastics.

Mr. Scalco was awarded the B.S. degree in physics from Drexel University in 1962, and has done graduate work in the same field at Temple University. He is a member of the Society of Plastics Engineers, The American Physical Society, and IEEE.



Robert L. Decker joined the Plastics Chemistry Research and Development Department at Bell Labs, Murray Kill, N.J. in 1970. His main interest is finding applications for recycled PVC. He is involved in the recompounding, testing and weathering of reclaimed PVC and other plastics.



Richard C. Donovan, after receiving a Ph.D. in Mechanical Engineering from the University of Pitteburgh in 1967, served as Assistant Professor at the same school in 1968.

Mr. Donovan joined Western Electric Company's Engineering Research Center at Princeton, N.J. in 1968 as a Member of Research Staff in plastics processing studies. He became Supervisor of the Plastics Processing Group in 1971 and in 1973 became Supervisor of the Materials Recycling Processes group which is responsible for developing new methods for recycling metals and plastics from telecommunications products.

In 1978 he became Department Chief in Corporate Product Planning, responsible for product management of interconnecting products and interdivisional products, including administration of development cases, product and technology allocations, and capital appropriations.



Dr. Anton F. Rodde is currently the Technical Publications Manager for the Western Electric Company. His work includes a number of previous assignments at Western's Engineering Research Center. As Research Leader in the Semiconductor Process department he was responsible for development of plasma processing for integrated circuit manufacture. Earlier work at the Center includes research and development of recycling processes in the area of critical materials and the development of high throughput production ion implantation systems for semiconductor doping. Dr. Rodde received a Ph.D. in physics from the Illinois Institute of Technology in 1970.

Service Service Service Service

AN ATTEMPT AT RECYCLING POLYOLEFINS FROM WIRE AND CABLE SCRAP

J. A. Falter E. Scalco

Bell Laboratories Murray Hill, N.J.

Abstract

Cable sheath, a large volume application of low density polyethylene, appears to be a potential outlet for polyethylenes reclaimed from wire and cable scrap. Three types of reclaimed polyethylenes were evaluated. It was found that by reprocessing or recompounding, the properties of two of the reclaimed materials were comparable to those of the virgin cable sheathing material. The properties of the third type of reclaim need further improvement to be reused as cable sheath.

Introduction

Substantial quantities of wire and cable scrap are generated each year by the Bell System. This scrap is made up of returned field cable and manufacturing scrap. As prices of raw materials continue to rise, reclamation of materials, such as metals and plastics, becomes more advantageous than in the past. In the Bell System poly(vinyl chloride) and polyolefins are the two major classes of plastic available for reclamation from wire and cable scrap and work is being done to reclaim them.

Through the coordinated efforts of personnel from Bell Laboratories, Nassau Recycle Corporation and Western Electric Company a new technology is being attempted for reclaiming plastics from communications cable and wire scrap. This system involves sorting, granulation, aspiration, electrostatic separation, flotatica, and melt screening processes. 1

The purpose of this paper is to relate some preliminary results of a recompounding study involving three polyolefin materials, with the objective of their reuse as sheath in new cable. In addition, results will be discussed of a low temperature impact study undertaken to establish criteria for testing.

Reclaimed Materials and Procedures

The three reclaimed materials studied were:

Type A - Principally high density polyethylene (HDPE) insulation reclaimed from relatively clean factory scrap

containing some polypropylene (PP) and $\sim 0.5\%$ contaminants.

- Typ B Primarily low density polyethylene (LDPE) containing ∿10% HDPE, ∿5% PP insulation compound and ∿0.5% contaminants. It was reclaimed from highly contaminated post-consumer, or field scrap.
- Type C Essentially LDPE sheath stripped off large cables from factory or field scrap, the primary contamination is ∿4-6% flooding compound.*

Recompounding and horogenizing were carried out by mixing the plastice for 7 minutes in a 6-inch two-roll laboratory mill at 160°C; plaques 0.075" thick were subsequently compression molded at 175°C at a low pressure for 3 minutes. Afterward the pressure was raised to 950 psi for 3 additional minutes followed by quenching in 10°C water.

The plaques were subsequently annealed at 70°C for 18 hours and conditioned at 23°C and 50% relative humidity for at least 24 hours before testing. All specimens were die-cut from the plaques. Except where otherwise noted, most properties were determined according to well known standards listed in Table 1.

Additives Study

Due to the nature and color of these reclaim materials and the relatively large quantity available, large volume applications seemed most appropriate. It was thus decided that an attempt should be made to use the reclaim in black cable sheath where electrical and colorability requirements are substantially less than those for primary insulations of communication wires.

However, the LDPE cable sheaths used in Bell System communication cables have other very stringent requirements such as: excellent resistance to environmental stress cracking; resistance to low

^{*} An asphaltic type flooding compound placed between the corrugated steel sheath and the LDPE sheath to retard corrosion.

temperature embrittlement, etc. Furthermore, they must perform well in a mainly outdoor environment for at least 40 years without significant loss of flexibility.

As stated above, the Type A reclaim is relatively free of contaminants and consists almost entirely of HDPE wire insulation, therefore it seemed appropriate to attempt its reuse first. A similar, but virgin natural HDPE of 0.945 g/cm³ density (ethylene-butene copolymer) was used for the initial reformulation study the aim of which was to search for an additive that, when mixed with HDPE, would modify it to have properties similar to those of LDPE cable sheathing compound.

An important property of LDPE cable sheath is its flexibility. HDPE has a flexural modulus approximately 4 times greater than that of LDPE and thus, if used as a sheath, will render most cables too stiff. It is primarily for this reason that the additives blended with HDPE were mainly rubbery (soft) materials and their degree of efficiency in lowering the flexural modulus was used as the initial screening criterion for a large number of commercially available and experimental additives. Classes of materials studied included chlorinated PE, copolymers of ethylene with vinyl acetate, vinyl acrylate, or propylene, several thermoplastic elastomers, butyl and nitrile rubbers, and terpolymers of ethylene-propylene-diene.

The flexural moduli of PE and a series of blends of HDPE with representative classes of these modifiers are shown in Table 2. In this table, HDPE and the blends were compared to two LDPE cable sheathing compounds: the base resin in LDPE-I is a blend of LDPE and about 5% of an ethylene-vinyl acetate copolymer, while that of LDPE-II is a low density copolymer of ethylene and butene-1 made by a new low pressure process.² The flexural modulus of the latter is 40% higher than the former although both compounds are used interchargeably.

Of the additives tested, based on their flexibilizing ability, two were selected for further study: a thermoplastic elastomer, TPE-I, consisting of a block copolymer of styrene-(ethylene butylene)-styrene extended with 47%, by weight, of a naphthenic-paraffinic oil blend, and a terpolymer, EPDM-I, of ethylene-propylene-diene extended with 43%, by weight, of a paraffinic oil.

In addition to the flexural modulus, tensile, cutthrough and low temperature impact properties of three polyethylenes, a blend of HDPE and 30% TPE-I, and one of 40% EPDM-I are shown in Table 3. It is clear from these data that the properties of the HDPE blends are commensurate with those of LDPE's, including low temperature impact as measured by low temperature brittleness (LTB), and flexural modulus.

In addition to requiring a higher concentration (40%) of EPDM-I than of TPE-I (30%) to reduce the modulus to an acceptable level, it was found from results of oven aging tests that the blend made with the former additive discolored, some oil

migrated to the surface, and the tensile properties deteriorated to an unacceptable level. The TPE-I containing blend, on the other hand, retained all of these properties at the same level as those of the LDPE controls. In addition, it is noteworthy that the yield strength of this blend measured at 80°C is higher than that of either virgin LDPE materials. This property is important in applications where pressurized cables are exposed to high temperature environments.

Evaluation of Reclaimed Polyethylene

I. Types A and B Materials

The results reviewed in the previous section indicated that HDPE can be modified, by the addition of 30% TPE-I, to yield properties similar to those of LDPE sheathing compounds. Thus, Type A, factory scrap reclaim was blended with the TPE-I and the results shown in Table 4 indicate that this material can be successfully recompounded for possible use as a cable sheathing material.

As indicated above, Type B reclaim consists of mainly LDPE, $\sim 10\%$ HDPE and $\sim 5\%$ PP, as determined by Differential Scenning Calorimeter techniques. Some of its properties are shown in Table 5. The LTB of this material is at least 20° poorer than the virgin sheathing material and its shear resistance (SR) is very low (790 lb.).

Although SR is not a specification requirement for sheathing materials, it has been included here since it is felt that this property gives a measure of general "toughness" and of how a sheath will resist cut-through and scraping during cable installation.

To improve the LTB of this reclaim it would be necessary to add a flexibilizer, however, this would render the resulting blend softer and the corresponding SR would be diminished to an even lower level. On the basis of these criteria, Type A, HDPE reclaim, was added to Type B in an attempt to increase the SR and TPE-I was added to this mixture to improve LTB.

The remaining data in Table 5 indicate that these properties thusly are improved. Nevertheless, these improvements do not seem sufficient to yield a material acceptable for cable sheath applications.

II. Type C Material

As already indicated, Type C material consists mainly of sheath stripped off large cables and contains, in the present case, 4% of an asphaltic type flooding compound. In Table 6 the performance of virgin cable sheathing compound LDPE-I is compared with that of Type C material.

The data indicates that even this small amount of flooding compound has a substantial negative effect on both LTB and SR. In the same table, it is shown that, by removing the flooding compound from Type C material, LTP and SR are improved by

over 15° and 450 lb., respectively: other properties are also significantly improved such that this material is believed to be acceptable for reuse in new cable. The flooding compound had been removed by washing with trichloroethylene. Further data on Table 6 indicate that addition of 10% TPF-I to the Type C material improves the LTB by 12° but lowers the SR to 1040 lb., an unacceptable level.

Low Temperature Brittleness

The ability of cable sheathing compounds to resist brittle failure due to impact at low temperatures is normally measured in the laboratory by LTB testing. Although most virgin polyethylene materials have an LTB <-76°C, this level of performance infrequently agrees with that of cable sheath in the field, as failures have been observed at substantially higher temperatures. Significant work3,4 on this problem has been reported and changes in the test method and specimen preparation have been proposed which substantially improve correlation of results of laboratory tests with field performance. The most significant change was the introduction of a notch in the tost specimens and definition of the distance of the notch from the clamp.

The present short study was undertaken in an attempt to establish criteria of sample preparation and method of testing such that test results for a large variety of materials to be tested would fall within the range of capability of the LTB apparatus, while using the same heat transfer medium (methanol). It is necessary to use the same heat transfer medium because its properties influence the outcome of LTB testing. For example, specimens of polybutylene sheathing compound notched with a razor blade edge were determined to have an LTB of 52°C and 36°C in water and methanol, respectively.

The optimum notch depth, for our purpose, was first determined by testing the two virgin LDPE cable sheathing compounds using specimens with varied notch depths. Notches were made initially using a razor blade whose exposed cutting edge (see Figure 1) had been carefully inspected and controlled to give a notch of reproducible depth. For this test the notch to clamp distance was 0.100" and, to minimize deformation during clamping, the loaded specimen clamp was first lightly tightened, then immersed into the constant temperature methanol bath for two minutes at which time they were removed from the bath, then tightened to 15 in.—1b. and immediately reimmersed.

The effect of notch depth on the LTB of these materials is shown in Figure 2 and, as one would expect, the LTB deteriorates as notch depth is increased. Although the two materials differ substantially in their notch sensitivity, it is clear that as the notch depth of about G.015" is approached the slope of a LTB notch depth curve becomes less steep. For this reason, a depth of 0.020" was chosen for use in further studies in an attempt to minimize the variation in test

results due to small notch depth differences.

Correspondingly, in Figure 3 it is shown that LTB improves as the notch-to-clamp distance is increased from 0.010" to 0.100". However, the slope of the LTB-distance curve decreases at a slower rate at notch distances less than approximately 0.050" therefore, a distance of 0.040" was chosen for use in further tests since only small variations in LTB would be expected by small deviations in the notch-to-clamp distance.

Although great care had been taken in introducing notches with razor blade edges, test results were not always reproducible. Therefore, as suggested by other workers, 4 specimens with molded-in notches were tested and reproducibility was acceptable. A schematic cross section of the mold rib used to form the notches is shown in Figure 4.

A comparison of LTB results, obtained from specimens with and without notches, for a variety of compounds described earlier, is shown on Table 7. As can be seen, the HDPE has a "notched" LTB of >30°C which indicates this material to be much more notch sensitive than either of the LDPE sheathing compounds. (Testing was not carried out above 30°C to avoid possible flashing of the heat transfer madium). The "notched" LTB of Type A material is also >30°C since it is primarily HDPE insulation compound.

The "notched" LTB of Type B material is -7°C and that of the fifty percent mixture of Type A and Type B materials is 30°C. Addition of 30% TPE-I to HDPE, to Type A material and to the 50/50 blend of Type A and Type B improved the notch sensitivity of each of the blends. The "notched" LTB of the virgin HDPE blend improved very substantially from >30 to -37°C. The "notched" LTB of the Type A material blend was -25°C which compares very well with those of the two virgin sheathing compounds (-22°C for LDPE-I and -33°C for LDPE-II). Although the LTB of the (50/50) Type A and Type B blend was improved from 30 to -10°C by addition of the TPE-I, this gain was not enough to make it suitable for cable sheathing.

Conclusions

The polyethylenes reclaimed from three types of scrap were Type A, mainly high density polyethylene (HDPE) insulation reclaimed from relatively clean factory scrap, Type B, mostly low density polyethylene (LDPE) sheath with $\sim\!10\%$ HDPE and $\sim\!5\%$ polypropylene reclaimed from post-consumer scrap, and Type C, a LDPE sheath stripped off large cables from factory or field scrap contaminated with $\sim\!4\%$ flooding compound.

It was found that blending the Type A reclaim with an oil extended thermoplastic elastomer resulted in a compound with potential reuse as sheath for new cable. In addition, it was determined that, after suitable removal of the flooding compound, Type C reclaim is recyclable as cable sheath.

Substantial improvements in the initially poor properties of Type B reclaim were effected by blending with Type A reclaim and the oil extended thermoplastic elastomer. However, these improvements were not sufficient for acceptability of this material as cable sheath. Work is continuing to further improve its properties.

Results of the low temperature brittleness study allowed a successful choice of test parameters such that reproducible data could be obtained for the various polyolefins studied using a single set of conditions.

Acknowledgement

The authors gratefully acknowledge the cooperation of W. H. Lockwood during the early part of this study and of their colleagues at Nassau Recycle Corporation, Western Electric Engineering Research Center and Western Electric Cable and Wire Product Engineering and Control Center.

References

- E. Scalco, R. L. Decker, R. C. Donovan, A. R. Rodde, "Recycling of PVC from Cable and Wire Scrap", proceedings of the 28th International Wire and Cable Symposium, Cherry Hill, N.J., November 1979.
- R. Bostwick, "An Improved Black Jacket Compound for Telephone Cables", Wire Technology, September-October, 1978, p. 50-54.
- K. Yamaguchi, H. Kishi, H. Takashima and S. Otomo, "Low Temperature Brittleness of Low Density Polyethylene for Cable Jackets", proceedings of the 24th International Wire and Cable Symposium, Cherry Hill, N.J., November 1975.
- G. M. Yanizeski, E. D. Nelson, C. J. Aloisio, "Predicting Fracture, Creep and Stiffness Characteristics of Cable Jackets from Material Properties", Proceedings of the 25th International Wire and Cable Symposium, Cherry Hill, N.J., November 1976.

a Black compound

TABLE 1 TEST PROCEDURES

Tensile Strength and Ultimate Elongation
ASTM D-412 using specimen die T-50
Flexural Modulus
ASTM D-790, Method I
Melt Index and Swelling Ratio
ASTM D-1238 at 190°C and 2160 g Load
Stress Crack Resistance and Resistance to
Process Degradation
ASTM D-1693

Low Temperature Brittleness
ASTM D-746 except 20 specimens were tested per
temperature and only complete breaks and samples
hanging by outer skin were counted as failures
Shear Resistance

Bell System material specification cut-through test using a 0.50 inch $45^{\rm O}$ wedge with a 0.0050" flat edge at 2.25"/min.

TABLE 2 FLEXURAL MODULUS

Туре	Concentration (% By Weight)	Flexural Modulus (10 ³ psi)
HDPE	then ere 100 de nos	104.5
LDPE-I	100	24.5
LDPE-II	100	34.4
HDPE +		
TPE-I	30	31.9
EPCM-I	10	39.2
EPM ¹	30	65.0
EVA ²	50	50.0
Batyl Rubber	40	47.0

¹ Ethylene propylene copolymer

TABLE 3

	MECHA	NICAL PRO	PERTIES		
	HDPE	LOPE-1	PODE-II	HDPE +30% TPE-1	HDPE + 403 EPDM-1
Ult. Tensile (psi)	3040	2370	2330	2360	1820
Ult. Elongation (%)	710	640	640	850	H90
Shear PEsistance (1b/in)	2530	1730	2780	1490	1690
Low Temp. Brittleness (°C) (T ₅₀)	<-16	<-76	<-76	<-76	<-76
Flexural Modulus (10 psi)	104.5	24.5	34.4	31.9	39.2
Yield Strength @ 80°C (psi)	1350	660	680	800	625
Oven Aging # 80°C					
Color	Va Septim	_a	_a	No Discoloration	Turned Brown
Oil Migration	anue géoc	_b	_b	None	Yes
Elongation Retention (%)	, 75 Sec.	55	50	55	6 40 6

b No oi: in compound

² Ethylene vinyl acetate

TABLE 4
MECHANICAL PROPERTIES OF TYPE A MATERIAL

TABI	LE 5	
MECHANICAL	PROPERTIES	

		Type A ¹	Type A
Ulc. Tensile	(psi)	3310	3526
Tensile 3 100% Elong.	(psi)	1720	1250
Ult. Elongation	(3)	810	900
Shear Resistance	(1b/in)	1620	1470
Flexural Modulus	(10 ³ psi)	75.2	23.3
Low Temp. Brittleness (T_{50})	(°C)	<-76	<-76

		Type B	Type A and Type B (50/50)	(50/50) +30% TPE-I
Ult. Tensile	(pai)	1590	1720	2170
Tensile @ 100% Elongati	on (psi)	1340	1570	960
Ult. Elongation	(%)	540	390	740
Shear Resistance	(1b/in)	790	1010	1150
Flexural Modulus	(10 ³ psi) 26.6	51.7	18.0
Low Temp. Brittleness (T ₅₀)	(°C)	-49	-62	-70

TABLE 6

MECHANICAL PROPERTIES OF TYPE C MATERIAL

		LDPE-I	Type C1	Type C ²	Type C ¹ 10% TPE-I
Ult. Tensile	(psi)	2370	1830	2080	1850
Elongation	(%)	640	600	650	750
Shear Resistance	(1b/in)	1730	1300	1750	1040
Melt Index	(g/10 min)	-	.53	.26	. 36
Swe'ling Ratio			1.4	1.4	1.3
Stress Crack Resistan	ice	0/10	0/10	0/10	0/10
Low Temp. Brittleness	(T ₅₀) (°C)	<-76	-58	-74	-70

¹ Cable Strippings

TABLE 7
LOW TEMPERATURE BRITTLENESS

	150'	-(°C)	
	Unnotched	Razora Blade Notch	Molded ^b Notch
LDPE-I	<-76	8	-22
LDPE-II	<-76	1	-33
HDPE	<-76	>30	>30
HDPE + 30% TPE-I	<-76	•	-37
Type A	<-76		>30
Type A + 30% TPE-I	<-76		-25
Type B	-49		- 7
Type A + Type B (50/50)	-62		30
(50/50) + 30% TPE-X	-70	0.000	-10

a Edge exposed 0.020", notch-to-clamp listance 0.040".

¹ HDPE insulation reclaim material

² Flooding Compound Removed with Trichloroethylene

b U-type 0.020", 0.340" notch-to-clamp distance.

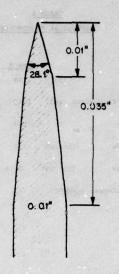


Figure 1 Razor Blade Edge

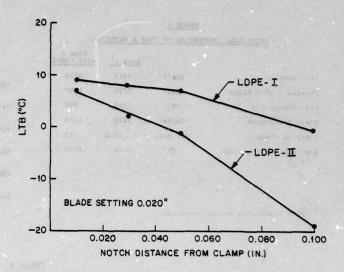


Figure 3 Low Temperature Brittleness vs. Notch-to-Clamp Distance

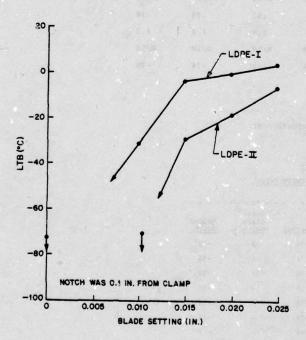


Figure 2 Low Temperature Brittleness vs. Razor Blade Setting

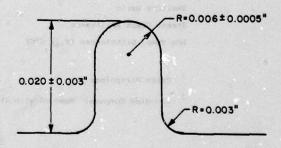


Figure 4 Mold Rib for Channel or U-Type Mold



Julia A. Falter received a B.S. in Plastics Technology from Lowell Technological Institute in 1971.
She joined the Plastics Chemistry Research and Development Department of Bell Telephone Laboratories at Murray Hill, N.J. in 1974. She has been active in studies of PVC jacket formulations, irradiated polyethylenes, and reclaimed polyolefins.



Emanuele Scalco joined Bell Labs in 1963 and is presently a supervisor in the Plastics Chemistry Research and Development department at Bell Labs in Murray Hill, N.J. He is responsible for developing methods of reclaiming extruded plastics, and for research and development of elastomers and radiation crosslinkable plastics.

Mr. Scalco was awarded the B.S. degree in physics from Drexel University in 1962, and has done graduate work in the same field at Temple University. He is a member of the Society of Plastics Engineers, The American Physical Society, and IEEE.

A METHOD FOR RESTABILIZATION OF ANTIOXIDANT DEPLETED LOW DENSITY POLYETHYLENE CONDUCTOR INSULATION

Frederick R. Wight

Bell Laboratories Norcross, Georgia 30071

Abstract

A coating material is described which restabilizes antioxidant depleted low density polyethylene conductor insulation. It is intended for field application on the insulation in pedestals or closures where insulation cracking is incipient. The coating resin serves as a reservoir for an antioxidant package which migrates slowly into polyethylene under field environments. Accelerated tests indicate substantial extensions of field life are possible with this material.

Introduction

Observations of premature embrittlement and cracking of low density polyethylene insulation (PIC) installed prior to 1971 has been well documented. Since that time insulation embrittlement, which is confined to aerial terminals and closures and above ground pedestals and terminals for buried cable, has been found to be slowly spreading northward to cooler climates. This in turn has contributed to rising maintenance costs for outside plant. While improvements in insulation

to rising main enance costs for outside plant. While improvements in insulation materials and stabilization have been made since 1971 concern over the rate of deterioration of early vintage PIC is high.

The B-insulation spray developed by Shea³ has found increasing popularity in the field for the temporary restoration of PIC insulation. Its primary purpose is as a coating to restore insulation integrity where cracking has already begun. However nothing exists today which actually retards the oxidative embrittlement process. If a method of retarding the cracking process and its northward migration can be found, considerable savings would accrue. One possible approach to retarding the rate of PIC cracking in the field is to introduce additional stabilizer into the low density polyethylene insulation to extend its lifetime.

The idea of restoring antioxidant to low density polyethylene (LDPE) whose

stabilizer has been depleted after years in the field is not new. Howard described a restorative treatment involving a multicomponent system applied on the affected insulation. Basically the system consisted of a coating material in a suitable solvent containing an antioxidant. The solvent is believed to act as a carrier for the anticxidant to allow it to migrate into the polyethylene. While Howard demonstrated the feasibility of this technique, the additive package was not optimized and no life projections were made.

Since that time it was also discovered that placement of highly stabilized sheets of polyethylene in pedestals heated to 90°C dramatically prolonged the life of the

PIC insulation in the pedestal.⁵ In this case, rather than relying on intimate contact between the insulation and antioxidant reservoir, antioxidant migration to the insulation occurs through the dead air space in the pedestal.

The methods of antioxidant restoration described above have been carefully examined using the B-spray lacquer as the primary vehicle. The results offer a very promising method for substantially prolonging the life of uncracked PTC in the field. The coating material is intended for use as part of a permanent rehabilitation program designed to minimize craft activity and is performed on pedestals or closures where cracked PIC is not present or has been removed.

Experimental

For our experiments the coating material consists of an aliphatic urethane lacquer

TABLE I

COMPOSITION OF LACQUER COATING

Ingredient	Parts by Weight			
Aliphatic Urethane	3			
Solvent System	92			

(Table I). The base resin is identical to the B-insulation spray although the solids content is slightly higher. This material was chosen for a number of reasons. The aliphatic urethane has outstanding long term thermal stability. We have found this resin to be soft and flexible after 7 years exposure in a pedestal in Tucson, Arizona. Forced air oven aging at 120°C for 8 months resulted in only slight discoloration. Its physical properties have been found quite suitable for this application and the solvent system is designed to be compatible with polycarbonate connectors.

TABLE II

ADDITIVES EVALUATED IN COATING

Hindered Phenols

- A01 4, 4' thiobis (di-tert-butyl-m-cresol)
- A02 Tetrakis [methylene-3 (3',5'-d1-tert-butyl-4-hydroxyphenyl) propionate]
 methane
- A03 Thio-diethylene-bis (3,5-di-tert-butyl-4-hydroxy) hydrocinnamate
- A04 N, N-Bis [3-(3,5-di-tert-outyl-4-hydroxyphenyl) hydrocinnamoyl]
- A05 3:1 condensate of 3-methyl-6-tertbutyl phenol with crotonaldehyde
- A06 Tris (3,5-di-tert-butyl-4-hydroxybenzyl) isocyanurate
- A07 Ontadecyl 3-(3',5'-di-tert-butyl-4-hydroxyphenyi) propionate

Synergists

(Peroxide Decomposers)

- SY1 distearylthiodipropionate
- SY2 dilaurylthiodipropionate
- SY3 pentaerythritol hexyl thiodipropionate
- SY4 Tetrikis (nonylphenyl) polypropylene glycol 425

Copper Deactivators

- CD1 Same as A04
- CD2 hydrazide derivative
- CD3 salicyloyl amino triazole
- CD4 proprietary compound

Initial tests were performed on .315" films of unstabilized LDPE dipped in the lacquer and hung to dry. Two coats were applied. Coating thicknesses were typically .002". Coatings were also applied to unstabilized LDPE insulated 22AWG copper.

Additives tested are summarized in Table II. The concentrations used in this report are all based on the percent by weight of stabilizer in the solid coating after drying. For initial screening of phenolic antioxidants a series of lacquer solutions were prepared containing 1 percent primary rhenolic antioxidant based on the weight of solids in the solution. Un-stabilized LDPE films (.015") were then treated with each coating and placed in a forced air oven at 90°C. The films were forced air oven at 90°C. periodically tested by differential thermal analysis (DTA) after removing the lacquer coating. The DTA oxidative inlacquer coating. duction times (OIT) obtained are used merely as a measure of the amount of antioxidant migrating into the polyethylene and in no way reflect ultimate lifetime. Unstabilized LDPE gives an induction period of 1 minute at 160°C. The induction period will increase with increasing stabilizer concentration. Higher test temperatures were used to obtain results in a relatively short time period.

Results and Discussion

Primary Antioxidant Screening

Results of the preliminary evaluation of phenolic antioxidants are shown in Table III. Note that all DTA measurements were made at 180°C except for A03 and A06 which were made at 190°C because of their higher induction periods. It is interesting to note that the absorption of stabilizer by LDPE is very rapid at 90°C even for the relatively nonvolatile stabilizers such as AC2 and A04. After 3 days the induction period for all samples has reached a plateau and decreases gradually from that point onward except for A06 which appears to have been retained the best in the polyethylene.

Howard, 6 in 1973, generated a 200°C DTA calibration curve for the concentration of AOI in LDPE. A concentration of 0.1% AOI in LDPE corresponds to an induction time at 200°C of roughly 40 minutes while an induction time of 8 minutes corresponds to .01% AOI. Clearly the 1.0% ACI in the lacquer provides far less stabilization to the LDPE than a fully stabilized (0.1%) LDPE sample. This point is crucial to our later discussion.

Table IV shows the effect of similar treatment at 70°C and 45°C. Note that at the

lower temperatures far less antioxidant is migrating into the LDPE. At 70°C, however, the trend among stabilizers is the same. That is, AO3 and AO6 look better than the others. Note again that AO6 appears to migrate more slowly and give high induction periods over a longer aging time.

Since 45°C is a temperature that is common in the field it can be seen that the level of stability that can be imparted to LDPE by this method does not appear significant. It is unlikely that an extension of field life by say, 20 years could be achieved, particularly when one considers that the tests performed thus far do not include copper and its strong procatalytic effect.

Screening of Synergistic Additives and Copper Deactivators

To improve the stability imparted by phenolic antioxidants alone, a series of stabilizer packages were made up, which included copper deactivators and synergistic components in conjunction with A03. A03 was used as the primary antioxidant because of its outstanding initial performance. However, as seen from Table III, A06 may have been a better choice in retrospect in view of its superior long term retention. These packages were added to the lacquer at a level of 1 percent each by weight of solids. LDPE films were coated and aged at 70°C. Results are shown in

TABLE III

ANTIOXIDANT MIGRATION AT 90°C IN

COATED UNSTABILIZED LDPE

Antioxidant	ant DTA Test		Induction Time (Min) After Days Aging at 90°C					
in Lacquer (1%)	Temperature (°C)	1 Day	3 Days	10 Days	42 Days	100 Days	200 Days*	
AO1	180°	8	11	7	5	2	1	
A02	180°	30	32	27	14	12	Notice 1	
A03	190°	28	23	15	9	6	order i fill	
A04	180°	10	10	8	9	4	3	
A05	180°	10	8	5	7	2	2	
A06	190°	10	12	12	14	11	8	
Untreated Contro	ol 160°	1		Embri	ttled in	55 Days		

^{*} All readings after 200 days taken at 180°C

TABLE IV

ANTIOXIDANT MIGRATION AT 70°C AND 45°C

INTO COATED UNSTABILIZED LDPE

Antioxidant	tioxidant DTA Test		OIT (Min	The Street Country of the Country of	OIT (Min) After Days at 45°C			45°C
in Lacquer (1%)	Temperature (°C)	1 Day	5 Days	20 Days	Temperature	2 Days	10 Days	20 Days
AO1	180	3	2	2	170	2	2	2
A02	180	5	7	6	170	3	6	4
A03	180	22	17	17	180	3	4	3
AOG	180	15	15	21	180	I	1	2

TABLE V

COPPER DEACTIVATOR AND SYNERGIST MIGRATION AT 70°C INTO COATED UNSTABILIZED LDPE

OTT (Min) at 180°C After Days at 70°C

	Olf (Min) at 180°C After Days at 70°C				
A/O in Lacquer	1 D	ay	5 Days		
1% Each	Al Pan	<u>Cu Pan</u>	Al Pan	<u>Cu Pan</u>	
Cu Deactivators					
A03/CD1	24	4			
A03/CD2	18	4			
A03/CD3	19	4			
A03/CD4	21	3			
Synergists			4		
A03/SY1	20		21	1822 (192.3)	
A03/SY4	45		43		
A04/SY1	18	3	16	1	
A03/SY2	36		31		
A03	22		17		

Table V. The effectiveness of the copper deactivator can be found by comparing the OIT on aluminum and copper pans. 7 In all cases, a significantly poorer OIT is obtained on copper pans. Note that where CD1 (A04) is used in conjunction with SY1, the material appears to have migrated as evidenced by the fact that it is functioning as a primary antioxidant (18 min on Al pans). However, as a copper deactivator it does not provide much relief from copper catalysis (3 min on Cu pans).

An added complication of this data, and an important one, is the fact that copper deactivators CD2, CD3 and CD4 as well as SY1 were only slightly soluble in the lacquer. Finally, note that SY2 and SY4 synergists gave significant improvements over A03 alone. As a result of these tests it was concluded that a copper deactivator cannot be effectively incorporated into LDPE by—this method. In addition, SY2 and SY4 appear to be effective synergists under these conditions. Since phosphite synergists are susceptable to hydrolysis we believe SY2 is the better choice.

Effect of Additive Concentration

Table VI shows the effect of stabilizer concentration on its degree of migration into LDPE at 45°C. The concentrations indicated here again are based on a percentage of the solids in the lacquer. Clearly the higher concentrations show a marked improvement in the quantity of stabilizer diffusing into the polymer. Also shown in Table VI is the effectiveness of A07 in conjunction with synergists SY2 and SY3 which appears to be very effective. SY3 is a liquid thioester synergist which was used in place of SY2 in an attempt to overcome a deficiency in SY2 which is its tendency to precipitate out of the lacquer solution before completely drying.

Attempts were made to improve the rate and degree of migration by introducing various solvents and oils that might act as carriers by swelling the LDPE. However, addition of toluene, sylene, or low viscosity mineral oils were found to produce no measureable improvement at 45°C.

TABLE VI

ANTIOXIDANT ABSORPTION AT 45°C

INTO UNSTABILIZED LDPE

Concentration of Stabilizers	OIT (Min) a	t 190°C After 7 Days	Days at 45°C
	1 Day	1 Days	14 Days
A03 and SY4			
1% each	3	8	5
3% each	17	52	50
5% each		85	80
5% A03; 5% SY2		43	44
5% A07; 5% SY2		91	76
5% A07; 5% SY3		87	89
2.5% A07; 2.5% A06; 5% SY3		77	
B-Spray		1@180°C	1@180°C

Oxygen Uptake Testing

To ascertain some measure of the expected lifetime of the samples in Table VI with 5 percent each of a hindered phenol and a synergist, we ran oxygen uptake tests at 100°C on a 22 AWG wire sample insulated with unstabilized LDPE. The samples were ccated with the restorative coating and aged for 1 week at 45°C. The lacquer coating was then removed before running the oxygen uptake. This latter step was necessary since as was seen earlier, an abnormally high amount of stabilizer diffuses from the coating into the LDPE at these higher temperatures.

Table VII shows the results of the 100°C oxygen uptake test. It demonstrates that a remarkable improvement in stability can be achieved by this method. Indeed the times to failure are comparable to LDPE fully stabilized (0.1% each) with A02 and CD5. Gilroy has generated failure data for LDPE stabilized with A02 and CD5 at temperatures as low as 60°C. For this system a 15 year life at 40°C was

Oxygen Diffusion Barrier Mechanism

predicted.

Further experiments suggest that this projection may be, if anything, conservative, since the experiment was performed after the coating was removed. Up to this point we have only discussed the use of a coating as a means to add stabilizer

to the LDPE. However, as discussed earlier the coating may also act as a barrier to oxygen. When a sample of unstabilized LDPE insulated copper was aged at 100°C by oxygen uptake with the B-Spray coating present, the time to the first failure was

oxygen uptake with the B-Spray coating present, the time to the first failure was 88 days. Recalling from Table VI the short DTA induction periods obtained on B-Spray treated LDPE, the long lifetime at 100°C seems to suggest that the coating itself is providing some additional protection.

TABLE VII

100°C OXYGEN UPTAKE

ON TREATED 22 AWG

	Time to Fin	rst Cracking
Stabilizer In Coating (5% Each)	Days	Years
A04/SY4	90	0.25
A07/SY1	106	0.27
A07/SY3	117	0.32
Unstabilized LDPE	3	0.008
LDPE/0.1% A01	11	0.030
LDPE/0.1% A02; 0.1% CD5	110	0.30

Quite possibly this protection could be in the form of an oxygen barrier much as the skin of an apple prevents oxidation of the meat. If the LDPE were stabilized to a level of 0.1% A01 its lifetime at 100°C would be only about 11 days. Table VI indicates that the level of stabilization provided by the B-Spray is far less and thus our results strongly suggest an oxygen barrier mechanism.

Limitations to Antioxidant Restorative Coating

One final question which we wished to answer was: How degraded could an insulation be and yet still be restorable? To answer this, we treated PIC samples from two field exposed pedestals which were exposed for 10 years in Florida. One pedestal was heavily degraded with over 80 percent of the insulation cracked, the other was only slightly degraded with less than 10 percent of the conductors having cracked insulation. Uncracked insulation samples only were removed from each pedestal and dipped in lacquer containing 5 percent each of A07 and SY3 synergist. After aging the coated conductors for 1 week at 45°C the coatings were removed and the insulated conductors subjected to oxygen uptake at 100°C. Whereas conductors from the badly degraded pedestal gave 100°C lifetimes from 6 to 30 days, the conductors from the lightly degraded pedestals showed lifetimes ranging from 63 to 119 days. This indicates that there is a limit to which we can expect improvement by stabilizer restoration. Fortunately, a restorative treatment such as described here would not be applicable to a terminal containing a high percentage of cracked PIC. Such terminals can only be rehabilitated by removing all the degraded wire work.

Summary and Conclusion

A coating material has been developed which acts as a stabilizer reservoir for PIC insulation. Application of this coating in the field to antioxidant depleted PIC will rostore antioxidant and extend the lifetime of the insulation to well beyond its original life expectancy. The coating resin is the same as used in the B-Spray lacquer. The stabilizer package consists of a mixture of a hindered phonol and a thioester synergist at a level of 5 percent each based on the weight of the dried coating. Based on the results presented it is believed that the hindered phenol portion of the package should consist of equal amount of AO6 and either AO3 or AO7. The AO3 and AO7 were found to migrate rapidly to a high initial level of stability while the AOG migrates to a lower level but retains that level over longer periods. The SY3, a thioester, was found to be the most suitable synergistic component. No improvements in performance could be obtained with the use of copper deactivators, partly due to their poor solubility in the lacquer solution. Current estimates indicate 15 to 20 years added life is possible by this method in the worst field conditions provided it is not used on terminals containing large number of cracked PIC wires.

References

- J. B. Howard, "Stabilization Problems with Low Density Polyethylene Insulations," Proc. 21st Int. Wire and Cable Symp., 329 - 341 (1972).
- B. B. Pusey, M. T. Chen and W. L. Roberts, Proc. 20th Int. Wire and Symp., 209 - 217 (1971)
- J. W. Shea, "Treatment of Degraded PIC Insulation in Pedestal Closures Associated with Buried Plant," Proc. 21st Int. Wire and Cable Symp., 70-74 (1972).
- 4. J. B. Howard, Bell Laboratories Internal Document
- 5. W. M. Martin, Bell Laboratories Internal Document
- J. B. Howard, "DTA to Predict Stability of Polyolefin Wire and Cable Compounds," SPE 31st ANTEC 19, 408 - 412 (1973).
- 7. F. R. Wight, "The Quantitative Differential Thermal Analysis Determination of Polyolefin Stabilization," Polym. Eng. Sci., 16, 652 (1976).
- 8. H. M. Gilroy, "Long Term Photo and Thermal Oxidation of Polyethylene," American Chemical Society, Division of Polymer Chemistry, Preprints, V. 19, No. 2. 839 (1978).



Frederick R. Wight joined the Transmission Media Laboratory of Bell Laboratories in 1972 after receiving a Ph.D in physical organic chemistry from the University of Georgia. At the present time he is a Member of Technical Staff in the Materials Group of the Interconnection Technology Laboratory at Bell Laboratories in Whippany, N.J.

Rehabilitation of Buried Air-Core PIC Cable Plant

R. P. Collins and W. S. Pesto

Bell Telephone Laboratories Norcross, Ga.

ABSTRACT

With the introduction of filled waterproof cable, a high level of reliability has been realized in buried cable installations. However, approximately 50% of the existing buried plant in the Bell System is still design is susceptible to conductor troubles caused by water entry, and in some instances, subject to conductor insulation cracking and flaking. As a result maintenance costs have continued to increase at a significant rate. These conditions tend to be most severe in buried ready-access distribution plant. keplace-ment on a wholesale basis is cost prohibitive, and therefore a more economical method of restoration has been developed. This procedure consists of systematic testing, inspection, diagnosis, and treat-ment of all defective elements in a hightrouble distribution area. Wet cable secreclaimed by pumping with are C-Reclamation compound, terminals are rebuilt and encapsulated to eliminate conductor defects and prevent future deterioration, and the area is converted to interface design using fixed count blocks to eliminate connecting access to cable pairs. Costs are substantially less than those of complete replacement, and tracking of four trial sites for to two years has shown the procedure to recover most of the defective pairs and reduce outside plant related troubles to near zero.

INTRODUCTION

Multipair telephone cable with plastic insulated conductors came into use in this country and abroad in the late 1950's. This cable which is commonly known as PIC cable (for Plastic Insulated Conductor) uses polyethylene for insulation and has an unfilled or air core. In the early days it was commonly believed that PIC cable, unlike the paper and pulp cables it replaced, was immune to effects of water, even if it managed to enter the core of the cable through sheath faults. With its

color code for easy pair identification and its reduced water sensitivity, PIC was the ratural candidate to use in the rapid expansion of telephone distribution plant during the 1960's. Not only was PIC cable used as standard for aerial plant, but it also provided the means to respond to growing public demand for "out-of sight" or buried telephone plant in new communities.

As shown in Fig. 1, since its beginning in the late 50's, air-core PIC cable has been used to build approximately 3.5 billion sheath-feet of buried plant. Since about 1970 this field of application has been taken over by filled waterproof cable, but even today roughly half of the buried plant in service is unpressurized air-core PIC. It is this segment of plant which the rehabilitation methods presented here address.

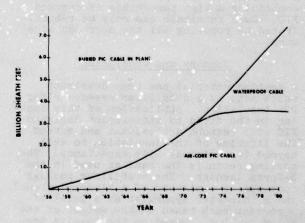


Figure 1

The majority of buried air-core PIC cable occurs in that segment of the network between the crossbox or interface and the subscriber. This portion of the network is grouped into Allocation Areas, which are contiguous geographic units of distribution plant of 500 to 2000 lines each. An Allocation Area normally consists of from one to five serving areas, each having its own feeder/distribution interface. While all areas of the plant may not have been upgraded from multiple design to serving area design, in most of the Bell System the plant has been organized and divided into Allocation Areas for planning and engineering. The Allocation Area is now the standard basic unit for planning. engineering, and operating the loop plant. In particular, many of the software systems now in use for tracking the performance and operating costs of outside plant use the Allocation Area as a minimum identified unit. Since a typical Allocation Area comprises an area of from 500 to 2000 stations, it also forms a workable quantity of plant for the systematic analysis and treatment program described here.

DISTRIBUTION AREA

Figure 2

To be more specific, a typical distribution serving area is shown schematically in Fig. 2. The feeder cable normally terminates in a flexibility point such as a crossbox or interface, and smaller air-core PIC distribution cables go out to terminals from which service wires feed each subscriber. The distribution cables are not pressurized, and are found to be either single jacket Aipeth, or double jacket PAP or PASP. The terminals are usually metal pedestals with the cable looped up and pairs exposed for service connection. Normally a pedestal will serve two to four subscribers depending on whether feed is along back lot lines or on the street. From an administrative standpoint this plant built in the 60's was

usually ready-access multiple design. That is, distribution pairs were multipled for possible assignment at several locations up and down a leg, and all cable pairs are accessible for connection at every terminal on a leg. An operational characteristic of this design is that normal service provision and changes requires daily access and manipulation of the cable conductors by station installers and repair people.

PROBLEM DEFINITION

It is now well known by operating forces that such buried, ready-access, aircore PIC distribution plant is susceptible to a number of failure mechanisms. These can be generally grouped into three major categories; defective cables due to water, environmental damage to conductors in pedestal terminals, and defective buried splices. The resulting condition is high defective pair rates, facility shortages, and high operating and maintenance costs. For example, while the defective pair rate from the main frame out is thought to average about 5% over the Bell System, it is common to find 15 to 20% of the distribution pairs defective beyond the interface in high trouble serving areas of this type. The average rate of customer troubles assigned to outside plant (code 4) is about 0.8 troubles per 100 stations per month, and the average loop operating cost is about \$5 per line per year, whereas these rates in serving areas candidate for rehabilitation can be ten times as great.

developing the rehabilitation In it has been most useful to methods. construct a unified picture of the numerous factors contributing to the defective pair problem. This view is shown in Fig. 3, which we call "The Infernal Triangle". The end result of defective pairs is caused by a combination of wet cables, wet buried splices, and deteriorated terminals. Moreover, there is an insidious interaction among these. For example, water in cable sections leads to conductor faults, which can lead to repair splices, which can be defective and lead to water entry and more pair faults, which often lead to access to pedestal terminals for trouble shooting and pair swapping, which aggravates the deteriorated conditions in the pedestal and causes more pair faults, causing more access and pair swapping, etc., etc. To make matters worse, there are many other factors which can exist in any combination to start or accelerate the cycle by causing one of the basic problems.

It is this unified view provided by the Infernal Triangle which forms the basis for the solution philosophy. That is, for a solution to be effective in reducing trouble rates, it must systematically recognize and deal with all of the basic

Do Sales Angle State State

INFERNAL TRIANGLE

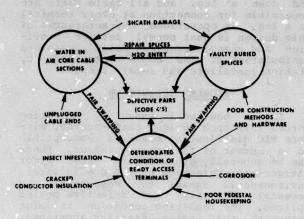


Figure 3

problems and their respective aggravators at once. Anything less will soon lead to a renewed ride around the Infernal Triangle and its ultimate fate of high trouble rates and operating costs.

The truth of this last statement is well known to operating people. There have been many attempts at rehabilitation in the past, but these usually involve either reclaiming some cables, or refurbishing some terminals, or rebuilding some splices, etc. This piecemeal approach never results in permanent operating improvement, and has convinced many that "rehabilitation" is futile.

Therefore, the primary characteristics of the rehabilitation method presented here are that it is systematic and comprehensive. The major steps are shown in Fig. 4, and these will be described in the following section.

REHABILITATION PROCEDURE

Identification of a worthy candidate area for rehabilitation is an essential preliminary to the actual procedure. While this is a complex process whose details are beyond the scope of this paper, its general features should be understood. Several manual and mechanized programs for tracking and analyzing the troubles and operating costs of specific segments of outside plant have become available to the Bell operating companies. Of particular importance to rehab are the Computerized Cable Upkeep Program (CCUAP), and the Trouble Report Evaluation and Analysis Tool (TREAT). CCUAP is a system which tracks and summarizes all cable repair activity by Allocation Area, described above. Similarly, TREAT is a computerized system

which accumulates and summarizes all customer trouble reports by cable number. Normally cable numbers can be mapped into Allocation Areas. The results form these two systems can be integrated with service order and assignment data in the Facility Analysis Plan (FAP) to develop a total operating cost per working line for each Allocation Area within a district. Under FAP the allocation areas can be ranked according to operating cost, and the contributors to cost analyzed to determine major causes i.e., whether high costs are due to cable troubles, terminal troubles, facility shortages, etc. The operating costs per line can then be combined with cost estimates for upgrading and rehabilitating the plant along with estimates of expected improvements in operating costs to develop an expected rate

REHABILITATION SEQUENCE

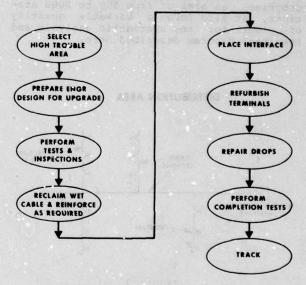


Figure 4

of return for rehab of each allocation area.

When the Allocation Areas are ranked in descending order of potential rate of return, the prime candidates for rehabilitation are obvious. It important to note, however, that this process of identification is thorough, systematic, and based on real operating data, not just a matter of opinion of various maintenance personnel in the district. Once an area has been identified by this process, then the steps of rehabilitation described below can begin.

(一) (1) (1) (1) (1) (1) (1) (1)

Characterization

In preparation for characterization, the outside plant engineer prepares for the field forces a set of cable plats and standard data forms on the serving area to be characterized. All results on every element of plant are recorded on these forms and returned to the engineer for analysis.

Characterization of the plant comprises two major components: pedestal (terminal) inspection, and cable testing. In pedestal inspection, every pedestal terminal is visited and inspected for broken wires, damaged insulation, insect damage, condition of sheath bonds, tangled conductors, insulation cracking, and transpositions (from pair swapping). All conditions are recorded on the worksheets along with the general condition rating as GOOD, FAIR, or POOR.

At the same time pedestals are visited for inspection, the service wires are tested. The vacant pair in each service wire is tested for leakage to ground with an ohmmeter. Any faults found are recorded on the worksheet according to pedestal address and address of customer served. while the craftsman is at each Also. pedestal, tests are made on the cable tions between pedestals to determine if sections are wet or dry, and to locate all sheath faults to ground. The water tests are made using the 176A Test Set. This set automatically compares the capacitive and resistive lengths of two vacant pairs within each section, and gives a direct indication of "wet" if the capacitive length is excessive. A decision threshold of 7% is built in to the instrument to allow for normal manufacturing variation. If the capacitive length is more than 7% above the resistive length the cable is declared wet, and if it is less than 7% above the resistive length, it is declared dry. As a result the craftsman records wet or dry on the worksheet for each cable section. In addition to the water test, each cable section is tested at this time for shield leakage to ground with an ohmmeter. If shield leakage to ground is found, the sheath faults are located and marked using a 173A Sheath Fault Locator or equivalent. The number and location of all sheath faults are recorded on the worksheets along with a simple schematic diagram to indicate any obstacles to repair of the cable, such as driveways, pools, etc.

At this point the field forces return to the engineer a complete set of data on every terminal and cable section in the candidate area indicating its exact

physical condition.

Diagnosis and Planning

In addition to repairing physical defects, it is also important to eliminate problems caused by routine craft activity. This is a common problem in areas of older ready-access multiple plant having high rates of inward-outward movement. This is overcome by upgrading to modern interfaced serving area design as part of the rehabilitation process. This upgrading reguires a few cables in the distribution area to be reinforced, an interface to be placed, and multiples in the distribution legs to be broken by reassignments.

Once the engineer has identified the cables to be replaced for upgrading, he must also make a decision on all remaining wet sections. Using the process indicated in Figure 5, he decides whether to reclaim by pumping (see Cable Treatment, below) or replace each section with filled Because most of the high trouble cable. plant of this type is in well established neighborhoods, the decision is usually in favor of reclaiming by pumping. Replacement often requires hand trenching and expensive reconstruction of lawns, fences, and patios so that pumping costs much less, even on small cables down to 50 or 25 pairs.

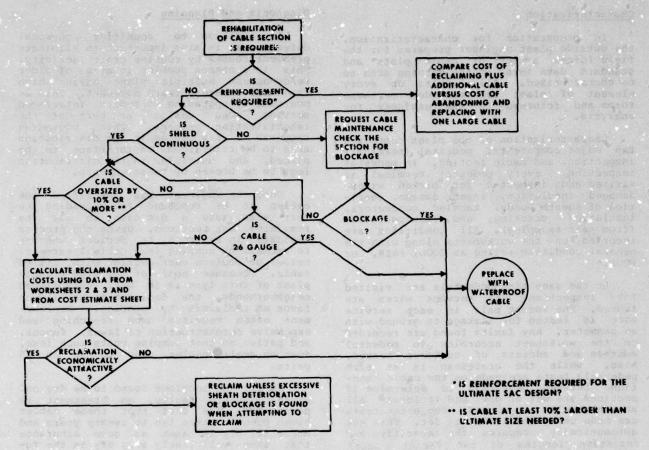
As for the sections found to be dry and without sheath faults, no treatment is prescribed. The fact that these cables haven been in place ten to twenty years and are still dry is taken as good assurance that they will likely stay dry in the fu-

As the result of this decision process, the engineer issues a work order covering every cable section, calling for either replacement, pumping, or no action. It is interesting to note in recent trials the breakdown of treatment has been

> Wet Cables 30% 25% Reclaim 5% Replace Left in Dry 65% Reinforce 5%

Certainly, not all the cables have to be either replaced or reclaimed when this diagnostic approach is used.

Similary, the engineer must make decisions on the treatment for terminals. Usually, because of the uniformity of conditions over an area, this can be done on a blanket basis for all pedestals. If pedestals are found to be in good condipedestals are found to be in good condi-tion, only topical treatment may be adequate. This includes placing fresh gravel in the base, tightening bonds, placing insecticide strips, and general clean-up. However, this good condition is



REPLACE VS RECLAIM DECISION

Figure 5

rarely the case in high trouble areas, so that complete rebuilding is called for.

Having received the work orders on terminals and all cable sections from engineering, the field forces undertake the physical rehabilitation. These steps are described in the following sections.

Cable Treatment

As indicated above, the treatment of wet cables includes either replacement with filled cable or reclamation by pumping. Replacement is quite straight forward using standard materials and methods of waterproof cable construction. Cable reclamation has been reported in earlier references, but essentially it consists of pumping the wet cable full of a low viscosity oil-extended urethane compound which forces out the water and later gels to form an impervious dielectric filler.

In 22 and 24 ga. cables this technique will usually recover all pairs with shorts, crosses, or grounds. The few opens caused by corrosion will not be recovered, but except in extreme cases these amount to only 1 or 2% of the cross section. Even in more fragile 26 ga. cables where some pairs can be forced open by the injection pressure, the recovery rate is normally 95% or better. Since most distribution cables are considerably oversize beyond the first section from the interface, this recovery rate is more than adequate for service requirements in stable neighborhoods.

An important part of the reclamation process is the repair of all sheath faults which were located in the earlier testing phase. This is necessary to assure that the filling compound will be pumped through the cable section and not out into the soil, and also to eliminate the original source of water entry.

Once the wet cables have been treated by reclamation or replacement, an important milestone has been reached: all cables in the rehabilitation area are dry and stabilized. No known wet sections are left in plant.

Terminal Treatment

The materials, hardware, and methods used in terminal rebuilding are selected to eliminate all of the problems indicated in Figure 3 and prevent their future occurance. The first step (Fig. 6) is to remove the old pedestal, dig down to



OLD PEDESTAL EXCAVATED Figure 6



NEW PEDESTAL PLACED Figure 8

provide some working slack in the cable, and cut back the sheath to expose fresh conductors and insulation. Next, (Fig. 7) the full cable core is spliced across using the 710 Modular Connector, and a fixed count terminal block is bridged onto the count assigned by the engineer to this location. Service wires are then transferred to the terminal block, and the old deteriorated loop of cable conductors cut away. New bonds to the shield are made, and separate flexible bond straps are attached.



OLD WIRE SPLICED OUT Figure 7



COMPLETED TERMINAL Figure 9

Once the wire work has been reconstructed, it is placed vertically in a special version of the standard Bell System buried closure, and a new pedestal housing set in place (Fig. 8). The terminal block is mounted on the pedestal backplate, and the new sheath bond straps connected to the housing. At this stage, using the information recorded during inspection, the craftsperson locates and repairs any service wire faults.

All pedestals in a leg are brought to this point prior to encapsulation, so that any remaining defects or errors can be found and repaired. When all wire work on the leg is verified to be correct, all of the rehab closures in the pedestals are encapsulated using standard re-enterable D-Encapsulant. Finally, fresh gravel is placed in the base of the closure to minimize condensation on the terminals. The result is then a completely rebuilt terminal, stabilized and protected against future deterioration (Fig. 9).

Final Test

When all legs have been rebuilt, all pairs are tested to the field from the interface. Opens, if any, are likely due to splicing errors in pedestals, and they can be corrected if the pairs are needed. Shorts, crosses, or grounds indicate leftin water or defective buried splices, and will be a continuing source of trouble. These faults must be located using bridge techniques and cleared by cutting out defective splices or reclaiming wet sections. In practice, very few of these residual problems occur.

RESULTS

Performance

This method was field trialed in four locations across the Bell System, and operating companies are now proceeding on their own. In the trial areas, typically 95% of the defective pairs have been recovered beyond the interface, i. e. defect rates have been reduced from around 20% to about 1%. However, the most important effect is in actual reduction of customer trouble reports and the resulting repair expenses. Figure 10 shows the rate of customer troubles cleared to outside plant in troubles per 100 stations per month in an actual trial project. This was a typical "high-trouble" area, and prior to rehab the rate was about 5 times the System average rate for all plant. After rehab the outside plant trouble rate went to 0.0 and has remained there since, now over two years.

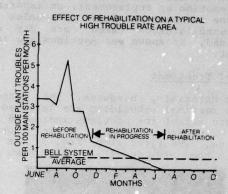


Figure 10

Based on knowledge of the specific materials and methods used, there is no reason to expect this rate to rise in the future. This same reduction to 0.0 has been repeated in all four trial areas.

Cost Effectiveness

The procedure described here is expensive, however it averages only 1/3 to 1/2 the cost of total cable and terminal replacement. Costs in trial areas have ranged from \$100 to \$200 per station, and a typical breakdown is shown in Figure 11. The benefits have been the elimination of an average of 5 troubles per 100 stations per month at a cost of about \$50 per trouble. This translates into an expense saving of \$30 per station per year.

If we assume 2/3 of the initial rehab cost is capitalized, and 1/3 is maintenance

TYPICAL REHABILITATION COST BREAKDOWN

Characterization & Eng	ineering 10%	
Cable Reclamation	30%	
Cable Replacement	10%	
Pedestal Rebuilding	35%	
Service Wire Repair	10%	
Miscellaneous	10%	
	Total 100%	-

Figure 11

expense, and that the improvement of eliminating the outside plant troubles has a lifetime of 10 years, then the after tax rate of return of the rehab project is over 14%. This is certainly sufficient to justify rehabilitation of many high-trouble areas without even taking credit for several other important benefits. In addition to the savings in routine repair expense, rehabilitation reduces many of the facility modifications and assignment changes required to provide new service in congested plant. It also reduces counts of other classes of troubles (caused by miscoding outside plant troubles) and troubles-not-found. And probably the most important benefit not yet quantified, the quality of customer service is greatly improved.

REFERENCES

- R. P. Collins and J. R. Apen, "A Complete Waterproof Cable System for Construction of Buried Loops", Proceedings of the International Symposium on Subscriber Loops and Services, May 1976.
- B. Pusey, M. Chan, and W. Roberts, "Evaluation of Thermal Degradation in Polyethylene Telephone Cable Insulation", Proceedings of the 20th International Wire and Cable Symposium, 1971.
- J. B. Howard, "Stabilization Problems With Low Density Polyethylene Insulations", Proceedings of the 21st International Wire and Cable Symposium, 1972.
- 4. S. Kaufman et al, "Reclamation of Water-Logged Buried PIC Telephone Cable", Proceedings of the 21st International Wire and Cable Symposium, 1972.
- 5. S. Kaufman et al, "The performance of Cable Reclamation", Proceedings of the 26th International Wire and Cable Symposium, 1977.
- R. Sabia et al, "Design Considerations, Chemistry, and Performance of a Reenterable Polyurethane Encapsulant", 24th International Wire and Cable Symposium, 1975.



R. P. Collins joined Bell Laboratories in Baltimore in 1962 with a B.S. in Mechanical Engineering from Miss. State University. In 1965 he received his M.S. in Engineering at the University of Maryland. He is presently Supervisor of the Transmission Media System and Applications Group in Atlanta, responsible for planning, systems studies, new product introductions, and rehabilitation developments in the cable and wire area.



W. S. Pesto is a member of the Transmission Media System and Applications Group at Bell Laboratories in Atlanta. He joined the company in Winston-Salem in 1961 and at present is responsible for developing methodologies for outside plant rehabilitation. Mr. Pesto received the A.S. degree in engineering from St. Bernard College, the B.S.E.E. degree from Auburn University and the M.S.E.E. degree from North Carolina State University.

The Relation between the Foaming Mechanism and Viscoelastic Properties of High Density Polyethylenes for Expanded Communication Cables

Masatake Matsui Yukio Morita

DATNICHI-NIPPON CABLES, LTD. Amagasaki, Japan

sections.

ABSTRACT

An experimental study of the expanded insulation for communication cables was carried out to determine the effect of rheological parameters on the foam structure. For the study, the chemical blowing agent (azodicarbonamide) was used to produce expanded insulations of highdensity polyethylenes. The quality of foam was determined from the newly introduced open cell parameter obtained using photomicrographs and rheological parameters were measured by a capillary rheometer. It was found that the open cell parameter correlates with the apparent viscosity, the non-Newtonian index, and the recoverable strain determined with two methods. These results were interpreted in terms of cell opening process.

1. INTRODUCTION

The foamed plastic insulation has been utilized for improving the duct usage by the reduction in the diameter of a core and the transmission characteristics of communication cables. It is necessary for the development of the higher quality expanded insulation to produce the insulation having more homogeneous foam structure. In the present paper, we shall try to investigate high-density polyethylenes suitable for manufacturing such insulations by a chemical blowing method. The largest problem in the material research is which of properties or characteristics affects on the homogeneous foamability and another is how to estimate the foam structure as quantitatively as possible. For the latter problem, the newer parameter will be introduced to represent the steric foam structure in section 5.2.1. and the former will be discussed in section 5.2.2.. At first let us review a few elements in conjunction to the form extrusion briefly in following

2. INITIAL CONSIDERATION

2.1 Foam Extrusion Process

It is well known that 'he extrusion process of the expanded insulation is a very complicated process, in which many physical and chemical processes are interacted each other, however, the foam extrusion process can be brokendown to elements, as shown in Fig. 1. What is evident from Fig. 1 is that the foam extrusion can be divided into two important prime processes, the non-Newtonian flow in the wire coating die and the phase transition or separation. Moreover, it can be considered that these prime processes are composed of rollowing three elements:

- the surface tension between the polymer melt and dissolved gases,
- (2) the solubility and diffusivity of dissolved gases,
- (3) the melt elasticity and viscosity of the polymer.

Authors will discuss a few points about these elements by briefly reviewing in the following sections.

2.2 Surface Tension

As well known, the surface tension is an important element in the foaming process, because the loaming the phase transition, in which a new process, because the foaming itself means surface is creating and developing. regard to the nucleation of micro foams, it is suggested that there are two types of nucleation, homogeneous nucleation and heterogeneous one (1, 2). In the nomogeneous nucleation, one phase in a state of supersaturation changes through the pressure drop to the new condition where two phases coexist. On the other hand, in the heterogeneous nucleation, bubbles grow on the surface of a pre-existing site, for instance, the surface of extrapped air or small particles. It is assumed that the latter is predominant in the actual foam extrusion, because the

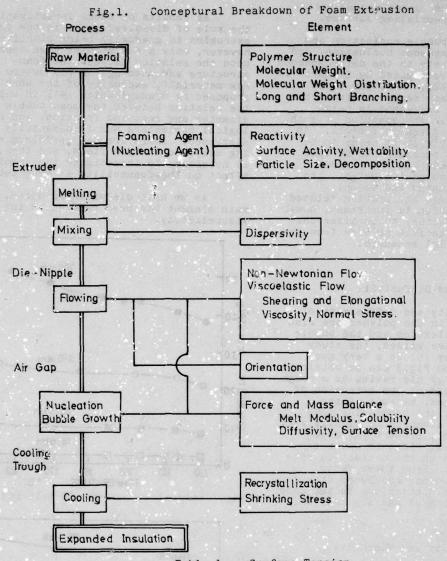


Table 1. Surface Tension

MATERIAL	CHARACTERIZATION	TENPERATURE RANGE (°c)	r 1) (dyne/cm)	dr/dī (dyne/cm·deg)	REFERENCE
HDPE	Mw: 6.7,000, 0,2 CH ₃ /100C	135 ~ 210	28.1	0.058	
LDPE	M:7,000 , 5.2 CH ₃ /100C	120 ~ 165	2 6.5	0.0 64	(3)
LDPE	M: 2,000 , 50 CHa/ 100C	115 ~ 195	25.9	0.0 60	
HDPE	Mv:8.0 X 10	146 ~ 200	r=58.0 - 0	.072 T (°K)	OA LATE
HDPE	Mv : 6.9 X 10 ⁴	ditto	d	itto	(4)
LDPE	Mn:1,0 X 10 ⁴	125 ~ 193	r = 57.1 - 0.	076 T (°K)	

(1) SURFAC TENSION)

decomposed solid residue of a chemical blowing agent or the undecomposed particle acts as the pre-existing surface.

The rate of bubble nucleation and growth in the homogeneous nucleation, and the bubble growth rate in the heterogeneous nucleation were investigated by Stewart (1) and Gent-Tompkins (2). Also the study of measuring the surface tension between the polyethylene melts and gases is being continued steadily. The examples of such studies (3, 4) are given in table 1. As is evident from Table 1, it seems to be quite all right to consider the surface tension is independent of the polymer structure such as molecular weight, its distribution, branching and so on. Accordingly, although the problem related to the surface tension is important, however, it is satisfactory to consider the element as a less serious problem from the viewpoint of material research.

2.3 Solubility and Diffusivity

The solubility and diffusivity of the dissolved gas in the polymer are also related to the nucleation and the bubble growth. As to these values, the study proposed by Griskey (5) is a very good example. Fig. 2 and Fig. 3 can be obtained using the results of his review as a rough estimation. In case of the extrusion of expanded insulations, because of the higher line speed, the processing time affected by these elements is usually very short. In addition, Stewart (1) made clarified that these elements are not affected very much on the nucleation rate and bubble number. From these facts mentioned above, we may concluded that these elements are not serious in the same sense as the problem of surface tension.

2.4 Melt Elasticity and Viscosity

For about ten years since 1970, the rheology of foam extrusion has been studied continuously. The influence of dissolved gases on the flow behavior of high and low density polyethylene melts was investigated using a capillary extrusion rheometer by Kwei-Blyler (6). Their results indicated that the addition of gas in the amount of 0.5% by weight to both polyethylene melts causes a viscosity reduction of approximately 20% at constant shear rate. According to Bigg et al (7), the reduction in viscosity of melt is inderendent of temperature over the range of temperature investigated. Moreover, Han-Villamizar (8) concluded the bulk viscosity of a melt containing blowing agent decreases with increasing concentration of the blowing agent.

As results of these investigations, the role of dissolved gases in the foam extrusion is gradually being clarified. however, only a few studies have been done upon the relation between the foam structure and rheological parameters of raw materials, exclusive of the work proposed by Oyanagi-White (91) in which the relation between the mean bubble diameter and occupied fraction, and rheological parameters was fundamentally discussed. There are many problems remaining unsolved in this field, and then, it is necessary to investigate the rheological effect on the foamability in more detail.

As we have discussed as above, the main element has been reduced to the melt viscoelastity.

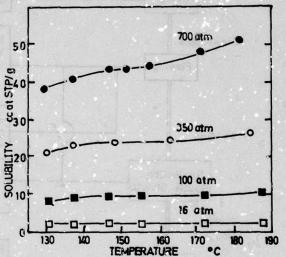


Fig. 2. Solubility between PE Melt and N2 gas

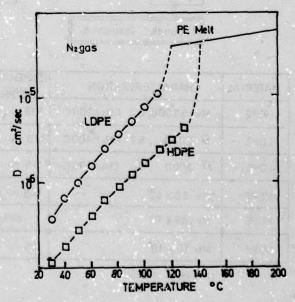


Fig. 3. Diffusion Coefficient

EXPERIMENTAL

3.1 Material

Four high density polyethylenes were used in the present work and are summarized in Table 2. These polyethylenes are still being developed by a resin supplier and were chosen so as to represent a range of melt rheological parameters. The blowing agent used in this experiment was Ficel EP-A (azodicarbonamide premixed with a small portion of a filler) supplied by Faiscns, U.K.. The concentration of the blowing agent was 1.0% by weight.

3.2 Capillary Rheometry

The raw polyethylenes with and without the foaming agent were extruded at 200°C from a constant load type capillary rheometer, KOKA flow Tester Model 302 (Shimadzu, Kyoto, Japan). Dies of diameter 1.0mm and length/diameter ratios (L/D) 1, 2, 10, and 20 were used. In order to minimize draw-down effects and measure the diameter of the extrudate exactly, the extrudate was cooled in the liquid having approximately same density as the melt investigated as soon as possible.

For flow in a capillary rheometer, the nominal snear stress at wall rw and the corresponding shear rate jw are defined as follows, respectively:

$$\tau \mathbf{w}' = \frac{P\mathbf{a} \cdot R}{2L}
\dot{\tau} \mathbf{w}' = \frac{4Q}{\pi R^3}$$
(1)

where Pa is the applied pressure in the reservoir, R is the capillary radius, and Q is the volumetric flow rate. These quantities may be made corrections for the excessive pressure and for the non-Newtonian behavior, respectively. The true wall shear stress tw can be calculated from the following relation (the Bagley correction (10)),

$$\tau \mathbf{w} = \frac{b_{\mathrm{a}}}{2((L/R) + n_{\mathrm{B}})} \tag{2}$$

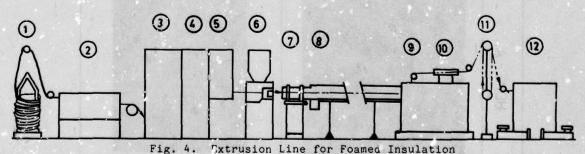
where n_B is the Bagley entrance correction. And the corrected shear rate at wall $\dot{\gamma}_w$ can be given by the equation (3) (10).

$$\dot{\mathbf{r}}\mathbf{w} = \left(\frac{3n \rightarrow 1}{n}\right) \cdot \dot{\mathbf{r}}\mathbf{w} \tag{3}$$

where $n = d(\log \tau w')/(\log \gamma w')$

Table 2. Polymers Investigated in Experiments

INDEX	DENSITY	MELT INDEX	FLOW RATIO	Mn	Mw	Q
HDPE-A	0.951	0.79	16.1	1.3X10 ⁴	10.0 X 10 ⁴	7.7
HDPE-B	0.954	0.76	15.7	1.3 X 1 0 ⁴	10.2X10 ⁴	7.8
HDPE-C	0,951	0.65	22.9	0.9X10 ⁴	10.5 X 10 ⁴	11.7
HDPE-D	0.947	0.43	26.3	1.07 X 10	18,0×10 [†]	16.8



- 1. Pay-off 2. Wire Drawing Machine 6. Extruder
- 3. Annealer
- 4. Preheater
- 5. Tension Helper

- Quenching Trough
 Water Spray Trough
- 10. Spark Tester
- 11. Dancer Roll Assembly 12. Take-up

Fig. 5 Photomicrograghs of Expanded Insulations (Magnification; x50)

MATERIAL SECTION	HDPE - A	HDPE-3	HDPE - C	HDPE-D
CROS S SECTION				
LONGITU- DINAL SECTION				

Fig.6. Optical Photomicrographs of Extrudates from Rheometer

Since polyethylene melts investigated in the experiment obey the power law (see Fig. 8), the apparent viscosity can be obtained from the following equation,

 $\tau = \eta \left(\dot{r} \right) \cdot \dot{r} \tag{4}$

where

$$\eta(\dot{r}) = K \dot{r} n - 1 \tag{5}$$

in which K and n are material constants, characteristic of the melt concerned.

3.3 Extrusion of Expanded Insulation

Expanded insulations were extruded using the wire coating line shown in Fig.4. For this experiment insulated cores were manufactured by coating about 0.35 mm expanded insulation on the conductor of 0.5 mm in diameter at a constant speed of 1500 m/min.

3.4 Observation of Foam Structure

Photomicrographs were made on cross and longitudinal sections of expanded insulations using a Scanning Electromicroscope Model JSM-50A (JEOL, Japan). For foamed extrudates of the capillary rheometer, the opticalmicroscopic observation carried out in the same manner as the case of expanded insulations (Model Ke, Nikon, Japan).

The void fraction (the occupied fraction of foams) of the expanded insulation was obtained measuring the relative density of foam insulations and raw materials.

4. RESULTS

4.1 Foam Structure

Representative SEM photomicrographs of cross- and longitudinal sections for the expanded insulations, which were manufactured under same condition, are shown in Fig.5. All insulations shown in Fig.5 have approximately same void fraction of 45 - 47%. These photomicrographs indicate that the mean diameter of the unit cell (the isolated spherical cell) are almost same because of premixing same amount of the blowing agent, however, there is large difference in the degree of opened cells among samples. It can be also recognized from Fig.5 that the degree of opened cells is not necessarily the same with each observed section. Even though there is few open cells in the cross section of a sample, many open cells are observed in the longitudinal section of the same sample.

Fig.6 shows typical photomicrographs of foamed extradates from the capillary rheometer at a constant load, namely, at

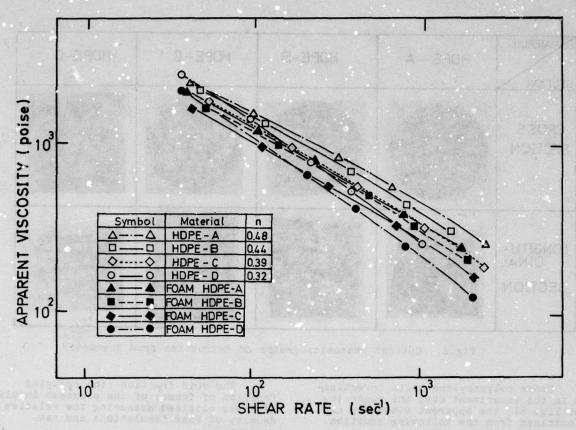


Fig.7. Apparent Viscosity of Polyethylenes with and without Foaming Agent.

a constant apparent shear stress. In this case, the stress of the melt received in die and the way of stress relief after emerging out of the die exit are reflected in the degree of opened cells. Fig.6 shows a interesting tendency, that, the open cell distribution of the cross section is localized in the neighbourhood of the flow center relatively, and furthermore, the opened cell observed in longitudinal section is elongated in the radial direction of extrudate.

To summarize the observation results, it is necessary to reconsider the one-dimentional observation.

4.2 Rheological parameters

4,2.1. Apparent viscosity

Fig.7 shows the apparent viscosities of raw polyethylenes and polyethylene/foam agent blends carculated by substituting the corrected shear stress and the corresponding shear rate into the power law given by the equation (4). The power law indices derived from the equation (5) are given in Fig.7. As shown in Fig.7, the

reduction in the viscosity of raw polyethylenes by pre-mixing with a foaming agent is recognized, and furthermore, the tendency of the viscosity reduction agrees with above-mentioned works (6-8).

4.2.2. End correction

A concrete example of the Bagley plot (10) (equation (2)) is given in Fig.8. It has been led to a strong suspicion that the Bagley plot has a poor linearity. In fact, according to recent studies (11, 12), the Bagley plot gave curved plots. However, since polyethylenes used in this experiment give approximately linear lines as in Fig.8, the end correction np seems to be able to estimated from the x-intercept of the line. The end corrections obtained using the above approximation are given in Fig.9. As is generally known, these value increase with shear rate.

Because it is assumed that the steady state flow cannot fully develope in the capillary flow of melts containing the foaming agent and the meaning of the end correction is not clear from the definition of end correction postulated for the

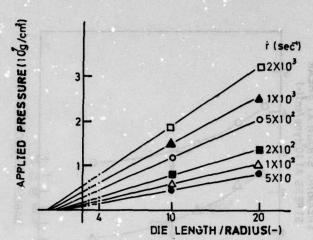


Fig.8. Bagley Plots

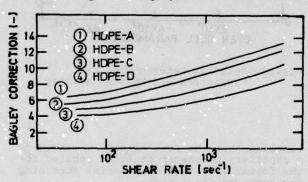


Fig.9. End Corrections

fully-developed steady flow, and then the end correction of melts containing the foaming agent does not be taken into consideration in this study.

4.2.3. Extrudate swelling

The shearing strain calculated from the following equation derived by McLucki-Rogers (11) is plotted in Fig.10.

$$\tau = G\left(\alpha - \frac{1}{\alpha}\right) \tag{6}$$

where α is the square of extrudate swelling ratio $(De/Do)^2$ and G is the shearing modulus, in which De and Do are the diameter of the extrudate and the die used in the experiment. For the relation between the die swell and the shearing strain, another hypothesis was proposed by Tanner (12). Plots given in Fig.10, however, give a good linearity.

5. DISCUSSION

5.1 Quantitative representation of foam structure

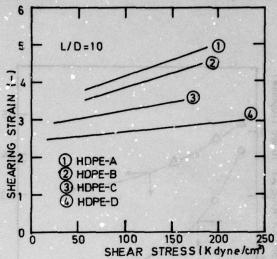


Fig.10. Recoverables Strains

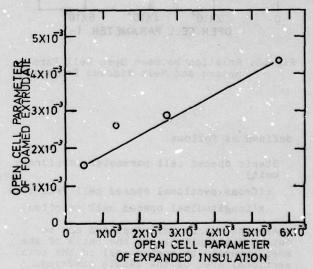


Fig.11. Open Cell Parameters

It seems complicate to classify the foam structure quantitatively in the case of not only expanded insulations but foamed plastic products. In the past, for the purpose of the semi-quantitative representation, several methods which included the measurement of mean bubble size and the sensuous ranking by eye, have been used for studies. For more exact analysis, Mihira et al (13) proposed the method suggesting the foam geometry statistically, but, their method cannot be applied to the case investigated. The reason is that, in spite of their assumption requiring a uniformly-distributed spherical bubble, actual foams include irregular opened cell. Although the complete representation of the steric foam structure seems to be the subject for a future study, in this paper, as an approach to represent the steric foam structure, we will introduce the parameter

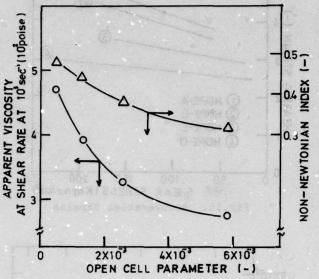


Fig.12. Relation between Open Ce 1 Parameters and Melt Viscous Properties

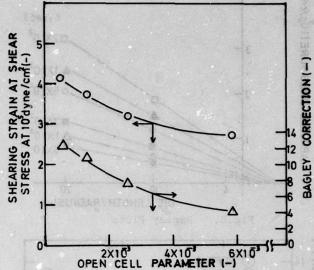


Fig.13. Relation between Open Cell Parameters and Melt Elasticity

defined as follows:

Steric opened cell parameter (arbitrary unit) (7

=(Cross-sectional opened cell fraction)
x(Longitudinal opened cell fraction)

where the opened cell fraction can be obtained graphically as the ratio of the area occupied by opened cell to the total sectional area of the sample observed.

Let us focus our attention on the foam structure of the expanded insulation. It should be emphasized that the degree of the opened cell is a more important factor than the mean-averaged diameter, because open cells cause pin-holes or harmful pockets in the insulation, which naturally affects the reduction in the dielectric characteristics and the transmission characteristics of communication cables. Accordingly, the steric representation given in equation (7) has an important mean actually.

The relation between the opened cell parameter defined in equation (7) of the foamed extrudates obtained from capillary rheometer and expanded insulations is shown in Fig.ll. As in Fig. 1, the opened cell parameter of the foamed extrudate is approximately proportional to the values of expanded insulations. We may therefore

conclude that the foam extrusion method by a capillary rheometer could be applied for the foamability test of material screening for expanded insulations.

- 5.2. Rheological parameters influencing on foam structure
- 5.2.1. Parameters related to viscous properties

Fig.12 shows the relation between the apparent viscosity calculated from the equation (4) and the non-Newtonian flow index estimated using the equation (5), and the open cell parameter described above. The values of the apparent viscosity shown in Fig.8 were calculated at a critical shear rate or slightly lower shear rate than the critical point (about 1 x 103 sec-1), where the well-known melt fracture phenomenon began.

It is apparent from Fig.12 that the apparent viscosity at the upper limit shear rate in the range of steady state are closely related to the opened cell structure and, as the viscosity at this point increases, the opened cell fraction decreases constantly.

For interpretation of this result, let us propose a hypothetic model for the cell opening process taken steps as

follows:

- the agglomeration of isolated spherical cells,
- (2) the interfacial rupture of the melt film separating each cell by the gas pressure difference,
- (3) the occurance of the opened cell.

According to the visual study on the die foaming process by Han-Villamizar (8), the bubbles begin to grow in the capillary die itself. If the above-proposed model is add to the result obtained by them, it is assumed that the initial agglomeration of isolated cells take place in die, too. Provided that there exist agglomerated cells in the die, the interfacial rupture of separating film depends on the viscosity of melt in higher shearing field. As the lower viscosity accelerates the thinning and slippage of the separating melt film and then the interfacial rupture occurs earlier.

Fig.12 indicates that the open cell parameter is dependent on the non-Newtonian index. The non-Newtonian index is a measure of the velocity of melt flow in die. The lower non-Newtonian index gives the more flat velocity profile. This fact suggests that the agglomeration in the cell opening process is accelerated in the fluid having the lower non-Newtonian index because of the relatively slowly flowing at the center.

Although Street (14) proposed with theoretical investigation that the growing of bubble is predominated by the biaxial extentional viscosity, which is approximately proportional to a 6-fold zero-shear viscosity, enough data for discussing this postulation could not be obtained in our work.

5.2.2. Parameters related to elastic properties

The influences of the elastic properties, the entrance correction obtained from equation (2) and the recoverable shearing strain from the extrudate swelling and equation (6), on the open cell parameter are shown in Fig. 13.

The Bagley entrance correction consists of two terms, a viscous component nc and an elastic component (Sp/2),

$$n_B = nc + (S_R/2)$$
 (8)

where nc is the Couette loss and S_R is the recoverable strain defined as;

$$S_R = (P_{11} - P_{22})/\tau w$$
 (9)

in which (F₁₁-P₂₂) is the normal stress difference in the direction of flow. The Couette component used to treat as a constant (0.77). Using this value along with the values given in Fig. 8, it becomes evident that the elastic component occupies the major portion of the Bagley correction.

Another parameter, which are related to the elastic properties of melt, is the extrudate swelling correlated to the recoverable shearing strain as reported in McLuckie-Rogers's work (11).

It is evident from Fig. 13 that both above parameters are influencing on the opened cell parameter of expanded insulation. The opened cell increases with decrease in the Bagley correction and with decreasing shear strain. If we consider the fact relative to the hypothetic model proposed in 5.2.1, it is assumed that the recoverable strain should be related the limiting quantity for the elastic rupture of the interface, especially in a rapid cell opening.

6. CONCLUDING REMARKS

The experimental study presented above has identified some important aspects of rheological significance in the extrusion of foamed insulation, and the following conclusions may be drawn:

- The newly introduced opened cell parameter appears to be useful for the representation of the steric foam structure,
- (2) The foam extrusion method using the capillary rheometer seems to be worth using as the screening for the foamability of materials,
- (3) The opened cell parameter correlates to the viscous properties of raw polyethylenes and decreases with increase in the apparent viscosity at higher shear rate and the non-Newtonian index,
- (4) The opened cell parameter relates also to the elastic parameters and decreases with increase in the recoverable strain,
- (5) These experimental results can be explained well by the hypothetic model proposed newly.

ACKNOWLEDGEMENT

The authors would like to acknowledge the continuing guidance and encour-

agement of Dr. H. Fujita. We also express our appreciation to Mr. K. Morita for the observation and testing of samples.

REFERENCES

- C.W. Stewart, "Nucleation and Growth of Bubbles in Elastomers," J.Polym. Sci., A-2, 8, 937-955 (1970)
- A.N. Gent and D.A. Tompkins, "Furface Energy Effects for Small Holes or Particles in Elastomers," J. Polym. Sci., A-2, 7, 1483-1488 (1969)
- G.L. Gaines, JR., "Surface and Interfacial Tension of Polymer Liquids -A Review," Polym. Eng. Sci., 12, 1-11 (1972)
- T. Sakai, "Surface Tension of Polyethylere Melt," Polymer, 6, 659-661 (1965)
- R.G. Griskey, "Behavior of Gases in Structural Foam during Molding," Mod. Plast., 72-76 (June 1977)
- 6. L.L. Blyler, JR. and T.K. Kwei, "Flow Behavior of Polyethylene Melts Containing Dissolved Gases," J. Polym. Sci., C-35, 165-176 (1971)
- 7. D.M. Bigg, J.R. Preston and D.Brenner, "An Experimental Technique for Predicting Foam Processability and Physical Properties," Polym. Eng.Sci., 16, 706-711 (1976)
- 8. C.H. Han and C.A. Villamizar,
 "Studies on Structural Foam Processing,
 "Polym. Eng. Sci., 18, 687-710 (1978)
- 9. Y. Oyanagi and J.L. White, "Basic Study of Extrusion of Polyethylene and Polystyrene Foams," J. Appl. Polym. Sci., 23, 1013-1026 (1979)
- E.B. Bagley, J. Appl. Phys., 28, 624 (1957)
- 11. C. McLuckie and M.G.Rogers, "Influence of Elastic Effects on Capillary Flow of Molten Polymers," J. Appl. Polym. Sci., 13, 1049-1063 (1969)
- 12. R.I. Tanner, "A Theory of Die-Swell." J. Polym. Sci. A-2, 8, 2067-2078(1970)
- 13. K. Mihira, T. Ohsawa and A. Nakayama,
 "Geometry of Polymeric Foam or
 Cellular Structures (I)," KolloidZ.u.Z. Polymere, 222, 135-140 (1968)
- 14. J.R. Street, "The Rheology of Phase Growth in Elastic Liquids," Trans. Soc. Rheol., 12, 103-131 (1968)

Masatake Matsui

Material Research Laboratory

Dainichi-Nippon Cables, Ltd.

Mr. Matsui graduated from Kyoto Institute of Technology with a M. Sc. degree in polymer chemistry in 1969.

Then he joined Dainichi-Nippon Cables, Ltd. and has been engaged in the research and development of plastic materials for power and telephone cables.

Mr. Matsui is currently chief engineer of Material Research Laboratory at Dainichi-Nippon Cables.



Yukio Morita

Material Research Laboratory

Dainichi-Noppon Cables, Ltd.

Mr. Morita graduated from Osaka University majoring applied chemistry in 1973.

Then he immediately joined Dainichi-Nippon Cables, Ltd. and has been engaged in the research and development of plastic materials for telephone cables.

Mr. Morita is currently a member of the Japan Society of Polymer Science.

EFFECT OF THERMAL AGING ON THE FLEXIBILITY AND CONDUCTIVITY OF PLATED AND UNPLATED COPPER CONDUCTORS

TSUTOMU INAGAKI

HUDSON WIRE COMPANY OSSINING, NEW YORK

ABSTRACT

The conductivity and flexibility of plated and unplated copper conductors were evaluated after thermal aging at 100°C to 250°C for times up to 2,000 hours. Effects of conductor size and construction on insulated and uninsulated stranded conductors were also evaluated. Optical microscopy, as well as SEM and EDAX analyses, were then conducted to correlate the observed results with the microstructure of the thermally aged specimens.

1.0 INTRODUCTION

Within recent years, a growing controversy has developed among researchers as to the effect of prolonged exposure to elevated temperatures of plated and unplated copper conductors with respect to maintaining the required flexibility and conductivity within prescribed limits. Several thermal aging investigations of plated copper conductors initiated by McCune, Bidwell, and others have revealed a rather perplexing difference in the obtained results. While McCune has found no detrimental degradation of either flexibility or conductivity even after extensive aging of silver plated copper conductors at 200°C. Bidwell has reported an unexpected degradation of the silver plate which may significantly reduce both the flexibility and conductivity at time and temperature parameters as low as 500 hours at 150°C. Specific effects of such degradation with thermal aging, if any, on these two properties are still unclear. Further, investigations initiated by MCAIR and Marshall Space Flight Center comparing plated and unplated copper conductors in regard to thermal aging effects on the flexibility and conductivity have revealed inconclusive results. The present investigation was conducted in an effort to reconcile these differing and/or inconclusive results as well as an attempt to quantitatively correlate the flexibility and conductivity as a function of time and temperature parameter.

2.0 EXPERIMENTAL PROCEDURES

20 foot loose coiled specimens were thermally aged in air utilizing a forced air Blue M oven with a Honeywell temperature controller. Silver, nickel and tin plated as well as unplated 20 AWG 19 end construction "true" concentric copper conductors were aged at 100°C, 125°C, 150°C, 175°C, 200°C and 250°C. Further, 12, 16, 20 and 24 AWG 19 end "unilay" concentric and "true" concentric silver plated copper conductors were thermally aged at the above temperatures to evaluate the effects of these additional parameters.

At appropriate intervals, the D.C. resistance, flex life and microstructure of the thermally aged specimens were evaluated up to a maximum of 2000 hours. D.C. resistance measurements were made on a Rubicon model 1622 Kelvin Bridge with a resolution of 0.5µR Measurements of resistance were taken over a 5 foot length with spring loaded pressure contacts. Flex life tests were conducted in a manner described in and in accordance with ASTM B 470. Transverse, longitudinal and oblique cross sections were evaluated on a Reighart metallograph at magnifications noted. Surface and elemental analysis were conducted on an AMR 1200 SEM and EDAX.

3.0 EXPERIMENTAL RESULTS AND DISCUSSIONS

3.1 EFFECTS OF THERMAL AGING ON THE D.C. RESISTANCE

All the conductor systems tested whether plated or unplated except for the nickel plated copper system exhibited significant increases in the D.C. resistance after prolonged exposure to air at elevated temperatures. The percent increase in resistance varied not only as a function of the time and temperature parameters but also as a function of the type of plating, type of stranding construction and the conductor size.

3.1.1. CHANGE IN D.C. RESISTANCE AS A FUNCTION OF THE PLATING MATERIAL

3.1.1.1. SILVER PLATED COPPER

As seen in figure 1a, silver plated copper conductors exhibited no change in resistance at aging temperatures up to 175°C even after exposure for 2000 hours. At 200°C and 250°C a significant change was observed with an increase in resistance of 2.5% and 4.0% respectively after exposure for

2000 hours. However, with increasing time, the resistance appeared to stabilize such that a leveling occurred after about 1500 hours. Metallographic examination of the thermally aged samples at 150°C and 175°C as seen in figure 2a revealed no disruption in the integrity of the silver plate with only a slight oxide formation visible on the surface. Although this oxide layer increased in thickness with time, it appeared completely coherent such that is afforded protection to the underlying silver plate. Further, EDAX analysis of the silver plate revealed no significant presence of copper to suggest extensive copper migration or the formation of diffusion reaction products.

At 200°C a significant change in the microstructure of the silver plate occurred. As seen in figure 2b, after aging for 2000 hours, irregularities were observed at the plate interface as well as some disruption in the continuity of the plate. EDAX analysis of the interfacial layer revealed no significant presence of silver to suggest the formation of a diffusion reaction product of silver and copper. The layer appeared to be a copper oxide layer resulting from the diffusion of oxygen through the discontinuities in the plate. At 250°C, a breakdown of the silver plate was observed after extensive aging. Along with a loss of the plate integrity, growth of the copper oxide layer and a coalescence of the remaining silver was observed as seen in figures 2c and 2d. Bidwell (2) observed similar tesults with silver plated copper conductors after thermal aging at $230^{\circ}\mathrm{C}$.

The silver plated copper conductor system appears quite stable at temperatures up to 175°C with no significant degradation of electrical properties although some oxidation of the surface which increases with time was evident. It appears that since silver oxide is itself a conductive material, contact and interstrand resistance factors are negligible and does not significantly alter the total resistance. At 200°C and 250°C, a significant increase in the resistance was observed. This increase appeared to be due to the degradation of the silver plate which occurs resulting in the exposure and oxidation of the underlying copper.

3.1.1.2. TIN PLATED COPPER

As seen in figure 1b, the tin plated copper conductor system exhibited an increase in resistance at all thermal aging temperatures. At 100°C and 125°C , the resistance was relatively stable with only a 1.2% increase after exposure for 2000 hours. At 150°C , 175°C and 200°C , significant increases in the resistance occurred with an increase of over 10% observed after aging for 2000 hours at 200°C .

Specimens aged at 100°C and 125°C exhibited both an oxidation of the surface and the formation of two distinct layers at the plate interface. As seen in figure 3a, the rapid growth of these layers resulted in the remainder of very little free tin on the surface. EDAX analysis revealed a signifi-

cant presence of copper in the layers such that they appeared to be some diffusion reaction product of copper and tin. McCune et al (1) have also observed the presence of these diffusion reaction products in tin plated copper conductors. Through X-ay diffraction techniques, these investigators have determined the products to be the brittle intermetallics Cu_3Sn (ϵ) and Cu_6Sn_5 (η).

After 300 hours of exposure at 150°C , only the two intermetallic compounds were present with no free tin visible. Further, numerous cracks radial in nature were observed extending through the length of the plate as seen in figure 3b. At 175°C and 200°C , severe cracking and lifting of the plate as well as oxide formation on the underlying exposed copper was observed as seen in figures 3c and 3d.

Although some increase in the resistance was observed at all aging temperatures, the tin plated copper conductor system was generally stable at 100°C and 125°C. The increase in resistance at these temperatures appeared to be due to oxidation of the tin as well as the formation and growth of the two intermetallic compounds. However at higher aging temperatures, cracks in the plate due to the brittle nature of these intermetallics and the subsequent oxidation of the underlying copper appeared to cause the further observed increases in the resistance. However it should be noted that in the present investigation all thermal aging was done in a static condition which may not reflect the true behavior. The true dynamic conditions (flexes and vibrations) which the conductors undergo during actual use should further accelerate and increase the observed degradation of the plate and the resistance cue to the formation of these brittle intermetallics.

3.1.1.3. NICKEL PLATED COPPER

The nickel plated copper conductor system exhibited no significant increases in the resistance even after thermal aging at 250°C for 2000 hours. Metallographic examination revealed the plate to be completely coherent with no evidence of diffusion reactions at the plate interface as seen in figure 4a. However as seen in figure 4b, extensive aging at 250°C resulted in significant grain growth and the occurrence of a creep phenomenon. Although the continuity of the plate was not disrupted even after exposure for 2000 hours, extensive deformation of the strands occurred. This behavior suggests that the failure of the nickel plated conductor both electrical and mechanical may occur due to this excessive creep deformation and not due to the plating as observed in the tin and silver plated systems.

3.1.1.4. UNPLATED COPPER

The unplated copper conductor system as seen in figure 1c exhibited significant increases in resistance with thermal aging at all temperatures. The resistance increase ranged from 2.5% at 100°C to almost 18% at 200°C after aging for 2000 hours. Metallographic examination revealed extensive

oxidation as well as a degradation of the strand surface as seen in figure 5a and 5b. Further, the adherence of the oxide to the surface was poor such that unoxidized copper was continually exposed leading to a rapid deterioration. Due to this deterioration, volume as well as contact resistance considerations appeared to result in the large observed resistance increase.

3.1.2. CHANGE IN D.C. RESISTANCE AS A FUNCTION OF CONDUCTOR CONSTRUCTION AND SIZE

As seen in figure 1d, the change in resistance after thermal aging was also a function of the type of stranding. A comparison of "Unilay" (unidirectional equilay concentric) and "True Concentric" (counterdirectional nonequilay concentric) after thermal aging revealed a considerable difference. In all cases the "Unilay" construction exhibited smaller increases in registance than true concentric constructions. This appeared to be due to the difference in the geometric packing between the two types of constructions which significantly changes the degree of exposure to the environment. As seen in figure 6, the unilay construction is a close packed configuration of strands as compared to true concentric. This not only necessitates a larger diameter for true concentric constructions which is undesirable, but creates larger spaces between strands for the passage of air. In other words the close packed nature of the unilay construction appears to protect the inner strands to some degree from oxidation whereas the true concentric construction due to the larger interstrand spacing does not.

As seen in figure 1d, the size of the conductor is also a factor after thermal aging in regard to changes in resistance. It was observed that the rate of increase was inversely proportional to the conductor size. The large increases in resistance after thermal aging is basically a surface oxidation phenomenon. Since the surface to volume ratio is inversely proportional to the conductor size, the smaller the conductor the larger should be the effect of thermal aging.

3.2 EFFECTS OF THURMAL AGING ON THE FLEX LIFE

As seen in figures 7a, b and c, considerable decreases in the flex life was observed in all plated and unplated specimens except for the nickel plated specimens after thermal aging. The silver plated copper conductor system exhibited a stable flex life at 150°C but decreased at higher temperatures. From microscopic observations it appeared the decrease was due to a diffusion bonding of silver which prohibited the adjacent strands from slipping and thus increasing the stiffness. Further at higher temperatures the degradation of the plate and subsequent oxidation of the copper effectively decreased the cross sectional area and contributed to the decrease in flex life.

The fin plated copper conductor system exhitited large decreases in the flex life at all thermal aging temperatures. The rapid decay of the flex life appeared to be due to both a bonding of the tin plate between adjacent strands and the

formation of the two brittle intermetallic compounds η and ϵ . Also, the rate of decay in the flex life with time was rayid and appears to be due to the rapid deterioration of the plate created by the formation of η and ϵ .

The unplated copper conductor system exhibited a relatively stable flex life at thermal aging temperatures up to 150°C with only a 4.2% decrease after 2000 hours. Due to the formation of oxides no bonding of adjacent layers was observed. Further, at these temperatures the oxidation was not severe enough to significantly reduce the cross sectional area. However at higher temperatures where extensive oxidation was observed, the rate of decrease of the flex life increased significantly.

The effects of the conductor size and construction are seen in figure 7d. Since the flex life is a function of the surface oxidation, the conductor size due to the respective difference in the surface to volume ratio is inversely proportional to the flex life. Significant differences were observed with a decay of only 10% for 16 AWG as opposed to 54% for 24 AWG.

Differences in flex life after thermal aging were also observed between true concentric and unilay constructions. As seen in figure 7e, the unilay construction in silver plated 24 AWG conductors exhibited a larger decrease in the flex life after thermal aging than true concentric. This appears to be due to the closer packing of strands in unilay which created more interstrand contact area and therefore a greater area for possible diffusion bonding. However, since the initial flex life of unilay constructions are greater, the absolute flex life after thermal aging was approximately the same.

4.0 CONCLUSIONS

All conductor systems whether plated or unplated except for the nickel plated copper system exhibited significant increases in the D.C. resistance and decreases in the flex life after thermal aging. The silver plated copper conductor system was stable up to 175°C, but at higher temperatures discontinuities in the plate and subrequent oxidation of the underlying copper as well as a coalescence of the silver plate resulted in increases in resistance and decreases in flex life. The tin plated copper conductor system though relatively stable up to $125^{\circ}\mathrm{G}$ exhibited large increases in resistance and dec ases in flex life at higher temperatures due to the formation and degradation of two brittle intermetallic compounds η and ε resulting in the exposure and oxidation of the underlying copper. The unplated copper conductor system exhibited the largest increase in resistance of all the conductors tested. However, since no interstrand bonding and/or diffusion reaction products were present the flex life was slightly better. Also due to strand packing considerations the resistances of unilay constructions were more stable than equivalent true concentric constructions. Further, the resistance and flex life is affected significantly by the

conductor size due to differences in the surface to volume ratio.

In this investigation the effect of thermal aging on plated and unplated conductors was determined in a static test condition. However, due to the reactions which were found to occur at the surface and plate interfacial boundaries such as the formation of brittle intermetallics in tin plated copper, the results may not reflect the true behavior of conductors in actual use. Therefore it is suggested that a more realistic test involving the integration of mechanical perturbations during thermal aging be more fully explored.

Although no deterioration of the conductivity or flex life was observed in the nickel plated copper system, an extensive creep phenomena occurred during thermal aging at 250°C. It appeared the nickel plating could withstand such temperature exposure without any detrimental effects, however, the base copper could not. Since the nickel plated system is used in high temperature applications of 250°C and above, a re-evaluation of the base material selection may be in order.

ACKNOWLEDGEMENTS

The author wishes to thank Mr. T. B. McCune and Mr. D. K. Sanghavi for their many enlightening discussions and helpful hints. The author also wishes to thank Miss Karen Biordi for her invaluable assistance in the experimentation.

REFERENCES

- 1 McCune, T.B.; Burn, J.H.; Busch, G.A.; Larson, D.J. Heat Aging Evaluation of Common Coated Copper Conductors, 19th IWC Symposium, Dec. 1970
- 2 Bidwell, L.R.; Thermal Aging of Silver-Plated Copper Aircraft Electrical Wire Technical Report AFML-TR-73-113 May, 1973
- 3 Nary, D.T.; The Effects of Environmental Aging on Plated and Unplated Copper Conductors McDONNELL AIRCRAFT COMPANY Oct. 1973
- 4 Shewmon, P.G.; <u>Diffusion in Solids</u> McGraw-Hill 1963
- 5 Butrymowicz, D.B.; Manning, J.R.; Read, M.E. <u>Diffusion Rate Data and Mass Transport Phenomena</u> <u>for Copper Systems</u> INCRA July, 1977
- 6 Dummer, G.W.A.; Materials for Conductive and Resiscive Functions Hayden 1970

BIOGRAPHY

Tsutomu Inagaki is a Supervisor of Product Engineering for the Ossining Division of the Hudson Wire Company. Since 1977 he has been involved in developing new nickel plated products, as well as designing high speed nickel plating equipment. As coordinator for research and development, he has also been involved in evaluating and developing current as well as new conductor systems.

Inagaki holds an MS degree in Metallurgical Engineering from the Polytechnic Institute of Brooklyn, and is a member of AAAS, AES, ASM and Sigma XI.

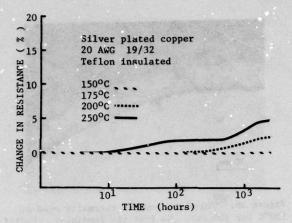


Figure la. Silver plated copper conductor

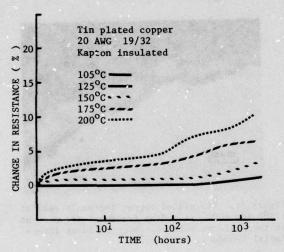


Figure 1b. Tin plated copper conductor

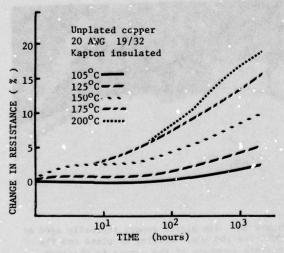


Figure 1c. Unplated copper conductor

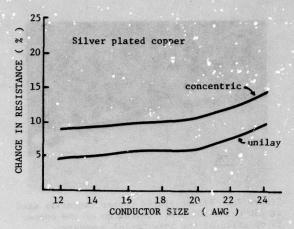


Figure 1d. The effect of strand construction on the resistance. Silver plated copper thermally aged at 200°C for 2000 hours.

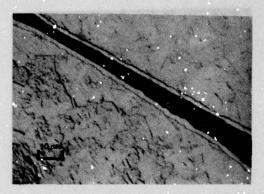


Figure 2a. Silver plated copper thermally aged at 175° C for 2000 hours. No loss of plate integrity observed.

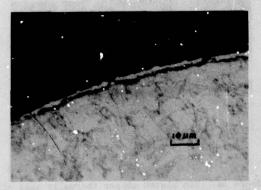


Figure 2b. Silver plated copper thermally aged at 200°C for 2000 hours. Evidence of interfacial layer as well as a discontinuity in the plate.

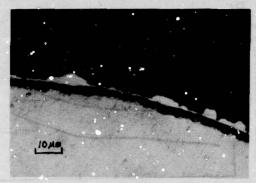


Figure 2c. Silver plated copper thermally aged at 250°C for 100 hrs. Oxidation of the copper is observed at the interfacial boundary.

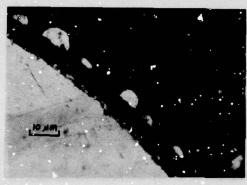


Figure 2d. Silver plated copper thermally aged at 250°C 2000 hrs. Growth of the copper oxide layer and a coalescence of the remaining silver is observed.

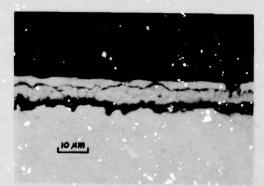


Figure 3a. Tin plated copper thermally aged at 125°C for 1000 hrs. The n and ϵ intermetallic of Cu-Sn is observed with very little free tin.

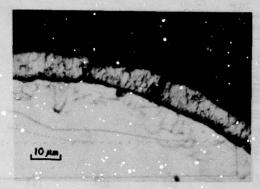


Figure 3b. Tin plated copper thermally aged at $150^{\circ}\mathrm{C}$ for 300 hrs. No free tin remaining. Radial cracks present in the plate.

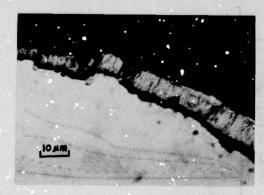


Figure 3c. Tin plated copper thermally aged at 175°C for 1000 hrs. Many fractures are present in the plate as well as copper oxide at interfacial boundary.

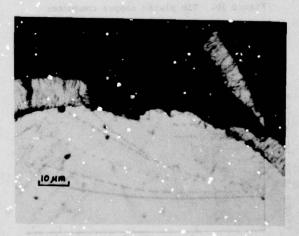


Figure 3d. Tin plated copper thermally aged at 200°C for 100 hrs. Lifting of plate and the complete exposure of the copper is observed.

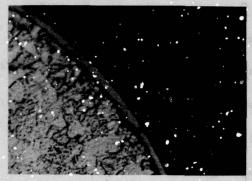


Figure 4a. Nickel plated copper thermally aged at 290°C for 2000 hrs. Plate is completely coherent with no irregularities at the interface.

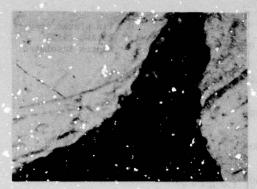
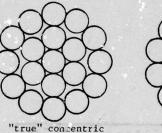


Figure 5b. Unplated copper the mally aged at 200°C for 2000 hrs. Extensive degradation of the surface due to oxidation is observed.



Figure 4b. Nickel plated copper thermally aged at 250°C for 2000 hrs. Significant grain growth and creep is observed.



"unilay" concentric

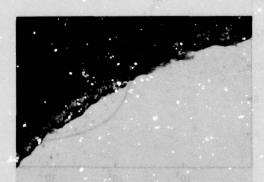


Figure 5a. Unplated copper thermally aged at $150^{\circ}\mathrm{C}$ for 2000 hrs. Thick oxide observed at the surface.

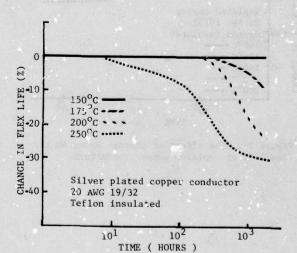


Figure 6. Geometrical configuration of strands in "unilay" concentric vs "true" concentric.

Figure 7. Silver plated copper conductor.

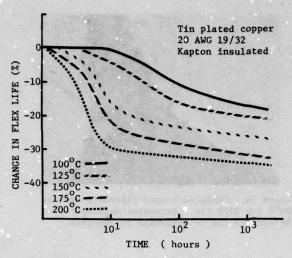


Figure 7b. The effect of thermal aging on the flex life of tin plated conductors. $% \left(\frac{1}{2}\right) =\frac{1}{2}\left(\frac{1}$

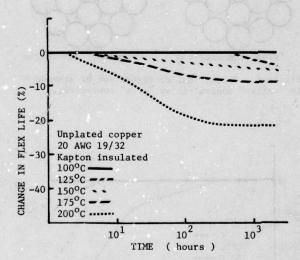


Figure 7c. The effect of thermal aging on the flex life of unplated copper conductors.

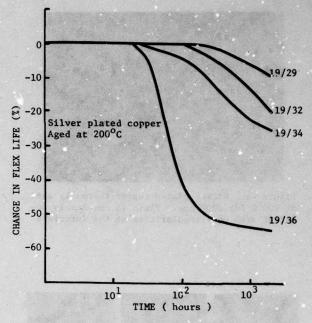


Figure 7d. The effect of conductor size on the flex life of silver plated copper conductors after thermal aging.

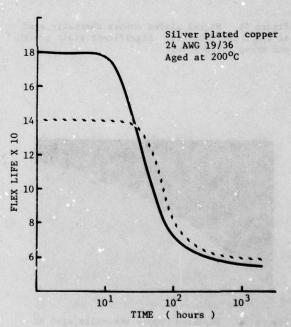


Figure 7e. The effect of strand construction in the flex life of silver plated copper conductors after thermal aging.

THE PERSON NAMED IN COLUMN TWO IS NOT THE OWNER.

ON THE NEED FOR METALLIC SCREENS IN THE SHEATHS OF TELEPHONE LOCAL-LOOP CABLES

H J C Spencer and G A Bartlett

British Post Office Telecommunications Headquarters

Summary

It is the common practice to use aluminiumpolyethylene laminate sheaths for dry local loop cables. The aluminium, typically a longitudinally applied foil 150 mm thick, is included to prevent the permeation of water vapour through the sheath. The introduction of petroleum-jelly filling removes the need for moisture barriers, but they have been retained in some designs of filled cables in the belief that they have valuable secondary functions, such as electrical screening. The paper considers the secondary functions in turn, with particular reference to distribution cables of up to 100 pair count. It finds that none constitute strong grounds for providing a moisturebarrier type screen in small local-loop cables, and some disadvantages are identified. The paper concludes that it is unnecessary to provide such screens in small filled cables, and probably unnecessary to provide them in large cables if these are filled.

The Primary Reason for Screens

It was realised soon after polyethylene was introduced as a sheath material that, although it was an excellent choice in most respects, it shared the weakness of other plastics in allowing the slow permeation of water vapour. Consequently the near infinite life expected of a telephone cable was unlikely to be achieved using sheaths made of polyethylene alone. The solution to this problem, jointly developed by Glover of the British Post Office (BPO) and Hooker of Telephone Cables Ltd, was the polyethylene/aluminium laminate sheath, which is now the preferred form of construction world wide. A paper to a conference in 1967 has shown that a polyethylene laminate sheath in conjunction with a moisture absorption medium in the cable core will ensure cable lives in excess of any conceivable system requirement.

Subsequently the use of polyethylene was extended to wire insulation and it is now the preferred material for this also. Polyethylene insulation did not, however, remove the need for the aluminium moisture-barrier because water vapour could still penetrate to the air spaces within cables. And polyethylene insulation brought with it a new problem. It was so good that in the event of

sheath damage water could enter a cable without causing an immediate fault. As the cable flooded, however, the transmission performance degraded and ultimately the water was piped to a vulnerable joint, causing a fault remote from the point of damage. This problem was in turn overcome by the development by British Insulated Callender Cables of jelly filling, the subject of an award winning paper to the 1968 Symposium. Jelly filling has another significant effect. In making a cable core impervious to water in liquid form, it clearly eliminates the need to prevent water vapour permeation through the sheath. It would seem logical, therefore, to cease to provide the moisture-barrier in filled cables. But this has not been the universal practice. Some telephone engineers, accustomed for many years to cables with substantial metal sheaths, have conservatively opted to retain the aluminium moisture-barrier even when the primary reason for it has been removed, in the belief that it has valuable secondary functions, such as forming an electrical screen. The BPO did not follow this line and the filled cables of up to 100 pair count it adopted as standard in 1968 have no screens. The aim of this paper is to review the value of the moisture-barrier as a screen in localloop cables for functions other than preventing the permeation of water vapour, and to consider whether in the light of extensive BPO experience of cables without such screens their retention is justified.

Possible Secondary Purposes of Screens

Mechanical Strength

Screens of the thickness required for a moisture-barrier, clearly contribute little to the mechanical strength of a cable. Other types of metallic screens have been developed with cable strength in mind, but reduce flexibility. There now appears to be a consensus of opinion that for cables placed in ducts polyethylene sheaths, typically 2 or 3 mm thick, depending upon cable diameter, give adequate protection.

For cables placed directly in the ground the standard polyethlene sheath, with or without a moisture-barrier, may not be sufficient. In these circumstances an additional rugged sheath is required, which can be very expensive. The BPO practice has been to protect directly-buried cables with steel-wire armour, although use has now commenced of the more economic loose plastic

oversheath construction described at last year's symposium.

Protection from Lightning Damage

This is a problem with many aspects. The extreme case is a direct strike which results in severe damage to, or destruction of a cable. Effective protection against a strike, or a near miss, requires such measures as placing the cable within a substantial welded steel tube, and the expense can only be justified in areas where strikes are frequent and soil resistivity high. This paper is concerned with the effects of lightning on conventional plastic sheathed cables in areas of moderate risk.

In areas of moderate risk non-conducting sheaths have obvious advantages on safety grounds. However, when the potential of the soil in which the cable is placed is raised by a lightning strike the electrical stress between the soil and the conductors within, will if high enough, rupture the sheath and, assuming the cable has no screen, damage the conductors. The critical distance between the point of a lightning strike and a cable, nearer than which damage to the conductors will result, is given by:-6

$$D = \frac{I \rho}{2MU} \tag{1}$$

where: D = distance in metres

I = peak strike current, kA

P = soil resistivity, A m

U = dielectric strength of cable, kV

For a given set of conditions a diagram can be drawn defining the critical target presented by a cable. Fig 1 is such a diagram for a modern BPO, filled, unscreened, distribution cable for which the critical distance in an area of high soil resistivity is of the order of 100 m.

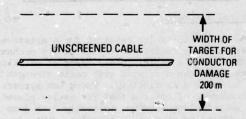


FIG 1. LIGHTNING TARGET - UNSCREENED CABLE

If, now, such a cable is given a metallic screen beneath the sheath the immediate effect is to reduce the thickness of insulation between the soil and the first conducting component of the cable, the screen, by the thickness of the core wrapping and the wire insulation, as illustrated by Figs 2 and 3.

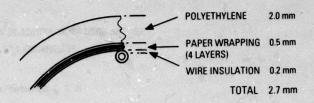


FIG 2. SECTION - UNSCREENED CABLE

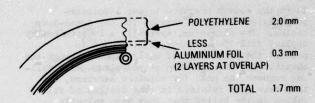


FIG 3. SECTION - SCREENED CABLE

The effect is particularly severe with small distribution cables. For example, the reduction for a 100 pair BPO cable with 0.5 mm conductors would be of the order of 35%. The inverse dielectric strength relationship of equation (1) leads to an increase in the critical distance for damage of over 50%, as shown in Fig 4.

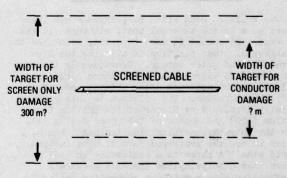


FIG 4. LIGHTNING TARGET - SCREENED CABLE

This assumes that the dielectric properties of the core wrapping and the wire insulation are as good as those of solid polyethylene, which is not the case. However, in the opposite sense is the effect of imperfections in the longitudinal seam in the screen, and of lack of concentricity between cable core and sheath. In practice the increase in the critical distance is probably of the order indicated. It is noteworthy that a corrugated screen reduces the effective thickness of the cable sheath much more severely than a smooth screen.

Clearly a cable with an earthed screen beneath the sheath is more likely to be damaged by lightning than one without. The effectiveness of the screen in protecting the conductors from damage is, therefore, all important.

A paper to the previous symposium indicated that the incidence of pin holes in the screen is unlikely to significantly degrade the performance of cables of the "dri-fill" type, and jelly filled cables are even less likely to be affected.

It is well known, however, that screens of the moisturebarrier type do not confer complete protection to conductors, and in the majority of lightning damage cases both the screen, if there is one, and the conductors are affected. It is necessary to add to Fig 4 another critical distance to define the area in which both screen and conductors will be damaged, for meaningful comparison with Fig 1. No theoretical studies or measurements have been noted in the literature bearing on the effect of the inclusion of an earthed screen on the critical distance for damage to conductors. A parallel can, however, be drawn between an insulated cable with an earthed screen when the sheath insulation has failed, and cables with conducting sheaths. Cables of this type have sheaths designed with a low transfer impedance, to reduce surge voltages on the inside of the sheath, and have improved insulation between sheath and conductor to withstand the residual surges. The "quality factor" 80 of such cables is assessed from the equation:

$Q = \frac{\text{peak dielectric strength of insulation (kV)}}{\text{Sheath transfer impedance (ohm/km)}} (2)$

By this criterion a moisture-barrier cable with sheath failure is of low quality.

A critical view that can be taken of the role of an earthed moisture-barrier screen is that it encourages breakdown of the sheath by increasing the electrical stress across it, and then forms an inadequate protection for the core, leading to conductor damage except, perhaps, in some very marginal circumstances. It is to be noted that Boyce advises that moisture-barrier screens should not be earthed. The BPO has embarked on a test program to quantify the effect of both earthed and floating screens.

Protection from Voltage Surges

Lightning strikes not close enough to damage cables can, never-the-less, induce voltage surge in conductors. These surges may have magnitudes of 10 kV, or more, which is sufficient to damage terminal equipment and to be a hazard to personnel. Surges can also be caused by faults in power systems.

Efficient and effectively earthed screens are capable of reducing voltage surges in conductors.

However, the circuits carried by the conductors are frequently extended beyond the bounds of cable screens, often with open wire drops. No matter how effective a cable screen may be, therefore, precautions such as the use of protective air gaps must be taken to prevent damaging voltages induced beyond the cable reaching equipment. This is particularly the case when the equipment is electronic rather than electro-mechanical. Any protection provided by screens in cables, is therefore, irrelevant.

Voltage surges in filled telephone distribution caties with screens, in an area of very high lightning exposure, were the subject of a paper at the
last symposium. Surges of up to 10 kV were reported,
excluding the effect of a lightning strike which
severely damaged a screened drop cable. Significantly it was noted that pair-to-pair surges were
the same as pair-to-screen, suggesting that they
all entered the cables by the drops.

Protection from Electrostatic Induction

Electrostatic effects may be encountered when cables run above ground for considerable distances in proximity to overhead high-voltage power lines. An earthed screen in the cable sheaths would reduce these effects. However, the use to which filled distribution cables are put makes it unlikely that any one of the conditions is met. The cables are filled for protection because they are placed underground, and being distribution cables they are rarely more than a few kilometres long.

For aerial cables there are several possibilities and practices vary between administrations. The cables may be filled or unfilled. If they are unfilled it can be argued that a moisture-barrier is required for its primary purpose, although this is questionable. The BPO practice is to use its standard, filled, distribution cable core for aerial cables, but in a figure-of-eight construction with a steel suspension strand. The suspension strand has an electrostatic screening effect.

Protection from Power Frequency Induction

Screens of the thickness typical for moisturebarriers have negligible effect at power frequencies. For example, a 150 mm screen in a 100 pair 0.5 mm cable would, attenuate 50 Hz interference by only about 0.2 dB when earth connections have zero resistance. A thicker screen would be more effective, eg a screen 1.5 mm thick, which could more properly be considered a sheath, would give an attenuation of nearly 8 dB. The screening effect is, however, critically dependant upon the resistances of the earth connections and if it is assumed that these are 5 ohms each then even a 1.5 mm screen would have a negligible effect over 1 kilometre. The screening effect is greater for longer lengths, because the earth resistances become less significant when compared with the sheath resistance and inductance. Even for a 10 km length, nowever, which would be exceptional for a distribution cable, the attenuation of a 150 μ m screen with 5 ohm earths would only be about 0.1 dB.

Because of the impractability of screening against power frequencies it is normal to design equipment such as telephone receivers to be insensitive to them.

Attenuation of Audio-Frequency Interference

The efficiency of a conducting screen in attenuating magnetic induction increases with frequency and can theoretically be significant at audio frequencies, as indicated by Fig 5. As for power frequencies, however, the effectiveness of the screen is very sensitive to the resistance of the earth connections at each end, as indicated by Fig 6.

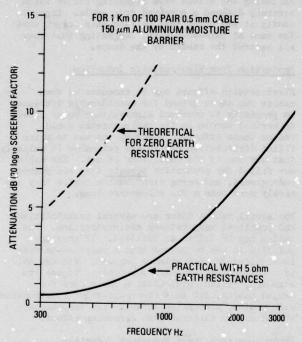


FIG 5 AUDIO SCREENING EFFICIENCY RELATED TO FREQUENCY

Perspective on the practical value of screens at audio-frequencies is given by the 8 ohms limit specified for exchange earth resistances by the BPO. To ensure that even this limit is complied with extensive, and expensive, earthing systems are necessary. It would be most uneconomic to seek to achieve earth resistances of the same order at the cabinets, pillars and terminal boxes in a distribution network.

In Britain, earth resistances at cabinets approaching 100 ohms are not exceptional, and for partyline working a subscribers earth resistance of 150 ohms has to be allowed for. Such values result in negligible screening effects.

The efficiency of a screen depends upon its resistance and, therefore, upon its thickness.

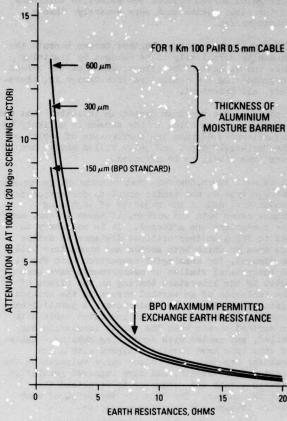


FIG 6. 1000 Hz SCREENING EFFICIENCY RELATED TO RESISTANCE OF EARTHS

The effect is, however, largely subordinate to earth resistance. Fig 6 shows that doubling, or even quadrupling the thickness from the BPO standard 150 µm would have negligible advantage with values of earth resistance likely to be met with in distribution networks.

The effectiveness of a screen at audio frequencies is also related to the length of cable, for the same reasons as at power frequencies. The effect is quantified in Fig 7. A length of 1 kV was taken for Figs 5 and 6 because it corresponds to a relatively long distribution cable in the British network, in which the average length is only about 400 m. However, the length effect is most marked for low earth resistance, and Fig 7 shows that for earth resistances met with in practice the improvement in screening with length is of little significance.

It appears that the audio frequency screening effect of a moisture-barrier is only likely to have benefits for long cable routes with earth resistances typical of those met at exchanges, eg for junction (toll) cables. For local-loops, and

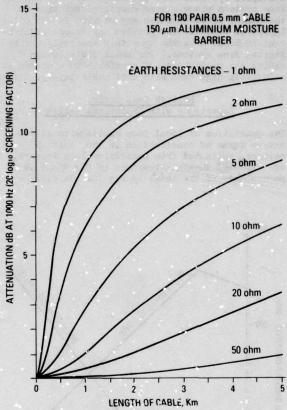


FIG 7. 1000 H7 SCREENING EFFICIENCY RELATED TO CABLE LENGTH

particularly for the small cables at the fringes of local networks, it appears to offer negligible benefits.

Attenuation of Radio-Frequency Interference

Theoretically the effect of a moisture-barrier type screen is very significant at high frequencies, as indicated by Fig 8. Induced signal levels are reduced by 30 dB and more, compared with unscreened cables, even when earth resistances are of the order of 100 ohms. The theory is supported by measurements of cable under controlled conditions, with all the pairs in the cable terminated at the cable ends. The same measurements, however, indicate that even in high signal strength localities transverse voltages within unscreened cables are very low, of the order of -80 dB (relative to 1 mw in 140 ohms). The possible attenuation of 30 dB by an earthed screen is not, therefore, significant for local-loop applications.

Measurements in actual networks give different results, however. Firstly there is a departure from the theory that the screening effect rises continuously with frequency. In practice it has

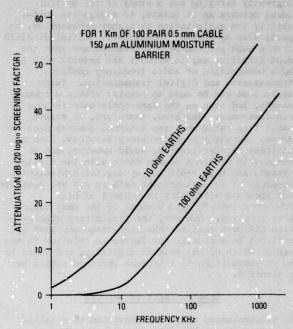


FIG 8. HIGH FREQUENCY SCREENING EFFECT RELATED TO FREQUENCY

been found to fall to zero at 1 mHz. The conclusion is that the earth connections existing at cabinets have an inductive component and the reactance of this rises with frequency, to effectively disconnect the screen.

The second significant result from tests in actual networks is that interference levels measured on pairs in cables terminated at the cable ends, but with other pairs left connected to their normal terminations, are considerably higher than those measured under the artificial controlled conditions. Levels of -60 dB are typical but there is a wide spread of measu ements. The conclusion is that the higher levels result from cross-talk between the pairs under test and other pairs, which are extended by plant with antenna-like properties, eg drop wire and MDF jumpers. This conclusion is supported by the correlation that exists between high levels of interfering signals, typically 20 dB higher than normal, found on a few "rogue" pairs, and the poor high-frequency cross-talk attenuation between the rogue pairs and othe s in the same group.

Analysis of network measurements made on both screened and unscreened cahles has failed to indicate any correlation between radio frequency signal levels and the presence or absence of screens, implying that any benefit screening may have is overwhelmed by other factors.

In considering the need for high-frequency screening in local-loop cables it is relevant to consider how they will be used in the future. The BPO is

currently carrying out a study of the British . local network as it exists, to assess its suitability for exploitation at higher frequencies, in particular by digital techniques. Initial findings from a vast program of measurements are that the most effective way to exploit the network will be by a combination of Ludio frequency analogue transmission and digital transmission. These techniques can be made to coexist within a common sheath, and even on the same cable pair in some circumstances. Any need, therefore, to screen cable from cable and from external sources does not arise. Existing high frequency services, such as analogue carrier systems, would however, not be compatible within a common cable with the digital systems and need replacing by digital equivalents. Analysis of the measurement data is not yet complete, and presents difficulty in respect of high frequency interference because of the many variables involved. However, the preliminary conclution has been reached that high-frequency pick up will not be a significant factor in relation to the exploitation of the network digitally, and there is no recommendation to introduce screened cables as a standard.

Disadvantages of Screers

In circumstances where the provision of metallic screens may have benefits, ever though this is not proven, and have no disadvantages, a policy of providing screens as an insurance could be justified, particularly if the additional cost is slight.

Electrical Protection

The possibility that cables with screens are more vulnerable to lightning dawage has already been discussed.

Mechanical Considerations

The handling properties of cables with the BPO standard 150 pm moisture-harrier screen are little inferior to those of cables without screens. If, however, thicker screens are used in search of greater electrical acreening efficiency the flexibility of cables is reduced and it may be necessary to corrugate the screen to restore it. The corrugations will increase the vulnerability to lightning damage.

Water Blocking

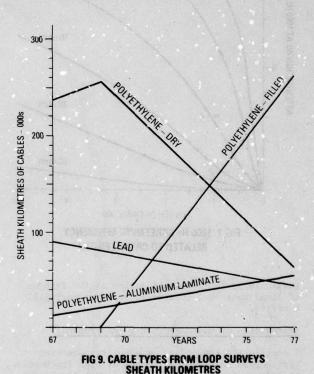
The presence of a screen makes it difficult to completely block a jelly-filled cable. While the core can be adequately protected the presence of the screen can prevent the sheath from making intimate contact with the core. Hence the screen may create longitudinal paths which can pipe water to unprotected joints.

Electrical Properties

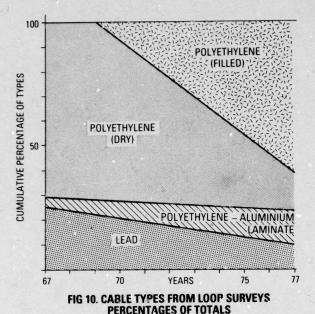
The proximity of a screen to a balanced conductorpair both increases its attenuation at highfrequencies and degrades the high-frequency crosstalk between pairs. The effect is a well known problem in exploiting junction (toll) concentriclayer audio cables with 1.5 and 2 mb/s PCM multiplex systems. BPO planning rules for digital line systems place a more severe restriction on the number of parts which may be used in the outer layers of cables. The problem may become significant in local networks when they are exploited by digital line systems. For small distribution cables the probability of proximity to a screen is relatively high even with unit cable lay-up.

British Post Office Experience with Unscreened Cables

The quantities of local loop cables with alternative forms of construction in the British network, estimated from successive loop surveys, are shown in sheath kilometres in Fig 9, and as percentages of the total in Fig 10. It will be



seen that for the past 12 years more than 70% of the total sheath kilometres has been unscreened. The screened cables are almost entirely in the pressurised main feeder network, and the unscreened cables, now largely jelly filled, are in the distribution network. In the BPO system the two parts of the network are clearly separated by flexibility cabinets, giving the opportunity to correlate differences of performance with the presence or absence of screens in the distribution cables. However, the possible areas of difference, largely protection and interference, are such that it is not easy to reach a quantified judgement.



Both screened and unscreened cables are occasionally damaged by lightning. Invariable the damage reports involve conductors, even in cables with moisture-barrier screens. The "pin-hole" problem referred to in the literature is virtually unreported. This is not to say that pin-holes never occur. In the main-feeder cables, which are pressurised by a flow system, pin holes to the screen would probably be masked by other sealing defects. In jelly filled distribution cables, pin holes to conductors may well be self sealing.

Inductive noise problems occur in both screened and unscreened cables. Solutions normally involve eliminating the source or improving the balance of affected circuits. Improvement by attention to screens, where they exist, is rarely practical and in high soil resistance areas noise is often earth borre.

A more positive judgement is possible for high-frequency interference. The current BPO 1 + 1 Subscribers Carrier is a low-cost, and now dated, equipment operating at frequencies of 40 and 64 kHz. It does not include compandors. Radio pick-up in localities with high field strengths has caused problems. These are avoided by prohibiting the use of the system on loops extended by more than 2 spans of drop or open wire. It has not been necessary to impose any restriction reluted to the absence of a screen in the cable sheath.

Conclusions

There is a sound theoretical case for the inclusion of a metallic moisture-barrier screen in the sheaths

of unfilled local-loop cables, although real-time experience is insufficient as yet to prove the need. The screen is also required in dry water-blocking cables, such as Dri-Fill and Telefloc. A metallic screen is not, however, required as a moisture-barrier in jelly-filled cables.

None of the secondary reasons considered for including a moisture-barrier for protection or as a an electrical screen appear strong and screens have disadvantages. It is concluded, therefore, that metallic screens should not be provided in the sheaths of jelly-filled distribution cables. The arguments used to support this conclusion have been quantified in relation to a 100-pair cable, the highest pair-count distribution cable used by the BPO. It is believed, however, the arguments can also apply to the higer pair-count main-feeder cables where these are jelly filled and the need for moisture-barrier type screens in these is very questionable.

Acknowledgements

The paper is published by permission of the Senior Director, Network Executive, of the BPO Telecommunications Headquarters. The authors are grateful to colleaguer at Telecommunications Headquarters for information and help in preparation of the paper. Particular thanks are due to S H Granger of the Local Line Task Force for information concerning high frequency interference and plans for future exploitation of local-loop cables, and to J O Colyer for advice on protection and interference aspects.

References

- D W Glover and E J Hooker, Post Office Flectrical Engineers' Journal, Vol.53 Page 253 January 1961
- 2. British Patent No.886417
- J C Harrison, Transactions of Plastics Institute, Vol.35 (No.119) Page 729 October 1967
- 4. N S Dean, The Development of Fully Filled Cables for the Distribution Network, Proc 17th International Wire and Cable Symposium
- 5. D R Bissell, D Chadwick and D C Smith, Petap Cable - A New Concept in Buried Cable Design, Proc 27th International Wire and Cable Symposium
- International Telegraph and Telephone Consultative Committee (CCITT), Joint Working Party CDF, Contribution No.13 April 1975
- 7. T K McManus and R Beveridge, A New Generation of Filled Core Cable, Proc 26th International Wire and Cable Symposium
- International Telecommunications Publication The Protection of Telecommunication Lines and Equipment Against Lightning Discharges, 1974
- Lightning, Vol.2: Lightning Protection, The Academic Press 1977, Page 810

- 10. J J Refi and M J Swiderski, Lightning Surges in Buried, Filled Telephone Distribution Cable, Proc 27th International Wire and Cable Symposium
- 11. H J C Spencer and L W Kingswell, The Application by the British Post Office of Carrier Techniques in the Existing Local Network, Conference Record, International Symposium of Subscribers Loops and Services, 1974

H J C Spencer PO/THQ/OP2 Lutyens House Finsbury Circus London EC2M 7LY Tel: 01-357 2235



Mr Spancer is Head of the Local Line and Junction Planning Division, (OP2), Telecommunications Headquarters, British Post Office. He is a Member of the Institution of Electrical Engineers

G A Bartlett PO/THQ/OP10.5.1 Carlton House Carlton Avenue East Wembley Middlesex HA9 8QH Tel: 01-908 1173



Mr Bartlett works for the External Plant Development Division, Telecommunications Headquarters, British Post Office. He is currently Head of Group dealing with the specification and development of twin and quad type cables. After graduating from the University of London in 1952 he gained experience in the Research Branch and Development Laboratories of the BPO. He is a Member of the Institution of Electrical Engineers.

THE DEVELOPMENT AND MEASUREMENT OF A WIDEBAND 12 PAIR CABLE

*H.L.Baker, **J.D.S.Hinchliffe, and **R.Mullins

*Rediffusion Engineering Limited

**Relipace Cords & Cables Ltd. - A member of the BICC Group

Abstract

The requirement specification for a 12 symmetrical pair broadband cable with stringent high frequency crosstalk protection ratios is set out. Such a cable has applications in the fields of HF television distribution systems and high speed data transmission. To achieve the target figures necessitated careful control of a number of experimental batches to optimise the design and processes.

To assure adequate production quality it is necessary to verify the crosstalk performance of all 132 pair combinations. The design of automatic test equipment to carry out these measurements and record the results or signal a defect is described.

1.0 Introduction

The six-pair wideband cable has now been the standard design for a number of years for television distribution systems based on the HF symmetrical cable, operating up to frequencies of approximately 12 MHz. This took the place of the earlier two screened quads for vision circuits and an audio quad. With the advent or potential of increasing numbers of channels, there has been a need for additional circuits, and with this in mind a 12-pair HF cable was proposed, which would also have applications in the data transmission field.

This paper describes the performance requirements for such a cable and the design considerations. The design/process development which has taken place over a period of years is then detailed. Finally, the paper describes the measurement requirements and, in particular, the design and development of a broadband Crosstalk Test Set to carry out automatically the measurement and recording of crosstalk coupling loss on all pair combinations in the cable.

2.0 Design Requirements

These were based on the requirements for an HF multipair distribution system with a bandwidth up to 12 MHz. In particular, attenuation leveis must be of the order of 10 dB/225 metres at 10 MHz with an impedance level conventionally in the 130 to 140 ohms band with a close tolerance on this level.

Far-End crosstalk coupling loss requirements for such systems are stringent and were set at levels of 53dB for the Power Average Crossview (PAX) and 48 d3 for the low pass limit on all pair/pair combinations. The usual considerations of minimising overall diameter and retaining some degree of flexibility also applied.

Whilst such design requirements were based primarily on the needs of an HF multipair television distribution system, similar types of cable are also required for PCM and digital applications.

3.0 Cable Design Considerations

The construction of a 12-pair cable to meet the design requirements of section 2.0 posed certain problems particularly with regard to the cable make-up to minimise pair/pair crosstalk coupling and at the same time minimise overall diameter. With regard to the latter, it was felt that the 12 pairs must be arranged in two layers of 3 + 9 and that the lay scheme for the individual pairs would have to take account of this. In addition, in view of the known difference in impedance level which can occur between pairs in inner and cuter layers, because of the proximity of the outer screen, it was necessary to space the screen from the outer layer to compensate for this difference.

First considerations indicated that the lay lengths of the pairs would be limited by both mechanical and electrical aspects. The latter precluded very short lays. For mechanical reasons the lay range can only be from 19mm to 90mm. limited at the low end by speed of twinner throughput and the requirement for ease of taping, and at the top end by the difficulty in maintaining constancy of lay lengths.

With the above considerations in mind, various cable designs were tried having the following basic parameters (conductor diameter was determined solely on attenuation level requirements):

Plain copper conductor - diameter 0.46 mm Polythene insulation to a diameter 1.34 mm Twinned and laid-up 9 pairs round 3 pairs Polythene inner sheath Conducting polythene or longitudinal aluminium tape screen Black polythene outer sheath diameter 11.9 mm

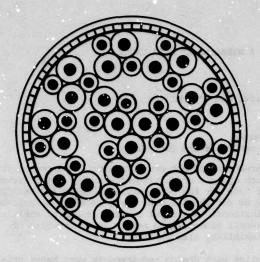


Fig. 1

12 Owist Cable

4.0 Experimental Work

In order to confirm whether the design objectives could be met a number of experiments were carried out on various modifications to the basic design of cable.

4.1 Experiment 1

This consisted of two cable types. The first being of 'qwist' construction, which is one with smaller audio pairs laid into the interstices of the larger video pairs, and the second cable being of conventional twisted pair construction (See Figures 1 and 2).

Both types were manufactured on a precision quadder and cross-stranded, nine units round three, on a detorsion strander, and subsequently an inner sheath of conducting polythene was applied followed by a conventional black polythene sheath.

Ten lengths each of 225 m of each cable type were manufactured with an appropriate lay scheme for the units.

There were considerable difficulties in meeting the crosstalk requirements on both qwist and pair types, individual adjacent pair combinations of the centre three pairs having coupling losses down to 35 dB.

Additionally, there were indications of difficulties on the centre to outer pair combinations of the pair type, and on adjacent pair combinations of the outer layer on both types.

The causes of these failures were attributed to two problems. Firstly, mechanical unbalance of the units either by eccentric core extrusion or mechanical deformation during manufacture and, secondly, particular twin lay combinations being unsuitable. The difficulty was in deciding how

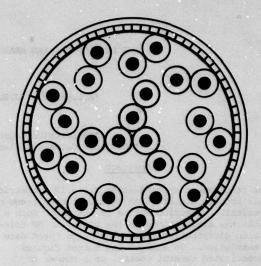


Fig. 2

2 12 Pair Cable

the two causes had interacted. It is generally assumed that if one particular combination is troublesome then this is a poor design of lay ratio. It is, therefore, prudent to make two separate manufacturing runs on any particular design before drawing any firm conclusions as to the cause of poor crosstalk performance.

In the case of this first experimental run it was decided from an examination of the results that the poor within centre performance was due to mechanical disturbance during the laying-up process and a new lay scheme reducing the lay lengths of the centre pairs was required. Additionally, a polyester tape should be applied over the centre pairs to improve the mechanical stability.

To determine the 'optimum' lay scheme to give the required crosstalk levels it was therefore decided to proceed with the qwist type cable only at the next stage this type being inherently more mechanically stable due to the interstitial audio cores.

4.2 Experiment 2

The second experiment containing the revised lay scheme with reduced lays on the centre units was split into two halves, one with a polyester tape over the centre and the other without. The best results showed that the crosstalk coupling loss improvement on the within centre pairs was marked — averaging 11 dB, but two of the centre to outer combinations were still poor with loss levels down to 41 dB and 44 dB average.

This necessitated a further minor change to the lay scheme, on one qwist each in the centre and outer layers. The effect of the polyester tape over the centre pairs was not significant.

4.3 Experiment 3

It was decided that the results of experiment 2 were sufficiently encouraging to proceed with a twelve pair cable (the ultimate objective), dispensing with the polyester tape and incorporating the two revised lays.

The results from this experiment indicated that the centre to outer and centre to centre problems had been overcome but there remained a particularly low combination on an adjacent pair combination in the outer layer of 41 dB and a further twin lay length modification was made to this pair.

4.4 Experiment 4

A further 10 x 225 m of cable was then manufactured and the results indicated that the crosstalk coupling loss levels were 2 to 3 dB below the required levels on the adjacent pair combinations of the outer layer.

There were also a number of poor individual results i.e. one bad result in an otherwise good combination, which in practice could lead to an excessively high rejection rate.

4.5 Final Development Phase

4.5.1 It was now felt that a substantial production run was needed to produce sufficient statistical information to confirm the design parameters and 10 km of cable was produced in two manufacturing batches. The crosstalk results confirmed that the design was good except for the 9 adjacent combinations in the outer layer still being approximately 3 dB below the required levels.

It was felt that as much improvement had been obtained from lay to lay ratio variation and it was likely that the third circuit crosstalk paths were the cause, either via the screen (in this case a carbon loaded polythene belt) or through the centre pairs.

An examination of the cumulative distribution of pair to pair couplings in batches of 30 coils of 6 pairs round a centre dummy and of 6 pairs round three audio pairs in otherwise identical unscreened cables resulted in the following:

Table 1

% of sample	Cable Type	Adj. Comb. dB min	Alt. Comb. dB min	Opp. Comb. dB min
95%	6 pr.	53	52	52
	9 pr.	50	54	53
90%	6 pr.	54	53	53
	9 pr.	51	56	54
50%	6 pr.	6 0	60	58
	9 pr.	58	62	58

From the above table it can be seen that the centre pairs seemed to degrade the average adj-

acent combinations by 3dB and improve the alternate combinations by 2 dB. It would, therefore, seem that if the influence of the centre pairs could be eliminated the troublesome edjacent combinations could be improved and a 2 dB degradation of the alternate combinations could be tolerated whilst still being within specification.

There was also evidence that by removing the screen further away from the cores on a six pair cable an improvement could be obtained on all combinations.

4.5.2 To confirm these points three experimental runs were manufactured. The first with the 9 cuter pairs around a dummy polythene centre, the second with a carbon loaded tape applied longitudinally over the centre three pairs and the third with an aluminium tape applied longitudinally over a natural polythene inner sheath of the same thickness as the carbon loaded type of the first two experiments. This was to maintain the same cable overall diameter. The results are tabulated in Table 2, but care must be exercised in drawing firm conclusions because of the small sample size.

Unfortunately combination 1 results on the aluminium tape cable suggested a manufacturing defect. In other respects, moving the screen further from the cable appeared beneficial.

Finally, 23 coils of this last type were manufactured to confirm this point giving results as in Table 3.

As will be observed an average 5 dB improvement had been realised and combination 1 proved to be a manufacturing defect.

The additional manufacturing batches have shown up a somewhat poorer combination of lays between two pairs spaced two pairs apart. One of the pairs is also involved in combination 9 of the adjacent combinations and it is felt that an alteration to that pair lay would be beneficial for the future.

In the meantime it has been acceptable that one particular pair should not carry HF TV signals, as 12 vision channels are not currently required.

The substitution of the aluminium screen for the carbon loaded sheath has degraded the NE crosstalk performance by up to 6 dB but this is still at an acceptable level.

Results on production quantities of similar cable give PAX coupling losses between 52 and 61 dB with an average of 54 dB, confirming the general level of the final experiment.

Sample size	Construction	PAX dB 9 adjzcent Average combinations - far end dB
22 coils	9 + 3 and carbon belt	1 2 3 4 5 6 7 8 9 51 53 49 51 56 53 52 54 48 52.0
5 coils	9 + dummy and carbon belt	54 59 50 56 61 50 52 56 52 54.5
10 coils	9 + 3 and carbon tape + carbon belt	56 52 50 54 55 51 56 53 51 53.0
5 coils	9 + 3 Poly belt + Al. tape	46 55 51 58 58 54 54 58 53 54.0

Table 3

Sample size	Construction	PAX dB 9 adjacent combinations - far end	Average db
22 coils 9 + 3 carbon belt		1 2 3 4 5 6 7 8 9 51 53 49 51 56 53 52 54 48	52.0
23 coils	9 + 3 poly belt Al. tape	56 60 57 59 57 53 58 57 53	57.0

5.0 Measurement Requirements

As well as the conventional production checks on conductance, insulation and capacitance, cables are subjected to pulse testing on HF impedance and internal reflections. It is important also to monitor the crosstalk performance between all pair combinations. In the HF band, because of the interaction between direct crosstalk and indirect crosstalk coupling paths, measurements made using a single frequency show considerable variations with frequency. It is therefore usual to make measurements using broadband white noise as the test signal and to compare the rms levels on the disturbed and disturbing pairs. Existing equipment for carrying out this test embodies manual switching for making the appropriate connexions to 6 pair cable and requires the operator to make adjustments and record the results for the 30 pair combinations.

With the doubling of the number of pairs the number of measurements required was more than quadrupled from 30 to 132 and this dictated a new approach.

6.0 Crosstalk test set design requirement

The major requirements for the new test set were that as far as possible measurements should be made and recorded automatically. The instrument was to measure over the spectrum 3 to 12 MHz total losses (cable plus crosstalk coupling) of 30 to 90 dB with an accuracy and resolution of \pm 1 dB and to accommodate wire diameters from 0.4 to 1.5

mm with a pair impedance of 100 to 170 ohms.

7.0 Instrument design

7.1 Test signal

In order to obtain a high spectral energy density a pseudo random binary pulse sequence (PRBPS) is used to derive the test signal. This is generated by a 10 bit TTL shift register clocked at 13 Mb/s which produces a sequence of 1023 bits having spectral components every 13 kHz. In order to remove the dc component and to enhance the HT spectrum the register output is gated with the clock to produce a biphase Manchester modulated signal. Filters are used to limit the frequency bandwidth producing a typical spectrum as plotted in Figure 3.

At the sending end each pair in turn is energised by a line driver comprising a pair of push pull power switching transistors applying 28V p-p to the line.

7.2 Pair selection

Balanced diode switches are connected to the near end and far end of each pair toterminate it or to transfer the gignal present to the level measuring system as required.

7.3 Level measuring circuit

The heart of the level measurement system is a diode operating as an rms detector the output of which is applied to a dc comparator having a stabilized reference. The output of the comparator is used to control the direction of a 1 dB stepping attenuator such as to bring the level of signal applied to the detector back to the reference level. The number of decibels in the attenuator in the equilibrium state is therefore a measure of the input signal level. When measuring disturbing signals an extra 30 dB of loss is introduced.

7.4 Digital control circuits

Hard wired TTL logic circuits are used to control the sequence of measurements, to control the operation of the diode switches selecting pairs under test and to step the measuring attenuator. After the 'Start' button has been manually operated the following measurement sequence ensues automatically. The test signal is applied to the first pair, the measuring circuit loss is adjusted as previously described and the numerical value of attenuation is stored temporarily. Next the measuring circuit is switched to the near end of the second pair and again adjusted. The new value of attenuation is subtracted from that stored and this difference representing the near end crosstalk coupling loss between pairs 1 and 2 is transferred to a first in first out (FIFO) memory. This process is repeated to measure and memorise the near end coupling loss between pairs 1 and 3, pairs 1 and 4 etc. etc.

When 11 measurements have been made i.e. all combinations involving pair 1, a hard shaking routine is set up between the FIFO memory and an electromechanical printer. The memory is emptied and the first row of results printed out.

Next pair ? is energised and in similar fashion the far end coupling loss to pair 1 is measured and memorised and then in succession the near end loss to the remaining pairs and the next row of results printed out.

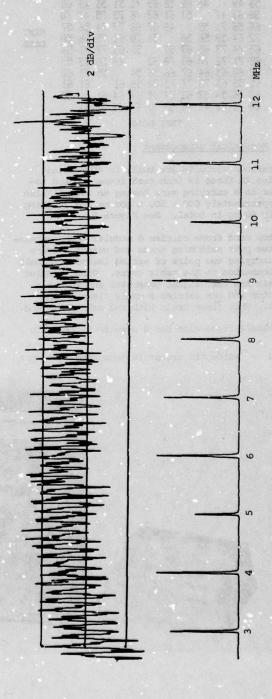
Each pair in succession is energised and the measurement sequence is arranged such that when the ordinal value of the energised pair exceeds that of the coupled pair the far end loss is measured and when the ordinal value of the coupled pair is the greater a near end measurement is made until all 132 pair combinations have been measured.

The resultant row by row printout appears in the format illustrated in Figure 4.

Provision is made in the instrument for manual stepping of the measuring sequence with an l.e.d. display of the results. Digital comparators are also embodied so that limits can be pre-set to halt the measurement sequence and warn the operator if there is excessive transmission loss due to an open circuit or if the crosstalk performance is below specification. Auxiliary outputs are avail-

able to interface with a VDU, a computer or other peripheral device.

Fig. 0 Test Signal Spectrum Plot



DISTURBED PAIR

Pair	1	, 2	3	4	5	6	7	8	9	10	11	12	
1 2 3 4 5 6 7 8 9 10 11 12	60 53 59 66 72 65 68 52 61 68	51 49 63 56 64 74 71 60 59 56	56 49 47 71 59 73 72 61 65 53	63 64 45 59 56 65 70 64 73 53	75 568 51 50 63 67 77 63	66 71 52 61 49 59 70 66 72 63	78 73 69 63 67 51 62 56 65	68 71 76 68 70 52 54 59 64	49 70 51 73 73 61 63 49 61 64	55 57 53 75 74 75 73 58 55	70 58 49 47 56 58 71 73 71 61	70 74 68 70 57 50 54 55 60 61	NEXT LOSS
		Ī				EXT							

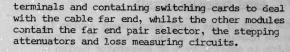
7.5 Mechanical arrangement

The various circuits are built in 4U modules carried in three 19 inch card frames housed together in a carrying case having an overall size of approximately $600 \times 500 \times 400$ mm and weighing nearly 60 kg in total. See Figure 5.

The top card frame carries 6 modules each containing two pair switching cards and output drivers and carrying two pairs of spring loaded terminals for connexion to the cable cores. Other modules contain the test signal generator and the pair selector and one carries a cable clamp in the front. This frame deals with the cable near end.

The middle frame also has 6 modules fitted with

Fig. 5 Automatic crosstalk measuring equipment



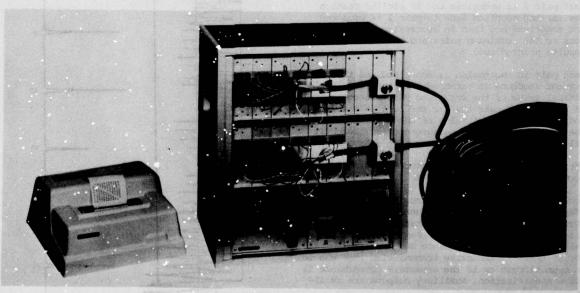
The bottom frame holds the power supplies, the sequence control circuitry, the output display and the peripheral interface units.

8. Conclusion

The development of a wideband 12 pair cable and test equipment for measurement of all crosstalk couplings has been completed to the stage where production of cable and equipment can be undertaken to meet the requirements of systems operating at frequencies up to 12MHz.

9. Acknowledgements

The A_{1} -thors wish to thank Rediffusion Engineering Limited and B.I.C.C. Limited for permission to publish this paper.





Redirfusion Engineering Limited, 187 Coombe Lane West, Kingston upon Thames, Surrey. KT2 7DJ

Mr. Baker is Head of the Cable Transmission
Department of Rediffusion Engineering Limited
which he joined in 1959 following a number of
years development experience. He has the responsibility of specifying or developing nearly all
the hardware used on HF cable TV systems from the
aerial through the down converters via cable and
repeaters to the subscribers' outlets. In 1974-6
he served as a member of the Joint BEC/BREMA/IBA
Working Group which produced the specification
for Broadcast Teletext. He is a Member of the
Institution of Electronic & Radio Engineers and
of the Society of Cable Television Engineers.



Reliance Cords & Cables Limited, Staffa Road, Leyton, London ElO 7PU

Mr.Hinchliffe has been Technical Director of Reliance Cords and Cables Limited since 1968. After gaining a BSc (Hons) at Leeds University, he joined BICC Limited in 1946 in their Telecommunications Laboratory. He transferred to BICC Helsby in 1954 becoming Technical Manager in 1959 in charge of the design and development of all types of plastics insulated cables. He is a Fellow of the Institution of Electrical Engineers and of the Society of Cable Television Engineers.

NON-CONTACT INK JET PRINTER FOR CABLE SHEATH MARKING

Wayne M. Newton

Western Electric Co., Inc. Norcross, Georgia

Abstract

A non-contact ink jet printer has been developed which is capable of printing on irregular surfaces, does not distort the cable sheath, will accommodate all new cable codes as they are added, provides selectable length marking of feet or meters and will operate at line speeds up to 1500 feet per minute.

The operating principles of the jet printer are presented to describe how characters are formed from the ink droplets. The microprocessor based control system and display for the printer, jet printing ink requirements and various inks investigated for cable sheath marking are presented. These inks include dye-type inks for marking PVC cable jackets and a special white pigmented ink developed for marking black polyethylene sheath.

Introduction

Sequential length, cable type, number of pairs, date of manufacture and manufacturing plant identification codes are commonly printed at intervals on the outer polyethylene cable jacket at the sheathing line. Mechanical, rotating drum type printers with metal print characters and various designs of ink transfer wheels are generally used to perform this printing. Entrance guides and cable support sheaves are used to properly position the cable under the printer drum. The printer is either friction driven by the cable or mechanically or electrically driven depending on the length marking accuracy required. Over the years, there have been improvements designed into the mechanical printers affecting print legibility, operation and maintenance. However, due to the mechanical nature of these printers, there are inherent limitations in their application, flexibility and operation. Also, improper operation such as excessive guide roll pressure can result in cable sheath damage.

This paper describes the development of an ink jet printer as a non-contact sheath marking device designed to overcome many of the limitations experienced with the mechanical markers.

Ink Jet Printer

Ink jet printing is emerging in correspondence quality "word processing" for office use, but major existing applications are for data printers, document handling systems, graphics systems and coding systems for the packaging industry. A commercially available jet printer utilized by the beverage industry was selected as the basic ink jet printing unit around which the non-contact sheath marker was developed.

The control unit and print station electronics of this printer are diagrammed in Figure 1. A microprocessor based control unit was added to the basic printer to store and output data to the main frame electronics corresponding to the length and code information to be printed.

An operator's control station consisting of a touch sensitive keyboard and LED display is interfaced to the control unit. This station, shown in Figure 2, permits the operator to monitor information which is being printed on the cable as well as enter new instructions for information to be printed on subsequent cables. Length measurement and marking in feet or meters can be selected from the keyboard for programming the marking of individual cables to correspond with either international or domestic length marking requirements.

Operating Principles

An ink jet printer employs the basic physical principles of ultrasonics and electrostatics on a fluid stream. While these effects are not new, only recently have they been combined to form a unique printing technology.

As background, the basic ink jet printing process is shown in Fig. 3. A conductive ink is forced under pressure through a small ultrasonically driven nozzle. The vibrating ink inside the nozzle cavity and resulting pressure waves cause the ink stream exiting the nozzle to break up into a stream of drops which are uniform in size and spacing. Surrounding the point where the drops break off from the stream is a charge electrode. A predetermined voltage is applied to the electrode as each drop separates from the

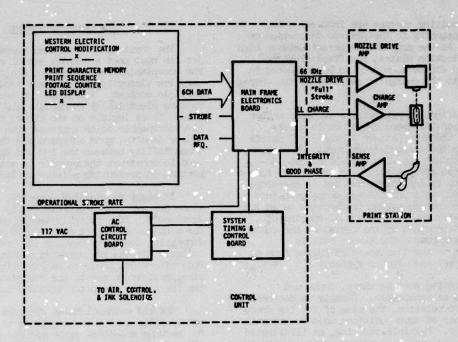


FIGURE 1: ELECTRONICS BLOCK DIAGRAM

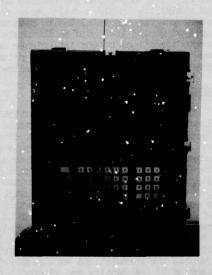


FIGURE 2: OPERATOR'S CONTROL STATION

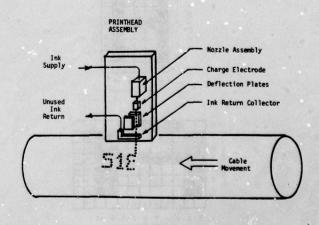
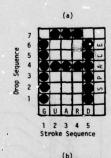


FIGURE 3: INK JET PRINTING PROCESS

stream. Resulting charges are induced on the drops corresponding to the desired deflection of each drop. As the drop stream passes between high voltage deflection plates, the fixed electrostatic field causes each drop to be deflected in proportion to the charge it received at the charge electrode.

This deflection generates a vertical column of up to seven ink drops on the cable corresponding to the drop pattern of the 5 x 7 matrix used to form the printed characters. The column, called a "stroke" may also contain spaces, depending on the character to be printed. To form a space, a drop is left uncharged and is therefore not deflected. All undeflected drops pass into a pick-up tube and are vacuum transported to an ink return tank for reuse. Horizontal spacing of strokes is determined by the travel of the cable under the printhead. The stroke rate is synchronized to the line speed by pulses from a measuring wheel and encoder system.

The printing must be sharp, dense and permanent to be acceptable. Density is determined by the ink formulation, the size of the ink drops and the number of drop positions used to assemble the character. Multiple stroking, as illustrated in Figure 4, is used to increase print density or make the characters "bolder". Sharpness is determined by the accuracy of drop placement which is a function of the drop formation, deflection, flight characteristics and in some respects the surface characteristics of the cable jacket. Permanence is a function of the ink's resistance to fading and interaction of the ink and the jacketing material for proper adhesion.



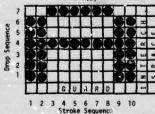


FIGURE 4: ALITERNATE CHARACTER CONSTRUCTION
(a) Single Stroke Character,
(b) Double Stroke Character

Ink Characteristics

The physical and chemical characteristics of jet ink must meet a complex set of requirements. For acceptable drop formation, the ink must have very low viscosity, low surface tension and small particle content. For proper deflection, the ink must be electrically conductive and uniform in mass. To be legible on the cable, the ink must have acceptable color contrast with the jacket, proper density, good adhesion and fast drying time. Compatibility between the ink and the materials used to construct the printer is also very important in preventing printer failure.

As might be expected, specific ink formulations are considered proprietary by their developers. If a suitable ink is not available for a unique application, the user must rely on a commercial source to develop the ink or else initiate his own ink research effort to do so. This effort can prove to be extensive for a complex application due to the restrictions on the ink for proper operation with the prirter.

MEX and methanol based dye inks which are commercially available were found to be suitable for marking non-black cable jackets such as grey PYC. As a result, jet printers are now being installed on two of our Alvyn cable sheathing lines. These printers will be using a black dye type ink. Similar units will also be used to code fiber optic ribbons in our new fiber optic cable production facility.

Marking of black polyethylene cable jackets with dye type inks was not successful because all colors of dye proved to be virtually invisible on black. It was concluded that a pigmented ink would be required to provide the desired opacity for good visibility on black cable jackets. A development program was initiated to determine if a suitable pigmented ink could be formulated and if major modifications to the jet printer would be required to accommodate this ink. The primary areas investigated are summarized as follows:

1. Operating Parameters

Conditions affecting the operation of the printer include both fixed and variable parameters. The drop frequency and jet diameter were considered fixed since they could not be changed without affecting the printer speed and resolution. The ultrasonic nozzle drive voltage and nozzle ink pressure are machine set up variables and the ink viscosity, density and surface tension are ink formulation variables. The interrelationship of these parameters have been modeled, confirmed with prototypes and reported by jet printer developers. Even so, many trials of various pigmented ink formulations were required to determine if ink density and viscosity parameters could be adjusted for proper operation within reasonable nozzle drive voltage and pressure settings. Gradually, a titanium

dioxide pigmented ink with sufficient density for good visibility on black and acceptable character formation was developed. Although nozzle drive voltages and pressure adjustments were more critical for the pigmented ink than for the dye ink, it was demonstrated that pigmented irk was feasible to pursue.

2. Ink Adhesion to the Cable

Initial trials with pigmented ink jet printing resulted in poor print adhesion to the polyethylene cable jacket. A unique ink which would remain fluid in the jet nozzle after an extended shutdown but would provide fast drying and good adhesion to the cable was required. Assistance was obtained from the Bell Laboratories Organic Materials Research and Development Group which was conducting research in ultraviolet curable coatings. resulting development was a pigmented ink with an ultraviolet sensitive resin system. The resin system chemically bonds the printing to the cable jacket as it passes under a high intensity ultraviolet light. The arrangement of printer components for this marking is shown in Figure 5.

Line speeds up to 200 feet per minute were run with resulting good ink adhesion using a 2.4 KW medium pressure U.V. lamp for curing. Higher line speeds are possible with the use of a more powerful lamp. Since this ink remains fluid until ultravioletly cured, drying problems and resulting blockages of the jet rozzle orifice are avoided even after a shutdown period of several days. Examples of printing with the white ink and the black ink are shown in Figure 6.

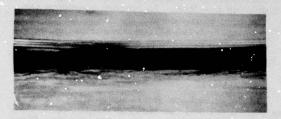
3. Long-Term Printer Operation

The most difficult problem encountered in using the new pigmented ink in the jet printer was achieving successful long-term operation. The two problem areas encountered were:

- Maintaining pigment dispersion and suspension in the ink
- Elimination of pigment accumulation and blockage of system filters



(a) Black Ink on Grey Vinyl Jacket



(b) White Ink on Black Polyethylene Jacket

FIGURE 6: EXAMPLES OF INK JET PRINTING

The first problem resulted from the TIO2 pigment settling out of suspension due to the very low viscosity of the ink. The ink is manufactured in a concentrated form and has sufficient viscosity to prevent the pigment from settling. However, when diluted to its low running viscosity, noticeable pigment settling occurs after 30 minutes. Meclanical stirrers were added to the ink supply and return tanks to overcome this problem. Also, the diameter of the ink supply tubing of the printer was reduced to increase the ink flow velocity and help maintain pigment suspension. Similarly, the ink supply line filter was kept as small as possible. These changes made it possible to maintain uniform ink dispersion during a long run and to minimize the startup dispersion stabilization time.

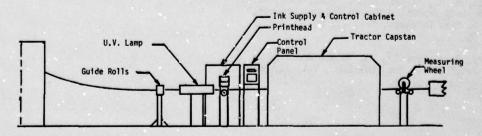


FIGURE 5: LOCATION OF NON-CONTACT PRINTER COMPONENTS

Pigment accumulation and blockage of system filters proved to be a more difficult problem to solve than was first anticipated. Although the ink was manufactured with an acceptable nominal particle size, pigment build-up occurred in the 10 and 20 micron system filters causing nozzle pressure variations and eventual filter blockage. To guard against the possible presence of a small amount of oversize particles, filtration through a depth type filter was added to the ink preparation procedure. This, along with other changes, virtually elimi-nated all filter accumulations and long term operation of the printer with the pigmented ink was possible. Laboratory operation has now been completed and the installation of a printer at two of our manufacturing plants for production trials of the pigmented ink has been scheduled for late 1979.

Conclusions

A high-speed ink jet cable marking system has been developed for marking length, cable code and other information on the cable sheath. Since this is a non-contact marking system, printing on irregular surfaces is possible and indentation and distortion of the cable sheath is avoided. The electronic control system provides full flexibility in selecting information to be printed and can be easily expended to perform other functions if required. If the initial plant trials of these printers are successful, usage is expected to gradually expand as the existing mechanical printers need replacement and other products are selected for marking.

Acknowledgements

The author wishes to acknowledge the contributions of H. N. Vazirari of Boll Laboratories in formulating the U.V. curable white ink and J. A. Hudson of Western Electric in designing the special electronic control system addition to the printer.

References

- Minto, Graemi S., "The Ink Jet Set," Penrose Annual 1978/79
- Beach, B. L., Hildenbrandt, C. W., Reed, W. H., "Materials Selection for an Ink Jet Printer," IBM J. Res. Develop., Vol. 21, No. 1, 1977, pp. 75
- Curry, S. A., Portig, H., "Scale Model of an Ink Jet," IBM J. Res. Develop., Vol. 21, No. 1, 1977, pp. 10

Wayne M. Newton Western Electric Co., Inc. 2000 N.E. Expressway Norcross, GA 30071



Wayne M. Newton is a Senior Development Engineer at the Western Electric Atlanta Works in Norcross, Georgia and is presently involved in Cable Sheathing Manufacturing Engineering. Prior to this assignment, he was active in sheath development and cable testing in the Western Electric Cable and Wire Product Engineering Control Center. Before that, he was engaged in Switching Systems Equipment Engineering.

Mr. Newton received a BSEE Degree from Clemson University in 1965 and holds two patents in the wire and cable field.

Y. Yamazaki

Tokyo, Japan

Nippon Telegraph and Telephone Public Corp. Nippon Telegraph and Telephone Public Corp. Tokyo, Japan

T. Ideguchi

S. Masaki

Nippon Telegraph and Telephone Public Corp. Tokyo, Japan

Summary

NTT is using Aluminum Sheath Cable as a countermeasure against induction interference from power transmission lines and electric traction lines. This cable has excellent electromagnetic sheilding characteristics. However, some weak points have appeared in its mechanical characteristics. Since 1974, NTT has researched a cable shielding structure design method which matches desired sheilding capability with mechanical characteristics, resulting in the New Aluminum Sheath Cable.

The new shielding cable is enclosed in a thinned and corrugated aluminum tube. Mechanical characteristics are greatly improved until they are as good as characteristics for other laminated sheath cables.

This paper describes electromagnetic shielding structure design method and mechanical and electrical characteristics for the New Aluminum Sheath Cable.

1. Introduction

The telecommunication network in Japan has become very widespread to satisfy increasing public communication demands. On the other hand, power transmission networks and electric traction networks have also expanded, to cope with economic development and energy demand growth. The heavily populated area in Japan is such that these three networks are densely installed side by side.
Therefore, induction problems have become more important than in the past. This condition is foreseen to change for the worse in the future, unless effective ccuntermeasures are successfully developed.

As one of the countermeasures against the inductive interference, NTT is now using Aluminum Sheath (AS) cable. The demand for AS cable has been increasing more and more in the past few years. Existing AS cable has excellent electromagnetic shielding characteristics and mechanical strength. However, this cable is covered by a relatively thick aluminum tube, which is very rigid. Therefore, installation efficiency is not very good, due to the cable rigidity. Cable sheath splices were prone to break down because of thermal stress in the cable sheath due to temperature changes causing expansion and contraction. So, it was desired to improve existing Aluminum Sheath Cables.

NTT minutely considered the relations

between the shielding sheath structure and its electromagnetic shielding characteristics and mechanical strength. It was made clear that it was necessary to not only improve mechanical characteristics by a change in cable structure, but also to compensate for worsened shielding characteristics due to structure change. In consequence, an optimum electromagnetic shielding structure design method was established, resulting in the New Aluminum Sheath Cable.

2. Aluminum Sheath Cable

2.1 Aluminum Sheath Cable

Electromagnetic shielding, to protect cable from induction interference, requires both a good conductive layer as an inner layer and a ferromagnetic layer as an outer layer in the cable sheath. Existing AS cable consists of a thick, smooth aluminum tube as a conductive layer and double low carbon steel tape armoring as a ferromagnetic layer.

Figure 1. shows AS cable structure.

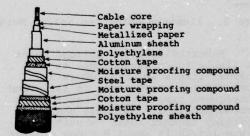


Figure 1. Existing Alminum Sheath (AS) Cable

2.2 Aluminum Sheath Cable Problems

The previously mentioned aluminum tube thickness ranges from 1.0mm to 1.5mm according to the cable diameter. Aluminum tube conductivity is excellent for electromagnetic shielding. On the other hand, from the standpoint of use as a cable sheath, mechanical characteristics, such as flexibility and the sheath splice ability to withstand thermal stress, are considerably worsened, compared with a general telecommunication cable because of the aluminum tube structure. Accordingly, the following restrictions and problems appeared in practical use.

2.2.1 Installation problems

The minimum permissible bend radius is very large, 10 times the cable outer diameter, so that the maximum cable outer diameter and the minimum manhole size are both greatly restricted in a practical installation in an underground conduit section.

The shielding sheath is not too flexible, so it is difficult to assure required slack when installing overhead cables.

2.2.2 Sheath splice problems

To protect the sheath splicing point from large thermal stress caused by aluminum tube expansion and contraction due to temperature changes, the cable sheath is spliced by a mechanically stout soldering method, using aluminum solder.

Figure 2 Shows the aluminum soldering splice method.

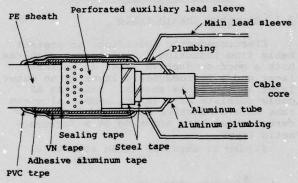


Figure 2. Aluminum Soldering Splice Method

Nevertheless, the spliced point is liable to be damaged due to the thermal stress in areas where the temperature change range is large and subsequent expansion and contraction become problems. As cable sheath splicing trouble ratio vs unit cable route length is about 8 times greater than the ratio of all cables other than As cable. This causes an increased maintenance workload.

2.2.3 Conductor insulation material limitations

The aluminum soldering method required applying high temperature, more than 200°C, to a small portion of the cable, plastic insulated conductors in cables cannot easily withstand such concentrated high temperature without damage. Therefore, paper insulated conductor cables are used.

When transmitting broadband signals, such as digital data and facsimile over AS cable connected to other plastic insulated conductor cable, the transmission system efficiency is restricted by the difference in high frequency transmission characteristics between AS cables and other plastic insulated conductor cables.

2.3 Requirements for New Shielding Cable

In order to solve the aforesaid problems, NTT has considered a new shielding cable, since 1974.

Requirements for new shielding cable are as follow.

 Electromagnetic shielding characteristics are equal to or better than existing AS cables.

(2) Mechanical characteristics such as flexibility and the sheath splice ability to withstand thermal stress, are equal to those of existing plastic sheath cables.

(3) New cable structure is also applicable to plastic insulated conductor.

3. New Shielding Cable Sheath Design Method

A sheath design method, which is a melding of mechanical characteristics and shielding characteristics, is described below. Mechanical characteristics improvement is intended through improving inner conductor sheath. The shielding characteristics are equal to, or better than, that of existing AS cable armored with low carbon steel tape.

3.1 Design Principle

The shielding factor of a sheath composed of inner conductor sheath and outer ferromagnetic sheath is expressed as:

$$\eta = \frac{Ro + Re}{Ro + (r+jx) + jxe + Re}$$
 (1)

where, Ro is the conducter sheath resistance (Ω/km)

(r + jx) is the additional impedance due to the magnetic flux in the steel armor. (Ω/km)

jxe is the external inductance of the sheath and ground return circuit. (Ω/km)

Re is ground resistance (Ω/km)

In Eq.(1), only Ro and (r + jx) are changed by sheath structure variation.

P means additional impedance ratio between new cable and standard cable. Q means conductor sheath resistance ratio between new cable and standard cable. These symbols are shown in Table 1. The following relation must be satisfied to realize $|n"| \leq |n'|$ from Eq. (1)

$$P \ge \frac{Q + Re''/Ro'}{1 + Re'/Ro'}$$
 (2)

· 图象是是一种企业的大型的企业的

Table 1. Various cable sheath impedances between new shielding cable and standard cable

	Conductor Sheath Resistance	Additional Impedance	Ground Resistance	Shielding Pactor
Stanuard cable	R ₀	r + jx	Re	n'
New Shielding cable	QR ₀	P(r+jχ)	Re'	η"

Here, we show the principle of the design, when 0.65mm-100pairs toll AS cable with 1.5mm smooth aluminum tube is used as the standard cable. Figure 3 shows the relation between P and Q, in the value where new cable has the same shielding factor as standard cable. According to this figure, the P value doesn't vary as much as the Q value, even if the Q value becomes far larger than 1.0, due to conductor sheath mechanical improvement. For example. if the Q value is less than 2.003.0, the value can be obtained by arranging the armoring method for low carbon steel tape used now, without increasing the tape quantity. So, it was first attempted to determine a conductor sheath structure satisfying the mechanical characteristics requirements, such as flexibility, bending and thermal stress characteristics. Next, it was attemped to arrange an armoring method using low carbon steel tape so that a P value corresponding to the resultant Q value could be obtained.

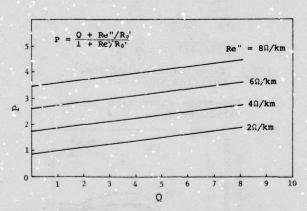


Figure 3. Relation between P and Q, in which new cable has the same shielding factor as standard cable.

(standard cable is 0.65mm - 100pairs toll)

As cable

3.2 Inner Conductor Sheath Design Method

At first, the following requirements were set up for the inner conductor sheath structure.

(1) The thermal stress and flexural rigidity becomes one-tenth of smooth aluminum tube used for cable shielding now, which is nearly equal to laminated sheath values.

- (2) The tolerable bending radius becomes six times the cable outer diameter.
- (3) The Q value is less than $2.0 \sim 3.0$.

A thin copper tube, corrugated copper tube, thin aluminum tube and corrugated aluminum tube were selected as the candidate structures satisfying the above listed requirements. Their mechanical characteristics were experimentally examined. The investigation showed that the bending radius was not satisfied in thin copper tube, corrugated copper tube and thin aluminum tube.

So, it was decided to use the corrugated aluminum tube as inner conductor tube.

Therefore, several experiment were conducted about mechanical characteristics, making several sizes of corrugated aluminum tube, as shown in Fig 4.

As a result, the following factors were clarified.

(i) Requirements (1) and (2) are satisfied at

$$\frac{t}{h} = 0.4 \text{ and } \frac{P}{h} = 5.0$$

(ii) Then, when 0.65mm - 100pairs toll AS cable is looked upon as standard cable, Q≤2.5 is obtained at t≥0.7.

This relation satisfied requirement (3). It was also clarified that this size corrugated aluminum tube can be made easily by the direct hot extruding method.

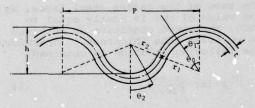


Figure 4. Corrugated aluminum tube model

3.3 Low Carbon Steel Armoring Design Method

3.3.1 Additional impedance equation

When current is flowing only in the inner conductor of the simple sheath model, which is composed of smooth inner conductor tube and outer ferromagnetic tube, shown in Fig. 5.

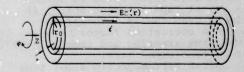


Figure 5. Simplified shielding cable sheath model

Additional impedance (r + jx) is described as follows

$$r+jx = \frac{Ez(r_0+t)-Ez(r_0)}{i}$$
 (3)

Where Ez(r) is the electric field intensity along the Z axis. In Eq.(3) Ez(r) is expressed in Bessel function by solving Maxwell's equation. The following approximate solution is obtained by using the resies form of Bessel function.

r+jx=
$$\frac{\gamma}{2\pi 6} \left\{ \left(\frac{1}{r_0} + \frac{1}{r_0 + t} \right) \text{ coth } \gamma t \right\}$$

- $\frac{2}{\sqrt{r_0 (r_0 + t)}} = \frac{1}{\sin h \gamma t}$ (4)

where $\gamma = \sqrt{j\omega\mu\sigma}$

- σ is ferromagnetic material conductivity.
- μ is ferromagnetic material complex permeability. $\bar{\mu} = \mu \, ' j \mu \, ''$

Here, the value of μ can be obtained by the following method. When the value of $|\gamma t|$ is far less-than 1.0, in which case the layer thickness is sufficiently thin, $\sinh \gamma t = \gamma t$ and $\cosh \gamma t = 1 + \frac{\gamma^2 t^2}{2}$ are obtained. (In the case of low carbon steel layer, as the value of $|\mu|$ is nearly equal to 3000, the above condition is obtained below 0.2mm tube thickness.) Therefore, the following relation is obtained.

$$r+jx = \frac{j\omega}{2\pi r_0} t \mu$$
 (5)

$$\mu' = \frac{2\pi r_0}{\omega +} x \tag{6}$$

$$\mu'' = \frac{2\pi r_0}{\omega t} r \tag{7}$$

As a result, μ ' and μ " are obtained by calculating Eqs. (6) and (7), using measured additional impedance values of thin ferromagnetic smooth tube (In the case of a low carbon steel Tube, less than 0.2mm thickness is considered).

Next, it was considered that the ferromagnetic layer would be formed in a spiral tape armoring shape, it could be used easily. Therefore, impedance correction factor between spiral tape armoring and smooth layer must be considered here.

Spiral ferromagnetic steel tape armor inductance, as shown in Fig. 6, is expressed by the following equation, by analyzing the spiral magnetic field, when tape is thin enough that eddy current will not occur.

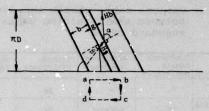


Figure 6. Spiral ferromagnetic steel tape armor model

$$\frac{r+jx}{jw} = \frac{t \cdot b \cdot \mu \sin^2 \varphi}{a(2\pi r \sin^2 \varphi + a \cos \varphi)}$$
 (8)

Smooth ferromagnetic tube inductance where tube wall is thin enough that eddy current will not occur, is expressed as follows.

$$\frac{\mathbf{r'}+\mathbf{j}\mathbf{x'}}{\mathbf{j}\omega} = \frac{\mathbf{t}\ \mu}{2\pi\mathbf{r}_0} \tag{9}$$

As a result, where ferromagnetic layer is thin enough that eddy current loss can be ignored, the following correcting equation is obtained.

$$A = \frac{r + jx}{r' + jx'} = \frac{k}{a} \left(1 - \frac{a^2}{4\pi^2 r_0^2}\right)$$
 (10)

If this relation is satisfied when large eddy current occur, the additional spiral armored ferromagnetic tape impedance can be expressed as follows:

$$r+jx = \frac{b}{a} \left(1 - \frac{a^{2}}{4\pi^{2}r^{2}}\right) \frac{\gamma}{2\pi 6} \times \left\{ \left(\frac{1}{r_{0}} + \frac{1}{r_{0}+t}\right) \cos h \gamma t - \frac{2}{\sqrt{r_{0}(r_{0}+t)}} \frac{1}{\sin h \gamma t} \right\}$$
(11)

3.3.2 Experimental equation verification

(1) Impedance correction factor verification

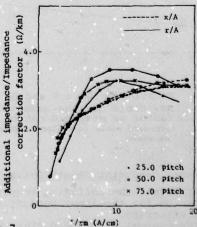


Figure 7.

Impedance correction factor verification

Low carbon steel tape is 0.8mm thick
and 25.0mm wide when warpped on

40.0mm diameter cable core.

Figure 7 shows the additional impedance divided by impedance correction factor, as related to magnetic field strength when low carbon steel tape 0.8mm thick and 25.0mm wide is wrapped around the 40.0mm outer diameter aluminum tube sheath with (1) 25.0mm pitch (φ =78.0°), (2) 50.0mm pitch (φ =66.5°) and (3) 75.0mm pitch (φ =53.0°). Characteristics for these three conditions agree well each other, so it is verified that the impedance correction factors can be used in ferromagnetic tape when eddy current occurs.

(2) Low carbon steel tape μ' and μ" values

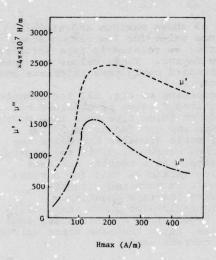
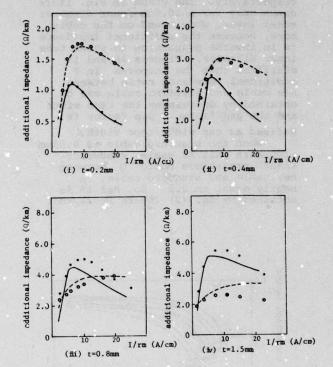


Figure 8. Low carbon steel tape μ value (measured)

Figure 8 shows low carbon steel tape μ ' and μ " values obtained by calculating Eqs. (6) and (7), using measured additional value for smooth low carbon steel tube 0.2mm thick, in which eddy current is very small, as related to magnetic field strength. Here, the additional impedance of a smooth tube was obtained by using the impedance correcting factor in the measured additional value for armored tape, which is 25.0mm wide and 6.2mm thick, wound so that it has 35.0mm inner diameter.



rigure 9. Additional impedance value as related to low carbon steel layer thickness

(calculated value { ______ }

measured value { ______ }

(3) Equation (4) verification

Figure 9 shows the additional impedance value for armored low carbon steel tapes (1) 0,2mm thick, (2) 0.4mm thick, (3) 0.8mm thick and (4) 1.5mm thick is comparing measured value and calculated value. Here, measured values are corrected by the impedance correction factor. Calculated values are obtained from Eq. (4). As a result, both values agree well with each other, so it is verified that Eqs. (4) and (11) are sufficiently useful in the design of low carbon steel tape armoring method.

3.3.3 Low carbon steel tape armoring design example

Low carbon steel tape armor is designed as follows, using complex permeability shown in Figure 9 and Eq. (11). Figures 10 and 11 show a calculated impedance correction factor example and |r+jx|max-t characteristics,

respectively. The graph in Fig. 11 is drawn only for a 10.0mm inner diameter steel layer, when wound on the cable core, because the additional impedance is in inverse proportion to steel tube inner diameter. Figures 10 and 11 clarified that the increase in P additional impedance ratio between new cable and standard cable can be obtained by decreasing the tape width and the gap factor. Gap factor is defined as gap width/tape width.

When the standard cable is $0.65 \,\mathrm{mm}$ -100pairs toll AS cable, conductor sheath resistance ratio Q between new cable and standard cable, is nearly equal to 2.5. So, P\(\text{2}\)1.15 is obtained by Eq. (2) (where Re=2\(\Omega/\text{km}\)).

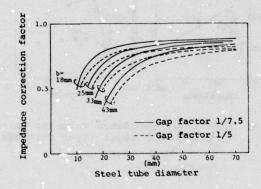


Figure 10. Calculated impedance correction factor

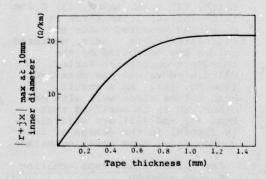


Figure 11 Calculated |r+jx| max - tape thickness characteristics result

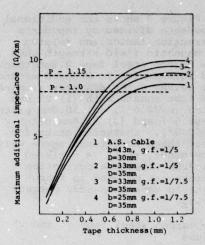


Figure 12. Low carbon steel tape armor design

Figure 12 shows maximum additional impedance value for low carbon steel tape armor as related to tape thickness and gap factor. These values are less than standard cable tape thickness and gap factor.

According to Fig. 12, for example, the required P value is obtained by using 0.7mm thick tape when tape width is 25.0mm and gap factor is 1/7.5 even if cable diameter increases due to forming corrugations in the aluminum sheath. As a result, the same shielding factor as that for a standard cable is obtained without increasing the tape quantity.

Figure 12 also shows that P=1.15

Figure 12 also shows that P=1.15 cannot be obtained by increasing tape thickness, using the same armor values as for current cable.

4. Trial Manufacture

According to the new shielding cable sheath design method, NTT made up plastic insulated conductor New Aluminum Sheath (NAS) cables. CCP-NAS cables are used for subscriber overhead distribution cable. Toll PEF-NAS cables are used for toll cable routes. Table 2 shows the trial manufactured NAS cables and Figure 13 and photograph 1 show the NAS cable structure.

Table 2. Trial manufactured NAS cables.

		Corrugated Aluminum Tube				Inner	Steel Tape			Weight
		Inner Diameter (mm)	Thick- ness (mm)	Corrugate Pitch (.mm)	Outer Diameter (mm)	PE Sheath Thick- ness	Thickness		Cable Diameter (mm)	(kgf/m
NAS cable 0.	0.5mm - 200P	26	0.8	11.0	32	1.0	0.8x25x2	2.0	45	3.3
	0.5mm - 400P	37	1.0	13.0	45	1.0	0.8x33x2	2.0	58	5.1
	0.9mm - 30P	20	0.7	9.0	25	1.0	0.6x18x2	2.0	37	2.1
	0.9mm - 100P	33	0.9	11.5	40.0	1.0	0.8x25x2	2.0	53	4.4
Toll PEF	0.65mm - 14P	11	0.7	9.0	16.0	1.0	0.6x18x2	1.5	27	1.2
NAS	0.65mm - 200P	36	1.0	13.0	44.0	1.0	0.8x33x2	2.0	57	4.9
cable	0.9mm - 100P	33	0.9	11.5	40.0	1.0	0.8x25x2	2.0	53	4.4
	0.9mm - 200P	45	1.1	14.5	53.0	1.0	0.8x33x2	2.0	66	6.8



0.9mm-100pairs Local-AS cable



0.9mm-100pairs CCP-NAS cable

Photograph 1 Cable structure

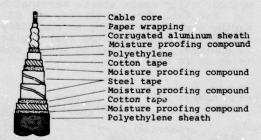


Figure 13. New Aluminum Sheath (NAS) Cable

5. Performance Test

NTT began performance tests on many kinds of cable characteristics in 1978.

5.1 Performance Test Outline

Performance tests were held at the Tukuba construction engineering office. Results were compared with values for existing Aluminum S.eath (AS) cable.

The factors examined in these tests are described below.

- (1) Shielding characteristics
- (2) Flexibility characteristics
- (3) Bending characteristics
- (4) Thermal stress characteristics.

5.2 Performance Test Results

5.2.1 Shielding characteristics

NAS cable shielding characteristics vs electric field intensity at low frequency (50Hz) was measured.

Shielding characteristics are shown in Fig. 14. NAS cables shielding characteristics are as good as existing AS cables at lower electric field intensity. However, at high electric field intensity, NAS cables have more effective shielding factor than existing AS cables.

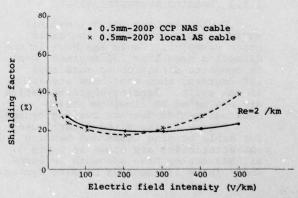


Figure 14. Shielding factor vs electric field intensity (at 50Hz)

5.2.2 Flexibility characteristics

A 50cm length of the sample cable is mounted so that one end is held firmly in place and is extended horizontally. A weight is loaded onto the other end of the cable. Flexibil-

ity was evaluated by the cable bend Table 3. Bending characteristics distance from the normal position.

The flexibility test method is shown in Fig. 15 and flexibility characteristics are shown in Fig. 16. NAS cables have much better flexibility than existing AS cables.

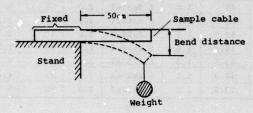


Figure 15. Flexibility test method

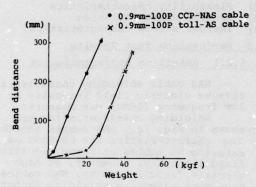


Figure 16. Flexibility characteristics

5.2.3 Bending characteristics

Cable was bent using a mandril whose radius was 6 times the cable outer diameter. Cable was bent in one direction more than 180 degrees, bent in opposite direction to more than 180 degrees, then bent back straight, in one cycle. Bending characteristics are evaluated by aluminum sheath buckings vs 180 degrees bending cycles.

Figure 17 shows the mandril used for cable bending tests and bending characteristics are shown in Table 3. All NAS cables have adequate performance for 6 180 degrees bending cycles.

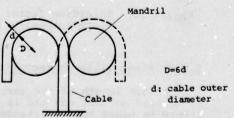


Figure 17. Cable bending test mandril

			Bending cycles			
Service and tak	Cables	1	6	8		
New	0.5mm-400P CCP-NAS cable	0	0	0		
cable	0.9-100P toll-PEF NAS cable	0	0	0		
Existing	0.5-400P local-AS cable	x	-	-		
cable	0.9-100P toll-AS cable	x	-	-		

Aluminum sheath is buclked.

5.2.4 Thermal stress Characteristics

Thermal stress was calculated by the thermal expansion of cable. Table 4 shows the thermal stress characteristics. NAS cable thermal stress is reduced to the point of a general laminated sheath cable thermal stress.

Table 4. Thermal stress

	Thermal stress (kgf/degree)	
New	0.5mm-400P CCP-NAS cable	2.8
cable	0.9mm-100P toll PFF-NAS cable	2.3
Existing	0.5mm-400P local-AS cable	7.6
cable	0.5mm-100P toll-AS cable	9.9

6. Sheath Splicing Tests

General sheath splicing methods for the plastic sheath cable become applicable to NAS cables. So, confirmation tests were made on cable sheath splicing method applicability.

6.1 Cable Sheath Splicing Method

NAS cable has the same core as the CCP cable or the toll PEF-LAP cable.

The Ready access terminal box is used in splicing for CCP-NAS cables. Figure 18 shows the cable splicing method, using ready access terminal boxes.
For toll PEF-NAS cables, the GS

taping method, involving an auxiliary lead sleeve plus Gas Stop (GS) taping, is applied. The GS taping method concept is shown in Fig. 19.

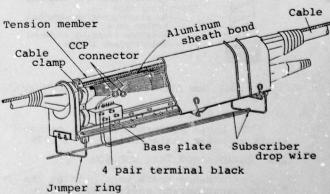
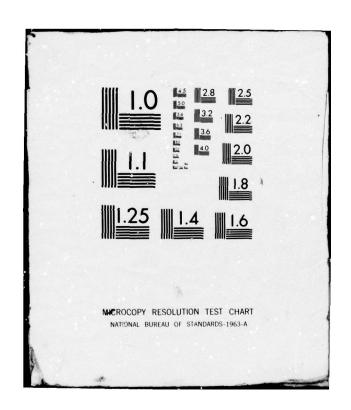


Figure 18. Ready Access Terminal Box.

ARMY COMMUNICATIONS RESEARCH AND DEVELOPMENT COMMAND -- ETC F/G 9/1 PROCEEDINGS OF THE INTERNATIONAL WIRE AND CABLE SYMPOSIUM (28TH--ETC(U) AD-A081 428 NOV 79 NL UNCLASSIFIED 3 of 5 AD-AO81428 2 4 PR. N R 7 118 R 2 III R OM



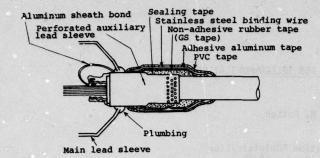


Figure 19. GS taping method

6.2 Confirmation Test

120 meter long NAS cables were installed in the high and low temperature experimental room, at Tukuba. Then, four splicing points were made at 40 meter intervals. 0.9mm-100pairs CCP-NAS cable and 0.65mm-14pairs toll PEF-NAS cable were used in this test.

Heat cycle tests (-20°C to +60°C temperature range, ten cycles) showed that there were no problems in any splice. This means that each splicing method has sufficient performance reliability for acceptable cable splicing.

7. Conclusion

NTT performed developmental research on New Aluminum. Sheath cable and examined performances for many kinds of cable characteristics. Results verified that New Aluminum Sheath cable satisfied the electromagnatic and mechanical characteristics requirements, and that the New Aluminum Sheath structure was applicable to plastic insulated conductors.

This New Aluminum Sheath cable will be extensively used in place of existing Aluminum Sheath cables in the future.

Reference

- U. Meyer; "Das magnetische Feld von Krarupdräten", E.N.T. Band I Heft 5, 1924.
- H. Otoy; "A Corrugated, Wire-Field Aluminum Sheath To Screen Telephone Cable From Inductive Interference", The 21st International Wire and Cable Symposium, 1972.
- N. Niimura; "Aluminum-Sheath Cable Used for Electromagnetic Shielding", JTR, Vol. 5, No. 1, 1963.



Yoshizi Yamazaki Nippon Telegraph and Telephone Public Corporation 1-1-6 Uchisaiwai-cho chiyoda-ku, Tokyo, Japan

Mr. Yamazaki, Staff Engineer of NTT's Engineering Bureau, is now engaged in developmental research on protection of telecommunication outside plant, cable gas pressurization monitoring system and so on.

He is a member of the Institute of Electronics and Communications Engineers of Japan.



Shojiro Masaki Tsukuba Construction Engineering Office, NTT Tsukuba-gun, Ibaraki, Japan

Mr. Masaki, Staff Engineer of NTT's Tsukuba Construction Engineering Office, is now engaged in developmental research on construction techniques for overhead telephone plant.



Tsuyoshi Ideguchi Ibaraki Electrical Communication Laboratory, NTT

Takai, Ibaraki, Japan Mr. Idequchi, Engineer of NTT's Ibaraki Electrical Communication Laboratory, is now engaged in research on telecommunication cable shielding method against external electromagnetic interference.

He is a member of the Institute of Electronics and Communications Engineers of Japan and the Institute of Electrical Engineers of Japan.

A SHOCK-ABSORBING JACKET FOR TELECOMMUNICATIONS CABLE

Harry M. Hutson

Rural Electrification Administration Washington, D. C. 20250

Abstract

For the past 25 years polyethylene has been the predominant type of overall jacket used for telephone cable. Unfortunately, this plastic jacket, unlike the previously standard lead sheath cables, insulates the shield from ground. Because of this insulative property, nearby lightning strikes can cause pinholes in the jacket which allow water to enter the cable core. In addition, high currents induced on the individual cable pairs cause shorts, opens, or damage to the electronic equipment used for carrier systems. REA has established a field trial to determine the effectiveness of using a semi-conducting jacket to eliminate these problems.

Introduction

Early buried cables employed a continuous lead sheath, in constant intimate contact with the soil, as both a moisture barrier and a protective shield against electrical surges. This provided excellent electrical protection, but the high cost of trenching it into place and the development of inexpensive, easily worked plastics caused the cable industry to turn to other designs.

Plastic jacket, paper-insulated cable which followed the lead sheath design was, at best, a compromise. Though the high dielectric strength of the jacket provided a fair amount of electrical protection, and it was much less expensive to install, surges did enter the cable. Furthermore, the low dielectric and vulnerability to moisture of the paper insulation resulted in extensive damage. To counter this situation a great deal of money was spent to design and maintain supplemental protection which limited voltages within the cable.

The next step was a plastic-jacketed and insulated design which provided acceptable

performance with the plant in use at the time of its introduction.

Today, however, we face a radically different situation. Material shortages and filled cable designs are driving the industry toward expanded insulations with dielectric strengths only one-half that of equivalent solid plastics. Also, electronics, which are highly miniaturized, such as carrier, attached to our cables are much more vulnerable to over-voltage surges than previous generations. Because of this situation, efforts are being undertaken to develop a cable design combining the shielding and protective characteristics of the lead sheath with the ease of installation and cost of modern plastic cables.

Source of Damage

Lightning, a short time high current discharge, is the most common source of damaging potentials on cable plant. Lightning is extremely variable in nature and characteristics. Bearing this in mind, the <u>typical</u> event, or flash, consists of 2-3 strokes, or periods of high current flow, separated by intervals of little or no flow spread over 0.3 second. The average initial stroke will attain a crest of 20kA; subsequent strokes will average 16kA; and the typical frontal di/dt of all strokes will be $22kA/\mu s$.

The frequency and severity of damage to be anticipated is a function of several factors, including the frequency and severity of lightning storms, the earth resistivity, and shielding obtained from local structures and terrain. Detailing the interaction of these factors is beyond the scope of this paper and is well covered in the literature.

With present cable designs, employing an insultated jacket over the conducting shield, there are several ways for lightning to cause damage:

1. The buildup of potential, resulting in dielectric failure of the jacket and arcing to the cable, causes pinholing. This is spread over a considerable distance and is created by dielectric failures and arcing from cable to soil (egress) as well as soil to cable (ingress). With respect to

ingress, the literature indicates that an arc through soil to an insulated cable may be three times as long as an arc to a cable which is in continuous conductive contact with soil. Also, the jacket of the latter cable will maintain nearly the voltage gradient of surrounding soil so that egress pinholes will not be formed.

2. Lightning currents carried on the shield induce potentials in core pairs, causing equipment failures and damage. With an insulating jacket, these currents may be "trapped" on the shield until they reach a remote ground, far removed from the original strike. Conversely, the conducting jacket permits the rapid draining of these currents as ground potential about the cable falls.

Florida Installation

In 1975, REA began work with Brand-Rex Compeny and Union Carbide to develop a telephone cable with a semi-conducting jacket for a field trial in a high lightning damage probability area. Semi-conducting compounds developed for use on buried power cables were originally considered, but they could not be extruded properly on equipment designed for telephone cables. As a result, a special compound was developed which could be extruded; it used Ketjin black in place of the more common carbon black.

A field trial site was selected along the Orange City Telephone Company's Graves to Deltona route. This central Florida location was chosen due to the area's high isoceraunic level (100 thunderstorm days per year) and the high resistivity of the sandy soil (450k - cm average for the route).

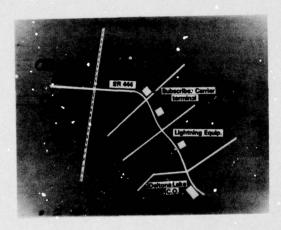


Figure 1 - Field Trial Route

Two 1.2kf lengths of 100-pair 22-gauge cable were prepared for the trial. The first, to serve as a reference, was of a standard telephone design: solid insulation, filled core, a 5-mil copper jacket, and a flooded shield to jacket interface. The second cable was of identical core and shield construction, but a 60-mil jacket of the experimental compound was placed in direct contact with the shield with no floodant over the shield.

The cables were trenched into the ground along the trial route at a 10-foot separation. Shields of both cables were bonded through normally and grounded at each end of the trial length to a driven ground. Ten pairs were selected from each cable for measurement. These conductors were electrically grouped together and isolated from the rest of the cable, other pairs, and ground at the beginning and end of the test section. At approximately the midpoint of the test section, the tunched pairs were accessed and recording voltmeters were connected between each group and shield. This configuration was maintained from September 1977 through October 1978, and data were recorded on a daily basis.

In October 1978, the configurations of the test sections were changed. The 10 measurement pairs in each cable were connected to the cable shield ground at each end of the test section. At the midpoint, the 10 tip conductors in each cable were connected to each other as were all ring conductors. The recording voltmeters were connected between these tip and ring bundles to measure metallic voltage. This configuration was retained from October 1978 through April 1979, when it was again changed.

In April 1979, a multi-channel surge recorder with improved response and capacity was obtained from Bell Telephone Laboratories. The configuration of the test section was changed and the recorder installed as in Figure 2.

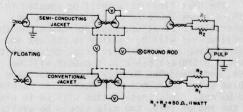


FIGURE 2 - TEST CONFIGURATION

One of the problems inherent in present designs of semi-conducting jacket material is an increase in its resistivity with age. As a result, in order to examine the potential decrease in conductivity, a dozen 18-inch samples of the semi-conducting jacketed cable were buried near the cable run with the intent of exhuming one every six months for laboratory evaluation of compound characteristics.

Results to Date

The data obtained from the recording voltmeter readings were as shown in Figures 3 through 8. Figures 3-5 are for the original configuration, while 6-8 reflect that in place after October 1978. Based on these data, it would appear that the semi-conducting jacket has a favorable impact on the reduction of surge voltages in paired communications cables.

In order to monitor the resistivity of the semi-conducting jacket, samples were exhumed and analyzed by the laboratories at Union Carbide, with the results shown in Figure 9. The nearly sevenfold increase in resistivity experienced in this cable would indicate that more effort needs to be made to obtain a stable compound. There has been a continuing effort by Union Carbide and others to develop a stable compound. In spite of this, the reduction of voltages on the semi-conducting jacketed cable indicates that the potential exists for improving electrical protection.

Future Trials

In view of the results obtained at the Orange City Telephone Company field trial, REA is planning a second trial in an effort to obtain an even more stable compound and to determine further the usefulness of this concept. The Orange City trial has not been abandoned, and we will continue to accumulate data which will be incorporated into a future report.

The next field trial will be located in the Nathans Creek Exchange of Skyline Telephone Membership Corporation, West Jefferson, North Carolina. It will be similar in concept and organization to the earlier trial except that several different cable pair counts will be used, and Brand-Rex Company will produce the cables using compounds from both Union Carbide and DuPont. This installation will be in place by the end of 1979, and data should be available beginning shortly thereafter.

Conclusions

Based on the Orange City trial, it would appear that semi-conducting jacketed telephone cable may have a place in the telephone industry in reducing lightning damage. Further work is required, however, to develop a suitable material for this use which will not degrade with time. Also, a cost/benefit evaluation of the final compound will be required to determine how widely

it should be employed throughout the country.

References

Lightning, Edited by R. H. Golde, Academic Press 1977

Earth Conduction Effects in Transmission Systems, by E. D. Sunde, Van Nostrand Co., 1949

The Protection of Telecommunications Lines and Equipment Against Lightning Discharges, CCITT, Published by ITU, 1974/78

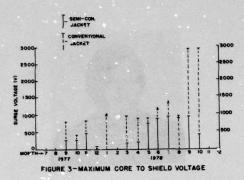
"Striking Back at Lightning", Kahelnews, Spring 79, Union Carbide Corporation

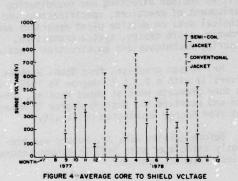
Lightning Protection of Buried Cable by Semi-Conducting Jackets, by H. D. Campbell, 14th Wire & Cable Symposium, 1965

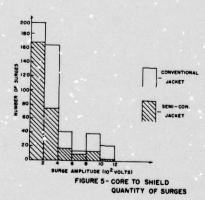
Conductive Coatings and Power Cable, by W. F. Jensen, Jr., RETEC of Soc. of Plastics Engrs., Toronto, 1976

Galvanic Behavior of Underground Cable Neutral Wires & Jacketing Material, by O. W. Zastrow, Materials Performance Vol. 16, No. 11, 1977

A Ground-Lightning Environment for Engineering Usage, by N. Cianos & E. T. Pierce, SRI Project 1834, August 1972







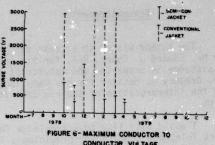
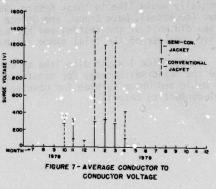
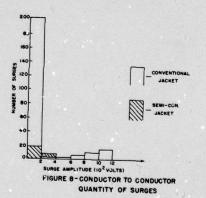


FIGURE 6- MAXIMUM CONDUCTOR TO CONDUCTOR VULTAGE





	BURIED CABLE	LABORATORY SAMPLE
INITIAL	1 A - cm	1k A - cm
'o mths.	425 A - cm	25t A - cm
te mths.	425 A - cm	-
24 mths.	_ "	_

FIGURE 9 - VOLUME RESISTIVITY ALONG CABLE LENGTH (0125°C)

Leading Market Commencer

<u>Acknowledgments</u>

The author wishes to express his gratitude to Mr. Edward J. Cohen, REA, for his indispensable assistance in preparing the manuscript and Mr. Gregory J. Hessler for his many long hours in the interpretation of the raw data into usable form.

I would also like to acknowledge The Winter Park Telephone Company for providing a location at its Orange City Telephone Company and its many engineers who gave me valuable assistance. I especially would like to thank Messrs. George W. Brown (deceased), Dave Brown, and George D. Nilsen did most of the testing and has been an active overseer of the trial since its beginning.

In addition I would also like to acknowledge the Brand-Rex Company for manufacturing the cable and Union Carbide for developing the semi-conducting material.



Harry M. Hutson is presently the Chief of the Outside Plant Branch of REA's Telephone Operations and Standards Division. His responsibilities include directing and coordinating development of practices, specifications and technical data on outside plant apparatus and hardware, cable design, system protection, measuring techniques and construction practices.

Mr. Hutson graduated from Johns Hopkins University with a B.S.E.E. degree in 1970. He has done graduate work at Johns Hopkins, Georgia Tech and received his Masters Degree in Management from George Washington University.

Before joining REA, Mr. Hutson was previously associated with Bell Telephone Laboratories, Atlanta, Georgia.

MODULAR UNIT DESIGN PULP CABLE

by

J.-P. Waucheul

R.L. Beauchamp

Northern Telecom Canada Limited Montreal, Quebec

ABSTRACT

Telecommunication companies, in general, have standardized on commercially-available 25-pair splicing modules for their outside plant cables. Operating economies are realized by utilizing the same 25-pair groups throughout the cable run.

This concept is easy to apply to PIC with its basic buildup of readily identifiable 25-pair units. Extension to existing pulp cables posed a problem because of the basic 50- and 100-pair unit construction.

Various design options have been proposed and implemented by the cable industry. Our approach, applicable to 22 AWG cables used for carrier transmission as well as the standard 24 and 26 AWG cables, is a new colour code scheme which retains all the advantages of regular pulp, with the added capability of modular splicing.

INTRODUCTION

Modular splicing systems have gained wide acceptance for cable installation. The connectors used accommodate 25 pairs and these pairs are identified throughout the cable run for ease of plant administration. To fully utilize this concept, it is essential that the cable construction permits easy identification of specific 25-pair groups.

Pulp cables are assembled using 50or 100-pair units with an overall binder. Modifications were required in the design to provide the modular capability.

STANDARD PULP CABLE DESIGN

In a cable three unit colours are used for position identification. Green, red or blue pairs form the outer layer of the respective units as shown in Table I.

There are nine basic twist lengths. This permits the use of different twists for adjacent pairs, alternate pairs, adjacent layers and alternate layers to provide good transmission properties. Indi-

vidual cotton binders provide the AWG identification, i.e. 26 AWG orange, 24 AWG red and 22 AWG white.

A multi unit cable is made up of one or more layers of units with spare pairs in the interstices. In the assembly of units into a cable, each layer contains one green unit flanked by alternating red and blue units. This provides a mirror image for identification of each unit position within the cable core, regardless of the direction of pull during installation. (Fig. 1).

LAYER OF PAIRS	PAIR COLOURS 100-PAIR UNIT	NO. OF PAIRS
Centre	Blue	3
1st Layer	Red	9
2nd	Green	15
3rd	Blue	21
4th	Red	24
5th	Green	28

TABLE I GREEN UNIT BUILDUP FOR STANDARD PULP

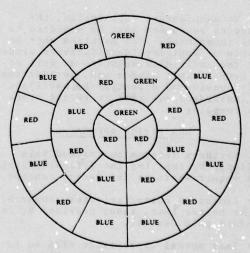


FIG.1 CORE BUILDUP FOR STANDARD PULP

These cables are randomly spliced within the individual units. Group identity is maintained throughout the cable run but is restricted to either 50 or 100 pairs. Thus, the advantages of using the 25-pair modular splicing technique for plant administration cannot be realized.

MULTIPLE UNIT PULP CABLES

It is possible, for example, to divide a 100-pair unit into four 25-pair subunits individually bound, or to divide a 50-pair unit into two 12- and two 13-pair subunits individually bound to provide 25-pair groups. Fig. 2.

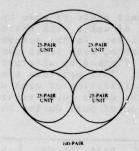


FIG.2 MULTIPLE UNIT PULP

One limitation inherent in this design is that the 100-pair and 50-pair units are larger than those of the standard design, resulting in a decrease in the maximum number of pairs which can be accommodated in a 3.5-inch or 4.0-inch cable duct system.

Also, in order to improve within unit crosstalk performance, a more complex system of twist lengths and pair spacing would be required (Reference 1).

To manufacture this design, the stranding equipment must be modified to be multi-functional. The machines must be capable of applying identification binders over the individual subunits as well as the overall unit binder and, in addition, it is considered essential to oscillate the individual subunits to reduce crosstalk coupling.

NEW DESIGN APPROACH

Northern Telecom approached this challenge by imposing the following stringent requirements on the design concept.

- Crosstalk characteristics comparable to, or better than, those provided by the standard pulp design.
- Same mutual capacitance with no increase in cable diameter for a given number of pairs.

- Easy separation of the four subgroups in the 100-pair unit or the two subgroups in the 50-pair unit.
- A design that is compatible with the existing colour code when old and new cables are spliced in the field; that is, it must be suitable for both modular and random splicing.
- The use of the standard colour code scheme for unit position and gauge identification.
- A design that requires no major changes in processing equipment while keeping the number of twist lengths to a minimum for inventory purposes.

COLOUR COORDINATED PULP CABLE

The construction of a 100-pair unit is shown in Fig. 3 and Table II (Reference 2).

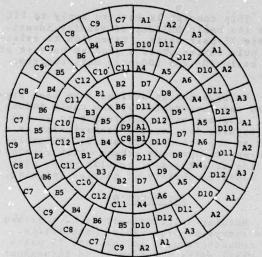


FIG.3 100-PAIR UNIT 24 AWG COLOUR COORDINATED DESIGN

Four 25-pair subgroups identified by the four-pair colours, red, orange, blue and green are used. Each layer is divided into two-pair colours in such a way that one half of the 100-pair unit contains two 25-pair groups. It will be noted that the unit lay-up provides for good separation of like pair twists and compares favourably with the conventional design. Six pair twists are used for each colour group, the individual pair twist being identified by a marking on the white wire of each pair. This marking is provided for identification during manufacture only and does not form part of the colour code. The twist scheme used for red and orange pairs is repeated for green and blue pairs, thus retaining a minimum of twist types.

Ring Condr.	Tip Condr.	Pair No.	Ring Condr.	Tip Condr.	Pair No.	Twist Type No.
Red	W/Bk	A1	Orange	W/Bk	B1	1
Red	W/O	A2	Orange	W/0	B2	2
Red	W	A3	Orange	W	B3	3
Red	W/R	A4	Orange	W/R	B4	4
Red	W/B	A5	Orange	W/B	B5	5
Red	W/G	A6	Orange	W/G	В6	6
Green	W/Bk	C7	Blue	W/Bk	D7	7
Green	W/0	C8	Blue	W/0	D8	8
Green	W	C9	Blue	W	D9	9
Green	W/R	C10	Blue	W/R	D10	10
Green	W/B	C11	Blue	W/B	D11	11
Green	W/G	C12	Blue	W/G	D12	12

Dash markings on white (W) condr. indicated as follows: /Bk - Black; /R - Red; /G - Green; /O - Orange; /B - Blue.

TABLE II PAIR TWIST SEQUENCE COLOUR COORDINATED DESIGN

A similar arrangement can be used for a 50-pair unit, in this case using only two-pair colours, say, green and orange for 22 AWG.

Gauge Identification

The colour of the outer layer of pairs in the unit are designed to provide the conductor AWG, as illustrated in Table III.

GAUGE	100-PAIR AND 50-PAIR UNITS
#26 AWG	Orange/Blue
#24 AWG	Red/Green
#22 AWG	Green/Orange

TABLE III GAUGE IDENTIFICATION

Mirror Identification

For a given gauge, all units are alike and the unit colours are obtained by overail cotton binders of green, red or blue. The use of these binder colours provides a mirror image and permits identification of each unit position within the multi-unit buildup of the cable as in the older cable designs.

TRANSMISSION CMARACTERISTICS

In the new design, the primary consideration was to maintain, or improve upon, the transmission characteristics of

the superseded regular pulp insulated cables. More specifically, the individual pair twist and pair positions within the unit were carefully chosen to optimize its crosstalk performance when used for digital transmission.

At the present time, large size 22 AWG pulp insulated pables are widely used for digital transmission in the trunk portion of the telephone network. Overall traffic demand determines the portion of the 50-pair units in the outer layer of cable that are assigned for digital transmission systems, such as T1-Carrier. Several lengths of cable are joined together to make up a standard 6000-foot repeater section. The controlling parameters affecting digital transmission are

- 1) Pair attenuation per repeater section.
- Near-end crosstalk coupling between pairs in opposite direction of transmission.
- Far-end crosstalk coupling between pairs in the same direction of transmission.

The pair attenuation of the new cable at carrier frequencies is equivalent to that of regular pulp insulated cable, as the basic pair design remains unchanged. Therefore, the same repeater spacings are preserved. In addition, as with regular pulp cables, the effects of Near-end crosstalk couplings are minimized by selecting non-adjacent units for opposite directions of transmission. This means that the within unit Far-end crosstalk couplings become the dominant interference source.

Cravis and Crater (Reference 3) have developed Far-end crosstalk requirements for the T1-Carrier system. These are presented in Fig. 4. The ELFEXT requirements in a repeater section are a function of the number of systems in the cable (n) and the standard deviation of the crosstalk distribution (σ). For n = 50, as versus 25, there is a 3 dB/octave increase in the system requirements for T1 operation.

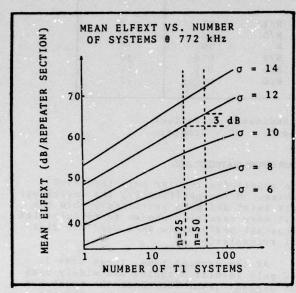


FIG. 4 FAR END CROSSTALK REQUIREMENTS FOR T1
CARRIER SYS (EM

Within unit Far-end crosstalk couplings have been measured on a number of modular unit and regular unit pulp cables. The average results for 50-pair, 22 gauge units are presented in Table IV. The overall crosstalk performance for the old and new designs are virtually identical. Compared with the system requirements, a 3 dB margin is provided.

E	LFEXT - 772	kHz dB/1000	ft.
	MODULAR CABLE	REGULAR CABLE	REQUIREMENT
Avg. (μ)	79.0	78.4	75.4
Std. Dev. (o)	12.6	12.5	12.5
1% worse than (1% wt.)	52.2	52.3	Large of the S

TABLE IV FAR END CROSSTALK RESULTS WITHIN 50-PAIR, 22 AWG UNITS

Although the above results would indicate that the crosstalk performance of the two cables are equivalent on a one-to-one basis, such a comparison is misleading as it does not consider the effect of modular splicing into 25-pair subgroups. From our analysis it was shown that, depending on the grouping of these 25 pairs within a unit, a significant crosstalk degradation can occur in a repeater section.

Figure 5 illustrates three possible groupings of 25 pairs within a unit. The ELFEXT crosstalk performance within each 25-pair group was measured and compared to the overall unit average. Results are presented in Table V.

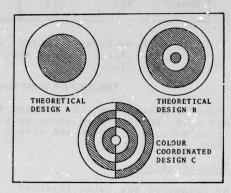


FIG.5 POSSIBLE GROUPINGS OF 25 PAIRS
WITHIN A 50-PAIR UNIT

	A			В	С	
	ŭ.	σ	μ	σ	ц	σ
Subgroup 1	72	11.5	74.8	11.8	77.8	11.3
Subgroup 2	81.6	14.1	80.2	12.8	79.2	12.4
Between sub- groups 1 and 2	70.9	11.5	79.2	12.8	79.9	13.2
Overall 50- pair unit for comparison	78.4	12.5	78.4	12.5	79.0	12.6

TABLE V FAR END CROSSTALK RESULTS WITHIN 25-PAIR GROUPS

For the concentric grouping of pairs in design A, there is about 10 dD difference in average crosstalk between the two 25-pair groups. The results for the centre 25 pairs are typical of crosstalk performance for individually bound 25-pair units. By comparison, for the optimum grouping of pairs in design C, the average crosstalk behaviour within each 25-pair group and within the overall unit are approximately equal. This means that no degradation in

crosstalk performance is experienced when utilizing modular splicing techniques as compared to the normal practice of random splicing within 50-pair units.

The significant difference between the various designs of Fig. 5 is in the arrangement of pairs within the unit. A detailed analysis of measurement data has established a strong correlation between the average pair separation and the average crosstalk for any grouping of 25 pairs. These results are plotted in Fig. 6.

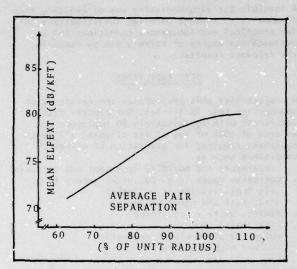


FIG 6 CROSSTALK VS. AVERAGE PAIR SEPARATION

CONCLUSIONS

Traditional practices of random splicing 50- and 100-pair units are beneficial in maintaining within unit ELFEXT crosstalk couplings in a repeater section at an acceptable system level. In order to provide this benefit for a modular splicing system, the lay-up of pairs within each of the 25-pair groups of modular unit pulp is arranged so as to meet the design constraints of overall size, transmission parameters and minimum in process inventory. Such an optimization is achieved by the colour coordinated design.

ACKNOWLEDGEMENTS

The authors wish to recognize the significant contribution made to this study by D.W. Taylor, co-inventor of the U.S. Patent - Reference 2 - previously with Northern Telecom. Also, P. Kish and Y. Le Borgne for their work in establishing the final design and the analysis of the transmission characteristics.

References

- (1) R.J. Oakley and R. Jaar, "A Study into Paired Cable Crosstalk", IWCS, Nov. 1973.
- (2) U.S. Patent 4 158 746, J.-P. Waucheul and D.W. Taylor, "Cable with Colour Coding Identification of Group", June 1979.
- (3) H. Cravis and T.V. Crater, "Engineering of Tl-Carrier System Repeatered Lines", Bell System Tech. J. March 1963.



Jean-Pierre Waucheul is Manager of Cable Materials, Research and Development, Cable Division, Northern Telecom Canada Limited. He worked three years for the "Cablerie de la Seine" in France before he joined the Design Department of Northern Telecom in 1976. He received a "Diplome d'Ingenieur Electricien" from L'Ecole d'Electricite et de Mecanique de Paris in 1972 and one from L'Ecole Nationale Superieure d'Electricite de Toulouse, section Electrotechnique in 1973.



Robert L. Beauchamp is Manager of Cable Development, Research and Development for Communications Cable. His 18 years' wire and cable experience have all been with Northern Telecom, except for two years with Bell-Northern Research. He received his B.A.Sc. degree in physics from the University of British Columbia in 1961

CORRELATION BETWEEN LABORATORY TESTS AND TEST SITE RESULTS OF TELECOMMUNICATION CABLES, SPLICES AND CLOSURES

by Georg Boscher and Wolfgang Giebel

SIEMENS AG, München

ABSTRACT

Laboratory investigations are correlated with test site results gained under real environmental conditions. For example:

- deviation of mutual capacitance of filled cables es buried versus identical cables stored at elevated temperatures;
- contact quality of splice connectors stored in closures under open air conditions and buried versus storage in temperature cycling;
- water vapor permeation of closures versus theoretical evaluations with data from short-term laboratory measurements;
- endurance tests concerning closure tightness in different climates;
- corrosion investigations of closures exposed to all possibly occurring media and measuring mechanical properties.

The results obtained are integrated into our specifications, representing generally acceptable criteria, although considering constructive and design-specific modifications.

INTRODUCTION

Although te:ecommunication cable networks represent a substantial value, operating and running costs of all components are required to be low. This goal can be reached by using appropriately and comprehensively tested components combined with simple installation techniques, by high quality standards, etc. in short, by a long maintenance-free life-time. As telecommunication cable networks have to cope with a multitude of environmental conditions a variety of adequate laboratory tests must be carried out prior to installation, in order to gain sufficiently exact predictions of operational reliability.

It is exactly here that the crucial point is reached: Climatic, mechanical and corrosive loads act simultaneously and their influence on the cable plant is known only inadequately, or not at all. Laboratory simulation frequently represents the behavior of samples under individual loads. Necessary test acceleration, artificial ageing and intensifying of test conditions lead to often highly inaccurate extrapolations.

A feasible but time-consuming way of avoiding this dilemma is to arrange parallel investigations under practical and laboratory conditions and to evaluate the degree of correlation by comparing the relevant results.

TEST FACILITIES

A project like this presupposes the existence of appropriate test facilities. Our central test department with approximately 80 employees on an area of 4000 m 2 has at its disposal all test equipment required for simulation of climatic conditions such as

- . temperature and humidity (constant and variable)
- . corrosive gases (e.g. \$02, H2S) vapors (e.g. salt fog), liquids (e.g. lgepal)
- . sand, dust and other pollution
- . dewing, white frost, icing
- . rain, hail, snow
- . solar and ultra-violet radiation
- . low and high pressure

and also for simulation of mechanical stresses, such as

- . vibration (harmonic and random)
- . shock
- . tensile forces (push, pull, torsion)
- . bending forces
- . impact
- . transportation
- . drop test

and of course all equipment necessary for measurement of the samples' properties.

Test site "Buchloe" is situated some 70 k:lometers south-west of München. There, on an area of approximately 50,000 m², installations of aerial, buried and underground or conduit cable plants can be realized. In aerial cable plants pole distance, height and tensile forces can be selected appropriately. Special arrangements permit manholes in buried or conduit networks to be flooded and accessories to be stored in water containers. Environmental conditions and operational behavior of samples are recorded by computer control, providing fast access to clearly arranged test results.

RESULTS

It is now approximately ten years ago since we first started projects investigating the correlation between laboratory tests and test site re-

Not the second second

sults. In the following we present a selection of the results obtained, knowing that it is far from complete. It would be beyond the scope of this presentation to deal with the great number of incividual results.

CABLE

In April 1974 we initiated the installation of a cable plant involving a total number of 15 cable loops, each 75 m long, containing 70 and 100 pairs respectively of AWG 26 and 22, buried at a depth of 80 cm. The installed cables were petrojelly-filled, with PE-insulated conductors and bonded aluminum-Pt cable sheath. Some of the cable loops were prepared with sheath damage and stored in the ground and in 1 m of water respectively.

The main purpose of this project was to study long-term protection of the conductors by the petro-je'ly in the case of cable sheath damage. We therefore supervized mutual capacitance, insulation resistance, and loss angle, and watched water ingress with the aid of Time Domain Reflectometer (TDR).

As one result, the three diagrams of fig. 1 show the measured relative deviation in percent of the mutual capacitance over a test period of five years.

It can be seen that over the observed period

- . the deviation of mutual capacitance is small
- . the mutual capacitance decreases with time
- the rate of decrease is influenced by the kind of filling compound
- mutual capacitance of units in the center of the cable core decreases more rapidly than of units in the outer layers and
- . smaller wire diameters show a faster response

Also in 1974, identical cables were stored in climate chambers at RT and at elevated temperatures such as 40°C, 55°C, 70°C and 80°C. The three diagrams of fig. 2 correspond to the diagrams in fig. 1. Here, in this accelerated procedure (elevated temperatures), some phenomena become clear:

The mutual capacitance as a function of time travels through a minimum. The decrease at the beginning is caused by swelling of the PE conductor insulation in the filling compound. The following increase is due to compound adsorption and absorption. These processes are accelerated by temperature. At temperatures exceeding 70°C the filling compound starts to melt, thus penetrating fast. Due to the higher compound surplus in the core center, units there are affected to a higher degree than in the outer layers.

There are good reasons to suppose that these processes act in a qualitatively uniform manner, but accelerated by higher activating energies, that is, higher temperatures. If we then feed all empirical data into a computer and take into consideration geometrical and material-specific properties, a fairly good half-logarithmic dependence is obtained. It indicates that for the change in mutual

capacitance an accelerating factor of 2.0 for each 10°C - increase in storage temperature is yielded (see fig. 3).

In other words, the behavior of mutual capacitance for a buried cable of the described type in its lifetime e.g. of 30 years is simulated by storing a suitable cable sample in $60^{\circ}\mathrm{C}$ over some 60 days.

SPLICE CONNECTORS

In 1971 we started an investigation concerning the splice connector AVH (=Aderverbindungshülse) which is the German version of the well-known B-wire-connector. The main interest lay in an accelerated procedure for predicting functional reliability. Besides this, we tested the function by varying conductor and insulation size and also material.

A total number of 5000 samples, in lots of 50 and 100, were subjected for weeks to elevated temperatures of 30°C, 50°C, 70°C and 90°C, and to temperature cycling. We also mounted 200 samples in closures and stored these closures under ground as well as under open air conditions over a period of eight years up to now. From over 60,000 single values the following diagram (fig. 4) shows the results of a particular sample combination having AWG 26 and PE insulation. In this diagram the mean value of change in contact resistance is plotted versus test time for various loads. All lots tested at constant temperatures, and even the samples in closures underground and under open air conditions, react qualitatively in the same way.

The diagram shows clearly that the process of natural ageing of samples inside closures under open air conditions is simulated by the laboratory test at 70°C. Because the average temperature 1 m under-ground in moderate climates (e.g. in Germany) is approximately 10°C, the results of the 30°C-test exceed those of buried samples. A test temperature of 90°C creates loose connections due to the kind of connectors and the results are therefore useless.

Storage of samples at elevated temperatures did not show the expected time-saving effect. We therefore started temperature cycling with various cycle durations, different temperature limits. We found out that temperature cycling represents a combination of deteriorating contact influences like micro-movements, growth of corrosive films, decreasing contact pressure and material degradation. Cycling conditions were finally fixed at -40°C ... +60°C according to the functional range of the connectors and to the maximum daily and scasonal temperature range. Cycling duration was set at eight hours.

The use of a frequency distribution diagram to examine contact reliability reveals that initially linear (Gaussian) distributions change into mixed distributions in the course of time. This is

caused by the fact that inherently inferior contacts deteriorate more severely than contacts that are good at the beginning. This becomes evident in the case of samples in closures that are buried or under open air conditions (fig. 5 and fig. 6)

Obviously it also appears under temperature cycling (fig. 7), but greatly accelerated. In order to compare the increase in contact resistance achieved by temperature cycling with that of natural ageing, we observed in particular all rapidly deteriorating values of the frequency distribution, practically forming a second branch of this curve. Correlating the standardized slopes of the temperature cycling with those obtained from buried and open air testing, we found relationship of life-time to number of temperature cycles as shown in fig. 8.

As expected, one temperature cycle simulates a load exceeding one year's storage in buried application, while representing considerably less than one year in open air conditions. This result has been verified for various applications of this particular contact system. We are presently investigating the extent to which these results are valid for other systems.

PERMEATION

Permeation in general is the ability of liquids and vapors to penetrate through solid materials. In the case of high water vapor permeation within a splice closure, mutual capacitance, insulation resistance and loss angle might be affected to an unacceptable degree. The selection of a plastic material with low permeation coefficient is therefore a decisive factor in closure development.

At the 1973 Cable and Wire Symposium in Atlantic City Siemens presented a paper (1) dealing with the theoretical evaluation of water vapor permetation. It was now of interest for us to see how these theoretical evaluations correlate with the values measured in practical application.

In 1970 we established another closure project in Buchloe with a total number of 45 closures under different conditions. All closures were without drying agent but with humidity sensors. Humidity was recorded in suitable intervals over a period of new eight years. The examples shown are closures in the ground and in 1 m of water with and without additional paper insulated cables.

The conclusions obtained from the diagrams No. 9, 10, 11, 12 are:

- Relative humidity in closures stored in the ground and in water behaves in the same way. The assumption of an outside relative humidity in the ground of 100 % is therefore correct (fig. 9)
- . The drying effect of the insulation paper is virtually as predicted (fig. 10)
- . The changes of relative humidity due to seasondependent temperature changes of +10°C are less

than +5 % r. H.

Theoretical evalutions and measured values correlate sufficiently after revising the formula in accordance with the empirically measured data (fig. 11 and fig. 12)

That means, that the formula in the above mentioned paper, with its correction, permits a good long-term prediction of relative humidity inside a closure if the initial conditions are known. Alternatively, the formula permits calculation of the proper amount of drying agent to limit the rate of relative humidity inside the closures.

ENDURANCE TESTS

Closures in gas pressure supervised systems are required to be tight and stay tight during application time. To prove the latter requirement we subjected closures to an endurance test with different temperatures and climates as well as with temperature cycling. In this test the closures in the various environments are loaded with graded pressures and the time to failure is recorded.

These pressure/time pairs are plotted on a doublelogarithmic form. Depending on the pressure grading, and considering the statistical distribution of failures this procedure permits long-term predictions for a certain failure probability.

During the development of the Universal Closure (UC) we tested not less than one thousand closures of different sizes, types (branch, tip, connection), mounting conditions etc. and fed the results together with up to 15 parameters of each closure into a computer. The next diagram shrws some of the results. To obtain a general view of the major facts, the single values are omitted (Fig. 13).

To interpret the results, it can be seen that . duration of tightness decreases with increasing temperature and that

nearly identical curves for 40°C/50 % r. H. and for 40°C/92 % r. H. show the influence of humidity on tightness to be negligible.

According to these results it becomes clear that we have not yet observed any leaks since we built an aerial cable plant in 1978 involving UC-Closures. When pressurized at 10 psig (\$\hat{\text{\text{a}}}\$ 1.7 bar) failures of closures under open air conditions are not yet to be expected. For builed and underground application life expectancy is (due to the lower temperature) approximately 50 years with 10 psig pressure supervision.

It has so far not been possible to integrate the time-consuming temperature cycling process in our results. We hope to submit these results in time for the oral presentation.

CORROSION

In every application closures have to cope with corrosion attacks. In aerial networks mainly

solar radiation combined with atmospherical characteristics (coastal or industrial areas,...) and extreme temperatures and temperature changes might affect closure reliability. Buried closures may be situated in acidic or alkaline, in household or industrial polluted soils, or in the vicinity of DC-driven trains or high-voltage cables causing stray currents.

Manholes within underground systems can be flooded with brack or salt water, NH₃- or any other polluted water.

Corrosion investigations are complicated by a lack of generally valid test criteria. Furthermore, closures are made of different materials having a varying response to corrosion.

However, to determine the functional reliability of closures under practical corrosion attacks it is sufficient to investigate the degree of corrosion stability of each part of the closure exposed to all possibly occurring media under obviously exaggerated conditions. (2)

For this, specimens of the polypropylene-ethylene-copolymer of the outer shell were exposed for a period of two years to the open air and sunshine in the desert climate of Arizona with the result that no deviation could be detected; also the ductility properties remained constant.

Of course tensile strength and elongation of specimens at various temperatures versus time were measured (fig. 14). The results including permeation rate and stress cracking resistance lead to the assumption that the plastic material is suitable for the required lifetime.

The sealing material was entirely tested in 1969.

Resistivity to sun radiation, proper adhesive behavior at high and low temperatures even in pressurized systems, compatibility with the cable- and closure components, and resistivity to soil acids and fungi and microorganisms were proven.

More than 100,000 screw-clamping closures using this sealing material mounted in 1970,and even more in the following years up to 1979 mainly in buried and underground application, prove also the functionability of the sealing material.

Stainless steel parts may be attacked under severe conditions. Provisions are made that even holes occurring in the metal parts do not disturb functionability. But holes could not be observed after a two years submersion in salt water, while the samples were exposed to air at least every 14 days for a weekend.

Beyond that, mounted closures were stored in . pH₃-, pH₁₀-, NH₃-solution, all at 40°C with intermediate exposure to air every three weeks . diesel fuel and gasoline at RT

- . salt water, surface active liquid (Igepal 10 %, $50^{\circ}\mathrm{C}$)
- . salt fog, S0 $_{2}-$ and C0 $_{2}-$ treatment in humid environment at $35\,^{\circ}\mathrm{C}$
- . solar and xenon radiation over 5000 h
- . cable filling compound
- open-air conditions (storage on a roof and at our test site Buchloe)

As some of the tests have now been running for more than 18 months (pH₂, pH₁₀, NH₂) without any leakage we are endeavouring to correlate the tests and actual life-time under normal and exaggerated conditions.

CONCLUSION

System resemblance of the components of tele-communication cable accessories permit analogue test procedures. On the other hand, the variation in material, type, size and application of these components calls for differentiated, design-specific tests. According to our findings, long-term predictions of e.g. contact quality, permeation, tightness and corrosion stubility only need a relatively short laboratory investigation. We therefore inserted those short-time tests into the adequate specifications. Taking into consideration constructive and application-specific characteristics, these specifications have become generally accepted. (3)

LITERATURE

- (1) D. Kunze, G. Boscher: Water vapor sorption of PE - a decisive factor for the operation behavior of PE - telecom. cable networks. Proceedings of the 22nd Wire and Cable Symposium Atlantic City, 1973
- (2) W. Giebel: Plastic closures and their metal components exposed to the open air, various soils and salt water Paper nr. 72, NACE, 1979
- (3) Siemens:
 Product specification for Universal Closures
 S 45050 T7009 P461

Georg Boscher received his Dipl. Phys. degree from the University of Munich in 1967. He started with Siemens at the Central Test Department, joined the Telecommunication Cable Division in 1971 and is now Department Manager for testing within the development area.

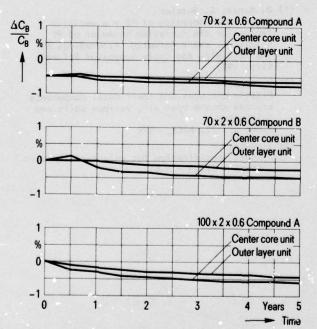
Siemens AG
NK E 32
Postfach 700 07 45
D-80C0 München 70

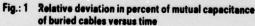
Wolfgang Giebel joined Siemens in 1964 after receiving an Engineer's degree from the Munich Polytechnic. After three years in the cable measuring department he became head of a laboratory responsible for development of telecommunication cable accessories. In 1978 he was put in charge of marketing and sales of telecommunication cable accessories. Siemens AG NK V 81 Postfach 700 07 45

D-8000 München 70









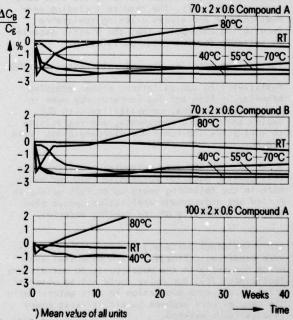


Fig.: 2 Relative deviation in percent of mutual capacitance ") of cables stored at elevated temperatures versus time

Street, Was Street, Street, Street, Street, St. of

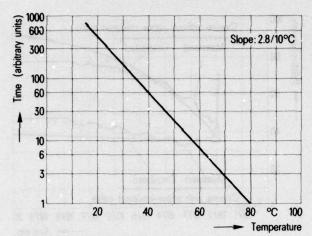


Fig.: 3 Relation between storage temperature and storage time for equivalent change in mutual capacitance

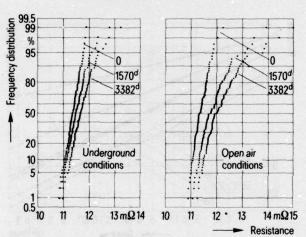


Fig.: 5 Frequency distribution of contact resistance after 0, and 6 1570 and 3382 days storage

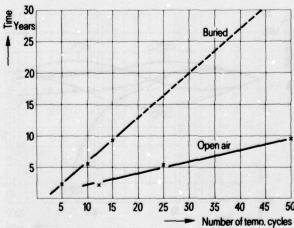


Fig.: 8 Relation of life-time to number of temperature cycles

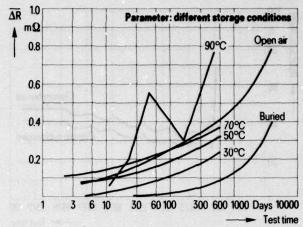


Fig.: 4 Mean value of contact resistance change versus test time

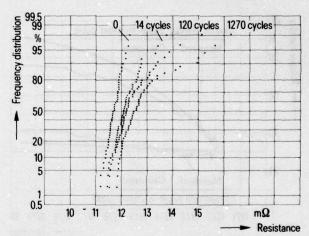


Fig.: 7 Frequency distribution of contact resistance after 0, 14, 120 and 1270 temperature cycles –40 °C ... + 60 °C/8h

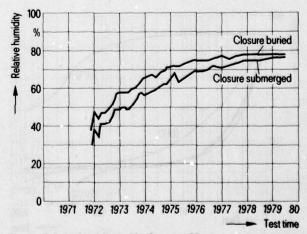


Fig.: 9 Relative humidity inside closures without paper-insulated cables versus test time

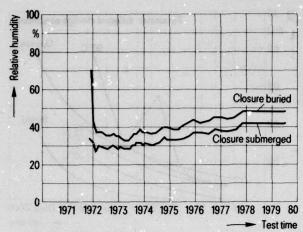


Fig.: 10 Relative humidity inside closures with paper-insulated cables versus test time

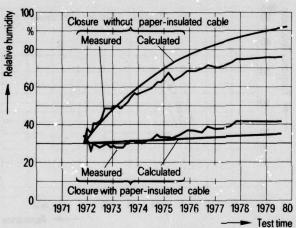


Fig.: 12 Relative humidity inside submorged closures with and without paper-insulated cables versus test time

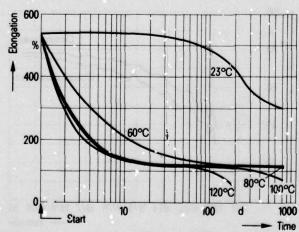


Fig.: 14 Results of tensile tests with Flostalen PP at different temperatures

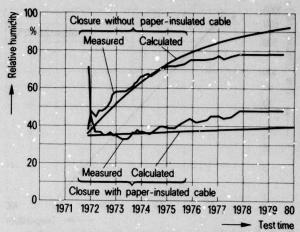


Fig.: 11 Relative humidity inside buried closures with and without paper-insulated cables versus test time

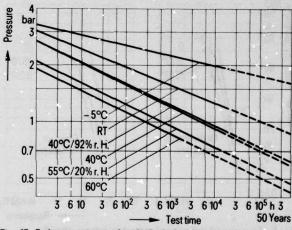
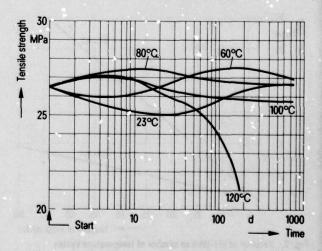


Fig.: 13 Endurance test results of UC-closures parameter: different test conditions



MODERN CONSTRUCTION METHODS TO COMBAT THE RISING IN-PLACE COSTS OF UNDERGROUND CABLES

T.M. Kochansky, P.E.

GTZ Service Corporation Stamford, Connecticut

ABSTRACT

Telephone companies have experienced a constant rise in the in-place costs of cable. Presently in GTE, the ratio of labor and material costs is approaching 65 percent and 35 percent respectively. This is an almost complete reversal of about 20 years ago. Since the operating company can do little or nothing to control the material cost, it must seek to control the in-place costs by reducing the labor cost component. Two methods can be employed to achieve this control for underground cables; these methods are: long cable pulls and preconnectorized cable plant. Long cable pulls entail extending cable nulling lengths beyond the traditional pulling lengths in order to reduce one or more splices. Preconnectorized cable plant (PRE-CON) pertains to factory connectorization of cable ends with 25 pair connector modules for the reduction of field splicing effort. A significant reduction in splicing cost can be achieved through the proper use of both concepts. This, however, requires careful planning and close coordination between the construction and engineering groups.

INTRODUCTION

The design of underground cable systems is dependent upon the design of the related conduit systems. The conduit network consists of duct runs some of which arc 70 or more years old. Several factors contributed to the designs of the past conduit systems; these are:

- 1. the "city street geometry";
- 2. cable reel lengths; and
- 3. branch cable and stubbing designs.

As a result, it was normal for a splice to occur at every manhole, and an average spacing would probably be somewhere around 400 to 500 feet between splices.

For many years, this was accepted as a normal situation without much consideration although newer conduit systems were being designed with longer section lengths, normally in the order of about 700 to 750 feet. Reel lengths for full size stalpeth cables are usually 800 feet. This seemed to point out that the procedure would be to design newer conduit sections to "reel length"

runs. Where possible, in older runs, more than one section would be pulled to eliminate a splice. Many times however, such a pull would be "too long" for a standard reel length and so two shorter reel lengths would be used. Today, cable can be ordered on oversize reels which somewhat reduces this problem.

As the installed cost of underground cable began to rise, Telcos became more interested in reducing splicing time. "Pull throughs" became more common and with the introduction of modular splicing, preconnectorized cable ends became possible. Both were directed at reducing the total splicing time required when installing new cables.

Today, the proper use of long cable pulls and preconnectorized cables can allow the Telco to achieve considerable cost reductions over more conventional methods.

LONG CABLE PULLS

Within the past few years, there have been a few good articles written about long cable pulls. 3.2.3 Some of what has been included in those articles will be reviewed here but only to assure continuity.

The term "long pull" implies a pull of longer than traditional pulling length and therefore could be considered as being more than a standard reel length of cable and involving one or more pull-through manholes.

There are three general areas for consideration in making long pulls; these are: conduit considerations, reel length considerations, and tension considerations.

Conduit Considerations The first consideration is whether or not the duct is large enough to allow the cable to be pulled through it. The old rule of thumb has been that the duct should be at least 1/2 inch larger in diameter than the cable. Pehrson points out that it is the diameter of the pulling eye that is more important and except for small cables, the diameter of the pulling eye (de) compared to the diameter of the cable (dc) can be estimated by the following expression:

For long pulls, the diameter of the duct should be at least $1.15d_{\text{C}}$ or (d_{C} + 0.5 inch) whichever provides the greater clearance.

The second consideration involving conduit is the condition and type of duct since the coefficient of friction (f) will be dependent upon these factors. The coefficient of friction can be described as the ratio of the force needed to pull the cable through the duct to the force normal (N) to the plane of the duct. In a horizontal plane, the normal force is equal to the total weight of the cable (W) which is the opposing force. Items which have an affect on the coefficient of friction include:

- 1. dirt or contamination;
- 2. type of surface;
- 3. lubrication of the cable;
- 4. duct deviations; and
- duct deformations.

Estimated frictional coefficients for lubricated polyethylene cables pulled through various types of ducts in good condition are shown below.

Type of Duct	<u>f</u>
Concrete	. 42
Fiber	. 44
Transite	.50
Plastic	.38
Tile	.20

One method of determining the frictional coefficient is to pull a piece of lubricated test cable of weight (W) through the duct and record the pulling tension (T) during the normal pulling speed. The coefficient of friction is then:

$$f = T/W = \tan \mathbf{w}$$
 (2)

Figure 1 shows this relationship. When the plane is inclined, the relationship shown in equation (2) is not really true 6 since the value of (f)compensates for the vertical component of the weight. This is covered in more detail in Appendix B.

Reel Length Considerations

An important factor in determing long pulls is the amount of cable which can be provided on a reel. Information of this type is available from the cable manufacturers, but it can be estimated if needed. The maximum amount of cable per reel is of course, limited by the physical dimensions of the reel. Figure 2 illustrates the various important dimensional characteristics of a reel. These include the flange diameter (F) and drum diameter (1), both of which are expressed in inches, the clearance (C) in inches from the last

vertical wrap of cable to the edge of the flange, and the traverse length (H), expressed in inches.

The number of vertical wraps (V_{W}) of cable on a reel can be determined by the following expression:

$$V_{w} = (F-D-2C)/2d_{C}$$
 (3)

The number of horizontal turns (Nw) can be calculated by:

$$N_W = (H/d_C) - 1$$
 (4)

Knowing these two factors, we can adapt the formula for the circumference of a circle to determine the contract of the contra mine the reel capacity (k_c) in feet, as follows:

$$R_C = (\pi / 12) (D + .5 V_W d_C) (Y_W N_W) (5)$$

The total weight (WTOT) is calculated by:

$$WTOT = R_{CW} + W_{REEL}$$
 (6)

Where: w is the weight per foot of the cable and WREEL is the weight of the reel.

Equation (5) is slightly in error since it considers the length (circumference) of each vertical wrap as the length of the central wrap. A more accurate but more cumbersome expression would be as follows:

$$R_{C} = \sum_{i=1}^{V_{W}} \left[(\mathbf{1}/12) (D + i \bullet d_{C}) N_{W} \right] (7)$$

In any design of long pulls, the engineer must verify that the estimated length can be provided by the manufacturer and that the construction forces have the necessary equipment to handle reels of that size and weight.

Tension Limitations

There are two limitations for pulling tension. The first is that the maximum pulling tension does not exceed the rated working load for wire ropes of the winch. Presently, the standard winch ropes have a rated working load of 6,500 pounds.

The second limitation is that the tension does not exceed the maximum allowable pulling tension (Tmax) for the appropriate cable. This is determined by the maximum allowable pulling tension per cross sectional area of the conductors used to make up the pulling eye. Although some variations exist concerning the number of conductors involved, $^{7.8}$ an approximation of the maximum allowable pulling tension is as foilows:

$$T_{\text{max}} = .6 \text{nAk}$$
 (8)

Subject to:
$$T_{max} \le 6500$$
 (9)

Where: n is the number of conductors in the cable, A is the cross sectional area of a single conductor in circular mils, and k is the allowable tension per conductor.

For copper and 3/4 hard aluminum conductors, k is equal to .008 lb/cir mil. When the wire diameter is expressed in inches, the area in circular mils can be found by using equation (10).

$$A = (\pi/4) (d_c)^2 (1.273 \times 10^6)$$
 (10)

Once the tension limitations are known, it is simply a matter of breaking down the layout of the contemplated pull into straight and curved segments and applying the following appropriate formula for each segment from the cable set up location to the pulling location.

Equation (11) is used to determine pulling tension for a straight segment, and equation (12) is used for a curved segment.

$$T = T_0 + Lwf \tag{11}$$

$$T = T_0 + wR \sinh \left[fL/R + \sinh^{-1}(T_0/wR) \right] (12)$$

Where: To is the holdback tension in pounds, L is the length of the segment, w is the weight of the cable in pounds per fcot, and R is the radius of the bend in feet.

The holdback tension is never zero since it is the tension for the previous segment. When the segment involved is the first segment, (T_0) is equal to the force required to overcome the inertia of the cable reel and pull the cable through the feeder into the duct. Yarious figures have been used for the initial (T_0) value, but I prefer to use 200 pounds. Appendix A shows the logic used to derive this figure.

Occasionally, nomographs have been used to circumvent the use of hyperbolic functions 9,10 as shown in equation (12), but these are often more difficult to use than either a calculator that has hyperbolic functions or a table of such functions.

An additional consideration for curved sections is the bearing pressure (P_B) against the side wall of the duct. This is calculated by:

$$P_{B} = T/R \tag{13}$$

Subject to:
$$P_B \le 150$$
 (14)

The location of the bend is important, especially when offsets are involved. When located near the pulling end, and when the radius of the bend is rather short, the denominator in equation (13) can be quite small in relation to the numerator and thus (P_B) can become large.

Other Considerations
The direction of a pull may be important as when bends are included in the section. Pulls should not be designed too close to the value of (Tmax) since conduit systems may contain unknown offsets especially in inner-city locations where congested sub-surface facilities are possible. In addition, unless excellent conduit location records exist, radii and location of bends will probably have to be estimated. Appendix B shows considerations for pulls involving inclines. In any situation, designs of long pulls should be a joint engineering and construction evaluative venture.

PRECONNECTORIZED CABLES

The introduction of modular splicing made preconnectorized outside plant catles possible. PRECON is simply plugging together the ends of multipair cables with modular type connectors in a simple manner so that time and effort of field splicing are minimized. I The Bell System's CONECS, which began in 1974 is similar in concept.

Advantages of these concepts in general, include higher productivity, better quality splices and cost savings. Less "open manhole" time is a decided advantage from a public relations standpoint.

Field evaluations of factory connectorized cables were made in several GTE operating companies prior to adopting PRE-CON as an approved concept for GTE.

While theoretically every splice has the potential to be a PRE-CON splice, in underground plant, only one end of the reel length of cable can be so equipped since the pulling eye is installed on the other end. Even so, test cases have shown that PRE-CON splicing times in the order of 25 percent of conventional splicing times or better are attainable. Splicing of the conductors in the field merely involves building the splice from the core by selecting and positioning the corresponding male and female connector modules (see Figure 4) and pressing them together with a hand crimping tool. Since the connectorized ends are built and tested under factory controlled conditions, more reliability is indicated than would normally be obtained with standard field splices.

<u>Considerations</u>
Factors to be considered include costs, splice locations, and cable lengths.

Although the splicing time is reduced, the material cost of the cable is increased since the manufacturer incurs additional costs to preconnectorize the cable. Engineering costs are slightly higher and placing costs are about the same or slightly higher.

when the following inequality holds true for a proposed project, PRE-CON is economically advantageous to the Telco.

 $M_S + E_S + P_S + nS_S > M_D + E_D + P_D + mS_D + (n-m)S_S$

(15)

Where: M_S is the material cost for standard (non-PRE-CON) cable, E_S is the engineering cost for standard cable, P_S is the standard cable placing cost, n is the total number of splices, S_S is the splicing cost per standard splice, M_P is the material cost for PRE-CON cable, E_P and P_P are the associated engineering and placing costs, m is the number of PRE-CON splices and S_P is the splicing cost per PRE-CON splice.

The locations of PRE-CON splices are important since the cable reels must be set up at the PRE-CON splice location and pulled in both directions away from it. In some situations, the better pulling arrangement may have to be given up in order to obtain the advantages of a PRE-CON splice.

Cable lengths must be considered since PRE-CON cables are supplied on reels with spacers to keep the vertical wraps of the cable from overlapping the connector bundles. About 90 percent of the length which would normally be provided can be obtained when factory PRE-CON is specified.

PRE-CON is not limited to factory applications since the Telco can utilize bad weather periods to preconnectorize their own cables thus maximizing splicing resources. This is more difficult for underground cables since the cable must be payed-out from the reel to take-up reel in order to connectorize the opposite end and they rewound onto a reel equipped with a spacer. This would not seem economical unless the magnitude of application was great enough to justify "shop" conditions. For buried or aerial applications where the exposed end can be preconnectorized without paying out of the cable, it may prove to be a viable concept.

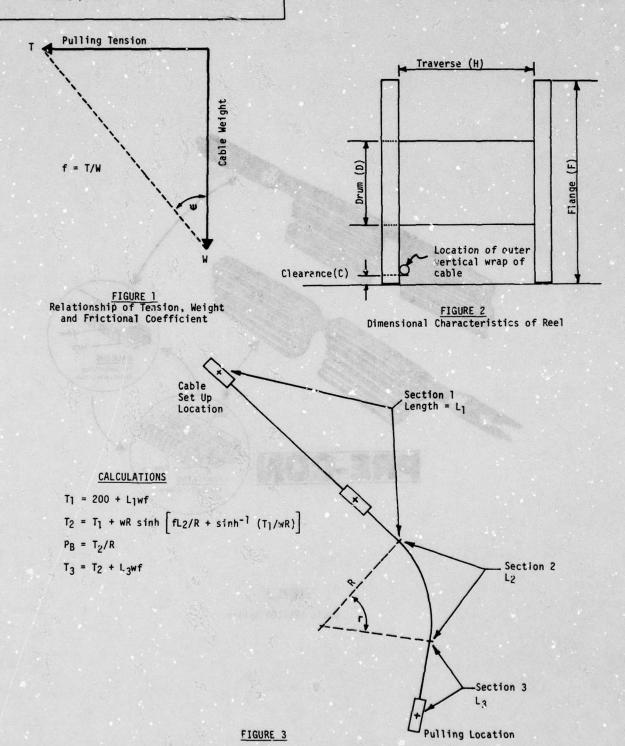
SUMMARY

Both the long pull and preconnectorized cable concepts offer opportunities for the Telco to hold down the installed cost of underground plant. Both concepts can be combined on a single project

and has indeed been done in the past. 13 Use of these concepts require more detailed engineering, close engineering and construction coordination and perhaps more installation time; however, the reduction in splicing time and associated costs will often easily offset the other increased costs. The opportunities for cost savings are only limited by the imagination of the Telco personnel.

REFERENCES

- 1 V.W. Pehrson, "Engineering For Cable Installation," <u>Telephone Engineer & Management</u>, 1 September 1977, pp. 73-80.
- William D. Kirkland, "Engineering and Pulling Long Cable Lengths Through Conduit Systems," <u>Telephone Engineer & Management</u>, 15 April 1974, pp. 86-91.
- ³ Nelson Jonnes, "Easing Those Long Cable Pulls," <u>Telepnone Engineer & Management</u>, 1 June 1978, pp. 82-85.
 - ⁴ Pehrson, p. 74.
 - ⁵ Ibid, p. 80.
- 6 W.G. McLean and E.W. Nelson, <u>Schaum's Outline</u> of Theory and <u>Problems in Engineering Mechanics</u>, 2nd ed. (New York: McGraw-Hill Book Company, 1962) p. 84.
 - 7 Pehrson, p. 73.
 - 8 Kirkland, p. 87.
- 9 GTE Practices, Section 912-300-901BC, Issue 2, September, 1974, "Selection of Ducts, Calculation of Pulling Tensions, Measuring for Cutting Lengths and Loading Cable Reels", British Columbia Telephone Company, p. 10.
 - 10 Information from a GTSW internal memorandum.
- 11 Tel Comm Products Division, PRE-CON Manual for Engineering and Construction of a Preconnect-orized Cable System (Saint Paul: 3M Company, 1977) p. 3.
- 12 D.R. Frey and G.S. Cobb, "CONECS A Complete Splicing System for Aerial, Buried and Underground Telephone Plant, "Proceedings of the 27th International Wire and Cable Symposium, November, 1978, p. 287.



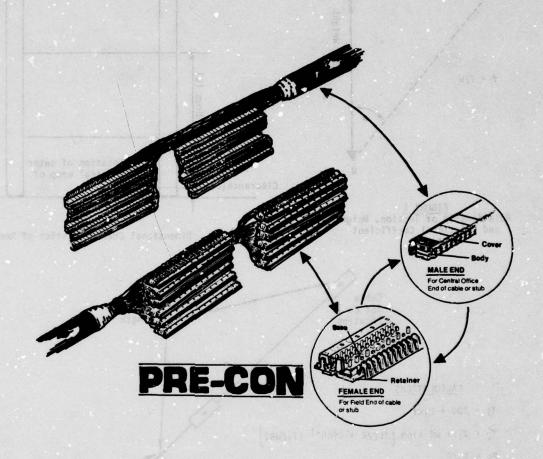


FIGURE 4

Basic PRE-CON Splice

APPENDIX A

Within this section we will consider the factors involved which determine the initial holdback tension (T_0), sometimes called the tail load. Calculations will be performed in two parts, i.e. the force (T_R) required to overcome the inertia of the static cable reel and then (T_F) which is the force needed to pull the cable through the feeder into the duct. For the first segment of a pull, it holds that:

$$T_{F} = T_{O} \tag{A-1}$$

Figure A-1 illustrates the condition for which calculations are to be made. The force needed to overcome the inertia of the cable reel can be determined by equation (A-2) which is an adaptation from a standard problem. $\mathbf{1}$

$$T_R = \overline{I} \alpha / r_1$$
 (A-2)

Where: $\overline{\mathbf{I}}$ is the mass moment of inertia taken through the axis at the cable reel hub, \mathbf{c} is the angular acceleration and \mathbf{r}_1 is the flange radius.

By taking some liberties, we can consider the cable and reel configuration as a hollow cylinder and calculate the value of $(\overline{1})$ as:

$$\overline{I} = M (r_1^2 - r_2^2)/2$$
 (A-3)

Where: M is the mass (W/g) of the cable and reel and r_2 is the drum radius.

The angular acceleration (a) can be determined by first calculating the linear acceleration (a), which is the charge in velocity from an idle condition to the pulling speed (v) during time (t).

$$a = v/t$$
 (A-4)

$$a = a/r_1 \tag{A-5}$$

Once (T_R) has been calculated, the general capstan equation can be used to calculate (T_F) .

$$T_F = T_R e^{-\Gamma}$$
 (A-6)

Where: e is the base of Napierien logarighms, s is the angle of wrap, and f is the coefficient of

If we consider the angle of wrap as the arc formed when the cable leaves the reel and travels through the feeder into the duct as shown in Figure A-1, a value of 3 π /4 radians should be

reasonable for (β). For the frictional coefficient, a value of .35 is selected as an estimate. Laminated plastic on steel usually is taken as f = .35 and although the feeder is aluminum, this should be satisfactory.

Using the following data, calculations were performed:

$$r_1 = 2.75 \text{ FT.}$$
 $r_2 = 1.75 \text{ ft.}$ $\alpha = .148 \text{ rad/sec}^2$

$$M = 8625Lb/32.2ft/sec^2$$

The angular acceleration was determined by considering a "jerky" start or a 3 second time period in which the pulling speed of 100 fpm is reached. The reflects a possible but not recommended acceleration!

 T_R is then calculated as 58 lb and subsequently plugged into equation (A-6) to determine a value of 132 lb for (T_F). A value of 200 lb for (T_F) or the initial (T_D) should be adequate for any situation.

REFERENCES

1 W.G. McLean and E.W. Nelson, <u>Schaum's Outline of Theory and Problems in Engineering Mechanics</u>, 2nd 3d. (New York: McGraw-Hill Book Company, 1962), p. 237.

Dudley D. Fuller, "Friction," <u>Standard Handbook for Mechanical Engineers</u>, 7th ed. (New York: McGraw-Hill Book Company, 1967), p. 3-35.

APPENDIX B

Within this section we will study the factors involved to pull a cable up an inclined plane. To set up the logic, we need to review the classic problem shown on Figure B-1 along with the free body diagram shown on Figure B-2. $^{\rm L}$

The problem is to determine the force (!) parallel to the plane that is needed to pull the block of weight (K) up the plane at a constant speed. Force (B) is the component of the weight which tends to pull the block back down the plane. The value of (P) is equal to the force needed to balance (P) plus the force needed to balance (P). Therefore:

$$P = K \sin \delta + fK \cos \delta \qquad (B-1)$$

Applying this to pulling an underground cable, equation (11) can be changed to:

$$T = T_0 + Lw \sin \delta + Lw_f \cos \delta$$
 (B-2)

If the cable were being pulled down the incline, the equation would be:

$$T = T_0 - (Lw sin a) + Lwf cos a$$
 (B-3)

From a purely theoretical viewpoint, it is better to pull downhill than uphill. In reality, physical considerations might make the reverse true.

Critical pulls include those involving "humps" or "dins" as these are vertical bends and bearing pressures may become great depending upon the location within the pull.

Another critical pull is when a curved section is involved on an incline. It would seem that the tension calculation is:

$$T = T_0 + \left\{ wR \sinh \left[\frac{1}{f} L/R + \sinh^{-1} \left(\frac{1}{f_0} / wR \right) \right] \cos \delta \right\} + Lw \sin \delta \qquad (B-4)$$

In any case, it is best that we not take ourselves too seriously and become enamored with the mathematics. Long pull problems might be likened to the bumblebee who never learned that he is an aeronautical nightmare for whom flight is impossible.

REFERENCES

APPENDIX C

Several methods have been used to calculate the tension around curved sections. The foundation for the various equations is the capstan formula as follows:

$$T = T_0 e^{\beta f}$$
 (C-1)

This has been considered as inaccurate, however, Kirkiand 1 has used a modification where (T_0) is not the holdback tension but the tension calculated as if the curved section was a straight section.

Rifenburg's 2 expression is also used. This expression and Buller's 3 are very close in results. Rifenburg's equation is:

$$T = T_0 \cosh (f \beta) + \sqrt{T_0^2 + (wR)^2} \sinh (\tilde{f} \beta) (C-2)$$

Buller's equation is:

$$T = wR \sinh \left[fL/R + \sinh^{-1} \left(T_0/wR \right) \right]$$
 (C-3)

The expression which I favor is similar to Buller's except that the value of (T_0) is added (see equation (12)).

The following comparison is made for the various methods where:

$$W = 5 \text{ lb/ft}$$
, L = 200 ft, f = .38, and $T_0 = 200 \text{ lb}$

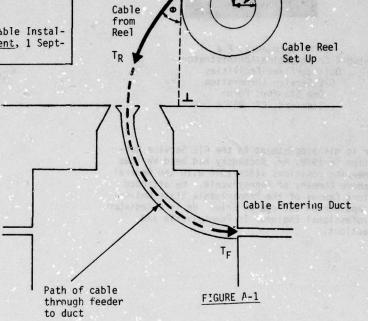
	β	_16	enston in	pounds a	s calcu	lated b	y equations
eg.	Rad.	R in ft.	<u>C-1</u>	<u>c-1*</u>	<u>C-2</u>	<u>C-3</u>	12
0	0	0	580	Eguat	ion_(11	1	
0	₹/18	1146	214	620	581	581	781
30	17/6	382	244	707	589	588	788
0	17/3	191	298	863	615	615	815
0	11/2	127	363	1054	658	660	860

Equation (12) is admittedly conservative for gentle curves; however, it is a compromise between equations (C-1) adjusted, and (C-3) for sharper curves. Based on my experiences in inspecting new conduit systems as they were being built, and knowing how irregularities are not always recorded, I prefer to be more conservative in the design of such pulls.

¹ Daniel Schaum. Schaum's Outline of Theory and Problems of College Phusics, 6th ed. (New York: McGraw-Hill Book Company, 1968), p.43.

REFERENCES

- William D. Kirkland, "Engineering and Pulling Long Cable Lengths Through Conduit Systems,"
 Telephone Engineer & Management, 15 April 1974,
 pp. 86-91.
- ² R.C. Rifenburg, "Pipe-Line Design For Pipe-Type Feeders," <u>AIEE Transaction</u>, Vol. 72, Part III, p. 1275.
- ³ V.W. Pehrson, "Engineering For Cable Installation," <u>Telephone Engineer & Management</u>, 1 September 1977, p. 75.



Flange Radius

Drum Radius

r1

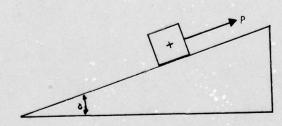


FIGURE B-1

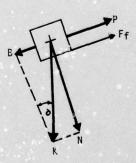


FIGURE B-2



T. M. Kochansky, P.E.

Network Construction Administrator Outside Plant Facilities
GTE Service Corporation
One Stamford Forum
Stamford, CT 06904

Prior to his appointment to the GTE Service Corporation in 1978, Mr. Kochansky had held various engineering positions since 1960 with the General Telephone Company of Pennsylvania. He attended the York Campus of the Pennsylvania State University and Gannon College in Erie. He is a Registered Professional Engineer in Pennsylvania and Connecticut.

SIMPLIFIED PRECONNECTORIZED CABLE SYSTEM FOR THE INTERNATIONAL TELEPHONE MARKET

J. Prosper and J.Z. Avalos

CABLES DE COMUNICACIONES, S.A.

ABSTRACT

The pre-connectorized cable program which several telephone Administration companies have tried and adopted, has been presented in previous Papers ¹²³ as a complete splicing system for outside plant installations. However, the success and efficiency of the system is subject to good planning and coordination between the project engineering and installation departments.

This Paper presents a simplified system which, we estimate, should be offered to the International Market using pairs and quads. This system requires a minimum of plannification and coordination and thereby reduces possible coding errors.

INTRODUCTION

Certainly the idea of shipping connectorized cables is not a new one since special communication cables terminated with pin-and-jack connectors are being shipped to the military and other jobs requiring it. Nevertheless this type of service could not be offered to the Telephone Plant because of design limitations and prohibitive cost. However with the development of the modular connector in the late 1960's the old idea of shipping pre-connectorized telephone cables was seen as a future reality. Finally in the mid 1970's, Bell System developed CONECS, a factory connectorized cable system, as a service to the outside telephone plant. This system would improve productivity reducing installation costs. In the years which followed, this program advanced at a faster pace covering as many splice situations as could be encountered in the field.

In 1977, our company's Investigation Department studied the possibility of adopting and offering this system to our customers. It was a considerable change in the Spanish telephone practices. Since then we have made a number of factory and field trials with the colaboration of the Spanish Telephone Company (C.T.N.E.). These trials have erabled us to establish our own concept and criteria plus valuable field results. Comparing these results with present and established preconnectorized programs, it is clear that the system can be a complicated one if the purpose is to cover all possible splicing situations employing all the hardware presently available to the outside telephone plant.

From our point of view, as cable manufacturers serving many companies, the idea of offering pre-connected cables is most attractive. However, if the system requires a considerable and complex effort from the several departments involved, it will not be practical and may defeat its purpose. Therefore, the connectorized cable system to be offered to our market and similar ones in other countries should be simple, eliminate unnecessary steps to avoid potential and costly errors, and improve coordination between the Engineering and Installation forces.

In order that a given project employing a preconnectorized cable system yield the lowest cost with the minimum of execution time, the project engineer must logically know the characteristics and limitations of the network in which the installation will be performed. Some of these are:

- Cable placing with a fixed or mobile reel
- Splicing points and distance between splices
- Possible obstructions

Additionally, a mechanical means to order specified lengths and type of cable termination will be needed. This is accomplished by a worksheet on which a cable to be installed is fully codified as to connector type, splice configuration and type, and closure preparation. Figure 1 on the following page shows a typical worksheet used by some American Administrations.

As can be observed, this type of worksheet with all its variables and alternatives requires hundreds of possible codes. This complexity may create dimensional and orientation errors by all personnel involved. Moreover the Project Engineer must be thoroughly familiar with the cable route and its limitations, specification (morksheet) rules, hardware availability, and be in constant coordination with construction personnel.

The complexity is understandable if the system is designed to cover all the splice configurations and existing hardware which some Administrations offer. However, many of the existing Administrations do not have a need for such a variety of accessories because of technological reasons or network needs. Accordingly, the pre-connected cable system to be

PART 1.	JOB NO:	REQUISITI	ON NO:	DATE:
	CABLE OR STUB TYPE:	NO.OF P	AIRS:	PRINT NO:
	PLACING REEL NO:	PLACING B	LOCK NO: BONE	WIRE: YES () NO ()
	SINGLE REEL: YES	() NO () CABL	E LENGTH:	BLOCK LENGTH:
PART 2.	PRE-CON CODE		has managed t	
		1 2		6 7 8
182 215 10	Director alder as , we	OUTSIDE	END	INSIDE END
PART 3.	OUTSIDE END (IF 10 T	YPE STUB, THIS END WI	LL HAVE A PRESSURE PLUG)	
MALE FEMALE BRIDGE CO	F MALE = 6 FEMALE = H = C BRIDGE CO = J	LEFT WALL MALE = A FEMALE = D BRIDGE CO = K	3. SPLICE CONFIGURATION IN LINE = I BUTT = B FOLDBACK = F	PC 6/48 = A LD10/42 = C PC 12/55 = D UP 1248 = E
BLANK EYE			4. CLOSURE/SHEATH PREP SINGLE SHEATH 1. TYPE, 18-TYPE = A 2C2A = M 2D2A = N	2C2A = R
STRAIG BRANCH CO SI	HT = S DE OF SPLICE = C SIDE OF SPLICE = F	To small by ent rights to small a smal	2-TYPE,16D1,PEDES-	2-TYPE = K PEDESTALS & CABINETS = L 4
PART 4. I	NSIDE END	sportess also st	e pag at without the	na leta kende je povijana i sije o
1.SEX AERIAL, MALE FEMALE BRIDGE CO FIELD	FEMALE = G FEMALE = H C BRIDGE CO = J	LEFT WALL MALE = A FEMALE = D BRIDGE CO = K	DIITT - D	PC 6/48 = A LD10/42 = C PC 12/55 = D UP 1248 = E
BLANK EYE	= B FIELD = R = E BLANK = B	FIELD = S BLANK = B	8. CLOSURE/SHEATH PREP.	DOUBLE OUGATU
6.BASIC STRAIG	SPLICE TYPE HT = S DE OF SPLICE = C SIDE OF SPLICE = F		SINGLE SHEATH 1TYPE, 18-TYPE = A 2C2A = M 2D2A = N 2-TYPE, 16D1, PEDES- TALS & CABINETS = B 16B1 = T 16C1 = C 16E2 = H 2O-,21-TYPE = F 30-,31-TYPE = G	DOUBLE SHEATH 1-TYPE,18-TYPE = J 2C2A = R 2D2A = S 2-TYPE = K PEDESTALS & CABINETS = L 8
M	ANHOLE CONFIGURATION	CO SP	T WALL LICE FIELD HT WALL	dio inserto di collegio della colleg

Figure 1 - Cable Coding Sheet

offered to these Administrations should be made simpler without diminishing the main objectives of higher field productivity and better splicing quality.

A SIMPLIFIED PRE-CONNECTORIZED CABLE SYSTEM

Basically, our idea of simplification is the result of a study and observation of the different steps required when connecting these modules at the factory and mating them in the field. It is well known that when preparing a cable end at a cable plant, the critical parameters are the cable orientation and correct dimensions. In the conventional system, the orientation is critical in order to attain a proper alignment when mating the female and male modules. These steps can be observed in figures 2 and 3.

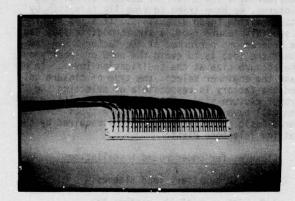


Figure 2
Conventional method

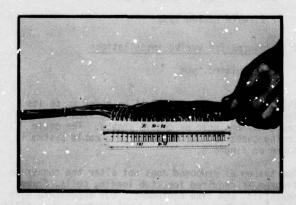


Figure 3
Orientation required

Although most companies keep records of their empty dects, these records do not give information regard-

ing actual duct conditions. The need to specify a given orientation requires previous knowledge of physical conditions and availability of the duct. To obtain this information a field trip must be made to assess the underground conditions.

In our proposed simplified system, we have eliminated the orientation parameters by means of a slight change in positioning the pairs in the connector module. This terminating method has i een designated as DOT (Dual Orientation Termination). Figure 4 shows this change.

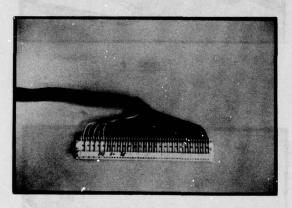


Figure 4
Improved method

The advantage of this method can be observed on figures 5, 6 and 7 which show the steps the splicer performs to obtain a proper orientation regardless of the cable position.

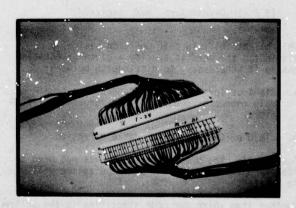


Figure 5

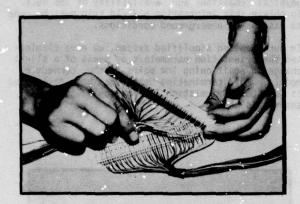


Figure 6

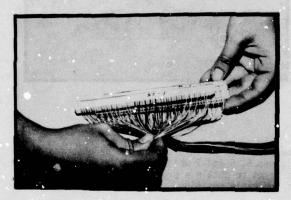


Figure 1

(5 & 6) Orientation not required

This slight shift in pair position basically eliminates the need to specify a given orientation making it unnecessary to distinguish between:

- Right or left wall when connecting a female or male connector module for underground installations
- b. Field or Central Office caple direction

Accordingly, the project engineer does not need to specify a duct or on which wall the splice will be located.

Another item which our code simplifies is the splice type and configuration. The configuration which more frequently is encountered in our outside telephone plant is the "in-line" type while the "foldback" is a special configuration usually employed on splicing load coils or when branching is required. In our coding system, we will specify

the straight, butt, branch, and load configurations. However, whenever a branch or load splice is required, the factory will terminate the cable in a foldback configuration. The other splice types, including the straight and butt types, will be furzished in the in-line configuration. Those required for pedestals as indicated in figure 1 are seldom used and therefore, for all purposes are not applicable to our installation practices.

Considering the points so far presented, our proposed system eliminates one block code since in our factory connectorized cable code system the established blocks 2 and 3 are combined in one.

As previously mentioned, the other critical parameter is the termination length prepared by the factory. This dimension will vary in accordance with the type of closure used and the sheath type, whether it is a single or double sheathed cable. Considering a few universal designs of splicing closures, we have tried to simplify this item by standardizing these dimensions. If a job requires a special closure type, a simple modification can be ordered and performed at the factory. In any event the idea is to avoid the need of specifying the closure size at the codification level. In our case the engineer selects the type of closure only and the factory is responsible of selecting the proper closure size. The proposed simplified system will have the following closure types covering three basic installation practices required by the Outside Telephone Plant:

- 1. Closures for underground installations
 - 1.1 With auxiliary lead sleeves
 - 1.2 With mechanical pressure box
- 2. Closures for aerial installations
 - 2.1 With free breathing type
 - 2.2 With sealed type
- 3. Closures for buried installations

Encapsulated type

These five closure types will be coded as to its type without indicating the closure size or if the cable has a single or double sheath. The cable coding sheet for our connectorized cable system is shown on figure 8.

The system as proposed does not alter the connexion program as required for stub loading coils, frame pedestals, and like equipment. Our experience with this simplified system has demonstrated a versatility which covers our needs with a minimum of complexity. Likewise the coordination between the project engineering and construction departments is clearly improved.

Installing connector modules under the system so far presented does not require modifications on the

STATE OF THE PARTY OF THE PARTY

CABLE CODING SHEET

PROJECT CABLE TYPE PLACING SEQUENCE REEL N°		PRINT N°	
SINGLE REEL: YES () NO (PRE-CON CODE	GLA OF STAR UNUGSO OF SLAR	
1 2 OUTSIDE END 3	ONE TERRITOR SERVED SAME AND AND	1 2 3 INSIDE END	
1. <u>SEX</u> Male = M Female = F Bridge = T Blank = B Pulling Eye = E	Butt = T Straight = S Branch = B Load = L	CLOSURE TYPE Pressurized: Lead sleeve = P Mechanical box= M Aerial: Free breathing = 0 sealed = C Buried = D	

Figure 8

hardware actually employed and the build-up diameter remains practically the same. Should the cable be required to be spliced on the opposite wall, the extra time and labor required by the installer does not impair the productivity of the system since the cable ends have been furnished with the DOT termination method.

PRE-CONNEXION OF QUADDED CABLES

Normally we should not expect difficulties in applying a factory connectorized cable program to quadded cables as well as to pairs especially since connector modules exist for the standard 14 quad unit. However, as it is well known, it is necessary to compensate capacitance unbalance parameters in order to obtain acceptable crosstalk characteristics. Usually, this is accomplished by an orderly pair transposition at the time the splice is performed. In this operation a considerable time is spent remeasuring all the capacitance unbalances on both cable lengths. Quads are then properly matched avoiding unpermissible unbalances which may result if a random splice is performed. Logically, the time and labor required increments splicing costs by a good percentage.

It is because of the need for balancing that preconnecting quadded cables at the factory is very attractive. Two cables can be connected with female and male modules to obtain the best compromising balancing situation. Nonetheless, our main concern resided in the fact that capacitance characteristics of a star type quad are susceptible to changes during cable placing manipulations. This could mean that balancing techniques performed at the factory may result in poor unbalances after the cables have been placed and connected.

In order to ascertain that connectorizing cable at the factory is the best compromise, exhaustive trials were made. Cables were laid flat on the ground and also went through several rewinding operations. We found, that in general, the capacitance unbalance readings at each stage did not vary substantially and the changes could be attributed mainly to the tolerance limits of the bridge used. Table I and II show a summary of the measured and compensated values.

Based on these promising results, we think that a factory pre-connected cable program can be applied to quadded cables obtaining practically the same values as a field balancing installation.

In our system, cables will be matched by means of a

CAPACITANCE UNBALANCE CHANGES

BEFORE AND AFTER UNWINDING (pF/Km)

	BEF	BEFORE		AFTER
	AVERAGE	MAXIMUM	AVERAG	E MAXIMUM
PAIR TO PAIR	33	205	34	246
PAIR TO GROUND	213	1200	225	1100

TABLE II

QUAD No.					QUAD No.			
CABLE	CABLE		pF/30	00m.	CABLE	CABLE	pF/3	300m.
"A"_	"B"		(1)	(2)	"A"	"В"	(1)	(2)
1	13		0	2	15	19	13	12
2	2		17	28	16	26	12	9
3	11		5	4	17	23	14	18
4	6		15 0	2	18	24	16	18 20
5	5		0	0	19	17	11	13
6	4		7	6	20	27	13	2
7	1		13	0	21	21	15	14
8	7		27	42 23	20 21 22 23	16	9	6
9	14		3	23	23	20	9	8
10	3		4 15	7	24	25	7	4
11	9		15	20 20 18 17	25 26 27	28	5	2
12	12		21	20	26	A (15 See 1995)	17	23
13	10		6	18	27	18	4	15
14	8		10	17	28	22	g b <u>allo</u> 94	-7
		AVERAGE	10.1	13.5		ant one was perturble television by the television	11.1	10.9
			(1)		IR CAPACITANCE ACCORDANCE TO	UNBALANCE SPLICING CARD		
			(2)	CAPACITANCE	F UNBALANCE AF	TER THE CABLES		

computerized program with a better reliability in a minimum of time. \\

Basically, the method is the usual one: a quad with the highest pair to pair capacitance unbalance on cable "A" should be spliced to a similar quad on cable "B". Signs are very important since the algebraic sum of these two unbalances should be the lowest absolute value. This means that if the unbalances to be matched have positive values, measured from a common reference, a pair of one of the quads should be transposed to obtain a "negative" unbalance value. When this process is performed on every pair of quads, a typical 14 quad splicing card may require the following connection:

CABLE A		CABLE B	CONNEXION
Quad 1	splice to	Quad 13	straight
Quad 2		Quad 2	Cross
Quad 3		Quad 11	Cross
Quad 13		Quad 10	straight
Quad 14		Quad 8	Cross

As can be observed, quads of cable "A" are sequentally connected on one of the modules while quads of cable "B" should be connected starting with quad No.13 in the first terminal, quad No.2 in the second, and so on until quad No.8 is connected to the lcst terminal

with the conductors of a pair transposed.

Results of economic studies show that a greater benefit could be obtained on pre-connecting quads than pairs. Table III compares the time units involved in splicing pairs and quads.

TABLE III

	NORMALIZED TO A	100 PAIR CABLE	
TYPE OF CABLE	CONVENTIONAL SPLICE	CONNECTORIZED SPLICE	VARIATION
Pairs	100	55	- 45
Quads (unbalan	107 ced)	55	- 52
Quads (balance	230 d)	55	-175

From the above table, we can appreciate the considerable time saving which is obtained on a balanced preconnected quadded cable when compared to a conventional splice. Another point to consider is that while a better return is obtained in connectorizing cables of 200 pairs and larger, a same relative return is obtained on cables with 50 quads (100 pairs). As we gain more field experience, actual savings on other sizes will be compared and confirmed.

FUTURE PLANS

To further simplify this system, we have also thought of using a unisex connector module. With this connector type, it will not be necessary to prefix cable direction. Another clear advantage of a unisex connector module is that factory or distribution centers can be stocked with cables pre connected on one or both ends with only one type of connector for all situations. Towards this end, AMP Inc. has already developed a hermaphroditic connector *.

The design which should fulfil our needs is still to be completed, however we expect to make a design recommendation to our connector supplier in the near future. Our aim is to improve the connector versatility such as to be used a number of times on as many splicing situations as necessary.

CONCLUSIONS

The connectorized cable system which has been developed in this study is based on the knowledge and needs of our national market and of the several international administrations which we serve. By eliminating several alternatives which are seldom used outside the American market, we were able to successfully train people in a very short time. In our major field experience ⁵, we realized that any

splicing situation can be pre-connected. Kowever, applying a complex system to an expanding telephone network impairs the basic advantages of a connectorized cable service. Accordingly, this simplified system should be very attractive to a telephone administration planning to splice pre-connected cables in a new or expanding cable network.

We have also presented results of a study on connectorizing quadded cables. The attractiveness of this service lies on the fact that quad balancing can be performed at the factory instead of on the field which requires excessive time and expertise. Applying this concept, we do not expect a change in transmission quality.

Based on our national market response, this connectorized cable system should be very attractive to those countries with similar needs and telephone network facilities.

REFERENCES

- Connectorized Exchange Cable Splicing (CONECS), by D.R. Frey and A.G. Hargee - Bell Lab. I.W.C.S.1976.
- CONECS. A Complete Splicing System for Aerial, Buried and Underground Telephone Plant, by b.R. Frey and G.S. Cobb, Bell Lab. I.W.C.S. 1978.
- Pre-Con Speeds Cable Reroute & Factory Splicing: a short cut for installation, from Telephone Engineer & Management Sept. 15,1978 and Telephony - June, 19,1978.
- The success story of pre-connectorized cable from Telephony - January 22, 1979.
- Internal Report. The story of Reallocating a Central Office empoloying pre-connectorized cables, from Cables de Comunicaciones, S.A. January, 1979.
- Pre-Con/MS², Pre-connectorized cable plant -Aerial and Buried from 3M Co. April 11, 1977.

ACKNOWLEDGEMENTS

The authors gratefully acknowledge the collaboration of the Quality Control and Electrical Measurement Laboratory Personnel. We are also grateful to Mrs. Maria P.Mendoza in preparing this document.



J. Prosper obtained his Technical Engineering degree in Telecommunication in 1973 from the University School of Technical Engineers (E.U.I.T.T.) in Telecommunication in Madrid. He joined the Research and Development Department of Cables de Comunicaciones S.A., Zaragoza, Spain in 1974. He is at present managing the Outside Telephone Plant Department in Madrid.



Juan Z. Avalos received his Bachelor in Electrical Engineering and Master in Mechanical Engineering from the City College of New York. Prior to joining Cables de Comunicaciones S.A., Mr. Avalos worked 12 years for General Cable Corp. He is presently working in the Cable Design and Engineering Department in Zaragoza. Mr. Avalos is an IEEE Member.

LIGHTGUIDE CONNECTOR COMPONENT CHARACTERIZATION

D. Q. SNYDER

Development Engineer

Western Electric Co.

Norcross, Georgia

Abstract

The primary lightguide connector component is a small chip produced from single crystal silicon and is used to very accurately position multiple fibers in a connector. An analysis of the chip geometry pointed out three major parameters that vary significantly due to the manufacturing process but must be kept within a one micron range in order to meet our desired loss objective. These critical parameters include groove width, side to side groove misalignment and overall thickness. Every wafer of chips is measured for these as well as other parameters with a toolmaker's measuring microscope and a electronic comparator both with a resolution to 0.1 microps.

Introduction

Specially designed silicon chips are being used for their ability to form geometric shapes to very precise tolerances. These chips are then used to sandwich a ribbon of 12 fibers between them, each fiber captured in a groove and thus precisely located. Identical connector halves, as described above are mated together and aligned with a second design chip. This technique allow us to obtain, for any two adjoining fibers, and axial misalignment of less than a few microns and therefore result in a very low connector loss.

To obtain this low loss several chip dimensional parameters must be monitored and checked very closely. A computerized chip measuring system was developed to facilitate the continuous monitoring of all necessary dimensional parameters. Groove width and groove misalignment along with other non-critical parameters are measured on a toolmaker's measuring microscope and the data points are directly transmitted into a desktop minicomputer. Chip thickness is measured on an electronic comparator and the data is also transmitted directly to the computer.

Parameters Determined With Measuring Microscope

Measured Parameter Description - Side Position

Silicon connector chips are currently received in the form of wafers and are retained in this form for all measurements on the microscope. Based on proven assumptions discussed below many parameters can be assumed uniform for an entire wafer. Both critical and noncritical parameters are measured on the microscope. The first and most important critical parameter is chip groove width (see Figure 1). All 12 grooves of a usable chip on each side of a wafer are measured and a mean and standard deviation is obtained for each side. It has been shown that the groove widths on the same side of a wafer do not vary within the accuracy of the instrument (approximately ±½ microns) but does vary between the two sides of the wafer. Groove spacing (see Figure 2), a well controlled parameter, is obtained as a by-product of the groove width measurement. This parameter is a function of the mask only and does not vary as a result of the chip manufacturing process.

Groove centering is the centering of the 12 groove complex relative to the edges of the chip and is considered a non-critical parameter since it is relatively easy to control (see Figure 2). This parameter is an important factor when fabricating array connectors and is defined as the distance from the edge of the chip to the top outside of the first land. By measuring a chip near the top of the wafer and hear the bottom of the wafer and both chips are in tolerance, all the chips on the wafer will be in tolerance.

Groove depth is the last parameter measured on the microscope and is also considered a non-critical parameter (see Figure 2). The chip is designed such that when the fibers lay in the grooves of the chip, they make contact with the sides only and not the bottom. Therefore, if the depth of the groove is below a certain minimum the actual depth is not critical and it is also an easy parameter to control. Groove depth is

considered to be uniform for the whole side of the wafer and is measured on each side of the wafer.

Results

As indicated above the results are tabulated as soon as the measurements are completed on each side. All data points are listed along with the calculated groove width of each groove and the calculated groove spacing including the mean and standard deviation for each. Groove centering and groove depth are also included along with the tolerances for each parameter, the product identification number and the date.

Measured Parameter Description - Edge Position

Groove misalignment is the second critical parameter and it can be measured on the same toolmaker's measuring microscope (see Figure 1). Groove misalignment is defined as the misalignment of the grooves between the two sides of the chip (see Figure 1). This misalignment has the effect of shifting all the fibers horizontally to one side or the other in the connector. Groove misalignment can be measured by mounting a wafer of chips vertically on a miscroscope stage and with the use of backlighting measure the amount of the offset or misalignment between the grooves on the sides of the wafer. The wafer can be turned over to measure the misalignment of the grooves on the other edge. The results can be plotted and thus the groove misalignment for any of the chips in a wafer can be determined. Results for each wafer are included in the data tabulation summary discussed below.

Thickness Parameter Determined With Electronic Comparator

Chip thickness is the third critical parameter and includes overall chip thickness as well as variations in the thickness across the chip (see Figure 1). With special wafer grinding and polishing techniques the major variation is the thickness between wafers rather than thickness variation within a wafer. To measure wafer thickness a commercial electronic comparator is calibrated using gage blocks with a conventional anvil mounted in the stand. A special flat contact point is used that doesn't penterate the grooves of the chip. Several thickness measurements are taken on the wafer, with the data being recorded in the computer and a mean and standard deviation is calculated.

Data Tabulation Summary

When all the chips are measured for a particular batch of wafers the data can be tabulated on a summary sheet for easy evaluation of the overall quality of each batch of chips. Included in the tabulation are all the critical parameters of the chips including groove width on both sides of the chip, chip thickness and groove misalignment. Also included on the summary is groove centering which is an important parameter in connector

fabrication. Other data is available but is not printed since it is not considered critcal and/or is usually well controlled.

Conclusion

Measurement of silicon chips for both non-critical and critical parameters using a toolmaker's measuring microscope and an electronic comparator is a very effective means of predetermining the quality of a connector dimensionally. With known critical parameters of chip groove width, chip thickness and groove misalignment the connector's dimensional quality is easily determined. Thus by selecting connector chips within certain tolerances on the critical parameters, the minimum transmission loss for a splice can be estimated.

References

- C. M. Miller, "Fiber Optic Array Splicing with Etched Silicon Chips," B.S.T.J., 56, 1977.
- D. Marcuse, D. Gloge and E. A. J. Marcatili, "Guiding Properties of Fibers" (Chapter 3 of Optical Fiber Communications," ed by S. E. Miller and A. G. Chyroweth) prepublished edition February 6, 1979.



Donald Q. Snyder, Western
Electric Company, 2000 N.E.
Expressway, Norcress, GA 30071.
Mr. Snyder joined Western
Electric in 1970 after receiving
his Bachelor of Science degree in
Mechanical Engineering from the
State University of New York at
Buffalo. He is currently working
on his Master of Science in
Mechanical Engineering at Georgia

Institute of Technology. Mr. Snyder has been involved with lightguide connectors and measurements for the last three years.

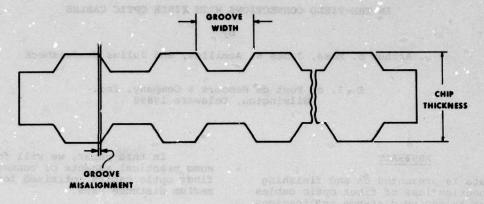


FIGURE 1
CRITICAL SILICON CHIP PARAMETERS

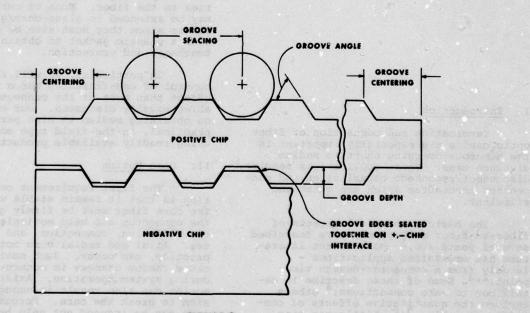


FIGURE 2
NON-CRITICAL SILICON CHIP PARAMETERS

IN-THE-FIELD CONNECTIONS WITH FIBER OPTIC CABLES

by

Arthur Z. Moss, James H. Aumiller, and Julius Uradnisheck

E. I. du Pont de Nemours & Company, Inc. Wilmington, Delaware 19898

ABSTRACT

Data is presented on end finishing and connection loss of fiber optic cables for short to medium distance applications. Core stability within the attached connector is discussed. The optical quality of the fiber end will be traced through a series of finishing steps using scanning electron microscopy. Dependence of connector insertion loss on end quality and core misalignment will be explored. A practical procedure for making field connections will be presented that allow rapid (five minutes), reliable, low loss, and economical field connections.

I. Introduction

Termination and connection of fiber optic cables are especially important in the numerous emerging short to medium distance uses. These applications require disconnect/reconnect capabilities and connection procedures which are quick and efficient.

The basic theoretical aspects of fiber-to-fiber connections were described several years ago. I More recent literature has emphasized applications - largely from a connector-design viewpoint. Some of these describe in detail how to make connections; there explore the quantitative effects of connector variables. Little has been published describing actual experience in real day-to-day applications. There remains little insight into what the user can normally expect.

In this paper, we will focus on some practical aspects of connectoring fiber optic cables optimized for short to medium distance uses.

We will discuss end finishing and connectoring of plastic-clad optical fibers, both silica core and plastic core, which are specially designed for 10 m to 1 km applications. These are step-index fibers characterized by 200 to 400 µm cores. The cores are surrounded by plastic claddings which provide protection, toughness, and large numerical apertures (light acceptance angles). Both hard and soft plastic claddings are available, imparting somewhat different properties to the fiber. Much of our discussion may be extended to glass-core/glass-clad fibers since they must also be coated with a plastic jacket to obtain adequate toughness and protection.

In particular, we will show that control of end-finishing has a larger effect than most of the connector variables usually discussed. Our emphasis is on obtaining medium to high performance practical, in-the-field type connections using readily available products.

II. Core Motion

The first requirement on a connection is that it remain stable with time. The core fiber must be firmly gripped by the connector and held motionless during end finishing, connection, and day-to-day use. Axial and radial core motion, in practice, can occur. Such motion will cause random changes in connection loss during system operation. Axial core motion can also result in enough protrusion to break the core. Forces on the core can be induced not only by a load or thermally induced tension on the cable, but also by a bend near the connector.

A typical method for achieving core stability is to epoxy the clad fiber into the connector ferrule. Both soft and hard claddings can be firmly affixed by maximizing the fiber surface exposed to the epoxy. However, cladding to core adhesion is much lower in soft-clad fibers than in hard clad, so that the core of the soft clad fiber remains freely moving.

The soft cladding is a spongy, pliable material that is easily torn or smeared. In Figure 1 the cladding has been peeled off the core by gently tugging with tweezers. Because of the relatively free motion of the core, it may recede leaving a hollow cylinder of cladding (Figure 2) or it may protrude (Figure 3). A surgical procedure is often recommended to remove the soft cladding at the fiber end and to carefully replace it (while avoiding damage to the delicate core) with a harder material. In contrast, the hard plastic cladding shows none of these characteristics; core/cladding adhesion is strong, the fiber can be clamped onto directly, and held motionless. The hard plastic clad fiber is placed straight into the connector ferrule and the end prepared.

III. Effects of Core Misalignment

Another requirement of a connection is that if light is to pass from one optical fiber to another with minimum power loss, the transmitting and receiving cores must be precisely aligned. Centering of the clad fiber in the connector and of the fiber core in the fiber are both essential. 3,4

The principal conclusion from most work dealing with connection loss is that lateral misalignment of transmitting and receiving cores contributes the largest amount to connection loss. 2, 4 Numerous calculations, some with experimental results have been presented which support this conclusion. Little actual experience has been reported.

Generally speaking, connectors can be machined to high tolerances in a fairly straightforward manner - although this by no means ensures that they always will be. However, as in wire coating technology, control of the hydrodynamic

forces in silica fiber coating operations is not so straightforward. It is a highly critical operation. We have determined the actual magnitude of the contribution of core misalignment to total connection loss, in a series of realistic connections using commercially available fiber and connectors.

Core-centering is generally described by percent displacement with respect to core diameter. Table I shows the percent core displacements of fiber samples used in our experiments. Also shown is the magnitude of the displacement and the silica core fiber diameters. In order to average out difficult-tocontrol variables, such as connector misalignment and end separation, each of two Sample Ends was connected to the same seven Test Ends. The results achieved with the two sample ends were compared. (Table II). Sample End #1, at 10%, represented a core displacement considered acceptable for most applications today. Sample End #2, at 25%, is unacceptable. The seven Test Ends cover a fairly typical (though weighted slightly to the high end) spectrum of displacement values.

Ends were finished by a procedure we will discuss in the following section. Each Sample End was rotated with respect to each Test End to determine the difference between the minimum and maximum power transmitted. We define this difference as Λ , the maximum loss attributable primarily to core misalignment. Because of potential damage to the ends during rotation, the end separation was not minimized for these experiments; only power differences were determined. Minimum overall connection loss was determined in the experiments to be described in the next section.

The statistical t-test for the mean Δ 's for the two sample ends showed that the results for 10% core offsets were statistically distinguishable from those for 25% offsets. At a 90% confidence, the difference of the means was 0.7 dB. Thus real world differences in core-centering due to connector/fiber tolerances can be large enough to have significant effect on connection loss. We included in Table II calculated mean values of Δ based on core overlap areas for each actual connection. The equation for overlap area, S, is

$$S = 2R^2 \left[\cos^{-1}\left(\frac{r}{2R}\right) - \frac{r}{2R}\sqrt{1 - \left(\frac{r}{2R}\right)^2\right]}$$

where

- R = core radius, assumed 200 μm. for both fibers.
- r = distance between core centers.

This equation represents the case for fibers with different displacements but equal core diameters and no end-to-end separation. We noted that the experimental results for both sample ends were a little better than calculated (1.5 vs 1.6 and 2.2 vs 2.8), but agreement was pretty good. The calculated values coincided with those obtained previously.

Using the above equation to predict the average (50% probable) Δ gave 1.1 and 1.9 dB for 10% and 25% displacement respectively.

These values represented the predicted loss if the connections in cur experiment had been made with no attempt to maximize or minimize the loss.

Finally using average optimized connection losses obtained with this system of fiber and connectors (which we'll discuss next), we estimated the maximum (or worst-case) overall connection loss for the 10% and 25% cases at 2.6 and 3.3 dB respectively (3.9 for the latter if we used the calculated values). This werst-case will occur in fewer than 3% of a randomized connection population. We also predicted from calculations the average (or 50% probable) loss expected for 10% and 25% displacements as 2.2 and 3.0 dB respectively.

Using calculated values, we have generated curves for maximum and average incremental connection loss (or A) for two identical ends as a function of core displacement. These are shown in Figure 4. The incremental loss is a slow function of core displacement; small changes in displacement have little effect. By using these calculated curves, it is possible to define with modest precision the sort of performance to expect from given fibers. As we will now show, if the performance appears to diverge significantly from the predicted value, inadequate end preparation is a likely culprit.

IV. End Finishing

With the optical core well centered and stabilized in a connector, the quality of the fiber end has an important effect on connection loss. Two types of end finishing are used for short to medium distance applications: cleaving and polishing. Proper cleaving can only be done by removing the plastic cladding

to expose the fragile glass surface. Plastic-core fibers can simply be cleaved with a razor. Both can be polished to improve the connection loss.

Figures 5 through 12 document the fiber surface quality at each stage of polishing, using hard-plastic clad. plastic-core and silica-core fibers. The photographs are scanning electron micrographs with 200X magnification. Surface features on the order of 1 µm - the wavelength region of interest - should be readily discernable to the naked eye. Accompanying the scanning electron micrographs are connection loss determinations.

The connection losses shown for most of the steps is the average of three determinations. At certain key steps, we determined the mean and standard deviation for tan. Connection loss was determined by placing a 2 m piece of cable between 820 nm LED and a silicon photodiode to obtain an initial power reading. Then, without disturbing the ends, the cable was cut in the middle, connectors applied, the ends finished as called for, and the connection assembled. Adjustments were made to minimize core misalignment. The ratio of the powers before and after connector insertion gave the connection loss. All connections were made without index-matching oil.

Figure 5 compares four commercially available silica core fibers which have been cleaved using a carbide razor and a flat surface. The plastic cladding was not first removed. 5a) through 5c) are soft clad; 5d), hard clad. In every case, the surfaces showed some features; a) was badly damaged; b) showed some clean optical surfaces, but was highly faceted, which will cause undesired refraction of the light; d) showed very cleas sarfaces with little faceting, but the core was damaged; c) was by far the best, though the surface does have some observacie features. The connection loss for samples similar to 5d) was 7.4 dB.

Find termination could stop here if the system Usually the high mean value and large uncertainty of the loss require users to polish the fiber ends.

Figure 6 shows the hard-clad fiber end after polishing with 600 grit emery paper. The surface was heavily pocked and scratched. The connection loss, 4.1 dB. Figure 7 shows an end polished with 600 grit paper followed by 4/0 grit paper. The end looked quite similar to

the previous one but there were fewer pock marks. The connection loss was 3.5 dB. These two steps served mostly to flatten the fiber end.

Figure 8 represents the first real polishing stap, removing most of the prominent surface features, leaving behind a speckled surface. This step followed the first two with 3.0 micron silicon carbide lapping film. The connection loss was 2.5 dB.

Figure 9 shows the results of the most critical step, polishing with clean 0.3 µm aluminum oxide lapping film. We noted a small amount of debris in the form of streaks on one side and a chunk on the other. This was readily removed in the final step, polishing with polishing microcloth, (Figure 10). We note that in our experiments, using the microcloth had no measurable effect on connection loss. In both cases it was 1.3 dB.

To prepare the end of the hard plastic-clad/plastic-core fiber is even simpler. Many users simply cut it with a sharp razor blade, obtaining a surface as shown in Figure 11. This is very similar in appearance to a cleaved glass end. Connection loss here was 4.7 dB. Now, skipping the three intermediate steps used on the silica-core fiber, Figure 12 shows the razor cut end polished with the 0.3 µm aluminum oxide film, followed by buffing with the polishing microcloth - yielding an essentially perfect surface. Connection loss here was 0.7 dB, better than the silica. We note that the theoretical limit of 0.3 dB exists because of Fresnel reflection losses in a dry connection.

Table III summarizes these results. We see that inadequate end-finishing had a much larger effect than had generally been attributed to it. It is often implied that the end quality will somehow take care of itself. But, today end quality may well be the major determining factor in connection loss.

Of course, connector design and core misalignment both influence the actual loss obtained in a given connection. However, we have made hundreds of connections following the procedure we described next, using inexpensive connectors. Only rarely does the loss exceed 2 dB, and virtually never, 3 dB. The steps outlined for the hard-clad silica fiber were performed by hand in about 30 seconds. Those for plastic fiber, in even less time.

V. End Preparation Technique

We are going to close with a very practical message: the end preparation techniques and connection losses discussed in this paper for hard-clad fiber optic cables are not laboratory curiosities but real, practical, low-cost and in use now.

We are going to flash through pictures of each step as it is being cone, spending about as much time as is actually spent to prepare an end. The technique is generally applicable to any kind of connector.

Step 1

Strip off approximately 4 cm of the outside (black) insulation using a No. 18 stripper hole. This outer jacket is Du Pont "Hytrel" polyester elastomer.

Step 2

Strip back the exposed "Kevlar" aramid fiber to approximately 0.5 cm.

Step 3

Strip the exposed "Hytrel" (white) back to the "Kevlar" using a No. 22 stripper hole. The fiber end will now be exposed.

Step 4

Take the stripped fiber end and push it in the end of the connector until it will go no further. Now crimp, epoxy, or use whatever method the type of connector requires to hold the fiber.

Step 5

Cut the protruding end of the fiber back so that approximately 1 mm still remains past the connector's nose. Now it is ready to polish.

Steps 6 - 10

Take the connector between the thumb and forefinger as if it were a pencil and lightly sand the end across clean sanding papers in the following sequence until no sanding lines appear on the paper. Be sure to blow grit off the end before going on to subsequent sanding steps:

- a) 600-A type paper (it is especially important to sand lightly here).
- b) No. 4/0 paper (5 7 strokes).
- c) Lapping film (3 micron silicon carbide).
- d) Lapping film (0.3 micron aluminum oxide).

Then, using a polishing microcloth, complete the smoothing process.

The final step is to complete the connection.

VI. Conclusion

- Axial core motion in connectors is minimized by hard-plastic clad fibers.
- For 10% core displacements the worst-case contribution to connection loss is 1.6 dB maximum. Connection loss is a slow function of displacement.
- End finish quality is extremely important for achieving low-loss connections. Plastic fibers are especially easy to finish.
- Easy, quick, low-cost, reliable, and low-loss field connections are here now.

REFERENCES

- D. Gloge, et al., Bell Systems Tech., <u>52</u>, p. 1563 (1963).
- K. J. Monaghan, IEEE Trans. CHMT-1, 282 (1978).
- W. Schumacher, Proc. Irc. Wire and Cable Symp., Oct. 1977.
- a) C. Kleecamp, et al., Designers Guide to: Fiber Optics, (Parts 1 to 4), EDN, 1979.
- K. J. Fentor, et al., Insulation/ Circuits, August 1977, pp 27 ff.
- A. Bickel, Course Notes, Fiber Optics, University of Rhode Island, June 1978.
- Z. Tadmor and R. B. Bird, Polym. Eng. and Sci., Vol. 14, 124 (1974).

TABLE I

OF EXPERIMENTAL ENDS

	8	Offset (µm)	Core Diameter (µm)
Test Ends:	11	21	194
	11	21	194
	13	25	191
	17	32	190
serio dita bei	17	33	196
	15	28	195
	14	28	203
Sample Ends:	10	19	193
	25	48	193

TABLE II

ON CONNECTION LOSS

Paggree I This is very sin	Loss	(aB)
Displacement for Sample End (%)	10	25
a. Experimental Maximum A	1.5	2.2
b. Calculated Maximum A	1.6	2.8
c. Calculated Average A	1.1	1.9
d. Experimental Minimum Connection Loss (See Section IV)	1.4	1.4
e. Estimated Maximum Con- nection Loss (a + d) (less than 3% of the total)	2.9	3.6
f. Estimated Average Con- nection Loss (c + d) (less than 50% of the total)	2.5	3.3

Minimum Theoretical Connection Loss: 0.3 dB

TABLE III

EFFECT OF END FINISHING ON CONNECTION LOSS IN HARD-PLASTIC CLAD OPTICAL FIBERS

Polishing Step	Connection Loss(dB)
A. Silica Core	
cleave	7.4
600 grit	4.1
4/0 grit	3.5±0.8
3.0 um silicon carbide	2.5
0.3 µm aluminum oxide	1.3
polishing microcloth	1.3±0.2
B. Plastic Core	
razor cut	4.7⊻2.1
0.3 µm aluminum oxide) polishing cloth	0.7±0.2
C. Theoretical Minimum (dry connections)	0.3



Fig. 1: Soft plastic-clad silica optical fiber. Cladding peeled from core.

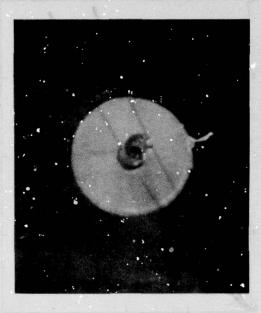


Fig. 2: Soft plastic-clad silica optical fiber. Hollow cylinder of cladding from which core has withdrawn.



Fig. 3: Soft plastic-clad silica optical fiber. Core protrudes well beyond cladding.

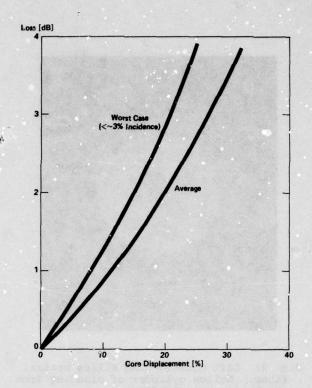
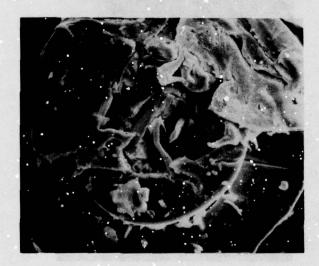
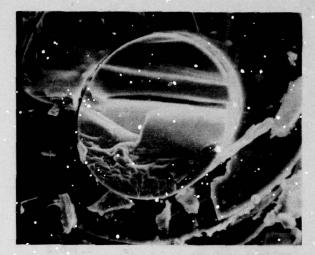


Fig. 4: Incremental connection loss from core misalignment.





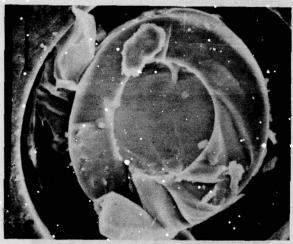




Fig. 5: Four cleaved silica core fibers. A-C) soft-clad D) hard-clad. Cladding has not been removed.

THE RESERVE AND ADDRESS OF THE PARTY OF THE



Fig. 6: Hard-plastic clad silica core fiber ground with 600 grit paper.

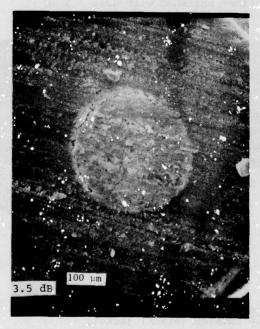


Fig. 7: Hard-plastic clad silica core fiber ground with 600 and 4/0 grit paper



Fig. 8: Hard-plastic clad silica core fiber polished with 3.0 µm silicon carbide after grinding.

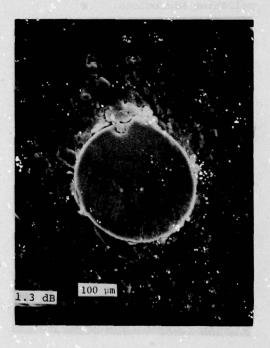


Fig. 9: Hard-plastic clad silica core fiber polished with 0.3 µm aluminum oxide film after 3.0 µm silicon carbide and grinding.

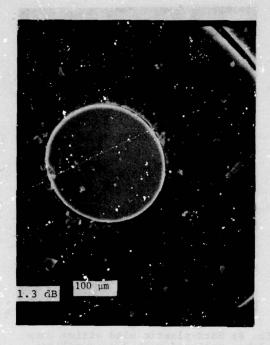


Fig. 10: Hard-plastic clad silica core fiber. Polishing completed with polishing microcloth.



Fig. 11: Hard-plastic clad plastic core fiber. Razor cut.

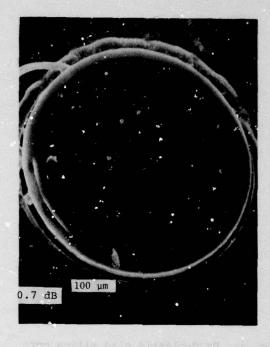


Fig. 12: Hard-plastic clad plastic core fiber polished with only 0.3 μm aluminum oxide and microcloth.



Fig. 13

Step 1 - Strip off approximately 4 cm of
the outside (black) jacket.

TO SEE STATE OF THE SECOND

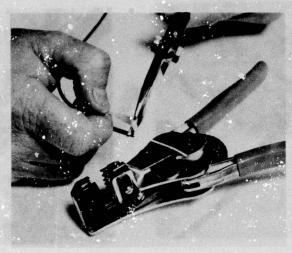
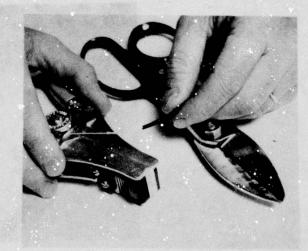


Fig. 14

Step 2

Strip back the exposed "Kevlar" aramid fiber to approximately 0.5 cm.





Step 3

Fig. 15: Strip the exposed inner jacket back to the "Kevlar".

Fig. 16: The fiber end will now be exposed.

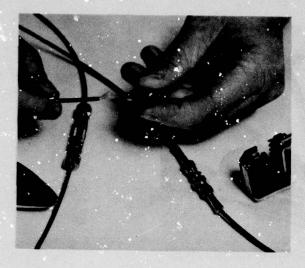
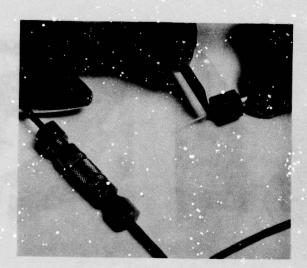


Fig. 17: Take the stripped fiber end and push it into the connector ferrule.



Fig. 18: Now crimp, epoxy, or use whatever method the type connector requires to hold the fiber.



Step 5

Fig. 19: Cut the protruding end of the fiber back so that approximately 1 mm still remains past the connector's nose. Now it is ready to polish.

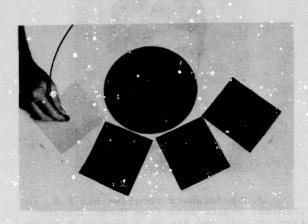




Fig. 20

Fig. 21

Steps 6 - 10

Take the connector between the thumb and forefinger as if it were a pencil and lightly sand the end across clean sanding papers in the following sequence until no sanding lines appear on the paper. Be sure to clean grit off the end before going on to subsequent sanding steps:

- a) 600-A type paper (it is especially important to sand lightly here).
- b) No. 4/0 paper (5 7 strokes).
- c) Lapping film (3 micron silicon carbide).
- d) Lapping film (0.3 micron aluminum oxide).

Then, using a polishing micro cloth, complete the smoothing process.

The final step is to complete the connection.



A. Z. Moss received his A.B. in Chemistry from Columbia University in 1968, and his Ph.D. in Physical Chemistry from the University of Illinois at Urbana-Champaign in 1973. He started with the Du Pont Textile Fibers Department upon graduation. There, he worked primarily in the area of textile flammability. Since 1977 he has been in the Plastic Products and Resins Department, working on PIFAX* Fiber Optic Cables. Dr. Moss's responsibilities include manufacturing and product development.

*Du Pont Trademark



J. H. Aumiller has been with Du Pont since 1961. He worked extensively on photo-imaging and organic adhesives in the Organic Chemicals Department. Since 1975 he has been in the Plastic Products and Resins Department, where for the last two years, he has worked on PIFAX* Fiber Optic Cables. Mr. Aumiller's responsibilities include technical service to Marketing.

*Du Pont Trademark



J. Uradnisheck received his B.S. in Chemical Engineering from Drexel University in 1971 and his Ph.D from Caltach in 1975. He started with Du Pont that same year and has been a Marketing Specialist for PIFAX* Fiber Optic Cables since 1978.

*Du Pont Trademark

LIGHTNING, TRANSIENT AND ELECTROMAGNETIC DISTURBANCES IN THE SWEDISH DEFENCE TELECOMMUNICATION NETWORK

Knut Egeland

S.E. Håkan Mörk

Defence Materiel Administration

Telefonaktiebolaget L M Ericsson

ABSTRACT

In 1975 the Defence Materiel Administration formed a working committee, AG-STÖR, with the task of increasing the availability in the telecommunication network. After an analysis of types of disturbances, including a lightning counter program and a lightning damage report system, the work has resulted in a number of specification standards and installation rules. The committee has initiated the design of material like a hybrid overvoltage arrester for protection of electronic equipment and a static power switch.

In the committee the Defence Materiei Administration, the Central Maintenance Workshops and Telefonaktiebolaget L M Ericsson are represented.

1. LIGHTNING DAMAGE INVESTIGATION AND LIGHTNING FLASH COUNTING PROGRAM

One of the main factors which reduce the availability of communication connections is lightning. Other types of overvoltages, for exemple induction from high voltage lines, are less frequent and normally easier to prevent during the planning of communication systems.

Lightning damages occur both on cables and on connected equipment. The majority of damages occur on telecommunication equipment and cables, however, power supply equipment is by no means immunc.

The lightning damage investigation is based on a very straight-forward report system where maintenance personal fill in details on a preprinted report form for damages which are suspected to have occured due to lightening. To make such a report system work the maintenance personal must be thorougly motivated, which has been achieved by:

- informing them of the result of each years investigation
- informing them of preventive measures resulting from the investigation
- keeping the details to be filled in to a minimum

It is estimated that 70 to 80 % of all lightning damages are reported and that about 95 % of reported damages are due to lightning. The number of reported damages per year divided into main categories are given in fig.1. A further division into types of equipments clearly points out the most sensitive types, i.e. those who should first be subjects of preventive measures.

Cable damages are responsible for a considerable part of the total maintenance time and cost. To reduce cable damages two protective measures shall be generally applied.

- All cable pair including spare pairs shall be protected at both ends with surge arresters of type rare gas tubes.
- All points where wires or cables are connected to a cable with different dielectric strength or different sheaths shall be protected with rare gas tubes.

For cable plants where maintenance statistics show repeated damages protection can be increased. The following points are likly to need further protection:

- loading coils
- transition between aerial and ground cable
- cables in the vicinity of high voltage lines.

The majority of damages occured on electronic equipment connected to relatively long cables. The preventive measures to reduce these damages was divided into two parts:

- specification of voltage durability for line equipment which will be reviewed in point 6 below
- specification of surge arresters for alectronic equipment, see point 7 below.

To evaluate the lightning damages and especially the results of preventive measures it is very helpful to have statistics on the amount of lightning. A lightning flash counting program was started in ten places in 1976. In 1977 the number of places was increased to twenty. The counters are of the CIGRE-type with vertical aerials. Data is collected manually in most places. Remote data collection is used in two places.

Measured keraunic levels for 1976-78 are given in fig. 2 with lightning flash density in fig. 3. Days with less than four countings are disregarded. In the evaluation of flash density it has been assumed that the counters will register flashes within a mean distance of 12.5 km and that 30 % of the registrations come from cloud-to-cloud flashes.

It is very interesting to look for relations between flash density and damages. Data for 18 places during 1978 is given in fig 4. It is obvious that a high keraunic level gives a high probability of damages. No correlation seem to exist between flash density and damages. This is probabley due to the fact that flashes will be registered within a very large area compared to the area where flashes will cause damage.

The investigation shows that preventive measures taken are adequate and will, when fully installed, greatly reduce damages.

2. STANDARD FOR EMC-SPECIFICATIONS

In a complex telecommunication center with equipment of varying generations and large differences in signal levels and power consumptions it is extremely important to have the interference levels under full control. From this aspect equipment include lightning, air conditioning, reserve power generators, alarm systems and so on as well as telecommunication equipment.

It is very time-consuming to make on site tests of all possible combinations of continuous operation, and virtually impossible to test all combinations of operation and on-off switching. These tests can be replaces by laboratory tests on single apparatus if and only if the emitted interference levels for all equipment are well below the sensitivity levels in receiving mode. The only existing standard covering both emitted and received levels is MIL-STD 461, 462 and 463 with Notices. The Military Standards specify default values of interference levels as well as measuring methods for both conducted and radiated emissions.

Since all the measurements specified do not apply to any one type of equipment, the measurements needed are chosen from a classification table where always applicable, sometimes applicable and rarly applicable measurements are given for different types of equipments.

All material tenders, now demand EMC-specifications according to MIL-STD from the suppliers. For existing telecommunication centers on site tests are made in combination with laboratory tests, resulting in modification of the worst emitters as well as the most sensitive receivers.

3. STANDARD FOR INSTALLATION OF TELEPHONE AND ELECTRICITY CABLES

The standard aim at a reduction of emitted and received interferences to improve the internal electrical environment of telecommunication centers. Cables are divided into three classes:

- Class S1: Disturbing cables, including electricity cables, reserve electricity and interruption free reserve electricity cables.
- Class S2: Neither disturbing nor sensitive cables like coaxial cables, waveguides and some alarm cables.
- Class S3: Sensitive cables like speech cables, some alarm cables and supervision cables.

Cables of different classes shall be installed separately, either on different routes or shielded from each other or for short routes kept a certain distance apart. Crossings shall be made at right angles. For frequencies above 200 kHz coaxial cables or waveguides shall be used. Aluminium or steel cable troughs are recommended, especially those types which are divided into two or more shielded troughs by metal walls. Every section of the troughs must be earthed. Metal cable screens and sheats on class S1 and S2 cables shall be earthed at both ends. On class S3 cables screen are normally earthed at one end only.

The electromagnetic coupling between two cables is determined by a number of factors like distance, length of parallellism and shielding effectiveness. The difficulty of shielding from low frequency magnetic fields result in a strong recommendation that lightning protection for both tele and power cables should be placed at the cable entrance.

4. DIRECTIVES FOR EARTHING

Earthing of a telecommunication center means physical connection to ground and/or connection to a reference potential within the center. The earthing system shall accomplish:

- operational earthing of low voltage
- protective earthing of high and low voltage
- interference reduction by earthing of metal parts
- lightning protection earthing
- equipotentialization within the center.

At the same time the earthing system must not cause disturbances by ground loops.

The internal earthing system is based on a heavy copper conductor, the inner ring conductor, separately installed on the outer walls. See fig.5. To this conductor all metal parts are connected one

way only. Metal cable sheats, overvoltage arresters, racks, water pipes, reinforcement irons etc. are all connected to this conductor. By installing this conductor separated from all other installations inspection of earth connections is made very easy.

The external earthing system, see fig. 6, starts with a heavy conductor of copper or galvanized steel installed in the ground encirceling the center. This outer ring conductors is connected to the inner ring conductor at several places, for example as close as possible to the overvoltage arresters. The earthing system then consists of earth rods for deep earthings and earth wires. Earth rods are used for overvoltage arresters, lightning rods, towers, masts and stay wires.

5. EMC-MEASUREMENTS ON POWER SUPPLY EQUIPMENT

During 1976 and 1977 the EMI environment in typical telecommunication centers was investigated. As power supply epuipments were suspected to generate the larger part of interferences, these were chosen as primary objects for investigation. Power supply equipment generally consists of:

- transformers
- diesel power generators
- rectifiers
- batteries
- DC/AC converters

Measurements show that interference levels during continuous operation in general conform with MIL-STD 461, 462.

However, during manual or automatic on-off switching of power supply equipment levels exceeding specified values by up to 70 dB were measured. Fig. 7 gives examples of measured levels of conducted interferences in dB uA/MHz and radiated interference in dB uV/m. MHz.

These measurements emhasize the importance of thorough specification work in tenders for new equipment, as well as continuing modification work on existing equipment.

6. DIRECTIVES FOR SPECIFICATION OF VOLTAGE DURABILITY FOR TELE-COMMUNICATION LINE EQUIPMENT

Equipment connected to external pairs, quad or coaxial cables must be able to withstand both transversal and longitudinal overvoltages. It is advantageous but not absolutely necessary if the voltage durability is in the order of 1 to 2 kV. It is necessary, though, that the voltage durability is a reasonable amount higher than the maximum signal level and that it is specified for both AC and surges. Generators used for testing voltage durability should have a fairly low internal impedance.

Longitudinal alternating voltage durability should be at least 2 kV, 50 Hz for 3°s for balanced lines. Transversal and longitudinal surge voltage durability should fulfil either of classes 1 to 6 below for surges of both polarities with pulse form 10,800 from a generator as in fig. 8. Class 1 should normally be specified.

Class	Pulse 1 peak vo	THE RESERVE THE PARTY OF THE PA	Maximum signal voltage DC + AC speak
1	1000	V	220 V
2	300	V	220 V
3	90	V	60 V
4	45	V	27 V
5	18	V	12 V
6	8	V	5 V

Intermediate amplifiers and repeaters should be specified according to the C.C.I.T.T. recommendations.

7. SPECIFICATION FOR OVERVOLTAGE PROTECTORS

This specification covers a family of overvoltage protectors for protection of pair or quad cables and equipment connected to these cables. The arresters shall allow longitudinal and/or transversal protection according to circuid diagrams in fig. 9.

The protection levels of the arresters shall conform with classes 1 to 6 in point 6 above. For class 1 only primary protectors are used, for the other classes both primary and secondary protectors are necessary. The components of the secondary protectors are chosen according to protection levels and transmission characteristics.

The protectors must be able to take at least ten current surges of pulse form 8/10 and peak current 10 kA with three minutes interval between surges without damage to any component. For pulse form 10/800 they must take at least 1 kA. If the protectors are overloaded they ought to fail in short-circuit mode.

The protectors should influence the matching between equipment and line as little as possible. For speech frequencies all classes must fulfil the requirements given in fig. 10. The demands for base band signals up to 108 kHz apply to class 6 only.

A protector family fulfilling this specification have been designed by L M Ericsson. The physical appearance is shown in fig. 17. These protectors are designed for indoor use and, when installed in a suitable box, for outdoor use. Mounting can be done in standard 19 inch racks on a mounting bar which takes 20 protectors or on walls using a bracket for one protector.



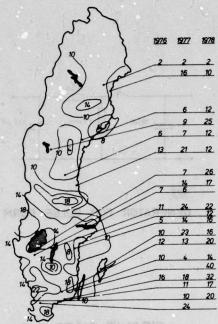
Knut Egeland graduated 1942 from the Technical institute of Stockholm, Sweden as electronic's engineer. After working for 6 years at L M Ericsson with design of electromechanical equipment he joined the Air Materiel Department of the Defence Materiel Administration. After working as head of cable and radio link networks he is now working with special technical investigations such as lightning and NEMP.



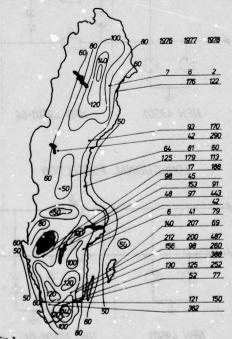
Håkan Mörk graduated 1972 from the Royal Institute of Technology. After working a year as researchengineer at the Institution for Plasma Physis he joined Telefonaktiebolaget L M Ericsson 1973. He is now Head of Technical section of Outside Plant Department of L M Ericsson.

	1975	1976	1977	1978
TELE EQUIPMENT	85	54	78	89
TELE CABLES	8	4	4	9
POWER SUPPLY EQUIPMENT	27	8	17	18
TELEPHONE SUBSCRIPTION	5	3	9	2
TOTAL	125	69	108	118

FIG 1. NUMBER OF REPORTED DAMAGES PER YEAR



LIGHTNING DAYS (days with more than 4 countings)
1958/62 medium valves



NUMBER OF LIGHTNING STROKES FER 100 km² AND YEAR 1958/62 medium values

PLACE	KERAUNIC LEVEL	NO 05 REG	FLASH DENSITY	DAMAGE 1 IMES	NO OF DAMAGED EQUIPMENT
1	17	639	91	1	1
2	25	2028	290	1	6
3	22	3098	443	1	1
4	26	1314	183	4	9
5	20	1050	150	1	1
6	12	291	42	1	1
7	40	2366	338	. 3	8
8	16	551	79	-	
9 1)	12	790	113		-
10	32	1767	252	2	14
11	10	852	122	2	2
12 1)	12	423	60	-	
13 1)	14	1818	260	2	3 2)
14 1)	20	3410	487	-	-
15	16	485	69	4-3	· -
16 1)	2	16	2		- · ·
17	12	1189	170	-	-
18	19	542	77	-	-

- 1) SOME PREVENTIVE MEASURES WAS TAKEN BEFORE 1978
- 2) ONLY UNPROTECTED EQUIPMENT WAS DAMAGED

FIG 4. RELATIONS BETWEEN LIGHTNING FLASH COUNTING AND REPORTED LIGHTNING DAMAGES 1978

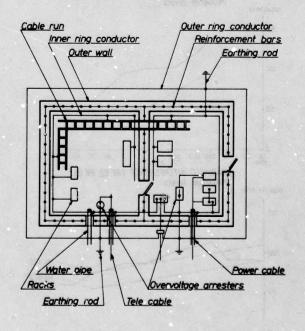


Fig 5. INTERNAL EARTHING SYSTEM

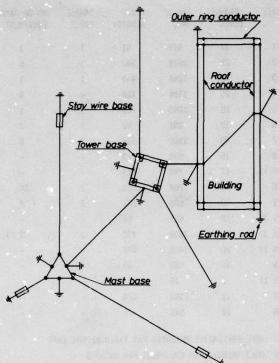
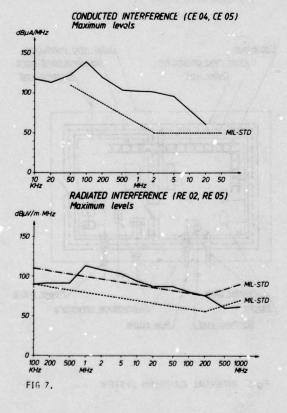


Fig 6. EXTERNAL EARTHING SYSTEM



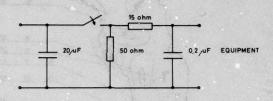
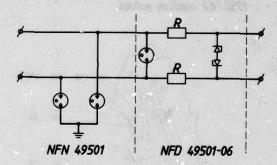


FIG. 8 GENERATOR FOR PULSE FORM 10/800

CIRCUIT DIAGRAMS

TRANSVERSAL PROTECTION



LONGITUDINAL PROTECTION

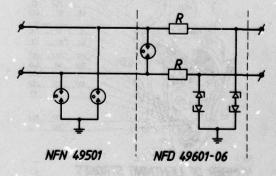
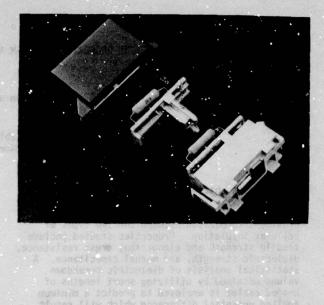


Fig.9

TRANSMITTED FREQUENCY KHZ	LINE IMPEDANCE OHM	ATTENUATION MAX DB	ECHO ATTENUATION MIN DB
0.3 - 3.4	600	1	16
4 - 108	150	0.5	. 24

FIG 10. TRANSMISSION CHARACTERISTICS OF THE PROTECTORS.

Physical Properties. To newcore the provide properties of team and team-able (mulation), newtone, were adjected to the following teams.



A COMPARISON OF THE PROPERTIES OF FOAM AND FOAM-SKIN INSULATION IN FILLED CABLES

Jeff Powers Garmon and Lawrence E. Davis

Superior Cable Corporation Hickory, North Carolina

ABSTRACT

Results obtained from the investigation of specific physical and electrical parameters of foam and foam-skin insulation are presented to provide a comparison between the two types of cellular insulation. Properties studied include tensile strength and elongation, crush resistance, dielectric strength, and mutual capacitance. A statistical analysis of dielectric breakdown values obtained by utilizing short lengths of unaged cables is employed to predict a minimum applied potential difference which will result in a failure of the cellular insulation. Furthermore, changes in the dielectric properties of foam and foam-skin insulation when subjected to accelerated heat aging are determined.

INTRODUCTION

Telephone cables comprised of cellular insulated conductors, which reportedly enjoy an economic advantage¹ over those units employing the more traditional solid insulation, have been monitored for several years in field installations²-³ and have been subjected to numerous laboratory investigations³-8. Two classes of cellular insulation, foam and foam-skin, have presently gained acceptance. Foam insulation consists of a single extrusion coating exhibiting a cellular structure throughout; whereas, the dual extrusion coatings characteristic of foam-skin insulation display an inner foam layer surrounded by a solid layer or "skin".

Data generated in this program from specific physical and electrical tests was used to provide a means of comparing the characteristics of high density polyethylene (HDPE) solid, foam-skin, and foam insulation. Furthermore, cables employing polypropylene (PP) and polyethylene-polypropylene (PE/PP) foam-skin insulation were evaluated to furnish a more general comparison of the two classes of cellular insulation. Both experimental and commercially available cables were included in the investigation.

Examination of the tensile, compression, abrasion, and dielectric properties of unaged specimens, as well as the changes in mutual capacitance and dielectric strength as a consequence of artificial aging provided a gauge for contrasting the behavior of foam-skin and

foam insulation. Of further interest was the dependence upon "skin" thickness of the physical and electrical properties of foam-skin coatings. Moreover, a possible correlation between dielectric strength measurements end the changes in mutual capacitance for pairs of cellular insulated conductors was sought. The procedures employed and the corresponding results are presented below.

THE TEST PROGRAM

Description of Evaluation Samples

Specimens subjected to comparative evaluation included uncabled primary insulation, singles removed from filled cable, and segments of finished cable. Only 24 AWG conductor cables were tested; furthermore, all cables considered were filled with compounds composed of petrolatum and polymers. Presented in Table I is a list of experimental and commercially available cables studied, which includes cables comprised of conductors coated with the following insulations: HDPE foam, HDPE foam-skin, PP foam, and PE/PP foam-skin. In addition, segments of cables consisting of HDPE solid insulation were tested to provide reference levels for measurements performed on cables employing cellular insulation.

It should be noted that the percentage of gas present in the primary insulations of experimental cable A was higher than would be observed in normal production. Also, during the fabrication of experimental cable C, foam-skin insulation exhibiting surface irregularities that can result from the primary extrusion process were included in the cable to determine to what extent the irregularities would be manifested in the electrical characteristics of the cable. Since this primary insulation met the in-process coaxial capacitance and "spark" testing requirements and could be buried within a reel and thus not be visually detected, the properties of the insulation displaying surface blemishes when subjected to post-production testing and accelerated thermal aging were of interest.

Test Procedures

Physical Properties. To compare the physical properties of foam and foam-skin insulation, specimens were subjected to the following tests: tensile strength, tensile elongation, crush resistance, and abrasion resistance. Dimensions

of the cellular insulation such as diameter over the dielectric (DOD) and "skin" wall thickness were determined by means of a micrometer and an American Optical microscope employing a 100X magnification.

Tensile and compression measurements were performed by employing a Baldwin Universal Testing Machine, Model 20B. A cross-arm speed of two inches per minute was utilized for tensile tests; whereas a 0.2 inch per minute speed was used for determining crush resistance. Tensile samples consisted of twelve-inch lengths of insulation carefully removed from an elongated conductor, while specimens undergoing crush analysis were single insulated conductors.

To assess the abrasion resistance of cellular insulation, a General Electric Repeated Scrape Abrasion Tester employing a 0.031 inch mandrel was utilized. Sampler of eighteen-inch long insulated conductor were each subjected to a total of ten measurements, the specimens being rotated by ninety degrees and advanced 1.5 inches after each measurement.

Electrical Properties. Parameters of an electrical nature considered in this evaluation were dielectric strength and mutual capacitance. Dielectric breakdown measurements were employed to study both unaged specimens as well as units subjected to accelerated heat aging; whereas, mutual capacitance observations were utilized to monitor changes occurring as a result of accelerated thermal aging.

Dielectric strength values for cable segments were determined by employing the DC cutput of a Hipotronics HD 100 Series Hipot Tester, which exhibited an upper limit of 40 kV. Two measuring techniques were utilized in Cris program.

One approach determined the DC potential required to cause a dielectric breakdown between the two conductors in a single pair. Specimens of cable exhibited a length of approximately eleven feet so that after preparation of the end portions for testing, a ten-fnot length was eval-uated. Sample preparation consisted of removing approximately six inches of jacket material from each end of the cable segment. Next, the shield was removed from the protruding, unjacketed portion such that the shield extending from the jacket was flared away from the conductors, thus avoiding possible nicks in the cellular insulation during subsequent testing. Approximately four inches of core wrap was removed from each end of the specimen; however, an adequate length of core wrap extended beyond the flared shield to prevent arcing to the shield. Individual conductors on the far end of the cable segment were separated to prevent shorting during the charging portion of the test, while the appropriate conductors on the near end were stripped of one inch of insulation and connected to the leads of the high-voltage tester. A dielectric breakdown measurement was performed by attaching the positive lead of the

high-voltage tester to one conductor of a chosen pair and the negative lead to the remaining conductor. The pair being examined was separated from nearby pairs to prevent arcing. The DC potential was applied continuously at a rate of 100 volts per second until breakdown was achieved.

The second method employed the same equipment, but different sample length, sample preparation, and measuring technique. Sample preparation involved removing the shield and jacket a distance of 24 inches from the near end of the twenty-three foot cable segment and 12 inches from the far end such that the core wrap was not nicked in the process. An 18-inch length of core wrap was then removed from the near end, while a 6-inch portion was removed from the far end of the cable. Approximately 3 inches of insulation was removed from all pairs at the near end, and the pairs were then bonded together by means of a bare 22 AWG conductor. All pairs at the far end were fanned, and at each end of the cable, dielectric tubing was placed over the pair to be analyzed. The tip and ring of the test pair were shorted and attached to the positive lead of the high-voltage tester, while the negative lead was employed to ground the bundle of remaining pairs and the shield. After the breakdown potential for a pair to all others and shield was determined, a second reading for dielectric failure was obtained to insure that only true breakdowns were subsequently analyzed. The DC potential difference was applied manually in a continuous manner at a rate of 500 volts per second until the breakdown potential was achieved.

Mutual capacitance values for pairs within a cable were determined by employing a General Radio 1650-A Impedence Bridge operating at 1000 Hz.

able segments exhibiting 300-foot lengths were positioned in a Blue M forced-draft oven capable at aintaining a constant test temperature, with variations in temperature of + 1°C between extreme locations within the oven. Individual conductors were fanned at the far end, and the conductors at the near end of the specimen were attached to a contact box located external to the oven, thus allowing for the monitoring of mutual capacitance during the thermal aging process without disturbing the position of the cable or leads. A constant temperature of 65° + 1°C was employed during the accelerated aging portion of this program.

Number of Samples Evaluated

The extent of testing was dependent on the nature of the test and upon the type of insulation being measured. Typically, a small sample population was employed for solid insulation, while more measurements were performed for specimens of cellular insulation. The average values for the tensile and compression properties were generated by measuring a minimum of five samples for each of ten colors of cellular insulation and then obtaining an average for each color. Subsequently, these ten values were averaged to provide the data presented in Table II. Each

average tensile and compression value was obtained, therefore, from the measurement of at least fifty specimens. Scatter in the data typical of scrape abrasion measurements required that a minimum of twenty conductors exhibiting cellular insulation be tested, corresponding to a minimum of two hundred observations for a given average value. A minimum of twenty measurements was employed to obtain average readings for the dielectric breakdown of cellular insulation, while the mutual capacitance of at least fifty pairs of conductors was monitored to obtain a single average value.

RESULTS

Unaged Specimens

Tests performed on specimens of uncabled primary insulation and subsequently cabled insulation revealed that, within experimental error, negligible changes were apparent in physical parameters as a result of cableing operations for both HDPE foam and HDPE foam-skin insulation. Table II provides a means of comparing the physical parameters obtained for the three types of insulation considered in this evaluation. standard error, one standard deviation divided by the square root of the number of samples considered, is also displayed in Table II in order to demonstrate the variations observed among specimens in a given test group. Consider, for example, the values for standard error associated with the tensile strength data for cables A and B. A standard error of 20 observed for cable A as compared to 68 for cable B was indicative of the greater variation in tensile strength values exhibited by specimens taken from cable B. Variations in the magnitude of measurements can be attributed to either inconsistency of the insula-tion and/or repeatability for a given test method.

Abrasion resistance was studied by employing a mandrel loaded with weights ranging from 300 to 600 grams. The results of these tests, as displayed in Figure 1, indicate that for cellular insulation possibly two mechanisms, crush and abrasion, are responsible for the eventual failure of the specimens subjected to the higher loads.

Data obtained from dielectric strength measurements is presented in Table III. In addition to providing values for average dielectric treakdown for a test cable, a prediction of a minimum range for dielectric failures, as provided by means of Weibull failure analysis, is presented. Weibull analysis is a statistical technique utilized for studying a small sampling of data and thereby gaining additional information about an entire population from which the data may be taken. By fitting the data to a mathematical expression cailed the Weibull Distribution, a prediction of the percent of all test specimens expected to fail at or below a given test value may be obtained. Appearing in Table III are expected dielectric breakdown values obtained by extrapolating data points plotted on Weibull probability paper. Typical Weibull plots of

dielectric breakdown for cellular insulated conductors, as measured by Method A, a DC wire-to-wire approach, appear in Figure 2. Possible pitfalls associated with the Weibull statistical approach are reported by Stone and Lawless⁹.

Aged Specimens

The effects of insulation expansion and of migration of filling compound into the insulation were observed by monitoring the mutual capacitance (Cm) of paired conductors within cable lengths subjected to a temperature of 65°C. Figure 3 depicts changes in mutual capacitance as a function of time of exposure to the elevated temperature. Only HDPE foam and HDPE foam-skin samples were evaluated in this program; however, similar tests performed by utilizing cables consisting of other types of cellular insulation have been reported by others^{5,7}. As seen from the plots of mutual capacitance (Cm) versus exposure time at the test temperature, pairs within a cable typically exhibited a decrease in mutual capacitance when the heat aging program was initiated, followed by a sometimes sharp and then gradual increase until at some time the mutual capacitance approached a constant value. Properly coated pairs displayed the above described behavior; whereas, cellular insulation exhibiting surface defects yielded mutual capacitance versus time curves which exhibited decidedly different rates of increase. Figure 5 illustrates these differences in the behavior of Cm as the cable was artificially aged. It is noteworthy that defective insulation in a filled cable can yield values for Cm, when measured prior to thermal aging, which cannot be distinguished from properly insulated conductors. Furthermore, cable C, an experimental HDPE foam-skin cable purposefully formed from conductors displaying adequate as well as defective insulation, passed the usual battery of post-production tests such as mutual capacitance, pair-to-pair capacitance unbalance, insulation resistance, and crosstalk. When subjected to dielectric strength measurements, the pairs from cable C exhibiting defective insulation were identified and corresponded to those pairs displaying large increases in mutual capacitance in Figure 5.

To further observe the effects of heat aging of cables comprised of cellular insulated conductors, dielectric strength measurements were performed utilizing cable segments artificially aged for designated periods of time. As presented in Figure 6, the magnitude of the average applied potential difference required to cause a dielectric breakdown between foam insulated conductors of a given pair increased with time of exposure to a test temperature of 65°C until a constant average value was attained. Similar behavior was noted for other cables comprised of both types of cellular insulation.

DISCUSSION

Unaged Specimens

Physical Properties. To compare the physical properties of foam, foam-skin, and solid insulation, consider the data presented in Table II, which lists values obtained from measurements of tensile strength, tensile elongation, crush resistance, and abrasion resistance, and Table I, which provides the percent of gas present in foam insulation and the "skin" thickness of foam-skin insulation. The values shown in Table II should be analyzed only with percentage of gas and "skin" thickness in mind.

Tensile measurements indicated that for HDPE insulation (cables designated as A, C, D, E, and Solid), solid insulation performed at a superior level, tut categorizing into three distinct groups (solid, foam-skin, and foam) appeared possible. However, closer scrutiny of available data revealed the contrary. For foam-skin compositions, tensile strength was observed to be directly re-lated to "skin" thickness when specimens from cables C, D, and E were compared. The average "skin" thickness and average tensile strength for specimens measured from cable C were 0.0021 inches and 1930 psi, while those units taken from cable D exhibited values of 0.0025 inches and 2606 psi, and samples from cable E displayed readings of 0.0025 inches and 2516 psi. Therefore, when tensile strength for foam-skin insulation is analyzed in conjunction with "skin" thickness, the apparent superiority of foam-skin over foam insulation is diminished somewhat so that a more appropriate ranking of insulation types may be solid and cellular, rather than the solid, foam-skin, and foam grouping mentioned previously. Moreover, to maintian proper coaxial capacitance, foam-skin insulated conductors displaying an increase in "skin" thickness may also exhibit a corresponding increase in the diameter over the dielectric (DOD) as well as a possible decrease in the percentage of gas in the foam beneath the "skin". All of the aforementioned changes tend to improve the physical characteristics of foam-skin insulation. It should be noted that cable A was comprised of HDPE foam displaying a percentage of gas (37%) higher than would be observed in production; therefore, higher tensile values would be expected for HDPE foam insulation exhibiting a 30-35 percent "blow", since a small change in percentage of gas content significantly affects physical parameters. Both polypropylene foam and PE/PP foam-skin insulation demonstrated values for tensile strength within the range of those observed for HDPE foam skin. However, as seen in Table I, the percent "blow" in the polypropylene foam insulation was less than that of the HDPE foam insulation tested; and the average skin thickness of 0.0029 inches exhibited by the PE/PP foam-skin insulation was greater than those specimens comprised of HDPE.

Testing for crush resistance revealed that all samples of foam-skin insulated conductors evaluated displayed somewhat higher values than

their foam counterparts. However, the degree of improvement of resistance to crush was minor when compared to crush parameters observed for solid HDPE insulation. The crush resistance values appearing in Table II are related to the magnitude of the compression speed employed during testing, and should therefore be compared only to published data obtained when identical test parameters were utilized.

When large loads (600 gm) were utilized for the scrape abrasion test, the number of cycles of the abrading mandrel required to remove sufficient insulation to reveal the copper conductor were within the same order of magnitude range for either type of cellular insulation; however, consistently higher values for abrasion resistance were obtained for foam-skin insulation than for Furthermore, the abrasion resistance of solid HDPE insulation was observed to be several orders of magnitude greater than that observed for cellular insulation. For smaller applied loads (300 gm), foam-skin insulation loses the consistent advantage over foam displayed when greater loads were utilized. This can be more clearly observed by referring to Figure 1 wherein abrasion resistance curves exhibit that possibly two phenomena are involved in causing scrape abrasion failures: abrasion and crush. When the number of cycles required for the abrading mandrel to cause a failure is plotted versus the applied load on a semi-logarithmic grid, two distinct linear relationships were observed for each curve, excepting that representing solid HDPE insulation. The two distinct linear plots for a given curve may be interpreted as meaning that abrasion was the primary factor involved when smaller loads were utilized; whereas both crush and abrasion were acting simultaneously when higher loads were applied. The crus resistance of foam-skin insulation was shown to The crush be greater than that for foam insulation; and at high applied loads employed during abrasion testing, curves for foam-skin were grouped above those for foam insulation. As observed in Figure 1, the curve representing PE/PP foam-skin specimens from cable F intersects the curve for HDPE foam cable A at lower applied loads. explanations may be given for this behavior: inherently greater crush resistance of the foam-skin insulation was no longer a factor in the scrape abrasion test, and the overall wall thickness for the foam-skin composite was less than that of foam-skin samples removed from cable C but was approximately the same wall thickness for the foam specimens measured. Again, referring to the curves in Figure 1, for values of applied load where abrasion is thought to be the contributing factor resulting in cellular insulation failure, HDPE foam-skin insulated conductors exhibited the greatest abrasion resistance, followed by HDPE foam, PE/PP foam-skin, and polypropylene foam. A vast difference in abrasion resistance characteristics was observed between curves representing HDPE solid insulation and those pertaining to cellular insulation of any composition or construction.

Electrical Properties. To establish a comparison between the dielectric strength of foam and foam-skin insulated conductors, refer to the data presented in Table III where the results of two measuring techniques are presented. First, consider the results obtained by employing Method A, a DC wire-to-wire process. The average applied DC potential required to cause dielectric breakdowns for a short cable length was from 15 to 100 percent higher for foam-skin insulation than for the foam insulation exhibiting the maximum average value. Cable C, exhibiting insulation with an average "skin" thickness of 0.0021 inches, demonstrated the 15 percent improvement in dielectric strength, while cable D, with a "skin" thickness average of 0.0025 inches, displayed the greater average value for dielectric strength. However, when the same measuring technique was employed to study air-core cable comprised of HDPE solid insulation, no reading less than 40 kV, the upper limit of the measuring device, was obtained. The values displayed in Table III for the standard error associated with each average value for dielectric breakdown indicate that larger variations from the average were obtained for foam-skin than for foam insulation. Such a trend may be explained by variations in the "skin" thickness observed from sample to sample within a given cable comprised of foam-skin insulated conductors. It should be noted that the aforementioned variations in "skin" thickness were observed for both experimental and commercially obtained cables, where the extruder was or may be assumed to have been operating under the specified tolerances. Based on average values for dielectric breakdown, grouping of insulation types into three categories (solid, foam-skin, and foam) appeared feasible; however, Weibull analysis of the data revealed that ranking according to average values was misleading. tical methods for determining minimum predicted values for the dielectric strength of the cable lengths indicated that only a minor difference existed between the performance of individual foam and foam-skin cables.

The Weibull distribution was employed to provide a statistical analysis of dielectric breakdown data to determine the predicted failure rate for a given applied DC potential. Using Weibull analysis involved plotting data on special probability paper, so constructed that data which followed the Weibull distribution would fall on a straight line. The data points were arranged according to magnitude, and the percent of samples failing at or below a given applied voltage (y-axis) was plotted versus the applied potential (x-axis). For large sample populations, the y-axis value (percentage of samples failed at or below a given applied voltage) for a corresponding x-axis value (applied voltage) was approximated by the cummulative percentage method, i/n, where the order number, i, was divided by the sample size, n. Data generated by measuring the dielectric breakdown of both foam and foam-skin insulation was subjected to Weibull analysis and plotted as shown in Figure 2, the reliability of

performing a dielectric strength measurement according to the procedure outlined for Method A was determined from the Weibull curve for any applied voltage by subtracting the corresponding values on the y-axis, in percent, from one hundred. The applied voltages for a Weibull 99% Reliability (99% of all samples predicted to fail above stated value) are presented in Table III and were obcained by extrapolating the Weibull plots to a horizontal line representing a y-axis value of 1.0%. Curves obtained from measurements of foam insulated cable resulted in a single straight-line fit of the data; whereas for foam-skin insulation, plots exhibiting a concave curvature were typical, indicating that two subpopulations were included in the data. When the two subpopulations were identified and plotted, straight-line fits to the data were obtained. By extrapolating the Weibull plots corresponding to each of the two subpopulations, a range for Weibull 99% Reliability was obtained and is presented in Table III. As seen in Figure 2, curves representing HDPE foam (37% "blow") and PP foam (30-35% "blow") appear to the left of both HDPE and PE/PP foam-skin insulation, and thus would appear to indicate that foam insulation is more susceptible to dielectric breakdown than foam-skin. However, comparison of the Weibull 99% Reliability values indicate that the lower portion of the range exhibited by the foam-skin constructions approaches those values displayed by foam insulation. For the five cables represented in Figure 2, expected dielectric breakdown values as indicated by Weibull 99% Reliability imply that no conclusive advantage is enjoyed by foam-skin insulation when contrasted with foam insulation. Small variations from the stated Weibull 99% Reliability for the foam insulation (cables A and B) could be obtained from straight-line fits to the data; however, the large range given for cables D and F represents the existence of two distinct sample populations resulting from dielectric breakdown testing. The large range for Weibull 99% Reliability values apparently inherent in the data obtained from foam-skin dielectric strength testing may be a manifestation of the magnitude and variation in "skin" wall thickness (Table I). It should be noted that the Weibull plot of data from cable C appears to "bridge the gap" between the other four curves displayed in Figure 2. Selected specimens from cable C, an experimental HDPE foam-skin cable, exhibited the smallest wall thickness and least variation from sample to sample of the foam-skin cables which were evaluated. Furthermore, these selected foam-skin specimens, when subjected to dielectric strength testing and subsequent Weibull analysis, behaved rather like their foam counterparts when the shape of the Weibull curves and the Weibull 99% Reliability values were compared.

Another technique, designated as Method B, for determining the dielectric strength of cellular insulation was employed whereby the DC potential difference was applied between one pair and the combination of all other pairs and shield. The average values for dielectric breakdown as measured for a given cable by employing

and the second second

either Method A or Method B were similar. For foam insulation, Weibull analysis of data generated from the two techniques revealed that consistently lower ranges for Weibull 99% Reliability were obtained by utilizing Method B. Furthermore, Weibull curves representing foam insulation as measured by utilizing Method B exhibited a concave curvature, which suggested that more than one population was being considered. It should be recalled that when Method A was employed, a straight-line fit was observed, indicating a single population or failure mode. Although only selected pairs within a cable binder unit were measured, it appears that the foam, and possibly the foam-skin insulation, was damaged during the testing process, thereby yielding a group of low values for dielectric breakdown corresponding to a second Weibull failure population not evidenced by the data generated from employing Method A. The existence of possibly two failure modes exhibited by employing Method B to determine di-electric breakdown for cellular insulation should be recognized if more than one pair from a given binder unit is tested.

Aged Specimens

The effect of accelerated thermal aging on segments of cable containing HDPE foam and HDPE foam-skin insulated conductors observed by monitoring changes in the mutual capacitance of pairs within the cable segments is depicted in Figure 3, where the percentage change in average mutual capacitance from the initial value recorded at 23°C is plotted versus time of exposure at 65°C. The measurements taken prior to and after thermal aging were performed at 23°C, while the remaining observations were made at 65°C, thus allowing for specimens to be maintained at a constant elevated temperature throughout the evaluation. As can be interpreted from Figure 3, an initial decrease in mutual capacitance was observed due to expansion of the insulation when the samples were first subjected to the elevated temperature. However, within 24 hours of the initiation of the aging program, a rather rapid increase in mutual capacitance values was sometimes observed, attributable to the migration of filling compound into the cellular insulation. Within a two-week interval, the rate of increase of the mutual capacitance had declined sufficiently for the curves plotted in Figure 3 to approach a constant value. The measurements performed subsequent to the aging program indicated that the change in average mutual capacitance for pairs within the aged cable segments was quite small. Residual swelling of the cellular insulation as well as entry of filling compound into the cellular structure were responsible for the difference noted in initial and final mutual capacitance values.

During the course of this investigation, it was observed that a possible correlation existed between the dielectric breakdown behavior of an unaged cable and mutual capacitance changes of specific pairs within the cable when a segment was subjected to accelerated heat-aging at 65°C.

During the fabrication of cable C, an experimental unit comprised of HDPE foam-skin insulated conductors, it was noted that lengths of primary exhibited surface irregularities, yet passed in-process coaxial capacitance and "spark" testing requirements. Two types of surface irregularities were observed; the solid skin portion of one segment was scraped by means of a small polymer fragment located near the die region of the extruder, while another segment of foam-skin primary displayed a rough "blister-like" surface blemish. As previously mentioned, both properly fabricated primary and those conductors coated with defective insulation were subsequently incorporated into cable C. Dielectric breakdown measurements performed by employing a short length of cable C and previously described Method A revealed several values whose magnitudes were considered low for the foam-skin construction. Weibull analysis of the data, depicted in Figure 4, indicated that when all data points were considered (acceptable insulation as well as the questionable insulation exhibiting surface irregularities), a plot, labeled as 1 and displaying concave curvature, was observed which suggested the existence of two subpopulations. When those pairs which exhibited surface irregularities were not considered, Weibull analysis yielded a straight-line fit to the dielectric breakdown data, as represented by curve 2 in Figure 4.

Observation of the changes in mutual capacitance of pairs contained in experimental cable C indicated that the foam-skin insulation displaying surface deformations aged differently from properly fabricated pairs. Higher average values for mutual capacitance were obtained for pairs containing damaged insulation than for those properly formed, as evidenced by the curves presented in Figure 5. The lower plot labeled as curve 1 indicates the aging behavior of pairs of conductors coated with properly fabricated foam-skin insulation; whereas, curve 2 represents data obtained from pairs exhibiting the aforementioned surface irregularities. The error bars for curves 1 and 2 were obtained by employing the standard error associated with each average mutual capacitance value; therefore, the limits for error are representative of the variations from pair to pair as well as variations in measured values due to experimental error. Deviations from the average mutual capacitance values for pairs displaying acceptable foam-skin insulation were small, as indicated by the magnitude of the error bars associated with curve 1. A contrasting behavior was observed for those pairs thought to exhibit surface irregularities, as depicted in curve 2 of Figure 5. To further demonstrate the aging behavior of foam-skin insulation exhibiting damaged "skin", consider curves 3 and 4 presented in Figure 5 which show the effects of heat aging on mutual capacitance values for individual pairs displaying damaged insulation. The error bars for curves 3 and 4 represent variations expected due to experimental error, since each data point refers to a single reading rather than an average value. It should be noted that the defective insulation was not of such severity to cause

cable C to fail normal post-production test procedures. Furthermore, mutual capacitance measurements of pairs within cable C prior to heat aging revealed no differences between properly formed and damaged "skin".

CONCLUSION

The average values obtained for the physical parameters considered in this program were typically somewhat higher for foam-skin than for foam insulation. However, when considering the variation in values from specimen to specimen within a given test unit, foam insulation was observed to be more consistent. The magnitude of the physical parameters for the foam-skin construction displayed a direct dependence upon "skin" thickness; whereby, a small increase in "skin" thickness resulted in a substantial improvement in physical properties. For the nominal "skin" thickness of 0.002 inches required to insure optimum economical product for foam-skin insulation, physical data reported herein indicated that when compared to solid HDPE insulation, both foam and foam-skin insulation exhibited similar behavior.

Both crush and abrasion were identified as the two mechanisms responsible for cellular insulation failure when large loads (500-600 gm) were employed in the scrape abrasion test. Thus, to obtain true abrasion resistance values, specimens should be subjected to small loads (300-400 gm).

Higher average values for dielectric breakdown were obtained for foam-skin insulated conductors than for those coated with foam insulation; however, the intrinsic dielectric strength for both types of cellular insulation were observed to be within the same range when Weibull statistical analysis was employed. Similar minimum dielectric breakdown values are projected for either type of rellular construction.

Based on both the physical and dielectric strength testing performed in this program, a grouping of insulation types into solid and cellular seemed more appropriate than a classification which ranked the two cellular types of insulation separately.

Artificial aging of cellular cable specimens revealed, as expected, small changes in mutual capacitance, not of a magnitude which would impair transmission properties. Furthermore, specimens subjected to thermal aging exhibited increases in dielectric strength as a consequence of insulation swelling and migration of filling compound into the cellular insulation.

A correlation between the results of dielectric strength measurements of unaged HDPE foam-skin insulation and the changes in mutual capacitance observed for cables containing HDPE foam-skin insulation when subjected to thermal aging was observed. Individual pairs of foam-skin

insulation, which exhibited surface defects and which passed normal production testing, aged differently from pairs displaying properly fabricated foam-skin. The dielectric strength measurements were capable of identifying the defective insulation which displayed unacceptable increases in mutual capacitance during the aging program.

REFERENCES

- [1] E. D. Metcalf, "Cellular Insulation as an Answer to Material Conservation", Proceedings of the Twenty-third International Wire and Cable Symposium, pp. 53-58, 1974.
- [2] J. Pritchett, E. L. Mather, and S. Verne, "Fully-filled Telephone Cable with Cellular Polyethylene Insulation after 10 Years Service", Proceedings of the Twenty-fourth International Wire and Cable Symposium, pp. 347-360, 1975.
- [3] S. M. Beach, K. R. Bullock, and D. F. Cretney, "The Properties of Cellular Polyethylene Insulated Filled Communications Cable and its Increasing Use", Proceedings of the Twenty-fourth International Wire and Cable Symposium, pp. 379-398, 1975.
- [4] E. J. Gouldson, M. Farago, and G. D. Baxter, "Foam-skin, a Composite Expanded Insulation for Use in Telephone Cables", Proceedings of the Twenty-first International Wire and Cable Symposium, pp. 158-172, 1972.
- [5] S. G. Foord, "Compatibility Problems in Filled Cellular Polyolefin Insulated Telephone Cables", Proceedings of the Twenty-second International Wire and Cable Symposium, pp. 23-29, 1973
- [6] G. A. Schmidt, "Life Prediction of Insulations for Filled Cables in Pedestal Terminals", Proceedings of the Twenty-sixth International Wire and Cable Symposium, pp. 161-180, 1977.
- [7] C. K. Eoll, "The Aging of Filled Cable with Cellular Insulation", Proceedings of the Twenty-seventh International Wire and Cable Symposium, pp. 156-170, 1978.
- [8] E. D. Metcalf, "Foam-skin Insulation for Filled Cable", Telephone Engineer and Management, pp. 132-134, April 15, 1979.
- [9] G. C. Stone and J. F. Lawless, "Weibull Statistical Analysis of Aging Tests on Solid Electrical Insulation", IEEE Transactions on Electrical Insulation, Volume EI-13, pp. 13-16, February, 1978.

ACKNOWLEDGMENTS

The authors thank Superior Cable Corporation for permission to publish this paper. The many measurements performed by M. Stearns, D. Coleman, and B. Beal are appreciated. Finally, thanks are due to R. Riley for typing the manuscript.

TABLE I. DESCRIPTION OF CABLES EVALUATED

wabwalla fi a	99(9f) = 5 U(A) W	Wire Size	Average "Skin" Thickness		
Designation	Type of Insulation	(AWG)	x (in)	σ	
Α	HDPE Foam 1	24		5.03	
В	PP Foam ²	24	- 		
c /	HDPE Foam-skin	24	0.0021	0.0004	
_ TT D	HDPE Foam-skin	24	0.0025	0.0006	
E	HDPE Foam-skin	24	0.0025	0.0006	
F	PE/PP Foam-skin	24	0.0029	0.0010	

NOTES: 1 Percentage of gas in insulation: 37%

Percentage of gas in insulation: 30-35%

TABLE II. PHYSICAL PROPERTIES OF CELLULAR AND SOLID INSULATION

Cable Strength (psi)		ength	Percent Elongation (%)		Crush Resistance (1bs)		Abrasion Resistance (Cycles at 600 gm)		Abrasion Resistance (Cycles at 300 gm)	
	x	σ/ N	×	σ/\sqrt{N}	×	σ/ √ N	x	σ/√N	x	σ/-√N
Α	1445	20	364	7	305	17	4.8	0.06	399	22
В	2528	68	950	144	367	5	4.6	0.3	111	42
С	1930	47	450	18	380	5	4.9	0.3	645	54
D	2606	66	563	12	414	5				
E	2516	98	584	7		_	<u></u> 0			_
F	2966	44	595	7	425	9	7.3	0.6	235	48
Solid	4110	49	870	8	1180		1043	168		_

TABLE III. DIELECTRIC STRENGTH FOR CELLULAR AND SOLID INSULATION

	METHOD A -	Dielectric	Breakdown 1 (kV)	METHOD B - Dielectric Breakdrwn 2 (kV)			
Cable	Average Value		Weibull \$9%	Average	Value	Weibull 99%	
Designation	x σ/√N		Reliability ³	x	σ/√N	Reliability ³	
А	10.9	0.14	9.0	9.5	0.3	5.5 - 8.5	
В	13.1	0.2	9.5	13.4	0.3	7.5 - 10.5	
С	15.3	0.6	9.5				
D	26.1	1.1	11 - 18	18.9	0.6	10 - 14	
F	20.6	0.8	11 - 18	20.0	0.5	11 - 18	
Solid	>40.0		20 A -	>40.0			

NOTES: 1 Method A: DC, wire-to-wire.

² Method B: DC, pair to all others and shield.

Weibull 99% Reliability: 99% of all samples are predicted to fail above stated value.

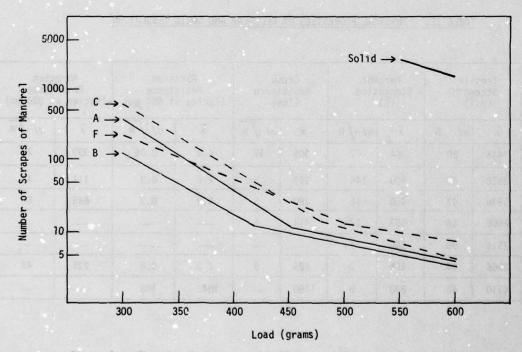


Figure 1. Abrasion Resistance of Cellular and Solid Insulated Conductors.

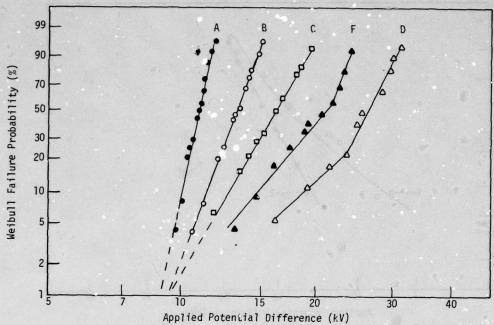


Figure 2. Weibull Analysis - Dielectric Breakdown of Cellular Insulation as Measured by Method A.

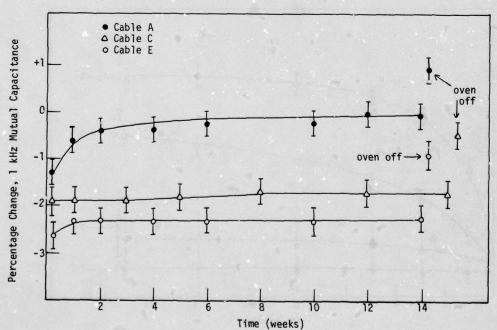


Figure 3. Percentage Change in Mutual Capacitance Versus Time of Exposure at 65°C for Cellular Insulation.

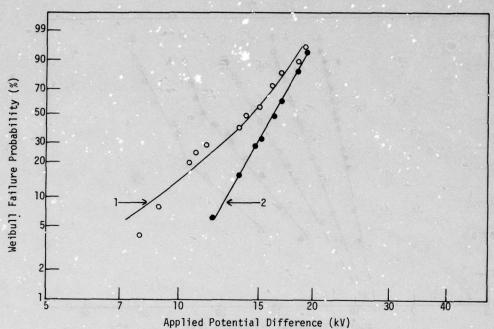


Figure 4. Weibull Analysis - Dielectric Breakdown Behavior for Foam-skin Cable C as Measured by Method A.

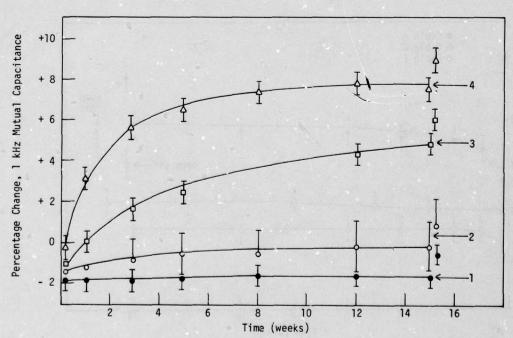


Figure 5. Percentage Change of Mutual Capacitance of Cable C Versus Time of Exposure at $65^{\circ}\mathrm{C}$.

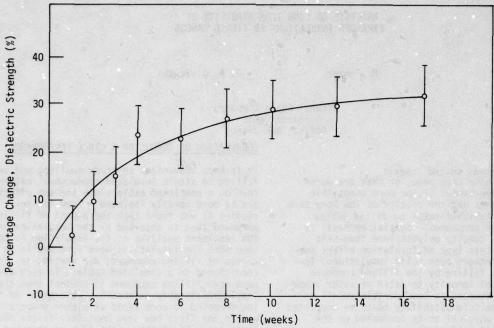


Figure 6. Percentage Change of Dielectric Strength Versus Time of Exposure at 65°C for a Cable Exhibiting Foam Insulation.



Jeff Powers Garmon is a Materials Engineer for the Technical Staff, Superior Cable Corporation. He received a B.S. degree in physics in 1970 from Berry Coliege, Mt. Berry, Georgia, and was granted a Ph.D degree in solid state physics in 1976 from Clemson University, Clemson, South Carolina. Prior to his work at Superior Cable, he was an Assistant Professor of Physics at Auburn University, Auburn, Alabama, and a Materials Engineer for Continental Telephone Laboratories.



Lawrence E. Davis is the Materials Engineering Supervisor for Technical Staff, Superior Cable Corporation. He received his B.S. degree in physics from Appalachian State University in 1969 and graduated with a Masters Degree in physics from the University of Wisconsin, Milwaukee, in 1974. Prior to joining Superior Cable, he was a Materials Engineer for Continental Telephone Laboratories.

ANALYSIS OF LONG TERM STABILITY OF EXPANDED INSULATIONS IN FILLED CABLES

M. Tenzer

J. A. Olszewski

General Cable Company -Research Center Edison, New Jersey

ABSTRACT

This paper reports on the recent advances that have been made, or that are under way, in the development of the more compatible filling compounds and the results of the long term transmission stability tests on filled cables employing these compounds. Special emphasis is placed on high density polyethylene foam-skin insulation as this type of insulation offers certain size advantages over solid insulation. Immunity to cell filling by the filling compound and the critical immunity to water or water vapor ingress are discussed in considerable detail in terms of transmission stability tests on completed cables and in physical tests conducted on the single insulated conductors.

INTRODUCTION

Foam skin insulated filled cables are receiving more favorable consideration as a replacement for solid insulated filled cables because of reduction in size and material conservation. It is anticipated that this trend will continue with the increasing restrictions on petro-chemical materials. The advantage of foam-skin is obvious the reduction of the dielectric constant of the insulation permits closer pair spacing and smaller overall dimensions for a given conductor size. We have developed a better understanding of the long term stability with respect to gradual migration of the filling compound into the cells, and the possible condensation of moisture into the cells in the presence of water. Advances are being made on new filling compounds and this paper will assess their influence on the long time stability of filled foam-skin cables.

The phenomenon of absorption of the petrolatum based filling compound components by polyethylene insulation is well known for some time, as for example, reported by Verne et al(1) and Jachimowicz et al(2). The absorption causes swelling of the insulation and may cause cell filling of expanded insulation. The process is both time and temperature dependent and varies to a large extent with the material systems involved. Viscosity of the filling compound, molecular weight distribution of the insulation/filler system and insulation cell structure were found to be important factors.(3)(4)

CORRELATION OF CONDUCTOR & CABLE PERFORMANCE

It is more convenient to study swelling and cell filling on single insulated conductors, rather than on a completed cable since the two effects can be more readily isolated. From earlier studies it was found that the amount of filling compound that is absorbed by the insulation and the resultant swelling of the insulation is the same when the insulations were immersed in an excess of filling compound; dip coated, or conditioned in a simulated cable. In each case much more filling compound is present than the insulation is able to absorb. Absorption of filling compound is more rapid at higher temperatureswithin the first few days most insulations absorb about one half of the weight that is absorbed Once saturation with filling comafter one year. pound occurs, under some circumstances migration of the filling compound proceeds into the cells. First an oily film is formed on the inner surface of the cell and with time some of the cells may fill. Figure 1 is a unique photograph of a frozen section of insulation taken with an optical microscope in which the arrow indicates a partially filled cell. In the cell below it, the filling compound has coated the inside of the cell, and is beginning to fill toward the center.

Electrical evaluation of cable transmission stability with time, primarily the stability of its capacitance, shows the net effect of both swelling and cell filling. Swelling causes decrease in capacitance due to increased separation between wires in the cable core, while cell filling causes increase in capacitance due to increase in the dielectric constant of the insulation next to the conductor. These two effects tend to counterbalance each other, although not necessarily as the same function of time. In this section of the paper, we will examine these effects for comparable filled cables employing the same type of filling compound (Q Series).

Typical weight gain and diameter changes conducted on solid and foam skin singles immersed in filling compound as a function of aging time and temperature are shown in Figure 2. It can be readily seen from the curves at 70°C that the weight gain has two distinct stages; i.e., first high rate of permeation into insulation material matrix which causes swelling and leads to a relative rapid capacitance decrease and then normally much slower rate of permeation for cellular insulations

and almost zero for solid insulations which causes no additional swelling. The lower the slope of the weight gain in the second stage, the lower is the rate of cell filling. As far as the first stage of weight gain and resultant swelling is concerned, it is more or less constant for given type of insulation material; i.e., high density polyethylene, polypropylene, etc.

However, all long term weight gain in the second phase cannot always be attributed to cell filling. Figure 3 shows an interesting case of abnormally high weight gain with aging at 70°C, with normal swelling behavior. This case was investigated further with the aid of a scanning electron microscope and it was found that the filling compound fractions accumulated in a gap between conductor and its insulation. This confirms the theory expressed by Verne(3) and Foord(4) that large or interconnecting cells are subject to greater rate of filling than small cells.

Figure 4 examines the long term mutual capacitance stability of filled solid and foam-skin cables at 70°C using the same insulation systems and filling compounds previously studied as singles. The change in mutual capacitance, referred to room temperature, is plotted as a function of time. It is apparent that at the start of aging the mutual capacitance of solid insulated cables drops while that of foam skin filled cables also drops but considerably smaller amount. This high rate of change is caused by the swelling effect in the insulation and the increase in conductor spacing. The foam skin insulations change less because of their greater resiliance and tendency to deforma-tion more. As the aging progresses, the capaci-tance of solid insulated cables stabilizes at about -1 to -2% change and is dependent on the filling compound and the type of insulation employed. The capacitance of foam skin insulations initially decrease -0.5 to -1.0%. As aging continues, the mutual capacitance begins to rise due to gradual cell filling. The rate of capacitance increase with time is a function of insulation/filler system, cable design and the temperature. However, for well designed systems it can be very small. For example, for 70°C the foam-skin insulated cables with Q Series filling compounds show only 1 1/2% increase of mutual capacitance (C_m) over a three year period. The actual changes in Cm would also vary with the size of the cable and the mechanical characteristics of the sheath and jacket materials.

The Q Series filling compound is a petrolatum base compound with modifiers that account for its significantly better performance. Preliminary data is also shown on a new B Series filling compound which will be discussed in a later section.

Yard aging tests were conducted for a period of five and one half years at the Research Center, Union, N. J., and mutual capacitance monitored periodically (Figure 5). As to be expected the changes in mutual capacitance were much slowed down and at least three years is required to reach the minimum mutual capacitance. (This is also

consistent with the room temperature data shown in Figure 2 on the single conductors.) This is further verified by the microphotograph (Figure 6) of a 25/22 foam skin insulated cable filled with Q Series compound after storage for 3 years in the reel yard at Bonham Texas. There is absolutely no evidence of any cell filling. The yard aging most nearly approximates the aerial plant; for the buried plant the temperature excursions are relatively lower. By proper selection of the insulation/filler system the rate of cell filling can be minimized over the expected service life of the cables.

LONG TERM STABILITY IN WATER IMMERSION

Improvements have been made in the stability of filled solid and cellular cables with respect to immunity to water since their introduction over a decade ago. Early problems with channeling of water between the cable core and sheath, and water ingress in the core have been virtually eliminated. Properly filled cables are now routinely capable of withstanding the industry standard pressure test under a 3' head of water with no longitudical water leakage for a minimum of 30 days.

Long term measurements have been made of the change in mutual capacitance for cable stored under water for 2000 days - 5 1/2 years. Figure 7 demonstrates that the relative rate of mutual capacitance change (LN Cm/Cmo) are very similar for both solid and foam skin HDPE utilizing the same filling compound. Both 22 AWG cores were incorporated in the same sheaths so that any water entry would have a very similar effect on both types of insulation. All samples were 30 ft. long, with 26 ft. length immersed in a 3 foothead of water at room temperature. Holes 3/8 in. diameter were cut through the sheaths, including the core tape, at intervals of 1 foot, and rotated at 90° from each other. (5)

Extrapolating the data of Figure 7 for W Series filling compound to 10,000 days, equivalent to 30 years of under water exposure, indicates an expected capacitance change of 14% for solid and 16% for foam skin insulation under these test conditions. Comparable data for the 0 Series filling compound has been in progress for approximately three years - but appears to be leveling off at an upper limit of about a 10% increase of Cm. Thus at room temperature, equivalent to buried plant, filled foam skin cables are comparable to filled solid cables with regard to their water stability. These data on filled cables also indicate they degrade much more gradually in comparison with water flooded air core cable where mutual capacitance can increase to 125% in a comparatively short time.

Concern has also been expressed that continuous channels can be formed in the filling compound if sufficient filling material is depleted from the interstices due to cell filling.(6) Experimental evidence to date on these new filling compounds/cable insulation systems with little or no appreciable cell filling, have a high degree

of immunity to water and water vapor ingress. It appears that any air which is expelled from the foam cells would remain as small discontinuous bubbles throughout much of the service life of the cable. This concept will be validated as more experience is developed on the behavior of these cables. Water immersion tests are also in progress at elevated temperatures (50°C) to accelerate the process of water permeation, but they have not proceeded for a sufficiently long time period to establish any meaningful correlation.

FILLING COMPOUND MODIFICATIONS

Petroleum Jelly is the underlying base of most cable filling compounds. However, by the very mature of its processing, it contains a wide range of molecular weight oils where fractions can permeate into polyethylene. Several experimental filling compounds are under investigation as alternatives to the present petrolatum based Q series.

All of these compounds have high surface tension and high melting points, they are pliable and tacky, and in addition, flexible over the temperature range that is encountered during the service life of the telephone cable. In order to have filling compounds available that do not fill the pores of the cellular insulation, initially two filling compounds were developed. These new compounds that are identified as the A, B and F Series do not contain petrolatum. Their base materials are uniform, well defined oils and their behavior and effect on the insulation are expected to be much less variable than that of petrolatum based compounds.

The absorption characteristics of these filling compounds at 70°C are indicated in Figure 8. The first tests were run on the A and B Series using a 55% expanded 8 mil wall of HDPE compound, followed by 2.5 mil skin of HDPE-Type D. Significant improvements in the absorption rate are shown after six months. Weight gain data was augmented by visual observations with the scanning electron microscope. After 4 1/2 months in Q Series compound many cells of the foam layer of insulation were completely filled (Figure 9a). To verify the observations on these specimens, the filling compound was extracted by a solvent and the empty cells verified by photomicrographs (Figure 9b).

Adjacent samples of insulation were also examined after immersion in the Aseries and B series compounds after both 4 1/2 and 6 months at 70°C. Microphotographs taken after 6 months clearly demonstrate that cell filling did not occur.

A second series of immersion tests were undertaken using the Type T HDPE material for the skin. In addition a new series of F compounds were introduced, very similar in composition to the B series. While the aging data for the F series shown in Figure 8 is not of long duration, it is highly encouraging, and appears more stable with respect to capacitance variation.

The behavior of these newer filling compounds are undergoing evaluation in experimental cables.

Figure 11 is the measured mutual capacitance at 1 kHz and verifies the lower absorption rate of the B Series using both liquid and semi-solid filling techniques. The same general performance is demonstrated for changes in attenuation for carrier frequencies at 772 kHz (Figure 12).

CONCLUSIONS

The results of the long term aging and water immersion tests on foam-skin high density polyethylene (HDPE) insulated filled telephone cables show that a proper design of insulation-filler system yields cables with sufficient stability of transmission characteristics to warrant adoption of this cable construction in the outside plant. By proper design of the filler/insulation system, cell filling by filling compound fractions (oils), can be insignificant or small within the expected service life span of filled cables, both in buried and aerial environment. Long term immunity to water at room temperature is equivalent to solid HDPE cables - continued evaluation is still required at elevated temperatures.

ACKNOWLEDGEMENTS

Special thanks are due to Ludwik Jachimowicz for his valuable suggestions and review of the manuscript, and to Gertraud Schmidt who directed the development of the filling compounds and provided the excellent microphotographs.

REFERENCES

- (1) S. Verne, R. T. Puckowski and A. A. Pinching, "Long Term Stability of Polyethylene Insulated Fully-Filled Telephone Distribution Cables", International Wire & Cable Symposium, Atlantic City, N. J., 1971.
- (2) L. Jachimowicz, J.A. Olszewski and I. Kolodny, "Transmission Properties of Filled Thermoplastic Insulated and Jacketed Telephone Cables at Voice and Carrier Frequencies", IEEE Communications Conference, Philadelphia, Pa., 1972.
- (3) S.G. Foord, "Compatibility Problems in Filled Cellular Polyolefin Insulated Telephone Cables", International Wire & Cable Symposium, Atlantic City, N.J., 1973.
- (4) S. Verne, A.A. Pinching and J.M.R. Haggar,
 Long Term Stability of Fully-Filled Cables",
 International Wire & Cable Symposium, Atlantic
 City, N.J., 1973.
- (5) J.A. Olszewski, "Immunity to Water of Foam, Foam-Skin and Solid Insulated Filled Telephone Cables", International Wire & Cable Symposium, Cherry Hill, N. J., 1975.
- (6) D. Mangaraj, M.C. Biskeborn and K.D. Kiss, "The Effect of Filling Compound on Cellular Insulation", International Wire & Cable Symposium, Cherry Hill, N.J., 1978.



1000X

FIGURE 1: DEMONSTRATION OF CELL FILLING OF A CELLULAR
INSULATION WITH A PETROLEUM BASED FILLING COMPOUND AFTER
EXPOSURE FOR 2 MONTHS AT 70°C.

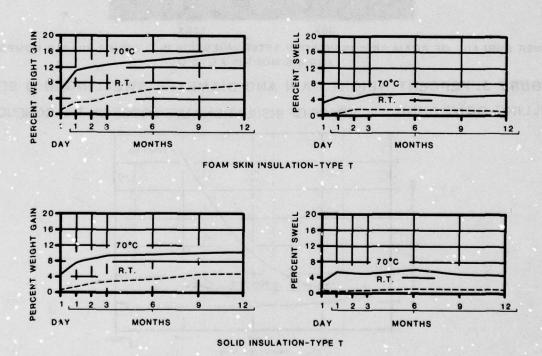
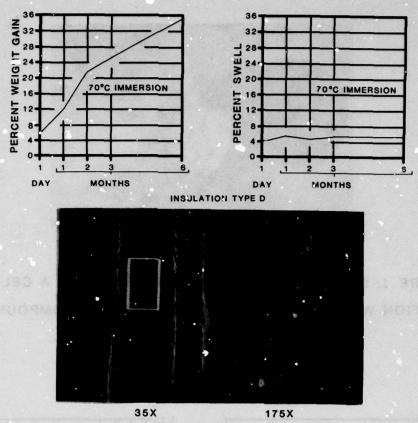


FIGURE 2: COMPARISON OF PERCENT WEIGHT GAIN AND PERCENT SWELL (Q SERIES FILLING COMPOUND).



INNER SURFACE OF FOAM SKIN INSULATION AFTER IMMERSION IN Q SERIES FILLING COMPOUND FOR 4.5 MONTHS AT 70°C

FIGURE 3: PERCENT WEIGHT GAIN AND DIAMETER SWELLING IN Q SERIES FILLING COMPOUND (CASE OF INSULATION TUBE LOOSE ON THE CONDUCTOR)

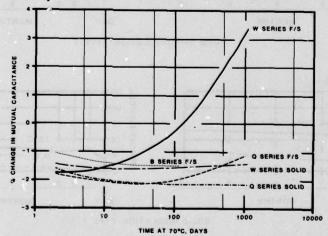


FIGURE 4: % CHANGE IN MUTUAL CAPACITANCE AT 1 kHz
AT 70°C (25/22 CABLE)
TYPE T INSULATION

三年 東京 大学 大学 大学 大学 大学 大学

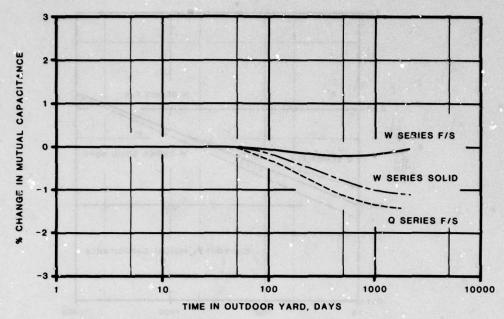


FIGURE 5: % CHANGE IN MUTUAL CAPACITANCE AT 1 kHz WITH YARD AGING AT UNION, NEW JERSEY. (25 PR/22 AWG)

TYPE T-INSULATION (HDPE)

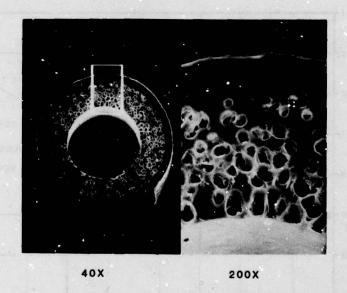


FIGURE 6: FOAM SKIN INSULATION REMOVED FROM CABLE AFTER
3 YEARS YARD AGING. (Q SERIES FILLING COMPOUND)

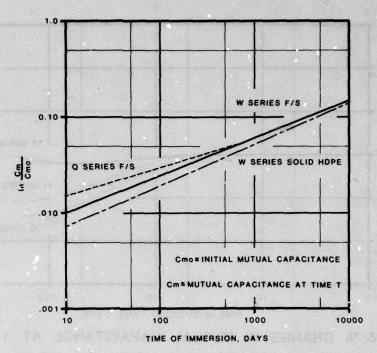


FIGURE 7: 1000 Hz MUTUAL CAPACITANCE STABILITY OF FILLED CABLES IN STANDARD WATER IMMERSION TESTS AT ROOM TEMPERATURE.

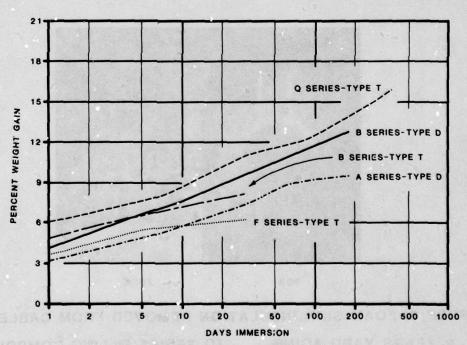
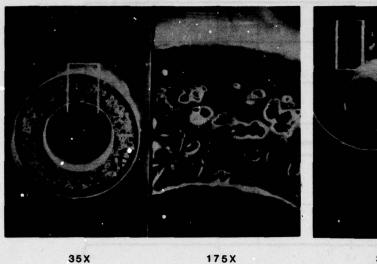


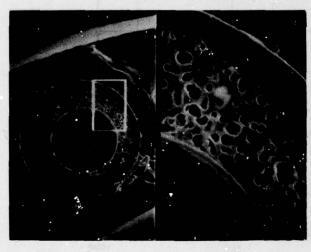
FIGURE 8: WEIGHT GAIN OF EXPERIMENTAL FILLING COMPOUNDS FOR FOAM-SKIN INSULATED CONDUCTORS AT 70°C



AS REMOVED

35X 175X
AFTER SOLVENT EXTRACTION

FIGURE 9: FOAM SKIN INSULATION AFTER 4½ MONTHS IMMERSION IN Q SERIES AT 70°C.



35X

175X

35X

175X

TYPE D INSULATION IN A-SERIES COMPOUND

TYPE D INSULATION IN B-SERIES COMPOUND

FIGURE 10: FOAM SKIN INSULATION AFTER 6 MONTHS INSERSION 70°C.

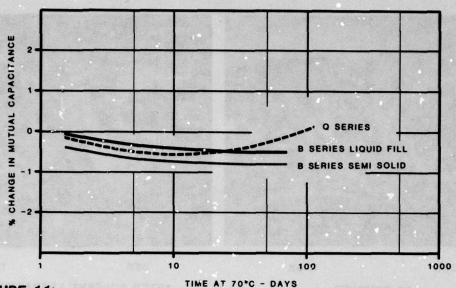


FIGURE 11:

% CHANGE IN MUTUAL CAPACITANCE AT 1 kHz WITH TIME AGED AT 70°C FOR 25 PR/22 AWG FOAM/SKIN FILLED CABLES.

TYPE T INSULATION

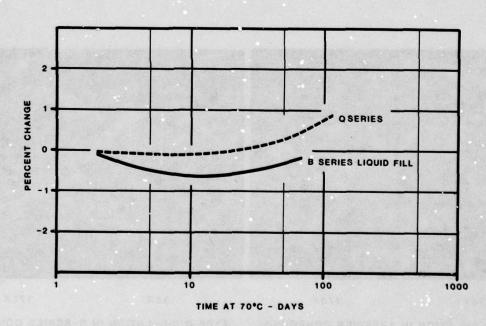


FIGURE 12: CHANGE IN ATTENUATION AT 772 kHz FOR FILLED FOAM-SKIN CABLES AGED AT 70°C.

TYPE T INSULATION

Milton Tenzer is Director, Research & Development, General Cable Company, Edison, N. J., a division of GK Technologies. Prior to joining General Cable, he was associated with the U. S. Army Communications R&D Command for over 30 years with major responsibilities in test equipment, microwave devices, electronic materials and transmission lines. He served as Co-Chairman of the International Wire & Cable Symposium from 1963 to 1978.



Jerzy A. Olszewski is Assistant Director Telecommunications Research at General Cable Company, Research Center, 160 Fieldcrest Avenue, Edison, N. J. 08817



COMPARTMENTALIZED LONGITUDINAL WATERPROOF CABLES

D.J. Dekker

J. Bruining

G.A.C. Schuring

Netherlands Postal and Telecommunications Services (PTT) Headquarters - Central Transmission Branch

Abstract

The need to maintain the quality of plastic insulated symmetrical cables and the wish to install coaxial cable systems without gas pressurisation led to cables that are made waterproof according to a compartment system with fault detection and localization facility. On the basis of given functional requirements some production techniques and blocking materials now being used are described. The influence on cable characteristics is discussed and fault localization techniques are described.

The topics mentioned in the abstract will be discussed in more detail in the following orresults of tests with filling materials, considerations on the choice of the compartment some examples of the application of the compartment system, the influence of water on the electrical characteristics of the cable core, method of fault localization and results.

Introduction

Since 1958 the Netherlands PTT has used plastic insulated cables in local networks only. Initially these cables were not provided with a metal screen. As the tightness of the plastic sheaths of these cables with respect to water vapour was bad, the cables were consequently highly sensitive to disturbances resulting from permeation of water. Therefore, the cables used later on were provided with an aluminium screen around the core and with an armouring. These cables - with a maximum capacity of 50 star quads - are used for the "standard connection points" now usually provided in newly to be built houses (preliminary installation). Such cables contain a relatively large number of joints which are injected with epoxy resin. 1 It was supposed that these joints would function as water blocks and hence it would not be necessary to make the plastic insulated cables watertight in longitudinal direction, for should a cable be damaged, only a short length of cable would be filled with water.

The Netherlands PTT was for the first time confronted with the necessity of making cables watertight in longitudinal direction, when plastic insulated cables were developed for trunk connections, the "low coupling level" type of cable.2 At the same time it was decided that the local plastic insulated cables should not only be used in the preliminary installation systems, but also to reconstruct the existing conventional parts of the local network in which lead sheathed cables with paper/air insulation are still in use. In case damage done to a sheath of a plastic insulated cable would not have been noticed, a cable length of 500 metres - between two joints - could be filled with water. Once it was decided to make plastic insulated cables longitudinally watertight, we made a start with a study of relevant documentation material. Next, in co-oreration with the manufacturers experiments were conducted. The compartment system as described in the present article was chosen. This system combines a discontinuous filling with a fault detection and localization facility.

Experiments with filling materials

The problem of making plastic insulated cables watertight can be solved in different ways: 3 , 4

- continuous filling; petroleum-jelly, powders
- and plastic foam can be used discontinuous filling: RTV (Room Temperature Vulcanising) rubbers, plastic foam or similar products can be used.

First the results of our own research work will be discussed.

Swelling powder

The first experiments were carried out with a powder made from tylose and polyolefin. Plastic insulated cables 150 x 4 x 0.5 filled with such powder were used in the local network on a limited scale only. We stopped using the powder for the following reasons:

- although the powder is not toxic it may nevertheless cause irritation in the respiratory organs when it flies about, so special safety

measures have to be taken during the manufacture and the jointing of the cables

- powders are sensitive to moisture; during the manufacture special precautions have to be taken and during the jointing work it may be troublesome if powder falls on the soil which is always humid
- the powder we examined is not resistant to bacteria and fungi
- filling the cable core with powder causes an increase of the mutual capacitance by about 10-20%
- the powders investigated are not compatible with an alarm wire because of the low insulation resistance
- in our opinion it is a drawback that the length over which water penetrates into the cable core is undefined.

RTV rubbers and petroleum jelly

When the idea of applying RTV rubbers was worked out it was decided that relevant experiments should be carried out on some test cables. The influence on the characteristics of cables filled with an RTV silicon rubber "Aquafoam" ⁵ (abbreviation AF) and those filled with a currently used petroleum jelly (abbreviation PJ) was examined during accelerated ageing.

In the study two wire constructions were involved, i.e.

- 0.5 mm conductors with solid PE insulation as applied in local cables (27 x 4 x 0.5)
- 0.8 mm conductors with cellular PE foaming rate 30% insulation as applied in the trunk cable with low coupling level (27 x 4 x 0.8). The following test cables were examine:
- unfilled cables (for reference purposes)
- cables provided with AF blocks at a mutual distance of two metres (i.e. filling degree 10%)
- cables fully filled with PJ.

 The AF is an RTV silicon rubber paste mixed with silicon oil. The PJ is a compound with a drop point of at least 70 °C. The choice of the PJ was based on BPO specification M142B and on DBP specification FTZ 72 TV 1. All the test cables were manufactured identically.

Advance study on ageing temperature and speed. A generally accepted method to speed up the ageing of plastics is to subject them to increased temperatures for a certain period of time. The relation between temperature and time, however, is not yet sufficiently known. To determine the most suitable ageing temperature the relation between temperature and time was studied on the basis of the swelling of the conductor insulation material in an abundance of a swelling medium (i.e. silicon oil and PJ). Tests were being performed on pressed plaques. The degree of swelling was regularly determined by weighing the samples. - solid PE (density 927 kg/m) MFI 0.3 gr/10 min), diameter 60 mm thickness 0.4-0.5-1.0

and 2.0 mm

Swelling media - silicon oil, viscosity 5.10^{-6} m²/s (the only component of AF which may cause the swelling) PJ (drop point 70 °C)

Temperatures - 30 - 40 - 50 - 60 - 70 and 80 °C.

As regards the 0.4 mm plaques after about two months the saturation point had not yet been reached at any of the temperatures mentioned. The increase in weight as a function of time however is so gradual that a final stage may be assumed.

with silicon oil there is an increase in weight first, but a decrease later consequent on the extraction of low-molecular fractions from the PE in the oil.

As with PJ the process depends on temperature and thickness of the samples; the change in weight is less than 0.4 %, i.e. at least ten times smaller than for PJ. The final stage will be reached after about one month.

Also extraction of low-molecular fractions from PE in the PJ is to be expected, but the absorption effect predominates. Results of the study concerning the influence of PJ are shown in the graphs of figure 1. After the samples were cooled down, there was no extraction of

silicon oil or PJ.

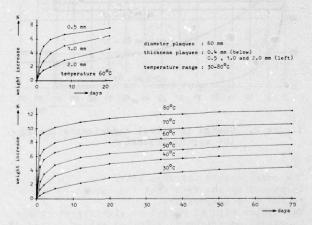


Figure 1 Weight increase of PEplaques in PJ

From the preliminary study it appeared that the process develops to rapidly in the temperature range above 60 °C, which is confirmed by relevant documentation material; exposure of cables filled with PJ to temperatures of 70 °C and higher causes ageing within a week. Moreover with cables stored in the bright sunshine and under tropical conditions temperatures of about 50 °C may occur. To be able to study the properties of the cables during the ageing process and to reduce the probability of rapid ageing to a minimum, an ageing temperature of 50 °C was chosen.

Cable ageing. The accelerated ageing process of the cables was followed for a period of two months.

Before and after that period electrical and mechanical tests were performed. During the ageing conductor resistance and mutual capacitance were recorded.

The following conclusions could be drawn.

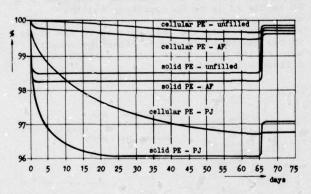
Mutual capacitance. The filling of the cable core results in an increase in mutual capacitance as shown in table 1.

table 1

Increase of mutual capacitance resulting from

cable type	filled with PJ	filled with AF
local cable 27. x 4 x 0,5	+16.0 %	+2.5 \$
trunk cable 27 x 4 x 0,8	+15.9 %	+2.5 %

As a result of the ageing the mutual capacitance also changes in those two months. The results are shown in the graphs of figure 2.



Change in mutual capacitance during figure 2. the ageing process

The considerable increase after the 65th day is caused by the fact that the cables cool down to the room temperature.

The cables with AF showed no significant change in mutual capacitance. With the cables filled with PJ, however, there were indeed significant changes.

The greatest - more or less permanent - change was found for cellular PE cables.

Capacitance unbalance. In none of the cables there were significant changes in the capacitance unbalance (couplings). Documentation material published at the end of 1975 about similar studies only makes mention of changes of the couplings within a star quad - under the influence of PJ - for wires with ring identification.

The conductor insulation of the cables used for the test described in the present article is either uncoloured (cellular PE) or coloured in the mass (solid PE).

Mechanical aspects. Before and after the ageing process the insulation of all the

cables was subjected to wrapping tests in accordance with:

- POTH Specification M142B para. 5.4 Appendix B FTZ Specification 72TV1 Appendix 3 para. 5.5 All cables underwent both tests successfully. Ageing had no adverse influence on tensile strength and elongation at break of the conductor insulation.

In cables on a drum PJ bags out, at any rate at somewhat higher temperatures; AF remains in place.

Other changes which were observed in electrical and mechanical characteristics are not significant.

Considerations on the choice of the compartment system

Depending on the standards applied in our judgement the various types of longitudinally watertight cables which were studied, all have their advantages and drawbacks. The Netherlands PTT draw benefit from the fact that it could continue to use conventional types of cables for a relatively long time to come, because highly advanced techniques are applied to balance symmetrical carrier cables; therefore, the frequency band on the existing cables could be widened such that it could largely cope with the increase in trunk telephone traffic. Moreover, prices for voice frequency cables for local networks were such that - from an economic point of view - it was not justified to use the more modern plastic insulated cables in capacities of 100 pairs and more. Until recently symmetrical plastic insulated cables were not yet used in trunk networks. However, after the development of the low coupling level trunk cable, this type of cable is increasingly being used for 2.048 kbit/s (PCM 30) transmission purposes. As a substitute for the symmetrical carrier cable the coaxial cable 1.2/4.4 mm will be introduced. The experience meanwhile obtained in local networks with plastic insulated cables shows that some kind of longitudinal watertightness is required for any cable with plastic insulated conductors. When the time had come that a decision should be taken on the manner of making cables watertight in longitudinal direction, we could choose from either using one of the wellknown methods, or developing a new system for this purpose. The latter possibility was chosen, in particular because the known methods did not comply with our wishes to maintain in a simple way the quality of the cable as a whole instead of only the core, for some tens of years. This especially holds for the metal sheath, which is to be found in any major plastic cable for the electrical screening of the cable core. Some minor fault in the sheath of an underground cable causes electrical contact between this metal screen and the soil, which may lead to corrosion. The cable sheath may lightly be damaged in various places. In particular in the case of stray currents

the metal screen may be corroded so

considerably that it will get cracked and eventually interrupted. Such interruptions give rise to a decrease of the transmission quality and may lead to vague complaints the cause of which is difficult to trace. It may It may be possible to observe damage to the cable sheath if the insulation resistance of the electrical screen with respect to earth is measured periodically, but this is not very practical, because normally this screen is earthed and such a method of quality control could be an impediment to applying a conductive

plastic sheath.

It was therefore decided that an "indirect" method should be used to signalize possible damage to the cable sheath. For this purpose an alarm wire was inserted in the cable core, and the core was not filled over the full length of the cable, but moisture blocks were provided discontiniously at regular distances. These blocks divide the cable core into compartments into which water may enter in case the cable sheath is damaged. The alarm wire consists of a copper wire of which the insulation has been perforated such that the conductor is not insulated over about 10 per cent of its length. After it is clear from the fact that the insulation resistance with respect to earth has decreased that water penetrated into a compartment, this alarm wire, together with a fully insulated conductor can be used to localize the fault.

For this purpose a measurement is made with a DC-bridge or pulse-echo equipment. Then the alarm wire can be used to determine exactly where the damage occurred with the aid of a cable tracer equipped with galvanic probes. Thanks to this system, only one compartment will be filled with water if the cable is damaged, and the damage can be repaired fairly easily by cutting the cable at a distance of one compartment length 1 at either side of the place of the fault and jointing and splicing a new piece of cable with a length 21.

For these repairs a suitable time can be chosen. The transmission is not affected by the penetration of water in a compartment. The mutual capacitance of the conductor pairs in symmetrical cables indeed becomes greater when water enters a compartment, but a compartment is relatively so very short that the effect of the increase in mutual capacitance on the transmission quality is practically nil. Measurements showed that the impact of a "drowned" compartment on cross-talk attenuation - also at higher frequencies (1 MHz) - is negligible. With coaxial cables the coaxial pairs are to a certain extent longitudinally watertight and completely transverse watertight, the alarm wire is part of the by-pack. So thanks to the compartment system it is possible not only to observe minor cable damage, but also to localize it by means of the alarm wire, and to have it repaired at a suitable time. It is still being studied whether it would be possible to dry a drowned

From an operational point of view an additional

advantage of the compartment system is that gas pressurization systems now being used with coaxial cables, become superfluous. As with the compartment system light damaging of the cable will certainly be signalized, we can do with a lighter armouring than would be necessary without this certainty. In case of the latter a heavier armouring will have to be applied than would have been necessary with a view to the desired tensile strength. With symmetrical cables the cable diameter need hardly be enlarged, for the mutual capacitance of the pairs is not notably increased by the provision of the waterblocks, while the filling material applied should have a low dielectric constant.

Summarising we can say that the Netherlands PTT opted for the compartment system for the following reasons:

Operational considerations

- universally applicable
- possibility to maintain the cable quality
- simple cable repairs.
- Economic considerations
- symmetrical cable, relatively cheap construction
- coexial (and optical) cable, no gas pressurization system

Functional requirements

System technique

The cable is made watertight according to a compartment system by providing the cable core with waterblocks at regular distances. Unless the applied filling material does not prevent the alarm facility to function within the blocks, the maximum length of a block is 25 cm. The distance between two successive blocks should be 2 metres.

Cable technique

The water blocks should not notably influence the mechanical properties of the cable. This applies in particular to the flexibility at the places where the blocks have been provided. The cable should further contain an alarm and fault localization facility. The operation of the alarm facility should be such that the insulation resistance between the alarm wire and the metal screen will have been decreased to at most 1 Mohm one hour after water has penetrated the cable and to at most 100 kohms after five hours.

Jointing technique

The jointing of the cable should not be affected adversely. If there is a water block at the point where the joint is made, this block should be easily removable without any special device being used. Remainders of the block should not be troublesome to the jointer and certainly not be detrimental to the jointing tools. It should further be possible to remove the sheath at the place of a block without causing damage to the conductor insulation.

Material

Without any safety precautions to be taken the cable with water blocks should not in any way be detrimental to a person's health. At normal cable temperatures, i.e. from -10 to +50 °C, the blocking material should not affect any other material used in the cable. The blocking material should not affect the electrical characteristics, not even in the long run. At temperatures from -10 to +50 °C the material should be plastic, but should not move in the cable core under the influence of

gravitation. (This will be checked by storing the cable in a climatic cabinet at 50 °C for a period of 30 days, and by determining the electrical characteristics and mechanical properties before and after this accelerated ageing.)

Longitudinal watertightness

All water blocks should be fully waterproof in longitudinal direction, also in the long run and after normal handling of the cable. The longitudinal watertightness is tested after pulling and bending the cable. Every individually tested block should with stand the pressure of a water column with a hight of one metre during 24 hours or an air pressure of 0.1 bar during 5 minutes.

Materialization of the compartment system

The above functional requirements were submitted to the cable manufacturers to be considered, requesting them to meet these requirements in such a way as seemed most suitable to them.

This approach resulted in different solutions. All solutions have one thing in common, however, the filling material is built up of two more or less liquid components which, as a result of a chemical reaction, are combined into a solid mass. The filling materials can further be divided into two categories, i.e.

1. filling materials expanding during the

reaction, and
2. filling materials not expanding during the
reaction.

As to the techniques to provide the filling material distinction ca be made between techniques whereby the whole cable core is filled at a time and techniques whereby this is done step by step during the stranding process.

Filling materials and application techniques

Some examples of the filling materials and their application techniques are described in the following.

PUR soft foam. An example of expanding filling material is a PUR soft foam, which results from the combining in the ratio 2: 1 of the components A and B.

Component A consists of polyaetherpolyol, a blowing agent, a catalyzer, a stabilizer

and silicon oil, component B is diffinylmethandiisocyanate. The following values are typical at a temperature of 20 °C:

component A component B relative density viscosity 1039 kg/m³ 1240 kg/m³ 0.370 Pas

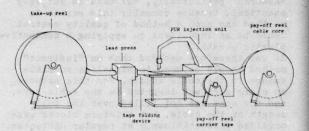


Figure 3 Principle of PUR injection and lead press

After the components have been combined the expansion is completed in a time lying between 40 and 220 seconds. After expansion in free air the weight of the PUR foam is $55 \pm 3 \text{ kg/m}^3$, the relative dielectric constant is 1.02. Two precision dosage pumps feed the components into a mixing chamber with a pressure of 80 to 200 bars; from this chamber a certain amount of the mixed compound is provided on a carrier tape at time intervals depending on the length of the compartment. This tape consists of a non woven polyester and is folded around the core in longitudinal direction. The filling material is deposited on the carrier immediately before the metal sheath is provided. When expanding the material penetrates through the carrier. The expansion takes place in a closed room, so there will be a certain overpressure in the space between two successive blocks. The principle of the application is found in figure 3.

RTV silicon rubber. The category of non-expanding filling materials includes a two-component RTV rubber which vulcanizes by means of an additive reaction

of an additive reaction. Such types of rubber are in general interded for application as cast rubbers which do not have to adhere. If applied as a means to make the cable longitudinally watertight, however, a certain degree of adhesion is necessary. But to avoid splicing problems the adhesion should not be too strong. Moreover, the rheological properties of the filling material should be such that it has a low viscosity during the injection, if the resistance to propagation is considerable (in the direction perpendicular to the conductors) and a high viscosity, if the resistance to propagation is small (in the longitudinal direction of the cable core). Moreover, once applied, the filling material should not drip from the cable before the wrapping has been provided.

For both adhesiveness and rheological properties a satisfactory solution was found by a well-balanced system of additives. As to the rheological properties figure 4 gives the relation between the shear tension τ and the shear velocity dv/dr of the compound. Only after the yield tension τ_0 has been exceeded does the filling material behave like a Newtonian liquid with a degree of viscosity that is determined by the angle α (a greater angle involves higher viscosity).

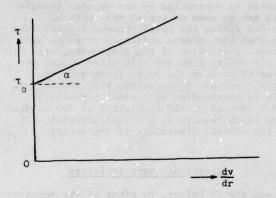


figure 4. Shear tension as a function of shear velocity of RTV-rubber

Although the compound can be applied in a oneshot method ~ like the expanding filling material described in the aforegoing - up till now this two-component silicon rubber is provided in successive steps, as shown in figure 5.

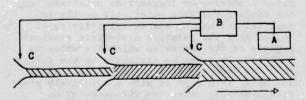
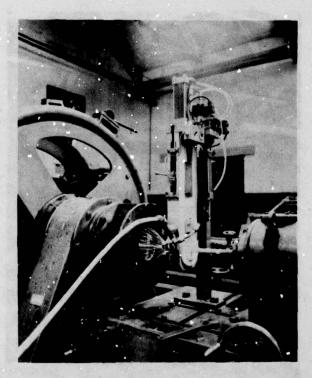


figure 5. Principle of a step by step technique in layer type cables

- A. trigger unit B. control unit
- C. injection unit

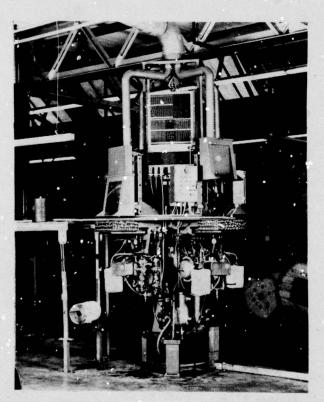
The trigger unit A is driven by the stranded cable core already fitted with blocks. It operates the injection units C through the control unit B which provides for the synchronization of the blocks in the different layers of the core. The injection points have been combined with the stranding nipples of the cable stranding machine. Apart from the shape of the nipple the viscosity, the injection pressure and the quantity of filling material are of importance for a satisfactory result. Thanks to the flexibility of the electronics of the control unit the number of injection points can be increased at random, so that the number of stranding elements of which the cable core is composed, is practically unlimited. In the manner described nearly all cable types can be made longitudinally watertight. By the order of the Netherlands PTT, for example, coaxial crbles with 6 and 12 pairs of 1.2/4.4 mm and optical cables with two units, each consisting of six 50/100 µm fibres, have successfully been treated in this way. Picture 1 shows an injection unit in the stranding line.



Picture 1
Injection equipment for RTV silicon rubber (AF)

Polyurethane compound. A third solution is a two component material based on polyur/thane that can be injected into the stranded cable core as a liquid and forms a golid water block after curing. The injection process - in principle discontinuous - takes place in the continuous extrusion process of a PE sheath for reasons of price and efficiency. In a revolving injection machine, as shown in picture 2, the cable core over which a PE sheath is to be extruded is led over a V-grooved wheel provided with four injection moulds that are one metre apart. The wheel is being driven by the cable itself. During one of its revolutions the complete injection process takes place:

- positioning of the cable core in the mould
- closing the mould
- high pressure injection of the two-component material
- opening the mould.



Picture 2
Revolving injection machine for polyurethane compound

The speed of this process is determined by the speed of the extrusion process of which it forms part.

The length of the block is defined by the length of the mould and the quantity of injected material. It is different for cables of various diameters. For a 200 pair cable the length of the block is about 20 cm; about 20 cc of material is used. The machine is suited for cables with a diameter of 6 mm and more. Because of the short curing time of the twocomponent material mixing takes place immediately before injection into the cable. To prevent curing inside the machine when the line has to be stopped it automatically cleans itself after a preset time has elapsed. The process is controlled by the process computer that can be seen on top of the machine. Besides giving the usual process commands the computer also checks injection pressure and volume, proportion of the components, etc. In all cables provided with water blocks the capacity between the pairs increases; the actual increase in capacitance is about 2,5%. This is compensated by a small increase in the thickness of the insulation of the conductors which results in a slight increase only of the overall dimensions of the cable.

Electrical characteristics

As was stated before, by means of the compartment system and an alarm wire a fault in a cable can not only be signalized, but also localized.

This system also allows for one compartment to be filled with water for a certain time. For some electrical characteristics the most important consequences of such a "drowning" will be discussed in the following.

The impedance of an alarm pair

In The Netherlands the cables in general are buried unprotected at a depth of at least 50 cm (local cables) or 70 cm (trunk cables). Should the cable sheath be damaged, water from the soil will - depending on circumstances after a shorter or longer time penetrate into the cable core. This water will mostly be polluted and has an average resistivity of 10 Q m. Also the relative dielectric constant depends on the degree in which the water is polluted. This can be explained by the fact that the free positive and negative ions in the water form dipoles with a relatively great dipole moment. Under the influence of an electric field E these dipoles are directed and consequently polarize the water.

As appears from $\mathcal{E}_{\mathbf{r}} = \frac{P}{\mathbf{\epsilon} \cdot \mathbf{E}} + 1$, in a static field the relative dielectric constant $\mathbf{E}_{\mathbf{r}}$ of a

substance (when ϵ_r >> 1) is directly proportional to the polarization P of that substance. The polarization is equal to the product of the number of dipoles per unit of volume and the magnitude of the dipole moments. The orientation of the dipoles takes some time and this means that the polarization and therefore the relative dielectric constant depends on the frequency of the electric field. The more the frequency increases the orientation of the dipoles will further remain behind the change in the direction of the electric field, and in the long run the dipoles formed by the positive and negative ions no longer follow this change at all.

what remains then is the polarization resulting from the permanent dipole moments of the water molecules and the relative dielectric constant is equal to that of non-polluted water, i.e. = 80.8

The quantitative effect of the mechanism described in the aforegoing on the mutual capacitance of an alarm pair in a cable in water with a resistivity P = 11.25 Ω m (by the addition of NaCl to purified water) is indicated in figure 6.

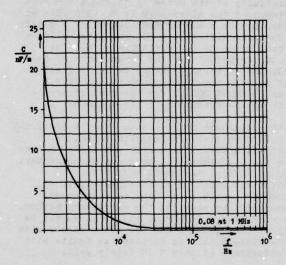


figure 6. Capacitance of the alarm pair in water with = 11.25 m

This mutual capacitance decreases as a function of the frequency from the extremely high value of 22.5 nF/m at 1 kHz to well over 0.08 nF/m at 1 MHz. The real part G and the imaginary part ω C of the admittance of this pair as function of the frequency is shown in figure 7. This figure also shows the value of ω C for a dry alarm pair.

In that case the conductance $G\approx 0$ (in fact $G\approx 1~{\rm d} S/m$ at 1 MHz).

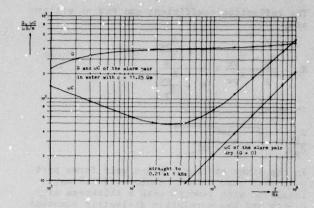


Figure 7 G and ωC of the alarm pair

Reflection coefficient and conductance to earth in a drowned compartment

From figure 7 it appears that at high frequencies the admittance of an alarm pair in a compartment filled with water with a resistivity of 11.25 $\Omega_{\rm m}$ is not much greater than the admittance of the alarm pair in dry condition. A further analysis of the magnitude of the reflection coefficient at 1 MHz at the change over from a dry to a wet compartment will have to reveal whether a fault can still be localized according to the pulse-echo method. In figure 8 the alarm pair is shown with an impedance $Z_{\rm p}$ in a dry compartment and an impedance $Z_{\rm pw}$ in a compartment filled with polluted water.

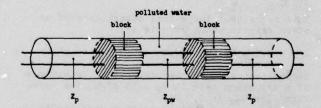


figure 8. Alarm pair in a compartment

At a frequency of 1 MHz we have in this situation:

$$Z_p = \sqrt{\frac{R + j_0 L}{G + j_0 C}} \approx \sqrt{\frac{L}{C_p}}$$

and

$$Z_{\rm pw} = \sqrt{\frac{R + j\omega L}{G_{\rm pw} + j\omega C_{\rm pw}}} \approx \sqrt{\frac{j\omega L}{G_{\rm pw} + j\omega C_{\rm pw}}}$$

The reflection coefficient can now be written

$$K_{r} = \frac{Z_{p} - Z_{pw}}{Z_{p} + Z_{pw}} = \frac{1 - \frac{Z_{pw}}{Z_{p}}}{1 + \frac{Z_{pw}}{Z_{p}}}$$

in which

$$\frac{Z_{pw}}{Z_p} = \sqrt{\frac{j\omega C_p}{G_{pw} + j\omega C_{pw}}}$$

In the trunk cable the alarm pair forms part of a star quad with conductors of 0.8 mm, insulated with fram PE with a thickness of 0.4 mm and has a relative dielectric constant $\epsilon_{rs} = 1.75$. The mutual capacitance of a normal pair in such a star quad C = 33 pF/m. If such a star quad lies in water with $\epsilon_{rw} = 80$, (in accordance with figure 6 this value will also be found in polluted water at 1 MHz) the mutual capacitance of a pair should be assumed to be the series connection of the coaxial capacitances C_k of the two wires:

$$C_{w} = \frac{C_{k}}{2} = \frac{\pi \cdot \varepsilon_{o} \cdot \varepsilon_{rs}^{k}}{2 \ln \frac{D}{d}}$$

taking into account that ξ_{rw} >> ϵ_{rs} . In water this capacitance will then be $C_{\text{w}}\approx 65~\text{pF/m}$. If the insulation of both conductors of a pair in a star quad is removed at one side over the full length, the mutual capacitance of this conductor pair in water with $\epsilon_{\text{rw}}=80$, calculated from the known dimensions, appears to be 300 pF/m.

In fact, however, the insulation of the conductors is not removed over the full length, but for 10% only.

This means that the mutual capacitance of an alarm pair in water amounts to:

$$C_{pw} = 0.9 \times 65 \text{ pF/m} + 0.1 \times 300 \text{ pF/m} \approx 88 \text{ pF/m}.$$

Taking into account that the mutual capacitance of a dry alarm pair is $C_p = 33~\mathrm{pF/m}$, the value found for C_{p_W} is 2.7 C_p . If it is assumed that there is a resistivity

If it is assumed that there is a resistivity of about 10 Ωm in the drowned compartment we find at 1 MHz (see figure 8): $G_{pw} \approx 3 \, \omega C_{p}$, so:

$$\frac{Z_{pw}}{Z_{p}} = \sqrt{\frac{j\omega C_{p}}{G_{pw} + j\omega C_{pw}}} = \sqrt{\frac{1}{3 + j3}} = \frac{1}{\sqrt[4]{18}} \approx 0.5$$

Then the reflection coefficient $K_r = \frac{1 - 0.5}{1 + 0.5} = 0.33$

If the resistivity of water is about 2.5 Ω m, the conductance G $_{pw}$ at 1 MHz may be assumed to be 2000 $\mu \mathrm{S/m}$ or G $_{pw}$ $\approx 4~\omega \mathrm{C}_{pv}$ \approx 12 $\omega \mathrm{C}_{p}$.

Then
$$\frac{Z_{pw}}{Z_p} \approx \frac{1}{\sqrt{12}}$$
 en $K_r \approx 0.5$.

It is not likely that the resistivity of the water in the soil will often be as low as 2.5 Ω_{m} .

On the contrary, in the majority of cases G_{pw} will be much smaller than ωC_{pw} and consequently

$$\frac{Z_{pw}}{Z_p} \approx \sqrt{\frac{C_p}{C_{pw}}} \approx \frac{1}{\sqrt{3}} \text{ en } K_r \approx 0.26.$$

A greater reflection coefficient at a high resistivity of the soil water can only be reached by an increased perforation rate of the insulation of the alarm pair. This is not very useful, however. A doubling of the perforation rate (from 10 to 20%) only leads to an increase in the mutual capacitance of the alarm pair in water from $C_{pw}\approx \beta~C_p$ to $C_{pw}\approx 4~C_p$, while in soil water with a resistivity of 10 Ω m $^G_{pw}$ will not be much more than 1000 $\mu \text{S/m}$. The conclusion to be drawn from the aforegoing consideration is that in general the reflection coefficient will be about 0.3.

As far as the conductance to earth of the alarm pair is concerned, figure 7 shows that with a resistivity of the water of 11,25 Ωm the conductance of the alarm pair is $G=230~\mu \text{S/m}$ at 1 kHz. So for a compartment length of 2 m this conductance will be $G\approx500~\mu \text{S}$. Extrapolation of this value to DC results in a value of 100 μS . Assuming that the conductance of one conductor to earth is about twice as great as that between the two conductors, we find a value of about 200 μS for the conductance to earth of one conductor of the alarm pair.

In this approach it is assumed that a compartment is completely filled with water. In practice, however, this will not always be the case and the alarm will be given much earlier. Also in view of the small reflection coefficient which is to be expected, it will seldom be possible to localize a drowned compartment by means of the pulse-echo method. The conductance to earth, too, will mostly be smaller than calculated; but measurements with a DC-bridge enable us to localize faults with a conductance of only 1 µS fairly well.

Influence of water on far-end crosstalk attenuation

In order to check the influence of water in the cable on crosstalk in everyday situations, first the following measurements were carried out on a cable of 500 m on drum:

- 1. the complex coupling G + jwC at 500 kHz 2. the far-end crosstalk attenuation at 500 kHz
- the far-end crosstalk attenuation at 500 kHz
 the far-end crosstalk attenuation at 1 MHz.

These measurements were performed on a dry cable and after two compartments had been filled with water.

This means that the cable is wet over a length of $^4\ \mathrm{m}_{\bullet}$

The modulus of k was calculated from G + $j\omega C$. The characteristics of all observations are indicated in the table 2.

Table 2

Far-end crosstalk attenuation in dry and wet cable

		Dr.	ry I	W	et e
Modulus of the complex couplings /k/ at 500 kHz	s (µS)	/k/≤30 pS 6.1 5.4 264	all values 14.3 67.5 288	/k/≤30 µS 5.4 5.8 264	14.2 67.3 288
Far-end prosstalk attenuation at 500 kHz	x (dB) s (dB) n	83 17 288		84 14 288	
Far-end crosstalk attenuation at 1 MHz	x (dB) s (dB) n	75 13 288		75 13 268	

The far-end crosstalk attenuation at 1 MHz has also been measured on a low coupling level trunk cable over a length of 3 km (PCM 30 regeneration section) under normal - i.e. dry - circumstances and after one compartment had been filled with water. This practical test confirmed that the drowning of a compartment does not influence the far-end crosstalk attenuation.

The fact that a wet compartment does not show any significant influence on the transmission characteristics means that even when cables are used for 2048 kbit/s PCM transmission, faults need not be cleared immediately.

Corrosion aspects of the alarm circuit

list.

Soil water - which owing to the presence of ions can be considered an electrolyte - may cause corrosion of the uncovered parts of both alarm wire and metal sheath. Two different metals, in our case copper and aluminum or lead, in an electrolyte form a galvanic cell. If the cell is closed, there will be corrosion at the anode. The degree of corrosion is determined by the magnitude of the cell current, which in turn depends on the nature of the metals, the resistivity of the electrolyte and possible external DC voltages (power supply, stray currents).

Local cables. In local networks the alarm wires are normally used to connect subscribers, so as to make quality supervision possible by means of routine testers. If in such a local cable an alarm pair is chosen having the full battery voltage between the two conductors, one of the conductors will soon be interrupted by corrosion when water enters the cable. So to avoid subscriber loop failure only one alarm wire is provided.

Figure 9 shows the normal situation for a subscriber's loop with an alarm wire. In the exchange the alarm wire is connected to the earthed positive pole of the power supply, via an inductive resistance in the power supply bridge.

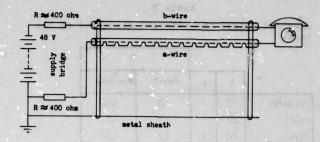


figure 9. Subscriber loop with alarm wire

The metal sheath is connected direct to the earth bar.

Now when, following some mincr damage, soil water penetrates a compartment, the galvanic corrosion cell is closed. The emf of this cell is about 2 V for copper and aluminium; the alarmwire is protected cathodically by the sheath as being a sacrificial anode. So, unlike the sheath, the alarm wire will not corrode. During a call this situation will even be more apparent, because a voltage equal to the product of line current and line resistance is superposed on the emf of the cell. This voltage is 10 to 15 V, the alerm wire remains cathode and the sheath remains anode. The resistance of the electrolyte between alarm wire and sheath under the most unfavourable circumstances will be about 5 kohm, so that in the situations sketched above the magnitude of the corrosion current is at most 0.4 mA and 2 to 3 mA respectively.

As far as the average telephone subscriber is concerned, the equipment will be idle for more than 95% of the time, so that under the most unfavourable circumstances the average corrosion current will have a value of about 0.5 mA. During a telephone call the increase in voltage may result in intensified reactions at both anode and cathode to such an extent that water is electrolyzed. An insulating layer of gas now formed will reduce the corrosion current.

The quantity of material M which is dissolved at the anode, is determined by the transported charge Q, the valence n and the atomic weight A of the material of which the anode is composed.

The value of M can be derived from the following formula:

$$M = \frac{A \cdot Q}{nE}$$

Where F is Faraday's constant (96487 C/mol). The specific values of the different materials used in cables are shown in table 3.

table 3

Specific values for material dissolved at the anode

			7.7	
	A	n	g/mAyr*	cm ³ /mAyr
aluminium	27	3	2.9	1.09
lead	207	2	31.1	3.0
iron	56	1	9.2	1,17
copper	63.5	2	10.5	1.18

* 1 mAyr (1 mAyear) = 31560 C

A cable with an aluminum sheath 0.2 mm thick and having a diameter of 10 mm contains 6.3 cm³ aluminium per metre of cable. In the situation sketched above not more than about 0.5 cm³ aluminium would corrode each year, so an interruption of the screen is nardly to be expected at short term. Corrosion by external causes, such as stray currents, have not been taken into account. 10

Because the insulation resistance of the subscriber's line, of which the alarm wire forms part, remains high and the conductor does not corrode, it is not strictly necessary to have the fault repaired within a short time. In local cables the alarm wire is the a-wire of the first star quad in the outer layer. Figure 10 shows a routing diagram of the circuits in local networks, together with the alarm wires.

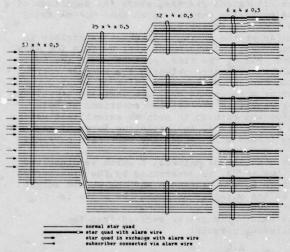


Figure 10 Local routing diagram of alarm wires

By means of the faulty wire in the exchange it is possible to determine which cable in the distribution network has been damaged.

Trunk cables. Also with trunk cables alarm wires are used to signalize water penetration. In this case however, the alarm wire is continuously monitored for insulation resistance and loop resistance. The principle of

the monitoring circuit is shown in figure 11.

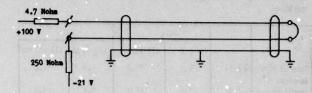


figure 11. Monitoring circuit trunk cables

In case of a sheath damage, followed by penetration of water in the core, the alarm wire shows a conductance to earth which is low compared with 4.7 M Ω. So the corrosion current flowing between alarm conductor and sheath will be 100 V/4.7 M $\Omega \approx$ 20 μ A. In this case, however, the alarm wire reacts anodically and the sheath cathodically, and the copper alarm conductor will corrode. The corrosion speed of copper is about 10.5 g (1.18 cm 3)/mAyr. This means that per day a quantity of copper equivalent to 0.14 mm of a conductor with a diameter of 0.8 mm would dissolve owing to corrosion. Therefore, only after a couple of days will the conductor be interrupted entirely. If action is undertaken to repair the fault immediately after the excitation of the alarm wire, fault localization is still possible by means of a DC measuring bridge.

Interruption of the alarm wire, however, presents no problems, because in a trunk cable - unlike local cables - the alarm wire does not form part of a transmission circuit. If the alarm wire is interrupted, the fault can be localized by means of pulse-echo measurements. Then again, it will not strictly be necessary to have the fault repaired at short term.

Methods to localize a drowned compartment

As far as fault localization in longitudinally watertight plastic insulated cables is concerned, distinction should be made between a conventional lead sheath, covered with bitumen, jute and steel tape armour on the one hand, and a plastic sheath on the other hand.

Let us consider a trunk cable with a conventional lead shoath and a plastic core with a compartment length of 2 metres. These cables are of such considerable length that the distance between one end of the cable and the place of a fault averages about 5 km. If we wish to determine the place of a drowned compartment in one measurement, the result of this measurement should show no greater inaccuracy than ± 2 m. A pulse shape often applied to localize faults in cables by means of the pulse-echo method is the 50 ns-sin puls. Its nominal pulse width corresponds with a length of cable which is significantly greater than a two-metre compartment, for this very reason the resolution of this pulse measurement is in fact too small.

This resolution could be increased by the upe of narrower pulses but would reduce the measuring range, which is already smaller than 5 km for a 50 ns pulse. Hence, in view of the small reflection coefficients to be expected and the insufficient resolution, as well as the required accuracy of about 2 m on an average fault distance of 5 km, pulse-echo equipment will in general be unfit for direct fault localization of a drowned compartment in the cable. As a rule proper direct fault localization will also be impossible with local cables. Although in local networks much smaller cable lengths are used than in trunk networks, data on length and situation of the cables are much less exact than for trunk cables. Another unfavourable factor is the relatively great pulse attenuation.

Under the circumstances a DC measuring bridge by means of which measurements can be performed according to the method of either Murray or Varley is more suitable.

The insulation resistance of the alarm wire to earth in a wet compartment is small (in the order of 10 to 100 k Ω) and a normal insulated wire of the same star quad can always serve to form a measuring loop. An experience d test officer can obtain surprisingly accurate direct localization results with a DC bridge and the probability of an accurate direct localization is no doubt greater with a DC bridge than with pulse-echo equipment. Nevertheless, even after a DC measurement, often a second measurement from a splice nearest to the probable place of the fault will be necessary to obtain the required accuracy of about 2 m (a currently used practice in localizing faults in underground cables).

The cable need not be opened for this second measurement, if the fault is localized by means of a cable tracer provided with galvanic probes or "prickers".

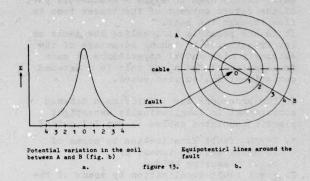


figure 12. Fault localization circuit

As shown in figure 12 in the exchange a tracer tone of 1 or 10 kHz is connected between the alarm wire and a free earth pin. A certain amount of current will leave the cable at the faulty point.

Consequently, in the soil a voltage will be built up as sketched in figure 13a. Over the place where the cable is damaged more or less circular equipotential lines could be drawn, as seen in figure 13b. With two prickers at a mutual distance of about 1 m the voltage is scanned along the cable trench.

The voltage between the two pirs can be read on a meter and is also audible with a headphone. As soon as the pins are on either side of the faulty point in a line of the same potential, the meter will show a minimum value and a tone will no more be heard.



By the performance of at least two measurements, mostly followed by a third control measurement, all perpendicular to each other as showed in figure 14, the point where the cable is damaged can be found with a great degree of precision.

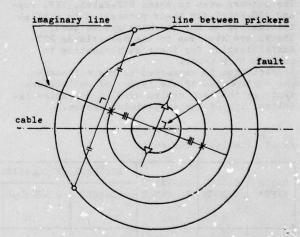


figure 14. Principle of fault localization
O first measurement
X second measurement

\(\triangle \) control measurement

This search method is based on the assumption that the cable has a metal screen that is fully insulated from earth by a plactic sheath or no metal screen at all. As far as longitudinally watertight local plastic insulated cables are concerned, this method to determine exactly where the fault occurs is used successfully after a first rough fault localization. It was possible, however, to use this fault localization method also for underground cables with a lead sheath. Although the relevent study has not yet been rounded off, it is already

clear that much benefit is drawn from the low soil resistivity in the Netherlands, which is, in fact, in most areas lower than 100 Ωm. Apparently, the impedance R_m + $j\omega L_m$ of the lead sheath armoured with two steel tapes, is sufficiently high to allow a measurable part of the return current of the tracer tone to flow through the soil. It is not possible lo localize the fault at low frequencies by taking advantage of the extremely high mutual capacitance at such

So the procedure for localizing a drowned compartment in longitudinally watertight plastic insulated cables is the following:

compartment filled with water.

frequencies of the alarm pair in a drowned

- 1. rough fault localization by means of a. pulse-echo equipment or b. DC measuring bridge
- 2. exact faul+ localization by means of the search method.

A survey of some fault localization under different circumstances is given in table 4.

Acknowledgements

The authors wish to thank NKF-Kabel, TKF, Pope and AEG-Kabel for their permission to publish information on the blocking system used. Thanks are also due to the Netherlands PTT Administration for their authorization to publish this paper. Appreciation is expressed to the colleagues who contributed to the laying of and measurements on the test cables used to determine the reliability of the compartment system.

Table 4 Fault localization results

			DESCRIPTION OF THE PARTY OF THE	
		 OF LOCALIZA	TION WITH	R
	DISTANCE TO FAULT	DC-BRIDGE	PRICKERS	ALARM

CABLE	CABLE	DISTANCE	ACCURACY	OF LOCALIZA	TION WITH	RESISTA	NCE OF	NUMBER OF
TYPE*	LENGTH	TO FAULT	PULSECHO	DC-BRIDGE	PRICKERS m	ALARM WIRE TO EARTH 10 ³ Ω	SOIL Ω m	CABLES IN TRENCH
1	3179	1945	25	2	exact	2.5	20	1
1	5527	. 988	-	5	1	15	300	5
1	6596	2421	-	6	exact	4000	140	2
2	1340	326	-	5	exact	380	100	1
2	500	300	- 1	1	exact	1000	160	and at mend
1	750	506	-	2	exact	10	735	5

*) 1. Trunk cable 0.8 mm conductor - foamed PE insulation length of compartment 2 m lead sheath, steel tape armouring

References

- 1. "Jointing of plastic-sheathed cables" ITU - Geneva 1978.
- Proc. 22nd IWCS p 150 "Symmetric cable either for loading without balancing or for PCM-transmission" D.J. Dekker, H.G. Dageförde, P. Zamzow.
- 3. Câbles et Transmission "La protection par barrières d'étanchéité du cable Paris-Lyon III a 18 paires coaxiales de 1,2/4,4 mm".

 J. Bendayan, M. Fouque, R. Mathieu.
- 4. Proc. 24th IWCS p 136 "Glassfibre armoured PIC trunk cable assembled with connecting plugs" H.G. Dageforde, P. Gregor, G. Thonnessen.
- 5. Proc. 24th IWCS p 361 "A new type of longitudinally waterproof telephone cable" Dr. F.H. Kreuger, H.L. Gorissen, J.F. Kooy and J.P.J. van Kesteren.
- 6. Proc. 24th IWCS p 365 "Change of crosstalk proporties in correlation with the interaction of polyethylene/petroleum-jelly" H.A. Mayer, H.J. Anderka and H.G. Dageforde.
- 7. Telephone Engineer and Management Aug. 1976 "The importance of shield continuity to good transmission" R. Rennaker.
- 8. Electrical Engineering Materials A.J. Dekker Prentice-Hall Inc.
- 9. Handbuch des Kathodischen Korrosionsschutzes W. v. Baeckmann, W. Schwenk.
- 10. Telephone Engineer & Management June 1978 "A solution to underground cable failures" K.E. Bow and L.G. Colter.

2. Local cable 0.5 mm conductor - solid PE insulation APL + PE scheath, insulated steel wire armouring



cable development group.

D.J. Dekker

Mr Dekker, who is a graduate of the Higher Technical College of Rotterdam, joined the Netherlands PTT-Administration as an apprentice at the Central Workshop in The Hague in 1939. His tasks within PTT included: maintenance of repeater stations and cable networks, technical

Mr Dekker is a member of both the C.C.I.T.T. and the IEC. For studygroup VI of the C.C.I.T.T. he acts as special rapporteur for questions concerning cables with plastic insulated conductors and he chairs the National Committee of the Netherlands of IEC TC 46.

development work and now he is chief of the



G.A.C. Schuring

Mr Schuring, who is an electronics engineer, started his professional career at the Dr. Neher Laboratory of the Netherlands PTT in 1960.

He did research work in the field of semiconductor materials and devices, such as transistors, Hall generators and laser components.

After two years at the PTT staff training centre, he joined the cable development group in 1972, in which he is mainly in charge of the electrical characteristics of telecommunication cables and of fault localization techniques.



J. Bruining

Mr Bruining is a graduate of the Higher Technical College of Leeuwarden. He has been employed with the PTT since 1966 and became a member of the cable development group in 1972. He is especially in charge of subjects regarding the mechanical and corrosion aspects of telecommunication cable coverings. In the field of cable standardization he is chairman of the National Committee of the Netherlands of IEC SC 46C.

MANUFACTURING GENERATION II FILLED SERVICE WIRE

by

J. M. Hacker

Western Electric Company, Inc. Baltimore, Maryland

ABSTRACT

A new water and flame resistant service wire is being manufactured at the Baltimore Works of the Western Electric Company. This new design, in addition to having increased mechanical integrity, is manufactured using contemporary concepts which have advanced the state of the art with respect to structural processability.

INTRODUCTION

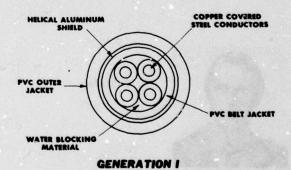
In an effort to convert the entire buried loop plant to a waterproof network, manufacture of an interim design of water resistant service wire began in the spring of 1973. While satisfying the immediate system needs for a structure which would inhibit water ingress and flame propagation, further research and development into upgrading structural integrity was vital. With an increasing number of states throughout the country enacting legislation for the mandatory installation of buried plant, customer demand for underground communication lines has been on the rise. Due to this increased demand, questions regarding the structural integrity of the service wire would be an area of continuous examination if allowed to remain unchecked.

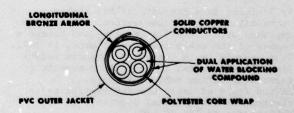
STRUCTURAL CONSIDERATIONS

The interim design of Filled Service Wire, similar in construction to PAP cable, attained the majority of its structural strength via four copper-covered steel conductors. The aluminum alloy shield, primarily an electrical drain and noise mitigator, contributed little to the overall breaking strength of the wire. Due to constant problems associated mainly with open shields in the service trench and shield breakage at the grounding lug, it was decided to transfer the basis of structural strength from the conductors to the shield. Additional benefits were realized by this transfer. With respect to installation, termination ease was augmented by replacing the copper-covered steel conductors with solid copper conductors, and the tougher

shield reduced the frequency of shield breaks at the termination point. With respect to manufacturing, the insulated conductor could now be drawn to size and annealed in tandem with the insulating line.

The manufacture of this new design posed a formidable problem: At the inception of the final design, basically a modified ASP construction (see Figure 1), how could a core whose outside diameter of 0.155" be armored with a corrugated longitudinal copper alloy armor at a "respectable" processing speed? Having defined a definite goal, the development of machinery and methods to produce this structure was undertaken.



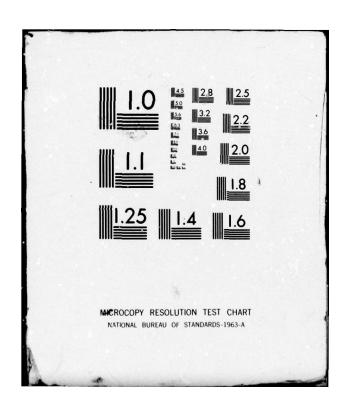


GENERATION II

FIGURE 1. DESIGN COMPARISON

CONTRACTOR OF STREET

ARMY COMMUNICATIONS RESEARCH AND DEVELOPMENT COMMAND -- ETC F/G 9/1 PROCEEDINGS OF THE INTERNATIONAL WIRE AND CABLE SYMPOSIUM (28TH--ETC(U) AD-A081 428 NOV 79 UNCLASSIFIED NL 4 of 5 AD-A08I428 Q (0) 1 P



MANUFACTURING CONSIDERATIONS

Culminating over three years of active effort on the part of the Bell Telephone Laboratories in Atlanta and the Western Electric Company at Baltimore, a structural design was arrived at and, after extensive field trial evaluations, manufactured for use in the Bell System as the link from the distribution point to the subscriber's premises.

An initial consideration in the design of the manufacturing process was that once the core sac was filled with waterproofing compound, it could not be disturbed by transporting it to subsequent operations (i.e., armoring, jacketing, etc.). The reason for this was that compound squeezing out of the core at the take up station would create an obvious housekeeping problem. Of even greater importance was that since some quantity of filling compound in the core sac would be lost during transport, the ability for the filled structure to retard the ingress of water would be obviously impaired. Using these considerations as design parameters, a tandem manufacturing line was designed and installed which combined six operations, similar to those performed on the interim design.

PROCESS DESIGN

The supply for the waterproofing/armoring lines is individual reels of twisted pairs insulated with a high molecular weight polyethylene (see Figure 2). The supply stands, a Western Electric Company design, maintain low and constant torque on the individual twisted pair supply reels to prevent excessive insulation shrinkback and conductor stretch.

The twisted pairs are then stranded in a layless fashion for pair counts in excess of two, but laid in parallel for the two pair design. Past data on a five pair service wire indicated that adverse capacitance unbalance effects were minimized using the layless approach rather than employing the conventional drum stranding method.

The twisted pairs are then grouped together and guided into an air cooled heat exchanger (see Figure 3). This exchanger, on the inlet side, retards counterflow of the filling compound out of the filling chamber during line shutdown. Exiting the inlet chamber, the core then passes through the filling chamber whose length prevents inadequate filling caused by compound cavitation and air entrainment at high manufacturing speeds. For pair counts in excess of two, an alternate filling method is available which changes the configuration of the core as it is advanced through the filling chamber to permit the entire periphery of the conductors to be exposed to the composition. Subsequently, the conductors are permitted to reform into the original core configuration with portions of the composition filling the interstices between the conductors. The reformation is facilitated by the changes in

strain produced by the elastic recovery of the conductors and the tension in the manufacturing line. I Since the core resides in the filling chamber for a very short time, a thin solidified skin of filling compound adheres to the outer surface of the insulated conductors. Viscous drag pulls along molten filling compound through the exit heat exchanger, air cooled like the inlet, and finally through a die which wipes the core to size. Water cooling, used in the past, was deemed unnecessary and in some aspects deleterious to the quality of fill. Vacuum/Pressure impregnation, also employed in the past, was found to yield a quality of filling equal to the present method.

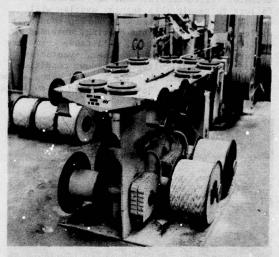


FIGURE 2. SUPPLY STAND

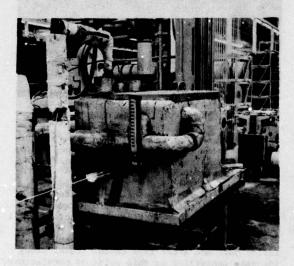


FIGURE 3. PRIMARY FILL TANK

The filled core is then enveloped longitudinally with a thin layer of polyester film (see Figure 4). The film, embossed for waterproofing compound retention, acrs as both a dielectric and mechanical barrier. The film embossment creates a mechanical wetting between the filling compound and itself and allows easier forming than a nonembossed polyester film of equivalent thickness. Since the core size is rather small, and the polyester is the only dielectric protection afforded to the cable between the conductor insulation and the armor, the degree of angular overlap, approximating that of larger diameter filled cables, must be retained. Failure to retain this angular overlap will result in arcing through the overlap causing dielectric heating. This heating, observed in earlier production trials, will cause premature failure of the polyester barrier, eventually leading to a high voltage breakdown condition between core to sheath. The wrapped core is then unitized and locked into orientation by applying a helical serving of polyolefin binder.

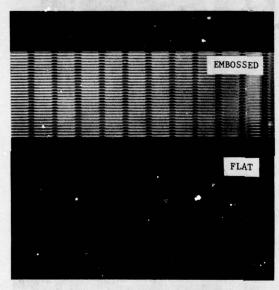


FIGURE 4. POLYESTER CORE WRAP

Up to this point of manufacture, the magnitude of development expended was overshadowed by the massive concentrated effort applied to the armoring/corrugating system.

The bound core is mechanically deflected out of its previously established line of travel and does not return to its original trajectory until it enters the forming apperatus along with the corrugated armor (see Figure 5). Since the filled core and armor tape cannot travel along the same centerline at this point of manufacture, one, or the other, must be displaced. Choosing the lesser of two evils, the filled core was chosen to be the displaced member. Approach angles on the deflection system were held to a minimum to prevent excessive sidewall pressure which would cause the filling compound to be

squeezed out of the structure. It was previously stated that the filled core could not occupy the same centerline of travel at this point of manufacture. The reason for this was the design of the armor accumulation system. Various existing methods of accumulation were considered, but due to the width, mechanical properties, and processing speeds of the copper alloy strip, it was ascertained that an open lattice of cumulative stock would diminish the possibility of mechanical damage during processing (see Figure 6). The accumulator, nested on an elevated level above the manufacturing line, receives the armor off of floor level mounted supply stands, up into the elevated accumulation lattice, and finally, back down to ground level where it enters the corrugator. The accumulator, in combination with an electrical resistance welder, allows continuous operation of the manufacturing line without shutting down to splice from pad to pad.

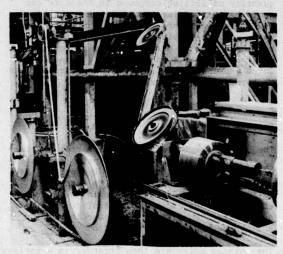


FIGURE 5. DEFLECTION SYSTEM

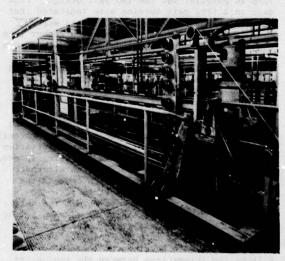


FIGURE 6. ARMOR ACCUMULATOR

The design of the corrugating rolls was arrived at by minimizing the deep drawing effect caused by an excessive number of corrugating teeth in contact with the stock material at any one point in time, and maximizing the corrugator roll pitch diameter. Programming the relationship between these parameters, using predetermined values for peak to peak amplitudes and corrugation count, various geometric combinations for the corrugating rolls were determined. Several iterations were then performed to compare the iconic model to existing larger size cable designs, in order to arrive at the optimum design. The rolls, theoretically optimized, performed well in actual practice. Hardness of the peaks and valleys in the armor tape were approximately 30 points higher on the Rockwell "B" scale than the midpoint between a peak and an adjacent valley. This selective hardening, while imparting higher resistance to penetration at the valleys, and of even greater importance at the peaks, did not overly work harden the armor to a point of nonductility. To insure ductility has not been lost in the finished structure, completed wire is wrapped around a 1½" radius mandrel for a number of convolutions, taken off of the mandrel and straightened out. It is wrapped around the mandrel again, taking care that the contact point of the sheath and the mandrel surface is approximately 180° from the previous sheath contact point, then removed and the armor is examined for cracks visible to the naked eye. The number of cracks observed to date have been well below accepted quality standards.

Once corrugated, the strip enters the armor former along with the previously deflected bound core (see Figure 7). A secondary application of filling compound is accurately metered between the bound core and corrugated armor as the armor is being formed into a tube. The metering device, accurate to less than 1% at full rate, is designed to linearly track the speed of the line to insure a constant volumetric quantity of fill per unit length at any line speed.

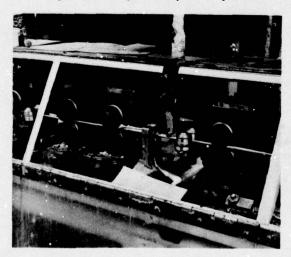


FIGURE 7. ARMOR FORMER

In forming a corrugated tube from narrow stock material one must carefully examine the mechanism involved. Softer shield materials such as aluminum need not conform to rigid forming parameters as do the harder materials such as copper alloys and stainless steels. Since the material must undergo a plastic deformation, the total work is a summation of the deformative work associated with bending the stock to shape, redundant work associated with internal deformation, and the work used to overcome the frictional resistances at the interface between the deforming metal and forming tools. 2 In order to achieve the final shape, the displacement work would remain fairly constant regardless of the forming method used. The redundant work can be somewhat reduced by minimizing edge stretch due to tensile stress unbalance between the midpoint of the stock material and the edges. The work to overcome frictional resistance can be greatly reduced, as in the case of this apparatus, by converting the majority of frictional forces, tending to retard linear motion, into inertial and rotational forces. Since the frictional resistance inherent to the tube forming apparatus used in the manufacture of this wire is low, tool wear and heat build up is minimal. What exits the forming apparatus is a formed tube, circular in cross section, which is fairly ductile.

The armored structure then passes into the extruder crosshead which utilizes specially designed poly (vinyl chloride) tooling which distributes the die pressure around the surface of the formed tube causing a thin wedge of the thermoplastic material to be injected between the overlap and underlap (see Figure 8). The shield circumference is not totally locked in by virtue of the corrugation profile, and the overlap/ underlap surfaces are allowed to shift in an oscillatory fashion during placement due to the resiliency of the thermoplastic material. Using a single extruder, the wedge and outer jacket over the armor are both applied simultaneously forming a monolithic covering in the completed

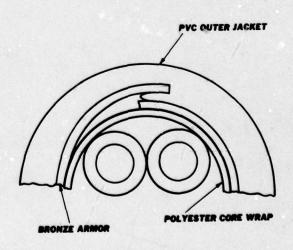


FIGURE 8. SHEATH DESIGN

product. Based on the results of a number of field trials, absence of the wedge would cause cracking of the armor and ultimately complete breakage of the structure. This cracking was due to the relatively small size of the cable core which the copper alloy armor envelopes, and the torsional rigidity of the completed wire. Large? size cables which are armored with the same type of material do not experience the aforementioned cracking and subsequently do not need to be jacketed in this manner. The jacketed wire is then sparktested at a direct potential of approximately 11 KV, sequentially marked every two feet with the cumulative footage length and Western Electric manufacturing location, and finally taken up onto a shipping reel.

CONCLUSIONS

This new design of filled Service Wire is as water and flame resistant as its forerunner. With the introduction of the previously outlined tandem method of manufacture, a structure with augmented mechanical integrity is now being produced at the lowest possible cost to the system.

ACKNOWLEDGMENTS

The author gratefully acknowledges the design efforts of the Wire Media Group of the Bell Telephone Laboratories, Atlanta, and the assistance of Engineering Personnel in the Outside Plant and Station Wire Development Group at the Baltimore Works who all enhanced the development of this project.

REFERENCES

- J. M. Hacker, U. S. Patent No. 3,885,380, May 27, 1975.
- G. E. Dieter, Jr., "Mechanical Metallurgy", Metallurgy and Metallurgical Engineering Series, 1961.
- J. M. Hacker, U. S. Patent No. 4,151,365, April 24, 1979.



Mr. J. M. Hacker, a Senior Development Engineer with the Western Electric Company at the Baltimore Works in Maryland, was graduated from the University of Maryland in 1970 with a Bachelor of Science Degree in Mechanical Engineering, and is presently engaged in graduate studies leading to an M.B.A. Degree at the Loyola College of Baltimore. He is currently responsible for the manufacture of all water resistant Service Wire at Baltimore. Mr. Hacker is a member of the Society of Plastic Engineers and has been granted a number of patents in the area of Outside Plant and Station Wire.

THE RESERVE AND THE RESERVE AN

APPLICATION OF SEISMOLOGY IN TELEPHONY

Louis Ance and Joseph P. McCann

Rural Electrification Administration Washington, D. C. 20250

Abstract

REA has adopted seismology for defining and locating rock in their construction contracts. This method of verifying rock locations will save telephone companies considerable amounts of money in construction by eliminating payments for rock cutting where ground could not be plowed due to improper plowing equipment. Seismology is also used to determine the best locations for cable plowing, pipe-pushes and underground duct systems.

Introduction

REA investigated several methods for defining and locating rocks and rock forma-One such method was rating tractors and defining their capability to plow or rip through different types of geological forma-REA soon learned that there were many variables involved in rating a tractor. Traction methods, accessories allowing plow blades to tilt and vibrate, considerations for the age and general condition of the tractor and the type of environment being dealt with all had to be considered. number of variables made it impossible to define the ripping or plowing ability of each tractor. Further research showed that the application of seismic testing in conjunction with USDA soil maps and available tractor rating information gave a practical solution to defining rock and rock formations.

Seismology

A seismograph is an instrument used to measure the travel time of a compressional (sound) wave artificially produced in the ground between the source and a detector. Past experience has shown that by using this simple procedure, a seismograph can be used successfully to indicate the type and composition of subsurface materials.

The velocities of sound waves differ greatly for different subsurface materials, depending upon such factors as hardness, degree of consolidation and density. The seismograph measures the velocity in each layer of material and thus allows subsurface identification and

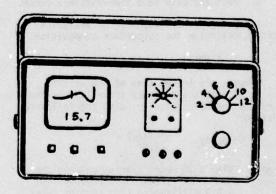
engineering classification.

A. Seismograph - The seismograph used in Figure 1 is an electronic device for measuring a short time interval with very high precision. The time interval is that required for a sound wave to travel through the earth for a distance of several tens or hundreds of meters. The sound is produced from a hammer flow. The arrival of the sound wave is detected by a geophone. This instrument is designed to measure only the upper layers of the earth. Figure 2

Equipment

The total time interval is rarely more than a few hundredths of a second and must be measured to an accuracy of 1/1000 of a second. Recent technological advances have allowed units to become more compact, easier to operate and less expensive.

FIGURE I



- B. Geophone The geophone is a sensitive device for detecting the ground vibrations produced by the arriving sound waves in the ground. A spur on the bottom of the geophone allows it to be embedded firmly into the topsoil for maximum effectiveness.
- C. <u>Hammer</u> A sledge hammer is all that is required to generate ground vibrations when conducting surveys involving depths at which cables are plowed. The hammer is fitted with a special switch which closes at the instant of impact.



D. Striking Plate - A striking plate should lay on the ground and be used to receive the hammer impact. The purpose of this plate is to achieve maximum energy transfer from the hammerhead into the ground.

Data Gathering Procedure

- Connect the geophone and hammer extension cords to the proper receptacles on the seismograph.
- Lay out a measuring tape along the ground to be surveyed, marking off increments to be used as hammering stations.
 - 3. Place a geophone at the starting point.
- 4. Turn the seismograph on, adjust the focus and intensity of the reference line on the cathode ray tube, adjust the gain, depress the "clear" function and then depress the "arm" function.
- 5. Pound a hammer on a striking plate at each marked location (clear and arm each time) and record the corresponding time readings at each location displayed on the seismograph.
 - 6. Plot the data on a time-distance curve.
- 7. Using either graphical or analytical methods, determine the subsurface composition.

Profiling the Subsurface

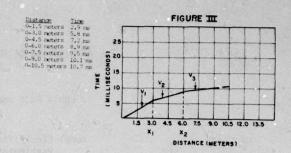
Knowing the travel time of the seismic wave as well as the distance travelled, we can calculate the wave velocity using the following equation:

$$Velocity = \frac{Distance}{Time}$$

Example: With a 10 meter spacing between the hammering location and geophone and a 2.5 millisecond time reading taken from the seismograph the seismic velocity would be:

Velocity =
$$\frac{10 \text{ meters}}{0.0025 \text{ sec.}}$$
 = 4000 m/sec.

A single velocity calculation gives a very general indication of subsurface composition. To increase the accuracy several time readings at different distances should be plotted on a graph. Some sample data and a corresponding graph is shown in Figure III.



Connecting the points plotted in Figure III with straight lines yields 3 lines with different slopes. Each slope corresponds to a different velocity and each velocity corresponds to a different subsurface material. The three velocities are as follows:

$$V_1 = \frac{3.0 \text{ m}}{5.8 \text{ ms}} = 517 \text{ m/sec}$$

$$V_2 = \frac{6.0 - 3.0 \text{ m}}{8.9 - 5.6 \text{ ms}} = 968 \text{ m/sec}$$

$$V_3 = \frac{10.5 - 6.0 \text{ m}}{10.7 - 8.9 \text{ ms}} = 2500 \text{ m/sec}$$

The hammer distances at which the changes in slope occur are designated x_1 and x_2 (See Figure III).

$$D_n = P(D_{n-1}) + \frac{x_n}{2} \sqrt{\frac{v_{n+1} - v_n}{v_{n+1} + v_n}}$$

Where:

Dn = depth of discontinuity

n = number of discontinuities - 1, 2, 3, 4,
etc.

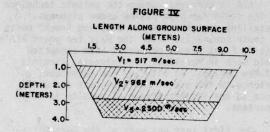
P = 5/6 or 0.85 or more accurately:

$$P = 1 - \begin{bmatrix} \frac{V_{n+1}}{V_n} \sqrt{\left(\frac{V_{n+2}}{V_n}\right)^2 - 1} & -\frac{V_{n+2}}{V_n} \sqrt{\left(\frac{V_{n+1}}{V_n}\right)^2 - 1} \\ \hline \sqrt{\left(\frac{V_{n+g}}{V_n}\right)^2 \left(\frac{V_{n+1}}{V_n}\right)^2} \end{bmatrix}$$

Substituting appropriate values and approximating, we find:

$$D_2 = 0.85(0.83) + \frac{6.0}{2} \sqrt{\frac{2500 - 968}{2500 + 968}} = 2.70 \text{ m}$$

Based on this data, a rough profile of the area surveyed would appear as shown in Figure IV.

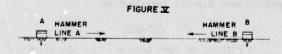


The computed depths represent an average value over the center two-thirds of the entire hammer line. For example, if the hammer line extends to a maximum distance of X max = 100 meters, then the computed depth is an average from roughly the 20 meter station to the 80 meter station.

In situations not requiring a high degree of accuracy, an approximation can be used to estimate the depth which hard materials are not present. Roughly, it can be said that no harder material exists within a depth of at least onethird of the maximum hammer distance.

Dipping Discontinuities

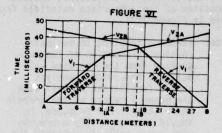
Up to this point it has been assumed that discontinuities are horizontal. The fact is each different layer of material is most likely at some incline. To establish the dip of a discontinuity, a traverse must be run in both the forward and reverse directions. Refer to Figure V. If the geophone was at position A for the first traverse, with the line of hammer stations extending to the right in the sketch, then a second traverse must be taken with the geophone at position B using the same hammer stations.



Taking another example, assume both a forward and reverse traverse were run and data obtained from both traverses was plotted on a graph. See Figure VI.

Note that the total time from A to B as well as the velocity V_1 must be the same for both traverses. If this is not the case, there is something wrong with the data.

By inspection of Figure VI or similar graphs the following conclusions may be drawn concerning the first discontinuity:



a. The depth to the V_2 material will be larger at the end of the traverse which shows the larger break distance, X_1 . In this example, X_{1B} (measured from point B) is larger than X_{1A} (measured from point A), so we conclude that the depth at B is greater than the depth at A.

b. Since the dip is proportional to the difference between X_{1A} and X_{1B} , we can make a rough estimate as to whether the dip is large or small. If X_{1A} and X_{1B} are equal, then the dip is zero and the surface is horizontal.

c. The true velocity V_2 is roughly equal to the average of V_{2A} and V_{2B} . $V_2 \cdot 2 \frac{(V_{2A})(V_{2B})}{V_{2A} + V_{2B}} \cdot 2 \frac{(1370)(2100)}{(1370) + (2100)} \cdot 1658 \, \text{m/sec}$

$$V_2 = 2 \frac{2A}{V_{2A}} + \frac{2B}{V_{2B}} = 2 \frac{(1370) + (2100)}{(1370) + (2100)} = 1658 \text{ m/sec}$$

$$D_A = \frac{X_{1A}}{2\sqrt{V_{2A} + V_1}} \frac{V_{2A} - V_1}{2\sqrt{V_{2A} + V_1}} \frac{10.8}{2\sqrt{1370 + 360}} = 4.1 \text{ m}$$

$$D_B = \frac{X_{1B}}{2\sqrt{V_{2B} - V_1}} \frac{V_{2B} - V_1}{2\sqrt{2100 + 360}} = 5.6 \text{m}$$

$$DIP \text{ ANGLE } \Theta = 1/2 \left[\sin^{-1} \left(\frac{V_1}{V_{2B}} \right) - \sin^{-1} \left(\frac{V_1}{V_{2A}} \right) \right]$$

$$DIP \text{ ANGLE } \Theta = 1/2 \left[\sin^{-1} \left(\frac{V_1}{2100} \right) - \sin^{-1} \left(\frac{360}{1370} \right) \right] = 2.7 \text{ degrees}$$

Based on this data a profile of the two earth layers would appear as illustrated in Figure VII.



Estimating Physical Properties of Earth Materials from Seismic Velocities

After analyzing the seismic graphs and determining the velocities and depths, estimate the compositon of the subsurface materials from the table in Figure VIII.

Note: Before attempting to estimate physical properties of the subsurface from the computed velocities, the seismic analyst should familiarize himself with the general nature of the terrain under study. For instance, he should know generally where the area water table is, whether the overburden is a product of weathering or underlying bedrock, whether it is mostly glacial drift over limestone, etc. Velocities alone are not a positive indication of material physical properties.

When estimating the type of subsurface, there are several general rules which the analyst should keep in mind as he studies the velocity chart. These rules are:

- Velocity is roughly proportional to a degree of consolidation, or hardness, of the rock or soil.
- 2. In unconsolidated materials, velocity increases somewhat with water content.
- Weather of a rock will greatly reduce its velocity.
- 4. A particular rock type will include a range of velocities, and these ranges may overlap for different rock types.
- Correlation of velocity with the type of earth material will depend to a great extent on the overall geological characteristics of the area under study.

6. Velocity measurements are very sensitive to dip of the interference. If high-precision measurements of velocity are required (for such purposes as estimating rippability under borderline conditions), always assume that a dip exists and follow the procedure for "Dipping Discontinuity".

It is entirely possible to use the seismic velocity data to determine such rock properties as rippability and bearing capacity. Such properties may differ with field conditions. Figure IX shows published data on rippability with a D7 tractor.

Field Experience

REA is currently using the seismic technique in the field for pipe-pushes under highways, installing duct systems and dafining "rock" units in their contracts. Over the past two years REA's Outside Plant Branch personnel have conducted field work in Maryland, Pennsylvania, Virginia and New Mexico. As with any new technique, experience in the use of the equipment and confidence in the interpretation of results is very important.

Our first test was made at the Agriculture Research Center in Beltsville, Maryland. The area is used for farming crops and should have contained little, if any, rocky areas. Our data verified this hypothesis. We had no difficulty in profiling the substrate. (See Figure X).

Our next trial at Commonwealth Telephone Co. in Dallas, Pennsylvania, was along a stretch of highway with noticeable outcrop of rock. We profiled the stretch for approximately one mile and defined the section in the area of the rock. Later, the telephone company installed the cable without difficulty and the rock outcrop was a large boulder. (See Figure XI). Additional field trials in Virginia and New Mexico provided information in the use and interpretation of equipment and data.

The REA field engineer located in Kentucky/ Tennessee reports excellent results in the use of this seismic technique for pipe-pushes under highways and for duct construction. One telephone company installed a 500 foot duct system without difficulty.

Several telephone companies have installed pipe under highways on the first or second attempt. Previously, construction crews made an average of five or six attempts to "push" pipe under a highway. Considering the cost of a five man crew and the associated equipment, the seismic technique paid for the instrument on the first underground highway installation.

Summary

A ripping or rock unit will be specified in the REA construction contract where a plow train capable of delivering a minimum of 55,000 pounds drawbar pull at 1.2 miles per hour forward speed is incapable of plowing cable at a specified depth. Where the capability of the plow equipment to deliver the specified drawbar pull is in question, the use of a refraction seismograph will be used by an engineer in determining if a rock or ripping unit is to be specified.

As the program gains acceptance and craftsperson gain experience in the use of the seismograph, the profiling of the borrower's right-ofway prior to construction may some future day become a reality.

Definitions

<u>Dip</u> - The angle of deviation from the horizontal made by a discontinuity surface. A horizontal discontinuity has a dip of 0 degrees.

<u>Discontinuity</u> - In reference to actual subsurface structure, the point or depth at which the material composition changes from a harder to a softer material, or vice versa. On a plot, the point at which the velocity slope changes value.

Profile - A cross-sectional representation of the earth surface.

<u>Survey</u> - The program of conducting a series of seismic traverses to accomplish a specific engineering purpose.

Time Reading - The measured time of travel of a sound wave through the earth from the hamwer to geophone.

<u>Traverse</u> - A line comprising the geophone position and the hammer stations. More exactly, a sequence of positions in a straight line along the earth's surface, comprising a fixed geophone position and several hammer stations, from which enough time readings can be obtained to construct and interpret one seismic plot.

<u>Velocity</u> - Speed of sound waves through a particular type of subsurface material. Velocity increases with increasing hardness of material, and usually falls in the range of 200 to 4600 meters per second.

<u>Acknowledgments</u>

We acknowledge the assistance of Messrs. Frank Whitehouse, George Pettross, Jr., Joseph C. McHale, and Ralph J. Fornaris in the compilation of data for this paper.

References

Engineering Seismology - Instruction Manual, Soiltest, Inc., first edition 1975.

Handbook to Ripping. Caterpillar Tractor Co., fifth edition 1975.

List of Published Soil Surveys, U.S.D.A. Soil Conservation Service - 1979

Biography

Louis Ance is on the staff of the Outside Plant Branch of REA's Telephone Operations and Standards Division. Previously he was a manager of Product Engineering, System Equipment Plant, Superior Cable and Equipment Division, Hickory, North Carolina. Most of his work has been in the field of outside plant application and designing and is the holder of 6 patents in Telephony.

Joseph P. McCann graduated from University of Maryland with a B. S. in Chemistry in 1956 and Newark College of Engineering with a M. S. in Engineering in 1968. He is presently an Outside Plant Engineer with the Rural Electrification Administration. Previously, he was associated with Bell Telephone Laboratories and is co-inventor of their design for filled cable.

FIGURE VIII

Table of Representative Velocity Values

(Note: Occasional formation may yield velocities which lie outside of these ranges)

Velocity in Meters/Seconds

Unconsolidated Materials

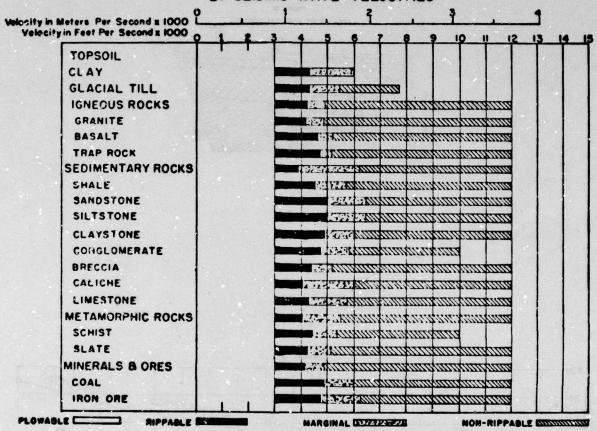
Most unconsolidated materials	Below 915
Soil - normal	245 to 460
- hard packed	460 to 610
Water	1525
Loose sand - above water table	245 to 610
below water table	460 to 1220
Loose mixed sand and gravel, wet	460 to 1050
Loose gravel, wet	460 to 915

Consolidated Materials

Most hard rocks	Above 2440
Coal	915 to 1525
Clay	915 to 1830
Shale - soft	1220 to 2135
- hard	1830 to 3050
Limestone - weathered	As low as 1220
- hard	2440 to 5485
Basalt	2440 to 3960
Granite and unweathered gneiss	3050 to 6100
Compacted glacial tills	
hardpan, cemented gravels	1220 to 2135
Frozen soil	1220 to 2135
Pure Ice	3050 to 3660

FIGURE IX

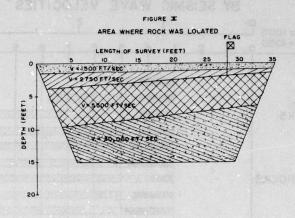
D7G RIPPER PERFORMANCE ESTIMATED BY SEISMIC WAVE VELOCITIES*

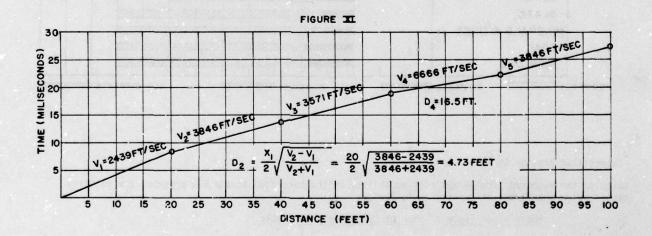


Based on the expected plowing and ripping ability of tractors used in the REA program, the velocity ranges below should be interpreted as follows:

Above water lable	In or Below the Water lable	2
0-914 m/sec	0-1524 m/sec	Plowable
914-1524 m/sec	1524-21	Rippable
1524 m, sec and up	2134 m/sec and up	Rock

^{*}Caterpillar Tractor Co.





DOSEARCH PROPERTY

LOW SMOKE AND FLAME SPREAD CABLES

L. J. Przybyla* E. J. Coffey+ S. Kaufman M. M. Yocum J. C. Reed D. B. Allen

Underwriters Laboratories
*Northbrook, Illinois
+Melville, New York

Bell Laboratories Norcross, Georgia E. I. Du Pont de Nemours Wilmington, Delaware

Abstract

Fire and smoke performance objectives for exposed installation of communications cables in air handling spaces were added to the 1975 National Electrical Code. A test was developed for flame and smoke measurement of cables. Tests were conducted and, based upon comparison of performance to acceptable wiring systems, several low smoke and flame spread cables were classified by UL.

Introduction

The National Electrical Code (NFPA No. 70) restricts the types of wiring permitted in air handling spaces in order to limit the spread of fire and smoke. All cables installed in the return air space above a suspended ceiling, often called a plenum, must be enclosed in metallic raceway or conduit. Alternately, specified metal sheathed cables may be installed without conduit. Exceptions to the conduit requirement are provided for communications, power-limited, and fire alarm cables that are listed as having "adequate fire resistant and low-smoke producing characteristics.

The three types of metal sheathed cables permitted are mineral-insulated metal-sheathed (Type MI⁵), metal-clad (Type MC⁶), and armored (Type AC⁷). Acceptance of these metal sheathed cables is presumed to be based on their similarity to a conduit system. The constructions of these cables are specified in the Code and in the Underwriters Laboratories (UL) Listing requirements. For exposed wiring other than the specified metal sheathed cables, the Code does not provide construction details. Instead it specifies apperformance requirement that the cables must have adequate fire resistant and low smoke producing characteristics.

When this performance requirement was first incorporated in the 1975 Code, an

appropriate test for assessing smoke and fire resistance did not exist. The Code writers did not know that it would be possible to develop cables to meet the Code intent. Their purpose in adopting a performance requirement was to encourage innovation in the development of highly fire resistant and low smoke producing cables.

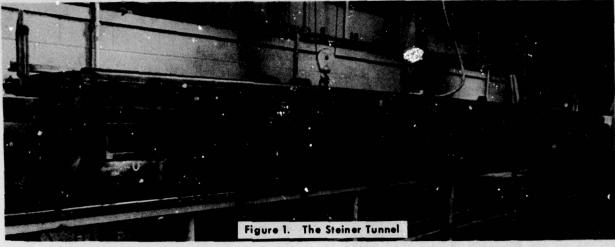
In response to the performance criteria in the Code, a test method was developed for measuring flame spread and smoke properties of cable, 8 and highly fire resistant and low smoke producing cables are now available. These cables are Classified by UL as meeting the intent of the Code.9, 10 The fire testing leading to the Classifications is the subject of this paper.

Experimental Plan

Fire experience has shown that enclosing cables in metallic conduit adequately limits the spread of fire and smoke from the cables within. Therefore, testing was conducted to compare flame spread and smoke from conventional cable enclosed in conduit with that from a new generation of highly fire resistant and low smoke producing cables. The new cables were judged to have "adequate fire-resistant and low-smoke producing characteristics" if, when tested without conduit, their flame spread and smoke production were less than or comparable to conventional cable in conduit.

Test Method

The test was developed and described by Beyreis et al.⁸ The test method utilizes the Steiner Tunnel (Figure 1). A single layer of cable or conduit is installed in a cable rack as shown schematically in Figure 2. The fire test is conducted with a 300,000 BTU/hour diffusion flame ignition source which engulfs the first 4-1/2 feet of cable rack for the 20 minute test duration. Air movement through the tunnel, controlled at 240 ft/min, exhausts combustion products while providing air for combustion.



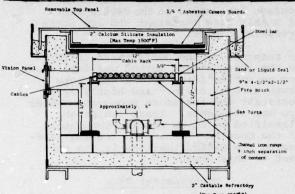


Figure 2. Cross Section of Tunnel Showing Mounting of Cable Rack

The relationship between flame propagation in this test and flame propagation in a simulated plenum has been investigated. 11,12 It was concluded that this test provides a severe fire environment in comparison to the fire in a simulated plenum. Therefore this test is a useful and conservative tool for judging the flame spread and smoke producing properties of cables.

Smoke is measured in the tunnel by means of a photocell and light source mounted across the 16 inch diameter exhaust duct. Optical density of the smoke is recorded during each test. Optical density is defined as log10 (Io/I) where Io is the incident light intensity and I is the light intensity which reaches the photocell after attenuation by smoke. Smoke which attenuates 90% of the incident light yields an optical density value of 1, 99% attenuation yields 2, and 99.9% attenuation equals 3. Optical density is used because it is linearly related to human visibility and directly proportional to the concentration of smoke particles. 14

Cables and Conduit Tested

Four different types of cable were tested;
1) telephone inside wiring cable, 2) telephone station wire, 3) power limited signal/fire alarm cable, and 4) coaxial cable. Two versions of each cable type were tested, conventional and highly fire resistant. The conventional cables were jacketed with PVC and insulated with either PVC or polyethylene (PE). The highly fire resistant cables were all insulated and jacketed with a fluorinated ethylene propylene copolymer (FEP). Further details of the cable constructions are given in Table I and Figure 3.

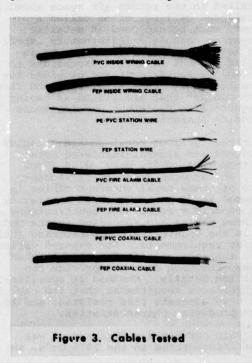
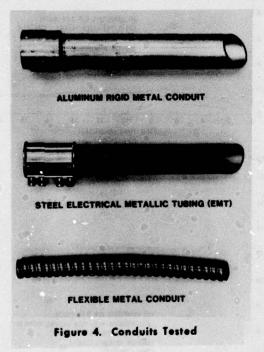


TABLE I
Cables Tested

Cable Type	AWG	Construction	Insulation Material	Jacket Material
Inside Wiring Cable	24	25 pairs	PVC	PVC
Inside Wiring Cable	22	25 pairs	FEP	FEP
Station Wire	22	4 wire quad	polyethylene	PVC
Station Wire	22	4 wire quad	FEP	FEP
Fire Alarm	18	6 conductors	PVC	PVC
Fire Alarm	18	6 conductors	FEP	FEP
Coaxial		RG-8 single	foamed polyethylene	PVC
Coaxial		RG-8 single	foamed FEP	FEP

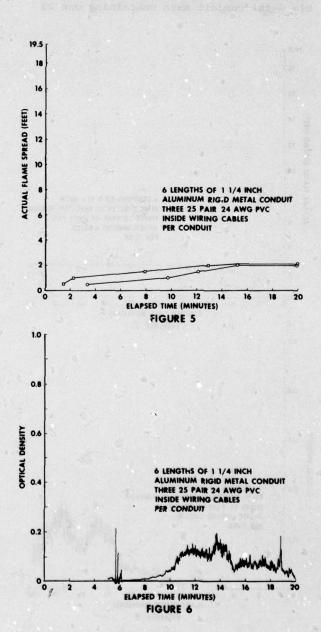
Four different types of conduit were used (Figure 4); 1) aluminum rigid metal conduit with threaded aluminum connectors, 2) steel electrical metallic tubing (EMT) with die cast setscrew connectors, 3) steel flexible metal conduit, without connectors, and 4) aluminum flexible metal conduit, without connectors.



Results

Telephone Cable

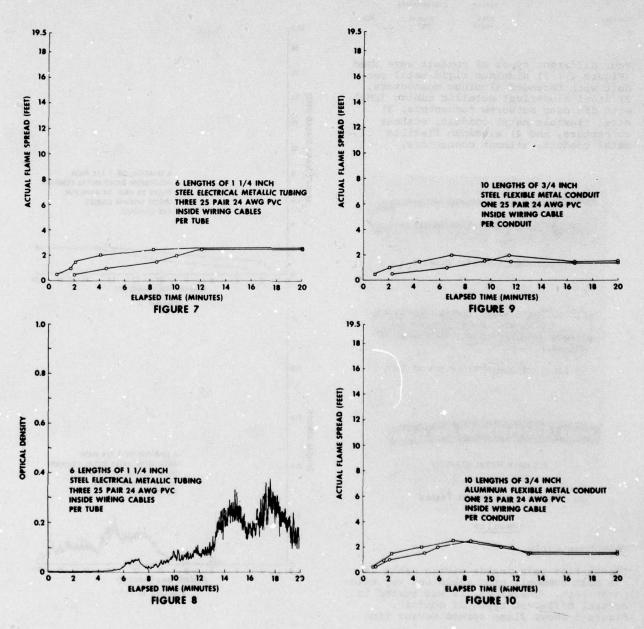
Twenty-five pair inside wiring cable is the most commonly used cable for key telephone sets. Therefore, it was tested in several different types of conduit. Figure 5 shows flame spread versus time curves for two tests of 25 pair inside wiring cable in aluminum rigid metal conduit. The cable rack was filled with 6 lengths of 1-1/4" conduit, each containing 3 lengths of 25 pair cable. In both tests the peak flame spread was very low - only 2 feet. Smoke from one of the tests is shown in Figure 6. Smoke production was very low; optical density, averaged over the 20 minute test period was only 0.05, with a peak optical density of 0.2.



Results for cable in steel electrical metallic tubing (EMT) are similar. Peak flame spread for 6 lengths of 1-1/4" steel EMT each containing 3 twenty-five pair cables, is only 2-1/2 feet (Figure 7). Smoke results for one test are shown in Figure 8. Average optical density for the two tests was 0.08, with a peak of 0.38 in one of the tests.

Flame spread versus time curves for 10 lengths of 3/4" steel or aluminum flexible metal conduit each containing one 25

pair cable are shown in Figure 9 (steel) and Figure 10 (aluminum). Peak flame spreads for cable in either conduit were only 2 to 2-1/2 feet. Smoke was negligible for cable in the steel conduit (Figure 11); average optical density for the duplicate tests was 0.007 with a peak of 0.06 in one of the tests. Cable in aluminum conduit emitted very little smoke, (Figure 12) but considerably more than cable in steel conduit; average optical density for the duplicate tests was 0.07, with a peak of 0.56 in one test.



Flame spread versus time curves for 18 lengths of 22 gauge, 25 pair FEP telephone cable are shown in Figure 13. The peak flame spread for both tests was 3 feet. Smoke was low (Figure 14). Average optical density for the duplicate tests was 0.08, with a peak at 0.35 in one test, (Figure 14). The total amount of smoke emitted, as measured by the average optical density, is similar to the smoke emitted by conventional cable in steel EMT.

Figure 15 shows flame spread versus time curves of two tests of quadded PE/PVC

2.0

1.8

1.6

1.4

1.2

1.0

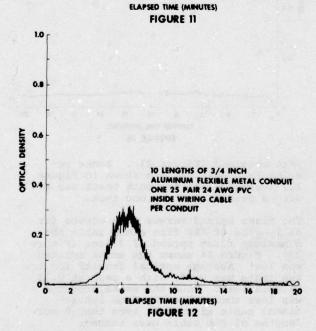
1.0 LENGTHS OF 3/4 INCH
STEEL REXIBLE METAL CONDUIT
ONE 25 PAIR 24 AWG PVC
INSIDE WIRING CABLE
PER CONDUIT

0.4

0.2

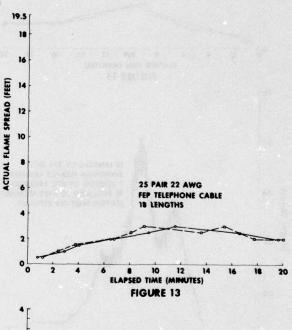
12

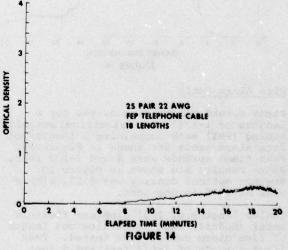
16 18

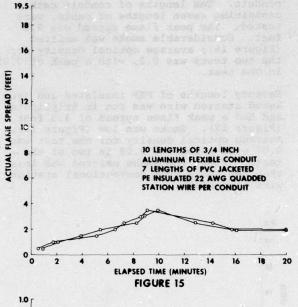


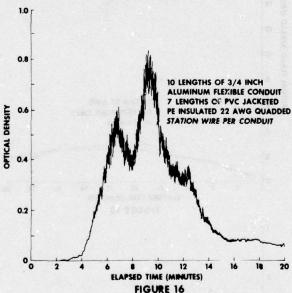
station wire in 3/4" aluminum flexible conduit. Ten lengths of conduit each containing seven lengths of cable, were tested. The peak flame spread was 3.5 feet. Considerable smoke was emitted (Figure 16); average optical density for the two tests was 0.2, with a peak of 0.85 in one test.

Seventy lengths of FEP insulated and jacketed station wire was run in triplicate and had a peak flame spread of 3.5 feet (Figure 17). Smoke was low (Figure 18). Average optical density for one test was 0.07 with a peak of 0.08 in two of the tests. Thus, the smoke emitted was less than the smoke from conventional station wire in conduit.





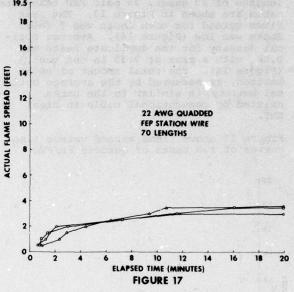


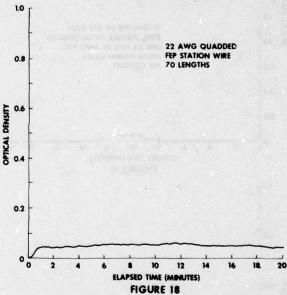


Fire Alarm Cable

Flame spread versus time curves for 6 lengths of 1-1/4" steel electrical metallic tubing (EMT) each containing 5 lengths of fire alarm cable are shown in Figure 19. Peak flame spreads were 4 and 3-1/2 feet. Smoke results are shown in Figure 20; average optical density was 0.13, with a peak of 0.70 in one test.

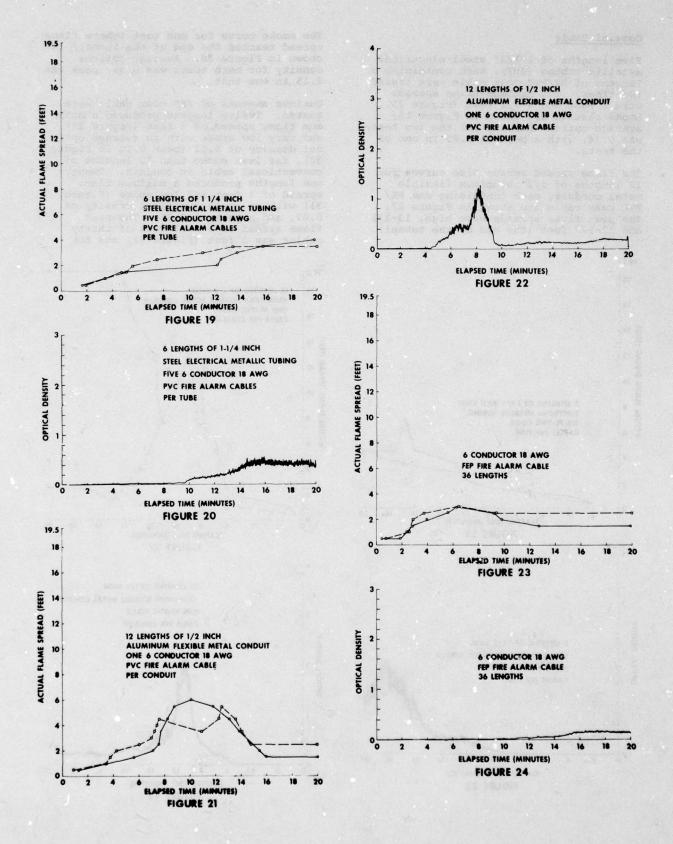
Twelve lengths of 1/2" aluminum flexible metal conduit, each containing one length of fire alarm cable, were tested. Peak flame spreads of 5-1/2 feet and 6 feet





were obtained (Figure 21). Smoke results from one test are shown in Figure 22; average smoke for both tests was 0.21, with a peak of 1.20 in one test.

The flame spread versus time curves for 36 lengths of FEP fire alarm cable show a maximum flame spread of 3 feet (Figure 23). Figure 24 shows the smoke emitted was low. Average optical density for the two tests was 0.04, with a peak at 0.15 in each test. Thus the smoke produced was less than the smoke from conventional cable in conduit even though more lengths of FEP cable were tested.



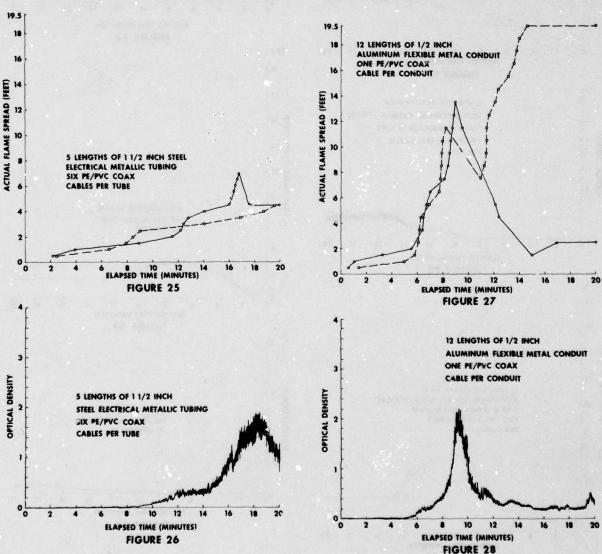
Coaxial Cable

Five lengths of 1-1/2" steel electrical metallic tubing (EMT), each containing 6 lengths of PE/PVC coax cable were tested two times. The maximum flame spreads were 7 feet and 4-1/2 feet (Figure 25). Smoke results are shown in Figure 26; average optical density for the two tests was 0.24, with a peak of 1.85 in one of the tests.

The flame spread versus time curves for 12 lengths of 1/2" aluminum flexible metal conduit, each containing one PE/PVC coax cable are shown in Figure 27. The peak flame spreads were high, 13-1/2 and 19-1/2 feet (the end of the tunnel).

The smoke curve for one test (where flame spread reached the end of the tunnel) is shown in Figure 28. Average optical density for both tests was 0.39; peak was 2.15 in one test.

Various amounts of FEP coax cable were tested. Twelve lengths produced a maximum flame spread of 3 feet (Figure 29) and very low smoke with an average optical density of 0.02 (peak 0.12 in Figure 30), far less smoke than 12 lengths of conventional cable in conduit. Twenty-one lengths produced a maximum flame spread of 3 feet and low smoke (Figure 31) with an average optical density of 0.07, and a peak at 0.25. The peak flame spread of a full rack of thirty cables was 3 feet (Figure 32) and the



average optical density was 0.15, with a peak in one test of 0.60, (Figure 33), comparable smoke to 30 lengths of conventional cable in conduit.

In addition to recording flame spread and smoke results, observations were made of the conduit and cables after each test. The aluminum rigid conduit was discolored but remained virtually intact. The steel EMT was discolored with the connectors melted in the fire region (which facilitated the release of smoke). The aluminum flexible tubing was partially melted while the steel flexible tubing was only discolored. The flexible tubing with interlocked but unsealed armor permitted smoke to issue along its length. The PVC cables were a combination of ash, char and melted jacket and insulation material depending upon the severity of fire envolvement. The FEP cable was melted in the fire region with the remaining sample appearing undamaged.

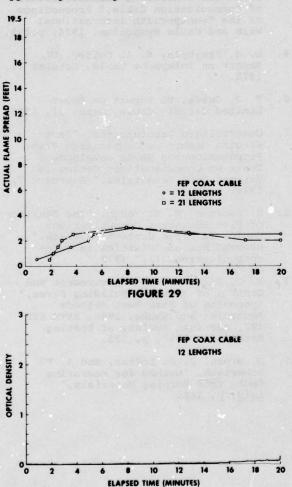
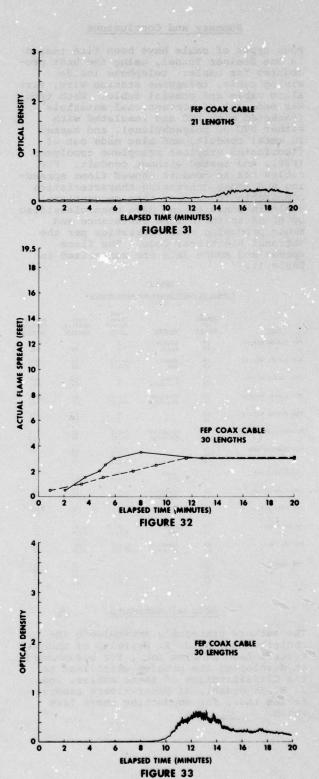


FIGURE 30



Summary and Conclusions

Four types of cable have been fire tested in the Steiner Tunnel, using the best procedures for cable: telephone inside wiring cable, telephone station wire, fire alarm cable and coaxial cable. Each type was made out of conventional materials (jacketed with PVC and insulated with either PVC or polyethylene), and tested in metal conduit, and also made out of fluorinated ethylene propylene copolymer (FEP), and tested without conduit. FEP cables not in conduit showed flame spreading and smoke generating characteristics comparable to or less than conventional cable in conduit, and have been classified by UL as to their fire resistance and smoke producing characteristics per the National Electrical Code. The flame spread and smoke data are summarized in

TABLE II
Summary of Flame Spread and Smoke Results

	Number of		Peak Flame Spread	Peak Optical	Average Optical
Cable	Cables	Conduit	Feet	Density	Density
PVC Inside Wiring	18	aluminum	2		
	18	rigid	2	.20	.045
PVC Inside Wiring	18	steel	2-1/2	.14	.069
	18	EMT	2-1/2	. 38	.094
PVC Inside Wiring	10	steel	2	.06	.008
	10	flexible	2	.04	.005
PVC Inside Wiring	10	aluminum	2-1/2	.56	.084
	10	flexible	2-1/2	.31	.051
PEP Inside Wiring	18		3	. 35	.12)
	18		3	. 25	.047
PE/PVC Station Wire	70	aluminum	3-1/2	.85	.222
	70	flexible	3-1/2	.66	.157
FEP Station Wire	70		3-1/2	.08	.069
	70	-	3-1/2	.07	-
	70	•	3-1/2	.08	
PVC Fire Alarm	30	steel	4	.70	.17
	30	EMT	3-1/2	.50	.09
PVC Fire Alarm	12	aluminum	6	.60	. 22
	12	flexiole	5-1/2	1.20	.19
FEP Fire Alarm	36	SART MATE IN	3	.10	.028
	36	•	3	.15	.043
PE/PVC Coax	30	steel	7	1.85	.37
	30	EMT	4-1/2	1.00	.11
PE/PVC Coax	12	aluminum	13-1/2	1.85	.45
	12	flexible	>19-1/2	2.15	.32
FEP Coax	12		3	.12	.015
	21		3	.25	.067
	30		3	.45	.13
	30		3	.60	.15

Acknowledgements

The authors gratefully acknowledge the contributions of J. R. Beyreis, of Underwriters Laboratories Inc., for his counsel in developing the program which lead to the Classification of these cables, and J. W. Skjordahl, of Underwriters Laboratories Inc., for conducting these fire tests.

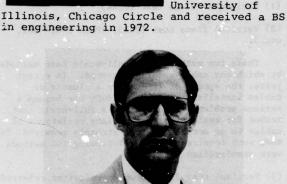
References

- 1. National Electrical Code, 1978
 Edition, National Fire Protection
 Association No. 70-1978, Section
 300-22(c).
- 2. ibid, Section 800-3(d).
- 3. <u>ibid</u>, Section 725-2(b).
- 4. ibid, Section 760-4(d).
- 5. ibid, Article 330.
- 6. ibid, Article 334.
- 7. ibid, Article 333.
- 8. J. R. Beyreis, J. W. Skjordahl, S. Kaufman and M. M. Yocum, "A Test Method for Measuring and Classifying the Flame Spreading and Smoke Generating Characteristics of Communication Cable," Proceedings of the Twenty-Fifth International Wire and Cable Symposium, 1976, p.291.
- L. J. Przybyla, E. J. Coffey, UL Report on Telephone Cable, October 11, 1978.
- T. J. Guida, UL Report on Power Limited Circuit Cable, March 21, 1979.
- 11. Underwriters Laboratories, "Fact-Finding Report on Comparative Flame Propagation and Smoke Development Tests on Communications Cables in Various Test Geometries," February 7, 1978.
- 12. S. Kaufman, M. M. Yocum, "The Behavior of Fire Resistant Communications Cables in Large Scale Fire Tests," proceedings of "Plastics in Telecommunications II," 1978.
- 13. R. G. Silversides, "Measurement and Control of Smoke in Building Fires," Symposium on Fire Test Methods Restraint and Smoke, 1966, ASTM STP 422, American Society of Testing Materials, 1967, p. 125.
- 14. D. Gross, J. J. Loftus, and A. F. Robertson, "Method for Measuring Smoke from Burning Materials," ibid, p. 166.



in engineering in 1972.

L. J. Przybyla is a Senior Project Engineer in the Fire Protection Department of Underwriters Laboratories, Inc. He has been in-volved in large scale fire testing and the development of fire test methods for wire and cable. He attended the University of



Stanley Kaufman is the Supervisor of the Materials Chemistry Group at Bell Telephone Laboratories in Norcross, Georgia. He received a B.S. in Physics from the City College of the City University of the City of New York, and a Ph.D. in Chemistry from Brown University. Before joining Bell Laboratories in 1970, he was a research scientist at the Uniroyal Research Center.



Joseph C. Reed is a Technical Specialist in the Fluoropolymers Division, Plastic Products and Resins Department, DuPont Company. He has been with DuPont for 30 years in various manufacturing, marketing and technical assignments. In recent years, his work

has focused on evaluating the behavior of fluoropolymer resins when used as electrical insulation on wire.



E. J. Coffey received his B.S. Degree in Electrical Engineering from the University of Notre Dame in 1952. He earned his Masters in Business Administration from the New York University in 1959. He is presently Associate Managing

Engineer with the Underwriters Laboratories. Mr. Coffey is also a member of Code Making Panel 6 of the National Electrical



Mary Margaret Yocum is a Western Electric employee who is assigned to Bell Laboratories in the area of flame retardant material development. She attended Cottey College and the State University of Iowa. Before Joining Western Electric she was employed by Continental Oil Company.



David B. Allen is a Senior Development Specialist in Fluoropolymers Division, Plastic Products and Resins Department, DuPont Company. He has been with DuPont for the past 25 years in various technical and marketing assignments, the last 20 years involved with Teflon fluorocarbon resins and since its introduction Tefzel fluoropolymer resins.

DEVELOPMENT OF FLAME-RESISTANT CABLES FOR INSTRUMENTATION AND COMMUNICATION

T. Yamamoto, Y. Takahashi and K. Nakano

The Fujikura Cable Works, Ltd., Tokyo, Japan

ABSTRACT

Having succeeded in the manufacture of flameresistant instrumentation cables, communication
cables and coaxial cables which can pass vertical
tray and vertical duct flame tests, we studied the
flame resistance of these cables. Intorducing a
new idea, cable oxygen index, its relation to the
results of cable flame tests was studied. As a
result, it was confirmed that the cable oxygen
index is effective for evaluation of the flame
resistance of cables.

1. INTRODUCTION

In recent years, power plants, large manufacturing plants, multistoried buildings, etc. are employing large quantities of power cables and control cables. In these plants, buildings, etc., a cluster of cables are installed in trays or ducts. If a fire starts, it spreads along these cables and the adjoining equipments catch fire, causing a serious damage. To minimize such damage, the cables must be resistant to flame and should not help the fire to spread even if it has caught fire. The flame-resistant power cables and control cables satisfying the above-mentioned requirements were developed already.

In recent years, those plants, buildings, etc. are employing large quantities of instrumentation cables, communication cables and coaxial cables to ensure complete automatic control and concentrated monitoring. As these cables are required to have high-quality transmission characteristics, polyethylene is widely employed for insulation, which is excellent in electrical and physical properties but is inflammable. It is, therefore, difficult to produce flame-resistant cables so far as polyethylene is used for insulation.

Vertical tray flame test and much severer vertical duct flame test are mainly employed for evaluation of the flame-resistance of cables in an actual fire. We have succeeded in the manufacture of instrumentation cables, communication cables and coaxial cables, which can pass the abovementioned flame tests. Reported hereinbelow are the results of he study of the flame resistance of these cables.

2. FLAME RESISTANCE OF CABLES

The following test methods are conventionally employed for evaluation of the flame resistance

of cables.

- (1) Horizontal flame test (UL44)
- (2) Vertical flame test (UL83, IPCEA-S-61- 402, etc.)

These two methods are small-scale test methods by which one cable sample is tested. In recent years, the spread of fire along a cluster of cables installed in a tray or duct has become a serious problem. Accordingly, a full-scale test method for evaluation of the flame resistance of cables in an actual fire was strongly required. To meet such requirements, the following two methods were standardized recently.

(3) Vertical tray flame test (hereinafter referred to as "VTFT")

This method was standardized in IEEE Standard 383 in 1974 (Ref. 1) and are widely employed.

(4) Vertical duct flame test (hereinafter referred to as "VDFT")

In plants, buildings, etc., catles are installed in closed ducts in most cases. If the cables catch fire under this condition, they will burn rapidly as the flames run upward because of ascending current and the temperature in the duct rises rapidly.

For evaluation of the flame resistance of cables under such condition, the VTFT employing an open tray is not sufficient. For this reason, VDFT was established in JCS 366 in Japan in 1978 (Ref. 2).

As shown in Fig. 1, a vertical tray is installed in the center of a metallic duct and 3,000 mm long cable specimens are installed on both sides of the tray at intervals of the half of their overall diameter until their total width reaches about 250 mm. The cables are burnt for prescribed time by a ribbon burner installed at a height of about 700 mm from the floor level in the duct. After stopping the burner, cables that are self-extinguishing without burning up to the top end of the tray are accepted and the time required until the flome is put out, the damaged distances of insulations and jackets are measured.

3. FLAME-PROOFING OF CABLES

To impart flame resistance to caples, the application of flame-resistant plastics is essential. For this purpose, it is necessary to have a correct understanding of burning phenomena in plastics and to use effective flame retardants in a suitable combination.

Plastics burn in the manner as described below. When a plastic material is overheated, its surface melts first and thermal decomposition occurs, producing an inflammable gas. This gas reacts with oxygen at temperatures above 500 to 600°C so rapidly as to give rise to combustion. The plastic material is overheated again by the heat energy released as a result of such reaction. Thus, the plastic material continues to burn through the repetition of the above-mentioned processes (Ref. 3, 4).

This continuous burning of plastics can be expressed as shown below. The heat energy is released through exothermic reactions between carbon monoxide and a highly reactive OH radical produced through the thermal decomposition of a plastic material.

Flame retardants to be used for retardation of burning of plastics are required to fulfil the following characteristics

- (1) To catch the OH radical which acts as a source of combustion
- (2) To shut off exygen supply
- (3) To prevent temperature rise by generating endothermic reactions

The fiame retardants will be described in more detail hereinbelow (Ref. 5, 6).

(a) Halogen base flame retaidant

Halogen is combined with the OH radical. The halogenated hydrogen produced at the time of burning is converted into an inert gas and reduces the oxygen concentration in the atmosphere. Accordingly, polyvinyl chloride (hereinafter referred to as "PVC"), chroloprene rubber, etc., which contain halogen elements, do not burn easily as compared with polyethylene (hereinafter referred to as "PE").

(b) Phosphorus base flame retardant

A phopshorus base flame retardant produces polyphosphoric acid through thermal decomposition. This acid forms a covering on the surface of the plastics to shut off oxygen from them.

(c) Antimony trisulfide

When this antimony is used in combination with a halogen base flame retardants, halogenated antimony is produced through thermal decomposition. When melted or evaporated, endothermic reactions are generated. When evaporated, the halogenated antimony is converted into an inert gas which reduces the oxygen concentration.

(d) Aluminium hydroxide

Aluminium hydroxide contains water of crystallization, which decreases temperatures by the latent heat when evaporated. Aluminium hydroxise also reduces the oxygen concentration by the vapour produced at the time of evaporation.

For imparting flame resistance to plastics, the above-mentioned flame retardants should be used in a proper combination in consideration of their workability, physical and electrical stability, costs, etc. Various plastics materials and their oxygen indexes representing their flame resistance (hereinafter referred to as "OI") are given in Table 1.

The OI is defined as the volume percentage of a minimum oxygen concentration which is necessary for a material to continue burning in a mixture of oxygen gas and nitrogen gas. The OI increases as the flame resistance of material increases. The method of evaluating the flame resistance of material in terms of OI is high in accuracy and excellent in reproducibility.

4. RESULTS OF THE FLAME TESTS FOR THE FLAME-RESISTNAT CABLES

Using the flame-resistant materials as described in the preceding chapter for jackets, insulations, etc., we succeeded in the manufacture of flame-resistant instrumentation cables, communication cables and coaxial cables that can pass VTFT or/and VDFT. At this time, we manufactured several trial cables using materials with different OIs, to obtain the basis for design of cables that can pass flame tests. The constructions of these cables and the results of their flame tests are given in Table 2. In VDFT, the PE insulated cables were burnt by the burner for 15 minutes and the PVC insulated cables for 20 minutes. The burning states in VTFT and VDFT are shown in Figs. 2 and 3, respectively.

As seen from Table 2, the cables consisting of an insulation made of PE, which is not flame-resistant, can pass VTFT. In this case, however, the OI of PVC used for jackets must be higher than that of the jackets of the PVC insulated cables. It will be seen that the cable that can pass VDFT must be produced by using materials with high OI for their jackets, insulations, binding tapes, etc. to enhance the OI of the whole cables.

5. DISCUSSION

The results of VTFT and VDFT reveal that the study of OI of jacket materials only is not sufficient for estimation of the results of flame test. As a cable is made of materials with different OIs, however, it is difficult to estimate the flame resistance of the whole cable clearly, and it is more difficult to compare the flame resistance of cables made of different materials. To facilitate our study, we introduced an idea of OI of the whole cable (hereinafter referred to as "cable-OI") by averaging the OIs of respective cable materials, and studied the correlation between the cable-OI and the flame resistance of cable.

Simplifying the model of flame-resistant cable as far as possible, we approximated the cable-OI by the following equation on the assumption that the cable-OI is equal to the value obtained by averaging the OIs of all combustible materials in terms of volume ratio:

OI = \sum_{k} Sk x OIk / \sum_{k} Sk x 100 % ····· (4)

where Sk : cross-sectional area of k-th cable material

Olk : oxygen index of k-th cable

material

The cable-OIs of the cables manufactured by way of trial are given in Table 2. The relation between cable-OI and the results of VTFT is shown in Fig. 4, while Fig. 5 shows the relation between cable-OI and the results of VDFT.

As seen from Figs. 4 and 5, in the same type of cable, a correlation exists between cable-OI and the damaged distance of jacket. It is, therefore, possible to estimate the flame resistance of cable by obtaining the cable-OI.

As the cable-OI is decreased, the damaged distance is increased, resulting in complete burning in the end. It is possible to estimate the minimum cable-OI necessary for a cable to pass flame tests, which are given in Table 3. These values can be used as a general guide to the design of flame-resistant cables.

For further examination of the flame resistance of cables, the following phenomena shown in Figs. 4 and 5 are worth notice.

- (1) It will be seen that PE burns more easily than PVC with equal OI. This may be because halogens in PVC catch OH radicals, and because PE melts more easily and produces larger quantities of energy.
- (2) Comparing PVC insulated cables with control cables (Ref. 7), which is shown in Fig. 4, it will be seen that the cables become more flamable as the conductor diameter increases. This may be because heat escapes from the burning area due to the heat conduction in the conductor, thus dropping the temperature in the burning area, as the conductor diameter

increases.

- (3) It will be seen that metalic shielded cables are noninflamable. This may be because the internal temperature drops due to the heatconduction effect as described in (2) above and because the metalic shieldings prevent the leakage of inflammable gas from the cable inside and the infiltration of exygen gas into the cable inside.
- (4) It will be seen that the cables filled with fillers are noninflamable. If there is a gap in the cable inside, the oxygen contained in such a gap contributes to burning.

Insulations of instrumentation cables, communication cables and coaxial cables are mostly made of PE as importance is attached to their transmission characteristics. Most of these cables have conductors of small diameter and are of multi-core construction. It is, therefore, difficult to impart flame resistance to these cables as compared with power cables and control cables for the reasons as described in (1) to (4) above.

In the future, efforts should be directed toward the following to improve the flame resistance of instrumentation cables, etc..

- (a) Development of PE with higher OI as a insulation material. Use of insoluble flame-retardant crosslinked polyethylene. Development of PVC with excellent electrical characteristics.
- (b) Filling the gap with fillers or the like and imparting flame resistance to them.
- (c) Use of a metallic shielding tape

6. CONCLUSION

We manufactured various types of flameresistant instrumentation cables, communication cables and coaxial cables, and confirmed that these cables can pass VTFT and VDFT. Introducing the concept of cable-OI, we approximated it by using very simplified models.

Comparing the cable-OI with the results of flame tests, it was found that a correlation exists between the cable-OI and damaged distance of jackets for the same type of cables, and it was confirmed that the cable-OI can be used for evaluation of the flame resistance of cables.

In the future, we will study the method of correcting the cable-OI depending on the difference in flame resistance between PE and PVC, the presence or absence of shielding tape, etc. Furthermore, we will make efforts to establish the method of estimating the flame resistance of cables with higher accuracy and reliability, and to develop flame-resistant cables that are more excellent in electrical characteristics and low in cost.

7. ACKNOWLEDGEMENT

The authors wish to express their thanks to many colleagues in The Fujikura Cable Works, Ltd who are engaged in the manufacturing and the development of flame resistant cables, and especially to the personnel of the Insulated Wire and Cable Group of our company who have supplied us with valuable data.

8. REFERENCE

- (1) IEEE Standard 383, Para 2. 5, 1964.
- (2) Japanese Cable Makers' Association Standard 366, 1978.
- (3) Kobe, "Kobunshi no Netsubunkai to Tainetsusei".
- (4) Z.E. Jollers, G.I. Tollers, Plastics and Polymer, vol. 40, <u>150</u>, 1974.
- (5) Eichhorn, Journal of Applied Polymer Science, vol. 3, <u>2511</u>, 1964.
- (6) Konishi and Hirao, "Nannenzai".
- (7) Yatsuhashi et al., Fujikura Technical Review, No. 57, 9, 1977.



Tomohiro Yamamoto

Engineer of Telecommunication Cable Engineering Dept.
The Fujikura Cable Works, Ltd.,
1-5-1, Kiba, Koto-ku,
Tokyo, Japan

Mr. Yamamoto received B.E. degree in electrical engineering from Kyusyu Unversity in 1967 and has been engaged in engineering of electronic and telecommunication cables. Mr. Yamamoto is a member of the institute of Electrical Engineers of Japan.



Yoshihiro Takahashi

Engineer of Telecommunication Cable Engineering
Dept.
The Fujikura Cable Works,
Ltd.,
1-5-1, Kiba, Koto-ku,
Tokyo, Japan

Mr. Takahashi received M.E. degree in electrical engineering from Yokohama National University in 1971 and has been engaged in engineering of electronic and telecommunication cables.
Mr. Takahashi is a member of the institute of Electrical Engineers of Japan.



Kousaku Nakano

Engineer of Material
Engineering Group,
Telecommunications
Research and Development
Dept.
The Fujikura Cable
Works, Ltd.,
1440 Mutsuzaki
Sakura-shi, Chiba-ken,
Japan

Mr. Nakano recived M.S. degree in chemistry from Gunma University in 1975 and has been engaged in research and development of plastic materials and manufacturing method for electronic and telecommunication cables. Mr. Nakano is a memeber of the Chemical Society of Japan.

Table 1 Oxygen indexes of cable materials

Materials	Symbols	01 (%)
Polyethylene	PE	17 - 18
Plame retardent polyethylene	FR-PE	23 - 25
Cross linked polyethylene	XLPE	17 - 18
Flame retardant cross linked polyethylene	FR-XLPE	23 - 28
Polyvinylchloride	PVC	23 - 24
Flame retardant polyvinyl- chloride	FR-PVC	25 - 42
Jute	Jute	20 - 21
Flame retardant jute	FR-Jute	30 - 40

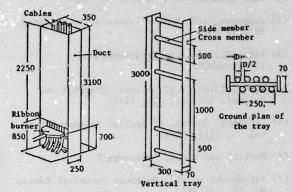


Fig. 1 Equipment of Vertical Duct Flame Test (dimensions in mm)

* The calorie of the burner is 70,000 BTU/hour.

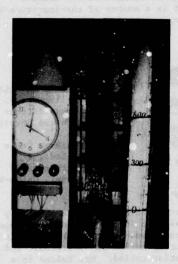


Fig. 2 Vertical Tray Flame Test



Fig. 3 Vertical Duct Flame Test

Table 2 Construction results of flame tests of trial manufactured cables

able	rip-	Name					Construc	Construction of cables	ables			Results of VIFT	of VIFT	Results of VDFT	of VDFT
		cables	Insula-	Insula- Fillers Bind-	Bind-	Shield-	Shield- Jackets Overall	Overal1	0×y	Oxygen index (%)	x (%)	Damaged	Flame	Damaged	Flame
	A DE		SHOTI		80 00 00 00 00 00 00 00 00 00 00 00 00 0	1000	ni W	(Approx.	Insula- Jac- tions kets		Cable-01 of ja	of nueing jacket time (mm)	nueing time (min)	of nucing jacket time (mm)	conti- nueing time (min)
-			PVC	Jute	FRT	-	FR-PVC	11.0	24	36.2	30.0	750	0	1550	0
7		FT-ICW	PVC	FR-jute	FRT	1	FR-PVC	11.0	24	36.2	31.8	700	0	1400	•
3	Instru-	100 *	FR-PVC	FR-jute	FRT	-	FR-PVC	11.0	32.5	36.2	34.1	650	0	006	•
4	menta-	0.5mm ²	FR-PVC	FR-jute	FRT	-	SFRV	11.0	32.5	42	37.3	650	0	750	0
5	tion		PE	PLY	ITI	-	FR-PVC	11.0	18	30	24.5	Bured	up in 5*		-
9	Cables		PE	Jute	PLT	1	FR-PVC	11.0	18	38	29.4	1050	2	1	'
1		FT-ICEV	PE	Jute	PLT	1	SFRV	11.0	18	42	31.6	006	2	Buned	up in 5
8		10c *	FR-PE	FR-jute	FRT		FR-PVC	11.0	24	38	33.1	800	-	Buned	up in 10
6		0.5mm ²	FR-XLPE	FR-jute	FRT	•	SFRV	11.0	28	42	35.5	850	0	1500	7
10			FR-XLPE	FR-jute	SFRT	•	SFRV	11.0	28	42	36.8	800	0	1200	•
11			FR-XLPE	000	SFRT	-	SFRV	11.0	28	42	36.9	950	0	1400	•
12		FT-ICEV-S FR-PE	FR-PE	FR-jute	FRT	CUL	FR-PVC	12.0	24	38	33.0	800	0	Burned	up in 11
13		10c *	FR-XLPE	-XLPE FR-jute	FRT	CUT	SFRV	12.0	28	42	35.4	700	0	1100	0
14		0.5mm2	FR-XLPE	FK-jute	SFRT	CUL	SFRV	12.0	28	42	36.6	750	0	950	•
15			PE	-	FRT	-	FR-PVC	21.5	18	32.5	27.2	1200	3	-	•
16	Communi- FT-CPEV	FT-CPEV	FR-PE	1	FRT	-	FR-PVC	21.5	24	32.5	28.9	1200	3	-	-
	cation	30F *	PE	1	FRT	1	SFRV	21.5	18	42	32.8	950	2	Burned	Burned up in 9
18	Cables	0.9mm	FR-PE	-	FRT	1	SFRV	21.5	24	42	34.6	800	0	Burned	up in
		FT-	PE	-	1	CUB	FR-XLPE	6.2	18	28	24.0	Burned	up in 6		-
20	Coaxial	Coaxial RG-59B/u	PE	1	SFRT	CUB	FR-PVC	6.2	18	36.2	29.1	950	7 2	Burned	Burned up in 8
	Cables	-L4	PE	-	SFRT	CUB	FR-PVC	14.0	18	36.2	30.5	006	3	Burned	Burned up in 9

PLY: Plastic yarn
PLT: Plastic tapes
FRT: Flame retardant tapes
SFRT: Spsecial flame retardant tapes

CUT: Cupper tapes
CUB: Cupper braids
SFRV: Special flame retardant PVC

: The time in minutes when the flames reached the end of the cables

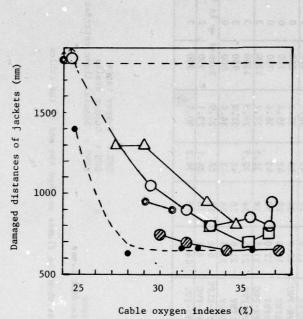


Fig. 4 Relation Between Cable Oxygen
Indexes and Results of VTFT

Ø FT-ICVV
O FT-ICEV
□ FT-ICEV-S

△ FT-CPEV

Frame resistant coaxial cables
Frame resistant control cables
3C x 5.5mm² (Ref. 7)

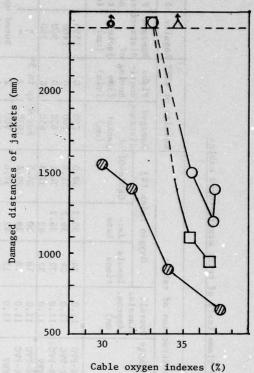


Fig. 5 Relation Between Cable Oxygen indexes and Pesults of VDFT

Table 3 Minimum cable oxygen indexes for passing the flame tests

Cables	Minimum cable-OI (%)	
1	VTFT	VDFT
PE insulated cables	26	34(burned for 15min.)
PVC insulated cables	26	29(burned for 20min.)

A FLAME RESISTANT POWER AND CONTROL CABLE INSULATION FOR MODERN ELECTRICAL APPLICATIONS

E.R. Kingsbury

A.C. Bruhin

A.F. Wu

General Electric Company Bridgeport, Connecticut

ABSTRACT

A non-chlorinated, crosslinked polyolefin wire and cable insulation, fully qualified to industry standards, has been developed by the General Electric Company, Wire and Cable Business Department Laboratories. The physical, mechanical, and electrical characteristics are discussed in comparison with specification requirements.

This insulation, when applied to a conductor, has demonstrated that it will meet the industry standard requirements even after being subjected to a simulated 40 years of life in a nuclear power generating station. This simulation testing included heat aging equivalent to 40 years of service at 90°C, a gamma radiation total dosage of 2.2 × 108 rads, and a 110 day simulated loss of coolant condition. After these severe environmental tests, cables built with this insulation still met the requirements of the IPCEA moisture absorption test (Electrical Method EM-60), and maintained their flame resistant characteristics.

INTRODUCTION

The increased concern with safety necessary in contemporary power generating stations and industrial facilities has brought about the need for continuous evaluation of specifications to define reliable wire and cable for these applications. In response to this need, design engineers must consider the environmental and operational conditions in which wire and cable must perform, and then write into the specifications test requirements that will demonstrate the capabilities of the wire and cable to satisfactorily perform in these conditions for the expected life of the installation. In performing this task he must consider that the resulting performance predictions will be based on accelerated test techniques.

Requirements for wire and cable used in power generating stations can be classified in two basic categories. The first category is the electrical requirements such as insulation resistance, power factor, dielectric constant, dielectric strength, etc., which are required to yield satisfactory operation under maximum rated load for the environmental conditions such as installation handling, elevated temperatures, moisture, crush and abrasion, and in nuclear stations, radiation and loss of coolant conditions, all of which are detrimental to proper electrical performance.

In response to the needs of the industry for a wire and cable design that would increase the operational safety of industrial installations and power generating facilities, a non-chlorinated insulation has been developed by the General Electric Wire and Cable Laboratories. The properties of this insulation have been established by an extensive test program that included physical and electrical testing to the requirements of industry standards, thermal aging to a simulated 40 year life, exposure to 220 megarads of gamma radiation, a 110 day loss of coolant condition test and vertical flame tests. The detailed test program and test results are presented in this paper.

QUALIFICATIONS TO INDUSTRY STANDARDS

Testing to IPCEA Standard S-66-524

In order to determine the physical and electrical characteristics of the insulation, it was subjected to the test requirements of IPCEA S-66-524. These tests, and the additional long term testing conducted, give the end user a background of extended test data and the service life experience showing that the wire and cable will safely meet the operational requirements of the installation. The authors of IEEE STD383-1974² have recognized the value of this type of background and have suggested that in order to conform fully to the IEEE standard, the insulation system and construction must conform to one of the major industry standards, such as IPCEA S-66-524. The results of the industry standard test program are presented in Table I.

Long Term Electrical Tests

Long term reliability of an insulation system is of prime importance to insure safe operation. Testing in addition to the requirements of IPCEA S-66-524 was conducted to determine the electrical stability of the insulation. Test samples consisting of #12AWG, 7 strand tinned copper conductor with 30 mils nominal of extruded insulation were immersed in 75° C water with a -600V dc voltage applied to the conductor for a period of 26 weeks. During this time measurements of stability factor, power factor, and specific inductive capacitance were made. As can be observed in the data shown in Figures 1, 2 and 3, the insulation is stable and maintains its electrical characteristics throughout the long test period. To further test the reliability of the insulation, an IR stability test in both 75°C and 90°C water with 600 volts ac applied to the conductor was conducted for a period of 60 weeks. The data in figures 4 and 5 shows the electrical stability which is an inherent requirement for insulation reliability.

Testing to IEEE Standards 323-19743 and 383-19742

The IEEE standards present the type testing required for qualification of wire and cable to be used in nuclear power generating stations. In addition to the IPCEA requirements the wire and cable must meet the following environmental test conditions.

- A. Normal service life simulation equivalent to 40 years service at rated temperature.
- Exposure to a total radiation dosage equivalent to 40 years of service.
- Exposure to a loss of coolant condition of radiation, heat, steam pressure and chemical spray.
- D. A vertical tray flame test with a gas burner flame input of 70,000 Btu/Hr.

The test samples subjected to the IEEE Standard 383 requirements are shown in Table II.

TAPLE I Insulation Characteristics

Test MCHTALIL	Unite	IPCEA Value	Typical Test Value
Tensile Strength, min.	psi	1800	2550
Elongation at rupture, min.	%	250	392
Air Oven Aging, 168 Hrs @121°C Tensile, min. retention	%	75	95
Elongation, min. retention	%	75	96
Solvent Extraction, max.	%	30	25
Heat Distortion, 121°C max. % of unaged value	%	30	9.6
Voltage Tests	Volts	Pass	Pass
Insulation Resistance K Constant, min.	-	10,000	63,000
Dielectric Constant 1 Day, max.	DIA	6.0	2.5
Increase in Capacitance 1-14 Dayş, max.	%	3.0	0.42
7-14 Days, max.	%	1.5	0.42
Stability Factor	-	1.0	0.09
Alternate to Stability Factor	d	0.5	0.02

Table II
Test Sample Description

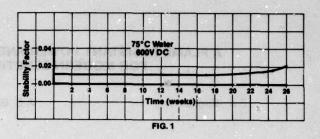
Conductor	Insulation	Binder	Jacket
1/C, 7 Strand, #12AWG, Tinned Copper	30 Mils Nominal	None	None
7/C, 7 Strand, #12AWG, Tinned Copper	30 Mils Nominal	Polyester Tape	45 Mils Nominal Neoprene

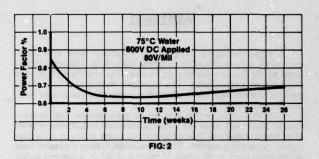
A. Normal Service Life Simulation

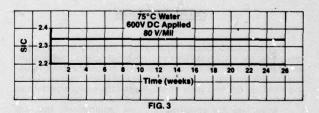
The Arrhenius technique is the accepted procedure for accelerated thermal aging and was used in this program to simulate 40 years of service life. The IEEE standards specify this technique and require that one of the test temperatures used to establish the Arrhenius plot shall be 136°C and that the other two test temperatures shall be at least 10°C apart. The standards, however, do not define the property to be measured or the end point to be used. In testing this insulation, percent elongation was selected as an indicator of aging since it is generally accepted as a reproducible test that reasonably predicts insulation degradation. The selection of the end point influences the slope of the Arrhenius plot and thus influences the life prediction. The end point normally selected is usually well below the absolute value of elongation required by the IPCEA standards for unaged material.

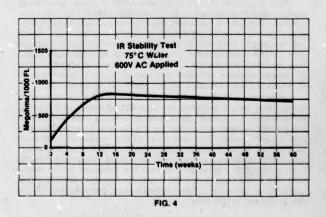
Since the Arrhenius technique has been established on the basis of the first order chemical reaction, the end point criteria cannot be arbitrarily selected but must be determined from the time-temperature test data plots so that it is associated with the first order chemical reaction only. Plots of the samples tested showed a relatively sharp reaction, a plateau of practically no change and a further or secondary reaction at test temperatures of 136°C, 150°C, and 160°C. The start of the plateau corresponded to an absolute elongation of 250% which was therefore selected as the end of life point. The use of an end point which is obtained from the first order reaction eliminates the possibility of obtaining misleading or possible invalid life expectancy data which: might occur if an end point that occurs after a secondary change is selected.

The simplified method for calculation of the regression line as shown in the Appendix to IEEE Standard 101-19725 was used to establish the Arrhenius plot shown in Figure 6. The raw data and the calculations for this plot are shown in Table III.









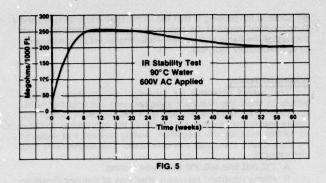


TABLE III
Arrhenius Calculations

1°C	T°K	$X = \frac{1}{T}$	X²	L	iog L =Y	log L = XY
136	409	2.4450×10 ⁻³	5.9780×10 ⁻⁶	960	2 9823	7.2916×10 ⁻³
136	409	2.4450×10-3	5.9780×10-6	1032	3.0137	7.3684×10 ⁻³
136	409	2.4450×10 ⁻³	5.9780×10 ⁻⁶	980	2.9912	7.3135×10 ⁻⁵
150	423	2.3641×10 ⁻³	5.5888×10 ⁻⁶	216	2.3344	5.5188×10 ⁻³
150	423	2.3641×10 ⁻³	5.5888×10-6	264	2.4216	5.7248×10
150	423	2.3841×10 ⁻³	5.5888×10-6	227	2.3560	5.5698×10*
160	433	2.3095×10 ⁻³	5.3336×10 ⁻⁶	65	1.8129	4.1869×10-
160	433	2.3095×10 ⁻³	5.3336×10-6	85	1.9294	4.4560×10
160	433	2.3095×10 ⁻³	5.3336×10-6	68	1.8325	4.2321×10~
Summi	ation 5	21.3558×10 ⁻³	50.7012×10 ⁻⁶		21.6740	51.6619×10-3

$$N = 9$$
Slope b = (N) ($\sum XY$) - ($\sum X$)($\sum Y$)
$$(N)(\sum X^2) - (\sum X)^2$$

 $= \frac{(9)(51.6619\times10^{-3}) - (21.3558\times10^{-3})(21.6740)}{(9)(50.7012\times10^{-6}) - (21.3553\times10^{-3})^2}$

= 8692

Intercept a =
$$(\Sigma Y) \cdot (b)(\Sigma X)$$

= -18.22

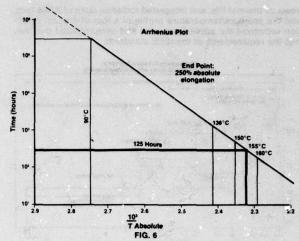
Temperature Rating for 40 Years (350, 400 Hours)

$$t = \frac{b}{Y-8} -273$$

$$= \frac{8692}{5.5445 - (-18.22)} -273$$

= 92.82°C

Temperature Rating For 125 Hours:



The predicted elongation of the insulation after aging for 40 years at a 90°C rated temperature is, therefore, equal to the minimum elongation requirements of IPCEA S-66-524 for **unaged** insulation. Based on the Arrhenius plot established from the aging data in Figure 6, an accelerated aging period of 125 hours at 165°C was established as simulating an excess of 40 years of service life at 90°C. The samples which were subjected to further environmental test requirements of the IEEE standards were subjected to these aging conditions.

B. Radiation Dosage

As part of the testing required for nuclear application, the test samples were exposed to a Cobalt 60 gamma field such that the average dose rate over the total exposure period was 500,000 rad per hour. The total exposure time was 412 hours, yielding a minimum dose of 222M rad to the cable. This dose simulates normal life (50M rads) plus the radiation predicted for a design base event (150M rads) plus 10% margin for a total of 220M rads. The test samples were rotated 90 degrees at intervals of approximately 100 hours of exposure. Irradiation was conducted in air at ambient temperature and pressure. Dosimetry was performed using a Victoreen Model 555 Integrating Dose Rate Meter and Probe. The total radiation dosage was applied prior to the loss of coolant condition testing to simulate a high dosage condition at the end of a 40 year life exposure. The samples were then exposed to the temperature, moisture, and chemical environments of a loss of coolant condition.

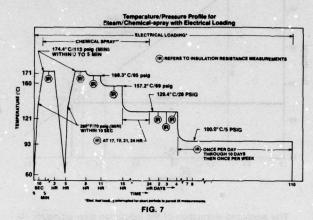
C. Loss of Coolant Condition

The loss of coolant condition testing simulates the environment to which the cables would be exposed if a pressurized water or a boiling reactor lost cooling water. This environment is simulated by the steam-temperature time conditions shown in Figure 7. These conditions were maintained for a period of 110 days, and a sodium hydroxide-boric acid chemical solution was sprayed on the test samples for the first 24 hours of the 110 day test period.

During the test period the cables were energized at 660 volts (10% above the rated voltage) and loaded with current levels determined from the IPCEA ampacity tables for cables in trays. This electric load was interrupted periodically so that insulation resistance measurements could be performed.

The test cables were installed on a mandrel, as shown in Figure 8, for the heat aging, radiation, and the entire loss of coolant condition simulation. At the conclusion of the 110 day period the test samples were removed from the mandrel, straightened, and reverse wrapped around a mandrel having a diameter of 40 times the cable diameter. The coiled samples were immersed in a tank filled with water for one hour and then subjected to an 80 volt/mil voltage withstand test for 5 minutes. The test samples which had been subjected to an environment equivalent to 40

years of thermal life, and integrated radiation dose of 220M rads, and the pressure/temperature profile of a loss of coolant condition withstood the applied potential and demonstrated that they met the requirements of the IEEE standards.



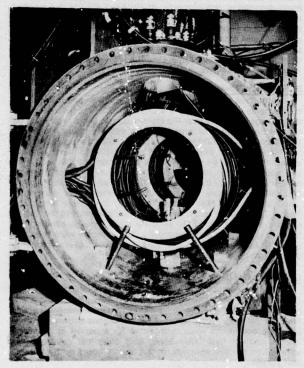


FIG. 8

D. Vertical Tray Flame Test

The IEEE standard for this test requires that a single layer of test cables be installed in a 12 inch wide, 3 inch deep, 8 foot long vertical metal cable tray. The layer of cable shail at least fill the center 6 inch portion of the tray with a separation of approximately one half the cable diameter between each cable. The cable mounted in the vertical tray was subjected to a flame from a ten inch wide gas burner with a heat input of 70,000 Btu's per hour, at an approximate temperature of 1500°F. The flame was applied 24 inches above the bottom of the vertical tray and three inches from the cable outer surface (per IEEE 383-74°). The flame was allowed to burn for a period of 20 minutes and was then shut

off. Criteria for passing is that the flame shall not propagate and burn the total height of the eight foot tray. The test cables did not propagate the flame and burned, including jacket char, a distance of approximately four feet.

Additional Testing

The overall objective for insulation development was not simply to meet the minimum specified requirements but rather to demonstrate the overall stability of the insulation system and insure satisfactory service for the life of the application. In order to further evaluate the insulation, testing beyond that required by the industry standards was conducted. This additional testing consisted of:

- A. 210,000 and 400,000 Btu flame testing.
- B. Flame retardant retention after loss of coolant condition test.
- C. Accelerated moisture absorption after loss of coolant condition test.

A. 210,000 and 400,000 Btu Flame Testing

High energy flame tests were conducted in a similar manner as the 70,000 Btu test of IEEE Standard 383-1974 except that the heat input to the burner was increased to 210,000 Btu and 400,000 Btu.

Single conductor cables of 14 Awg, 2 Awg, and 500 MCM gauge sizes were tested with a 210,000 Btu/hr flame source and a single layer of test samples in the tray. The flame source was spaced three inches from the cable. The maximum flame damage observed was 4 feet, 3-1/2 feet, and 3-1/3 feet respectively.

A seven conductor, 12 Awg cable was tested with a 210,000 Btu/hr flame source and a single layer of test samples in the tray. The flame source was spaced 13-1/2 inches from the cable. The maximum flame damage observed was 6-1/2 feet. This test was repeated with enough test samples to yield a 40% tray fill condition of loosely laid cables to allow air flow between the samples. The maximum flame damage observed in this test with 52 sample lengths of cable in the tray was 6 feet.

A 40% tray fill condition with seven conductor, 16 Awg cable test samples was subjected to a 400,000 Btu/hr flame source. The flame source for this test was spaced 20 inches from the cable. The maximum flame damage observed in this test with 106 sample lengths of cable in the tray was 7-3/4 feet.

Samples of seven conductor cables, thermally aged to a simulated 40 years of service life at 90°C, were subjected to 70,000 Btu and 210,000 Btu vertical tray flame test. No flame propagation occurred. The maximum burned length was 5 feet.

This flame testing shows that the insulation will meet the test "pass" criteria of IEFE 383-1974 when subjected to test conditions which exceed the required industry standards.

B. Flance Retardant Retention

Chlorinated insulations, while exhibiting a good degree of flame resistance, decompose with aging and may be subject to dehydrochlorination occurring under conditions of high temperature, pressure and moisture. Since these conditions occur during the actual life of a cable and are amplified during loss of coolant conditions, the insulation fire retardant system is not based on chlorine but on a proprietary flame retardant system. In order to evaluate the flame retardant stability, a standard wet chemical analysis was made on the insulation compound which had been subjected to the environmental conditions of aging, radiation and loss of coolant condition to determine the flame retardant retention. The results are presented in Table IV. The data is well within the accuracy of measurement and indicates that 100% of the flame retardant was retained.

To further demonstrate the stability of the flame retardant system, 1/C power cables, and singles removed from multiconductor control cables, which had experienced the total aging, radiction, and DBE environments, were subjected to the UL VW-1 and the IPCEA S-19-814 single conductor vertical flame test. All samples passed the test.

DOTO TOTAL BEAUTIFUL PROGRAMMENT OF THE P

TABLE IV

Flame Retardant Stability

(Flame Retardant Remaining After Conditioning)

	Con			
Cable Type	Aging	LOCA (Days)	Irradiation (M rads)	Flame Retardant Remaining (%)*
7/C Control				
Sample 1	125Hrs @165°C	110	220	95
2		110		98
3		110	220	100
1/C Power				
Sample 1	125Hrs @165°C	110	220	98
1		110	220	96
3			1	100

*Mean of Measured Values:

Standard Deviation:

The flame retardant system used in this insulation is extremely stable and not significantly affected by environmental

C. Accelerated Moisture Test After Loss of Coolant Condition Test

Although not required by any industry standard, the insulated test samples which had previously been heat aged, irradiated, and exposed to the loss of coolant condition testing, were subjected to the accelerated moisture test method EM-60 of IPCEA S-66-524.1 The data observed on a typical sample is noted in Table V.

TABLE V

	IPCEA Requirements	After Test Values
1 Day		
SIĆ	6.0 max	2.66
% Power Factor, 80V/mil		1.45
Stability Factor	1.0 max	0.23
14 Days		
SIC	6.0 max	2.74
% Power Factor, 80 V/mil		1.37
Stability Factor	1.0 max	0.21
1-14 Days		
% SIC Increase	3.0	3.00
Alternate Stab. Factor	0.5	0.02
7-14 Days		
% SIC Increase	1.5	1.11

As can be determined by the above data, the insulation after a simulated 40 year life, an integrated radiation dose of 220M rads and a simulated design base event, meets the requirements of accelerated moisture testing for new insulation. This indicates that the materials used have a high degree of stability and demonstrates the ability of the insulation system to provide long reliable service.

CONCLUSIONS

This insulation offers considerable advantages over insulation systems presently being used. This insulation has the ability to withstand the simulated environment of 40 years of life, demonstrates stable electrical properties in water (EM-60 testing) even after exposure to the qualification test of IEEE 383 and 323 Standards, and exceeds any established flame test requirements.

It is believed that this insulation has established a milestone in flame, moisture and radiation resistant power and control cables. The insulation offers the electrical power generating stations and industrial facilities the reliable service that is essential in modern industry.

ACKNOWLEDGEMENTS

The authors wish to acknowledge the invaluable help of Dr. S.B. Hamilton, Manager of General Electric Wire and Cable Engineering, Dr. E.F. Holub of the Corporate Research and Development Center, Mr. J.E. Betts of General Electric Wire and Cable Insulation Development, Dr. Y. Kim, and Dr. M. Kijapp of General Electric Wire and Cable Insulation Development, D. Breeding, T. Kurien, J. Mallick, and C. Wallace of the General Electric Wire and Cable Materials Analysis and Testing Laboratory, and J. Galloway, of General Electric Wire and Cable Marketing Section.

REFERENCES:

- IPCEA Pub. No. S-66-524, NEMA Pub. No. WC7-1971 (R1976) including revisions 1 through 6. "Cross-Linked-Thermoset-ting- Polythylene-insulated Wire and Cable for the Trans-
- mission and Distribution of Electric Energy"

 2. IEEE STD. 383-1974, ANSI N41.10-1975, "IEEE Standard for Type Test of Class IE Electric Cables, Field Splices, and Connections for Nuclear Power Generating Stations'
- IEEE STD. 323-1974, "IEEE Standard for Qualifying Class IE Equipment for Nuclear Power Generating Stations
- IPCEA Pub. No. S-19-81 (Fifth Edition), NEWA Pub. No. WC3-1969 (R1974) including revisions 1 through 6 "Rubber-Insulated Wire and Cable for the Transmission and Distribution of Electrical Energy"

 5. IEEE STD. 101-1972m "IEEE Guide for the Statistical Analysis
- of Thermal Life Test Data"



ALFRED C. BRUHIN received a B.A. degree in Physics and Mathematics from LaSalle College and did graduate work in Physics at Temple University. Mr. Bruhin came to the General Elec-tric Company in 1961 as a Development Engineer in the Re-Entry and Environmental Systems Department. While with this Department he held a number of positions including Project Engineer for the Biosatellite Electrical System, and then became Manager of Electrical Power Equip-ment Engineering. At present he is Manager of Product Development Engineering, Wire and Cable Business Department, Bridgeport, CT. In this capacity he is responsible for the design and development of new and improved cables and cable systems, and for the development of electrical testing technology for the Department.



EARL R. KINGSBURY received a B.S. degree in Mechanical Engineering from the University of Maine in 1947. From 1947 to 1951 he worked for Uni-Royal as a machine designer. From 1951 to 1977 he was employed at the Revere Corporation of America as Project Engineer and Engineering Manager for fluid system components and wire and cable. He is presently a Product Development Engineer with the Wire and Cable Business Department of the General Electric Company, Bridgeport, CT.



ALEX F. WU received a B.A. degree in Chemistry from Southern Connecticut State Coilege in 1975 and a Masters degree from the same institution in 1977. He joined the Wire and Cable Business Department of the General Electric Company, Bridgeport, CT, in 1975 as an Insulation Development Chemist. In this capacity he is responsible for the origination and development of compounds used as insulation and jacketing for wire and cable.

ALL LIQUID FIRE RETARDANT URETHANE CASTING RESINS

Melvin Brauer and Thaddeus Kroplinski

NL Industries, Inc. Hightstown, NJ 08520

ABSTRACT

Two all-liquid fire retardant urethanes, i.e., no filler added, are described. Both products have oxygen indices exceeding 30 and have UL-94 ratings of V-0. The elastomers are extremely resistant to hydrolysis, process easily, and have good electrical and physical properties. Both products are fungus resistant, and they are non-corrosive to copper.

INTRODUCTION

Flame retardant (FR) polyurethanes have been described in the literature for approximately 20 years. A voluminous amount of studies have shown that urethane combustibility can be reduced by the incorporation of halogens, phosphorous, nitrogen, boron or antimony. The synergistic effects of phosphorous/halogen and halogen/antimony combinations have also been well documented. It is also well known that polymer structural characteristics such as aromaticity, crosslink density and stereo chemistry will have significant effects upon the combustibility of polyurethanes. 5, 6

Furthermore, even more subtle structural characteristics such as the degree of unsaturation and the incidence of carbonyl groups can affect urethane flammability.^{7,8} Unfortunately, the factors which lead to a reduction in urethane combustibility often compromise the utility of a urethane product.

The foam industry has been a leader in urethane flame retardance research, and there is a multitude of published FR urethane foam compositions. However, we have found that FR foam technology is not suitable for the development of flame retardant, two component potting and encapsulating compounds. Traditionally FR foam producers have utilized halogens in combination with phosphorous to achieve the desired FR properties. In some instances totally non-reactive additives have been used. In other cases combinations of reactive and non-reactive FR components have been employed. We have found that these formulations will revert during the more demanding hydrolytic scability tests required

by the telecommunications and electronics industries. Moreover, these type of formulations melt and drip when burned and thus have a UL 94 rating of V-II, rather than the more desirable rating of V-O which is assigned to self extinguishing, non-dripping materials. The use of the newer iso-cyanurate FR foam technology leads to compositions which have V-O ratings, but the products are too brittle for many of the usual casting resin applications.

Over the past two years our laboratory has developed FR technology which ailows us to formulate two component, all-liquid casting systems which have excellent hydrolytic stability, good electrical and mechanical properties and which have markedly reduced combustibility. The performance of this technology, as typified in two systems, FR-3 and FR-4, is described below and compared to our earlier FR urethanes, FR-1 and FR-2, which used conventional technology.

DISCUSSION

Early Development

Our first FR urethane product was an all-liquid, two component casting system which cured at room temperature to a 55A durometer elastomer. This system utilized non-reactive additives to provide 5% chlorine and 1.5% phosphorous. The product had an UI of 26. Many types of ronreactive additives were screened during the development of FR-1. The typical classes of compounds screened are shown in figures 1A-1E. The product ultimately employed the chlorinated phosphate ester shown in figure 1B. Although the roduct was suitable for the intended use, with respect to electrical, processing and FR properties, we were not entirely satisfied with the urethane. The elastomer reverted in boiling water and melted and dripped during OI and UL 94 tests. The crosslink density and aromaticity of the system was subsequently increased by substituting polymeric MDI (functionality 2.7) for pure MDI (functionality 2.0). This polymer change did not substantially improve the hydrolytic stability or the FR properties of the system. To correct the hydrolytic stability deficiencies we adopted another approach in the development of FR-2.

In formulating FR-2 we employed a synergistic combination of antimony oxide and chlorine. By eliminating the phosphate linkage, which our investigation showed was the primary site of hydrolytic cleavage, and substituting a very stable halogenated cycloaliphatic hydrocarbon, we expected to dramatically improve the hydrolytic stability of our FR product. This expectation was fully realized. After seven days in boiling water, FR-2 lost only 5 units hardness. However in achieving the improved hydrolytic stability, we had severely compromised our processing properties.

The principal drawback to FR-2 was a rapid settling and hard packing of antimony oxide in the polyol portion of the system. Furthermore, FR-2 also cripped during burning and had a UL 94 rating of V-II, despite an OI rating of 28.

Due to the severe processing and storage problems associated with filled urethanc systems, we ultimately abandoned this approach to FR casting systems and explored the use of isocyanurate technology.

Our early isocyanurate experience confirmed data in literature which indicated that a casting compound based on the total conversion. of isocyanate to isocyanurate leads to very brittle material. When the systems were modified with 0.1 to 0.5 equivalents of 400-2000 MW diols, more extensible isocyanurate-urethane elastomers were produced. However, these systems tended to gas during cure, possibly due to the formation of CO₂ and carbodifmide linkages as a side reaction. Moreover, we found that the dry heat aging of these materials was poorer at temperatures below 150°C than their 100% urethane analogs. Reluctantly we abandoned this approach, and over a two year period developed more fruitful methods of producing FR urethane casting systems.

New FR Potting Compounds

Processability. The technology we developed culminated in two products, FR-3 and FR-4, which typify our FR formulation capabilities. Both liquid casting systems combine the excellent processability of conventional all-liquid FR casting systems with the high heat and moisture resistance of filled FR polyurethanes, without sacrificing electrical, physical or flame retardant properties. As shown in Table 1, the viscosities of FR-3 and FR-4 components are low enough to permit penetration of the potting compounds into small interstices often present in tel communications and electronic devices. The reasonably balanced mix ratios should minimize errors due to dispenser drift. The freezing point of the components range from 10°F to 25°F, and heated shipments or heated storage facilities should not be required until the later months of the year. However, in the event of freezing, all components revert back to true solutions when stored above their freezing points.

Physical Properties. The two all-liquid FR casting systems, FR-3 and FR-4, were formulated to exemplify our newly developed FR technology with respect to physical properties. As shown in Table 2, FR-3 is a relatively soft (75A) extensible (70% elongation) potting compound, while FR-4 is a much harder (65D) material. FR-3 and its variants should find use where a lower modulus and greater extensibility are needed. Cur data indicate elongations on the order of 100% to 150% could be developed which would posses essentially the same processing, electrical, aging and flammability characteristics of FR-3.

FR-4 is a high strength (4000+ psi) material which has much lower elongation than FR-3. However, the 12% elongation of FR-4 is considerably more than we would expect to obtain from other rigid potting compounds such as polyesters and epoxies of similar electrical properties. FR-4 and its variants should find use in applications where high strength and rigidity are the most important physical requirements.

Electrical Properties

The electrical properties of FR-1 - FR-4 are presented in Table 3. For comparison data a 65D durometer, non-fire retardant ricinoleate based polyurethane is also included as the control. The low dissipation factors of FR-3 and FR-4 (.02 and .01, respectively) represent significant improvements over those obtained with FR-1 and FR-2. In fact, the dissipation factors of the new FR systems are comparable to what is obtainable from a non-FR polyurethane with a comparable polymer backbone and hardness. The volume resistivities of the new systems fall in the 10¹³ to 10¹⁴ ohm-cm range, and the dielectric constants range from 3 to 5. As would be expected the softer, less crosslinked system has the highest dielectric constant. These values are comparable to what can be achieved by older technology, as exemplified by FR-1 and FR-2, and should be acceptable for most applications.

Flammability. The flammability characteristics of FR-3 and FR-4 were studied and compared to our earlier compositions FR-1 and FR-2. The oxygen index test (ASTM 2863), the vertical burn test (ASTM 586) and the UL 94 vertical brun test were used to study subscale system responses to heat and flame. We also studied the effects of dry heat (100°C for 7 days) and humidity (95% RH/100°C for 7 day3) aging under accelerated conditions. These tests are useful for characterizing and screening the effects of subscale samples of material under controlled laboratory conditions. The data should not be construed to indicate the behavior of the compositions in an actual fire.

The new casting systems, FR-3 and FR-4, combine two FR features not heretofore available from extensible and hydrolytically stable elastomers. The two products were found to have oxygen indices in excess of 30 and were found to be non-dripping in all three of the tests conducted. By contrast FR-1 and FR-2 had oxygen indices

well below 30 and dripped during all flammability tests. Exceptionally short burn times of less than 2 seconds were noted for FR-3 and FR-4 in the 568 vertical burn tests. By contrast, FR-1 had a burn time of almost 4 seconds, and FR-2 burned at a rate of 10.9 cm/sec. in the same test. A ncn-FR urethane with a crosslink density midway between that of FR-3 and FR-4 burned at a rate of 13.9 cm/sec. The complete combustion of FR-2 was totally unexpected in view of its relatively high OI of 28.

When the burned samples of FR-2 were examined, we found that combustion along the entire sample was limited to a very low volume of material. In fact, we could characterize the burning as being essentially limited to outer surfaces. Evidently, the greater part of the burning was due to a settling of the FR additives which resulted in a two-phase elastomer. Obviously one phase had very poor flammability characteristics. This experience rather dramatically showed the need for using more than one type of FR test to adequately assess the relative combustion characteristics of polyurethanes. A summary of the initial combustion characteristics of the urethanes is found in Table 4.

The results of the accelerated aging tests (see Tables 5 and 6) were equally as encouraging as the initial FR screening tests. The oxygen indices of FR-3 and FR-4 increased, rather than decreased, after the accelerated aging tests, while only slight increases in burning times were noted. FR-3 exhibited some degradation due to the severe accelerated humidity aging condition, as evidenced by intermittent dripping during the UL 94 tests. By contrast, FR-1 could not be tested after humid aging, since it reverted, and it burned 5.4 seconds longer after the dry heat exposure. FR-2, the filled FR urethane, exhibited longer burn times than either FR-3 or FR-4 after dry heat aging and wet heat aging, but it was not completely consumed in the vertical burn tests as it had been originally. These drastic differences in burning behavior are attributed to differences in filler distribution within a relatively small (300g) casting.

Taken or balance we believe the data indicate that the new compositions exhibit exceptional FR properties which are well maintained in adverse environments

Cure Rate. Two practical aspects of any casting resin system are the rate of cure under various conditions, and the properties of the system before and after full cure is reached. These time dependent characteristics will often dictate how soon after potting a unit can be moved or used.

The rates of cure of FR-3 and FR-4 were studied at 25°C, 60°C, 80°C and 100°C. The optimum cure conditions for these temperatures are 7 days, 16 hours, 5 hours and 2 hours, respectively. The time to reach approximately 70% of cure at 25°C and 60°C is 2 days and 2 hours, respectively.

The cure times were determined on the basis of physical-time correlations using 1/8 inch thick samples. The optimum cure time will vary if thicker samples are used, since longer times will be needed to reach equilibrium temperatures.

Partially Cured Properties. During this study we also monitored the burning characteristics, hydrolytic stability and electrical properties of FR-3 and FR-4 as a function of time at 25°C. We were surprised to find that both compounds fully developed acceptable values for all three of these properties within 24 hours after curing at 25°C. As shown in Table 7, there is less than a 1.5% change in weight when the compounds are boiled in water even when the time of the cure was varied between 1 day and 7 days at 25°C. The maximum hardness change noted during these experiments was only 12 units.

The combustion and electrical characteristics of the compounds over the 7 day cure period changed even less than the hydrolytic stability. The burning times changed by no more than 1 second, and the largest change in burning lengths was only 0.5 centimeters. Similarly, there were only insignificant changes in the volume resistivities and dielectric constants during the cure period. The dissipation factors of both compounds even after only 1 day of cure at 25°C were less than 0.1. The characteristics of developing fully acceptable properties before full cure is obtained should allow short and less than optimum elevated cure temperatures to be used in conjunction with subsequent post cures at ambient conditions.

Miscellaneous Tests. As reported earlier, we used a one week immersion in boiling water as one means of testing for hydrolytic stability. The maximum hardness loss was only 12 units while weight gains of no more than 1.4% were noted. These results are as good as we have obtained previously in formulating non-FR ricincleate based polyurethanes, and better than values generally obtained from polyether or polyester based urethanes of similar hardnesses. As shown in Teble 8, the new FR potting compounds also exhibited good dry heat aging characteristics. Weight losses and hardness gains were no more than 1.5% and 14 hardness units, respectively, after exposure to 107°C for 500 hours.

Both compounds proved to be non-corrosive to copper when subjected to the Western Electric copper corrosion visual and electrical tests described in MS 17000, and they do not support fungus growth when tested per ASTM G21. A complete list of test methods is presented in Table 9.

SUMMARY AND CONCLUSIONS

This paper has described two new all-liquid FR polyurethane casting compounds. The properties of the compounds have been compared to conventional all-liquid FR polyurethane and filled FR polyurethane casting resins. It has been

demonstrated that the new FR casting compounds retain all the processing advantages of conventional all-liquid FR systems, while suffering from none of their disadvantages. The new compounds exhibit exceptional hydrolytic stability which is coupled with electrical and mechanical properties that are well suited for applications in telecommunication and electronics industries.

REFERENCES

- W.C. Kuryla and A.J. Papa, Flame Retardancy of Polymeric Materials, Marcel Dekker, Inc., New York, 1975.
- J.W. Lyons, The Chemistry and Uses of Flame Retardants, John Wiley and Sons, Inc., New York, 1970.
- J.K. Jacques, Trans. J. Plast. Inst., Conf. Suppl., No. 2, 33, 1967.
- W.M. Lanham, U.S. 3,075, 927 (to Union Carbide Corp.), Jan. 20, 1963.
- K.C. Frisch, J. Cellular Plastics, Vol. 1, April, 321-330, 1965.
- A.J. Papa and W.R. Proops, J. Applied Science, Vol. 17, 2463-2483, 1973.
- E.A. Dickert and G.C. Toonp, Modern Plastics, Vol. 42, 197, 1965.
- C.B. Quinn, J. Polymer Science, 15, 2587-2594, 1977.



Melvin Brauer NL Chemicals/NL Industries, Inc. P.O. Box 700 Hightstown, NJ 08520

Melvin Brauer received his B.A. degree from Hunter College and did graduate work at this College. Prior to joining NL Industries in 1972 he was employed by Hercules Incorporated as a propellant development chemist. Since 1973 he has been exclusively involved in the development of potting encapsulation and cable reclamation compounds. He holds numerous patents in connection with this work



Ted Kroplinski
NL Chemicals/NL Industries, Inc.
P.O. Box 700
Hightstown, NJ 08520

Ted Kroplinski received his B.S. degree from Rutgers University and his M.S. from the New Jersey Institute of Technology. Prior to joining NL Industries in 1965, he was employed by the U.S. Envelope Company as an adhesive chemist. At NL Industries his work involves the development of polyurethane adhesives, coatings, and elastomers. Since 1972 he has been Section Leader for the urethane laboratory. He has written three papers and has several patents.

TABLE 1 HANDLING AND PROCESS CHARACTERISTICS

SYSTEM	FR-3	FR-4
Prepolymer designation	EV740	EV741
Polyol designation	EP1435	EP1433
Prepolymer Weight (%)	37	39
Polyol Weight (%)	63	61
VISCOSITY DATA		
Prepolymer Viscosity (cps)	1300	2400
Polyol Viscosity (cps)	1770	6200
Mix Viscosity (cps)	1500	4200
COMPONENT PHYSICAL PROPERTIES		
Prepolymer Density (g/cc)	9.99	16.02
Polyol Density (g/cc)	10.47	10.91
Prepclymer Freezing Point (*F)	16	10
Polyol Freezing Point (°F)	10	25
Prepolymer Flash Point (°F)	440	430
Polyol Flash Point (°F)	485	490

TABLE 2

PHYSICAL PROPERTIES OF FR-3 AND FR-4

PROPERTY	<u>FR-3</u>	FR-4
Hardness (Shore Units)	75A	65D
Tensile Strength (psi)	1240	4500
Elongation (%)	70	12
Tear Strength (pli)	211	158
Density (g/cc)	1.26	1.27

TABLE 3 ELECTRICAL PROPERTIES OF FR URETHANES

	FR-1	FF-2	FR-3	FR-4	NON FR CONTROL
Kerdness (Shore Units)	55A	60D	75A	65D	65D
Dielectric Countant @ 1KHZ	4.2	3.0	4.9	3.1	3.0
Volume Resistivity (ohm-cm)	3x10 ¹²	3x10 ¹⁴	4x10 ¹³	4x10 ¹⁴	2×10 ¹⁵
Dissipation Factor	0.19	0.05	0.02	0.01	0.01

TABLE 4 FLAMMABILITY CHARACTERISTICS OF FR URETHANES

	<u>FR-1</u>	FR-2	FR-3	FR-4	NON FR CONTROL
ASTM D-568					
Vertical Burn Test					
Extent of Burning (cm)	2.9	consumed	2.3	1.9	consumed
Time of Burning (sec.)	3.8		1.5	2.1	
Burning Rate (cm/min.)		10.9			13.9
ASTM D2863					
Oxygen Index					
X .	25.7	27.7	32.1	33.6	20.8
UL94 Vertical Burn Test					
Classification	V-II	B-V-II*	V-0	V-0	В

*The burning characteristics of this composition varied, due to rapid settling of the FR fillers.

TABLE 5

FLAMMABILITY CHARACTERISTICS OF FR URETHANES AFTER DRY HEAT AGING*

	FR-1	FR-2	FR-3	FR-4
ASTM D-568				
Vertical Burn Test				
Extent of Burning (cm)	3.4	1.8	2.5	1.9
Original Value	2.9	consumed	2.3	1.9
Time of Burning (sec.)	9.2	9.2	1.2	1.2
Original Value	3.8	consumed	1.5	1.1
ASTN D2863				
Oxygen Index				
or in the state of the state of	25.8	28.3	34.9	37.4
Original Value	25.7	27.7	32.1	33.6
UL94 Vertical Burn Test				
Classification	V-II	V-II	V-0	V-0
Original Classification	V-II	B-V-II	V-0	V-0

*7 days @ 100°C

TABLE 6

FLAMMABILITY CHARACTERISTICS AFTER HUMID AGING*

	_FR-1	FR-2	FR-3	FR-4
ASTM D-568				
Vertical Burn Test				
Extent of Burning (cm)	reverts	3.3	2.7	2.2
Original Value	2.9	consumed	2.3	1.9
Time of Burning (sec.)		4.8	3.2	1.4
Original Value	3.8	consumed	1.5	1.1
ASTM D2863				
Oxygen Index				
		27.7	35.3	37.4
Original Value	25.7	27.7	32.1	33.6
UL94 Vertical Burn Test				
Classification		V-II	V-II	V-0
Original Classification	V-II	B-V-II	V-0	V-0

*7 days @ 95% RH/100°C

TABLE 7
PROPERTIES OF CURED AND PARTIALLY
CURED POTTING COMPOUNDS

	FR	-3	FR	1-4
Cure Condition	1 day @ 25°C	7 days @ 25°C	1 day @ 25°C	7 days @ 25°C
Tensile Strength (psi)	806	1240	2842	4220
Hardness (Shore)	58A	75A	55D	65D
Dielectric Constant @ 1KHZ	4.7	4.2	3.2	2.7
Dissipation Factor @ 1KHZ	0.078	0.024	0.041	0.012
Volume Resistivity ohm-cm	3.7x10 ¹³	4.8x10 ¹³	2.6x10 ¹⁴	1.7x10 ¹⁴
Oxygen Index	31.6	31.8	33.3	33.5
UL94 Rating	V-0	V-0	V-0	V-0
Extent of Burning (cm)	1.9	2.4	1.5	1.9
Burning Time (sec.)	2.0	1.2	1.0	1.2
Hardness after 7 days in boiling water	64A	66A	60D	53D
Weight Change after 7 days in boiling water, %	-0.22	+1.4	-0.34	+1.0

TABLE 8
MISCELLANEOUS TEST RESULTS

RESULT			
FR-3	FR-4		
non-corrosive	non-corrosive		
1.4	1.0		
9	and mark		
14	6		
1.5	1.0		
	non-corrosive 1.4 9		

TABLE 9 TEST METHODS LIQUIDS Viscosity Brookfield Viscometer Density AOCS-To-1B-64 Pour Point ASTM-D97 Flash Point ASTM-D1310 SOLIDS Dielectric Constant ASTM-D150 Dissipation Factor ASTM-D150 Volume Resistivity ASTM-D257 Insulation Resistance Western Electric MS17000 Tensile Strength ASTM-D412 Elongation ASTM-D412 Hardness ASTM-D2240 Density ASTM-D792 Copper Corrosion Western Electric MS17000 Fungus Resistance ASTM-G21 Oxygen Index ASTM-D2863 Extent of Burning ASTM-D568 ASTM-D568 Time of Burning Burning Rate ASTM-D568

UL94

UL94 Rating

FIGURE 1A

Oligomeric Chloroalklyl Phosphonate

FIGURE 1D

$$\begin{array}{c|c}
Br & Br & Br & Br \\
Br & Br & Br & Br \\
Br & Br & Br
\end{array}$$

Decabromodiphenyl Oxide

FIGURE 1B

2,-2-Bis(chloromethyl)1,3-propylene-Bis[Bis(2-chloroethyl]phosphate

FIGURE 1E

 ${\tt Dodecachloro-dodecahydro-dimethanodibenzo-cyclooctene}$

FIGURE 1C

$$\left(\begin{array}{ccc} CH_2 - CH_2 - CH_2 - O \\ | & | \\ Br & Br \end{array}\right) - P = O$$

Tris(dibromopropyl)phosphate

The Performance of Polyvinyl Chloride Communication Cables in a Modified Steiner Tunnel Test

Inderjit L. Wadehra

International Business Machines Corporation Kingston, New York

Abstract

Modified Steiner Tunnel Test results are presented for polyvinyl chloride communication cables. It was demonstrated that the cables could have both low flame spread and smoke emission, depending on their arrangement in the test tray. Flame spread and smoke emission values were favorable to those obtained with fluorinated ethylene propylene (FEP) cables but increased significantly when the cables were placed inside electrical metallic tubing.

Background

In 1975, the National Electric Code (NEC) was changed to reflect a new requirement for the following types of circuits: Remote Control, Signaling and Power Limited, and Communications, Classes 1-3 respectively. Articles 725 and 800 now state that the conductors (wiring) for such circuits are to be installed in accordance with Article 300, with the exception that "Conductors listed as having adequate fire-resistant and low-smoke producing characteristics shall be permitted for ducts, hollow spaces used as ducts, and plenums ...".

The code does not indicate the levels of performance relative to fire-resistant and low-smoke producing characteristics nor the test methods for determining such characteristics.

Test Method

Recognizing the need for standards for testing cables and regulating their use (in conformance with the NEC), the Underwriters Laboratories (UL), in collaboration with Bell Labs, developed a feasible test method. 2 Using a Steiner Tunnel as the testing facility, the method differs only slightly from ASTM E-84. A cable rack is used for mounting the samples in the upper part of the tunnel and the test time is extended from 10 to 20 minutes.

The two Laboratories presented their test results at an ad hoc committee meeting (set-up by UL) in Chicago, April 25, 1978. 3,4 The presented data indicated that (a) both cables with Polyvinyl Chloride (PVC) Jackets and those with PVC insulation exhibited a maximum flame spread of 19-1/2 feet after 20 minutes while emitting copious amounts of smoke, (b) PVC/PVC cables when installed in electrical metal tubing, although meeting the intent of the NEC, still exhibited considerable smoke and flame spread, and, (c) Fluorinated Elthylene Propylene (FEP)/FEP cables exhibited a lower level of smoke emission and had a smaller flame spread than did the PVC type cables.

Cost Impact

Most commonly-used communication cables use PVC insulation and/or Jackets. The use of either conduits or FEP cables would result in a significant cost increase. A typical PVC cable costing \$0.055 per foot would cost \$0.58 per foot in FEP. And if it's installed in electrical metallic tubing/conduit, there would be an additional tubing cost of approximately \$1.00 per foot plus installation costs. Accordingly, studies were undertaken at IBM to:

- Obtain a better perspective of the Modified Steiner Tunnel test.
- Explore the possibilities of reducing the PVC cables' smoke and flame spread through specimen (cable) arrangement/ separation in the test tray.

Materials Tested

Cables tested in this study are described in Tables 1 and 2. The description includes their construction (Table 1) and the amounts of combustibles and their oxygen index (Table 2).

Electrical Metallic Tubing

Steel, electrical metallic tubing, Underwriters' Laboratories listed (Issue #HZ-460), having a nominal internal diameter of 1-1/4 inches, was fitted with die-cast zinc and setscrew connectors.

Test Procedure

The testing was conducted at United States Testing Company, Hoboken, N.J., using a modified Steiner Tunnel (Figures 1 and 2). (The test conditions and method were essentially the same as those presented at the Chicago Meeting and already described). The tunnel, 25 ft. long (test flame length was 4-1/2 feet), was completely sealed except for a flame and air inlet at one end and an exhaust duct at the opposite end. The cable rack permitted flame involvement of the entire cable. It also increased the radiant heat from the roof of the tunnel, thus making the test much more severe than that of ASTM With the input air velocity controlled at 240 feet per minute, the exhaust gases were monitored for smoke density and temperature. A photometer, installed across the exhaust duct to monitor the smoke, had its output recorded for 20 minutes.

A smoke emission value was obtained in the following manner. Because the amount of light transmitted to the photometer decreases as the smoke increases, the area under the correspondingly decreasing light's plotted output curve was divided by the area under a curve obtained by burning untreated red oak lumber during a 10 minute ASTM E-84 calibration test. The quotient was then multiplied by 100.

The flame travel, observed through windows in the tunnel, had a possible maximum of 19-1/2 feet.

Results

Table 3 presents the results obtained when five PVC cables were progressively spaced in the test tray. With no separation the cables exhibited total combustion, producing the maximum flame spread possible 19-1/2 feet. In addition, a very high smoke development measurement of 745 was recorded.

When the cables were placed one inch apart, the maximum flame spread possible was reached 2 minutes 7 seconds sooner than when there was no spacing between the cables. This change was attributed to a "complementary" effect that happens when cables are in close proximity. However, in the test, as the separation distance

increased, the complementary effect decreased, resulting in an increasingly lower flame spread that became self-extinguishing (Experiments 3, 4, and 5).

In the last cables-only experiment (6), the cables were bundled together. Even though it took longer to attain, the flame spread increased three feet over that of the previous experiment (5) when the cables were four inches apart.

Table 4 contains the flame spread and smoke emission test results for four additional cable sets. In every case there was a reduction in flame spread and smoke emission when the cables were separated (four inches). Thus, a reduced flame spread with flame extinguishing capabilities, along with less smoke can be achieved with controlled separation of polyvinyl cables.

Table 5 illustrates the results obtained with bundled polyvinyl chloride cables encased by electrical metallic tubing (EMT). A test performed with seven bundles, with each bundle containing six cables equally spaced, (Experiment 7) exhibited the maximum flame spread possible along with a very heavy concentration (995) of smoke.

The results of Experiment 8 were obtained with a gable setup identical to that of Experiment 7 except that the cables were placed in EMT. The flame spread was still significant (six feet) with a very high smoke emission (620). Thus, EMT does not really reduce flame spread and smoke emissions to levels generally considered low or comparable to FEP cable.3 However, placing the test specimens (EMTs) in the tunnel one foot behind the burner slightly reduced the flame spread (to five feet) but significantly lowered the smoke emission (to 260) - see Experiment 9. These reductions were attributed to the mixing and dilution of products of pyrolysis of PVC with incoming air (at a velocity of 240 feet per minute) before ignition.

Conclusions

The results of the discussed test indicate that polyvinyl chloride communication cables can, when adequately spaced, have a low flame spread, self-extinguishing properties, and low smoke emissions. The PVC cable-only separation experiments were definitely better than those obtained when the cables were installed in electrical metallic tubing, comparing favorably with tests obtained with FEP cables.

References

- National Fire Protection Association, National Electrical Code 1975, Sections 300, 725 and 800.
- Beyreis, J. R., Skordahl, J. W., Kaufman, S., and Yocum, M. M. "A Test Method for Measuring and Classifying the Flame Spreading and Shoke Generating Characteristics of Communication Cable," 1976 International Wire and Cable Symposium Proceedings, pp 291-295.
- Underwriters Laboratories "Fact-Finding Report on Comparative Flame Propagation and Smoke Development Tests on Communication Cables in Various Test Geometries," February 7, 1978.
- 4. Underwriters Laboratories Memorandum to Members of Ad Hoc Committee to Determine Requirements for Cables for Use in Air Handling Plenum, March 21, 1978.

Inderjit L. Wadehra obtained his M.S., with honors, from Punjab University, India, in 1956 and his Ph.D. in chemistry from McGill University, Montreal, Canada in 1964. He joined IBM in 1967 as a staff chemist and is presently a



senior engineer in the materials laboratory at IBM's Kingston, New York facility. Dr. Wadehra is presently responsible for material selection and process development. This includes investigating structural materials, adhesives, organic coatings, and dielectric materials to ensure the right material for a specified application, and tests for product performance, reliability and safety in proposed or defined installation environments. He is an active member of the American Chemical Society and the Society of Plastics Engineers.

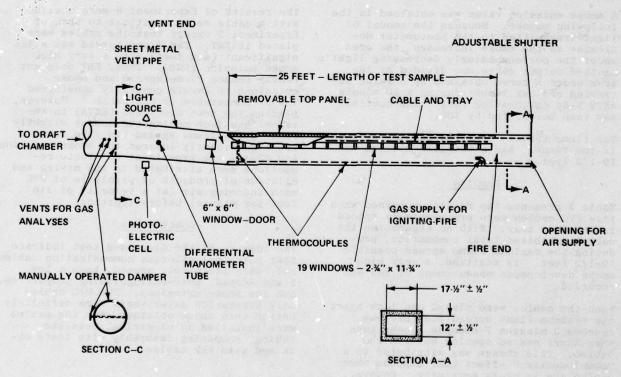


FIGURE 1 STEINER TUNNEL - SIDE VIEW

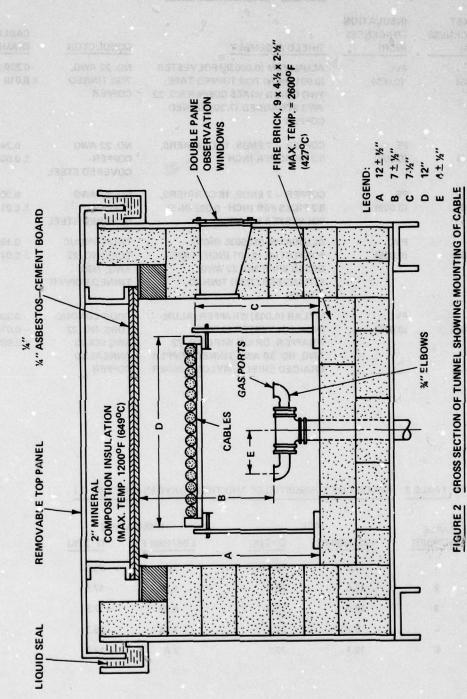


TABLE 1 CABLE DESCRIPTION

CABLE NUMBER	JACKET (THICKNESS INCH)	INSULATION (THICKNESS INCH)	SHIELD ASSEMBLY	CONDUCTOR	CABLE OUTSIDE DIAMETER (INCH)
-1	PVC (0.035)	PVC (0.009)	ALUMINUM (0.00035) POLYESTER (0.001 INCH) 7/30 TINNED TAPE; TWO DRAIN WIRES COPPER NO. 22 AWG STRANDED (7/30) TINNED COPPER	NO. 22 AWG, 7/39 TINNED COPPER	0.280 x 0.175 ± 0.010
2	PVC (0.031)	PE (0.009)	COPPER — 7 ENDS, 16 CARRIERS, 8.2 PICKS PER INCH	NO. 22 AWG COPPER- COVERED STEEL	0.240 ± 0.007
3	PVC (0.040)	PE (0.009)	COPPER — 7 ENDS, 16 CARRIERS, 8.2 PICKS PER INCH; 0.002 INCH POLYESTER WRAPPED	NO. 22 AWG COPPER- COVERED STEEL	0.260 ± 0.01
4	PVC (0.035)	PVC (0.009)	ALUMINUM (0.00035 INCH) — POLYESTER (0.001 INCH) TAPE — DRAIN WIRE NO. 22 AWG STRANDERS (7/30) TINNED COPPER	TWO CONDUC- TORS, NO. 22 AWG, 7/30, TINNED COPPER	0.180 ± 0.015
5	PVC (0.030)	PVC (9.017)	MYLAR (0.003) WR APPER; ALUM- INUM-POLYESTER (0.0025) WRAPPER; DRAIN WIRE NO. 22 AWG; NO. 30 AWG TINNED COPPER BRAIDED SHIELD; NYLON BINDER	FOUR CONDUCTORS, NO. 22 AWG SOLID ANNEALED COPPER	0.300 -0.015 + 0.035

TABLE 2 AMOUNT OF COMBUSTIBLES AND THEIR OXYGEN INDEX (O · I)

CABLE	JACK		INSULA	TION
NUMBER	LBS/1000 FT	O·I(%)	LBS/1000 FT	O · I (%)
1	12.3	24.1	3.3	25.3
2	14.0	23.0	4.25	~17.5
3	18.8	23.4	4.24	~17.5
4	9.77	24.1	1.64	25.3
5	19.1	22.1	3.8	~17.5

TABLE 3 EFFECT OF SPACING ON THE PERFORMANCE OF CABLE NO. 1 IN TUNNEL TEST

			TEST		SPREAD		
EXPERIMENT NUMBER	CABLE ARRANGEMENT	NO. OF LENGTHS	(MINUTES)	TIME MIN/SEC	DISTANCE FEET/INCH	DEVELOP	MENT
9981.582	FULL TRAY	42	20	3:05	19:6	10 MINS	715
		(Manual Est				15 MINS	730
						20 MINS	745
2	ONE INCH APART	9	20	2:58	19:6	10 MINS	315
						15 MINS	320
						20 MINS	325
million	TWO INCHES APART	5	20	3:00	10:0	10 MINS	195
TE MUNIC						15 MINS	205
					4.1.14DCG 123	20 MINS	215
4 97	THREE INCHES APART	4	20	1:55	4:0	10 MINS	185
						15 MINS	210
				20.29	SI TREAT OF	20 MINS	235
5	FOUR INCHES APART	3	20	1:50	2:0	10 MINS	150
						15 MINS	165
				200		20 MINS	175
6	PLACED TOGETHER IN	3	20	4:17	5:0	10 MINS	125
CARLES STATE	CENTER					15 MINS	135
						20 MINS	140

TABLE 4 EFFECT OF SPACING ON THE PERFORMANCE OF CABLES NO. 2 – 5 IN TUNNEL TEST

		FLAME SPREAD					
CABLE NO.	CABLE ARRANGEMENT	NO. OF LENGTHS	DURATION (MINUTES)	TIME MIN/SEC	DISTANCE FEET/INCH	SMOKE DEVELOP	MENT
2	FULL TRAY	44	20	3:09	19:6	10 MINS 15 MINS	590 600
						20 MINS	610
	FOUR INCHES APART	3	20	2:24	7:0	10 MINS	135
						15 MINS	150
						20 MINS	160
3	FULL TRAY	40	20	2:44	19:6	10 MINS	735
						15 MINS	755
						20 MINS	760
	FOUR INCHES APART	3	20	4:52	15:0	10 MINS	195
						15 MINS	205
						20 MINS	210
4	FULL TRAY	59	20	2:16	19:6	10 MINS	610
						15 MINS	610
						20 MINS	615
	FOUR INCHES APART	3	20	1:50	6:0	10 MINS	90
						15 MINS	110
						20 MINS	130
5	FULL TRAY	35	20 '	5:34	19:6	10 MINS	840
						15 MINS	880
						20 MINS	905
	FOUR INCHES APART	3	20	4:06	4:0	10 MINS	190
						15 MINS	210
						20 MINS	230

TABLE 5 STEINER TUNNEL DATA WITH CABLE NO. 1 INSTALLED IN ELECTRICAL METALLIC TUBING

			ENTOWER	FLAME	SPREAD		
EXPERIMENT NUMBER	CABLE ARRANGEMENT	NO. OF LENGTHS	DURATION (MINUTES)	TIME MIN/SEC	DISTANCE FEET/INCH	SMOKE DEVELOP	MENT
316 AH	FULL TRAY	42	20	5:05	19:6 A - 2/4 - 2/0	10 MINS 15 MINS 20 MINS	715 730 745
7 07 934 985 93 948 93	SEVEN BUNDLES WITH SIX CABLES IN EACH BUNDLE SPACED EQUALLY	42	20	8:00	23+(19:6 , ₂₄ +	10 MINS 15 MINS 20 MINS	895 985 995
8 6 1 6 6 6 6 6 6 6 6 6 6 6 6 6 6 6 6 6	SEVEN EMTS WITH SIX CABLES IN EACH EMT PLACED TOGETHER IN CENTER	42	25	13:51	6:0	10 MINS 15 MINS 20 MINS 25 MINS	80 435 570 620
9	SEVEN EMTs WITH SIX CABLES IN EACH EMT PLACED TOGETHER IN CENTER	42 (-1 TO 23 FEET)	25	14:50	5:0 Day 10:58.49 R31/835	10 MINS 1E MINS 20 MINS 25 MINS	35 135 235 260
10	THREE EMTS WITH SIX CABLES IN EACH EMT SPACED FOUR INCHES APART	18 (0 TO 24 FEET)	25 1939 181 50 57	13:45	5:0 	10 MINS 15 MINS 20 MINS 25 MINS	115 255 385 465

Name of the Asset of the Asset

IMPROVEMENT AND APPLICATION OF POLYMER CLAD OPTICAL FIBER FOR COMMUNICATION USE

Nobuo Ohmori Hiroshi Kajioka Takashi Shimada Shoji Shinzawa Kazuhiko Takada

Hitachi Cable, Ltd. Tokyo, Japan

ABSTRACT

Notwithstanding many advantages, there yet remain some problems limiting the application of polymer clad optical fibers. This paper deals with key problems and their solutions.

The temperature dependence of the transmission loss is clarified by the microbending loss due to the outer diameter deviation of the plastic jacket at low temperature. After an improvement the additional loss caused by a temperature change between -20°C to 60°C was reduced to less than 2 db/km.

The length dependence of the numerical aperture is more intensive than for the silica clad step index fiber, because there exists a strong mode coupling.

The relation between the numerical aperture and the excitation condition was investigated. As a result the loss due to the length dependent numerical aperture is about 4.3 dB. Although the theoretical value is 0.4, the effective value of the numerical aperture is nearly 0.18.

A polymer clad fiber connector whose size is compact and almost similar to that of the silica clad fiber was developed. Its loss is less than 1.5 dB.

1. INTRODUCTION

A polymer clad fiber (PCF) has been developed for short optical links. The large core diameter and the easiness of manufacture are the main advantages. Further depending on the purity of the fused silica as the fiber core, its transmission loss is less than 10 dB/km.

There are several problems to be solved before PCF is practically applied. The first one is that its transmission loss after plastic jacketing process drastically increases in the low temperature region.

This may be one of the most serious problems of PCF.

In order to use PCF for a transmission line, a maximum transmission loss in the temperature range from at least -20° to 60° must be assured. Chapter 2 describes the improvement of the transmission loss in the low temperature region by reducing the microbend due to plastic jacketing.

The second problem is the difficulty of the estimation of the transmission properties in the transient state. Because there exists a strong mode coupling in PCF, length and mode dependent attenuations are more intensive than in the silica

clad multimode fiber. In Chapter 3 the length dependent numerical aperture is investigated and the additional loss at sending end is Charified. Chapter 4 describes an optical cables using

Chapter 4 describes an optical cables using PCF. Three different types; spacer type, unitype and bundle type are described. The general transmission characteristics and mechanical properties are shown.

For the application example a cable containing eight PCF cores used in a fiber optic link installed in an electric power station is introduced.

The third problem is the development of a low loss and reliable connector. Fixing the polymer cladding is very influential so as to prevent the fiber core from thrusting from the connector end face. In Chapter 5 a PCF connector who se size is compact and almost similar to that of a silica clad fiber is described.

2. IMPROVEMENT OF TRANSMISSION LOSS AT LOW TEMPERATURE REGION

Plastic jacketed optical fibers suffer from an increase in loss at low temperatures due to microbending by shrinkage of the plastic jacket. PCF has a higher temperature dependence of transmission loss than the silica clad multimode optical fiber. One reason is a material discontinuity at the core-cladding interface; silica core-polymer cladding. The discontinuity causes mode coupling. A second reason is the change of the refractive index of the silicone resin polymer at the cladding. The refractive index of silicone increases as the temperature descends, and therefore the relative index difference decreases at low temperatures. In other words, the power contained in the higher guided modes spills out to that of the radiation modes. This loss increase of PCF becomes remarkable after plastic jacketing. In order to reduce this loss increase microbending induced on the PCF by jacketing must be made as small as possible.

In plastic jacketing there are many factors which cause a mechanical stress on PCF such as the outer diameter deviation, eccentricity, Young's modulus, the extrusion condition and so on. After an experimental study on PCF whose structual parameters are listed im Table 1, the authors reached the conclusion that the first factor is the most dominant for the loss increase in the low temperature region.

Table 1 Parameters of PCF

Core Diameter	150 µm
Cladding Diameter	300 µm
Jacketing Diameter	600 μт
Numerical Aperture	0.4 (L = 2 m) 0.18(L = 1000 m)
Attenuation Constant at \(\sim = 0.84 \) \(\mu \) m	5 ~ 8 dB/km
6 dB Bandwidth	20 ~ 30 MHz · √km

Let $\Delta\alpha$ denote the loss increase at -20°C as compared to 20°C. Fig. 1 shows the experimentally determined relation between $\Delta\alpha$ and the mean value to peak deviation Δ D of the outer diameter of the plastic jacket. The mean value of the diameter is 600 μ m. The relation in Fig. 1 is obtained under the excitation condition of the steady state which is to be discussed in the following chapter. From Fig. 1 the following relation can be derived:

 $\Delta\alpha \approx 0.15.\Delta D$ (dB/km) (1) Fig. 2 shows the temperature dependence of the transmission loss at the wavelength of 0.84 µm. In Fig. 1 the white and black circles correspond to the loss increases $\Delta\alpha$ before and after taking certain measures to decrease the diameter deviation of the nylon jacketing, respectively.

Fig. 3 shows one of the measured longitudinal

irregularities of the jacket diameter.

Through the above mentioned improvement it has become possible to manufacture PCF whose transmission loss at -20°C is less than 10 dB/km at the wavelength of 0.84 µm.

3. TRANSMISSION CHARACTERISTICS OF PCF IN THE TRANSIENT STATE

The atteruation $\alpha_{\tilde{m}}$ of the m-th mode group is given as

$$\alpha_{\rm m} = \alpha_{\rm core} + \frac{{\rm m}^2}{{\rm M}^2 \sqrt{2{\rm M}^2 - 2 \cdot {\rm m}^2}} \quad \alpha_{\rm clad}$$
 (2)

where M is the maximum mode group index which is calculated by the following Eqn. (3), and α core and α clad are the attenuation constants of the core and the cladding, respectively. (1)

$$M = \frac{2\pi}{\lambda} \quad a.MA \tag{3}$$

where λ is the wavelength, a is the core radius and NA is the numerical aperture. The value α clad has the order of 1 to 5 x 10 dB/km. At first it was thought that the transmission loss of PCF became large essentially because of the high attenuation of the cladding. As for the baseband bandwidth it seems to be narrow according to the theoretical index difference. Actually, however PCF has a low transmission loss of about 5 dB/km and a bandwidth of about 70 MHs α which is almost similar to that of a silica clad step-index fiber with NA = 0.2. All these properties come from the high attenuation of the higher modes due to the silicone cladding and the effect of strong mode coupling.

In order to analyze the mode distribution the far-field pattern (FFP) of optical power is usually applied. In this experiment a dome type light emitting diode (LED) is used. Fig. 4 shows the FFP of a short piece of PCF, where the gap d between the butt end of the PCF and LED is adopted as a parameter of the excitation condition. According to Fig. 4 it is said that the mode distribution of a short piece of PCF depends strongly on the excitation condition. The state under which the propagating modes are affected by the excited modes is called the transient state. On the other hand as the fiber length increases, the mode distribution becomes independent of the excitation condition. This state is called the steady state of the mode coupled multimode fiber. Fig. 5 shows the FFP of one kilometer PCF. It can be seen that it is not the excitation condition but the property of PCF itself such as mode attenuation and mode coupling coefficients that determine the FFP. The characterization in the steady state is explained by the coupling matrix. [2] In Fig. 6 the relation between the 90 % NA NA90 and the loss due to the length dependent NA ANA is shown.

The NAgo is defined by the measured FFP as NAgo =
$$\sin \theta$$
 go (4)

Let us consider the output optical power P2 from a piece of PCF whose length is L.

$$P_2 = P_1 \cdot 10^{-(\alpha_e \cdot L + n \cdot A_s \Rightarrow A_{NA})/10}$$
 (5)

where P_1 is the power from the LED pigtail, α_e is the attenuation constant of PCF in the steady state, As is the splicing loss, and n is the number of splicing. $\mathcal{O}_{\mathbf{e}}$ is measured by the dummny fiber method. In Eqn. (5) the term ANA is the most important because it depends on the excitation condition. Fig. 7 shows the relation between the 90 % NA and the fiber length. According to Fig. 7 the loss due to the length dependet NA can be obtained by getting the value of the numerical aperture at the end of the LED pigtail. It is also seen that the 90 % NA of 2 m PCF is about 0.4 and almost equal to the theoretical value calculated by the refracive index difference between the core and the cladding. The 90 % NA in the steady state is nearly 0.18. It takes about one kilometer for PCF to reach the steady state. It is possible to estimate the output power at the end of an arbitrary length of PCF with Fig. 8. The loss due to the length de-pendent NA becomes about 4.3 dB until the propagation along the PCF changes from the transient state in to the steady state.

The baseband transfer function of a multimode fiber is expressed by

$$g(\omega, L) = \sum_{n=1}^{M} P_0(n) \exp(-\alpha_n \cdot L - j \cdot \omega_n \cdot L), \quad (6)$$

where $P_0(m)$ and \mathcal{T}_m are the power of the m-th mode group at L=0 and the mode group delay time of the m-th mode group, respectively. The latter is expressed by

$$\tau_{\mathbf{m}} = \frac{\mathbf{n}_1}{\mathbf{c}} \left(\frac{\mathbf{m}}{\mathbf{H}}\right)^2 \tag{7}$$

where c is the light velocity in free space, n_l is the refractive index of the core. then the baseband attenuation characteristics are obtained by

$$A(W,L) = 20 \log |G(W,L)|$$
 (8)

Fig. 8 shows the frequency characteristics of the baseband attenuation of one kilometer PCF, where A clad is taken as a parameter. The difference between the curves calculated and observed is caused by the effect of the mode coupling.

Fig. 9 shows the length dependent 3 dB and 6 dB baseband bandwidth of the same PCF piece.

The 6 dB handwidth in the range L km is approximately expressed by the equation.

$$B(L) = B_0 \cdot L^{-0.5}$$
 (9)

The bandwidth B_0 at 1 km falls between 20 and 30 MHz.

4. POLYMER CLAD FIBER CABLES

As shown in Fig. 10 three types of PCF cable have been developed. The first one is a spacer type cable, the second is a unit type and the third is a bundle type. In the spacer type cable PCFs are separately laid in the grooves of the spacer. As a strength member stranded steel wires or FRP rod are used. No transmission loss increase is observed after the cabling process. The unit type cable consists of some plastic jacketed cord units in which several PCFs are accommodated with strength member material and the units are stranded together with a suitable lay length. The unit cord can be independently used as an indoor cable. The general properties of the spacer type and the unit type cables are listed in Table 2.
According to table 2 thewe two different type cables can meet the condition for usual installation and

Table 2 Characteristics of PCF cables

handling procedures.

	mbes -1 (*05- 5	Spacer Type	Unit Type
Attenuation		Less than 8 dB/km	Less than 8 dB/km
Ba	ndwidth	20-30MHz -/km	20-30MHz./km
	mber of Fibers Cable	up to 12	up to 36
St	d. Length of	500 or 1000 m	500 or 1000 m
0	erall Diameter	up to 20 mm	up to 20 mm
We	ight	up to 150 g/m	up to 100 g/m
9	Bending Radius Repitition	100 mm 10 times	50 mm 10 times
108	Tensile Strength	100 kg	50 kg
rt	Impact	3 lbs.ft	3 lbs.ft
1 Properti	Twisting Angle Load	90°/n 25, kg	90°/m 25 kg
Schanical	Vibration	15 mm, 10 Hs 106 times	45 mm, 10 Hs 106 times
Mech	Compression	100 kg/ 50 mm width	100 kg/ 50 mm width

Two pieces of PCF cable were installed in an electric power station for the use of a fiber optic link. The cable structure is shown in Fig. 11. In this cable, eight cores of PCF are compartmentalized into four grooves of the spacer. So each groove accommodates two cores of PCF with woolen string cushion material wound around PCFs. Small size connectors and the splicing method expressed in the next chapter are also applied to this link.

The general characteristics of the indoor cable are listed in Table 3. As one of the mechanical properties th loss characteristics under compression are shown in Fig. 12. The transmission loss is restored to the initial value when removing the compression force.

Table 3 Mechanical Properties of PCF indoor Cable

Test Items	Results	Condition
Bending	Passed. (No Fiber Breaks after 2000 times at 30 mm radius)	Bending Radius: 30 mm, Repitition: 10 times in both ways.
Twisting	Passed. (No Fiber Breaks after 1000 times)	10 turns/m in both ways, Repitition: 10 times.
Impact	Passed. (No Fiber Breaks at 6 lbs.ft)	3 lbs.ft
Tensile	Passed. (No Fiber Breaks at 100 kg)	Load 50 kg.

As one of the applications of PCF, a 84-core bundle fiber has been developed. This bundle comprises PCFs whose core are made from nonjurified silica. This bundle is being practically used with couplers at both ends as a high voltage isolator. The general longitudinal insulation characteristics are mentioned in Table 4.

The bundle and its coupler are shown in Fig. 13.

Table 4 Insulation Characteristics of PCF Bundle

Test Items	Results	Condition
A.C. Breakdown Voltage	Passed.	A.C. 230 KV,
D.C. Breakdown Voltage	Passed.	D.C. ± 225 KV, 30 min.
A.C. Corona Breakdown Voltage	Passed.	A.C. 25 KV, 30 min.
Impulse Breakdown Voltage	Passed.	±550 EV, 3 times
Switching Surge Breakdown Voltage	Passed.	±40 KV, 3 times

Remarks 1) Sample Length for Corona Test: 0.2 m, Sample Length for Other Tests: 1.5 m.

> 2) Environmental Condition: Room Temperature, 40 60 ≸ RE.

One of the most difficult problems in the development of the bundle was to fix the 84 PCFs at the end face. The heat cycle test, bending test and twisting test were applied to the bundle to guarantee that the PCFs do not thrust from the end face. In order to meet the requirement, the sheath structure, the material selection and the end fixture have been surveyed and successful results were obtained. The mechanical properties are listed in Table 5.

Table 5 Mechanical Properties of PCF Bundle

Test I tems	Results	Condition
Bending	Passed. (No Loss Changes after 300 times at 10 mm radius)	Bending Radius: 25 mm, Repitition: 50 times in both ways.
Twisting	Passed. (No Loss Changes after 100 times)	5 turns/m in both ways, Repitition: 20 times.
Tensile	Passed. (No Loss Changes at 12 kg load)	Load 10 kg between end fixtures.

5. CONNECTOR AND SPLICING

A compact connector for PCF has been developed as shown in Fig. 14. The coupling method of the connector is as follows: an opposing pair of the plug is mated and srially butted to each other in a metal receptacle. Thereby the optical fibers are precisely aligned in the lateral direction. Comparing with that of a silica clad multimode mode fiber in addition to the accuracy of dimensions of the components and assembling, the characteristics of the PCF connector is strongly influenced by the end face condition of the fiber. Because the cladding is made of silicore polymer which is soft and brittle, fixing the fiber in the connector plug is very difficult.

Many kinds of investigations were made for each assembling process of the connector in order to fix firmly the cladding of PCF at the end face of the plug. Among them, selection of adhesive, adhering condition, aging of materials are very important. The developed connector has many excellent features such as a small size similar to that of the silica clad fiber, low connection loss and no thrusting of the fiber from the connector end face. The total length of the plug is about 40 mm including the reinforced part of the plug neck, and the length and the outer diameter are 8 mm and 3 mm, respectively.

The connection loss is less than 1.5 dB.
Table 6 explains the general properties of the PCF connector.

Table 6 General Characteristics of PCF Connector

Test Items	Results	Condition 20°C		
Initial Value	Avg. = 1.0 dB Max. = 1.3 dB Min. = 0.8 dB Std. dev.=0.09dB			
Temperature	Loss Increase: Less than 0.3 dB	-20°C to 60°C.		
Rotation	Loss Increase: Less then 0.2 dB	An pendendry Ale		
Repitition	Loss Increase: Less than 0.15dB	500 times		
Heat Shock	Loss Increase: Less than 0.1 dB	-20°c/60°C, 30 cycles.		
Static Tensile	No Loss Changes	Load: 30 kg, 1 min.		
Vibration	No Loss Changes	Amplitude: 1 mm, Frequency: 16.7 Hz, 2.5 x 10 ⁵ times.		

Fig. 15 shows the splicing structure of PCF. It is necessary for the jointed part of the silica core to be surrounded with the cladding material because the silicone cladding of the fiber has been removed before the silica core jointing. In the splicing section the space between the jointed silica core and the protection glass tube is filled with silicone polymer for the cladding.

6. CONCLUDING REMARKS

Some problems, which must be overcome before polymer clad optical fiber can be used practically are investigated and discussed. The temperature dependence of the transmission loss has been improved and the additional loss at -20°C is reduced to less than 2 dB/km.

The transmission characteristics in the transient state is made clear and thus the output power at an arbitrary length of the fiber can be precisely estimated.

A compact low loss and reliable connector has been developed.

7. REFERENCES

- B. Gloge and E. A. J. Marcatili; "Multimode Theory of Graded-Core Fibers, "B.S.T.J., <u>52</u>, 9 (Nov. 1973), pp.1563-1578.
- H. Kajioka; "The Transmission Theory of Modecoupled Multimode Fibers Based on Scattering Matrix, "The Transactions E of the Institute of Electronics and Communication Engineers of Japan, Sept. 1979. (to be published)

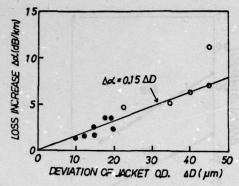


Fig.1 The relation between the loss increase at -20°C and the diameter deviation of the plastic jacket of the polymer clad optical fiber investigated.

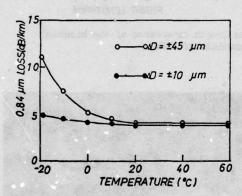
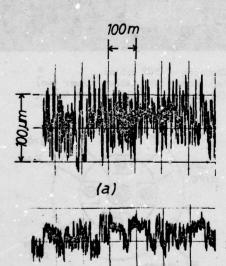
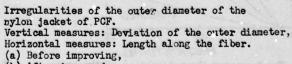
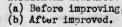


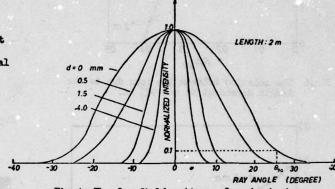
Fig.2 The temperature dependence of PCF at the wavelength of 0.8% um.



(b)







The far-field pattern of a short piece of PCF. Fig.4

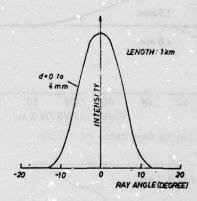


Fig.5 The far-field pattern of a long piece

- Bold Committee Committee

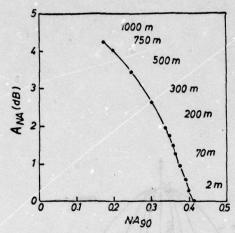


Fig.6 The relation between the loss due to the length dependent NA and 90% NA.

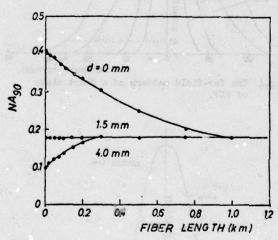


Fig. 7 The length dependence of 90% NA.

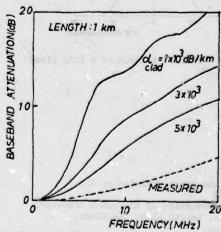


Fig. 8 The frequency characteristics of the basebend amplitude attenuation of PCF.

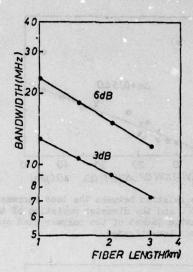


Fig.9 The length dependence of the baseband bandwidth of PCF.

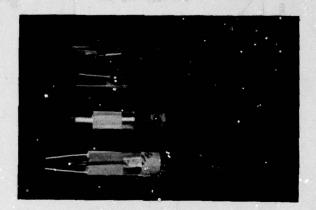


Fig.10 Examples of PCF cables
(a) Spacer type cables (lower two)
(b) Unit type cables (upper two)

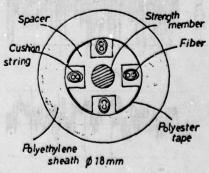


Fig.11 8-core PCF cable installed in an electric power station.

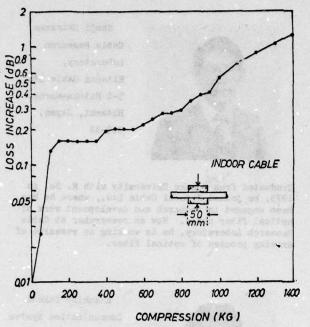


Fig.12 The transmission loss vs. compression characteristics of PCF indoor cable.

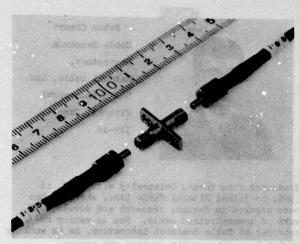


Fig.14 PCF connector

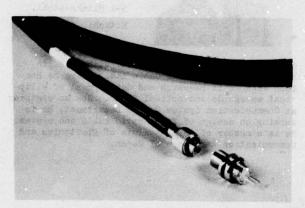


Fig.13 PCF bundle and its coupler

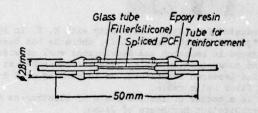


Fig.15 Splicing of PCF

AUTHORS



Nobuo Ohmori Cable Research Laboratory, Hitachi Cable, Ltd. 5-1 Hitaka-machi Hitachi, Japan, 319-14

Graduated from Tohoku University with M. E. in 1966, he joined Hitachi Cable Ltd., where he has been engaged in design, research and development work of communication cable. Now as senior researcher, at Cable Research Laboratory, he is working on R & D of fiber optic devices and system. He is a member of the Institute of Electronics and Communication Engineers of Japan, and IEEE.



Hiroshi Kajioka Cable Research Laboratory, Hitachi Cable Ltd., 5-1 Hitaka-machi Hitachi, Japan, 319-14

Graduated from Kyoto University with M. E. in 1973, he joined Hitachi Cable, Ltd., where he has been engaged in research and development work of wide band communication cable. Now as researcher at Cable Research Laboratory, he is working on R & D of fiber optic cable.

He is a member of the Institute of Electronics and



Communication Engineers of Japan.

Takashi Shimada Cable Research Laboratory, Hitachi Cable Ltd., 5-1 Hitaka-machi, Hitachi, Japan, 319-14

Graduated from Nagoya University with M.E. in 1974, he joined Hitachi Cable Ltd., where he has been engaged in research and development work of fiber optic devices. Now as researcher, he continues to work on R & D of fiber optic devices and system. He is a member of the institute of Electronics and Communication Engineers of Japan.



Shoji Shinzawa
Cable Research
Laboratory,
Hitachi Cable Ltd.,
5-1 Hitaka-machi,
Hitachi, Japan,
319-14

Graduated from Tohoku University with M. Sc. in 1973, he joined Hitachi Cable Ltd., where he has been engaged in research and development work of optical fiber cable. Now as researcher at Cable Research Laboratory, he is working on research of drawing process of optical fiber.



Kazuhiko Takeda Communication System Design Dept., Hitaka Works, Hitachi Cable Ltd., 5-1 Hitaka-machi, Hitachi, Japan 319-14

Graduated from Tohoku University with B. E. in 1970, he joined Hitachi Cable Ltd., where he has been engaged in research and development of elliptical waveguide and optical fiber. Now as engineer at Communication System Design Department, he is working on design of fiber optic cable and system. He is a member of the Institute of Electonics and Communication Engineers of Japan.

UV CURED RESIN COATING FOR OPTICAL FIBER/CABLE

C. L. Schlef, P. L. Narasimham and S. M. Oh

ITT EOPD Roanoke, Virginia 24019

Glass optical fibers were fabricated using various UV curable resins as protective coatings. These fibers were evaluated for their mechanical and optical performance, and the results compared to fibers coated with silicone resin, plus an extruded jacket of thermoplastic copolyester material. The advantages and disadvantages of the use of UV curable resins as optical fiber coating materials are discussed.

Introduction

One of the primary requirements in the production of glass optical fibers and cables is the preservation of the strength of the glass fiber itself. Theoretically, glass is one of the strongest materials known to man, having a strength (for SiO₂) of nearly 14,000 N/sq mm. 1 However, in practice this strength is never realized. Strength degradation occurs when submicroscopic cracks (<100 Å long) are present in the surface of the glass and these microcracks act as stress concentrators. These cracks may be created when the pristine glass surface comes into contact with any form of solid matter, including dust particles in the air.

A second cause of strength degradation is stress corrosion or static fatigue. In stress corrosion, water molecules from the environment react with the glass at the tips of microcracks under the influence of stress. This causes subcritical cracks to slowly grow with time until the stress intensity at the tip of at least one crack reaches the critical level. The crack then propagates very rapidly and failure occurs.^{2,3}

In order to preserve the strength of glass fibers, it is necessary to do two things: first, the pristine surface must be protected from all types of mechanical damage. Second, the surface must be protected from attack by ambient moisture. These two purposes can be

accomplished with some degree of success by coating the bare glass with a protective material immediately after the fiber is formed from the melt.

Many different single and two layer coating systems have been employed in producing optical fiber. One system is the application of a soft, thermally cured, primary coating by dip coating on line, followed by an extruded coating of a harder thermoplastic material. The primary coating consists of a silicone resin which provides minimal mechanical protection, but serves as a "cushion" against microbending. The harder secondary coating provides full mechanical protection and is moderately successful as a moisture barrier.

Since silicone resin is thermally cured and is dependent upon radiant and convective heat exchange for curing, it imposes an upper limit on the rate at which the fiber may be drawn. This is brought about by the fact that the coating must be relatively well cured before it exits the curing oven and contacts any of the fiber handling equipment.

The curing rate of UV curable resins is dependent only upon the intensity of UV light available to initiate cross linking of the polymer. UV lamp systems are available in a wide range of power output and bulb lengths. If UV curable resins are employed as primary coating materials, they will not severely limit the draw rate. Thus, higher draw rates may be employed and will reduce the total cost of glass optical fiber fabrication. Also, some UV cured coatings provide better mechanical and moisture protection than the silicone resin-thermoplastic double coating. These facts make UV curable resins very attractive as glass optical fiber coating materials. This paper evaluates the potential use of UV curable resins as coating materials for optical fiber.

Experimental Procedure

All fibers were drawn using oxy-hydrogen flames as the heat source. In drawing the fibers, all draw conditions except the coating material were kept the same. The UV curable resin was applied by dip coating. The resin was cured immediately using a UV lamp system with variable power supply. Fibers were drawn at rates ranging from 30-60 m/min.

In all cases, the diameter was optically monitored with a Milmaster diameter sensing device and controlled with a Milmaster closed loop feedback controller. The coating thickness was kept at 100 μm making the total od approximately 327 μm with a single UV cured coating.

Some of the fibers were drawn from solid synthetic silica (Suprasil ® or SS2) rods. Since the refractive index of UV curable resins is higher than that of fused silica, fibers drawn from solid silica do not transmit light and were used only for strength testing. Fibers drawn from graded index preforms were optically evaluated for attenuation, dispersion and numerical aperature. Some of the graded index fibers were over coated with a secondary extruded coating of a thermoplastic copolyester. Several received a secondary coating and immediate curing in a nitrogen atmosphere.

Three types of tests were performed for strength evaluation:

- a. Proof tests: the entire length of the fiber is progressively subjected to a specified stress. This may be done on-line as the fiber is drawn, or off-line. The fiber may be tested several times at different stress levels.
- b. Dynamic tensile tests: two meter gauge length specimens of the fiber being tested are stressed to failure at a selected strain rate. A plot of probability of failure versus breaking stress is made based on Weibull statistics.
- c. Fatigue tests mandrel method: the mandrel method of fatigue testing (described in detail elsewhere)⁵ was used to determine the fatigue paramater, N, for fibers coated with various materials and combinations of materials.

Results and Discussion

Table 1 lists the properties of the various UV curable resins employed as protective coatings in the present study.

All the UV curable resins are formulations consisting of an oligomer, multifunctional monomers and a photo initiator. However, the physical properties of these cured resins can be varied by changing the oligomer and/or using multifunctional monomers. For example, formulations with mono-functional monomers yield films which are soft and flexible when cured, whereas use of multifunctional monomers yield tough, rigid films. The cure rate of these resins can be increased to some extent by increasing the photo initiator concentration. However, this will reduce the pot life of the resin.

Optical Performance

Table 2 lists the optical properties of graded index fibers coated with different UV curable materials, before and after a secondary coating of an extruded thermo-plastic copolyester. The optical losses for the fibers coated with a UV curable material are consistent and also compare favorably with that of a fiber coated with a silicone resin and an extruded jacket of a thermoplastic copolyester. If fibers are coated with a material having a lower refractive index than glass, cladding modes with higher losses are generated. These cladding modes make the measurement of transmission loss and design of optical fiber systems diffi-In fibers having UV cured coatcult. ings, cladding modes with higher losses are stripped away since UV cured resins have a higher RI than glass, and this may be a desirable property. However, in the case of graded index fibers, it However. was difficult to define the core-cladding interface because of this effect. Also, these materials cannot be used as a primary coating on plastic clad silica (PCS) fibers, because the coating itself acts as the optical cladding, and the light will be stripped from the fiber.

Graded index fibers coated with UV cure resins were also extruded with a thermoplastic copolyester as a secondary jacket in order to study the compatibility of these resins with the thermoplastic material, and also the effect on optical and mechanical properties. It can be seen from these results that the extrusion of a secondary jacket of thermoplastic copolyester over the UV cured resin compare favorably with silicone coated fibers with respect to the optical properties, as shown in Table 2. The transmission increase is due to reduction in microbending losses. The effect of the secondary coating over UV cured resin coated fiber on mechanical performance will be discussed later.

A DESCRIPTION OF THE PARTY OF T

In order to simulate the double jacketing design for fibers, graded index fibers were first dip-coated with a soft UV curable resin, and a secondary hard coating of UV curable resin was applied later. The two dip-coating processes resulted in a fiber of 508 μm od starting with a bare fiber of 127 μm od.

The optical properties of these fibers are given in Table 3. It can be seen that the optical losses compare favorably with a silicone coated and a copolyester extruded fiber. This coating procedure can be employed successfully without affecting the optical properties of the fibers.

Mechanical Performance

The static fatigue results for fibers coated with UV curable resin are given in Table 4. The stress values at time to failure of 10,000 and 1,000 seconds are given for comparison of the performance of different coatings. The value of the fatigue parameter N, also gives some idea of the fatigue behavior and is, in part, affected by the coating material. The stress levels can be compared at a given time to failure for different resins, and this data also gives some comparison. is seen from the data that the stress levels fall in the range of 2700-3300 N/sq mm (at 10⁴ s). However, in the case of resin #2, there is a marked increase in the stress levels, as compared to the other values. It is possible that this may be explained in terms of the adhesive strength between the coating and glass surface as described below.

A primary coating of a silicon; resin does not adhere strongly to the glass fiber surface and UV curable resins seem to have better adhesion. It was found that resin #2 has the strongest adhesion to the fiber, as compared to the other coating materials, as implied from coating strippability tests. The effect of adhesion may be an increase in the static fatigue limit in the case of fibers coated with resin #2. Increased adhesion between fiber and resin may help prevent a build-up of moisture at the interface, and thus can improve the fatigue characteristics. The type of bonding between the glass resin interface is not known.

The dynamic tensile test results are given in Table 4. In all the cases, the Weibull plot is unimodal, and the maximum and average values fall in the same range. Thus, it is seen that UV curable resin coatings do not degrade the fiber strength, and in some cases, improve the fatigue characteristics. The above strength data is further supported by

proof-test strength of these fibers. Table 4 also lists the results of prooftest strength of fibers coated with different UV curable resins. It can be seen from these results that several kilometer lengths of these fibers passed proof-test strength levels of 690 and 1380 N/sq mm. It can be concluded from these results that fibers coated with UV curable resins retain the initial strength and fatigue resistance of optical fibers.

Advantages and Disadvantages

There are several advantages to the use of UV curable resins over the thermally curable resins. One of the major advantages is the potential increase of draw speed, which will reduce the cost of fiber production.

UV curable resins consist of a one-part system with a shelf life of 3-6 months, compared to the pot life of 2-3 hours for the mixed thermally curable resin.

UV curable resins have good adhesion to various substrates. They are available in a range of viscosities and mechanical properties. They have good wettability and low volatility. They can be easily applied by dip coating.

A disadvantage of UV curable resins is that most of them contain multifunctional acrylates. Acrylates are a potential health hazard and must be used with greater care than is necessary for the use of silicone resins.

Conclusions

On the basis of the work described above, it may be concluded that UV curable resins are very promising candidates for use as coating materials in the production of optical fibers. Draw speeds may be increased. These materials perform very well in preserving the strength of the fiber, are easy to apply, and have no detrimental effect on optical characteristics of the fibers. The fact that cured properties may be tailored to suit specific needs makes them very attractive for use with fibers fabricated for special applications. The disadvantage of their toxicity can easily be overcome by use of proper handling techniques.

Acknowledgment

The authors wish to express their appreciation to Robert A. Spencer and David R. Hollandsworth for their assistance in the preparation and testing of the fibers used in these experiments.

37

References

- R. H. Doremus, Glass Science, John Wiley & Sons, New York, 1973, P.284
- 2. R. J. Charles, W. B. Hillig, Symp. on Mechanical Strength of Glass, Union Sci. Continentale du Verre, Charleroi, Belgium, 1962, P. 511
- W. B. Hillig, R. J. Charles, High Strength Materials, V. F. Jackey, Ed., Wiley., New York, 1965, P. 682
- D. M. Spero, Choosing UV Hardware -Promises, Performances, Prices, 4th Int. Conference on Radiation Curing, Chicago, 1978
- C. K. Kao, M. Maklad, V. Schurr, <u>Topical Meeting on Optical Fiber</u> <u>Transmission II, February 22-27, Williamsburg, VA Paper #TUAR</u>
- 6. W. Rowe, Molecular Design in the Formulation of Radiation Cure Systems, 4th Int. Conference on Radiation Curing, Chicago, 1978
- 7, Hiroshi Shimba et. al., Preprints of ACS/CSJ Chemical Congress, Honolulu, Hawaii, April 6, 1979, P. 77
- 8. H. N. Vazirani et. al., Topical
 Meeting on Optical Fiber Transmission
 II, February 22-27, 1977, Williamsburg, VA Paper #TUB3-1



Charles L. Schlef graduated from the University of Missouri - Rolla, with a B.S. in Ceramic Engineering in 1970. He received an M.S. in Ceramic Engineering from the same institution in 1976. In August of 1976, he joined ITT Electro-Optical Products Division where he is a fiber optic engineer working in the areas of fiber strength inprovement and drawing/coating process development. He is a native of St. Louis, Missouri. Mr. Schlef is a member of the National Institute of Ceramic Engineers, the American Ceramic Society, The Society of Glass Technology (England) and Keramos.



Pundi L. Narasimham is an applications engineer in the fiber optics laboratory at ITT EOPD, Roanoke, Virginia. He received a B.S. in Chemical Engineering in 1974 from Osmania University, India; an M.S. in Chemical Engineering from Indian Institute of Science, India, in 1976; and another M.S. in Polymer Science and Engineering from Washington State University in 1978. His areas of interest include fiber strength improvement, mechanical properties, and the development and evaluation of polymeric coatings and coating techniques. He is a member of ACS and SPE.



Shin Moo Oh is a senior engineer in the fiber optics laboratory at ITT EOPD, Roanoke, Virginia. His responsibilities include research and development of optical fibers to achieve improved strength and durability. He earned a B.S. and M.S. in Ceramic Engineering from Han Yang University, Seoul, Korea in 1967 and 1969, respectively. He received another M.S. and a Ph.D. in Ceramic Engineering from Iowa State University in 1973 and 1975, respectively. He is a member of the American Ceramic Society, NICE, and the Society of Glass Technology.

Table 1. Properties of UV Curable Resins.

	ers.	PROPERTIES						
				MECHANICAL				
I.D.#	MATERIAL	Viscosity @25°C (cps)	Density @25°C (gm/cc)	RI @25°C	Hardness Shore A	Tensile (N/mm ²)	Elong.	Modulus 9 1% Elong. (N/mm ²)
Resin #1	Urethane Acrylate	6000	1.12	1.54	37	31.0	15	434.5
Resin #2	Polyene/Polythiol Ester	4000	1.25	1.51	80	10.3	30	689.7
Resin #3	Urethane Acrylate	20,000	1.10	1.523	84	19.3	50	89.7
Resin #4	Epoxy Acrylate	6500	1.13	1.5	niesā +	et atese	Ţ	•
Resin #5	Polyurethane	2000	1.08	1.51	35	23.5	100%	eth •
Resin #6	Urethane Acrylate	13,000	1.13	1.53	57	6.9	84	4.8

Table 2. Comparison of Optical Data of UV Cured Resin Coated Fibers Before and After Secondary Jacket Extrusion.

A hai kerel		OPTICAL DATA Before Secondary After Secondary					
	feet distant	Jacketing		Jacketing			
COATING MATERIAL	CABLE LENGTH (m)	Attenuation @0.85 µm (dB/km)	Disp. @ 0.9 μm (ns/km)	Attenuation @0.85 µm (dB/km)	Disp. @ 0.9 μm (ns/km)		
Resin #1	753	5.27	1.76				
Resin #2	650	5.22	0.59	3.41	0.91		
Resin #3	985	4.56	1.48	3.86	1.70		
Resin #4	1135	5.83	0.98	6.68	0.57		
Resin #5	1120	3.05	2.21	3.63	2.15		
		fore 201 s. 13		manage the min Tax			

Table 3. Optical Data of Double UV Coated Fibers.

I.D.	Coating Combination	Optical Da		
		Attenuation @ 0.85 µm	Dispersion @ 0.9 µm	NA
		(dB/km)	(ns/km)	
Fiber #1	With Resin #5 only	3.58	<.2	0.21
	Resin #5 + Resin #2	4.54	<.2	0.20
Fiber #2	With Resin #5 only	3.74	<.2	0.24
	Resin #5 + Resin #2	4.10	<.2	0.24
Fiber #3	Silicone + Thermoplastic Copolyester	3.00-4.00	0.5-1.5	∿0,21

Table 4. Mechanical Performance Data of UV Cured Fiber.

Coating Materials Static Fatigue Test		Dyramic Tensile Test				Proof Test*				
N		Breaking Stress (N/mm ⁻²) @ 10,000 s @ 1,000 s		Stress (N/mm ⁻²) M Max Min Average				Tested (km) Fiber Length	Stress Level # of (N/mm ⁻²) Break	
								2.0	1379	0
Resin #1	17	2763	3160	29	5545	1841	5159	2.94	690	0
								3.1*	690	0
Resin #2	27	3457	3769	69	6408	5414	5780	3.1*	1379	0
Resin #3	23	2740	3023	-	-	77.0		0.9	690	0
Resin #4	23	2932	3236	40	6497	2380	5759	1.0	690	0
Resin #5	19	2638	2980	50	5863	5000	5456	-		-

*All fibers have 127 μm od except *marked fibers (i.e., 102 $\mu\text{m})$

EFFECTS OF SINGLE-MODE FIBER NA ON OPTICAL AND MECHANICAL PROPERTIES

F. I. Akers, A. R. Asam, M. S. Maklad

ITT ELECTRO-OPTICAL PRODUCTS DIVISION Roanoke, Virginia 24019

Abstract

Single-mode fibers, ranging in numerical aperture (NA) from 0.1 to 0.2, were fabricated using core glass systems of SiO2/GeO2 and SiO2/P2O5. These fibers were evaluated with respect to bending and microbending losses using equipment specially designed to isolate these variables. Bending and microbending losses were also measured in fibers having four different combinations of hard and soft primary and secondary jacket materials. Single mode fibers were evaluated for dynamic tensile strength and for fatigue.

Introduction

Single-mode fibers are being used as media for rotation and accustic sensors which are based on optical phase change detection. Deployment of these sensors will require long lengths of fiber to be coiled onto small diameter mandrels.

The optical loss of a single-mode fiber can increase through radiation due to curvature and microbending. In addition, a tightly coiled fiber is subjected to tensile stress which will reduce the time to failure.

This paper discusses the evaluation of unstressed attenuation as well as bending and microbending losses in 0.1 to 0.2 NA single-mcde fibers having compositions of SiO₂/GeO₂ and SiO₂/P₂O₅. Bending and microbending losses were also measured in fibers having four different combinations of hard and soft primary and secondary jacket materials. In addition, furnace drawn single-mode fibers were tested for tensile strength and fatigue.

Experimental

Single-mode fibers were fabricated at ITT-EOPD. The optical cladding material used was B_2O_3 doped SiO_2 while core materials were either GeO_2 or P_2O_5 doped SiO_2 . Fibers were designed to have a mode diameter (V) of 2.2 at 0.63 μ m.

The fibers were dip coated on line during the drawing operation with a silicone resin primary coating and extruded with a secondary jacket of polyester to a final diameter of 0.40 mm. Additionally, one high NA single-mode fiber was drawn with four combinations of coating types: two silicone resins having Shore A hardness values of 35 and 70 and two polyester formulations having hardness values of 40D and 72D.

The single-mode fibers were evaluated in several ways. First, the unstressed attenuation of each fiber was measured at 0.63 µm, 0.83 µm, and 1.03 µm while a 105-m length of the fiber was loosely strung around two 30-cm diameter drums spaced 15 m apart. Secondly, the excess bending loss was measured at 0.63 µm as a function of fiber turns around mandrels having 12.7-mm, 9.5-mm, 6.4-mm, and 3.2-mm diameters. Thirdly, the excess attenuation at 0.63 µm was measured in 24 locations for each fiber as the fiber was subjected to microbends using a specially designed microbend test fixture. As a final evaluation of fiber optical performance in a simulated sensor configuration, 30 m of 0.19-NA single-mode fiber was tightly coiled onto an 8-mm diameter mandrel and the loss was measured as a function of coiled fiber length.

The mechanical performance of several fibers was evaluated by determining fiber dynamic tensile strength and by determining fiber static fatigue characteristics. The dynamic tensile tests used variable strain rate control and employed two-meter gauge lengths to determine the probability of failure as a function of failure stress. Static fatigue testing was performed on small diameter mandrels in air under ambient conditions, which resulted in determination of the fatigue resistance parameter, N.

Results and Discussion

The results of the unstressed attenuation measurement are reported in Table 1.

Table 1. Single-Mode Fiber Loss Data.

Loss (±0.3 dB/km)
(@.83 μm) (@1.03 μm)
2.4 2.4
17.4 NE
8.7 5.0
11.0 35.2

NE = Not Evaluated

Table 2. Microbend Loss Test Result Summary.

Fiber	Core		Excess	Loss (dB)
Number	Dopant	<u>NA</u>	Mean	Std Devn
EMT-20721	GeO ₂	.11	4.3	1.9
EMT-20738	F ₂ O ₅	.11	8.4	3.0
EMH-20495	GeO ₂	.21	0.0	0.1
EMH-20627	P ₂ O ₅	.17	0.8	0.2

The lowest unstressed attenuation was found in the 0.11-NA germanosilicate fiber. It can be seen that the high NA fibers typically have baseline attenuation values higher than those for the low NA fibers. This increase in loss for high NA single-mode fiber is attributed to Rayleigh scattering from increased core dopant levels necessary to achieve high NA values. It can also be seen that P2Os doped SiO2 core fibers have higher losses than the GeO2 doped SiO2 core fibers.

The results of the bend loss tests are shown in Figure 1. Only the results of the 6.4-mm and the 3.2-mm mandrel tests are shown, since all fibers were insensitive to wrapping onto both the 12.7-mm and 9.5-mm mandrels. While both low NA fibers exhibited excess losses of about 20 dB on the 6.4-mm mandrel and about 25 dB on the 3.2-mm mandrel, the 0.21-NA germanosilicate core fiber had no significant loss increase after 20 wraps on the 3.2-mm mandrel. The 0.17-NA phosphosilicate core fiber showed no loss increase on the 6.4-mm mandrel but did suffer a loss increase of 30 dB after 20 turns on the 3.2-mm mandrel.

Figure 2 graphically illustrates the relationship between fiber bend loss and fiber NA. Except for the 0.17-NA phosphosilicate core fiber, bending loss is shown to be directly related to NA.

The results of the microbending evaluation are shown in Table 2. The results show high NA fibers to have very small, if any, microbending losses while the low NA fibers exhibit significant losses. Also, in both cases the P_2O_5 doped core fiber has a greater loss than the GeO₂ doped core fiber.

The results of the jacket evaluation are shown in Figures 3 and 4. Figure 3 shows the bending loss results after 20 turns on the 6.4-mm and 3.2-mm mandrels while Figure 4 shows the microbend loss results. Figure 3 shows that all jacket combinations are similar in their effects on bending losses except for the hard/hard jacket combination which shows significantly lower loss. The microbending tests showed similar results. The jacket combination of soft silicone and soft polyester was easily damaged by the test apparatus and broke repeatedly. The hard/hard combination proved most resistant to microbending induced losses.

The results of the 30-m wrap onto an 8-mm mandrel are shown in Figure 5. The data show a nearly linear increase in excess loss with wound fiber length to a maximum of 0.21 dB at 30 m.

The results of the dynamic tensile tests are shown as Weibull plots in Figures 6 and 7.

Fiber A (Figure 6) shows very high strength with a unimodal distribution of breaking strength. The high mean and minimum strength of 5413- and 4827-N/mm² are comparable to values achieved with high strength flame drawn fibers. No large flaws were encountered in the short lengths tested. Fiber B (Figure 7) had a unimodal failure distribution but with a very low slope. In addition, the minimum strength point on the Weibull plot indicates the presence of a "low strength tail." Variations in strength from fiber to fiber may be attributed to contaminants in the furnace atmosphere and to nonuniformity in the fiber coating.

The results of the static fatigue tests are plotted in Figure 8. Statistically, fibers A and B exhibited about the same resistance to fatigue having N values of 20 and 23 respectively. These results compare favorably with high strength flame drawn fibers for which an N value of 22 is typical.

Conclusion

In conclusion, the unstressed loss as well as bending and microbending losses were measured in single-mode fibers as a function of NA and core composition. In addition, the dynamic tensile strength and fatigue parameter of single-mode fibers were evaluated. Bending and

microbending losses in 0.2 NA germanosilicate core fibers are negligible. Single-mode fibers exhibit variability in strength which must be eliminated before fibers can be deployed in tightly coiled configurations.

Acknowledgement

This work was performed under contracts from the Naval Research Laboratory and the Office of Naval Research.



Frank Akers is an engineer in the Optical Fiber Development Group at ITT EOPD. His responsibilities include preform development for both multimode and single mode optical fibers. He received his B.S. and M.S. degrees in Chemistry from Virginia Polytechnic Institute and State University.

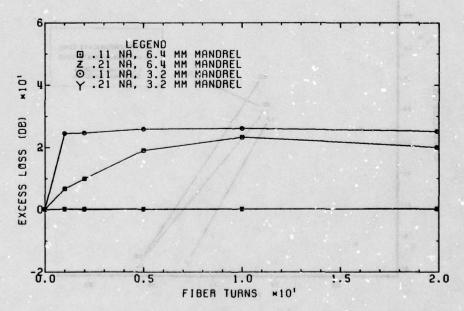


FIGURE 1A. BEND LOSS RESULTS: GEO2 DOPED CORE FIBERS

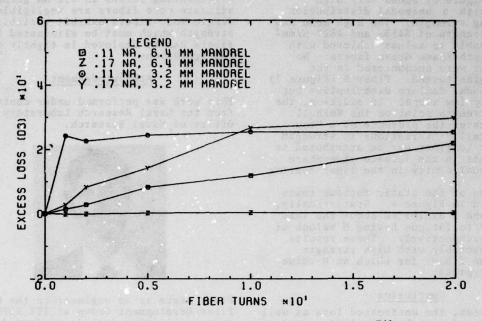


Figure 1b. Bend Loss Results: P205 Doped Core Fibers

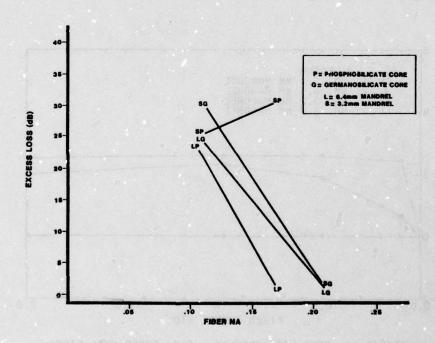
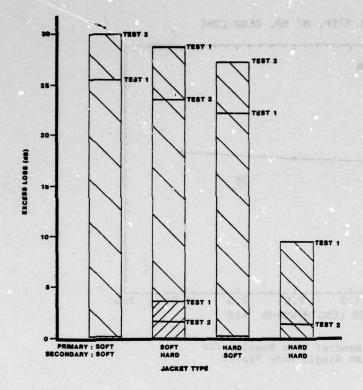


Figure 2. Excess Bending Loss after 20 Fiber Turns.



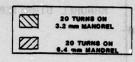
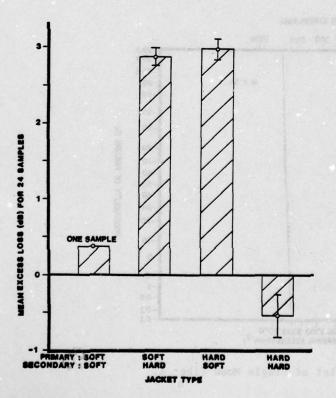


Figure 3. Single Mode Fiber Jacket Evaluation Bend Test Results.



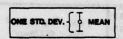


Figure 4. Single Mode Fiber Jacket Evaluation Microbending Tests Results.

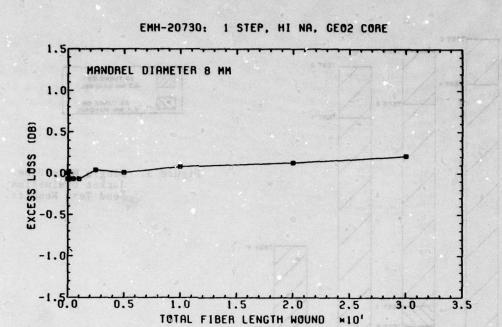


Figure 5. 8 mm Mandrel Test Results for High NA Single Mode Fiber.

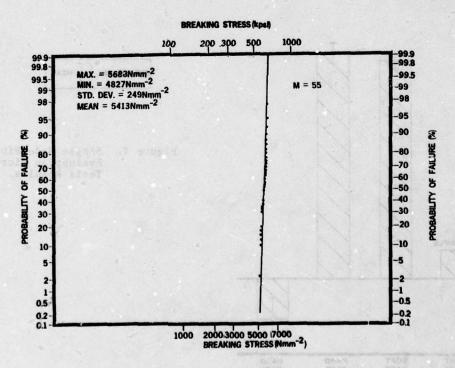


Figure 6. Weibull Plot of Single Mode Fiber A.

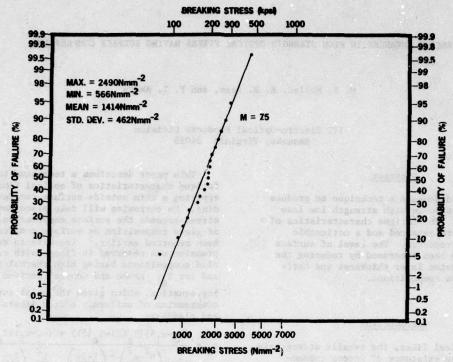


Figure 7. Weibull Plot of Single Mode Fiber B.

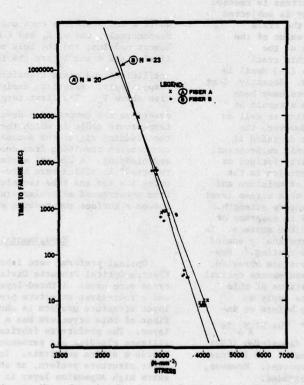


Figure 8. Static Fatigue of Single Mode Fibers in Air.

RECENT ADVANCES IN HIGH STRENGTH OPTICAL FIBERS HAVING SURFACE COMPRESSION

404 678 mm 669

M. S. Maklad, A. R. Asam, and F. I. Akers

ITT Electro-Optical Products Division Roanoke, Virginia 24019

Abstract

This paper discusses a technique to produce surface compression in high strength low loss optical fibers. The fatigue characteristics of these fibers were measured and a noticeable improvement is reported. The level of surface compression has been increased by reducing the surface compression layer thickness and optimizing the glass compositions.

Introduction

For an optical fiber, the tensile strength is dependent on the existence of stress concentration at micro-cracks or flaws on the fiber surface, such that the fracture stress is reached at the deepest flaw. As the fiber is subjected to a tensile load, the stress at the crack increases substantially over the value of the externally applied stress because of the leverage introduced by the long thin crack geometry. The Si-O bond strength (2-3 Mpsi) is exceeded and the crack propagates. Recently, long length high strength optical fibers have been reported. 1,2 This development is a result of careful preform and fiber processing as well as the high purity of glass used. However, the initial high strength of fiber is degraded if subjected to tensile load in a humid environment. This degradation is caused by static fatigue or stress corrosion. The stress corrosion is the flaw propagation in the presence of moisture and eventual failure of glass fibers at a stress level less than that of the initial fracture strength. Several approaches were developed to suppress or prevent stress corrosion at the fiber surface. In one approach, the fibers were hermetically sealed in a thin metal sheathe by freeze coating.3 However, grain boundary corrosion, surface abrasion, cyclic fatigue of metal coating and excess optical fiber loss are some of the limitations of this technique. Another approach is to apply a chemically durable Si3N4 coating before an inline organic protective coating.4 The Si3N, is deposited using a chemical vapor deposition (CVD) technique during the drawing process. An increase in the fatigue parameter n was reported. However, the initial fiber strength was degraded.

This paper describes a technique to improve fatique characteristics of optical fibers by applying a thin outside surface compression cladding. No corrosion will take place until tensile stress exceeds the surface compression. Effects of glass composition on surface compression have been reported earlier. Increase in surface compression was observed ir fibers with core and clad compositions having high thermal expansion and low Tg. Krohn and Cooper derived the following equation, which gives the axial surface compression of uniformly coated fibers having core and cladding:

$$\sigma_{Z} = \frac{(\alpha_{2} - \alpha_{1}^{*}) (T_{g}(2) - T_{g}(1)) + (\alpha_{2} - \alpha_{1}) (T_{g}(1) - T)}{\frac{1}{3K_{1}^{*}} \left(\frac{b^{2} - a^{2}}{a^{2}}\right) + \left(\frac{1 - 2\nu}{E}\right) - \frac{b^{2}}{a^{2}} \left(\frac{1 - \nu}{E}\right)}$$
(1)

where a and b are the core and fiber radii respectively, and ν , E, and K are Poisson's ratio, Youngs modulus, and the bulk modulus, respectively, and α and T_g are the thermal expansion coefficient and glass transformation temperature, respectively. Asterisks designate glass properties above T_g . The first term in Equation 1 describes the compression developed in the temperature range in which the core is fluid and the cladding rigid; the second term describes the compression resulting from cooling both rigid core and cladding. A 20-kpsi surface compression was reported in silica core boro-silicate clad fibers using the rod and tube technique. Fiber prepared from prestressed molecular stuffed preforms showed a surface compression of 30 kpsi. 7

Experimental

Optical preforms were fabricated at ITT Electro-Optical Products Division. Two preform types were used: a three-layer structure preform and a four-layer structure preform. The three-layer structure preform is shown in Figure 1. The fiber of this structure has a thin outside silical ayer. The preform is fabricated with a borosilicate cladding and germanium silicate core inside a silica substrate. In processing a four-layer structure preform, as shown in Figure 2, an extra high expansion layer is introduced first

Sefore the optical cladding and optical core. Fibers with different silica cladding thicknesses were prepared by reducing the silica layer thickness in the finished preforms.

Preforms were drawn into fibers and coated in-line with a primary coating of a silicone resin and a secondary copolyester coating for mechanical protection.

In the weakest link model⁸ a plot of ln ln [1/(1-F)] against ln σ for a given length showed a steep straight line, indicating that a single Weibull distribution is present where F is the probability of failure and σ is the fracture stress level.

Dynamic strength of optical fiber is evaluated at a 20% minimum strain rate using 20 specimens. The strength distribution is presented as a Weibull plot. Fibers were fatigue tested using the mandrel technique, which is described elsewhere. 9

Results

Figure 3 illustrates the Weibull distribution of two three-layer fibers. Fiber 1 has unimodal distribution in the Weibull plot, which indicates the absence of large surface flaws. On the other hand, fiber 2 has lower strength and multimodal Weibull distribution. This strength degradation in fiber 2 is associated with preform processing. Static fatigue testing of strong fibers with unimodal Weibull distribution produced a consistent fatigue parameter value n, compared to large fluctuation in n values associated with weak fibers. To compare fatigue characteristics of fibers it was found necessary to compare only strong fibers with unimodal Weibull distribution.

Figure 4 shows a comparison of fatigue curves for two three-layer structures and a plastic clad silica (PCS) fiber. Fibers with surface compression show a shift towards higher stress values, which is more pronounced in fiber A. Fiber A has a 1-µm thick SiO₂ layer and a 56-kpsi shift in the fatigue curve as shown in Table 1. Fiber B, with a thick cladding, shows only a 19-kpsi shift.

Figure 5 shows the results of fatigue testing on four-layer structure fibers. Fiber A indicates a larger shift than that exhibited by PCS fibers, which also demonstrate the effect of thinner cladding on surface compression. As shown in Table 1, the shift is equal to 68 kpsi and the compressive layer thickness is 1 µm. The shift is reduced to 33 kpsi for a 3-µm thick SiO, layer.

It can be concluded from Table 1 that improved fatigue characteristics can be achieved by reducing the surface compression layer thickness.

In conclusion, two types of optical fibers having surface compression layers have been fabricated. The dynamic strength and static fatigue were measured for both of these fibers. The effect of surface compression layer thickness was studied and the improvements in fatigue characteristics were demonstrated.

Acknowledgments

This work was supported by Navy NOSC, Contract Number NO0123-79-C-0301. The authors wish to thank NOSC for its support and for permission to present this paper.

References

- Maklad, M. S., Asam, A. R., "Long Length High Strength Optical Fibers," 27th Int. Wire and Cable Symposium, Cherry Hill, N. J., Nov. 14-16, 1978.
- DiMarcello, F. V., Hant Jr., A. C., Williams, J. C., and Kurkjian, C. R., "Improved Long Length Strength of Furnace-Drawn Silica Fiberguides," 154th Meeting of the Electro-Chemical Soc., Pittsburgh, Pa., Oct. 15-20, 1978, pp. 391-393.
- Robertson, G. D., Pinnow, D. A., and Wyscoki, J. A., "Metal-Coated Fiber Optical Waveguides," presented at the Glass Division Fall Meeting of the Am. Ceramic Soc., Bedford, Pa., Oct. 12-14, 1977.
- Hiskes, R., "Improved Fatigue Resistance of High Strength Optical Fibers," Topical Meeting on Optical Fiber Communication, March 6-8, 1979, WF6.
- Maklad, M. S., Kao, C. K., "Fatigue Characteristics of Optical Fibers Having Large Surface Compression," ibid, TUC3.
- Krohn, D. A., and Cooper, A. R., "Strengthening of Glass Fibers: I Cladding," J. Am. Ceramic Society, 52 (12), (1969), pp. 661-664.
- Mohr, R. K., El-Bayoumi, O. H., and Hojaji, H., "Static Fatigue in Glass Fibers Having Surface Compression," presented at 80th Annual Meeting of the Am. Ceramic Soc., Detroit, Mich., May 6-11, 1978.
- Kurkjian, C. R., Albarino, R. V., Krause, J. T., Vazirani, H. N., Dimarcello, F. V., Torza, S., and Schonhorn, H., "Strength of 0.04-30 m Lengths of Coated Fused Silica Fibers," J. Appl. Phys. Lett., 28, pp. 558-590 (1976).
- Rao, C., Maklad, M., Goell, J., "Testing of Tensile Strength of Optical Waveguides," Topical Meeting on Optical Fiber Transmission II, Williamsburg, Va., Feb. 1977.



Dr. Maklad was born in Egypt and received a BS in Chemistry and Physics and an MS in Physics from Cairo University in Cairo. He held a scientist position with Egypt Atomic Energy Commission from 1962-1967 to study the radiation effects on glass and develop radiation shielding glass windows and glass dosimeters. In 1970 he received his Ph.D in Ceramic Engineering from the University of Missouri-Rolla. As a post-doctorate fellow, Dr. Maklad was engaged in fiber optic development at Catholic University in America from 1971-1974. Currently Dr. Maklad is a Principle Scientist at ITT Electro-Optical Products Division.



Mr. Akers is an engineer in the Optical Fiber Development Group at ITT Electro-Optical Products Division. His responsibilities include preform development for both multimode and single mode optical fibers. He received his BS and MS degrees in Chemistry from Virginia Polytechnic Institute and State University and is a member of the American Chemical Society.

Table 1. Fatigue Improvement in Three- and Four-Layer Type Fibers.

Fiber Type	Sio Outer Layer Thickness (µm)	*(kpsi)
3-layer A	. i .weileche bei j	56
В 32	4	19
4-Layer A	Miking, W., Bellin, J., J.	68
Actual Burns	dit lesi 30 eo yeldek	33

*Shift in fatigue curve, compared to PCS fiber.

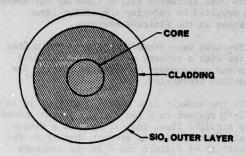


Figure 1. Three-Layer Structure Fiber Cross Section

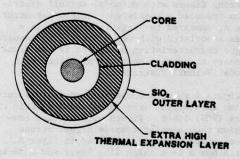


Figure 2. Four-Layer Structure Fiber Designed to Increase Surface Compression.

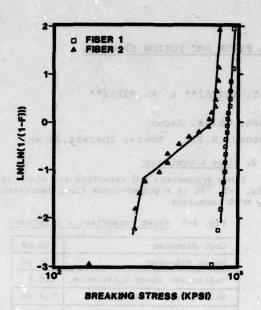


Figure 3. Comparison of Weibull Plots of Three-Layer Durable Fibers.

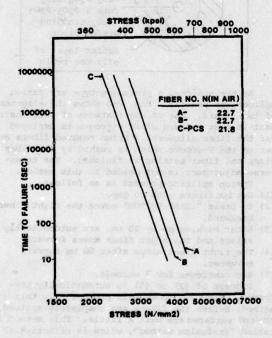


Figure 4. Comparison of Durable Fibers in Static Fatigue Test (Three-Layer Structure Fibers).

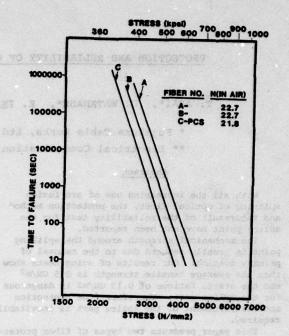


Figure 5. Comparison of Durable Fibers in Static Fatigue Tests (Four-Layer Structure Fibers).

PROTECTION AND RELIABILITY OF OPTICAL FIBER ARC FUSION SPLICING

T. ARAI*, O. WATANACE*, K. INADA*, S. SEIKAI** & M. HIRAI**

- * Fujikura Cable Works, Ltd. Sakura, Chiba, Japan
- ** Electrical Communication Laboratory, N.T.T. Tokai, Ibaraki, Japan

Abstract

With all the increasing use of arc fusion splicing of optical fiber, the protection method and the result of the reliability test for the splice point have not been reported.

The mechanical strength around the splicing point is greatly reduced due to the removal of primary coating. Our results of aging tests show that the average tensile strength is 0.5 GN/m² and the static fatigue of 0.13 GN/m2 is dangerous for the splice part. Therefore, the protection and reinforcement of the splice part is inevitablly required.

This paper presents two types of fiber protector. One is V-grooved substrate, on which the splice part is fixed with silicone adhesive. The other consists of two pieces of metal plate, between which the splice part is sandwitched with hot-melt film. The change of the splicing characteristics by heat cycle test, high temperature aging test and humidity aging test were measured. The results showed that both of them were very practical and reliable.

1. Introduction

As the splicing method of optical fibers, V-groove substrate method and arc fusion splicing method are mainly used. The merit of the former is that the instrument is simple and low splicing loss can be easily obtained with the precision cutting of V-groove. Increasing of the splicing loss with time, however, is unavoidable due to the evaporation of the matching oil or due to the decrease of hold power of the adhesive agent.

Compared with V-groove method, arc fusion splicing method formerly required complicated instruments, much time and skillful technique. Recent development of an automatic arc fusion splicer employing a fixed V-groove makes it possible to splice even single-mode fibers easily in short time.

Therefore, arc fusion method will be widely used in the field, but the evaluation of this method from the viewpoint of reliability has not been made. It is very important because improper protection method causes not only the fluctuation of the splicing loss by ambient temperature but also the failure of the splice part.

This paper describes what is the most important to the protection for the arc fusion splicing part and explains two reliable and practical methods.

2. Fiber & Equipment

Fiber parameters and structure are shown in Fig. 2-1. It is a graded-index fiber manufactured by MCVD technique.

Fig. 2-1 Fiber Parameters & Structure

Core diameter	50 μm
Outer diameter	125 µm
Refractive index difference	1.0 %
Buffer layer diameter	0.4 mm
Jacket diameter	0.9 mm
Jacket o	f nylon
Jacket of	95-SiO2 9205-B2O3 adding

As the splicer, a prefusion-type arc fusion splicer was used[1]. Fig. 2-2 shows the alignment of two fibers. One of the faatures of this instrument is that a fixed glass V-groove is employed for the fiber alignment. Nylon removed fibers are set on the V-groove which is pushed by the fiber clamp and fiber setting is finished. The transverse adjustment is not needed in this method.

Fusion splicing process is as follows.

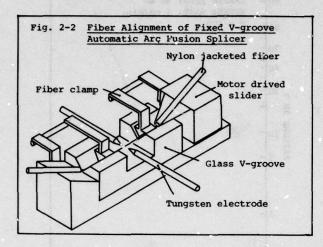
- (1) Set two fibers with no gap.
- (2) To press "START BUTTON" moves the right fiber backward.
- (3) After backing up by 20 µm, arc automatically arises and the right fiber moves forward.
- (4) The right fiber stops after 60 μm forward movement.
- (5) Arc continues for 7 seconds.

Process of (2) to (5) is automatically performed. Fig. 2-3 shows this process. In this method, before the fibers are completely spliced, the end surfaces are melt a little. This method is called "Prefusion method", which is effective to the compensation of fiber end surfaces and to the prevention of the bubble growth during fusion[2].

The arc arises between the tungsten electrodes whose gap is 1.4 mm. The arc current is about

20 mA and controlled with the triac.

Fig. 2-4 shows the histogram of splicing loss of the graded-index fiber. The average splicing loss is 0.08 dB.



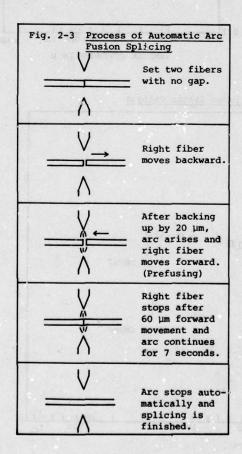
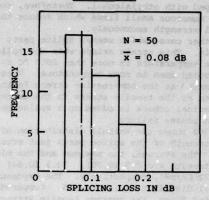


Fig. 2-4 Splicing Loss of Graded
Index Fiber

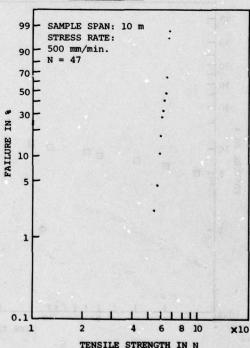


3. Mechanical Strength of Spliced Part

At present, tensile strength of a jacketed fiber is reaching its theoretical limitation. Fig. 3-1 shows the Weibull distribution of the jacketed fiber used in this experiment. The average tensile strength is 65 N i.e. 5.4 GN/m². This value can be obtained with a clean drawing furnace and proper primary coating, which prevent the fiber surface from being damaged by dusts, moisture and so on.

In splicing, however, primary coating must be completely removed. Because the rest of the primary coating causes the axial offset in the fixed V-groove type splicer.

Fig. 3-1 Tensile Strength of Jacketed Optical Fiber



We usually remove nylon jacket and primary coating with a wire stripper and wipe fiber with a gauze damped with ethylalcohol. Therefore, removed fiber has numerous small flaws which reduce the mechanical strength enormously.

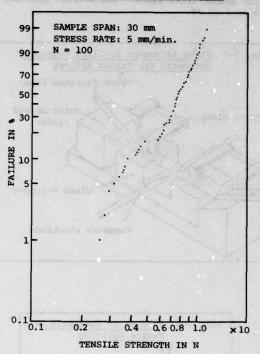
The other cause which weaken splice parts is heat strain. This strain arises when the splice part whose temperature is more than 2000 °C is rapidly cooled down to room temperature. This strain remains as the compressive stress in the surface and as the tensile stress in the center. When mechanical schock is added to a splice part, the strain causes failure.

Fig. 3-2 shows the Weibull distribution of the tensile strength of the splice parts just after splicing. The average, the maximum and the minimum tensile strength are 8.5 (0.70), 10.1 (0.84) and 2.6 N (0.22 GN/m^2), respectively. The exponent of the Weibull distribution is about 5. Compared with the jacketed fiber, the average tensile strength is reduced to one tenth and the dispersion is large.

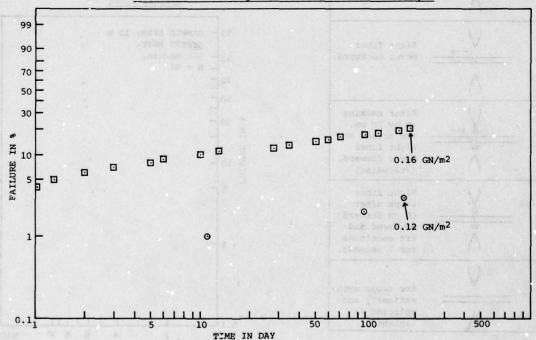
Fig. 3-3 shows the result of the static fatigue test. The loads are 0.08, 0.12 and 0.16 GN/m2, respectively. The number of samples is 100. The splice part is coated again with silicone resin. In six months, there is no failure to the load of 0.08 GN/m², but 3 samples were broken to the load of 0.12 GN/m² and 20 samples to the load of 0.16 GN/m2. In order to obtain long-term reliability, the static fatigue on splice parts must be at least less than 0.08 GN/m2.

These experimental results show that machanical strength of splice parts is so greatly reduced that we have to take special precautions to protect splice part.

Fig. 3-2 Tensile Strength of Spliced Parts Just After Splicing



Flg. 3-3 Time to Failure of Spliced Parts under Static Fatigue



4. Design of Protector

The most important characteristics for the protector of the arc fusion splice part are as follows.

(1) Protect the splice part from external schocks.

(2) Short operation

(3) Not to add stress to the splice part

In order to satisfy the conditions (1) and (2), it is enough to cover the splice part with a hard material like a stainless sleeve and fix it with a strong, rapid-curing adhesive like an epoxy resin. Importance of the condition (3) can be understood by calculating the internal stress caused by the protector due to temperature change. The splice part is assumed to be protected as shown in Fig.4-1. Increase of the ambient temperature expands the fiber, epoxy resin and stainless sleeve. The tensile stress added to the fiber is

$$f = E_1 \cdot \frac{E_1 A_1 k_1 + E_2 A_2 k_2 + E_3 A_3 k_3}{E_1 A_1 + E_2 A_2 + E_3 A_3} \cdot \Delta T$$
 (Eq. 4-1)

E₁, E₂, E₃: Young's modulus of fiber, epoxy resin and sleeve, respectively

A₁, A₂, A₃: Cross section area of fiber, epoxy resin and sleeve, respectively

k₁, k₂, k₃: Linear expansion coefficient of fiber, epoxy resin and sleeve, respectively

ΔT: Temperature increase

If ΔT is 60 deg., f becomes more than 0.2 GN/m² which is sufficient to cause failure. For the prevention of this stress, use of soft adhesive is effective. Young's modulus of epoxy resin is about 2400 kg/mm², but the value of soft adhesive like silicone resin is less than 1 kg/mm². In this case, the expansion of stainless sleeve is relaxed by silicone resin and shall not add any stress to the fiber. Soft adhesives are favorable for the protection of the splice part.

Another disadvantage of the sleeve type protector is that the splice part might bend in the sleeve as shown in Fig. 4-2. This bending causes not only the excess splicing loss but also the failure of the splice part. This bending is, here, approximated with sine function. The minimum radius of the bending is

$$R = \frac{L^2}{2\pi^2 d}$$
 (Eq. 4-2)

L: Bending period

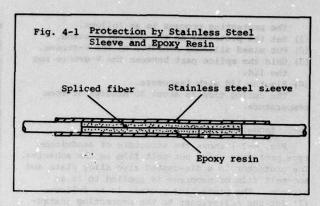
d: Inner diameter of sleeve Bending stress caused by curvature R is

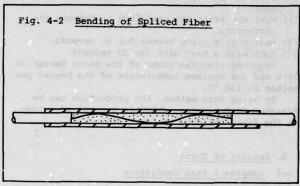
$$T = \frac{DE_1}{2R}$$
 (Eq. 4-3)

D: Outer diameter of fiber

In case L = 20 mm, d= 1 mm, D = 125 μ m and E = 7500 kg/mm², T is 0.23 GN/m². This bending stress which is easy to occur in the sleeve is also very dangerous to the fiber. Therefore, the structure of the protector must be designed to hold splice part in straight.

From the discussions mentioned above, it is proved that the most important point in the protection of the splice part is to hold the fiber in straight with a soft adhesive. In section 5, two types of the protector based on this idea is described.

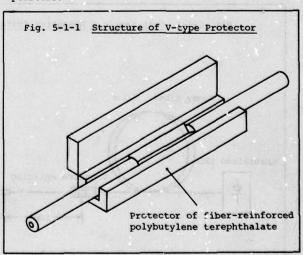




5. Tested Protectors

5-1 V-type Protector

Fig. 5-1-1 shows the structure of the V-type protector. The splice part is put on the V-groove and held by the lid. The material is fiber-reinforced polybutylene terephthalate resin. As the adhesive, RTV silicone composed of base and hardner is chosen. It is very reliable as the coating material as well as elastic to the wide range of temperature.



The protecting process is as follows.

- (1) Set the protector on the protector stand.
- (2) Put mixed silicone adhesive on the V-groove.
- (3) ,Hold the splice part between the V-groove and the lid.
- (4) Fix the lid with fasteners.

The curing time is about 30 minutes at room temperature.

5-2 Sandwitch-type Protector

Fig. 5-2-1 shows the structure of sandwitchtype protector using hot-melt film as the adhesive. The protector is a die-casted zinc alloy plate and hot-melt film of neoprene is applied to it in advance. The protecting process is as follows.

- Set the splice part to the protecting instrument.
- (2) Pull the lever and sandwitch it between the protectors.
- (3) Heat with a plane heater for 30 seconds.
- (4) Cool with a heat sink for 30 seconds.

Required electric power of the plane heater is 15 W and the maximum temperature of the heated protector is 130 °C.

By using this method, the protection can be finished in 2 minutes, which is a great advantage in the fiber splicing in the field.

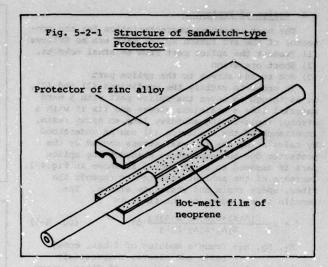
6. Results of Tests

6-1 Samples & Test Conditions

Test samples were prepared and measured in the form of Fig. 6-1-1. One test sample have five splice points. Two samples, i.e. ten splice points were tested to each aging test. Initial splicing loss of the splice point is less than 0.1 dB.

Four protection methods including two methods for comparison were tested.

- (Me-1) Stainless sleeve with epoxy resin
- (10 minutes curing)
 (Me-2) V-type protector with epoxy resin
 (10 minutes curing)



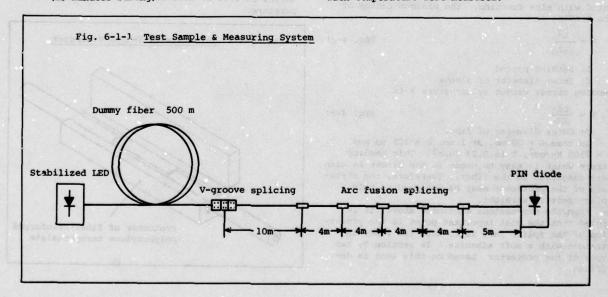
(Me-3) V-type protector with silicone resin (30 minutes curing)

(Me-4) Sandwitch-type protector with hot-melt film (1 minute curing)

Three kinds of aging tests were performed to each method.

- (A) Heat cycle test 80 cycles (6 hours/cycle) High temperature: +60 °C Low temperature: -20 °C
- (B) High temperature aging test 80 °C, 480 hours
- (C) Heat & humidity aging test 60 °C, 95 %RH, 480 hours

Tensile strength and splicing loss before and after the aging tests and splicing loss fluctuation with temperature were measured.



6-2 Tensile Strength

Table 6-2-1 shows the result of tensile strength of protected splice parts before and after the aging test. Tensile strength by Me-1 was not measured because of many failures after the aging tests. Me-2 presented the maximum tensile strength but it was reduced by humidity. Tensile strength by Me-3 was increased by aging, especially showed

high strength to humidity.

Hot-melt film whose strength reaches its full strength soon after cooling preserved its characteristics after the aging test. Therefore, it is the most excellent adhesive from the viewpoint of field operation.

Table 6-2-1 Change of Tensile Strength

			N =	10, mit:	N.
		Me-1	Me-2	Me-3	Me-4
Initial strength	Ave.	20	25	10	17
(24 hours after	Max.	28	32	11	23
protection)	Min.	13	17	9	/ 11
After heat cycle	Ave.		16	16	19
test	Max.	1	19	19	22
and the second second	Min.		13	13	14
After high	Ave.		20	20	15
temperature	Max.	\	24	24	20
aging test	Min.		17	17	11
After heat &	Ave.		22	22	18
humidity aging	Max.	1	26	26	23
test	Min.		18	18	10

6-3 Excess Splicing Loss

The change of the splicing loss after the aging tests are shown in Table 6-3-1. More than half of the splice points by Me-1 were broken in all tests as expected. One splice point by Me-2 was also broken in high temperature aging test. Special

precautions must be taken to employ hard adhesives. Fxcess splicing losses by Me-3 and Me-4 were all less than 0.02 dB, so that both of them are very reliable methods.

Table 6-3-1 Excess Splicing Loss by Aging Tast

(Average excess loss per 1 point in dB, N=10)

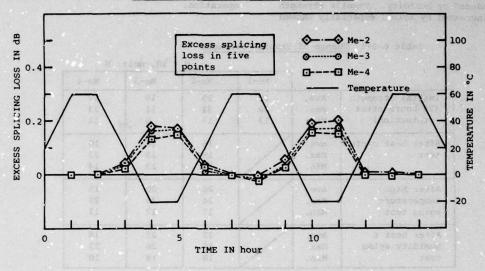
	Me-1	Me-2	Me-3	Me-4
After heat cycle test	Failure of 7 points	0.03	0.02	0.02
After high temperature aging test	Failure of 8 points	Failure of l point	0.01	0.02
After heat & humidity aging test	Failure of 5 points	0.07	0.02	0.02

6-4 Splicing Loss Fluctuation by Temperature

Fig. 6-4-1 shows the temperature dependence of splicing loss. All of the protectors except Me-1 showed excess splicing loss of 0.02 dB at low tem-

perature region. It was caused by the microbending of the spice part due to the shrinkage of the protector and the adhesive.

Fig. 6-4-1 Temperature Dependence of Splicing Loss



7. Conclusion

Tensile strength of the arc fusion splicing part is reduced to less than one tenth of jacketed fiber. The best method to protect this splice part is to hold it in straight with a soft adhesive.

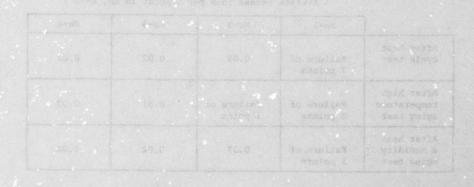
On the basis of this idea, the V-type and the sandwitch-type protector were manufactured and tested. The results of the aging tests showed that both of them are very practical and reliable.

Acknowledgment

The authors would like to thank Dr. N. Uchida of Electrical Communication Laboratory in N.T.T. and Mr. S. Tanaka of the Fujikura Cable Works, Ltd. for their continuous encouragement through this work.

References

- T. Arai et al., "Arc Fusion Splicing of Low-Loss Single-Mode Fiber". IOOC' 79
 M. Hirai et al., "Melt Splice of Multimode Opti-
- [2] M. Hirai et al., "Melt Splice of Multimode Optical Fiber with an Electric Arc". Electron. Lett. Vol.13, 123(1977)



Authors



Takatoshi Arai

The Fujikura Cable Works, Ltd. 1440 Mutsuzaki Sakura-shi Chiba-ken 285 Japan

Takatoshi Arai was born in 1953. He joined the Fujikura Cable Works, Ltd. after his graduation from Tokyo University in 1976 and has been engaged in research and development of optical fiber and its splicing. He is a member of the Institute of Electronics and Communication Engineers of Japan.



Okosu Watanabe

The Fujikura Cable Works, Ltd. 1440 Mutsuzaki Sakura-shi Chiba-ken 285 Japan

Okosu Watanabe was born in 1945 and graduated from Musashi Institute of Technology with a B.E. degree in telecommunication engineering in 1968. He joined the Fujikura Cable Works, Ltd. in 1968 and has been engaged in research and development of automatic telephone cable splicing machine, alarm system for telephone cable plant and optical fiber splicing. He is a member of IECE of Japan.



Koichi Inada

The Fujikura Cable Works, Ltd. 1440 Mutsuzaki Sakura-shi Chiba-ken 285 Japan

Koichi Inada was born in 1941. He joined the Fujikura Cable Works, Ltd. after his graduation from Yokohama National University in 1963 and has been engaged in research and development of high frequency coaxial cable, leaky wave coaxial cable, super conducting cable, millimeter waveguide and optical fibers. In 1976, he received Ph.D. degree from Tokyo Institute of Technology. He is now a head of optical fiber and cable development section and a member of the Institute of Electronics and Communication Engineers of Japan and the IEEE of the U.S.A.



Shigeyuki Seikai

Ibaraki Electrical Communication Laboratory, N.T.T. Tokai Ibaraki-ken 319-11 Japan

Shigeyuki Seikai was born in 1945 and received Ph.D. degree in engineering from Osaka University in 1974. After he joined the Ibaraki ECL in 1974, he has been engaged in research and development of millimeter waveguide, optical cable splicing and designing of optical fiber cable. He is a staff engineer, Optical Transmission Line Section in Ibaraki ECL and a member of the Institute of Electronics and Communication Engineers of Japan.



Masataka Hirai

Ibaraki Electrical Communication Laboratory, N.T.T. Tokai Ibaraki-ken 319-11 Japan

Masataka Hiral was born in 1946. He joined the Ibaraki ECL after his graduation from Waseda University in 1969, and has been engaged in research and development of aluminium composite materials and optical cable joint. He is a staff engineer, Optical Transmission Line Section in Ibaraki ECL and a member of the Institute of Electronics and Communication Engineers of Japan and the Institute of Metals of Japan.

经验的的复数形式

NON-DESTRUCTIVE METHOD OF MEASURING OPTICAL LOSS OF MULTI-MODE FIBERS

Y. Y. Huang and J. A. Olszewski

Research Center General Cable Company 160 Fieldcrest Avenue Edison, New Jersey 08817

ABSTRACT:

The conventional method of optical loss measurement requires cutting off 2 meter length of fiber or optical cable in order to establish the optical signal input level. Repeated measurements during cable manufacture, cable installation and fiber splicing result in substantial loss of length.

A new technique of fiber loss measurement was developed which utilizes two directions side coupling of optical beam into a fiber cladding and then into its core, which is based on the phenomenon of evanescent field penetration and fiber "microbending" respectively. The subject paper describes in detal this new method and the accuracy of the obtained results.

INTRODUCTION:

The motivation for this work was to provide a convenient arrangement of optical signal launching and detection at remote ends of fibers when aligning their two ends prior to fusion splicing in the field. This paper presents a method of side coupling of an optical beam into a fiber cladding and then into its core based on the phenomena of evanescent field penetration and fiber microbending respectively. With this approach, a technique of fiber attenuation measurement is developed that avoids damage to fiber or loss of significant cumulative fiber or cable length in measurements.

EXPERIMENTAL TECHNIQUE:

The experimental arrangement is shown in Figure 1. A stable He-Ne laser beam, of 1 mm diameter A is passed through a linear polarizer, a quarterwave retarder, a beam splitter and a right angle prism. The two collimate parallel laser beams, of nearly equal power, are focused by means of convergent lenses and totally reflected at the common midpoint of the fused quartz dove prism top surface, O. Two similar mode converters, cladding mode strippers, mode scramblers and V-vacuum chucks are adjacently aligned around point 0, the center of symmetry. When measuring the optical attenuation of a fiber by the subject method, it is necessary to remove the fiber coating, if any, about 2 meters from one of the fiber ends for a distance of about 25 cm, a distance separating two

V-vaccum chucks. This straight, bare fiber section is suspended just above the top surface of the prism, its alignment over focal point 0 is maintained with two V-groove vacuum chucks. An optically polished surface of a 25.4 mm diameter stainless steel disc of about 50 mg, weight W., mounted on a fine vertical position control device, is slowly lowered, contacts the fiber surface and finally rests upon point 0 (see Figure 2). This arrangement causes a considerable amount of the light power to couple and propagate in both directions in the fiber. The fiber axis on each side of coupling point 0 is sequentially deformed by a mode converter and a mode scrambler, which results in conversion and propagation of suitable mode distribution in the fiber core. The remaining unwanted cladding modes are stripped with symmetrically positioned mode strippers. Signals D (1) and D(L) are produced at the ends of the fiber length 1 and L respectively. The fiber is then disengaged from the apparatus and rotated 180° about point 0 to affect position reversal of their ends. Signal

D_v(1) and D_v(1) are obtained at fiber ends, with lengths 1 and 1 respectively, by following this procedure.

Measurements were made on three multimode gradedindex fibers produced by Corning Glass Works. The characteristics of the fibers are listed in Table 1.

THEORETICAL CONSIDERATIONS:

The subject launching technique is very similar to that used to excite modes in planar optical film via a prism. Since the fiber side and dove prism at point 0 are in good contact, only a microscopic air gap is usually present between them. The bidirectional waves of the incident light cones in the dove prism undergo total internal reflection at prism top surface point 0. Evanscent fields occur in this gap and then extend into the cladding region, thus resulting in leaky modes excitation. In a ray diagram, each of such leaky modes corresponds to an emitting ray from fiber surface point 0. Figure 3 shows one of those rays with propagating direction () . The directional angles are found to be related to focal distance of lens, and separating distance between incident laser beam and lens axis, H, according to

$$\cos \theta_{m} = \left[\frac{n_{p}^{2} n_{f}^{2} + (n_{f}^{2} - n_{p}^{2}) (H/f_{0})^{2}}{n_{p}^{2} + (H/f_{0})^{2}} \right]_{n_{f}}^{\nu_{2}}$$
(1)

A STATE OF THE STA

Here \bigcap , and \bigcap are the refractive indices for the prism and the fiber cladding respectively. As such ray propagates along undisturbed fiber, the ray angle \bigcap with respect to fiber axis in a free space can be expressed by

$$\theta = Sin^{-1} \frac{n_e H}{f_e (n_p^2 + H^2/f_e^2)^{\frac{1}{2}}}$$
(2)

It should be noted that Equation (2) assumes that $\phi = 0$ and $\rho \approx 0$.

In fact, fiber attenuation implies power substraction from core modes. Therefore, conversion from leaky to core modes is necessary to achieve the measurement objective. In a low loss multimode fiber, less mode conversion occurs spontaneously. However, it is shown theoretically that $\binom{4}{2}$: (1) when a fiber is subjected to axial perturbation, a significant mode coupling is introduced if the spatial frequency of a particular spectral component of such perturbation approaches the phase differences between the coupled modes, and (2) as a fiber undergoes constant curvature, the coupling strength among modes is in inverse quadratic proportion to phas difference. The use of mode converter described above results in a constant curvature of the fiber in the compressed segment which converts some of the leaky modes into their near neighbor high order core modes. The purpose of passing the fiber through a mode scrambler is to produce a varying periodical wavelength of fiber axis from 1 to 3 mm in order to accomplish near steady-state fiber modal excitation.

In the derivation of the fiber attenuation expression for a given wavelength, a realistic assumption was made that the leaky mode attenuation of the two fiber segments from coupling point 0 to the mode converters are equal. The assumption, if not valid, may introduce only a small error because the involved fiber lengths are short and equal. The purpose of rotating the fiber 180° about point 0 is to eliminate coupling and conversion factors appearing in the derivation. The attenuation in terms of dB for net length, L - { can be expressed as

RESULTS AND DISCUSSION:

With the subject side launching arrangement, the coupling efficiency for 125 um fiber diameter is approximately 2%. The angular power distribution of such excited leaky modes is shown in Figure 4, curve (a). From this curve it can be seen that the peak power distribution occurs between 1° and 3° which is consistent with the values calculated using Equation (2) and substituting experimentally measured values for H, f., n and n (6mm < H < 1mm, f = 20cm and n = 1,458). For fiber sample A, the far-field radiation patterns obtained at a distance of 2 meters from mode converters with and without the mode scrambler

are also shown in Figure 4, curve (b) and (c) respectively. It appears that the use of the mode scrambler, causes a strong mode coupling effect. Table 1 lists measured attenuation values for three multimode graded-index fibers as determined by this technique as well as by the standard method. The attenuation values of three fibers measured by the technique described herein were found to be about 6% higher than those determined by the standard end launching method. The reasons for the dispartiy in measured attenuation by the two methods are as follows: In the subject method, initially excited modes are nearly all leaky modes. A part of the leaky modes is converted into core modes by the fiber microbending effects. Some of these modes that have strong persistance can propagate along the fiber over a significant distance. Therefore, the observed attenuation is masked by a certain amount of persistent leaky mode loss. However, the attenuation of multimode graded-index fiber, measured by standard method, also incorporated a small amount leaky mode losses which may not be so significant as in the former case. In addition, high order core modes excited by the subject method may be more pronounced than those produced by the standard method.

The accuracy of the attenuation measurement can be determined by output signals ratio from the fiber ends by slightly varying the launch point. Based on the results obtained using three low loss graded-index multimode fibers, the measurement uncertainty is approximately \pm 0.3 dB. The dominant cause of this relatively high deviation is believed to be due to the fiber surface imperfection such as fiber surface flaws.

We have proposed and demonstrated the feasibility of using fiber side launching technique to measure fiber attenuation non-destructively. This technique may also be used to provide the intermediate access points in the light wave communication system.

CONCLUSIONS:

- Non-destructive attenuation measuring technique described herein offers a novel approach to measurements on multimode optical fibers and yields results of reasonable accuracy.
- Fiber side coupling and mode converting, employed in this attenuation measuring technique can be controlled to provide finite narrow guided mode excitation for evaluation of differential mode attenuation in multimode optical fibers.

TABLE 1

EXPERIMENTALLY DETERMINED ATTENUATION FOR THE THREE MULTIMODE GRADED-INDEX FIBERS

				Net	Attenuation, dB @ 63	32 nm
Number Number	Diamete Fiber	Core	N.A.	Length L - (,km	Standard 0.1 N.A. End Launch Method	Subject Method
A	125	58	0.16	1.10	12.7 <u>+</u> 0.1	13.5 <u>+</u> 0.3
В	125	60	0.17	0.71	8.9 <u>+</u> 0.1	9.4 <u>+</u> 0.4
C	125	62	0.17	0.44	5.3 <u>+</u> 0.1	5.6 <u>+</u> 0.3

REFERENCES:

- J. A. Olszewski, G. H. Foot, and Y. Y. Huang, IEEE Trans. on Communications, COM-26, 7, 991 (1978).
- 2. P. K. Tien, Appl. Opt. 10, 2395 (1971).
- D. Marcuse, Theory of Dielectrical Optical Waveguides, (Academic, N.Y., 1974).
- 4. H. G. Unger, Planar Optical Waveguides and Fibers, (Clarendon Press, Oxford, 1977).
- R. Olshansky, M. G. Blankenship, and D. B. Keck, in Second European Conference on Optical Fiber Communication, Paris (1976).





J. A. Olszewski

Y. Y. Huang

The authors are with General Cable Company, Research Laboratories, at 160 Fieldcrest Avenue, Edison, New Jersey 08817. Dr. Y. Y. Huang is Senior Research Engineer in charge of optical measurements and J. A. Olszewski is Assistant Director of Research, Outside Plant Cables.

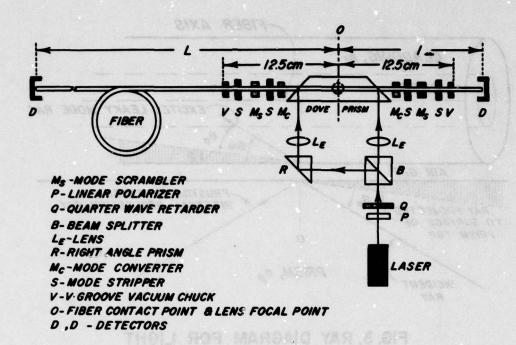


FIGURE 1: EXPERIMENTAL ARRANGEMENT FOR NONDESTRUCTIVE FIBER LOSS MEASUREMENT.

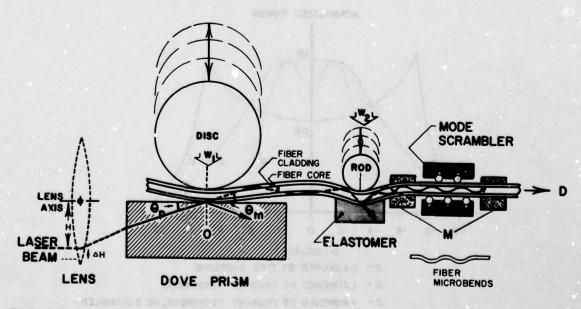


FIGURE 2: COUPLING MECHANISM FOR INTRODUCING LASER BEAM INTO CLADDED FIBER CORE.

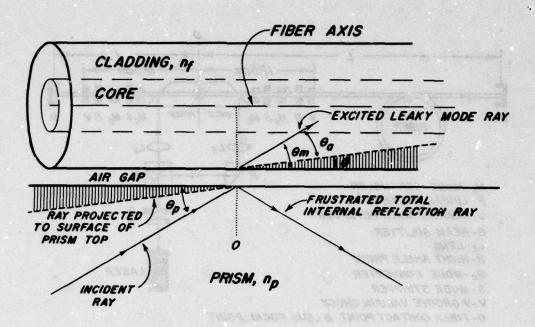
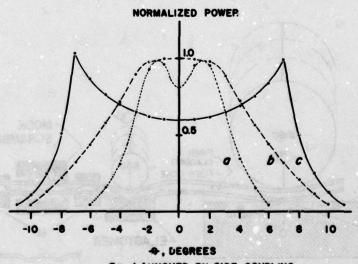


FIG. 3. RAY DIAGRAM FOR LIGHT COUPLING INTO FIBER



0- LAUNCHED BY SIDE COUPLING.

b- LAUNCHED BY PRESENT TECHNIQUE.

C- LAUNCHED BY PRESENT TECHNIQUE, NO SCRAMBLER.

FIG.4: FAR FIELD RADIATION PATTERNS OF A MULTIMODE GRADED INDEX FIBER.

INSTALLATION AND FIELD MEASUREMENT EQUIPMENT FOR OPTICAL COMMUNICATION CABLES

F. Krahn, W. Meininghaus, D. Rittich, K. Serapins, J. Gladenbeck

Felten & Guilleaume Carlswerk AG, Cologne, West Germany

Summary

This paper deals with the installation of optical communication cable routes and subsequent testing. The cable, field splicing, test and measuring equipment are described. Details are given on the installation and testing of two optical cable routes, namely, the field trial system for the Deutsche Bundespost in West Berlin with the cables laid in ducts and an experimental cable route for the Danish Post Office with the cables buried by the conventional ploughing technique.

Introduction

Research and development on optical communications systems began about 15 years ago. In the meantime, fibres, optical transmitters, receivers and fibre-fibre jointing techniques have been developed, so that in laboratories optical systems with bitrates 1 Gbit/s and repeater distances up to 53 km are now possible.

Despite this advanced development stage and the advantages of optical systems compared with conventional systems, use on a worldwide scale will only be feasible when the handling, i. e., installation, splicing, testing and measurement are no more difficult than for conventional systems. We have therefore developed optical cables, splicing tools and test and measuring equipment which can be used not only in laboratories but also under adverse field conditions, thus proving their feasibility in practical use.

Optical Cable

The graded-index fibres for the cable were made at the Philips glass works, Eindhoven/Netherlands, with the PCVD process' evolved by the Philips Research Laboratory in Aachen/Germany. They have a core of 50 um and a cladding of 100 um diameter.

Six loosely secondary-coated fibres were stranded around a Kevlar tensile member, wrapped with Hostaphan and polyethylene tapes and covered with an extruded polyethylene sheath giving an outer diameter of 7,0 mm⁵. This basic unit was combined with two copper 0.9/2.25 mm star-quad units to produce a cable core with an outer diameter of 15 mm. The sheath over the core consists of aluminium-laminated polyethylene.

The overall cross-section of the cable, which has a diameter of 19 mm, is shown in Fig. 1.

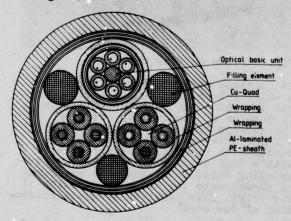


Fig. 1 Cross section of the optical cable

antide practical and all	
This cable has the followi	ng technical
data:	
Weight:	250 g/m
Tensile strength:	2500 N
Minimum bending radius:	100 mm
Average fibre loss:	
STATE OF THE PARTY	< 4 dB/km ($\lambda = 850 \text{ nm}$)
Average excess loss due	(11 - 0)0)
to cabling:	<0.2 dB/km
Avenage miles basedenin-	
including material dispers	ion el 5 ne/lm
including material dispers	(10% 1107 110)
Permissible temperature	(10% varue)
range:	-10°C to+50°C
	-10 0 00+30 0

Splices and Connectors

Fixed splices

For fixed splices, welding the fibre butts together has been found the best method even for use in the field. A compact welding unit developed for this purpose is shown in Fig. 2

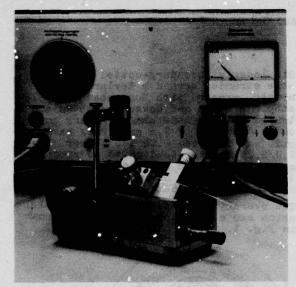


Fig. 2 Fibre welding unit

It consists of a power supply unit and a welding head. During the welding process the joint can be inspected and an impression of its quality obtained. The average splice loss is less than 0.2 dB. After welding, the splice is coated with Zapon varnish and sleeved with a thin metal tube having plastic crimping sections at the ends which can be shrunk onto the secondary coating of the fibre. This provides adequate protection of the weld.

Detachable Splices

The principle of the detachable splice (3-needle joint) is as follows:- The fibres to be joined are aligned in a channel formed by three identical polished rods arranged in the form of a triangle. The channel has a diameter of a few um narrower than the fibre diameter. To provide strain relief, two 0-rings are clamped with union nuts onto the secondary coating of each fibre.

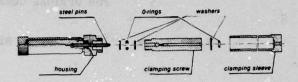


Fig. 3 Detachable splice

The average loss per splice is less than 0.25 dB with index matching liquid. It remains constant at temperatures varying from -30° to +80°C.

Connectors

The optical connectors make use of the precision of watch jewels. These jewels have a concentric bore slightly in excess of the fibre diameter. They are cemented to metal tubes of slightly smaller diameter than the jewels. The fibres to be joined are fed through the metal tubes into the jewel bores and fixed with an adhesive. To make a connection the metal tubes are inserted in casings, aligned by two parallel steel cylinders which form a V-groove, and fixed with two shorter steel cylinders by tightening the union nuts.

Typical connector losses are less than 1 dB without index matching liquid.

Test and Measuring Equipment

Fault locator

The fault locator makes use of the pulse reflection technique well-known in testing conventional cables. The basic design is shown in Fig. 4.

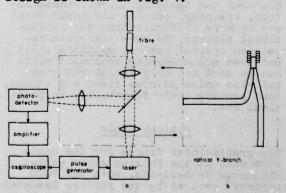


Fig. 4 Basic design of the optical fault locator

The locator contains a laser light source with driver, an optical system with beam splitter and an optical receiver⁶. The length resolution, limited by 10 ns laser pulse width is approx. ± 1 metre. This is amply sufficient for practical work.

Using a conventional beam splitter in the fault locator would necessitate very critical adjustment, and any solution found would be highly sensitive to vibration and shock. For this reason, the beam splitter was replaced by a low-loss Y-branch consisting only of fibres? This device permitted a highly compact instrument to be built. One port of the Y-branch is bonded to the emitting surface of the laser and the other to the light-sensitive surface of the APD. (Fig. 4b) The stem is terminated with a connector which permits coupling to the fibre under test.

This set-up has remarkably low losses so that a dynamic range of more than 70 dB can be achieved. This range covers twice the loss in the fibre $(2 \cdot \mathbf{Q} \cdot 1)$ under test and the loss at the fracture $(2 \cdot \mathbf{Q} \cdot 1 - 10\log R \le 70 \text{ dB})$.

Detection of the reflected pulse is thus possible up to 7 km, if a fibre break is absolutely clean (R=0.04) and assuming an attenuation of 4 dB/km. But even with the worst possible fracture encountered in practice ($R=4\cdot10^{-4}$) 8.9 detection is still possible over a length of 4.5 km.

Attenuation meter

Cut-off method

The equipment consists of an emitter and a receiver in separate units. The emitter unit contains an infrared semiconductor light source with regulated optical output.

The attenuation is measured by connecting the emitter and receiver to the fibre to be measured and setting the receiver to a zero dB reading. A second measurement on a short piece of this fibre gives a direct digital reading in dB with an accuracy of 0.1 dB. The dynamic range of the equipment is 50 dB.

To facilitate measurements on field sections two matched receivers can be used.

Backscattering method

With the backscattering method 10 the fibre loss is obtained as a function of the location.

The principle of our backscattering meter is shown in Fig. 5.

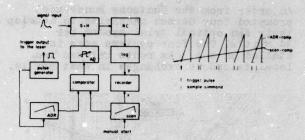


Fig. 5 Principle of the backscattering meter

The backscattered signal, which appears periodically, is scanned by a sample-and-hold circuit. If the scan rate is low, each point of the curve can be examined several times. The average signal can be derived from the subsequent RC network.

The sample-and-hold circuit is driven by two ramp generators through a comparator. The length of one ramp corresponds to the time window selected. The length of the other ramp corresponds to the measuring time selected.

The optical dynamic range corresponds to a fibre attenuation of 13.5 dB. It can be increased by changing the amplification of the backscattering signal.

Using improved electronic circuits, a good linearity (0.1 dB), a good long-term stability and an insensitivity to the first light pulse reflected at the beginning of the fibre to be measured was achieved.

Dispersion meter

The device used to measure dispersion, i. e., the broadening of a light pulse launched into a fibre, consists of a transmitter and receiver unit. The transmitter uses a semiconductor laser which, driven by an avalanche transistor, launches extremely short light pulses (half-width about 0.2 ns) into the fibre to be measured. The receiver detects these signals with an APD which contributes 0.2 ns to dirac pulses. The output signal can be displayed on a sampling oscilloscope or pen recorder or be read directly into a commuter which calculates the pulse broadening or the transfer function.

Cable Installation

Field trial system in Berlin

An order from the Deutsche Bundespost prompted four German companies to develop their own optical trial system for 34 Mbit/s. The four systems were installed on a 4.3 km route between two local telephone exchanges in West Berlin.

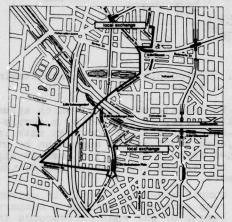
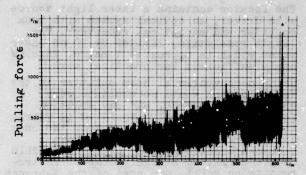


Fig. 6 Cable route for the field trial system in West Berlin

The cable used in our system has already been described (The indoor cables are sheathed with PVC instead of Al-laminated-PE). All outdoor cables had to be pulled into ducts. For the 4.3 km route we used cable lengths, two of which (52 m and 94 m long) are laid in the terminal stations. The shortest outdoor cable length was 288 m and the longest 1011 m. Because of the small pulling forces required for the optical cable a new winch was constructed. As the cable route contained many curves (one section up to 20 bends), guiding wheels were installed in some manholes to reduce the friction of the cable so that the entire length of cable could be pulled into the duct. The pulling forces were controlled at the winch and the actual forces on the cable measured by a special device developed by the Deutsche Bundespost Research Centre. This device was installed between the cable and the pulling rope and the measured values were transmitted by the Cu-quads in the pulled cable to a recorder. Static pulling forces up to 2000 N and additional dynamic forces up to 500 N were measured (Fig. 7) but no fibre break occured.



Pulled cable length

Fig. 7 Pulling forces on an optical cable

For the purpose of testing, the optical fibres of 9 cable sections were connected using different techniques. Of the six parallel fibres each contains two plugged connectors of the watch jewel type. The remaining six joints per fibre were made in two different ways: Permanent fusion splices on three fibres and semi-permanent joints of the 3-needle type on the other three.

All these joints and connections, including the conditioning of the fibre end faces, were made in the manholes.

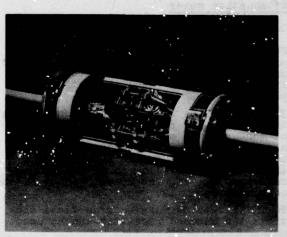


Fig. 8 Cable sleeve

Fig. 8 shows a cable sleeve in which the joints were encased. The coupling losses reached in this trial system were <0.2dR for welded splices and <0.25 dB for 3-needle joints.

The 4.3 km trial route has the following transmission characteristics (average for the six fibres):

- Optical attenuation at 850 nm wavelength: 22.2 dB

(including splices and connectors)

- Dispersion (50% at 900 nm wavelength;
half-amplitude line width of the scurce
1.6 nm): 1.5 ns.

These values have not been changed since the installation in July 1978, despite the fact that index matching liquid is used for the 3-needle joints.

Experimental route for burying optical cables

Cables for long haul transmission are usually buried in soil. In order to test whether the ploughing technique, which the Danish Post Office uses for most of its trunk cables, can be adapted to optical cables, the behaviour of glass fibre cables was studied during and after the ploughing. The experimental cable route is shown in Fig. 9.

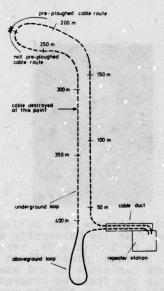


Fig. 9 Cable route for ploughing experiments

Two cables, each of which having a length of 500 m, were ploughed into the ground. The construction of the cable core has already been described. One of the cables had an Al-laminated-PE sheath and the other a 1.2 mm PE-covered Al-tube. The Al-tube was loosely extruded over the cable core with a clearance of 1 mm to permit subsequent use of a gas monitoring system.

The ploughing method can be described as follows: The cable reel is fixed in front of the plough and the cable brought over the plough and through the cable guide on the cutter into the soil. The laying depth was 1 m as is normal. The plough was pulled by two caterpillars, each of which had 100PS (Fig. 10).



Fig. 10 Ploughing of an optical cable

The following field experiments were made with the two cables:

Before ploughing: The attenuation of each fibre was determined. The six fibres of the cable were spliced together and the total attenuation and pulse broadening measured.

During ploughing: The first cable sections were ploughed into pre-ploughed routes. This is normal for conventional cables too, in order to remove big stones and other obstacles. The second cable sections were ploughed into routes which were not pre-ploughed. During installation the attenuation of all six fibres was observed.

The ploughing even in the not preploughed route caused no problems. The attenuation of the cable increased during laying by <0.1 dB/km.

After ploughing: The pulse broadening of the actual fibre length of each cable decreased during ploughing from 1 ns to 0.7 ns for the 3 km fibre length. This was probably due to an increase in mode mixing.

The cables were intentionally destroyed by an excavator. The actual fibre breaks did not occur exactly at the point damaged by the excavator. The maximum distance between this point and the fibre breaks was 5 m for the cable with the Al-laminated-PE sheath and 35 m for the cable with the Al-tube-PE sheath, the latter being caused by the 1 mm clearance between Al-tube and cable core.

This means that future cables should have a construction providing better adhesion between all cable elements. Should a cable be destroyed the defective cable length would be kept to a minimum.

After destruction, the cable was repaired by the fibre-fibre welding technique already described. The joint boxes were installed and buried in the soil without any problems. The cables will remain buried for testing the long-term behaviour.

Conclusion

The experiments described in this paper show that with the equipment developed for this purpose optical cables can be installed, connected and tested even under adverse field conditions. Further improvements will naturally be found for all items, even though development of optical communication systems has already advanced from the laboratory stage to actual practice.

References

- Kao, K. C.; Hockham, G. A. "Dielectric Fibre Surface Waveguides for Optical Frequencies" Institution of Electrical Engineers Proceedings, 113 (1966) 7, pp. 1151 - 1158
- Baack,C.; Elze, G.; Walf, G. "Feasibility of Optical Gigabit Transmission Systems" Supplement to the Proceedings of 4th Eur. Conf. on Opt. Comm., Genua, 1978, pp. 44 46
- 3. Nakagawa, K.; Ito, T.; Aida, K.
 Takemoto, K.; Suto, K. "32 Mb/s Optical
 Fibre Transmission Experiment with
 53 km Long Repeater Spacing" Supplement
 to the Proceedings of 4th Eur. Conf.on
 Opt. Comm., Genua, 1978 pp. 102 105
- 4. Geittner, P.; Küppers, D.; Lydtin, H.
 "Low Loss Optical Fibres Prepared by
 Plasma Activated Chemical Vapor Deposition (CVD)" Appl. Phys. Letters 28
 (1976) 11, pp. 645 646
- Weidhaas, W. "Optical Fibre Cables and Accessories" Proceedings of 3rd Eur. Conf. on Opt. Comm., München, 1977, pp. 47 - 49

- 6. Rittich, D.; Meininghaus, W. "Meßgeräte für die optische Nachrichtentechnik" Frequenz 32 (1978) 12, pp. 350 - 356
- Kalmbach, U.; Dittich, D. "Abzweig für Lichtleitfasern" Nachrichtentechn. Z. 31 (1978) pp. 423 - 425
- Ueno, Y.; Shimizu, M. "Optical Fiber Fault Location Method" Appl. Optics 15 (1976) pp. 1385 - 1388
- Rittich, D. "Detektierung und Lokalisierung von Faserbrüchen in optischen Nachrichtenkabeln" Nachrichtentechn. Z. 30 (1977) pp. 841 - 842
- 10. Barnoski, M.K.; Jensen, S.M. "Fiber Waveguides: A Novel Technique For Investigating Attenuation Characteristics" Appl. Optics 15 (1976) pp. 2112 - 2115

flood cables, the behaviour of the



Friedrich Krahn was born in 1939. He graduated from the University of Minster in 1970 with a Dr. rer. nat. in Physics. He then joined Felten & Guilleaume Carlswerk AG and was first engaged in the field of innovation and diversification. In 1973 he was appointed head of the department for fibre optics research and development.



Dieter Rittich was born in 1951. He studied at the Ruhr-Universität of Bochum and graduated in 1976 in electrical engineering. He is at present employed by Felten & Guilleaume Carlswerk AG and works on optical communication systems in the research und development department.



Wolfgang Meininghaus was born in 1947. He studied electrical engineering at the Ruhr-Universität of Bochum and graduated in 1974. He then joined Felten & Guilleaume Carlswerk AG, Cologne, and has since been working on the development of measuring equipment for optical fibres.



Klaus Serapins was born in 1936. He studied electrical engineering at the Ingenieur-Schule Cologne. He graduated in 1961.
Since 1976 he has been involved in the development of connectors and splicing equipment for optical communication systems.



Jürgen Gladenbeck was born 1939. He studied physics at the universities of Bonn and Cologne.
Since joining Felten & Guilleaume in 1966 he has worked on various projects in the materials research section and is currently engaged in the development of splicing and testing techniques for optical fibres and cables.

UP-DATE ON THE OPTICAL PERFORMANCE OF FIELD INSTALLED FIBER OPTIC CABLES

J.B. Masterson

J. Peveler

Research Center General Cable Company Edison, New Jersey 08817

INTRODUCTION:

Optical fiber cables have been developed for use in communication circuits which have high information bandwidth and low susceptibility to electromagnetic interference. With the advent of the injection laser, high intensity sources were available which operate at discrete wavelengths and which can be easily coupled to glass fibers. Similar advances have occurred in solid state detectors, modulators and low loss optical fiber cables. Optical communication systems have been installed which incorporate these optical components and cables.

This paper discusses the design criteria for the cables used in several installations. (1) (2), (3), the unique problems inherent in each installation and the resultant performance of the cable after installation.

CABLE DESIGN:

The construction of an optical fiber cable must take into consideration the optical, mechanical and physical characteristics of the glass fiber itself. Torsional and micro and macro bending effects on the fiber must be minimized. (4) (5) Internal stress and surface flaws in the glass must be screened to insure long cable life. (6) (7) The optical cable design must be such as to allow for a great amount of field handling such as bending, pulling and flexing without degrading optical performance.

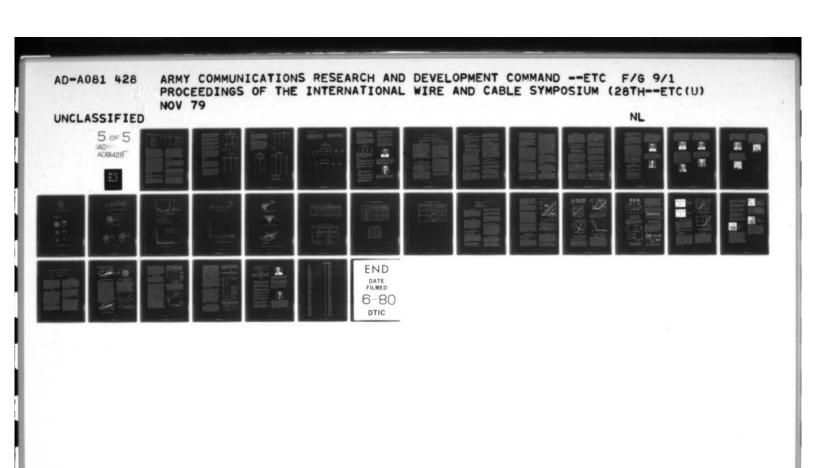
It is expected that the handling of the cable in the field and during installation will follow conventional methods established for conventional communication cables. The field personnel are the same people who are skilled in good installation practices. The equipment to be used in an optical cable installation is for the most part standard for all cable installations. The cable design should, therefore, be capable of withstanding conventional methods and equipment.

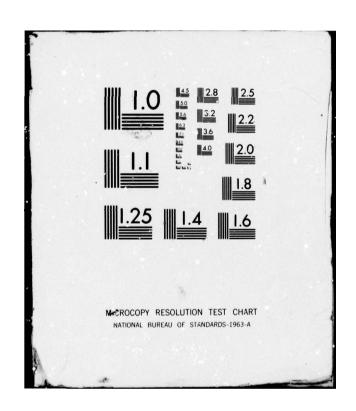
Optical cables are usually much smaller in size than conventional metallic conductor cables. This inherent small size, due to the size of the fibers themselves, reduces the cable weight per meter.

Pulling and handling forces during installation are much lower than for conventional cables. The smaller volume of the optical cable enables the manufacturer to place much longer cable lengths on a reel. Typical cable lengths of several kilometers have been produced. There longer lengths require new considerations for field installations. The number of field splices can be reduced and thereby system reliability is improved, A reduction in the number of splices further reduces the cost of the installed link.

The field environment for an optical cable is essentially the same as the conventional cable it replaces. Temperature cycling, severe heat or cold, wind and ice loading, hydrostatic water pressure, corrosive gases and liquids and dynamic vibration occur throughout the field. Cable materials must be selected which are essentially chemically inert to corrosion, thermally stable and which have a projected acceptable service life. These materials must be capable of withstanding the rigorous field exposures with a minimum of degradation. The materials incorporated in the cable design must be compatible with one another as well as the field environment.

The cables and their respective installation discussed in this paper are of the floating ribbon design where the ribbon is recessed from the protective sheathing. The fibers were positioned side by side in a laminated tape or ribbon. The ribbon of fibers was then positioned in a helically grooved core, which provided excess fiber length in the cable design.





CABLE INSTALLATIONS:

The cable installations discussed in this paper are as follows:

Year	User	# of Fibers	Length Day	Type Of Installation	Application
12/76	Arnold Engineering (Air Force)	6 9147	2.2 km	Buried	High Speed Data (150 MBPS)
4/77	General Telephone Co. of California	6	9 km	Duct Duct	Voice (1.5 MBPS)
9/77	Kennedy Space Center NASA	11	2 km	Duct	High Speed Data (150 MBPS)
10/78	Belgium Telephone Co. GTE/ATEA	6	10 km	Buried	Voice (34 MBPS)
10/78	Union Pacific Railroad	6	1.3 km	Aerial	Video (6MHz)

Direct Burial

The Arnold Engineering installation and the Belgium Telephone Company installation were very similar in number and frequency of obstacles along the route. The Arnold Engineering Center is a complex of engineering test centers which are interconnected with power, communication, gas, water, high pressure steam and air services. In the short length of two kilometers more then ninety transverse obstacles had to be crossed. The cable was threaded under these obstacles with only two splices required for the entire installation. The optical fiber cable was installed simultaneously with four other conventional communication cables in the same trench.

The GTE/ATEA cable in Belgium required an excessive amount of handling in order to meet local installation requirements and at the same time reduce the number of splices. This cable route passes through a conjested urban area of Brussels. The local requirement necessitated opening and closing approximately 100 meters of trench a day in the city. As the trench was opened the cable was placed in the trench and the trench closed at day's end. Where street crossings or utility services occurred the cable was removed from the reel and coiled into a large figure 8 adjacent to the trench. The cable was then pulled through pipes under roads and driveways and under transverse services. After pulling under the obstacle the cable was then rewound on the reel for the next installations section. Due to the congestion of Brussels, the cable was re-reeled several times before a reel was completely installed. No fiber break has occurred in the field as a result of the extensive mechanical handling during either the Arnold or Brussels installation.

Duct Installations

The General Telephone Co. of California installation and the Kennedy Space Center installation were examples of long lengths of optical fiber cable pulled into existing ducts.

The installation in ducts of cable up to 1 km in length required that the cable be pulled through several manholes which are intermediate along the route. Guides and pulleys were used where necessary to correct for misalignment of the ducts. Bends of 90° have been made within a manhole using especially constructed quadrants on which several rollers were mounted.

Devices have been used in both the GTE California and Nasa in Florida installations for monitoring pulling tension. In both installations the maximum permissible pulling tension was 900 pounds. A load cell monitor at the cable pulling eye, intermediate manhole running line tensiometer and winch line tensiometer have been used to measure the drag on a one kilometer pull. In all instances it was not necessary to exceed the maximum pulling tension in order to install a kilometer length. The maximum pulling tension measured on the load cell at the pulling eye of the cable during the NASA installation was 360 pounds. The length of the cable pull was 3114 feet.

Aerial Installation:

A kilometer of figure eight design optical fiber cable was installed at the Union Pacific Railroad in Denver, Colorado. This first railroad installation was aerially placed on a pole line adjacent to the rail yard. The route of the cable proceeds from the yard office across the rails to a remote TV camera station. Some 15 to 20 railroad tracts were crossed and the trains were continuously moving and being switched during the installation.

Splicing:

Fiber splices must meet two basic requirements, low insertion loss and sufficient mechanical strength in the splice area. The splicing loss can be low if there is no mismatch in either dimensions, concentricity, profile or numerical aperture. Mechanical misallignment due to offset, gap, tilt and fractured end cuts will increase the splice loss.

The ultimate splice is one that is optically transparent, minimizing both signal distortion and attenuation.

The installed cable link loss after splicing is usually less than the sum of the individual lengths measured before splicing. In a multimode fiber each mode has a different attenuation coefficient. The attenuation measured on a length of fiber is the ratio of the power transmitted to the power launched and this ratio is the average attenuation of the modes propagated. If a short length is measured, less than the steady state coupling length, then the measured attenuation with all modes excited will be

greater than the steady state coupling condition. (8)
The splicing loss and the non steady-state loss are
difficult to seperate. Actual field splice losses
are generally washed out by the improvement due to
equilibrium and in many instances the calculated
field splice loss appear as amplifiers.

The cable installation at the Arnold Engineering Center utilized a wet splice connector. An index matching fluid was used to improve the coupling across the splice. Typical splicing loss for this connector was found to be 1.7 dB.

The General Telephone of California and the GTE/ATEA cable installations were made with connectors which ultilized an index matching epoxy cement in the splice junction. Splice losses as low as 0.5 dB have been achieved with this method.

The NASA and Union Pacific installations were made using a fuse splicing technique. (9) Fuse splicing introduces the lowest loss value of the three methods employed. The insertion loss of fused splices ranged from 0.1 to 0.3 dB in the laboratory.

Fuse splicing requires an electric arc to melt and weld the fiber ends together. The electric arc creates a problem in areas where an explosive atmosphere exists. The technique had to be modified for use in manholes where both toxic and explosive gases can accumulate. A sealed chamber was designed and constructed for use in the manholes. The chamber was pressurized with a neutral gas and all splicing of fibers was accomplished within the chamber. This equipment was used for the NASA installation.

PERFORMANCE DATA:

NASA

The data for the NASA installation is given in Table 1. As can be seen from the attenuation and bandwidth data, the attenuation of the installed cable was approximately 0.4 dB higher than the cabled value and 0.7 dB higher than the fiber data. Since the installed lengths were less than the manufactured lengths, the slight increase in attenuation is partially due to non-equilibrium lengths (less than one kilometer) measured for field data.

The System & Splicing loss data indicates the sum of the individual section attenuation measurements before splicing and the attenuation after making two fuse splices. In one case, fiber splice #1 at manhole 034, was defective. It was decided not to reopen and remake this fiber splice since all the other ten(10) splices were of an acceptable level. The average change in attenuation after splicing the individual sections was +0.4 dB for two splices or 0.2 dB per splice.

TABLE 1 NASA

ELEVEN FIBER SYSTEM, 1985 METERS AVERAGE ATTENUATION AND BANDWIDTH

			Fiber 1	Data
Cable	Length (km)	BW (MHz)	dB/km
1	1.0		844	5.0
2	1.0		1108	5.2
3	0.9		982	7.1
Average			978	5.8
	Cable o	n Reel	Installed Cable	Change
	BW (MHz)	dB/km	dB/km	₫B
1	829	5.6	5.8	÷0.2
2	984	5.7	6.2	+0.5
3	1145	7.1	7.4	+0.3
Average	986	6.1	6.5	

Attenuation of 820 nm.

SYSTEM AND SPLICING LOSS

	Sum of Indiv. Fibers dB/1985 Meters	Measured after Splicing dB/1985 Meters	dB Change for 2 Splices
1	13.1	21.0	defective
2	13.7	12.4	-1.3
3	13.7	13.9	+0.2
4	12.4	13.1	+0.7
5	12.4	11.6	-0.8
6	12.9	13.0	+0.1
7	15.2	14.5	-0.7
8	14.7	13.0	-1.7
9	13.2	11.1	-2.1
10	10.3	11.5	+1.2
11	10.3	11.3	+1.0
Avera	ige 12.9	13.3	

The data for the GTE/ATEA installation is given in Table 2. The installed cable measurements were approximately 0.1 dB lower than the cabled data. Even though extensive cable handling was required to thread the cable around successive obstacles, no change occurred as a result of handling during the installation. The data for the cable on the reel shows an increase due to cabling of 1.8 dB over the fiber values.

The System and Splicing Loss data is given in Table 2B. Each repeatered section represents approximately five individual lengths on which measurements were made. The sum of the individuals is compared to the section length after splicing. It can be seen that the improvement due to splicing non-equilibrium sections more than compensates for the insertion loss of the splices themselves. In four splices, high splicing losses were encountered. Fiber 5 in section 1 and fibers 4, 5 and 6 in section 3 were respliced recently. The order of improvement of the respliced fibers is typified by fiber 5 of section 1, which improved by 5.4 dR.

TABLE 2A GT&E ATEA

BRUSSELS TO VILVOORDEN SYSTEM

SIX FIBER SYSTEM, 10,513 METERS.

ATTENUATION AND BANDWIDTH

	Fiber Data		
Cable	BW (MHz)	dB/km	
1	566	4.4	
2	631	4.4	
3	487	4.6	
4	516	4.6	
5	562	4.6	
6	523	4.7	
7	590	4.7	
8	740	4.6	
9	Cable not	used in system	
10	597	4.8	
11	2,	4.7	
12	427	4.7	
Average	564	4.6	

			Installed	
	Cable o		Cable	Change
Cable	BW (MHz)	dB/km	dB/km	₫B
10,20	712	4.8	5.1	+.3
2	706	5.3	5.2	2
3	490	5.6	6.4	+.8
4	727	7.2	7.8	+.7
5	557	6.4	6.1	2
6	632	7.2	6.9	3
7	536	6.8	6.7	1
8	697	6.7	6.1	6
9	Cable	not used in	system	
10	539	7.1	6.8	2
11	800	7.1	6.6	5
12	656	6.1	5.6	4
Average	e 644	6.4	6.3	

Attenuation at 820 nm

TABLE 2B
GT&E ATEA
SYSTEM AND SPLICING LOSS

System 10,512 meters Repeater spans (meters)

Fiber No.	Section 1*	Section 2**	Section 3*** 3258 m
1. a.	21.1	23.0	20.4
b.	22.0	22.3	19.5
c.	+.9	22.3 7	19.5 9
2. a.	21.0	21.2	21.3
b.	20.9	22.0	19.4
c.	20.9 1	22.0 +.8	19.4 -1.9
3. a.	20.1	21.7	18.8
b.	20.7		19.0
c.	+.6	22.4 +.7	19.0
4. a.	21.9	21.5	18.2
b.		22.0	21.0
c.	$\frac{21.2}{7}$	+.5	+2.8
5. a.	21.2	22.1	19.6
b.	27.5		33.7
c.	+6.3	21.5	+4.1
6. a.	21.5	22.4	19.7
b.	21.4	21.7	23.0
c.	2	6	+3.3
-			

- a. Sum of individual fibers
- b. Measured, after splicing
- c. Change in attenuation
- * Span includes 5 splices
- ** Span includes 5 splices
- *** Span includes 4 splices

The attenuation and bandwidth data for the Union Pacific Railroad system is given in Table 3. The attenuation on the installed cable mounted on poles improved over the reel values. The improvement was found to be 0.5 dB. The measurements were made on essentially long lengths and therefore correlate well.

The System and Splicing Loss for the installed cables indicates essentially no difference between the 3pliced cable and the sum of the individual lengths. The average change due to splicing is 0.1 dB.

TABLE 3
UNION PACIFIC RAILROAD

FIVE FIBER SYSTEM, 1562 METERS.

ATTENUATION AND BANDWIDTH AT 820 nm

		Fiber	Data	Cable	on Reel	Initial Installation	Initial Change in
Cable	Length km	BW (MHz)	dB/km	BW (MHz)	dB/km	dB/km	Att. (dB)
1	.739	420	4.6	730	5.3	5.5	+.3
2	.832	352	4.5	444	5.3	4.1	-1.3
	1.562 A	ve. 386	4.5	587	5.3	4.8	

SYSTEM AND SPLICING LOSS

		Installed Len	gths	After		
Fibers	Cable 1dB	Cable 2	Cables 1 & 2	Splicing dB/1562	<u>n</u>	Change in Atten. (dB)
1	4.1	3.2	7.3	8.4		+1.1
2	4.5	3.2	7.7	7.3		4
3	4.0	3.1	7.1	6.5		6
4	4.0	3.8	7.8	7.7		1
5	3.8	3.4	7.2	7.5		+.3
		Ave	erage 7.4	7.5		

Field Monitors on Attenuation

The General Telephone of California, the NASA and the Union Pacific Railroad systems have been monitored for attenuation changes on the field. The General Telephone of California system had an increase in attenuation of 0.3 dB/km during the first two months of monitoring. No appreciable changes occurred and the monitor was removed after approximately two years.

The NASA cable was spliced into five loops of 4 km each and the attenuation of each loop measured. Loop number five (5) was monitored continuously from February of 1978 to May, 1979. The attenuation change in loop 5 decreased during the cold season by 0.2 dB and increased during the warm season by 1.0 dB. A cyclical change has been noted with an average change of 1.8 dB in 4 km.

$\begin{array}{c} \underline{\text{TABLE 4}} \\ \text{Attenuation Change with Time} \end{array}$

dB/4km at 820 nm.

Loop	11-78	6-78	<u>dB</u>
1	20.44	21.09	+0.65
2	21.54	23.37	+1.83
3	21.52	24.08	+2.56
4	23.26	25.64	+2.38
5	25.60	27.53	+1.93

The Union Pacific Railroad cable has a thermo couple mounted on the cable. It is continuously monitored to record temperature changes in the aerial installation. The attenuation of the loop increased by 0.3 dB when the temperature went down to -10F and decreased by 0.2 dB when the temperature increased to 110 F.

Conclusions

The optical cable installations discussed herein have demonstrated the ability of optical cables to be installed using similar techniques and equipment as standard telephone cables.

A variety of installation types, (duct, buried and aerial) have been accomplished with minimum optical transmission degradation.

Attenuation monitoring of several installations indicated changes in system loss due to time and temperature,

References:

- J.A. Olszewski, G.H. Foot, Y.Y. Huang, "Development and Installation of an Optical Fiber Cable For Communications", NTC '77, December 1977.
- G. Bahder and J.A. Olszewski "Experience To-Date with Optical Fiber Cables" 26th IWCS, Cherry Hill, New Jersey, November 1977.
- J.A. Olszewski, A. Sarkar, Y.Y. Huang, "Optical Fiber Cable For Tl Carrier System" 25th IWCS, Cherry Hill, New Jersey, November 1976.
- S.E. Miller, E.A.T. Marcatili and T. Li
 "Research Toward Optical-Fiber Transmission
 System" Proceedings of the IEEE, vol. 61,
 pp. 1703 1751, (1973).

- W.B. Gardner, "Microbending Loss in Optical Fibers", BSTJ, vol. 54, p. 457 (1975); D. Marcuse, "Microbending Losses of Single-Mode, Step-Index and Multimode, Parabolic - Index Fibers", BSTJ, vol. 55, p. 937 (1976).
- R.E. Love, "The Strength of Optical Waveguide Fibers" Proceedings of Soc. Photo - Optical Instrument Engineers, vol. 77, p. 69 - 77 (1976).
- B. Justice, W.E. Snowden and D.M. Jenkins, "Water Integrity of Optical Fibers", Final Report on NELC # N 00123-75-C-1061, (1975).
- D. Marcuse, "Theory of Dielectric Optical Waveguides", Academic Press, New York (1974).
- Y. Kohanzadek, "Hot Splices of Optical Waveguide Fibers", Applied Optics, vol. 15, p 793, (1976); D.L. Bisbec, "Splicing Silica Fibers with an Electric Arc", Applied Optics, vol. 15, p 796, (1976).



Joseph Masterson is Assistant Director of Research And Development, Fiber Optics, with the General Cable Company Research Laboratory in Edison, New Jersey. He has been involved with the design and installation of fiber optic cables. He received his BSEE degree from Newark College of Engineering and an MS in Operations Research and Systems Analysis from Polytechnic Institute of Brooklyn.



John Peveler has been with the General Cable Company Research Laboratory since January 1963. He has been involved in telephone and coaxial cable evaluation and more recently in Fiber Optical Cable Development.

HIGH DENSITY MULTICORE-FIBER CABLE

- S. Inao*, T. Sato*, H. Hondo*, M. Ogai*, S. Sentsui*, A. Otake*,

 K. Yoshizaki*, K. Ishihara**, N. Uchida**
 - * The Furukawa Electric Co., Ltd. Marunouchi, Tokyo, Japan ** Ibaraki Electrical Communication Lab. Tokai, Ibaraki, Japan

Abstract

High density optical cables using multicore fibers was designed and manufactured. High density subunits were fabricated by stranding 6-core fibers, and the cable was made after unit stranding sub-units. Cables with an outer diameter of 12 mm had 252 cores and that with a 28-mm outer diameter, 1,512 cores. Their densities are 20 times higher than those of conventional optical fiber cables. Cable loss, bandwidth, temperature and mechanical performance were the same as those of conventional optical fiber cables. Crosstalk was over 40 dB. Multicore fibers were tested for splicing and branching for each of their cores, with good results. Multicore fibers permit a reduction in manufacturing cost through less manufacturing materials and processes required. It also reduces the splicing work to ultimately bring down optical cable manufacturing

Introduction

Optical fibers have low loss and wide band characteristics and are regarded promising as future communication media.

The development of optical fibers has progressed rapidly, and a single mode fiber with a loss of 0.2 dB/km at a 1.6 μm wavelength has been reported(1). Fibers with losses below 3 dB/km can be obtained fairly easily at 0.85 μm wavelength(2). The development of optical fiber cables is also progressing satisfactorily(2).

An important factor in introducing optical fibers for commercial use is to increase the economic efficiency of optical fiber cables. One way to increase the fiber economic efficiency is to make fiber diameters thin and reduce the material cost per unit waveguide. However, thin diameter fibers are difficult to handle, and their fiber strength lowers. The cost to produce preforms by the MCVD process could be reduced by making fiber core diameters thinner. However, the cost of cladding

quartz cannot be overlooked, and much cannot be expected from thin diameter fiber

The core diameter of each core in a multicore fiber(3) is thin. However, the fiber diameter is 125 to 150 μm , and there will be no problem in handling fibers, or about fiber strength. Fibers can be fabricated at a reduced cost. Nevertheless, this fiber has some problems related to branching and splicing - such as separating signals from different cores. Provided these problems could be solved, these fibers would be extremely promising. It can be pointed out that optical fiber cables have failed to fully utilize the merits of thin diameter which optical fibers offer, in order not to increase fiber losses. However, high density optical fiber cables have to be developed to utilize the merits of thin diameter if optical fibers are to expand their application range.

We produced high density subunits (1.9 mm outer diameter and six fibers) using multicore fibers and obtained economical and high density cables by stranding subunits and by stranding units to obtain a cable. Compared with the ribbon type cable developed by Bell Telephone Laboratories, this cable has a lower fiber density. However, to secure lower cabling loss and a mechanically stably, cables were used a unit construction. This cab has 252 cores when its outer diameter is This cable 12 mm, and 1,512 cores when the outer diameter is 28 mm. A terminal for this cable, which will be an important element in utilizing this cable for commercial use, was also developed, and satisfactory results could be derived in branching and connection.

The purpose of this paper is to report a design and characteristics of a multi-core fiber cable and the development of a terminal for this cable.

Fabrication

Multicore Fiber

The multicore fiber has a construction shown in FIG. 1 and is fabricated in the following steps (Fig. 2):

- (1) First, a preform rod with a GeO₂ P₂O₅ SiO₂ core and P₂O₅ B₂O₃ SiO₂ cladding is fabricated by the MCVD process.
- (2) Seven preform rods are placed in a quartz pipe.
- (3) The pressure inside the pipe is reduced, and the quartz pipe is heated by an oxygen-hydrogen burner for collapsing to fabricate a multicore fiber preform.
- (4) Fibers are then drawn. Fibers thus drawn are primary coated with a modified silicone and are again coated with another silicone to make cabling easy and increase the fiber strength.

Two types of fibers were produced - 125 and 150 μm in fiber outer diameter. Fibers with sizes thicker than these are difficult to bend and handle. thinner than these sizes are subjected to a limitation in terms of connection, fiber loss and band characteristics. A silicone buffer layer is used to reduce loss increases caused by microbends. Under the present cable manufacturing technology, the high density characteristic which optical fibers offer is sacrificed in order to reduce loss increases by cabling and to give mechanical strength to cables. Silicone for the buffer layer is colored to make optical fiber identification easy. No degradation of fibers by coloring has been observed in any of the cabling processes.

The parameters of these fibers are shown in Table 1. Loss and band characteristics of these fibers are also snown. The figures show that these fibers develop high losses in a long wavelength band.

High Density Subunit

To best utilize the advantage of thin diameter which optical fibers have, six buffer coated fibers, without coating nylon on the fibers, which is usually done, were stranded around a stainless-steel tension member with an outer diameter of 0.4 mm. A silicone resin was filled among the fibers, which were squeezed by a die. The fibers were heat baked to obtain a circular 6 fiber. These fibers were coated with nylon in the same process to make a 1.9 mm subunit, FIG. 4.

The subunit contains a multicore fiber and single-core fibers so that loss changes at various processes can be compared with single-core fibers. The configuration of this subunit is shown in FIG. 5.

The subunit is fabricated to make nylon skin peeling easy. Each fiber can be separated easily by removing nylon by using a wire stripper.

High Density Optical Cable

Six high density subunits are stranded around an FRP tension member 2.0 mm in outer diameter together with PP yarn and are taped to structure a unit with an cuter diameter of 7.4 mm. To make cabling easy, up to subunits are made high dense, and the cable has the same construction as that used in other optical fiber cables developed in Japan after the unit construction. This unit is then LAP sheathed and cabled to obtain Type I. Type II is produced by stranding six units around a tension member, taping them and by LAP sheathing them. The cable outer diameters of Types I and II are 12 and 22 mm, respectively. The cable lengths are 300 and 250 m, respectively. In this cable, GI singlecore fibers were used for the purpose of comparison. If multicore fibers only were used, Types I and II cables would have $7 \times 6 \times 6 = 252$ and $252 \times 6 = 1,512$ cores, respectively.

Optical Performance

Transmission Loss

Excess loss by microbends may be observed when stranding subunits, coating nylon, unit stranding and when sheathing (4).

These cable losses could be measured by a monochromator in a wavelength range of 0.8 to 1.6 μm with bare fibers after drawing and by an LED at 0.85 μm in processes after drawing.

A light beam that passed through a dummy fiber with a single core for a distance of 500 m was injected at a V-groove splicing for single-core fibers. The multicore fiber was butt-joint spliced with a thin diameter fiber having a core diameter of 15 μm and a length of 100 m.

Fiber losses at various processes are shown in Table 3. Loss increases by cabling were below 0.1 dB/km in average with multicore, monocore and colored buffer fibers. No difference due to fiber type could be traced.

Regarding fiber loss spectra, the mode near the cut off propagates at the incident edge unless a higher mode does not propagate for long distance in the case of multicore fibers, FIG. 6. In this instance, loss is measured rather largely. A gentle loss curve can be obtained when the mode near the cut off is removed by bent near the fiber incident edge.

Compared with monocore fibers, loss increases generate in a long wavelength region by an increase in OH losses caused by thin core diameters (5). Multicore fiber was observed loss increases by imperfectness of waveguide, also. However, loss increases during cabling is small, and these loss increases generate during fiber fabrication.

Baseband Response

Basically, there should be no difference in baseband response between mono- and multicore fibers. However, bandwidth does change as the core diameters of fibers are made thinner $^{(5)}$. No comparison can be made for multicore fibers as preforms are not the same. However the thinner core diameter, bandwidth is narrower for monocore fibers from same preform rod. Bandwidths were measured with bare fibers and cables by the swept frequency method at 0.85 and 1.3 um wavelengths. Because cable lengths were short, no 6-dB loss could be measured. Therefore, the baseband loss α was converted from the loss for 1000 MHz assuming $\alpha = kf^2$. No clear-cut process variation could be observed as fiber lengths differed considerably. However, a slight band increase is considered possible.

Temperature and Heat Cycle Performance

Temperature characteristics of multicore fibers were measured between -40 and
+60°C. Measurements were made by winding
a Type I cable on a drum and placing it in
a constant temperature oven, changing the
temperature by 10°C. Four types of fibers
were measured: the center and a side core
of a multicore fiber, and colored and noncolored conventional monocore fibers. All
the fibers developed no loss variation
down to -30°C. At -40°C, the monocore
fibers generated a 0.4 dB/km loss increase.
A side core in a multicore fiber developed
a 0.1 dB/km loss increase, while the center
core generated no change at all. (Fig. 7)

In the high temperature range, no loss change could be detected at all up to 60°C.

Similar measurements were also made with bare fibers, but no loss changes could be traced. The heat cycle mode was $20^{\circ}\text{C} + -30^{\circ}\text{C} + 20^{\circ}\text{C} + 60^{\circ}\text{C} + 20^{\circ}\text{C}$ in cycles of 24 hours. None of the fibers developed loss changes.

Crosstalk

Crosstalk between two cores is larger with multicore fibers than with monocore fibers. In measuring crosstalk, a system shown in FIG. 8 was used, and optical intensities were compared by time differences of photo exposure, instead of using a branching fiber, in order to avoid cross-talk at the spliced section. A He-Ne laser was injected into a fiber with a core diameter of 15 μm and outer diameter of 125 μm , and the laser beam was injected into the multicore fiber by butt splicing the multicore fiber with the other fiber. Except for the cores injected with a beam, fibers were moved and adjusted so that the light could not be seen in the cores by observing the other edges by a microscope. The other edge of the multicore fiber and the fiber with a 15-µm core diameter and 125-µm outer diameter were butt spliced to attain the maximum level, to measure the level of the main waveguide. Crosstalk was measured by moving the fiber, butt jointing and splicing with the other core. The measurement resolution was within 1 dB, and all the cores showed more than 41 dB. The optical level of the cladding section was 46 dB, and this value was made a measurement limit.

Distance characteristics of fiber crosstalk were measured together with cable crosstalk by cutting fibers in 1-km lengths. The levels were all inside the measurement error. Crosstalk increased when fiber lengths were shortened to a few meters. (Fig. 9) Losses occurring at fiber splicing sections radiate. However, large crosstalk generates near the incident edge where radiation is not perfect. No problem is expected as a light does not transmit actually.

Bend and Side Pressure Test

Multicore fiber, loss increases by bend or side pressure, and crosstalk variation were studied. Loss increases of multicore fibers by bends and side pressure are about 1/3 those of GI fibers, and this can be attributed to effects by thin core diameters. No change in crosstalk could be detected when loss increases by side pressure and bends were not large.

Mechanical Performance

Multicore fiber cables were measured for items shown in Table 5 to study their mechanical characteristics. Conditions and results for each item are shown side by side. The mechanical tests confirmed that there was no large difference with conventional cables and that a high density cable could be produced by using this construction.

Branch Fiber

Multicore fibers will have significance as high density transmission media only after mutually independent signals transmit inside each of the cores in a multicore fiber. To transmit independent signals inside multicore fibers, a branch fiber to connect a plurality of ordinary single-core fibers with a multicore fiber is indispensable. Branch fibers inject optical signals that transmit in individual ordinary fibers into a multicore fiber and take out optical signals of specific cores in a multicore fiber for injection into ordinary fibers.

These branch fibers are required to fulfill the following two requirements:

- (1) Splicing loss (insertion loss) between individual fibers and desired specific cores in a multicore fiber is small.
- (2) Splicing loss (crosstalk) between individual fibers other than those allocated for combinations and cores in a multicore fiber is large.

FIG. 10 shows an example of constructing a branching fiber. One fiber with an outer diameter equivalent to the core pitch of a multicore fiber and with a core diameter equivalent to the multicore fiber core diameter is placed in the center. Around this fiber, six other similar fibers are bundled tightly. The groove of thin diameter fibers is fixed so that their edges have the same flat circle, and are aligned in such a manner that the core axis of each fiber coincides with the axis of each core of the multicore fiber. The fibers are then fixed.

It is not easy to fix thin-diameter fibers in a 1-6 arrangement. In the method used this time, one fiber was inserted on the lowest layer of the V-groove of a fiber with a 60° vertical angle, as shown in FIG. 11. The next upper layer had two fibers, and one next three fibers. The uppermost layer had four fibers, or a total of ten fibers were inserted and pressed in the V-groove. It was easy to form a 1-6 arrangement with seven fibers excluding three fibers on the vertex of the triangle.

To obtain a branch fiber for a multicore fiber with an outer diameter of 150 μm , core diameter of 20 μm , and a core pitch of 50 μm , a multicore fiber was butt jointed, as shown in FIG. 10, with a fiber 50 μm in outer diameter and 20 μm in core diameter fixed as in FIG. 11, to fabricate a branching fiber. Insertion loss and crosstalk characteristics of this branching fiber are 4 dB and over 30 dB respectively.

Splicing

Splicing characteristics of small core-diameter fibers have to be fully studied prior to splicing multicore fibers. In multicore fibers, loss increases caused are constant when misalignment/core radius are constant. This does not change even with fibers with thin diameter cores of about 20 μm . Consequently, a higher alignment accuracy proportionate with the portion of the core diameter that has become small is required.

The largest difference between splicing methods for multicore fibers and conventional single core fibers is that alignment in two right-angle directions is not sufficient and that alignment by fiber rotation becomes essential for multicore fibers.

When making connector splicing, rotary alignment is possible by jointing plugs, in which center cores are fixed to match the centers, are jointed through a sleeve and by rotating one plug. However, rotation alignment is not necessarily easy with fusion splicing, which method is now popular. The trouble is to realize rotation of fibers in a space without their centers deflecting.

A vacuum V-groove and crude rotary mechanism were mounted on the fusion splicing tool used this time, for alignment at fiber center and core position alignment by rotation. The vacuum groove maintained the fiber position so that the fiber center did not move off center even if the fiber rotated.

After axial alignment in this fasion, the fibers can be fusion spliced under the same conditions as those for splicing regular single core fibers.

The rotary mechanism is extremely simple as shown in FIG. 12, and the tool does not become complex merely because it is for splicing of multicore fibers.

Splicing losses for each core after the same fiber was spliced repeatedly five times.

Future Design

The high density cable using multicore fibers had a loss increase of below 0.1 dB/km by cabling, and satisfactory results could be obtained in mechanical, temperature, and crosstalk characteristics. These positive accomplishments show that this cable construction is promising.

Nevertheless, it will be necessary to fabricate multicore fibers with losses of 2.5 dB/km at 0.85 $\mu\,m$ and of 1.0 dB/km at

 $1.3~\mu\text{m}$, or better, as is the case with monocore fibers, excluding loss increases at long wavelengths by thinner fiber core and excluding those caused by imperfectness in fiber fabrication.

Crosstalk was measured at λ = 0.63 µm. It will be necessary to measure at 0.85 and 1.3 µm wavelengths which are actually used. A good prospect could be obtained regarding fiber branching and splicing. However, a study to make isolation larger and crosstalk at the jointing section smaller will be needed. The practicality for multicore fibers will generate only after these peripheral technologies have been completed.

In terms of manufacturing process flow, multicore fiber cables contain fibers each of which has seven cores. Compared with ordinary optical-fiber cable manufacturing process, one process step can be omitted. Therefore, multicore fibers have a cabling advantage in addition to its advantage as a fiber, when discussing about production cost. Furthermore, cables containing multicore fibers can be made thinner for the same number of cores, and splicing can be done for the seven cores at the same time. Therefore multicore fibers offer technical and engineering advantages. All these characteristics will be useful in increasing the economical efficiency of optical fiber cables.

The study has shown that fiber high density can be realized by introducing subunits. By combining subunits and multicore fibers, high density optical cables have been realized after subunits at the cost of space factor, notwithstanding the fact that a unit construction, which has less loss variation, is used.

Reference

- 1. T. Miya, Y. Terunuma, T. Hosaka and T. Miyashita, "Ultimate Low-Loss Single-Mode Fiber at 1.55 μ m," Elec. Lett., 15 No. 4 (15th Feb. 1979), pp. $106\overline{-1}08$
- H. Ishihara, M. Tokuda, N. Uchida, S. Inao, M. Hoshikawa and K. Inada, Technical report of IECE in Japan, CS78-173 (Dec. 1978)
- S. Inao, T. Sato, S. Sentsui, T. Kuroha and Y. Nishimura, "Multicore Optical Fiber," Technical Digest of Papers of the Topical Meeting on Optical Fiber Transmission 3, Williamsburg, Virginia (Feb. 1979), pp.
- W. B. Gardner, "Microbending Loss in Optical Fibers," B.S.T.J., <u>54</u>, No. 2 (Feb. 1975), pp. 457-465

5. Unpublished

Shozo Inao was born in 1938, graduated from Waseda University in 1962, and joined the Furukawa Electric Co., Ltd. in 1962 and has been engaged in research and development of millimeter waveguides, coaxial cables and pair cables, and now development of optical fiber cables. He is an assistant manager of Optical Transmission Department of Telecommunication Laboratory in Chiba Works, and a member of the Institute of Electronics and Communications Engineers of Japan.



Tsuguo Sato was born in 1939, graduated from Science University of Tokyo in 1963, and joined the Furukawa Electric Co., Ltd. in 1957 and was engaged in chemical analysis and now development of optical fibers. He is a Chief Engineer of Optical Transmission Section in Central Research Laboratory.



Hirotoshi Hondo was born in 1945, graduated from Tohoku University in 1969, and joined the Furukawa Electric Co., Ltd. in 1969 and has been engaged in coaxial cables and broadband pair type cables, and now designing optical fiber cables. He is a Chief Engineer of Optical Transmission Department of Telecommunication Laboratory in Chiba Works, and a member of the Institute of Electronics and Communications Engineers of Japan.

Shintaro Sentsui was born in 1947, graduated from Tokyo University in 1970, and joined the Furukawa Electric Co., Ltd. in 1970, and has been engaged in research and development of superconductive coaxial cables, and now designing and evaluation of optical ribers. He is a Chief Engineer of Optical Transmission Department of Telecommunication Laboratory in Chiba Works, and a member of the Institute of Electronics and Communications Engineers of Japan.



Mikio Ogai was born in 1948 and graduated from Tokyo University in 1970 with a BS in Electrical Engineering, and then joined the Furukawa Electric Co., Ltd. After engaged in the development of MM-waveguide and its application system for five years, he worked for the National Radio Astronomy Observatory and engaged in the development and construction of MM-waveguide system for VLA Telescope in New Mexico for two years. He returned to the Furukawa in 1977 and has been engaged in development of optical fiber communication systems. Now he is a chief engineer of fiber jointing section of the Telecommunication Laboratory, and is a member of IECE in Japan and a member of IEEE.

Akihiro Otake was born in 1949, graduated from Tohoku University in 1974, and joined the Furukawa Electric Co., Ltd. in 1975 and has been engaged in development of coaxial cables, and now designing optical fiber cables. He is a Senior Engineer of Optical Transmission Department of Telecommunication Laboratory in Chiba Works.





Kazuto Yoshizaki was born in 1928, graduated from Tokyo University in 1952, and joined the Furukawa Electric Co., Ltd. in 1952 and was engaged in research and development of millimeter waveguides, antenna, and optical fiber cables. He is a Manager of Engineer Department of Head Office, and a member of the Institute of Electronics and Communications Engineers of Japan.



Koushi Ishihara was born in 1943, received the M.S. degree from Yamanashi University in 1969, and joined the Electrical Communication Laboratory in 1969, and has been engaged in research and development of cable structure, and now designing optical fiber cables. Mr. Ishihara is a Assistant Chief of Optical Transmission Line Section in Ibaraki ECL, and a member of the Institute of Electronics and Communication Engineers of Japan.



Naoya Uchida was born in 1939, graduated from Kyoto University in 1962, and joined the Electrical Communication Laboratory in 1963, and has been engaged in research and development of acousto-optic light deflectors and modulators, electro-optic waveguide modulators, and now designing, fabrication, and evaluation of optical fiber cables and related techniques. Dr. Uchida is a Chief of Optical Transmission Line Section in Ibaraki ECL, and a member of the Institute of Electronics and Communications Engineers of Japan and the Japan Society of Applied Physics.



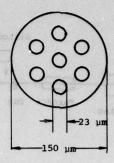


Fig. 1 Construction of Multicore Fiber

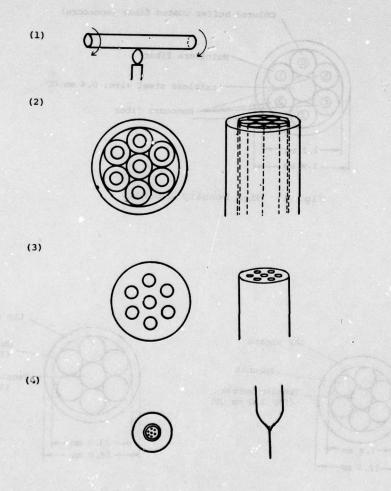


Fig. 2 Multicore Fiber Manufacturing Process

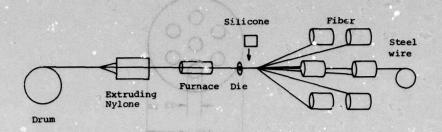


Fig. 3 High Density Subunit Manufacturing Process

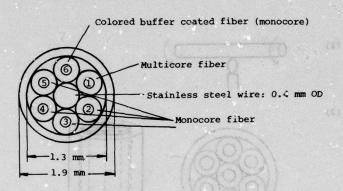


Fig. 4 High Density Subunit

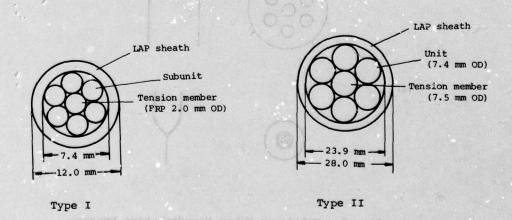
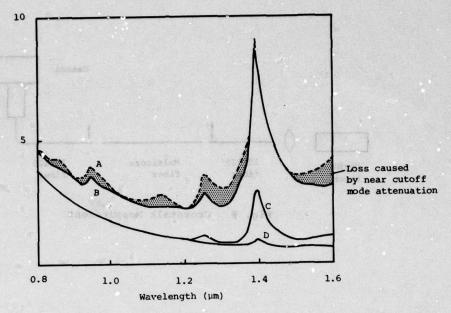


Fig. 5 High Density Cables



- A: Multicore fiber without mode trap
- B: Multicore fiber with mode trap
- C: Monocore fiber (typical: 50 µm core dia.)
- D: Monocore fiber (OH free: 50 µm core dia.)

Fig. 6 Loss Spectral Curves of the Fibers

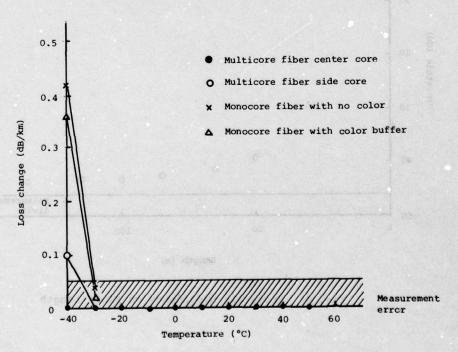


Fig. 7 Temperature Dependency Loss

A STORY AND STORY

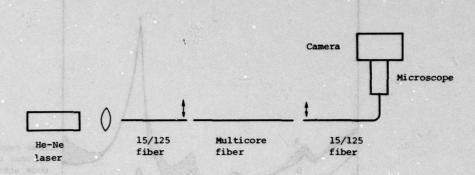


Fig. 8 Crosstalk Measurement

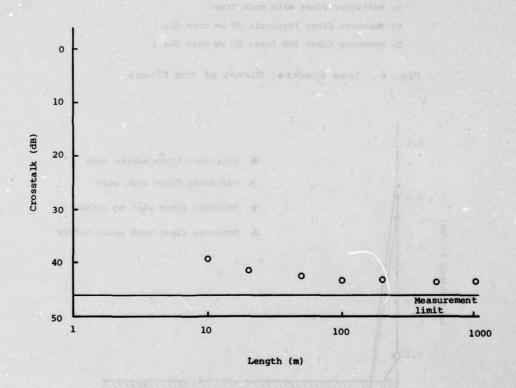


Fig. 9 Crosstalk Dependency on Fiber Length

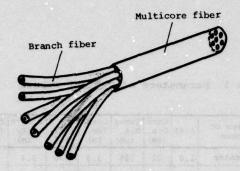


Fig. 10 Fundamental Configuration of Branch Fiber

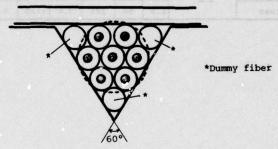


Fig. 11 Fiber Alignment in Branch Fiber

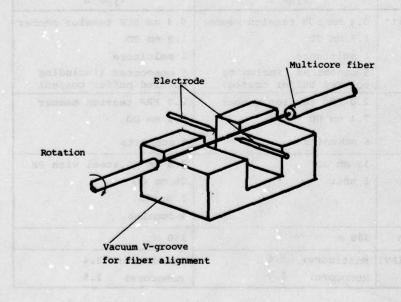


Fig. 12 Alignment Jig for Multicore Fiber Fusion Splicing

Table 1 Parameters of Typical Fibers

Kind of Cable	Color of Buffer	Place of core	Δ(%)		Outer Dia. (µm)	Loss* (dB/ km)	fc* (MHz- km)	Loss** (dB/km)	fc** (MHz· km)	Primary Dia. (μm)	Buffer Dia. (µm)
Multicore	Trans-	Center	1.0	22	125	3.3	530	2.4	620	200	400
	parent	Side (AV)	1.0	22	17.73 6 (13	3.4	610	2.2	430		
	Green	Center	1.0	22	125	3.2	410	2.7	520	200	400
		Side (AV)	1.0	22		3.4	820	2.5	370		
Monocore	Trans- parent		1.0	50	125	2.5	1060	0.6	680	200	400
	Green		1.0	50	125	2.6	1120	0.6	510	200	400

* \ \ = 0.85 um

** \ = 1.3 um

Table 2 Parameters of the Cable

	Type I	Type II
Subunit	0.4 mm SUS tension member	0.4 mm SUS tension member
	1.9 mm OD	1.9 mm OD
	1 multicore	1 multicore
	5 monocores (including colored buffer coated)	5 monocores (including colored buffer coated)
Unit	2.0 FRP tension member	2.0 FRP tension member
	7.4 mm OD	7.4 mm OD
	6 subunits	6 subunits
Cable	12 mm OD	7.5 mm OD steel with PE
	1 unit	28 mm OD
		2 units
		4 dummies
Ļength	300 m	250 m
Loss (AV)	Multicore: 3.4	Multicore: 3.4
	Monocore: 2.7	Monocore: 2.6

Table 3 Loss Charge and Baseband Response Versus Manufacturing Process

a traisfea	elustan \$ sp	less quas	CUE 1 1	and a		Baseband			
: hos nim	Kind of Cable	Un- packaged		Unit	Cable LED	Un- packaged		Cable	
	190 am	Spectral				0.85 μm	1.3 µm	0.85 μm	1.3 µm
	Multicore(14)	3.34	3.41	3.40	3.42	542	423	682	519
Type I	Monocore (8) (Transparent)	2.57	2.63	2.62	2.68	846	610	1042	713
	Monocore (2) (Green)	2.62	2.68	2.70	2.71	1012	620	1096	721
U margan	Multicore(14)	3.41	3.43	3.39	3.42	389	510	416	630
туре п	Monocore (8) (Transparent)	2.48	2.51	2.53	2.50	963	530	1082	610
	Monocore (2) (Green)	2.51	2.50	2.59	2.57	1096	518	1165	690

Table 4 Crosstalk

		Center 1	Side 2
Center	: 1		41 dB
Side	2	41 dB	
Side	3	42 dB	42 dB
Side	4	43 dB	45 dB
Side	5	43 dB	45 dB
Side	6	41 dB	46 dB
Side	7	42 dB	45 dB

Table 5 Mechanical Performance and Test Condition

	Result	Cond	ition		
Tensile strength	70 kg load 150 kg load	No less change 0.1 dB increase			
	250 kg load	Breakage			
Crushing test	700 kg load 900 kg load	No loss change 0.1 dB increase No mechanical damage	50 mm x 50 mm plate Rate of loading: 5 mm/min		
Mandrel strength test	50 kg load 150 kg load Center Side	0.2 dB increase	2 m cable segment D = 500 mm θ = 90° P = 50 kg, 150 kg		

STRESS-STRAIN BEHAVIOR OF OPTICAL FIBER CABLES

Peter R. Bark
Siecor Optical Cables, Inc.
Horseheads, New York
Ulrich Oestreich, Gunter Zeidler
Siemens AG, Telecommunication Cables
Munich, West Germany

A. Abstract

Based on fracture mechanics and fatigue tests, the paper discusses design considerations and test methods of optical fiber cables which offer reliability, long lifetimes and stable operating characteristics under installation and use conditions. Cable strains up to 1% and operating temperatures from -50°C to +80°C can be achieved by utilizing the loose, filled buffer concept without effect on the long-term mechanical and optical performance of fibers.

B. Introduction

The difference in the stress-strain behavior of copper wire and optical glass fiber dictates different cable design principles. Glass fibers are, in effect, incompatible with cable materials in two fundamental respects: Young's Modulus and coefficient of thermal expansion. Glass fibers do not show a yield point as copper wires; the stress-strain characteristic is linear up to the fracture load. The challenge of optical cable design is to deal with these facts and produce reliable cables with long life expectancies and premium, stable transmission characteristics.

C. Fiber Properties

Results of extensive tests on doped deposited silica fibers can be summarized as follows:

1. Strength of Optical Fibers

- 1.1. Strength of optical fibers is mainly determined by surface flaws which are randomly distributed along the fiber. Fiber strength is thus a statistical property, and data from fiber fracture tests is usually presented in a form of frequency distribution. This strength distribution for a given fiber strongly depends on sample length, loading velocity and environmental conditions. The longer the fiber, for example, the higher the probability of failure under a given stress.
- 1.2. If fibers are not stressed, their mechanical and optical properties remain unchanged, even in the presence of humidity, water, strong acid and basic chemicals.
 - 1.3. Surface flaws can grow in the presence

of stress. Thus fibers which are stressed due to tension, torsion or sharp bending are subject to static fatigue, resulting in a strength deterioration over time.

1.4. Usually optical fibers are subjected to a strength screen testing over the total length during manufacture. Thus weak fibers are eliminated and, as a result, the frequency distribution is truncated.

Static fatigue tests on screen tested fibers indicate that for long-length fibers (several kilometers as used in telephone cable plants) permanent stress levels of approximately one-third of the screen test do not affect fiber strength for a typical 20- to 40-year lifetime. For short-term, short-length applications the allowable permanent stress level may be higher.

2. Scattering Effects in Optical Fibers

Each optical fiber radiates when bent. This radiation of power is caused by a number of modes which are no longer guided and are coupled out of the core. The smaller the bending radius, the higher the amount of scattering. Bending radii above 50 mm, as applied by stranding in multifiber cable structures, do not result in measurable losses, even in lengths up to one kilometer or more. However, when an optical fiber is locally deformed on a microscopic scale, the transmission properties can be drastically affected. This microbending effect is determined by the amplitude and period of local distortions of the fiber coating and/or fiber buffering as well as by the fiber geometry and numerical aperture.

D. Optimization of Cable Designs

Reflecting fiber properties and based on test results, cable structures can be developed which offer reliability, long lifetimes and stable operating characteristics under installation and use conditions. To achieve hest performance levels economically, cable designs have to be optimized for the type of applications.

Optical fiber cables are strained under field conditions. This is especially important for aerial cable installations where the tensile reinforcement of the cable is permanently loaded by the cable's weight and additionally by ice and wind. Also for other types of installations, the cable is under tensile load during and, to a degree, after installation. In most cases the pulling load is applied to a randomly-bent, long cable and coupled by frictional forces to the outer cable sheath. Not only the kind of installation, but also the type of fiber, the link length performance and the lifetime expectancy determine the cable design.

Typical long-distance applications, such as T3 telephone trunks, require performance stability during life environment and failure probabilities in the order of 0.1% or less for a 30 km fiber link over a 20- to 40-year lifetime. Because of a high transmission rate over long lengths, changes of fiber attenuation, bandwidth and NA have to be very low.

To meet these requirements, the mechanical performance of the cable has to be optimized. The cable structure must create an operating "window" where the fiber can move relative to the rest of the structure without being stressed. Cable designs capable of decoupling the inevitable stresses of the installation environment from the fiber are "slotted core", "spacers" or "loose tube buffers"3. All of these cable designs provide space to accommodate a certain fiber excess length n. Thus the fiber tensile stress can be controlled or even kept to zero in all plannable situations during cable life. The only residual stress left is that due to fiber bending as a result of stranding; this amount, however, can be kept below the allowed one-third of the screen test level if the cable is designed appropriately.

Typical short-distance applications, as in industrial instrumentation or computer application, tolerate, in most cases, failure probabilities of 1% for a 3 km link over a 5- to 10-year lifetime. Very often high-NA, larger-corediameter fibors are being used; changes of one to two dB/km during life environment are acceptable. For this case a tight-fiber buffer seems to be the adequate design concept. The permanent fiber stress will be higher than in the loose buffer design; the fiber strain is directly proportional to the cable strain.

E. Fiber Tensile Strain In Different Cable Structures

Figure 1 schematically compares the fiber tensile strain for a given cable strain for tightly- and loosely-buffered structures.⁵

1. Tight Cable Structure

In the tight structure (A in figure 1), the cable tensile forces are coupled statistically to the fiber mainly in bends or by lateral compression. Because of material irregularities, these loads always induce a certain degree of microbending. Therefore the fiber strain, which is directly proportional to the cable strain, usually is associated with an excess of attenuation. In addition, the fracture probability increases

exponentially with fiber strain.

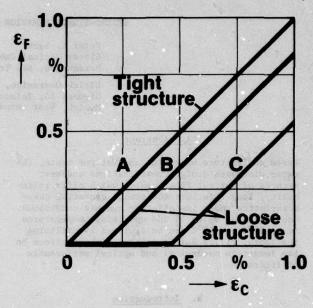


Fig. 1: Fiber Strain ϵ_F Vs. Cable Strain ϵ_C For Tightly and Loosely Buffered Fibers

2. Loose Cable Structure

In the loose structure (B and C in figure 1), however, the fiber strain is smaller than the cable strain because the cable cross section provides a certain fiber excess length n.

2.1. Unstranded Cables - In single-fiber cables containing a loose buffer tube, the elongation/contraction window where the fiber remains stress free is determined by the inner fiber clearance W and average helix period P of the fiber inside the loose tube (see figure 2):

$$\eta_{\rm T} = \frac{\pi^2 w^2}{2P}$$

Typically η_T is in the order of 0.1%, i.e. the fiber in a 1000 m single-fiber cable is approximately 1001 m long. Figure 3 shows the relationship between fiber excess length η_T and helix period P for a given fiber OD and a given tube inner diameter. At the moment, where η_T increases higher than approximately 0.1%, an increasing radiation due to macro and microbending creates an undesirable excess attenuation. Furthermore, at smaller helix periods P, the fiber bending stress surpasses the allowable maximum long-term stress for very low failure probabilities.

Figure 4 demonstrates the importance of very precisely controlling fiber helix period P and fiber excess length n_{T} during manufacturing. Smaller amounts of n_{T} result in a lower performance cable strain behavior. An excess length n_{T}

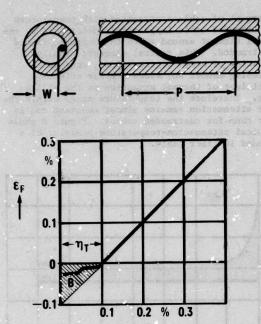


Fig. 2: Fiber Strain ϵ_F Vs. Cable Strain ϵ_C for a Single-Fiber Cable (Loose Tube Buffer). η_T : Fiber Excess Length (Allowed Tube Strain)

EC

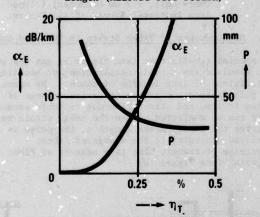


Fig. 3: Excess Attenuation α_E and Helix Period P vs. Fiber Excess Length η_T (Straight Loose Tube, W = 0.8 mm)

which is higher than calculated creates excess attenuation during buffering/cabling.

The contraction of a ceble structure is mainly determined by the temperature coefficients of the different cable components. Because of the big difference of the coefficients of thermal expansion between cable plastic materials and silica fiber, temperatures below -30°C cause cable shrinkage which results in increasing fiber excess length and excess attenuation. Figure 5 shows a

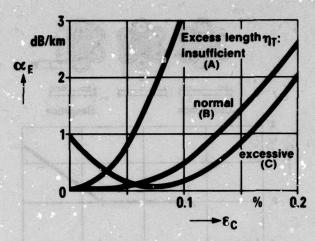


Fig. 4: Excess Attenuation α_E vs. Cable Strain ϵ_C for a Single-Fiber Cable (W = 0.7 mm)

typical attenuation-temperature dependence of an unstranded single-fiber cable. By using stiffening members having a similar coefficient of thermal expansion to silica, the excess attenuation beyond -30°C can be reduced.

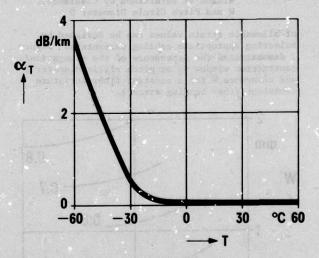


Fig. 5: Excess Atteruation α_T vs. Ambient Temperature T of a Single-Fiber Cable (Loose Cable Coil, 1 m Diameter)

2.2. Stranded Cables - The elongation/contraction window in stranded cables in not only determined by the fiber clearance W inside the buffer Lube, but also by the stranding lay length L and the pitch circle diameter D (see figure 6). This stranding-induced fiber excess length n_T is considerably bigger than in unstranded loose-tube cable designs. On straining a stranded cable, the fiber moves laterally toward the center of the cable core. The fiber remains unstressed until it contacts the inner wall of the buffer jacket adjacent to the central member. Typical values of n_S in stranded general-purpose cables are in the range of 0.3 to 0.5%. Cables with a broad range

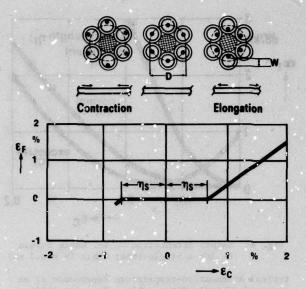


Fig. 6: Fiber Strain ϵ_F vs. Cable Strain ϵ_C for a Stranded Cable

η_S: All wed Elongation/Contraction Window as Determined by Clearance W and Pitch Circle Diameter D

of allowable strain values can be designed by selecting appropriate cabling parameters. Figure 7 demonstrates the dependence of the elongation/contraction window η_S on pitch circle diameter D and clearance W for a constant fiber curvature (constant fiber bending stress).

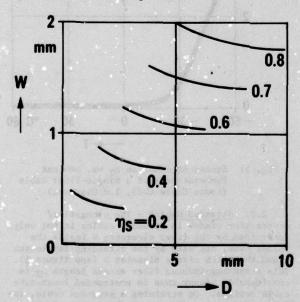


Fig. 7: Relation of Elongation/Contraction Window η_S, Pitch Circle Diameter D, Buffer Clearance W. Constant Fiber Curvature (Bend Radius 80 mm)

The amount of cable contraction with temperature in a stranded cable is primarily determined by the centrel element around which the buffered fibers are stranded. This central element, usually consisting of steel or fiberglass, acts as a stiffening member and shows similar effective coefficient of thermal expansion as the silica fiber. Therefore the temperature range within the fiber attenuation remains almost constart and is wider than for unstranded cables. Figure 8 shows a typical attenuation-temperature behavior of a stranded 10-fiber cable.

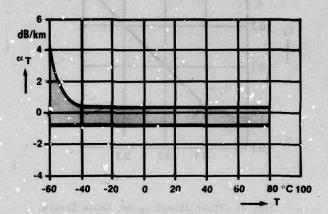


Fig. 8: Excess Attenuation α_T vs. Ambient
Temperature T of a 10-Fiber Cable (Loose
Cable Coil, 0.7 mm Diameter). Toned
Area Indicates Spread of All Fibers.

F. Measurements of Fiber Strain in Stressed Cables

A special tensile test (see figure 9) was designed to simulate the actual installation and handling conditions of long lengths of cable. By means of a pulse response neasurement device, change of transit time and attenuation due to cable straining can be monitored. When the cable strain surpasses the fiber excess length n, the pulse is delayed according to the elongated fiber. Increase of transit time is a measure of fiber strain (see figure 10).

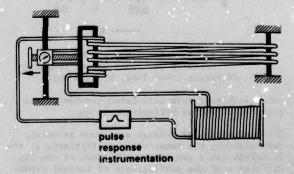


Fig. 9: Long Length Tensile Test Setup

At the same time pulse peak power and the total pulse energy decrease because of increased

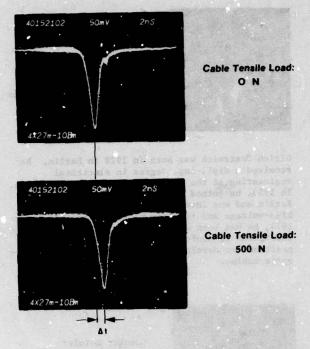


Fig. 10: Pulse Response Measurement of A Strained Fiber vs. Cable Tensile Load

microbending losses. The weakly-coupled modes, which are mainly present in the pulse tails, are stripped off more easily than the lower order modes. Therefore when calculating, the attenuation from the peak power of the pulse response is smaller than the attenuation derived from the integrated pulse erergy. In the following figures the excess attenuation data are based on the pulse energy changes, including all higher and lower order modes.

By measuring the transit time at different cable stress levels, the following data are obtained from the test:

- cable tensile load (F)
- cable strain (EC)
- fiber strain (ϵ_F)
- excess attenuation (α_E)

The following figures 11 and 12 summarize the results for an unstranded single-fiber cable and a stranded 10-fiber cable. These tests confirm the calculated design parameters. While the allowed elongation windew for the single-fiber cable is in the range of 0.1%, the tested 10-fiber cable with relatively small values for W and D has an operating range of $\eta_S=0.3\%$ cable strain. For both types of cable the attenuation increases approximately at that stress level where the allowed elongation window is surpassed and the fiber is subjected to tensile 3 tress. The excess attenuation was measured to be reversible in the range shown in the graphs.

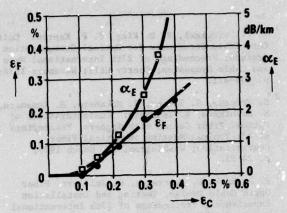


Fig. 11: Fiber Strain ϵ_F and Excess Attenuation α_E vs. Cable Strain ϵ_C in a Single-Fiber Cable (W = 0.77 mm)

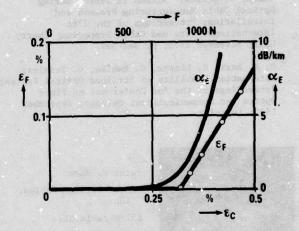


Fig. 12: Fiber Strain ϵ_F and Excess Attenuation α_E vs. Cable Tensile Force F and Cable Strain ϵ_C in a 10-Fiber Cable (W = 0.55 mm, D = 3.5 mm)

G. Summary

It has been demonstrated that the stability of optical and mechanical properties of optical cables can be optimized for the type of application. Fiber reliability and long-term stability can be achieved in cable structures using a loose fiber buffering. This cable structure can be designed to provide an operating "window" where the fiber can move relative to the rest of the structure without being stressed. By correct dimensioning of fiber clearance, average helix period, pitch circle diameter and lay length, practical cable tensile forces and cable strain during installation and under life result in zero fiber strain.

- T. S. Swiecicki, F. D. King, F. P. Kapron: Unit Core Cable Structures for Optical Communication Systems; Proceedings of 27th International Wire and Cable Symposium; Cherry Hill; November 1978; p. 404-411.
- S. Yonechi, S. Tanaka, T. Nakahara, H. Kumamaru, M. Hoshikawa, K. Ishihara: Characteristics of Optical Fiber Cables with Spacers; Proceedings of the Topical Meeting on Optical Fiber Communication; Washington, DC; March 1979; p. 24-25.
- P. R. Bark, U. Oestreich, G. Zeidler: Fiber Optic Cable Design, Testing and Installation Experiences; Proceedings of 27th International Wire and Cable Symposium; Cherry Hill; November 1978; p. 379-384.
- T. Kobayashi, Y. Sugawara, R. Yamanchi, K. Inada, N. Uchida: Stress in Fibers During Optical Cable Manufacturing Process and Installation; Proceedings of the 27th International Wire and Cable Symposium; Cherry Hill; November 1978; p. 362-369.
- P. R. Bark, H. Liertz, G. Mahlke, G. Zeidler: Attenuation Stability of Strained Optical Cables; Proceedings of the 2nd Conference on Fiber Optics and Communications; Chicago; September 1979; in print.



Peter R. Bark
Siecor Optical Cables,
Inc.
631 Miracle Mile
Horseheads,
New York 14845

Peter Bark holds a bachelor of science degree from the Technical University at Munich. He also received his doctorate in engineering from the same institution in the field of molecular beam physics. He has been employed by Siemens AG in Munich, West Germany since 1971, in several positions in the telecommunications field. His principal assignments were in optical communications cabling, interconnecting hardware and subsystems, where he made a number of key contributions. Among his assignments in optical communications, he was a development engineer for cable filling compound physics and for optical cables and the supervisor of development and pilot plant manufacturing for optical waveguide systems. Peter Bark is now vice president for engineering at Siecor Optical Cables, Inc.



Ulrich Oestreich Siemens AG Telecommunication Cables Munich, West Germany

Ulrich Oestreich was born in 1928 in Berlin. He received a dipl.-ing. degree in electrical engineering at the Technical University in Berlin. In 1953, he joined the Siemens-Cabel-Works in Berlin and was involved in the development of high-voltage and telecommunication cables. Since 1974, he has been with the telecommunication cable department in Munich, where he holds a managing position for developing and manufacturing of fiber optic cables.



Guenter Zeidler Siemens AG Telecommunication Cables Munich, West Germany

Guenter Zeidler was born in 1940 in Rosshaupt, Germany. He studied from 1959 to 1964 at the Technical University of Munich. He holds a dipl.-ing. degree in electrical engineering and a PhD in physics. In 1965, he joined the Munich Telecommunication Central Labs of Siemens AG, working in the laser field. He changed to the Siemens Research Labs in 1972, holding managing positions in the field of fiber and integrated optics. Since 1976, he has been with the telecommunication cable department in Munich and is now responsible for the development and manufacturing of fiber optic cables and ancillary hardware.

DESIGN AND PERFORMANCE OF A CROSSPLY LIGHTGUIDE CABLE SHEATH

P. F. Gagen and M. R. Santana

Bell Laboratories Norcross, Georgia

ABSTRACT

A high-strength, torque-balanced, crossply sheath having multiple layers of steel reinforcing strands applied with opposite lay directions has been developed for the Bell System, ribbon-type, light-guide cable. Compared to earlier single-ply cable sheaths: (i) tensile strength has been doubled, (ii; tensile creep has been virtually eliminated, (iii) bend, kink, handling, and impact performances have been improved, and (iv) diameter and bending stiffness have remained constant. As a result, the crossply cable is suitable for a wider range of temperatures and applications. Sheeth design and performance will be discussed.

INTRODUCTION

Bell Laboratories has in recent years been very active in the development of lightguide communi-cation cables. Earlier cables^{1,2} were designed for underground installations having a limited temperature range (no steam conditions). In May 1977, the first lightguide communication system offering a wide range of telecommunication services to customers carried commercial traffic in the Chicago loop area.² Although all the lightguide cables were successfully installed without any optical fiber breaks, the experience helped identify desirable design changes in the single-ply cable sheath. Changes such as: (i) a higher cable tensile strength and (ii) improved handling by eliminating the tendency of the cable to twist when bent were needed. In addition, around that same time, experiments showed that the tensile creep of the single-ply sheath was not acceptable. Hence, a new high-strength, torque-balanced, crossply cable sheath was developed.

Lightguide cables with the new crossply sheath will be used in underground and aerial applications of the Bell System standard lightwave transmission system (designated FT3) operating at 44.736 Mb/s (DS3 rate). The first installation of this system is scheduled for the first half of 1980 with a service date in late 1980.

GPTICAL CABLE DESIGN

Because of the small size, vulnerability, and relatively large number of optical fibers involved, it was decided that craftpersons should handle groups of fibers rather than individual fibers. This together with the concept of array splicing³, evolved into the use of fiber ribbons⁵⁻⁷ consisting of linear arrays of fibers as a first step in fiber packaging. Although the ribbon structure provides good initial protection for the fibers, a reinforced sheath is needed for protection against handling and installation stresses in typical outside plant applications.

Both the single-ply and crossply cable designs are modular in the sense that the sheath is identical regardless of the number of ribbons contained. Typically, an optical-fiber ribbon has twelve fibers. For this case, the minimum number of fibers in a cable is 12 (one-ribbon cable) and increases in multiples of 12 up to 144 (twelve-ribbon cable). For both cable designs, the ribbons are stacked on top of each other to form a rectangular array, and the array is twisted to improve its bending properties.

Single-ply Design

Figure 1 shows an exploded view of the single-ply cable design. Briefly, the twisted ribbon core is longitudinally wrapped with a thermal barrier to prevent the outer sheath extrusions from damaging it. The sheath consists of a high-density polyethylene (HDPE) inner sheath over which a relatively thick polypropylene twine layer is helically applied. The sheath strength members (steel wires) are then helically applied over the twine layer and an HDPE outer sheath is extruded over them. Note that only one layer of wires is present; therefore, the cable will have a tendency to twist under a tensile load (not torque balanced). The thick polypropylene layer was intended to provide thermal protection and cushioning from impact loads for the ribbon core.

A complete description and mechanical properties of this design was reported in the 1977 International Wire and Cable Symposium (Reference 1).

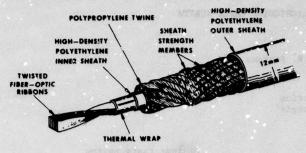


FIGURE 1. SINGLE-PLY LIGHTGUIDE CABLE

Crossply Design

Figures 2 and 3 show an exploded and a crosssectional view of the crossply lightguide cable design. The sheath consists of an HDPE inner sheath over which a relatively thin layer of polyester tape is applied to serve as a bedding for the first reinforcing wire layer which is followed by an HDPE extrusion. The second layer of wires is applied (again over a thin layer of polyester tape) and the outer sheath of HDPE is extruded over it. The two layers of wires have opposite lay directions, and their lay lengths are adjusted to eliminate the tendency to twist under a tensile load (torque balanced). Note that the diameter remained constant even though there are two layers of reinforcement in the crossply sheath design. This was accomplished by replacing the thick polypropylene layer of the single-ply sheath with a thinner polyester layer in the crossply sheath. Thermal measurements of the ribbon core during extrusion showed that the polypropylene and the polyester layers were equally effective thermal barriers. In addition, the polyester layer enhances registration of the strength members by allowing the wires to compress into it and thus form a trough which holds the wire in place during extrusion. In the following sections, the crossply sheath mechanical properties will be discussed, and it will be shown that they are either superior or equivalent to the single-ply sheath.

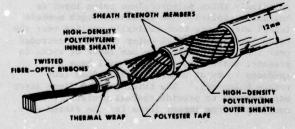


FIGURE 2. CROSSPLY LIGHTGUIDE CABLE

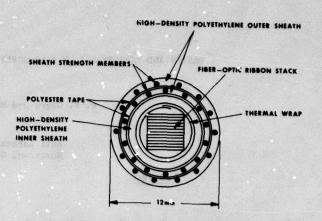


FIGURE 3. CROSSPLY CABLE CROSS SECTION

TENSILE PERFORMANCE

Based on field installation experience, it was decided that a significant increase in cable tensile strength was required for general outside plant applications. The number of sheath strength members was doubled for the crossply cable to approximately double the tensile stiffness of the sheath. The results, illustrated in Figure 4, show the stiffness of the single-ply and the crossply cables to be approximately 900 lb/% and 1800 lb/%, respectively. The cable tensile behavior is linear up to about 1% elongation. However, the fibers limit the amount of elongation allowed since they should not be stretched past their proof-test-level strain. For FT3 the fibers will have a minimum proof-test stress level of

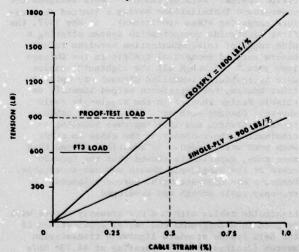


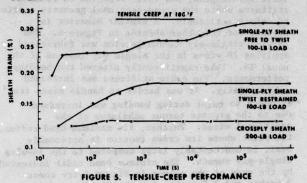
FIGURE 4. LIGHTGUIDE CABLE TENSILE PERFORMANCE

5x10* psi or approximately 0.5% strain. Hence, the dotted line in Figure 4 represents the cable elongation (0.5%) and load (900 lb) when the fibers are at the proof-test level. A factor of safety of two thirds is applied to the cable proof-test load to protect against short-term static-fatigue failure of the glass fibers during installation. Hence, the FT3 tensile rating of the crossply cable will be 600 lb. In the future, as the fiber prooftest strain increases toward 1%, the tensile rating of the cable can increase accordingly. The existing cable sheath and pulling eye hardware can support a 1500-lb load.

TENSILE CREEP PERFORMANCE

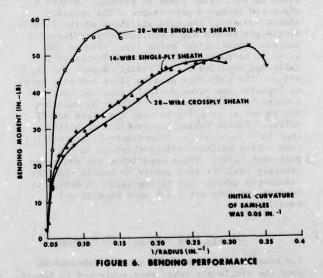
Tensile-creep properties of the single-ply cable were characterized. These measurements were important since the allowable cable strains were small. Strain due to tensile creep should be limited to an acceptably small portion of the allowable cable strain to keep from: (i) reducing the cable tensile rating and (ii) breaking fibers from excessive strain during installation.

A series of tensile-creep tests were performed on the single-ply sheath for different load conditions and temperatures. Samples were hung vertically in an environmental chamber, a 100-1b weight was attached to the samples to apply a constant load, and the elongation of the sample was measured versus time. Typical results are shown in Figure 5 for a chamber temperature of 180° F. The upper curve represents a sample that was free to twist during the test. For the middle curve, the sample was restrained from twisting during the test, but was otherwise free to elongate. As a reference point, the 100-1b load would stretch the single-ply samples to about 0.12% without creep effects. As seen in Figure 5, the total strain, including creep, could approach two to three times the anticipated short-term strain. A comparison of the free-to-twist and twist-restrained results suggests two causes for tensile creep in the single-ply sheath: (i) twist elongation where the sheath elongates as the wires untwist and (ii) radial migration of the wires into the soft twine layer where the sheath elongates as the wires move in slightly toward the center of the cable. The difference between the upper and middle curves in Figure 5 correlated well with the elongation due to the measured amount of untwist of the sample. Since the crossply is torque balanced (no tendency to twist) and does not contain a soft twine layer (inhibits radial movement of the wires) it was expected that its tensile-creep performance would be dramatically improved relative to the single-ply sheath. In fact this turned out to be true. The lower curve in Figure 5 shows the crossply cable has negligible creep at 180° F under a 200-lb load (which is equivalent to a 100-lb load on the single-ply sheath). The crossply tensile creep was also negligible for a 1200-lb load at 180° F. Hence tensile creep is no longer a concern for installations involving very hor sunny days or installations in ducts near steam heating where temperatures could range from 150 to 180° F.



BEND PERFORMANCE

Bending properties of optical cables including bending stiffness, handleability, and minimum bend radius are important. The bending properties of several designs were characterized by determining curvature as a function of applied bending moment. Results for three designs: (i) the single-ply (14-wire) cable, (ii) a 28-wire version of the single-ply cable, and (iii) the crossply (28-wire) cable are indicated in Figure 6.



The 14-wire single-ply sheath curve in Figure 6 can be divided into three general regions: (1) a relatively high initial stiffness region where the wires and polyethylene (PE) matrix are under the same bending strain, (ii) a region of moderate stiffness where the wires slip relative to the PE and are able to average the bending strain over their lay lengths, and (iii) a region of reduced stiffness where the cross-sectional geometry starts to deform noticeably. A similar behavior is evident for the other sheaths in Figure 6. The 28-wire single-ply sheath version was fabricated by applying 28 wires in the single ply instead of the usual 14. This significantly altered the bending performance. The cable stiffness was increased substantially. It was harder to handle since its tendency to twist during bending was increased due to the greater torque unbalance of the additional wires. Further, its minimum bend radius, the point where its cross section is noticeably oval, is unacceptably large compared to the 14-wire single-ply sheath. The minimum bend radii indicated by the ends of the curves in Figure 6 are about 7 inches and 3.5 inches for the 28-wire and 14wire single-ply sheaths respectively. The difference between the cables was attributed to the interaction of the wires and the soft twine layer. When tests were continued beyond the minimum bend radius, the wires on the inside of the bend would start to buckle into the twine layer and initiate a sheath kink. This condition developed at a larger radius for the 28-wire version.

The crossply cable minimum bend radius is improved since no soft twine layer is present. Figure 6 shows the improved performance. The crossply sheath has about the same stiffness as the 14-wire single-ply sheath and a minimum bend radius of 3 inches. Removing the twine layer allowed the wires to be positioned nearer the center of the cable and provided firmer radial support for the wires. The polyester bedding layer not only helps to register the wires during stranding, but also reduces the cable bending stiffness by reducing the amount of coupling between the wires and PE matrix. Cables having longitudinal or helical gaps in the polyester, like Figure 2, are stiffer than cables having complete coverage in the polyester layer. Field experience has shown the crossply cable is much easier to handle than the single-ply cable. The torque-balanced design is neutral and does not twist upon bending and handling.

IMPACT, BEND AND TWIST PERFORMANCE

The crossply cable showed a general improvement over the single-ply cable when subjected to impact, bend, and twist tests. Tests were performed on cables containing 144 fibers. The crossply cable survives a single impact of 30 ft-1b (0.25-inch diameter striking mandrel), or 400 cyclic impacts of 4.75 ft-1b (0.5-inch diameter mandrel) without damage. In bending, 1400 cycles of ±90° over a 4.9-inch radius bend caused no damage. In twist

the cable endured without damage 2000 cycles of ±180° twist while rolling back and forth over a 6-inch diameter sheave. These crossply results are similar to the single-ply cable in single impact and bending, but are significantly better in cyclic impact and twist.

SUMMARY

Table I summarizes the rated properties of the crossply lightguide cable design. The crossply design will be used in the Bell System standard FT3

TABLE I

Value*	Comments
12-144	Ribbon structure
0.48 in.	
80 lb/kft	design of tenns to smile of a
1800 15/%	olemais geographications him Transports in the interesting of the
600 1ь	Assumes 5x10 ⁴ psi fiber proof-test level and safety factor
9 inches	Includes a safety factor
30 ft-1b	0.25-inch diameter striking mandrel
400 cycles	4.75 ft-lb impact, 0.5-inch diameter striking mandrel
2000 cycles	±180° of twist
1400 cycles	±90° bend over a 4.9- inch radius
	12-144 0.48 in. 80 lb/kft 1800 lb/% 600 lb 9 inches 30 ft-lb 400 cycles

* The criterion for the ratings is no sheath and/or fiber damage.

lightwave inter-office trunk transmission system. The weight and tensile stiffness are nominal values and will vary slightly depending on the fiber content of the cable. Compared to the single-ply cable, the crossply cable:

- has the same diameter and bending stiffness.
- (ii) has about double the tensile strength,
- (iii) is torque balanced,
- (iv) has negligible tensile creep,

- (v) has improved kink resistance and handling,
- (vi) has overall improved impact, bend, and twist performance, and
- (vii) is suitable for a wider range of temperatures and applications.

ACKNOWLEDGMENT

The successful design and fabrication of the crossply lightguide cable is due to the efforts of many individuals at Bell Laboratories. Special thanks are extended to J. W. Elling and G. M. Yanizeski for their contributions in cable testing.

REFERENCES

- M. J. Buckler, M. R. Santana, and S. C. Shores, "Design and Performance of an Optical Cable", 26th International Wire and Cable Symposium, Cherry Hill, N. J., November 1977.
- T. C. Cannon, D. L. Pope, and D. D. Sell, "Installation and Performance of the Chicago Lightwave Transmission System", IEEE Transactions on Communications, Vol. COM-26, No. 7, July 1978.
- M. I. Schwartz, "Optical Fiber Cabling and Splicing", Technical Digest of Papers of the Topical Meeting on Optical Fiber Transmission I, Williamsburg, Virginia, January 1975, p. WA2.
- C. M. Miller, "Fiber Optic Array Splicing with Etched Silicon Chips", B.S.T.J., Vol. 57, No. 1 (January 1978), pp. 75-90.
- R. D. Standley, "Fiber Ribbon Optical Transmission Lines", B.S.T.J., Vol. 53, No. 6 (July-August 1974), pp. 1183-1185.
- M. J. Saunders and W. L. Parham, "Adhesive Sandwich Optical Fiber Ribbons", B.S.T.J., Vol. 56, No. 6 (July-August 1977), pp. 1013-1014.
- M. J. Buckler, M. R. Santana, and M. J. Saunders, "Lightguide Cable Manufacture and Performance", B.S.T.J., Vol. 57, No. 6 (July-August 1978), pp. 1745-1757.
- T. C. Cannon and M. R. Santana, "Mechanical Characterization of Cables Containing Helically Wrapped Reinforcing Elements", 24th International Wire and Cable Symposium, Cherry Hill, N. J., November 1975.



P. F. Gagen (Paul) is supervisor of the Optical Cable Design Group. The Group is responsible for developing a family of fiber optic cables for the Bell System lightwave communications systems.

Since joining Bell Labs in 1970, he has been involved with the development of control systems for remotely-steerable underground tunneling devices, equipment for handling large coaxial cables in the field, and automated interconnection systems for telephone central offices.

Paul has a B. E. degree from the Cooper Union College, and a M.S.M.E. from New York University. He is a member of Tau Beta Pi, Pi Tau Sigma, and his hobbies include varied sports activities.



Manuel R. Santana received a Bachelor of Science degree in Electrical Engineering in 1970 from the University of Hartford and his Master of Science degree in Electrical Engineering in 1971 from the Georgia Institute of Technology. Since 1970, he has been employed by Bell Laboratories at Norcross, Georgia, where he is presently a member of the Technical Staff in the Fiber Optic Transmission Media Department. His present assignment is on optical-fiber cable design, analysis, and testing. He is a member of the IEEE.

AUTHOR INDEX

kers, F. I 333,	340	Masterson, J. B.	30
llen, D. B.,	281	Matsui, M	12
nce, L	273	McCann, J	27
rai, T	344	Morishita, M	
sam, A. R 333,	340	Morita, Y	12
umiller, J. H	212	Mork, H	22
valos, J. Z	201	Moss, A. J	2
aker, H. L	153	Mullins, R	15
ark, P. R	385	Muninghaus, W	3
artlett, G. A	145	Nakajima, J	
auchamp, R. L	179	Nakano, K.	2
rowicz, L	32	Nantz, T	
scher, G	184	Narasimham, P	3
auer, M	305	Newton, W	1
ooks, R. M	58	Oestreich, V.	3
own, W. E	11	Ogai, M	3
	299	Oh, S. M.	3
1. (1. 1. 1. 1. 1. 1. 1. 1. 1. 1. 1. 1. 1. 1	254	Ohmori, N.	3
Impbell, B. D.	18	Okubo, M.	200
[2] - 현존 경험 전환, 14, 15 - 1 : 1 : 1 : 1 : 1 : 1 : 1 : 1 : 1 : 1	281	Olszewski, J. A.	3
이 마스트를 잃었다면 하면 나는 아이를 하는데 하면 하면 하는데	118	Otake, A.	3
이 경기에 가장 아니는 이 이 이 아들은 전투에 이 전투에 가장하고 있다면 하는데 하는데 이 시간 이 시간 때문에 되었다.	232	Ouchi, Y.	2016
cker. R. L.	96	Pirotta. R.	
	254	Presto, W. S.	1
vereaux, R. C.	11	Prosper, J.	2
novan, R. C.	96	Przybyla, L. J.	2
	225	Reale, P. J., Jr.	
[1] - 1 - 1 - 1 - 1 - 1 - 1 - 1 - 1 - 1 -	225		2
	105	Reed, J. C.	
im, G.	1	Reed, W.	
incis, P. C.	65	Rittich, D.	3
		Rodde, A. F.	
	391	Santana, M. R.	3
	232	Sato, T.	3
	184	Scalco, E	
	357	Schlef, C.	3
2. N. J.	258	Schuring, G. A.	2
II, L. J	78	Seikai, S.	3
, G. J	65	Sentsui, S	3
(1884년) (1884년) 1884년 (1884년) 1884년 1 1884년 - 1884년	153	Serapins, K.	3
(BENERAL SERVICE SERVI	344	Shimada, T.	3
	370	Shinzawa, S.	3
경험 🗢 시간에 있다면 있는데 그 사람이 가면 이 가는데 그리는데 하는데 보고 있다면 하는데 보고 있다면 하는데	352	Snyder, D. Q.	2
bis, P.	53	Spencer, H. J. C.	1
HE 12 : 6 전 [1912] 1약 [2012] 1인	174	Stephens, W. J.	
	165	Streu, R. J.	
	344	Tachigami, S	
	137	Takahashi, Y.	2
(2000년) [2] (이 12일에 기업하다 (2010년) [2010년) (12일 12일 12일 12일 12일 12일 12일 12일 12일 12일	370	Takeda, K.	3
E	37	Tenzer, M	2
[2] 15 15 16 16 16 16 16 16 16 16 16 16 16 16 16	370	Tisdale, M. W.	
	319	Uchida, N	3
ıfman, S	281	Umezu, H	
vazoe, H.	21	Uradnisheck, J	2
kawa, S	21	Wadehra, I. L.	3
caid, J	- 1	Watanabe, O	3
	299	Waucheul, J. P.	1
그들이 가는 사람이 되는 이 것 같아 되는 것이 없는 것이다.	191	Wight, F. R.	1
	244	Wu, A. F	2
	357	Yamamoto, T.	2
	305	Yamazaki, Y.	1
nch, J	78	Yocum, M. M.	2
aklad, M. S	340	Yoshizaki, K.	3

